STEPS TO CREATING A CO-CULTURE TO INVESTIGATE REACTIVE SPECIES IN NEURODEGENERATION

CHARLOTTE HOWARD

A thesis submitted in partial fulfilment of the requirements of Nottingham Trent University for the degree of Doctor of Philosophy (PhD)

September 2019

Copyright Statement

ABSTRACT

Introduction

Neurodegenerative disease's such as Alzheimer's and Parkinson's disease are becoming more prevalent as the aging population increases. Multiple factors are implicated including impaired protein degradation, mitochondrial dysfunction and oxidative stress; whose mechanisms may be interconnected in the so-called 'Neurodegenerative Bermuda triangle'. Understanding these hallmarks is essential for developing new therapies to help ameliorate symptoms of neurodegenerative diseases.

Methods and Aims

Human neuronal (SH-SY5Y) and glial (U-87MG) cell lines were used to investigate oxidative stress mediated neurodegeneration. Reactive species (RS), specifically peroxy radicals and superoxide radicals were produced using 2,2'-Azobis(2-methylpropionamidine) dihydrochloride (AAPH; a ROS generating lipid peroxidation agent) and rotenone (a mitochondrial disruptor that inhibits complex I), respectively. Using fluorescence probes, cellular function assays, PCR analysis, protein expression and proteomics the effects of RS in neural cells both in mono and co-cultures were investigated.

Results

AAPH and rotenone were shown to have divergent effects on neural cells exposing the differences between these cells. Furthermore, AAPH was found to induce greater lipid peroxidation than rotenone, suggesting different toxins induce specific RS. In particular, the NRF2-antioxidant response element was highlighted as a key pathway activated by oxidative stress. Experiments with primary embryonic cortical neuronal cultures show the limitations of *in vitro* differentiation models. Thus, steps to create a co-culture were investigated, demonstrating the difficulties associated with co-cultures but showing how neuronal susceptibility to RS was altered by glial cells.

Conclusion

This body of work highlights AAPH for future investigations into lipid peroxidation. Furthermore, the results herein suggest differentiation methods should be considered when evaluating RS susceptibility. Finally, initial investigations have determined how transwell inserts can be used to create co-cultures between neural cells with materials needing to be considered for future studies. Conditioned media provides an alternative way to investigate secreted factors where potential pathways have been determined for future studies.

TABLE OF CONTENTS

FIGURE LIST

TABLE LIST

ABBREVIATIONS

1-methyl-4-phenyl-1,2,3,6-tetrahydropyridine	MPTP
2,2’-Azobis[2-methylpropionamidine] dihydrochloride	AAPH
2’,7’-dichlorofluorescein	DCF
2’,7’-dichlorofluorescin diacetate	DCFDA
3-(4,5-dimethylthiazol-2-yl)-2,5-diphenyltetrazolium bromide	MTT
4-(2-hydroxyethyl)-1-piperazineethanesulfonic acid	HEPES
4-hydroxynonenal	4-HNE
5’,6,6’-tetrachloro-1,1’,3,3’-tetraethylbenzimidazolylcarbocyanine iodide	JC-1
6-hydroxydopamine	6-OHDA
Adenosine triphosphate	ATP
Alzheimer's disease	AD
Ammonium persulfate	APS
Amyotrphic lateral sclerosis	ALS
Antioxidant response element	ARE
Aromatic amino acid decarboxylase	AADC
Ascorbic acid	AA
Bicinchoninic acid	BCA
Bovine serum albumin	BSA
Brain derived neurotrophic factor	BDNF
Central nervous system	CNS
Chymotrypsin-like activity	CLA
Complementary DNA	cDNA
Core particles	CP
Cytochrome c	Cyt c
Data dependent acquisition	DDA
Data independent acquisition	DIA
Deoxyribonucleic acid	DNA
Dihydronicotinamide-adenine dinucleotide phosphate	NADPH
Dimethylsulfoxide	DMSO
Dopamine trasnporter	DAT
Dopaminergic	DA
Dulbecco’s Modified Eagle Medium	DMEM
Dulbecco’s phosphate buffered saline	DPBS
Dynamin related protein 1	DRP1
Electron transport chain	ETC
Ethylenediaminetetracetic acid	EDTA
Extracellular acidification rate	ECAR
Extracellular matrix	ECM
Foetal bovine serum	FBS
Glial fibrillary acidic protein	GFAP
Glutathione	GSH
Glutathione peroxidase	GPX
Glyceraldehyde 3-phosphate dehydrogenase	GAPDH
Growth derived neurotrophic factor	GDNF
Heat shock factor	HSF

Heat shock protien	HSP
Horse radish peroxidase	HRP
KELCH-like ECH associated protein	KEAP
Lactate dehydrogenease	LDH
L-dihydroxyphenylalanine	L-DOPA
Lewy bodies	LB
Malondialdehyde	MDA
Mitochondrial DNA	mtDNA
Mitofusin	MFN
Monoamine oxidase	MAO
N, N, N',N'-Tetramethylethylenediamine	TEMED
NADPH oxidase	NOX
Neurodegenerative Bermuda triangle	NBT
Neurotrophic tyrosine kinase receptor B	NTrkB
Nicotinamide adenine dinucleotide	NADH
Nitric oxide synthase	NOS
Non-essential amino acids	NEAA
Nuclear erythroid related factor	NRF
Optic atrophy 1	OPA1
Oxidative stress	OS
Oxygen consumption rate	OCR
Parkinson's disease	PD
Peroxiredoxin	PRDX
Polyester	PET
Polymerase acrylamide gel electrophoresis	PAGE
Post-translational modification	PTM
Proliferator-activated receptor coactivator gamma coactivator 1α	PGC-1α
PTEN-induced kinase-1	PINK1
Quantitative real-time polymerase chain reaction	qRT-PCR
Reactive nitrogen species	RNS
Reactive oxygen species	ROS
Reactive species	RS
Real-time cell analysis	RTCA
Regulatory particle	RP
Retinoic acid	RA
Ribonucleic acid	RNA
Sequential acquisition of all theoretical mass spectra	SWATH-MS
Small interfering ribonucleic acid	siRNA
Sodium dodecyl (lauryl) sulphate	SDS
Standard deviation	SD
Standard error of mean	SEM
Substantia nigra	SN
Superoxide dismutase	SOD
Thiobarbituric acid reactive substances	TBARS
Thioredoxin	TXN
Tris buffer saline	TBS

Tris-acetate EDTA	TAE
Tyrosine hydroxylase	TH
Ubiquitin carboxy-terminal hydrolase L1	UCH-L1
Ubiquitin proteasome system	UPS
Vesicular monoamine transporter 2	VMAT2

CHAPTER 1

GENERAL INTRODUCTION

1.0 General Introduction

1.1 Parkinson's Disease

With people living to greater ages in developed and developing countries, neurodegenerative diseases such as Alzheimer's and Parkinson's disease (AD and PD, respectively) are becoming more prevalent. PD is the second most common neurodegenerative disease (Gitler et al., 2017; Maniati et al., 2019), first described as "the shaking palsy" in 1817 (Parkinson, 2002). The core clinical features recognised in PD include: bradykinesia, tremor and rigidity (Carta and Hirsch, 2018) though more recently, studies have identified non-motor features preceding these motor symptoms such as hyposmia, sleeping disorders, depression and constipation (Schapira et al., 2017). Underlying these clinical features are neuropathological hallmarks including loss of dopaminergic (DA) neurons in the substantia nigra (SN) and intraneuronal inclusions referred to as Lewy bodies (LBs; Walker et al., 2019). LBs are immunoreactive for α-synuclein, 3-nitrotyrosine, neurofilament, synphilin-1, ubiquitin and ubiquitin-pathway related proteins (Collier et al., 2017; Voronkov et al., 2018; Walden and Muqit, 2017). Yet despite multiple decades of studying PD, the cause and underlying mechanisms for PD's pathology are still unknown.

1.1.1 Familial Parkinson's disease

PD can be separated into two types: familial and sporadic. Familial PD patients have shown increased levels of oxidized lipids and proteins (Sanders and Timothy Greenamyre, 2013), as well as decreased levels of reduced glutathione (GSH; H. Wei et al., 2019 , theorized to contribute to protein accumulation and aggregation. In familial patients, mutations in α-synuclein (Ingelsson, 2016), parkin (Kitada et al., 1998), ubiquitin carboxy-terminal hydrolase-L1 (UCH-L1; Nishikawa et al., 2003), PTEN-induced kinase-1 (PINK1; Valente et al., 2004) and DJ-1 (Vincenzo Bonifati et al., 2003) have been documented.

Mutations (Polymeropoulos et al., 1997) and overexpression (Singleton et al., 2003) of wild-type α-synuclein, a 140 amino acid protein substrate for the ubiquitin proteasome system (UPS) (M C Bennett et al., 1999; Shimura et al., 2001; Tofaris et al., 2001) show increased protein misfolding and aggregation (Feany and Bender, 2000; Goedert, 2001; Ludtmann and Abramov, 2016). Furthermore α-synuclein mutants are more resistant to proteolysis (Sakai et al., 2019) and demonstrated a longer rate of proteasomal degradation relative to wildtype α-synuclein (Bennett et al., 1999). In addition, a study using transgenic mice overexpressing α-synuclein showed mitochondrial function was impaired while oxidative stress (OS) increased (Ludtmann et al., 2018; Song et al., 2004). *In vitro* studies using SH-SY5Y cells overexpressing α-synuclein demonstrated

increased caspase 3 activity alongside decreased cell viability (Perfeito et al., 2017). In addition, lower levels of superoxide dismutase and glutathione, responsible for scavenging superoxide, hydrogen peroxide and hydroxyl radicals (Marí et al., 2013; Nakamura et al., 1997; Ruszkiewicz and Albrecht, 2015) were observed. SH-SY5Y cells transfected with mutant α-synuclein also exhibited decreased cell viability, condensed nuclear apoptotic bodies and increased intracellular reactive oxygen species (ROS; Ju et al., 2017). Together, these studies suggest mutant α-synuclein accumulates suggesting protein degradation clearance is impaired contributing to OS.

Parkin, an E3 ubiquitin ligase, is responsible for protein ubiquitination, targeting substrates to the 26S proteasome for degradation (Imai et al., 2000). Parkin can localise to mitochondria, playing a role in inhibiting mitochondrial-dependent cell death by preventing swelling and caspase release (Darios et al., 2003). In addition, leukocytes from patients with parkin mutations showed selective impairment of complex I in the electron transport chain (ETC) of mitochondria. In both familial and sporadic PD patients parkin deficiencies and mutations are associated with mitochondrial dysfunction and OS (Müftüoglu et al., 2004). Studies of parkin-null flies support this as they displayed altered mitochondrial morphology and tissue degeneration in wing flight muscles and spermatocytes (Greene et al., 2003). In another study, overexpression of mutant parkin increased cellular markers of OS while wildtype parkin expression reduced these markers (Hyun et al., 2002). Parkin-null mice exhibited lower levels of oxidative phosphorylation, weight gain and antioxidant capacity. These mice also showed increased RS mediated tissue damage suggesting parkin regulates mitochondrial function and protects cells from OS (Palacino et al., 2004). Other parkin-null mouse models support decreased antioxidant capacity as lower levels of reduced glutathione were measured (Itier, 2003). Therefore due to parkin-null mice having decreased antioxidant capacity they are more susceptible to RS damage, which is evident in parkin-null mice brains which display elevated oxidised protein and lipid levels (Palacino et al., 2004). In another study, RS are suggested to inactivate parkin (Winklhofer et al., 2003). Therefore, low levels of parkin suggest decreased antioxidant capacity resulting in RS induced damage, leading to mitochondrial dysfunction propagating more RS and further parkin inactivation, creating a vicious cycle of damage possibly leading to cell death. Together, studies suggest parkin mutations result in protein accumulation, mitochondrial dysfunction and RS generation.

In rare familial forms of PD, mutations in ubiquitin C-terminal hydrolase L1 (UCH-L1), a deubiquitinating protein have been observed (Leroy et al., 1998; Shimura et al., 2001). Proteins in the UCH family are involved in the hydrolysis of small C-terminal ubiquitin adducts (Pickart and Rose, 1985). Due to their substrate specificity it is proposed UCH proteins are involved in ubiquitin recycling rather than deubiquitination (Bishop et al., 2016; Larsen et al., 1998). Four isoforms are

reported: UCH-L1-L4 (Mayer and Wilkinson, 1989; Shinohara et al., 1993; Wilkinson, 1995) where UCH-L1 is neuron-specific (Wilkinson et al., 1989). In a German family with familial PD, a missense mutation was observed in the gene coding UCH-L1 resulting in partial loss of hydrolase activity (Leroy et al., 1998). In mice with intragenic deletion of UCH-L1, neuron-specific phenotypes and severe neurodegeneration was observed (Lee and Hsu, 2017; Saigoh et al., 1999). Due to UCH-L1's specific ubiquitin hydrolase activity it is suggested to regulate cellular levels of free ubiquitin in neurons (Kang et al., 2018; Larsen et al., 1998). Furthermore, recent studies suggest that UCH-L1 undergoes S-nitrosylation both *in vitro* and in rotenone induced PD mouse models, resulting in structural instability. This provides a nucleation point allowing α-synuclein to aggregate faster (Kumar et al., 2017). Furthermore, lipid metabolites can react with UCH-L1; mutagenesis studies demonstrate that Cys90 and Cys152 are the main sites for this (Kabuta et al., 2008), ameliorating OS by scavenging the reactive metabolite, 4-hydroxynonenal. Therefore, UCH-L1 mutations show reduced hydrolase activity causing lower levels of free ubiquitin or structural changes but also impact levels of OS, and adversely affect protein degradation via the UPS suggesting proteasomal dysfunction contributes to PD pathology.

Mitochondrial dysfunction has also been suggested in familial PD pathology where patients have shown PINK1 mutations. Both wildtype and mutant PINK1 localise to mitochondria (Valente et al., 2004). Wildtype PINK1 appears to have a protective effect against apoptosis by suppressing cytochrome c release, repressing mitochondrial-dependent cell apoptosis via caspase activation (Beilina et al., 2005; Chen and Chan, 2009; H. L. Wang et al., 2007). Furthermore, PINK1 is imported into healthy mitochondria where it can undergo cleavage by proteases, once N-terminally cleaved, PINK1 is then degraded via the proteasome. However, upon mitochondrial dysfunction PINK1 is no longer imported and accumulates on the outer mitochondiral membrane activating parkin, where together PINK1/parkin aid mitochondrial quality control by moderating proteins and mediating their clearance (Chan et al., 2011; Sarraf et al., 2013). For example, mitofusin-1 and -2 are targeted for degradation to prevent fusion of damaged mitochondria, maintaining a healthy mitochondrial network (Tanaka et al., 2010; Xu et al., 2011). In *Drosophila,* PINK1 inactivation resulted in progressive loss of DA neurons. However, treating inactivated PINK1 *Drosophila* with antioxidants such as vitamin E or superoxide dismutase (SOD) suppressed ommatidial degeneration. This suggests PINK1 maintains neuronal survival by preventing OS (Wang et al., 2006) . Similar results were found in human DA neuroblastoma SH-SY5Y cell lines, where PINK1 deficiency lead to mitochondrial dysfunction and increased OS (Wood-Kaczmar et al., 2008). SH-SY5Y cells that had PINK1 knockdown mediated by siRNA showed decreased cell viability, mitochondrial membrane potential, mitochondrial respiration and ATP levels alongside increased apoptosis (van der Merwe

et al., 2017). Other studies support these findings as PINK1-knockdown primates also demonstrate neuronal degeneration (Yang et al., 2019). These studies suggest mitochondrial dysfunction and OS may underlie DA neuronal loss.

DJ-1, is another genes reported to be involved in the OS response with mutations in DJ-1 associated with functionally inactive protein leading to early-onset PD (Bonifati et al., 2003). Initially, DJ-1 was identified as an oncogene able to transform cells weakly on its own but more strongly when combined with *ras* (Nagakubo et al., 1997). DJ-1 is also reported as a circulating tumour antigen in breast cancer (Le Naour et al., 2001), a regulatory component of the RNA-binding complex (Hod et al., 1999) and a hydroperoxide-responsive protein that responds to oxidative stimuli such as hydrogen peroxide (H_2O_2) or paraquat, suggesting antioxidant properties (Mitsumoto and Nakagawa, 2001). In neuronal cell models, DJ-1 can form large molecular complexes, where these associations depend on the proteins oxidative state (Piston et al., 2017). DJ-1 can be oxidised on Cys106, which resides in a hydrophobic pocket, resulting in conformational destabilisation and loss of function (Filosto et al., 2011; Kiss et al., 2017). However, this oxidation is not a simple 'on-off' switch but acts in a biphasic manner, regulated by OS levels, resulting in changes to cell physiology (Filosto et al., 2011). The importance of the oxidative state of DJ-1 has been highlighted by Saito *et al.* who have observed oxidised DJ-1 in both neurons and glia of PD brains, and levels appear to decrease with disease progression (Saito et al., 2014). Furthermore, DJ-1 is also associated with dopamine metabolism, where oxidised intermediates of dopamine found in neuromelanin have been implicated in non-motor symptoms of PD (Schapira et al., 2017). *In vitro* knockdown of DJ-1 in SH-SY5Y studies have shown α-synuclein accumulation and aggregation (Xu et al., 2017a). Furthermore, the Met26I DJ-1 mutation affects its interaction with SUMO-1, enhancing mitochondrial removal resulting in greater susceptibility to dopamine toxicity (Strobbe et al., 2018). Therefore, DJ-1 is a multifunctional protein involved in regulating transcriptional processes, mitochondrial and antioxidant capacity, playing a key role in neurodegeneration.

While only a small percentage of PD sufferers carry hereditary familial mutations, the mutations provide valuable information about the possible mechanims underlying neurodegeneration (summarised in table 1.1). Indeed, both familial and sporadic PD display a similar phenotype and thereby potentially share common underlying pathways. Consequently, familial PD patient studies can provide an insight into possible pathways underlying the pathogenesis of sporadic PD (Gandhi and Wood, 2005). Understanding this pathology will help us generate novel therapies for many who suffer from this incurable but common neurodegenerative disorder.

Table 1.1 Summary of genes associated with familial Parkinson's disease and what neuropathological hallmarks they infer. *Adapted from* Ferreira and Massano, 2017; Nuytemans et al., 2010.

Gene	Function	Neuropathology	References	Infers
α-synuclein	Role not fully understood but believed to be involved in neurotransmission. Substrate for ubiquitin proteasome system. Misfolding associated with mitochondrial dysfunction.	Neuronal degeneration in the SN alongside LB's.	Bennett et al., 1999 Song et al., 2004 Ju et al., 2017 Perfeito, Ribeiro and Rego, 2017	Protein homeostasis impairment Mitochondrial dysfunction
Parkin	E3 ubiquitin ligase involved in proteasome-dependent protein degradation. Mainly localised to mitochondria and involved in mitochondrial function. Mutants show elevated oxidised protein and lipid levels.	Neuronal degeneration in SN.	Greene et al., 2003 Itier et al., 2003 Winklhofer et al., 2003 Palacino et al., 2004	Protein homeostasis impairment Mitochondrial dysfunction Oxidative stress
Ubiquitin C-terminal hydrolase 1 (UCH-L1)	Deubiquitinating protein and regulates free ubiquitin levels. Nucleation point allowing α-synuclein aggregation.	Neurodegeneration.	Kumar et al., 2017 Larsen et al., 1998 Leroy et al., 1998 Saigoh et al., 1999 Shimura et al., 2001	Protein homeostasis impairment
PTEN-induced putative kinase 1 (PINK1)	Localised to mitochondria suppressing mitochondrial-dependent cell apoptosis. Knockout showed mitochondrial dysfunction and oxidative stress.	Neuronal degeneration in SN accompanied by LB's.	Clark et al., 2006 Park et al., 2006 van der Merwe et al., 2017 Wang et al., 2006	Mitochondrial dysfunction Oxidative stress
DJ-1	Multiple functions including redox reactive signalling intermediate. Dopamine metabolism.	Not reported.	Filosto et al., 2011 Kiss et al., 2017 Mitsumoto and Nakagawa, 2001 Piston et al., 2017 Saito et al., 2014 Strobbe et al., 2018 Xu et al., 2017	Oxidative stress

1.2 The Neurodegenerative Bermuda Triangle

As human samples are difficult to obtain and post-mortem samples are limited as well as ethically demanding, *in vitro* and *in vivo* models have been generated to replicate the neuropathological hallmarks of PD and understand the disease process. Early research used mitochondrial complex I inhibitors such as 1-methyl-4-phenyl-1,2,3,6-tetrahydropyridine (MPTP), rotenone or paraquat to reproduce selective degeneration of DA neurons both *in vitro* and *in vivo* mice (Manning-Bog et al., 2002; Seniuk et al., 1990) and primate (Park et al., 2019) models. However, these models did not completely reproduce PD as they missed the other hallmark: LB's. Later models with chronic infusion of rotenone in rodents (Betarbet et al., 2000; Visanji et al., 2016) and in particular MPTP in mice (Fornai et al., 2005) have proven more successful as α-synuclein positive aggregates were detected, though these are difficult to replicate consistently.

Our knowledge has increased substantially using familial PD findings in combination with both *in vitro* and *in vivo* models; from these, multiple factors have been implicated in LB formation and DA neuronal degradation. These include: impaired protein degradation (McNaught and Jenner, 2001), mitochondrial dysfunction (Naoi et al., 2009) and oxidative stress (Ischiropoulos and Beckman, 2003); whose mechanisms may be interconnected in the so-called 'Neurodegenerative Bermuda triangle' (figure 1.1).

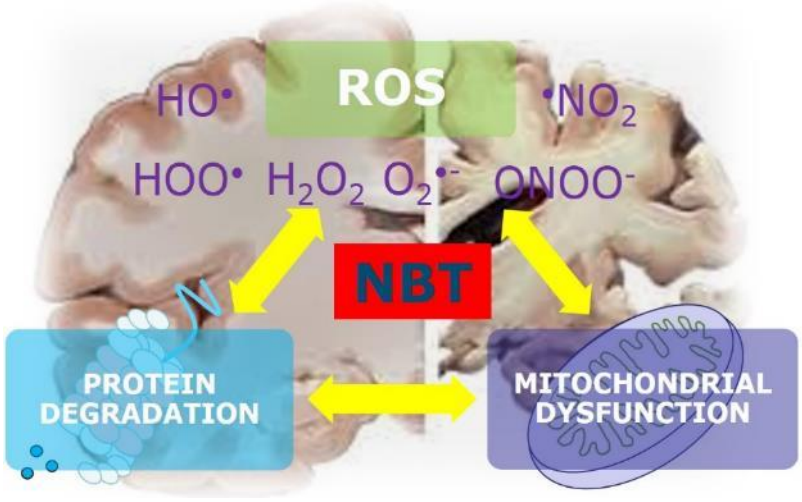

Figure 1.1. Schematic representation of the 'Neurodegenerative Bermuda Triangle' leading to neuronal loss in Parkinson's disease*. Known risk factors for the pathology of PD include impaired protein degradation, mitochondrial dysfunction and reactive oxygen species (ROS) which seem to be interrelated events that underlie neurodegeneration.*

1.2.1 Mitochondrial Dysfunction

1.2.1.1 Role of mitochondria

More so than other organs, the brain has a higher energy demand and thus utilises mitochondria to provide ATP via oxidative phosphorylation (Franco-Iborra et al., 2016), as other sources such as fatty acid oxidation are too slow or produce high levels of ROS (Schönfeld and Reiser, 2013). As such neurons almost exclusively rely on mitochondria for ATP.

Mitochondria generate ATP via the transfer of electrons along a series of complexes which together make up the electron transport chain (ETC), where the electrons reduce molecular oxygen to two molecules of water (Franco-Iborra et al., 2015; Grimm and Eckert, 2017; Vos et al., 2015; see figure 1.2). Briefly, this involves complex I transferring electrons from nicotinamide adenine dinucleotide (NADH) to the ubiquinone pool, while a proton is concurrently pumped through the inner mitochondrial membrane (Benit, 2004). Complex I is the main source of leaking electrons leading to ROS (Andreazza et al., 2010) and associated with mitochondrial dysfunction in neurodegenerative diseases (Jha et al., 2017; Ruan et al., 2017). Whereas complex II is involved in the Krebs cycle as well as the ETC and encoded completely by nuclear DNA, which transfers electrons from succinate to the ubiquinone pool (Zeviani, 2004). Complex III is also linked with electrons leaking leading to ROS (Borisov, 2002). Electrons are subsequently transferred from the ubiquinone pool to cytochrome c, while a proton is simultaneously pumped from the mitochondrial

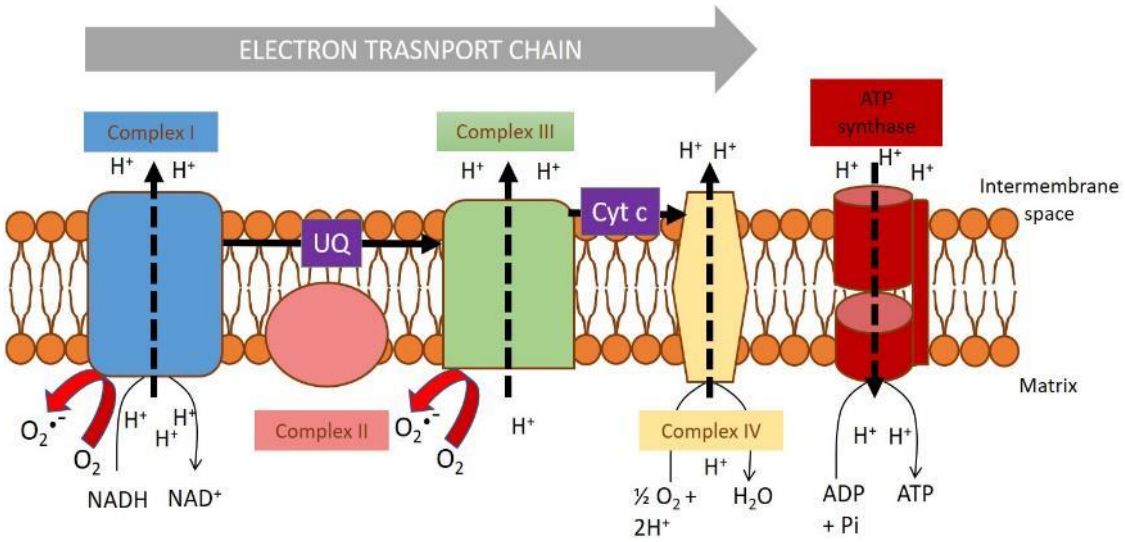

Figure 1.2 Reactive oxygen species generation via the electron transport chain. *Electrons are passed through complex I to ubiquinone (UB) and then to complex III. Cytochrome c (Cyt c) then transfers the electrons to complex IV where they react with molecular oxygen to produce water. Meanwhile ATP synthase synthesises ATP using the proton electrochemical gradient. Superoxide is mainly formed at complex I and III where electrons can leak from. Adapted from Grimm and Eckert, 2017; Vos et al., 2015.*

matrix space to the intermembrane space (Haut et al., 2003). Complex IV, also referred to as cytochrome c oxidase is the final complex involved in electron transfer, catalysing the transfer from cytochrome c to reduce molecular oxygen producing two molecules of water, while coupling proton pumping across the inner mitochondrial membrane (Diaz et al., 2006). The final complex in the ETC, complex V, ATP synthase is located in the inner mitochondrial membrane and synthesises ATP from ADP using the proton electrochemical gradient to provide energy for this reaction (Jonckheere et al., 2012).

In addition to providing energy, mitochondria provide essential metabolic intermediates, are involved in calcium buffering and regulating apoptotic processes ensuring cellular homeostasis (Friedman and Nunnari, 2014; Onyango et al., 2010; Su et al., 2010). As such, mitochondrial dysfunction plays a key role in contributing to physiological processes in health. This is especially true in the brain as neurons are post-mitotic and irreplaceable in particular regions, and therefore sensitive to accumulation of oxidative damage and defective mitochondria during aging (Kowald and Kirkwood, 2000; Terman et al., 2010). Furthermore, neurons contain different compartments including the cell body, axon, dendrites and synapses and as such, mitochondrial distribution is paramount to sustaining specific energy requirements (Lin and Sheng, 2015; Obashi and Okabe, 2013; Pernas and Scorrano, 2016). The importance of functional mitochondrial distribution in synapses has been demonstrated in studies where peroxide production is greater in rat synapses relative to other compartments (Borrás et al., 2010, 2003; Ohashi et al., 2016), and synaptic mitochondria are more susceptible to calcium induced depolarization in older animals (Lores-Arnaiz et al., 2016), suggesting greater sensitivity to mitochondrial dysfunction with age. Whereas, astrocytes, a sub-type of glial cells responsible for supporting neurons and regulating OS (Allaman et al., 2011; Gan et al., 2012; Vargas and Johnson, 2009), possess filopodial and lamellipodial extensions that are too narrow to accommodate mitochondria. As a result, astrocytes rely on glycolysis and glycogenolysis, in addition to oxidative phosphorylation to satisfy their energy demands (Hertz et al., 2007), suggesting they are less susceptible to mitochondrial-induced oxidative stress.

1.2.1.2 Mitochondrial dysfunction during aging and neurodegeneration

As mitochondria play a central role in energy metabolism and redox homeostasis, mechanisms of age related mitochondrial dysfunction are the subject of many studies to understand both normal aging and neurodegenerative disorders (Grimm et al., 2016). Multiple forms of familial PD are linked with gene mutations such as; PINK1, parkin and DJ-1, which are associated with the surveillance and protection of mitochondria (Chu, 2010; Fukui and Moraes, 2007). Furthermore, mitochondrial

dysfunction, reduced ATP levels, enhanced ROS levels (Sharma et al., 2014), toxic protein accumulation (Goedert et al., 2017) and failure of mitochondrial quality mechanisms (Green and Van Houten, 2011; Tatsuta and Langer, 2008; Ved et al., 2005), such as mitophagy (Ni et al., 2015; Wai and Langer, 2016; Youle and Narendra, 2011) contributes to mitochondrial DNA (mtDNA) mutations and damage. Together, these aberrations are associated with a greater risk of PD (Reeve et al., 2013; Schapira and Gegg, 2011).

Mitochondrial proteins are encoded by both their own mitochondrial DNA (mtDNA) within mitochondria and nuclear DNA, within the nucleus, where the quality control of mtDNA is not as efficient as nuclear thus, mtDNA mutations are more likely (DeBalsi et al., 2017). This may account for why complex I is more susceptible to dysfunction as mtDNA encodes 7 of the 13 subunits (Paradies et al., 2010). Accumulation of mtDNA mutations has been associated with age related diseases (Aon et al., 2016; DeBalsi et al., 2017; Kauppila et al., 2017; Kujoth, 2005) including both familial and sporadic PD. Further supporting this, a mouse model of PD showed mtDNA damage in DA neurons contributing to dysfunction (Pickrell et al., 2011). Where upon stress mitochondrial mutations can change mitochondrial biogenesis as described below, attributing to the cells lack of ability to dilute out these mutations (Guerra et al., 2019).

More recently, genes associated with mitochondrial biogenesis have become important in understanding mitochondrial dysfunction. Familial PD associated gene mutations including DJ-1, α-synuclein and parkin, have also been observed to affect fission and fusion (Van Laar and Berman, 2013). Furthermore, peroxisome proliferator-activated receptor coactivator gamma 1α (PGC-1α), is considered the master controller of mitochondrial biogenesis, which has been found to be impaired or have decreased levels in PD patients (Cronin-Furman et al., 2013; Pacelli et al., 2011). Further supporting this, increased levels of PGC-1α lead to higher expression of mitochondrial subunits attenuating rotenone induced neuronal loss (Zheng et al., 2010).

To decrease mtDNA mutations mitochondria can divide (fission) and fuse (fusion) to maintain a homogenous mitochondrial population and mix mitochondrial content (Chan, 2012; Grimm and Eckert, 2017; see figure 1.3). Fission and fusion is also used to maintain growth, shape and mitochondrial distribution (Calkins and Reddy, 2011; van der Bliek et al., 2013) with repetitive cycles regulating morphology and dynamics (Sharma et al., 2014).

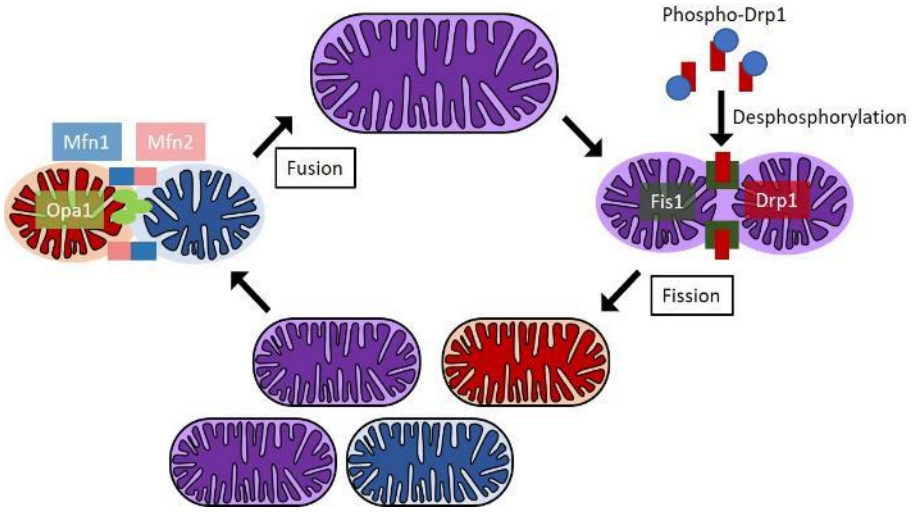

Figure 1.3 Schematic representation of mitochondrial fission and fusion. *Phosphorylated-dynamic related protein (Drp1) is mainly localised to the cytoplasm, once dephosphorylated Drp1 is recruited to the mitochondria via fission protein 1 (Fis1). Drp1 subsequently forms spirals around mitochondria promoting constriction followed by fission. Pro-fusion proteins mitofusin 1 and 2 (Mfn1 and Mfn2) are localised to the outer mitochondrial membrane while optic atrophy 1 (Opa1) is localised to the inner mitochondrial membrane. Mfn1 and Mfn2 oligomerization tethers adjacent mitochondria promoting outer mitochondrial membrane fusion while Opa1 promotes inner membrane fusion. Adapted from Grimm and Eckert, 2017.*

Mitochondrial fission enables proliferation of mitochondria for renewal and redistribution (Pernas and Scorrano, 2016). Fission is regulated by dynamin related GTPases such as dynamin related protein 1 (DRP1), which can be regulated by post-translational modifications such as phosphorylation or dephosphorylation (Campello and Scorrano, 2010). Inactive DRP1 is cytosolically located and dephosphorylation results in activation and relocation to the mitochondrial membrane (Bradshaw et al., 2016; Han et al., 2008; Uo et al., 2009). DRP1 mutations result in aberrant mitochondrial morphology, a heterogenous population and non-uniform distribution of mtDNA, resulting in increased RS leading to increased apoptosis (Knott et al., 2008; Oettinghaus et al., 2016). Further supporting the importance of DRP1, DRP1 knockout Purkinje cells exhibit mitochondrial swelling, impaired ETC, increased oxidative stress and autophagy marker accumulation leading to neurodegeneration in the cerebellum (Kageyama et al., 2012). In addition, mouse synaptosomes showed increased DRP1 levels during aging (Stauch et al., 2014), suggesting DRP1 as a potential player in neurodegeneration.

Fusion counteracts fission, allowing mitochondria to interact and communicate with each other (Chan, 2006), while regulating mutated mtDNA (Benard and Karbowski, 2009; Hung et al.,

2018). Like fission, dynamic related GTPases are utilised in this process where mitofusin 1 and 2 (MFN1/2) are responsible for outer membrane fusion, whereas optic atrophy 1 (OPA1) promotes inner membrane fusion (Friedman and Nunnari, 2014; Silva Ramos et al., 2019). Mutations in MFN2 or OPA1 results in autosomal dominant peripheral neuropathy resulting in mitochondrial fragmentation (Carelli et al., 2015; Knott et al., 2008). Low stress is believed to trigger mitochondrial fusion, in contrast prolonged stress favours fission (Fischer et al., 2012; Rahim et al., 2016), where free radicals increase activation of mitochondrial fission proteins. The ratio of fission to fusion determines mitochondrial length and closed network formation (van der Bliek et al., 2013).

Fission/fusion is integrated with other mitochondrial quality control mechanisms, including the removal of aged/damaged mitochondria via mitophagy (Haroon and Vermulst, 2016; Lou et al., 2020; Youle and Narendra, 2011). Impaired mitophagy has been suggested to contribute to mitochondrial dysfunction during aging (Diot et al., 2016) and found in post-mortem PD brains (Beal, 2003; Ryan et al., 2015; Yakhine-Diop et al., 2019), as well as dopaminergic neurons from patients with sporadic or familial PD (Burbulla et al., 2017; C. Wang et al., 2018). Furthermore, a study showed autophagy related genes Atg4B, Atg5, Atg16L1, and histone deacetylase are downregulated in the peripheral blood cells of PD patients (Miki et al., 2018).

Autophagy involves the lysosomal removal of the intracellular contents of a cell, including proteins and organelles that maintain cellular homeostasis (Santambrogio and Cuervo, 2011; Wang et al., 2016). Autophagy can be divided into 3 main categories: microautophagy, macroautophagy and chaperone-mediated autophagy. Microautophagy involves the lysosomal membrane engulfing a small cytoplasmic portion (Mizushima et al., 2008; Oshima et al., 2019). Whereas macroautophagy entails content engulfing via an autophagosome or phagophore. The mature autophagosome subsequently fuses with the lysosome, degrading its membrane and contents via lysosomal proteases (Cuervo and Wong, 2014; Lieberman et al., 2020). Finally, chaperone mediated autophagy consists of specific protein degradation via chaperones such as HSP70, which then interacts with lysosomal membrane receptor LAMP-2A (Cuervo and Wong, 2014; Loos et al., 2017; Martinez-Vicente and Cuervo, 2007).

Deficiencies in macroautophagy leads to protein aggregation contributing to neurodegeneration (Anglade, 1997; Scrivo et al., 2018). As neurons rely on mitochondria to maintain their energy levels (Kann and Kovács, 2007) they need to replace damaged mitochondria. Macroautophagy (mitophagy) regulates this process, whereby mitochondria are selectively sequestered and delivered to the lysosome for degradation (Lemasters, 2014; Manzoni, 2017). This involves proteins such as p62/SQSTM1, OPTN or NDP52 on the outer mitochondrial membrane

acting as a mitophagy receptor (containing a LIR motif), which facilitates the interaction with LC3 family members to recruit autophagosomal machinery (Harris et al., 2018; Zhang and Ney, 2009; see figure 1.4). Alternatively, PINK1 accumulates on dysfunctional mitochondria to mark them for lysosomal degradation (Ivankovic et al., 2016; Narendra et al., 2008). PINK1 subsequently phosphorylates and recruits parkin to the surface of mitochondria (Shiba-Fukushima et al., 2012) activating parkin's E3 ligase activity (Kane et al., 2014; Kazlauskaite et al., 2014). This leads to the ubiquitination of mitochondrial surface proteins tagging them for proteasomal or autophagy degradation (Chan et al., 2011; Harris et al., 2018; Yoshii et al., 2011; see figure 1.4). Therefore, unsurprisingly mutations in PINK1 and parkin can lead to accumulation of dysfunctional mitochondria and increased oxidative stress (Lubbe and Morris, 2014; Obeso et al., 2017; Redmann et al., 2016, 2014).

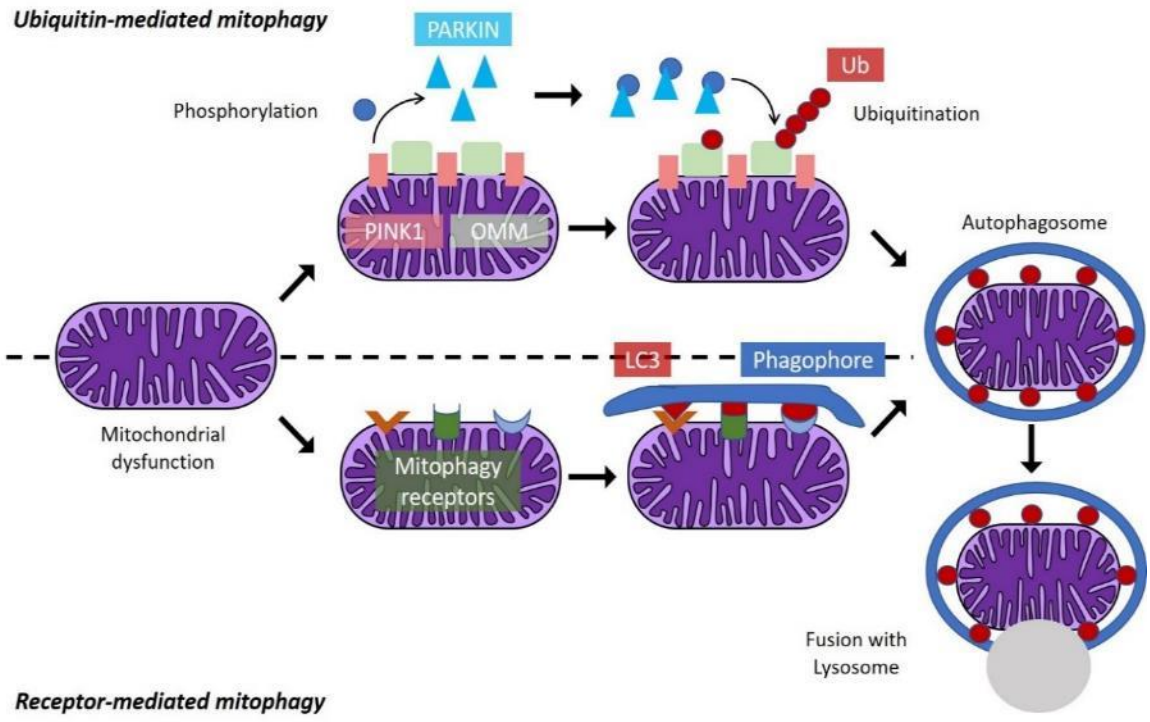

Figure 1.4. Schematic representation of mitophagy mechanisms. *When mitochondria become dysfunctional, they can be degraded via ubiquitin- and receptor-mediated mitophagy. Mitochondrial dysfunction can lead to PINK1 localising to the outer mitochondrial membrane where it recruits and phosphorylates Parkin. Phosphorylation activates Parkin's E3 ligase activity leading to ubiquitination of outer mitochondrial membrane (OMM) proteins facilitating phagophore formation. Alternatively, mitochondrial dysfunction can lead to several receptors being expressed on the OMM resulting in LC3 on the phagophore binding. The resultant phagophore expands enclosing the damaged mitochondria forming an autophagosome which can fuse with lysosomes allowing degradation via lysosomal enzymes. Adapted from Harris et al., 2018.*

Most importantly in neurodegenerative diseases dysfunctional mitochondria are associated with increased RS levels (Islam, 2017; Liu et al., 2017). As mentioned previously electrons are passed down the ETC to produce ATP but dysfunctional mitochondria lead to electrons 'leaking', which react with molecular oxygen generating superoxide, which is described in greater detail below. Therefore, inducing oxidative stress using mitochondrial inhibitors is a common strategy to investigate the role of ROS in neurodegeneration.

1.2.2 Oxidative stress

Redox reactions consist of the transfer of electrons resulting in oxidation (loss of electrons) or reduction (gain of electrons). These redox reactions are central to biological functions including metabolism and respiration (Franco and Vargas, 2018). In aerobic organisms, oxygen is the main oxidising agent, the main source of ROS and subsequent reactive nitrogen species (RNS). Redox biology has been implicated in health and disease, which is mostly attributed to altered reactive species (RS) homeostasis. Redox reactions in cells consist of electrons transferring between molecules, which cycle between an oxidised and reduced state to regulate metabolism and cell signalling (Paul D. Ray et al., 2012; Trachootham et al., 2008). This redox homeostasis is an integrated process between neurons and glia (Baxter and Hardingham, 2016).

Oxygen is of great importance for neural cells as they have a high metabolic rate and reduced regenerative capacity relative to other organs. As a result, the brain is more susceptible to damage via oxidative and nitrosative stress; as such these stresses are implicated in a variety of neurodegenerative diseases (Halliwell, 2019; Koskenkorva-Frank et al., 2013). However, despite being recognised as an underlying mechanism in neurodegeneration, understanding how these stresses contribute to the development and progression of neurodegenerative diseases is not fully understood. As such, a greater understanding as to how these processes are involved in neurodegenerative disease will lead to the identification of novel therapies.

1.2.2.1 Generating reactive oxygen and reactive nitrogen species

The brain utilises mitochondria to provide ATP via oxidative phosphorylation (Franco-Iborra et al., 2016). Mitochondria also regulate cell survival and contain redox enzymes (Danial and Korsmeyer, 2004; Karbowski, 2010) such as superoxide dismutase (SOD). Increased RS levels are mainly attributed to mitochondrial dysfunction (Schapira, 2008) though dopamine oxidation, xanthine oxidase and NADPH oxidase (NOX) also contribute (Gandhi and Abramov, 2012a; Winterbourn and Hampton, 2008; see figure 1.5).

Incomplete reduction typically occurs as electrons can 'leak' from the ETC during oxidative phosphorylation. Such leaks initially result in superoxide ($O_2^{\cdot-}$) formation (Fariss et al., 2005). The $O_2^{\cdot-}$ levels generated are relatively low and therefore neutralised by matrix localized antioxidants. However, if the ETC complexes become impaired or dysfunctional $O_2^{\cdot-}$ levels can significantly rise, and redox homeostasis can become unbalanced. If not scavenged, $O_2^{\cdot-}$ is dismutated to hydrogen peroxide (H_2O_2) by superoxide dismutase (SOD). Multiple enzymes remove H_2O_2 including: peroxiredoxins (PRDXs), glutathione peroxidases (GPXs) and catalase (Birben et al., 2012; Schafer and Buettner, 2001). H_2O_2 oxidises PRDXs at cysteine within the active, which is subsequently reduced by thioredoxin, thioredoxin reductase and NADPH or glutathione (Park *et al.*, 2016). GPXs are also oxidised by H_2O_2 and then reduced by glutathione (GSH). In contrast, catalase is localised to peroxisomes (Winterbourn and Hampton, 2008) and decomposes H_2O_2 to water and oxygen. If H_2O_2 is not dismutated, iron catalyses the Fenton reaction producing hydroxyl radicals. Hydroxyl radicals are the most reactive ROS, which can damage protein, lipids, carbohydrates, DNA and initiate lipid peroxidation by removing an electron from polyunsaturated fatty acids (Birben et al., 2012).

Ultimately, the generation of $O_2^{\cdot-}$ results in a cascade of other RS that each have unique properties and biological targets (see figure 1.5). For example, H_2O_2 lacks a charge and can therefore diffuse across membranes, while $O_2^{\cdot-}$ is charged and has limited permeability (De Grey, 2002). Furthermore, H_2O_2 reacts with cysteine and methionine residues within proteins while $O_2^{\cdot-}$ reacts preferentially with iron sulphur centres and nitric oxide (D'Autréaux and Toledano, 2007). Therefore RS characteristics will determine their ability as damaging or signalling molecules (Winterbourn, 2008).

In addition, ROS can generate reactive nitrogen species (RNS) such as nitric oxide ($^{\cdot}NO$) and peroxynitrite ($ONOO^-$) (Sultana et al. 2013; see figure 1.5), which are involved in signalling and neuronal damage (Cobb and Cole, 2015). $^{\cdot}NO$ like $O_2^{\cdot-}$ is a short-lived diffusible molecule involved in inflammation and synaptic transmission (Moncada and Bolanos, 2006). L-Arginine, NADPH and oxygen act as substrates for nitric oxide synthase (NOS) producing $^{\cdot}NO$, citrulline and water (Smith and Lassmann, 2002) while using cofactors flavin mononucleotide, flavin adenine dinucleotide, tetrahydrobiopterin, haem and NADPH. However, if tetrahydrobiopterin levels are depleted NOS can produce $O_2^{\cdot-}$ (Moncada and Bolanos, 2006). If $O_2^{\cdot-}$ reacts with $^{\cdot}NO$ peroxynitrite is produced. This reaction primarily occurs where superoxide is produced due to its short lifetime. Peroxynitrite can subsequently undergo protonation and homolytic cleavage producing nitrogen dioxide ($^{\cdot}NO_2$) and hydroxyl radicals (Hogg and Kalyanaraman, 1999). Therefore, a variety of RS can be generated which can react with various targets (summarised in table 1.2).

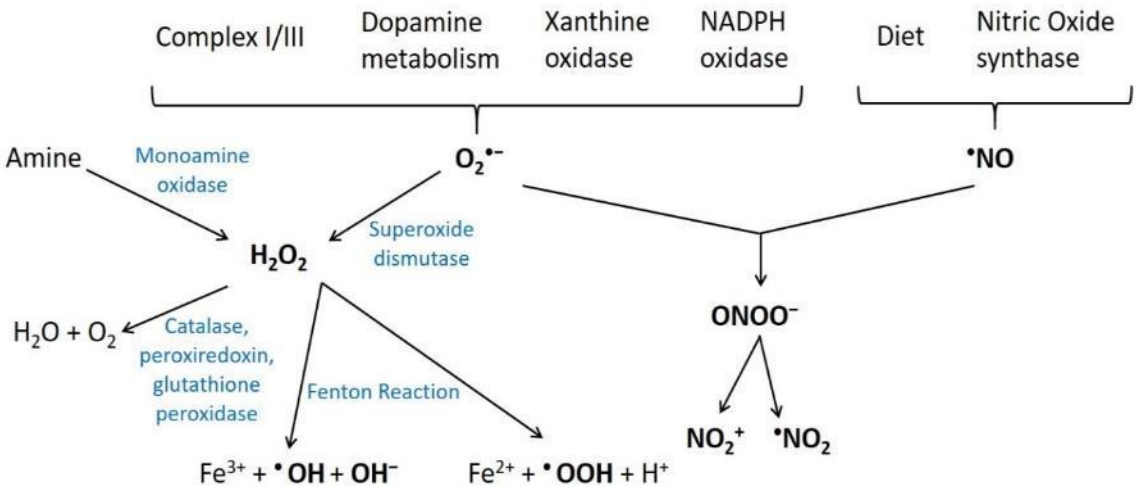

Figure 1.5. Superoxide generations leads to a cascade of other reactive species. *Superoxide can be dismutated to hydrogen peroxide (H_2O_2) via superoxide dismutase. H_2O_2 can also be generated by monoamine oxidase. Subsequently, the toxic H_2O_2 can be reduced to water and oxygen via detoxifying enzymes catalase, peroxiredoxin and glutathione peroxidase. However, if the levels of H_2O_2 are too great to be detoxified then the high levels of iron in neurons can result in the Fenton reaction resulting in peroxy and hydroxyl ROS. Alternatively, superoxide can react with nitric oxide from diet or nitric oxide synthase to generate peroxynitrite, which can degrade into nitrogen dioxide radicals. Adapted from Winterbourn, 2008.*

RS are chemically reactive due to the possession of an unpaired electron making these molecules unstable. Under natural conditions these are involved in cellular activities such as inflammation, cell survival, stressor response and multiple diseases including; cardiovascular disorders, allergies, cancers and neurodegenerative diseases (He and Zuo, 2015; Zuo et al., 2015, 2014). High levels of these RS can lead to disruption of the redox balance between prooxidant and antioxidant levels leading to alterations in cellular function and possibly cell death (Zuo et al., 2015). This redox balance can be disrupted by inflammation or mitochondrial dysfunction (Rego and Oliveira, 2003; Sharma and Nehru, 2015). Furthermore, protein aggregates can result in inflammation leading to RS upregulation and subsequent OS (Wyss-Coray and Mucke, 2002; Zuo et al., 2015). It should also be noted that OS can result in post-translational modifications to proteins leading to aberrant proteins, which can then aggregate causing inflammation (Bantle et al., 2019; Burns and Wang, 2017). Therefore, disruption of redox homeostasis can result in a feed forward loop leading to cell damage and ultimately death.

Thus, to aid in attenuating OS, antioxidants such as glutathione or vitamin C and E are suggested as possible treatments. Unfortunately, antioxidant treatments have yielded mixed results. In some *in vitro* studies antioxidants have been successful in reducing OS and neuronal

degeneration (Ambrogini et al., 2019; Then et al., 2010). Further *in vivo* treatment with vitamin E for 2 years attenuated functional decline in AD patients (Ittner et al., 2010) and early life supplementation with vitamin E appears to reduce the risk of PD (Miyake et al., 2011). However, others report that 5 months treatment with orally administered vitamin E had no effect in PD patients (Pappert et al., 1996). Although another more recent double blind test showed vitamin E supplementation yielded more promising results (Taghizadeh et al., 2017). These controversies are possibly due to the limited amount of vitamins passing into the blood from the intestine as tocopherol can pass through the blood brain barrier (Peltzer et al., 2018). As such, understanding possible downstream effectors of OS may be critical to develop novel therapies for neurodegenerative diseases such as PD.

Table 1.2 Summary of reactive species generated, and potential targets identified.

Oxidant	Formula	Reaction Equation	Target	Outcome	Ref.
Superoxide	$O_2^{\bullet-}$	NADPH + 20_2 ↔ $NADP^+ + 2O_2^{\bullet-}$	Mitochondrial uncoupling	Activates nucleotide-sensitive mitochondrial proton transport	(Echtay et al., 2002)
Hydrogen peroxide	H_2O_2	$2O_2^{\bullet-} + H^+ \rightarrow O_2 + H_2O_2$ Hypoxanthine + H_2O + O_2 ⇌ Xanthine + H_2O_2 Xanthine + H_2O + O_2 ⇌ uric acid + H_2O_2	STAT6	Cyclooxygenase-2 expression and prostaglandin release	(Park et al., 2012)
Hydroxyl radical	$HO^{\bullet}$	$Fe^{2+} + H_2O_2 \rightarrow Fe^{3+} + OH^- + HO^{\bullet}$	Unsaturated fatty acids in membranes	Lipid peroxidation, production of 4-hydroxynonenal	(Sultana et al., 2013a)
Nitric oxide	$^{\bullet}NO$	L-Arginine +3NADPH + H^+ + $4O_2$ ⇌ 2Citrulline + $2^{\bullet}NO$ + $4H_2O$ + $3NADP^+$	Neuronal plasticity via cGMP and ERK	Improves neuronal plasticity	(Gallo and Iadecola, 2011)
Peroxynitrite	$ONOO^-$	$O_2^{\bullet-} + {}^{\bullet}NO \rightarrow ONOO^-$	Tyrosine hydroxylase	Inhibit tyrosine hydrogenase, decreased dopamine levels	(Ara et al., 1998; Park et al., 2003)

1.2.2.2 Antioxidant defences

As cellular RS levels increase for signalling during metabolic processes and inflammation it is important for the brain to have suitable defence mechanisms to scavenge and dispose of excess RS to return redox balance. As such, the brain has multiple enzymes that catalyse the breakdown or removal of RS including superoxide dismutase (SOD), catalase, peroxiredoxins (PRDX), glutathione peroxidases (GPX), glutathione (GSH) and a few other molecules.

Within the central nervous system there are 3 isoforms of SOD; cytosolic CuZnSOD1, mitochondrial MnSOD2 and extracellular SOD3. These enzymes are responsible for removing

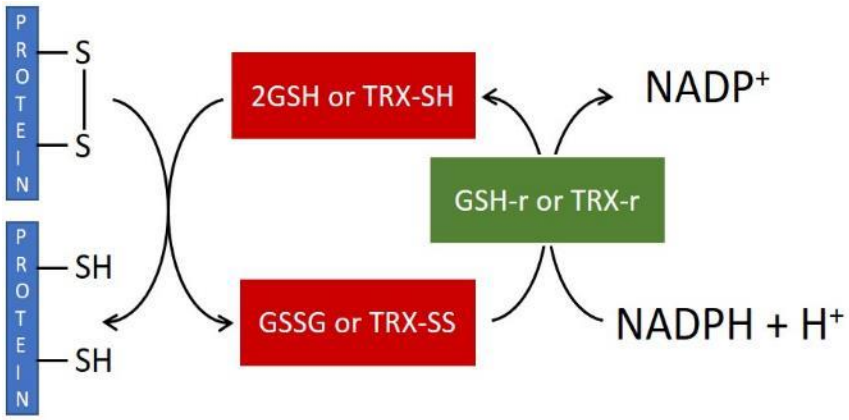

Figure 1.6. Schematic representation of glutathione and thioredoxin coupling antioxidant systems. *Thiol groups on various proteins can be oxidised to produce disulphide bridges (SS). Glutathione (GSH) or thioredoxin (TRX) can reduce disulphide bridges back to thiol groups while being oxidised producing oxidised glutathione disulphide (GSSG) and oxidised thioredoxin (TRX-SS). GSSG and TRX-SS can be reduced by glutathione reductase (GSH-r) and thioredoxin reductase (TRX-r), respectively, in the presence of NADPH allowing constant recycling of these proteins so they can act as antioxidants. Adapted from Espinosa-Diez et al., 2015.*

superoxide by catalysing its dismutation to hydrogen peroxide and oxygen (Dasuri et al., 2013; Y. Wang et al., 2018).

Catalase is one enzyme responsible for the removal of hydrogen peroxide, present in the cytosol, mitochondria and peroxisomes but has a minor role with low levels of hydrogen peroxide but is more important when levels are higher (Gandhi and Abramov, 2012). Peroxiredoxins (PRDXs) have more recently be identified to be important for the removal of hydrogen peroxide (Stöcker et al., 2018). There are 3 classes of PRDXs in animals; typical 2-cysteine, atypical 2-cysteine and 1-cysteine with 6 isoforms across these classes (PRDX1-6; Rhee, 2016). For all PRDXs the thiol group of the active site cysteine is oxidised to sulfenic acid resulting in a disulphide bond (see figure 1.6; Espinosa-Diez et al., 2015). This disulphide bond is reduced by thioredoxin (PRDX1-5) or glutathione (PRDX6; Poole et al., 2011; Turner-Ivey et al., 2013) and is responsible for the removal of hydrogen peroxide in the cytoplasm and mitochondria (Hall et al., 2011). PRDXs are catalytically slower than glutathione peroxidases, but are present in large amounts within the cytosol and organelles to compensate for this (Rhee et al., 2005). Furthermore, it is important to note that hydrogen peroxide partially inactivates PRDXs possibly to allow cell signalling (Halliwell and Gutteridge, 1991; Rhee et al., 2005) but more PRDX is synthesised to remove excess hydrogen peroxide (Georgiou, 2003).

Glutathione peroxidase (GPX) is another enzyme responsible for reducing hydrogen peroxide but also lipid peroxides using GSH as the electron donor (Dasuri et al., 2013; Gandhi and Abramov, 2012). GPX is present in both the mitochondria and cytosol (Conrad and Friedmann Angeli, 2018). Glutathione (GSH) is a tripeptide of glutamate, cysteine and glycine serving to protect against OS (Dasuri et al., 2013; Gandhi and Abramov, 2012) in both a direct and indirect manner. Directly via oxidation of cysteine residues and indirectly, GSH reduces peroxides (Miller et al., 2018) by becoming oxidised to a disulphide bridge (GSSG), which can be reduced back to GSH by glutathione reductase in the presence of NADPH, which donates an electron for the reduction (Dringen et al., 2000; Dringen and Hirrlinger, 2003; see figure 1.6). Interestingly, GSH levels are lower in neurons than glia; the latter assisting neuronal GSH levels by supplying cysteinyl-glycine, the precursor of GSH (Dringen et al., 2005; Dringen and Hamprecht, 1997). Furthermore, glia appear to be more resistant to RS possibly due to the higher GSH levels and accelerated GSH synthesis under stress relative to neurons (McBean, 2017).

In addition to enzymes, there are also some low molecular weight antioxidants within the central nervous system (CNS), such as ascorbate (vitamin C) and tocopherol (vitamin E; Rice, 2000). Typically, intracellular mammalian levels of vitamin C range from 0-5 mM (Du et al., 2012) with neurons exhibiting 10 mM (Harrison and May, 2009), suggesting it plays an important role in survival. Further supporting this, knockout of sodium vitamin C transporter 2 in mice resulted in decreased ascorbate levels in the blood, brain and tissue and these mice died within a few minutes of birth (Sotiriou et al., 2002). Vitamin C is water soluble and at physiological pH exists as ascorbate which acts as an electron donor (Nishikimi, 1975; Rice, 2000). Neurons readily uptake ascorbate whereas astrocytes uptake dehydroascorbate and convert this to ascorbate (McBean, 2017).

Voltammetry reveals that vitamin C can lose two electrons for reducing other molecules, but commonly functions as a one electron reducing agent as oxidation of ascorbate produces monodehydroascorbate radical, which exhibits resonance stabilisation (Deakin et al., 1986; Smirnoff, 2018). As a result of stabilisation monodehydroascorbate radicals do not react readily with oxygen or other molecules to generate more radicals but act as effective radical scavengers, in particular superoxide (Cabelli and Bielski, 1983; Smirnoff, 2018; Wenzel, 2003). This is supported by studies that show that superoxide levels and markers of oxidation, such as lipid peroxidation and carbonyl levels are reduced by vitamin C (Das et al., 2019; Kondo et al., 2008; Patra et al., 2001; Wenzel, 2003).

Vitamin E, like vitamin C, can scavenge superoxide but with a lower affinity as demonstrated by the higher rate constant (Gotoh and Niki, 1992). Vitamin E, also known as

tocopherol, is important for the oxidative status of the brain where greater levels are observed in astrocytes relative to neurons (Lee and Ulatowski, 2019; Makar et al., 2008). Vitamin E is taken up from the intestine (Traber et al., 1990) via eight different isoforms; α-, β-, γ-, and δ- tocopherol (saturated) and tocotrienols (unsaturated) which exhibit antioxidant activity. *In vitro,* α-tocopherol is the most reactive (Burton and Ingold, 1986) due to the α-tocopherol transfer protein (α-TTP) (B. Li et al., 2013) and redistributes to other tissues. Both oxidative status and vitamin E levels affect expression of α-TTP in the brain (Ulatowski et al., 2012) where levels also vary depending on specific areas. Interestingly, expression of α-TPP is highest in cerebellar astrocytes (Hosomi et al., 1998), suggesting greater levels of vitamin E in astrocytes (Lee and Ulatowski, 2019; Makar et al., 2008).

Vitamin E has established a role in neurological health via mitigation of OS, as severe and prolonged deprivation leads to neurological damage (Takahashi et al., 2017). Furthermore, AD and PD patients exhibit lower levels of vitamin E in the blood and cerebral spinal fluid, although other studies contradict this (reviewed in Chang et al., 2018). However, it is believed that vitamin E localises mainly to cell membranes where it reduces lipoprotein oxidation by scavenging peroxyl radicals (Mocchegiani et al., 2014; Niki, 2014). Furthermore, more recently vitamin E has been demonstrated to suppress ferrotopsis *in vitro* preventing phospholipid oxidation, which leads to cell death (Wortmann et al., 2013). Therefore, vitamin E appears to play a key role in neurological health by modulating OS.

DJ-1 is also reported to be involved in the OS response and mutations in DJ-1 are associated with the protein becoming functionally inactive resulting in early-onset PD (Bonifati et al., 2003; see section 1.1.1). DJ-1 is thought to act as an antioxidant via oxidation of its Cys106 residue (Taira et al., 2004). In support of this, the auto-oxidation of DJ-1 eliminates RS *in vivo* and *in vitro* (Taira et al., 2004; Yokota et al., 2003). Interestingly, OS has been shown to induce DJ-1 expression (Mitsumoto et al., 2001). DJ-1 is required for nuclear factor erythroid 2-related factor (NRF2) activity (Clements et al., 2006), as it affects NRF2's association with the inhibitor protein Kelch-like ECH associated protein 1 (KEAP1), which ubiquitinates NRF2 (Dhakshinamoorthy and Jaiswal, 2001; Itoh et al., 1999). NRF2 is a leucine zipper transcription factor involved in the regulation of antioxidant pathway gene activation (Cho et al., 2006). Once dissociated from KEAP1 NRF2 becomes stable and translocates to the nucleus (Chen and Kong, 2004; Nguyen et al., 2005). There it forms heterodimers with other regulators inducing and driving the expression of antioxidant genes (Lee et al., 2003a) and detoxification enzymes (Alam et al., 1999; Tonelli et al., 2018) mentioned previously (Chen et al., 2014; see figure 1.7).

1.2.2.3 Oxidative and Nitrative stress during neurodegeneration

As mentioned previously RS can be generated from a variety of sources (see figure 1.5), which are balanced by a variety of antioxidant defences that can be activated by RS sensitive transcription factors. In addition to activating transcription factors, oxidative and nitrative stress can cause a variety of post-translational modifications (PTMs) to different amino acid residues in various proteins. Despite understanding the encoding genome, the proteome is approximately 2-3 orders greater in size, suggesting PTMs play an important role in homeostasis. PTMs can result from enzymatic and non-enzymatic attachment of chemical groups to amino acid sides chains (Walsh et al., 2005), which influence their structure and cellular functions. Furthermore, dysregulation of PTMs is associated with aging and is known to affect disease conditions (Cloos and Christgau, 2004; Gorisse et al., 2016; Liddy et al., 2013). PTMs can be divided into enzymatically and non-enzymatically driven reactions, involving covalent cleavage of peptide backbones or covalent additions to amino acid side chains. Redox PTMs are non-enzymatic PTMs that depend on reactive species which involve covalent additions to side chains (summarised in table 1.3).

These covalent additions by redox PTMs can be reversible or irreversible. For example carbonylation is a common oxidative PTM where a carbonyl moiety such as aldehyde, ketone or lactam is added to proteins (Møller et al., 2011). Carbonylation can occur on several residues including arginine, histidine, lysine, proline, threonine and cysteine where cytoskeletal proteins such as neurofilaments and tubulin are particularly susceptible to carbonylation (Bizzozero, 2009).

Nitration was initially believed to be an irreversible redox PTM, produced by RNS that react with tyrosine residues generating 3-nitrotyrosine (Sadowska-Bartosz et al., 2014) but dinitrase enzymes have been frond that reverse this PTM (Deeb et al., 2013). Furthermore, nitration appears to be highly selective with only specific tyrosine residues being nitrated, with only a fraction of the proteome being affected (Radi, 2013). This suggests nitration is highly regulated and it is when PTMs are no longer regulated this PTM contributes to neurodegeneration. This is supported by studies which demonstrate that 3-nitrotyrosine is associated with nitrative stress during aging (Bandookwala and Sengupta, 2020). More specifically, α-synuclein nitration appears to promote LB formation due to the PTM decreasing its solubility (He et al., 2019). Furthermore, tyrosine nitration of complex I in SH-SY5Y cells has been shown to irreversibly inhibit complex I in the ETC, (Murray et al., 2003; Yamamoto et al., 2002) and hence associated with decreased ATP synthesis alongside enhanced apoptotic and necrotic cell death (Davis et al., 2010). Therefore, tyrosine nitration PTMs may contribute to neurodegeneration via promoting protein aggregation or mitochondrial dysfunction.

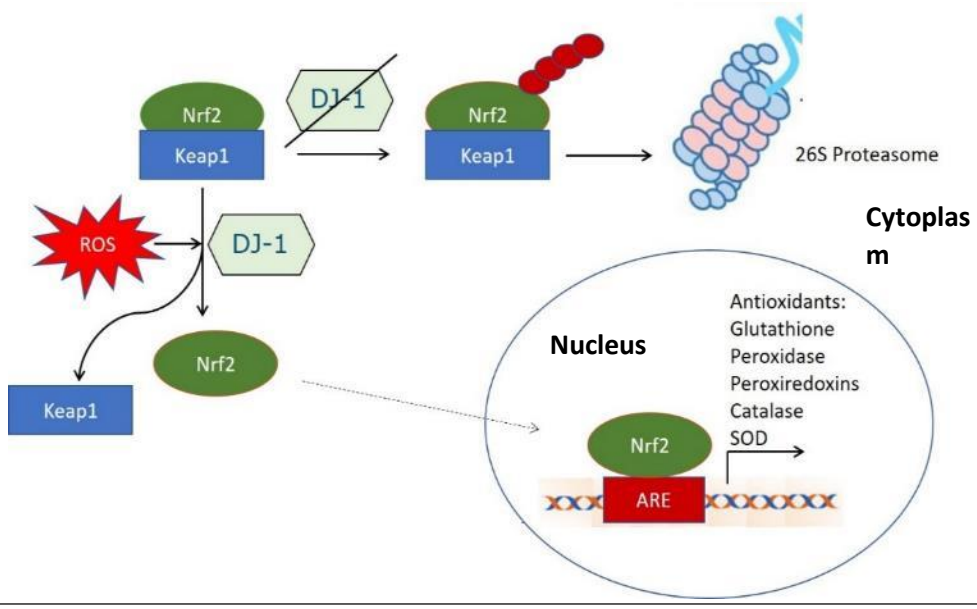

Figure 1.7. Schematic representation of NRF2-ARE pathway activated by reactive species. *Under normal conditions NRF2 associates with KEAP1 in the cytoplasm where it becomes ubiquitinated as a signal for proteasomal degradation. Under oxidative stress reactive oxygen species (ROS) levels increase resulting in dissociation of NRF2 from KEAP1. This allows NRF2 to translocate to the nucleus where it binds to the antioxidant response element (ARE) upregulating transcription of antioxidants such as glutathione, glutathione peroxidase, peroxiredoxins, catalase and superoxide dismutase (SOD). Recently, DJ-1 is also believed to be important for aiding NRF2's dissociation from KEAP1. Adapted from Chen et al., 2014.*

RNS can also cause another reversible PTM referred to as S-nitrosylation, which occurs in the presence of a transition metal that accepts an electron (Smith and Marletta, 2012), targeting the thiol groups of cysteine and methionine residues (Nakamura and Lipton, 2016; Stamler et al., 1997). Like other redox PTMs, S-nitrosylation is associated with neurodegenerative diseases (reviewed in Nakamura et al., 2013). Similar to nitration, S-nitrosylation can inhibit components of the ETC (Di Giacomo et al., 2012; Montagna et al., 2020) including complex I (Chouchani et al., 2013). S-nitrosylation can further affect mitochondria as nitrosylation of cys644 in DRP1 enhances its oligomerization and GTPase activity, resulting in excessive mitochondrial fragmentation leading to synaptic loss and neuronal damage (Cho et al., 2009; Z. Zhang et al., 2016). Furthermore, parkin S-nitrosylation is linked to autosomal recessive juvenile onset Parkinson's, contributing to abnormal mitochondrial dynamics by effecting E3 ligase activity in a biphasic manner (Yao et al., 2004).

RS can also lead to lipid peroxidation. This alters lipid-lipid interactions, ion gradients, membrane fluidity and membrane permeability (Borst et al., 2000a; Saleh et al., 2010). In addition, lipid peroxides are labile and can degrade causing additional toxicity. For example, ferrous irons can react with lipid peroxides generating corresponding alkoxyl radicals that can propagate

peroxidation reactions or aldehyde degradation products such as 4-hydroxynonenal (4-HNE) and malondialdehyde (MDA), which are highly reactive (Gaschler and Stockwell, 2017).

4-HNE can form stable adducts with proteins changing their function by modifying histidine, arginine, lysine and cysteine residues (Higdon et al., 2012), which can only be removed via controlled degradation of the protein. However, if not degraded these proteins can accumulate causing toxicity, where HNE forms adducts with mitochondrial respiratory chain subunits RS levels can increase (Harris et al., 2015; Lee et al., 2012; Reed et al., 2008). Mitochondrial HNE modifications can overwhelm autophagy as HNE concentration increases in neurons, contributing to mitochondrial dysfunction (Dodson et al., 2017; S. Zhang et al., 2017). In addition to mitochondrial dysfunction, lipid peroxidation products such as 4-HNE can induce oligomerisation of α-synuclein resulting in toxicity in SH-SY5Y cells and Parkinson's disease (Näsström et al., 2011; Shamoto-Nagai et al., 2018).

MDA like 4-HNE is another by product of lipid peroxidation where levels have been found to be 10-fold higher in the SN of post-mortem PD brains compared with other regions as well as age matched control (Całyniuk et al., 2016; Gökçe Çokal et al., 2017). Farias *et al.* also demonstrated increased levels of MDA and lipid hydroperoxides, both indicators of lipid peroxidation were elevated in the blood of PD patients (de Farias et al., 2016). Additionally, Farias *et al.* also showed that while MDA was present in both early and late phases of PD lipid hydroperoxides were only significantly higher in late stage PD, suggesting lipid peroxidation is associated with disease progression. As such MDA is another marker of oxidative stress, which is supported by prior vitamin E administration lowering MDA and protein carbonyl levels (Jhoo et al., 2004). MDA can also form protein adducts via modification of the lysyl residues of a protein (Barrera et al., 2018). Once formed MDA and 4-HNE can be reduced to alcohol by aldo-keto reductases or alcohol dehydrogenases or oxidised to acid by aldehyde dehydrogenases (Barrera et al., 2015).

Table 1.3 Summary of post-translational modifications associated with oxidative stress. Adapted from Santos and Lindner, 2017; Didonna and Benetti, 2015.

Post-translational modification	**Reversible/ irreversible**	**Target amino acid residue**	**Example**	**References**	**Infers**
Carboxylation	Irreversible	Lysine, proline, arginine, threonine, histidine, cysteine	Cytoskeletal proteins neurofilament and tubulin	Bizzozero, 2009	Protein aggregation
Nitration	Reversible	Tyrosine	α-synuclein promoting LB formation Complex I inhibition	Takahashi et al., 2002 Murray et al., 2003 Yamamoto et al., 2002 Davis et al., 2010	Protein aggregation Mitochondrial dysfunction
S-nitrosylation	Reversible	Cysteine, methionine	Complex I inhibition DRP1 activation Parkin inactivation UCH-L1 inactivation	Di Giacomo et al., 2012 Sun et al., 2007 Chouchani et al., 2013 Cho et al., 2009 Zhang et al., 2016 Yao et al., 2004 Kumar et al., 2017	Mitochondrial dysfunction Protein aggregation

In conclusion, RS can alter cell signalling but also cause changes via modification of protein structures (table 1.3). These protein modifications can be reversible or irreversible leading to either loss or gain of function. These modifications may lead to aberrant proteins that can accumulate forming toxic aggregates. Alternatively, cell toxicity can be caused by modifications of important machineries such as the complexes in mitochondria or proteasome, suggesting links between oxidative stress and the other hallmarks of neurodegeneration. Alternatively, lipid peroxidation can produce other molecules such as 4-HNE and MDA which are markers of oxidative stress but can also form protein adducts leading to proteotoxic stress.

1.2.2.4 Generating oxidative stress to model neurodegeneration

Excessive RS levels are associated with numerous pathologies (Poprac et al., 2017). The importance of redox balance is highlighted by the numerous biological mechanisms for combatting their toxic nature, including a variety of antioxidant enzymes. These RS appear to contribute to the pathology of various neurodegenerative disorders. Therefore multiple models have been used to investigate the role of RS in both signalling and neurodegenerative disorders (Reczek and Chandel, 2015).

Currently, most methods rely on the application of RS directly or indirect by increasing RS levels by inhibiting antioxidant pathways via drug treatment and/or genetic approaches to mimic neurodegenerative process. 6-hydroxydopamine (6-OHDA); a commonly used catecholaminergic neurotoxin, enters neurons via dopamine transporters resulting in catecholamine quinone formation leading to OS. In addition, 6-OHDA may inhibit complexes I and IV in the ETC (Glinka and Youdim, 1995) although this is not confirmed (Storch et al., 2000). Intracerebral injection of 6-OHDA resulted in increased levels of ROS including hydrogen peroxide, superoxide and hydroxyl radicals (Heikkila and Cohen, 1973).

The most common way to induce RS is by using ETC inhibitors, particularly complex I inhibitors as complex I activity is reported to be reduced in the SN of PD patients (Blesa et al., 2015; Franco-Iborra et al., 2016; Schapira, 2008). Some of these reagents include rotenone, a ETC complex I inhibitor or antimycin A, a ETC complex III inhibitor, resulting in increased mitochondrial superoxide production resulting in OS (L. Wang et al., 2015). MPTP is another drug that causes Parkinsonian symptoms and dopaminergic neurodegeneration when humans and sub-human primates have been systemically injected (Choudhury and Daadi, 2018). MPTP is catabolised by MAOB in glia producing MPP^+ which accumulates within dopaminergic neurons via dopamine transporters. Once within the neurons, MPP^+ can then inhibit complex I generating ROS (Coyle and Puttfarcken, 1993).

Alternative genetic approaches for inducing RS include mutations in α-synuclein, parkin and PINK which results in mitochondrial dysfunction leading to increased levels of RS (Blesa et al., 2015). Furthermore, evidence of point mutations in mtDNA may also be associated with complex I deficiency or mitochondrial dysfunction in PD (Hauser and Hastings, 2013), resulting in RS generation. Similar results were found in human neuroblastoma SH-SY5Y cell lines where PINK1 deficiency lead to mitochondrial dysfunction and increased OS (Wood-Kaczmar et al., 2008).

Genetic DJ-1 mutations promote its proteasomal degradation, promoting OS (Bonifati et al., 2003; Miller et al., 2003). DJ-1 null mice did not show widespread neuronal loss, however, they were more susceptible to toxins (Goldberg et al., 2005; Kim et al., 2005). This was supported in human neuronal cell lines where DJ-1 knock down resulted in cells being more susceptible to toxins (Taira et al., 2004; Yokota et al., 2003). Mutant forms of DJ-1 are reported to be unstable relative to wildtype DJ-1 (Di Nottia et al., 2017; Macedo et al., 2003). In models of Neuro2a cells where DJ-1 was down-regulated neurons were more susceptible to H_2O_2 induced death. However, these cells were rescued with overexpression of wildtype DJ-1 but not mutant DJ-1 (Yokota et al., 2003). This suggests DJ-1 protects neurons from OS while mutant DJ-1 loses this function.

In conclusion there are multiple ways to generate RS such as directly exposing cells to RS, using reagents that inhibit pathways that reduce RS levels, or modulating scavenger enzymes either chemically or genetically. Establishing what species are generated from each toxin in precise locations will aid in establishing a better understanding of their role in signalling and damage in neurodegenerative disorders such as PD.

1.2.3 Impaired protein degradation

Although gene defects are not always present in sporadic cases, impaired protein handling is suggested to play a role in the pathogenesis of PD as part of the NBT. Protein degradation is important for removing aberrant toxic proteins that can accumulate and compromise cellular function and viability. Cytoplasmic inclusions known as Lewy bodies are a pathological feature of PD present in DA neurons of the SN and cerebral cortex (Braak et al., 1995). Formation of these LB's is poorly understood, however, aberrant protein aggregation appears to occur when the cells ability to remove abnormal, mutated or oxidatively modified proteins is exceeded, or mechanisms of removal are impaired or inhibited (Lefaki et al., 2017). Studies have shown increased levels of oxidatively damaged proteins, protein aggregation and accumulation of poorly degraded proteins within LB's (Thibaudeau et al., 2018). Oxidatively damaged protein levels are greater in the SN of PD brains, evidenced by elevated protein carbonyls and 4-hydroxynonenal (HNE) protein adducts (Shahmoradian et al., 2019; Zhao et al., 2017). Evidence also suggests a general increase in protein

aggregation in the SN (Grünblatt et al., 2018). Together, multiple studies implicate impaired protein degradation or uncontrolled production of abnormal proteins plays a role in PD (Mcnaught et al., 2001; Walden and Muqit, 2017).

1.2.3.1 The ubiquitin proteasome system

1.2.3.1.1 Structure and Function

To prevent protein accumulation and aggregate formation under normal conditions intracellular proteins can be degraded in an ATP-dependent manner involving the ubiquitin proteasome system (UPS; Hough et al., 1986). This system is tightly regulated and plays a major role in cellular processes including: cell proliferation, differentiation, protein transport, antigen processing, DNA repair and apoptosis (Komander and Rape, 2012; Livneh et al., 2016). More recently studies have shown that the proteasome is also involved in proteolytic cleavage affecting protein function altering downstream processes (Olshina et al., 2018). The proteasome is one mechanism of aberrant protein removal which has been reported as impaired or with reduced subunit expression in nigral

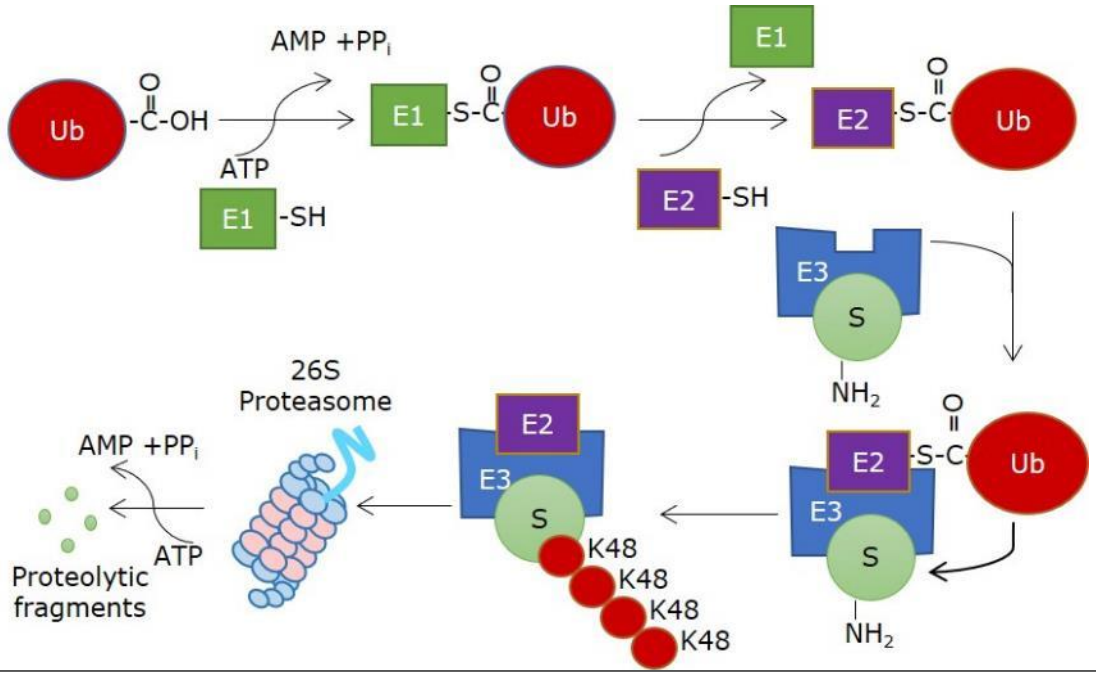

Figure 1.8. Schematic representation of ubiquitin conjugation to target substrates to the ubiquitin proteasome system (UPS). *Free ubiquitin (Ub) is initially activated by E1 in an ATP-dependent step to form a thiol-ester bond between E1 and the carboxy-terminus of Ub. Ub is transferred to E2 via a trans-thiolation reaction. E2 associates with E3 which has a substrate already bound. Ubiquitin is then transferred to the substrate forming an isopeptide bond with a lysine residue in the substrate. Successive addition of Ub to initial Ub creates a polyubiquitin chain. If conjugated to K48 this is recognised as a signal for degradation by the 26S proteasome. Adapted from Glickman and Ciechanover, 2002.*

post-mortem tissue (McNaught et al., 2003). Proteasome degradation involves ubiquitin; a 76-amino acid globular protein, covalently added post-translationally.

Ubiquitin conjugation proceeds via a three-step cascade mechanism involving E1, E2 and E3 enzymes (Figure 1.8; Glickman and Ciechanover, 2002). E1, the ubiquitin activating enzyme, activates ubiquitin in an ATP-dependent manner producing a high-energy thiol-ester intermediate with the carboxy-terminal glycine of ubiquitin. Subsequently, E2, a ubiquitin conjugating enzyme, accepts activated ubiquitin from E1 via a trans-thiolation reaction and transfers ubiquitin to the substrate that in some cases is specifically bound to E3, a ubiquitin protein ligase. Generally, ubiquitin is conjugated to the substrate through an isopeptide bond with the ε-NH_2 of a lysine residue in the substrate (Ciechanover and Brundin, 2003). Successive addition of ubiquitin molecules to the initial ubiquitin conjugated to the substrate creates a polyubiquitin chain (Kwon and Ciechanover, 2017). Different linkages in these polyubiquitin chains can exhibit distinct functions. Polyubiquitin chains linked through lysine 48 (K48) residues target proteins for degradation via the 26S proteasome (Chen and Sun, 2009).

The 26S proteasome is composed of complexes centred on the 20S proteasome core particle (CP) which is capped at both ends by the 19S regulatory particles (RPs), regulated by multiple chaperones (Bedford et al., 2010). The 20S CP structure displays a cylindrical structure made up of four heptameric rings composed of seven α and β subunits stacked as a α_7-β_7-β_7-α_7 arrangement giving a pseudo-sevenfold symmetry. The α-subunits form the outer ring while the β subunits form the inner (Groll et al., 1997). The 20S CP is responsible for degrading proteins in mammals via three enzymatic β-subunits (Deshmukh et al., 2019; Unno et al., 2002) which have chymotryptic, tryptic and post acidic-like hydrolysing activity. The CP acts as a channel with an open and closed conformation, where by itself it is closed due to the highly conserved N-terminals of the seven alpha subunits (Groll et al., 2000). The narrow channel in combination with the enzymatic specificity minimises non-specific proteolysis.

The 19S RP is responsible for controlling entry to the CP channel and consists of 2 major assemblies defined as the lid and the base, each of which consist of nine subunits (Finley, 2009; Kwon and Ciechanover, 2017). Rpn11 is the key component of the lid which is a metalloprotease deubiquitinating enzyme situated above the Rpt entry port ring (Pathare et al., 2014; Verma, 2002; Worden et al., 2014). The base consists of a hexamer of non-redundant ATPases containing Rpt1-6. These ATPases convert the energy from ATP hydrolysis into mechanical force. Within eukaryotes it is believed that these different Rpt subunits evolved for recognising ubiquitin signals for degradation. However, currently it is unknown if the 6 subunits hydrolyse ATP in a random,

sequential or concerted manner (Beckwith et al., 2013; Peth et al., 2013; Rubin, 1998). Within the Rpt subunits is a coiled coil helix domain which promotes assembly of the ring via contacts with other regions of the base and lid. These subunits also contain an OB domain which restricts access through the entry port (Lander et al., 2012; Lasker et al., 2012). The ring also has Rpn1, Rpn2 and Rpn13 subunits, which can dock ubiquitin both directly and indirectly (Hamazaki et al., 2015; Husnjak et al., 2008).

In addition to ubiquitin, molecular chaperones are essential for folding proteins, refolding damaged proteins and targeting irreversibly damaged proteins to the UPS for degradation (reviewed in Balchin, Hayer-Hartl and Hartl, 2016). Many of these chaperones are heat shock proteins (HSPs). Transcription of these HSPs is controlled by heat shock transcription factor 1 (HSF1), which is constitutively expressed in most tissue and cell types where post translational modifications modulate its activity (Xu et al., 2012). Under normal conditions HSF1 is a monomer localised to the cytosol but under stressful conditions HSF1 homotrimerises, becoming active and translocating to the nucleus (Rabindran et al., 1993; Utani, 2010). Once in the nucleus, HSF1 binds to the cis-regulatory element of DNA (the heat shock element) leading to an increase in HSP expression (Jacob et al., 2017).

One member of the HSP family particularly important in response to ROS is HSP70, which participates in protein trafficking, early stage protein folding and refolding or degradation of aggregate peptides, especially those modified by RS (Bukau et al., 2006; Lazarev et al., 2016). HSP70 recognises early stage protein folding via short hydrophobic regions that are rich in leucine residues (Rudiger, 1997). If folding is not possible HSP70 associates with co-chaperones to promote degradation (Fernández-Fernández et al., 2017).

1.2.3.2 Proteasome dysfunction during aging and neurodegeneration

Rare forms of familial PD have shown mutations in UCH-L1, a deubiquitinating enzyme suggesting protein degradation and the UPS may play a role in neuronal loss. Furthermore aggregates have been detected in neurons within the SN of PD patients (Braak et al., 2003), suggesting protein homeostasis disruption. In addition, proteasome activity declines in the brain and spinal cord with aging (Finley, 2018).

Proteasome catalytic activity and subunit levels are reported to decline in SN post-mortem tissue but not the cortex or striatum of PD patients (Mcnaught et al., 2001; McNaught et al., 2003). This suggests DA neurons may be more vulnerable to dysfunctional UPS in sporadic PD. Furthermore rats treated with rotenone for 5-7 days to model PD exhibit significantly decreased

proteasomal activity in the ventral midbrain but not in striatal or cortical regions (Betarbet et al., 2006). Additionally, greater levels of ubiquitinated proteins in DA neurons were detected in rotenone treated rats relative to controls, while 20S proteasome levels did not change suggesting loss of proteasomal activity and not subunit levels (Betarbet et al., 2006). *In vitro* SK-N-MC neuroblastoma cells treated with rotenone for 3 weeks showed an increase in proteasomal activity suggesting an initial compensation followed by a significant reduction in activity after 4 weeks (Betarbet et al., 2006). This suggests continuous rotenone exposure eventually overwhelms the proteasome, possibly via generation of RS and subsequent accumulation of oxidised proteins.

Oxidatively modified proteins are present in LB's within the SN of PD patients (Giasson, 2000; Luk, 2019). One method of degrading oxidatively damaged proteins involves the 20S proteasome (Lefaki et al., 2017) via ubiquitination or in an ATP-dependent manner (McNaught and Jenner, 2001; Shringarpure et al., 2003). *In vitro* studies with SH-SY5Y cells treated with rotenone showed reduced proteasomal activity with concurrently increased levels of oxidatively modified proteins, suggesting impaired proteasomal function leads to increased levels of damaged proteins (Shamoto-Nagai et al., 2003). In addition, Shamoto-Nagai *et al.* also report proteasomal subunit oxidation. Additionally, a study suggests the 26S proteasome is more vulnerable to OS than the 20S proteasome alone (Raynes et al., 2016; Reinheckel et al., 2000). RNS such as nitric oxide and peroxynitrite directly added to cell lysates also resulted in decreased 20S activity (Chou et al., 2010). Together, this suggests that both ROS/RNS can affect proteasome activity directly by modifying subunits leading to high levels of aberrant proteins, or indirectly through overwhelming the UPS with oxidatively damaged proteins resulting in protein aggregates and degeneration.

Accumulation of misfolded proteins leads to upregulation of HSPs to assist in refolding damaged proteins or sending irreversibly damaged proteins to the UPS for degradation (Ciechanover and Brundin, 2003; Esser et al., 2004). For example, astrocytes are reported to have high levels of HSP25 under basal conditions but accumulate following proteasomal stress (Goldbaum et al., 2009). Furthermore, mutations in molecular chaperones have been associated with neurodegeneration (Gorenberg and Chandra, 2017). In AD patients, HSP90 levels have been reported to be elevated in cytosolic and membranous fractions (Dou et al., 2003; Gracia et al., 2019). Another study has shown that S-nitrosylation of the critical thiol group of HSP90 abolishes its ATPase activity required for its function as a molecular chaperone (Martinez-Ruiz et al., 2005; Nakamura and Lipton, 2017). Additionally, upregulation of HSP70 prevented neurodegeneration in *in vivo* PD models (C.-W. Zhang et al., 2016). It is also important to note that aggregates have been found to contain chaperones such as HSP70 and HSP27 (Ito et al., 2002; Rideout and Stefanis,

2002).Together, these studies suggest changes in molecular chaperones, possibly via higher RS levels, contribute to misfolded protein accumulation, aggregation and cell death.

1.2.4. Links between mitochondrial dysfunction, oxidative stress and impaired protein degradation

The pathogenesis of neurodegenerative diseases is still unclear yet is vitally important due to the ever-growing aging population. While there are a variety of neurodegenerative diseases each affecting different brain regions, they share two key characteristics: insoluble protein aggregates and neuronal degeneration (Merlini and Bellotti, 2003). Post-mortem PD patient brains have shown reduced proteasome activity in the nigral striatum (McNaught and Jenner, 2001; McNaught et al., 2003) alongside mitochondrial dysfunction (Goedert et al., 2017; Loeb et al., 2010; Luth et al., 2014) and increased levels of oxidatively modified proteins, lipids and DNA (Goedert et al., 2017; Ischiropoulos and Beckman, 2003; Jenner and Olanow, 1996). Therefore, there is evidence for multiple systems being affected in neurodegeneration and it is reasonable to investigate if these factors are interrelated.

A possible unifying mechanism that can induce protein aggregation and neuronal degeneration involves the pathways that reactive oxygen and nitrogen species can drive. This is supported by increased levels of oxidatively modified proteins, DNA and lipids observed in post-mortem PD tissues (Goedert et al., 2017; Ischiropoulos and Beckman, 2003) as well as in familial cases, as mentioned previously. While this does not confirm that OS is the sole reason for the pathogenesis of neurodegeneration, it establishes a role for OS that links with the other hallmarks of neurodegeneration.

If antioxidant systems are overwhelmed alongside decreased mitochondrial function, OS has been shown to increase susceptibility to proteotoxic stress (Breitzig et al., 2016; Harris et al., 2015; Xun et al., 2012). RS can affect proteostasis directly via post-translational modifications or affecting degradation via the proteasome. Modifications of proteins can result in gain or loss of function due to secondary and tertiary structure alteration (Nedić et al., 2013; Perez et al., 2009; Trougakos et al., 2013). As a result of these PTMs, proteins can misfold exposing hydrophobic regions which aggregate together (Weids et al., 2016). Aggregates can accumulate and overwhelm the UPS by forming stable insoluble complexes which can lead to cell death (Espay et al., 2019; Lindersson et al., 2004). As a result of reduced proteasome activity, oxidatively modified proteins can accumulate resulting in more aggregates and inclusion body formation. Consequently, cellular dysfunction and apoptosis ensues (Demasi and Davies, 2003; Ding et al., 2004; Rideout et al., 2001). More recently, aggregates have been demonstrated to be delivered to mitochondria resulting in

mitochondrial dysfunction (Ruan et al., 2017) linking OS, dysfunctional protein degradation and the apoptotic process.

Rotenone, which inhibits complex I, shows a dose dependent decrease in UPS activity in HEK, SK-N-MC cells, and SH-SY5Y cells (McLennan and Degli Esposti, 2000; Shamoto-Nagai et al., 2003) whereas other inhibitors of ETC complexes (e.g. antimycin or potassium cyanide) did not result in proteasome inhibition. Furthermore qRT-PCR revealed α- and β-subunit expression was the same regardless of rotenone treatment suggesting possible PTMs are affecting proteasomal activity (Chou et al., 2010). In addition, a previous study demonstrated α-tocopherol attenuated rotenone induced proteasome inhibition (Betarbet et al., 2006), though an alternate study contradicted this (Chou et al., 2010). Others showed pesticides effect mitochondrial morphology and function but also inhibited 20S and 26S proteasome activity (Chen et al., 2017). It is also important to note that cells treated with proteasome inhibitors exhibited increase RS levels (Dröge, 2002). Livnat-Levanon *et al* have also demonstrated defective mitochondria induce RS and proteasome disassembly (Livnat-Levanon et al., 2014), which is supported by Rinaldi *et al* that show Rpn11-m1 mutated proteasome also exhibited increased levels of intracellular RS (Rinaldi et al., 2002). Whilst controversy remains on how proteasome activity is decreased under stress, RS and mitochondrial dysfunction appear to contribute to altered proteostasis and subsequent cell death.

The link between dysfunctional proteostasis and RS is further highlighted by both pathways possessing common factors such as molecular chaperones including HSP27, HSP70, HSF1 and antioxidant response proteins such as NRF1 and 2. Small heat shock proteins such as HSP27 provide high affinity platforms for unfolded protein preventing aggregation under stress (Kayser et al., 2013; Somara and Bitar, 2006). These small HSPs are highly regulated by PTMs such as those that result from RS (Clements et al., 2007; Song et al., 2014). Furthermore, HSP27 targets damaged or mutated proteins to the UPS for degradation (Li et al., 2013; Outeiro et al., 2006). Additionally, HSP27 levels have been seen to be increased in astrocytes of PD patients (Shimura et al., 2017).

HSP70, unlike HSP27 is a highly abundant HSP with various roles but is mainly involved in the correct folding of newly synthesised proteins, and refolding proteins that are misfolded or aggregated (Garrido et al., 2012). HSP70 is composed of 2 domains: an amino terminal ATPase domain and a carboxy terminal substrate binding domain made up of a helical segment and β-sandwich domain where the latter recognises hydrophobic amino acids (Hartl et al., 2011; Rüdiger et al., 1997). Furthermore HSP70 is reported to mediate dissociation and re-association of the 26S proteasome during adaption to OS (Grune et al., 2011).

These chaperones are regulated by heat shock factors (HSFs) where HSF1 is the dominant highly conserved transcription factor (Åkerfelt et al., 2007). Under normal homeostasis, HSF1 remains inert as inactive monomers bound to chaperones such as HSP70 and HSP40. Stress results in chaperones binding aberrant proteins releasing HSF1 whereupon it undergoes phosphorylation, trimerization and nuclear localisation (Anckar and Sistonen, 2007). HSF1 can also sense OS via 2 cysteine residues (Ahn and Thiele, 2003) and upon activation, HSF1 binds to the consensus heat shock element within the promoter regions of HSP genes, resulting in their activation and gene expression to aid in controlling responses to oxidative and proteotoxic stress (Anckar and Sistonen, 2011).

Transcription factors such as nuclear erythroid factor 1 and 2 (NRF1 and NRF2) are also influenced by oxidative stress. NRF2 has a short half-life of approximately 10-20 minutes (Bryan et al., 2013) and is regulated by the UPS as KEAP1 acts as a redox switch, via its cysteine 151,273 and 288 residues, where under normal homeostasis KEAP1 binds NRF2 facilitating its ubiquitination and degradation via the proteasome (figure 1.8). Whereas upon OS NRF2 is released allowing its phosphorylation by a variety of kinases (Huang et al., 2015) and subsequent translocation into the nucleus via importins (Silva-Islas and Maldonado, 2018). Once in the nucleus NRF2 can bind to the ARE in the promoters of multiple genes including antioxidants such as catalase, SOD, glutathione synthesis proteins etc., but also increases proteasome subunits levels and ubiquitination related genes during OS (reviewed more thoroughly in Korovila et al., 2017; Kwak et al., 2003). Human embryonic stem cell studies also showed NRF2 controlled proteasome maturation and proteasome-related chaperones (Jang et al., 2014).

NRF1 is homologous to NRF2, and also undergoes nuclear translocation upon deglycosylation competing with NRF2 for the ARE (Lee and Ryu, 2017), but is also is regulated by proteasomal degradation despite differing in regulatory mechanisms and cellular localisation (Ohtsuji et al., 2008). NRF1 appears to be important in proteasome subunit regulation as NRF1 has been identified as a key transcriptional regulator of proteasome genes in neurons. This is demonstrated by NRF1 knockout mice, which showed reduced expression of genes encoding for the 20S and 19S subunits along with impaired proteasomal function (Lee et al., 2011). Further supporting this, low concentrations of proteasome inhibitors induce NRF1, whereas higher concentrations lead to NRF1s inactivation (Radhakrishnan et al., 2014; Vangala et al., 2016). Therefore, both NRF1 and NRF2 are regulated by the proteasome via OS and help to return cells to homeostasis by upregulating antioxidant genes but also proteasomal subunits to degrade already modified proteins or aggregates (see figure 1.9).

In conclusion, while it is unclear what initiates neurodegeneration to produce these hallmarks, they appear to link in various feedback loops to try and return cells to homeostasis. Due to how difficult it is to determine the start of neurodegenerative pathogenesis it would be more beneficial to determine if there is a linking cofactor which can provide therapeutic potential.

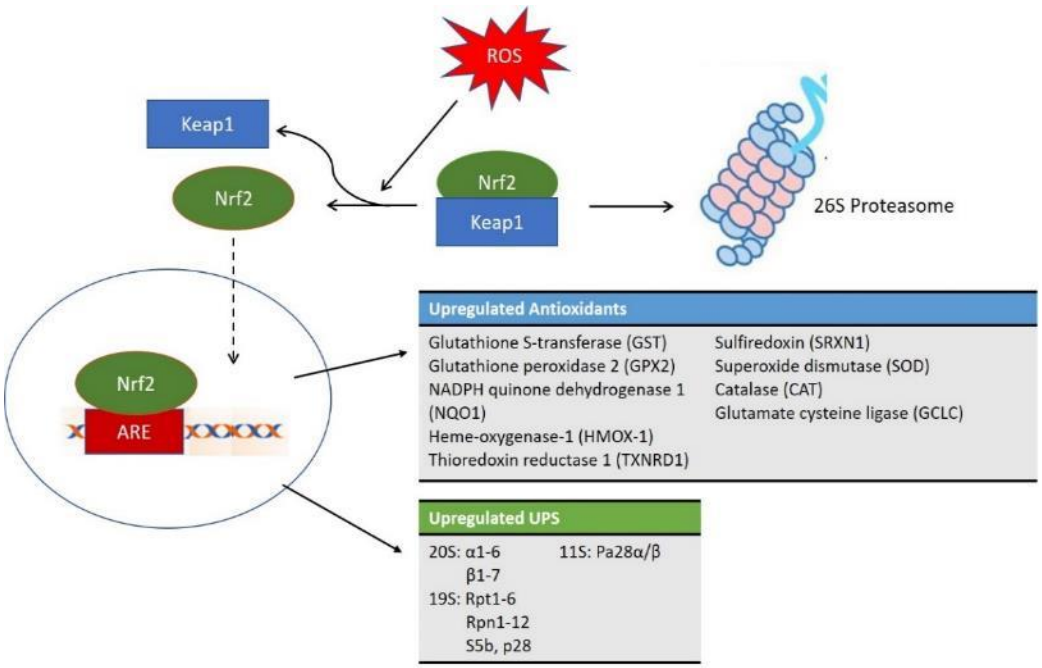

Figure 1.9. Overwhelming the cells antioxidant systems results in defence mechanisms being induced. *During oxidative stress NRF2 dissociates from KEAP1 leading to nuclear translocation and upregulation of a variety of antioxidants and ubiquitin proteasome system (UPS) subunits to come to the cells defence against oxidative stress. Adapted from Korovila et al., 2017 and Chen et al., 2014.*

1.3 Co-Culture

1.3.1 Glia in neurodegeneration

Although neurons were once the focus of neurodegenerative research, many are realising the immune system may be involved in PD aetiology suggesting neuroinflammation may not just be a consequence of neuronal dysfunction or degeneration. Glia are the most abundant cell in the brain and can be separated into 3 types: oligodendrocytes, microglia and astrocytes which are the most populous (Herculano-Houzel, 2009; Verkhratsky et al., 2012). Neuronal degeneration in PD is associated with neuroinflammation which is mediated primarily by microglia (Kempuraj et al., 2016) and less so by astrocytes and oligodendrocytes (Perry, 2012). A greater density of activated microglia have been observed in the SN of PD patients and associated with DA neuron loss in PD (Ghadery et al., 2017). Activated microglia have also recently been reported in the SN and striatum

of animal models (Pisanu et al., 2014; Stott and Barker, 2014). In addition to microglia, astrocytes are also key in neurological disorders as reactive astrocytes are a key aspect of PD (Boillée et al., 2006; Koprich et al., 2008; Miklossy et al., 2006).

Astrocytes are large stellate cells with multibranched processes extending their branches from the soma which divide into secondary branchlets, tertiary leaflet and end feet that encase blood vessels but also ensheath neuronal synapses (Bushong et al., 2002; Khakh and Sofroniew, 2015).

In PD patients studies have shown increased GFAP expression, a marker of astrocytes (Manocha et al., 2017), where vimentin and nestin have also been shown to be upregulated in reactive astrocytes (de Pablo et al., 2018). The role of astrocytes in neurodegeneration is further highlighted by studies showing α-synuclein positive astrocytes correlating with nigral neuronal death (Cavaliere et al., 2017). Furthermore, PD models show astrogliosis following dopaminergic neuronal death (El Massri et al., 2016; Hirsch and Hunot, 2009), whilst administration of 6-OHDA also resulted in increased GFAP expression (Ganapathy et al., 2019). These studies suggest that OS plays a role in astrogliosis.

Interestingly, it is believed that astrocytes are more resistant to stress than neurons as aggregates are more commonly found in neurons (Jansen et al., 2014). Further supporting this, the UPS in glia has been shown to be more active than in neurons both *in vitro* and *in vivo* (Sung and Jimenez-Sanchez, 2020). The increased resistance of astrocytes to OS may help to reduce proteotoxic stress, since astrocytes contain one of the highest cytosolic concentrations of glutathione, (approximately 8-10mM in primary astrocytes) in mammalian cells (Makar et al., 2008; Raps et al., 1989; Yudkoff et al., 1990). Additionally, higher levels of DJ-1 in astrocytes have been observed in post-mortem PD samples relative to neurons suggesting astrocytes attempt to combat OS during neurodegeneration (Frøyset et al., 2018; Neumann et al., 2004). In addition, the importance of astrocytes in combating neural OS is supported by the high level expression of detoxifying enzymes and transporters such as ascorbic acid, glutathione and its precursors (Allaman et al., 2011; Asanuma et al., 2019). Astrocytes also display greater levels of NRF2 than neurons (Jimenez-Blasco et al., 2015), which regulates the expression of catalase, peroxiredoxin 6 and glutamate-cysteine ligase; the latter being an enzyme involved in the first step of glutathione synthesis (Dowell and Johnson, 2013; Lee et al., 2003).

Overall, these studies suggest neurons are not the only cells that need to be considered when studying neurodegeneration as other cells display different capabilities and functions. In particular, astrocytes seem to have different mechanisms for coping with OS and need

consideration when examining neurodegeneration as they appear to be key for understanding underlying pathways and may support neurons in some way.

1.3.2 Neuron-glial crosstalk

Currently, most studies involve the study of monocultures to understand intracellular mechanisms involved in the pathogenesis of neurodegeneration. However, in the brain there is a not a single cell type, but a complex network of different cells composed of different ratios depending on the brain region. The importance of these networks is highlighted by the SN having the lowest glia to neuron ratio in the brain (von Bartheld et al., 2016), which may explain the selective vulnerability of dopaminergic neurons in Parkinson's disease. Therefore, understanding not only intracellular mechanisms but also intercellular and feedback mechanisms are important for understanding neurodegeneration.

Glia dynamically interact with neurons by responding to neurotransmitters and in response regulate neuronal and synaptic function by releasing gliotransmitters (Araque et al., 2014; Eroglu and Barres, 2010; Perea et al., 2014). For example, astrocytes can secrete neurotrophic factors such as glial derived neurotrophic factor (GDNF) and brain derived neurotrophic factor (BDNF), which are essential for dopaminergic neuron survival and development (Pöyhönen et al., 2019). Furthermore, astrocytes use a malate-aspartate shuttle to transport various nutrients and metabolic precursor to neurons. One of the most important shuttles that astrocytes possess is the glutamate-glutamine shuttle allowing collection and conversion of glutamate from the extracellular space secreted by neurons into glutamine, which is shuttled back to the presynaptic terminal of synthesis and is critical for glutamate synthesis, acting as an essential neurotransmitter (Murphy-Royal et al., 2017). In addition to helping neurotransmission astrocyte-neuron crosstalk is important for dendritic growth, synapse formation and removal of dysfunctional synapses through both soluble factors and direct contact (Haim and Rowitch, 2017; Stevens et al., 2007).

Astrocytes release glutathione, which is subsequently broken down into γ-glutamyl group and cysteinyl glycine via γ-glutamyl transferase. Ectopeptidases then break down cysteinyl glycine into cysteine and glycine which are taken up by neurons. Therefore, astrocytes help provide neurons with components to generate glutathione to aid with OS (Bolaños, 2016; McGann and Mandel, 2018). Additionally, astrocytes protect neurons from OS via DJ-1 as astrocytes with DJ-1 knocked out exhibited impaired glutamate uptake (Kim et al., 2016). This leads to higher levels of extracellular glutamate leading to neuronal excitotoxicity, which is a known cause of neurodegeneration (Jakaria et al., 2018). The importance of DJ-1 from astrocytes in neuroprotection is highlighted by knockout DJ-1 astrocytes displaying reduced ability to protect

neurons against PD models using rotenone (Larsen et al., 2011). Further supporting astrocytes protecting neurons from OS is a study where NRF2 overexpression in astrocytes delayed disease onset in mouse models with mutant α-synuclein expression in neurons (Gan et al., 2012).

Therefore, studies suggest that crosstalk between astrocytes and neurons is important for controlling neuronal and synaptic function but also aids with OS. As such, there is a greater need for co-culture systems to investigate the crosstalk between different cell types in the CNS to establish an *in vitro* model that replicates more *in vivo* like conditions for the development of novel therapies for neurodegenerative diseases.

1.4 Aims of the study

The overall objective of this study is to investigate the role of OS during neurodegeneration and start development of a neural co-culture model. This will be achieved through establishing the consequences of different RS on individual neural cell types. These investigations will allow greater understanding of these cells prior to developing a neural co-culture. As a result, the pathways underlying neurodegeneration can be investigated and future novel therapies for neurodegenerative diseases proposed. Hence the main aims of this study are:

- To generate OS using different oxidising agents, rotenone (a complex I) and AAPH (an oxidising agent), in neuronal and glial monocultures whilst also investigating other factors such as mitochondrial and proteasome dysfunction to investigate pathways involved in the pathology of neurodegeneration. This has the potential to determine if specific RS influence the hallmarks of neurodegeneration in various ways in different neural cells.

- To investigate these RS inducing agents in a differentiated model to greater mimic more *in vivo* like conditions to determine a more representative model of the human brain, allowing downstream effects of RS to be determined.

- Finally, crosstalk between neurons and glia will be investigated in a co-culture. When investigating, these secreted factors will be probed from conditioned media and non-contact co-cultures. This has the potential to identify possible protective secreted factors which may provide future novel therapies for neurodegenerative diseases.

CHAPTER 2

MATERIALS AND METHODS

2.0 Materials and Methods

2.1 Materials

2.1.1 Cell Culture

2.1.1.1 Cell Lines

SH-SY5Y cell line acquired from the European Collection of Authenticated Cell Cultures (ECACC; Salisbury, UK)

U-87MG cell line acquired from the European Collection of Authenticated Cell Cultures (ECACC; Salisbury, UK)

2.1.1.2 Reagents

B-27™ Supplement (50X), serum free (17504044) – ThermoFisher Scientific, Loughborough, UK

Dulbecco's phosphate buffered saline without Ca^{2+} and Mg^{2+} (17-512F) – Lonza, Slough, UK

Foetal bovine serum (10270-160) – ThermoFisher Scientific, Loughborough, UK

Gibco Dulbecco's Modified Eagle Medium/ F12 Ham (DMEM: F12) 1:1 with 15 mM Hepes L-Glutamine without phenol red (21041025) – ThermoFisher Scientific, Loughborough, UK

GlutaMAX™ supplement (35050061) – ThermoFisher Scientific, Loughborough, UK

Hybri-max sterile, filtered dimethylsulfoxide (DMSO; D2650-5X10ML) – Sigma Aldrich, Dorset, UK

Lonza Dulbecco's Modified Eagle Medium/ F12 Ham (DMEM: F12) 1:1 with 15 mM Hepes L-Glutamine (LZBE12-719F) – Scientific Laboratory Suppliers, Nottingham, UK

MEM Eagle non-essential amino acid solution (100X) (13-114E) – Lonza, Slough, UK

Neurobasal™ Medium (21203049) – ThermoFisher Scientific, Loughborough, UK

Opti-MEM™ reduced serum media (31985062) – ThermoFisher Scientific, Loughborough, UK

Penicillin-Streptomycin (17-603E) – Lonza, Slough, UK

Trypsin-10X (BE02-007) – Lonza, Slough, UK

2.1.1.3 Plasticware

15 ml and 50 ml red capped tubes – Sarstedt, Leicester, UK

6 well, 12 well, 24 well and 96 well sterile tissue culture plates – Sarstedt, Leicester, UK

Cell culture flasks (T25, T75, T175) – Sarstedt, Leicester, UK

Cryovials – Sarstedt, Leicester, UK

E-plate L8 (300600840) – ACEA Biosciences, US

E-Plate Insert 16 (6465382001) – ACEA Biosciences, US

Pipette filter tips (10 µl, 200 µl and 1000 µl) – Dutscher Scientific, France

Polypropylene sterilin tubes – Sarstedt, Leicester, UK

TC insert for 24 well plate, PET membrane bottom, transparent, pore size 0.4µm sterile,

non-pyrogenic/endotoxin-free, non-cytotoxic (83.3932.041) – Sarstedt, Leicester, UK

Seahorse XF24 cell culture microplate (100777-004) – Agilent, Santa Claret, US

Sterile serological pipettes (1 ml, 5 ml, 10 ml, 25 ml) – Sarstedt, Leicester, UK

Thermo Scientific™ Nunc™ Lab-Tek™ Chmaber Slide system 8 wells – Fisher Scientific, Leicester, UK

2.1.2 Laboratory reagents

2,2'-Azobis[2-methylpropionamidine] dihydrochloride (AAPH; 440914) – Sigma Aldrich, Dorset, UK

2',7'-Dichlorofluorescin diacetate (DCFDA; 4091-99-0) – Sigma Aldrich, Dorset, UK

3-(4,5-dimethylthiaol-2-yl)-2,5-diphenyltetrazoulium bromide (MTT; M2128) – Sigma Aldrich, Dorset, UK

2-mercaptoethanol (M6350) – Sigma Aldrich, Dorset, UK

Ascorbic acid (A5960-25G) – Sigma Aldrich, Dorset, UK

α-tocopherol (T3251) – Sigma Aldrich, Dorset, UK

Accugel 29:1 (40% solution) acrylamide (A2-0068) – Geneflow Ltd., UK

Adenosine 5'-triphosphate (ATP; A3377) – Sigma Aldrich, Dorset, UK

Agarose (A9539) – Sigma Aldrich, Dorset, UK

All-trans retinoic acid (R2625) – Sigma Aldrich, Dorset, UK

Ammonium persulphate (A3678) – Sigma Aldrich, Dorset, UK

Bicinchoninic acid (B9643) – Sigma Aldrich, Dorset, UK

Bio-Rad protein assay dye reagent concentrate (5000006) – BioRad Laboratories Ltd, Hertfordshire, UK

Bovine serum albumin (BSA; A2153) – Sigma Aldrich, Dorset, UK

Click-iT™ Lipid Peroxidation Imaging Kit - Alexa Fluor™ 488 (C10446) – ThermoFisher Scientific, Loughbourough, UK

Copper phthalocyanine 3,4',4'',4''' terasulphonic acid tetrasodium salt (245356) – Sigma Aldrich, Dorset, UK

Copper (II) sulphate (451657) – Sigma Aldrich, Dorset, UK

Copper (II) sulphate solution (C2284) – Sigma Aldrich, Dorset, UK

Dimethyl Sulfoxide (DMSO) (472301) – Sigma Aldrich, Dorset, UK

Dual-colour prestained precision plus protein™ standards, 10-250 kDa (161-0374) – BioRad Laboratories Ltd, Hertfordshire, UK

EZ-PCR Mycoplasma Test Kit (20-700-20) – Biological Industries, Staffordshire, UK

Fluorescein Diacetate – Sigma Aldrich, Dorset, UK

Folin-ciocalteu phenol reagent (F9252) – Sigma Aldrich, Dorset, UK

GAPDH positive control siRNA (4390849) – ThermoFisher scientific, Loughborough, UK

Glycine (G8898) – Sigma Aldrich, Dorset, UK

Glutathione fluoremetric assay (CS1020) – Sigma Aldrich, Dorset, UK

Hanks balanced salt solution (HBSS CAMGPR) – Brainbits, Springfield, US

Hellmanex III (Z805939-1EA) – Sigma Aldrich, Dorset, UK

InstantBlue™ stain (SKU: ISB1L) – Expedeon, Cambridge, UK

iScript™ cDNA Synthesis kit (1708890) – BioRad Laboratories Ltd, Hertfordshire, UK

iTaq™ universal SYBR® green supermix (172-5120) – BioRad Laboratories Ltd, Hertfordshire, UK

JC-1 (CAY15003-5 mg) – Cambridge bioscience, Cambridge, UK

Laemli buffer (S3401-10VL) – Sigma Aldrich, Dorset, UK

Laminin (L2020-1MG) – Sigma Aldrich, Dorset, UK

Lipofectamine 3000 – ThermoFisher Scientific, Loughborough, UK

Methanol (67-56-1) – Fisher Scientific, UK

Mitotracker™ Red CMXRos (M22425) – ThermoFisher Scientific, Loughborough, UK

N-Succinyl-Leu-Leu-Val-Tyr-AMC (7-amino-4-methylcoumarin; BML-P802-0005)– Enzo Life Sciences, Exeter, UK

N,N,N',N'-Tetramethylethylenediamine (TEMED; T9281) – Sigma Aldrich, Dorset, UK

NRF2 siRNA (4392420) – ThermoFisher Scientific, Lougborough, UK

Paraformaladehyde (158127) – Sigma Aldrich, Dorset, UK

Pierce ECL Western blotting substrate (32106) – ThermoFisher Scientific, Loughborough, UK

Pierce LDH cytotoxicity assay kit (88953) – ThermoFisher Scientific, Loughborough, UK

Poly-L-lysine (P4707-50ML) – Sigma Aldrich, Dorset, UK

Potassium sodium tartrate tetrahydrate (217255) – Sigma Aldrich, Dorset, UK

Precision plus protein™ Kaleidoscope standards (161-0375) - BioRad Laboratories Ltd, Hertfordshire, UK

Protease inhibitor cocktail (P8340) – Sigma Aldrich, Dorset, UK

Protein carbonyl colorimetric assay kit (10005020) – Cambridge bioscience, Cambridge, UK

RIPA buffer (R0278) – Sigma Aldrich, Dorset, UK

RNeasy mini kit (74134) – Qiagen Ltd, UK

Rotenone (R8875-1G) – Sigma Aldrich, Dorset, UK

RT^2 First strand kit (330404) – Qiagen Ltd, UK

RT^2 Profiler™ PCR Array Human Oxidative Stress Plus (PAHS-065YC-6) – Qiagen Ltd, UK

RT^2 SYBR Green ROX qPCR Mastermix (330524) – Qiagen Ltd, UK

Scramble control siRNA (sc-37007) – Santa Cruz biotechnology, USA

S-nitrosylation protein detection kit (10006518) – Cambridge bioscience, Cambridge, UK

Sodium azide (S2002) – Sigma Aldrich, Dorset, UK

Sodium carbonate (451614) – Sigma Aldrich, Dorset, UK

Sodium dodecyl (lauryl) sulphate (SDS; L22040-1000.0) – Melford biolaboratories Ltd., Suffolk, UK

Sodium hydroxide (795429) – Sigma Aldrich, Dorset, UK

SYBR safe DNA gel stain (S33102) – ThermoFisher Scientific, Loughborough, UK

TBARS assay kit (CAY100090 55-96 wells) – Cambridge bioscience, Cambridge, UK

Tris(hydroxymethyl)aminomethane (Tris; B2005) – Melford biolaboratories Ltd., Suffolk, UK

Triton™ X-100 (T8787) – Sigma Aldrich, Dorset, UK

Trypan blue (T8154) – Sigma Aldrich, Dorset, UK

Tween ® 20 (274348) – Sigma Aldrich, Dorset, UK

XF real-time ATP assay (103592-100) – Agilent, Santa Claret, US

2.1.3 Equipment

ACEA Biosciences – RTCA iCELLigence, San Fracisso, US

Bio-rad cell counter – BioRad Laboratories Ltd, Hertfordshire, UK

Bio-Rad Mini-Protean III system – Biorad laboratories Ltd, Hertfordshire, Dorset, UK

Bio-Rad T100 thermocycler – Biorad laboratories Ltd, Hertfordshire, Dorset, UK

BMGLabtech CLARIOSTAR plate reader – BMG labtech, Aylesbury, UK

Corbett Rotor-gene 6000 real-time PCR machine – ThermoFisher Scientific, Loughborough, UK

ErgoOne ® Multi-channel pipette – StarLab Ltd, Milton Keynes, UK

ErgoOne ® Single-channel pipettes (0.5-10 µl, 2-20 µl, 20-200 µl, 200-1000 µl) – StarLab Ltd, Milton Keynes, UK

EVOS FLOID cell imaging station – ThermoFisher Scientific, Loughborough, UK

Incucyte S3 live-cell analysis system – Sartorius, Goettingen, Germany

ImageQuant™ Las 4000 – GE healthcare life sciences, Buckinghamshire, UK

Leica DMI8 inverted microscope – Leica Microsystems, GmbH, Manheim, Germany

Leica TSC SPS II confocal microscope – Leica Microsystems, GmbH, Manheim, Germany

Nanodrop 8000 spectrophotometer – ThermoFisher, Scientific, Loughborough, UK

Nikon Eclipse TS100 inverted microscope – Nikon, Japan

Nikon digital sight DS-Fi2 – Nikon Instruments Inc., Japan

Nikon digital sight DS-U3 – Nikon Instruments Inc., Japan

Seahorse XFe24 analyzer – Agilent, Santa Claret, US

StepOnePlus™ real-time PCR system – Applied biosystems, Foster City, CA, USA

2.1.4 Antibodies

Table 2.1 Primary antibody list detailing their molecular weight, characteristics, applications, dilution factor and the company they were purchased from.

Name	Specificity	Host Species	Concentration for each application		Supplier (Cat No)
			WB	IF	
Anti-β III tubulin	**50 kDa**	Mouse, polyclonal	1:1000	1:500	Abcam (ab41489)
Anti-nuclear erythroid-derived 2 like factor (NRF2)	**68/110 kDa**	Rabbit, polyclonal	1:1000	1:200	Genetex (GTX103322)
Anti-S100	**21 kDa**	Mouse, monoclonal	1:500	N/A	Abcam (ab14849)
Anti-Synaptophysin	**38 kDa**	Rabbit, monoclonal	1:1000	1:100	Abcam (32127)
B512	**α-tubulin, 50 kDa**	Mouse, monoclonal	1:2000	N/A	Sigma (T6074)
DJ-1	**20 kDa**	Rabbit, polyclonal	1:10000	N/A	Genetex (GTX132552)
GFAP	**50 kDa**	Rabbit, polyclonal	1:1000	1:250	Genetex (GTX108711)
HSF1	**82 kDa**	Rabbit, Polyclonal	1:1000	N/A	Cell signalling technology (4356T)
HSP27	**23 kDa**	Rabbit, polyclonal	1:1000	N/A	Genetex (GTX112964)
HSP70	**72/73 kDa**	Rabbit, polyclonal	1:1000	N/A	Cell signalling technology (4872T)
Lamin A/C	**74/ 63 kDa**	Mouse, monoclonal	1:2000	N/A	Cell Signalling Technology (4777S)
MFN1	**84 kDa**	Mouse, monoclonal	1:1000	N/A	Santa Cruz (SC-166644)
OPA1	**92 kDa**	Mouse, monoclonal	1:1000	N/A	BD Bioscience (612606)
pDRP1	**82 kDa**	Rabbit, Polyclonal	1:1000	N/A	Cell Signalling Technology (3455S)

Peroxiredoxin 6	**25 kDa**	Mouse, monoclonal	1:1000	N/A	Abcam (ab16947)
SOD1	**18 kDa**	Mouse, monoclonal	1:1000	N/A	Cell Signalling technology (4266T)
Ubiquitin (P4D1)	**Ladder**	Mouse, monoclonal	1:1000	N/A	Cell Signalling technology (3936T)

Table 2.2 Secondary antibody list detailing their dilution factor and the company they were purchased from.

Name	Concentration	Supplier (Cat no.)
Polyclonal horse anti-mouse IgG HRP conjugated antibody	1:1000	Cell signalling technology (#7076)
Polyclonal goat anti-rabbit IgG HRP conjugated antibody	1:1000	Cell signalling technology (#7074)
Alexa Fluor 488 donkey anti-mouse IgG	1:500	Invitrogen Ltd (A21202)
Alexa Fluor 488 donkey anti-rabbit IgG	1:500	Invitrogen Ltd. (A21206)
Alexa Fluor 350 goat anti-mouse IgG	1:500	Invitrogen Ltd. (A11045)

2.2 Cell culture

2.2.1 Maintenance of human cell lines

SH-SY5Y and U-87MG cells were cultured in sterile growth media composed of DMEM: F12 with a 1:1 ratio of 15 mM Hepes L-Glutamine (Scientific Laboratory Suppliers, Nottingham, UK) supplemented with 10% (v/v) heat inactivated foetal bovine serum (FBS; ThermoFisher Scientific, Loughborough, UK), 100 units/ml penicillin (Lonza, Slough, UK), 10 µl/ml streptomycin (Lonza, Slough, UK) and 1% (v/v) non-essential amino acid solution (100X; NEAA; Lonza, Slough, UK) in tissue culture flasks. These flasks were maintained at 37°C in a humidified atmosphere of 95% (v/v) air and 5% (v/v) CO_2. Once the cells reached 70-80% confluence they were passaged using trypsinisation. To achieve this, cells were briefly washed twice with Dulbecco's phosphate buffered saline without Ca^{2+} and Mg^{2+} (DPBS; Lonza, Slough, UK), where washes were retained to remove all traces of serum. Cells were then incubated with 250 µg/ml trypsin (300 µl for T25 flasks and 900 µl for T75 flasks; Lonza, Slough, UK) for approximately 3 minutes at 37°C. Trypsin was quenched with serum containing growth media and added to the previous washes prior to harvesting cells by centrifugation at 300*g* for 5 minutes. The supernatant was discarded, and the resultant pellet was re-suspended in fresh growth media and the required cell number (17000 cells/cm^2) was transferred into sterile tissue culture flasks containing pre-warmed growth media.

2.2.2 Co-cultures

2.2.2.1 Contact co-cultures

Cells were split as detailed in section 2.2.1. Cells were subsequently pelleted and counted as detailed in section 2.2.5. Cells were again seeded at total density of 17000 cells/cm^2 where half of the cell population were SH-SY5Y and half were U-87MG cells. This resulted in a 1:1 seeding ratio.

2.2.2.2 Non-contact co-cultures

Cells were split as detailed in section 2.2.1. Cells were subsequently pelleted and counted as mentioned in section 2.2.5. Inserts were incubated with growth media for 5 minutes prior to seeding to improve adhesion to the cell insert material. Cells were seeded at 6900 cells/cm^2 in both cell inserts and the 24 well plate to maintain a 1:1 ratio and allowing for differentiation.

2.2.2.3 Conditioned media

Cells were seeded at 6900 cells/cm^2 to allow for differentiation over 5 days. Media was collected from U-87MG cells at 5 days to aid SH-SY5Y differentiation. In addition, following 5-day

differentiation cells were treated with 1 mM AAPH or 0.5 µM rotenone for 48 hours and media was collected. The collected conditioned media was frozen immediately at -20°C until needed. When cells were ready for treatment cells were treated with a 1:1 ratio of conditioned media and fresh media to account for the loss of nutrients in the conditioned media.

2.2.3 Cell count and seeding

To estimate cell numbers cells were counted using a haemocytometer where the cell density was estimated using the following calculation:

$$\frac{Cells}{ml} = Average\ cell\ count\ (1\ mm^2) \times 10^4 \times dilution\ factor$$

To achieve the required cell density within a known volume of growth media, the cell number was subsequently used in the following calculation:

$$Volume\ required\ for\ desired\ cell\ number\ (ml) = \frac{Desired\ cell\ number}{\frac{Cells}{ml}}$$

The appropriate cell density was then seeded into the required tissue culture flask and incubated at 37°C in a humidified atmosphere of 95% (v/v) air and 5% (v/v) CO_2.

2.2.4 Cryopreservation of cells

For long term cell preservation, cells were frozen in liquid nitrogen. Cells were seeded in T25 flasks and harvested whilst in the log phase of growth. Cells were briefly washed twice with DPBS to remove serum and washes were kept before incubating cells with 250 µg/ml trypsin for approximately 3 minutes at 37°C. Trypsin was quenched with growth media and added to the DPBS washes prior to centrifugation at 300*g* for 5 minutes. The supernatant was then discarded and the pellet was re-suspended in 1 ml of ice-cold freezing media (10% (v/v) dimethyl sulfoxide (DMSO) in sterile DMEM: F12 with a 1:1 ratio with 15 mM Hepes L-Glutamine growth media supplemented with 10% (v/v) heat inactivated FBS, 100 units/ml penicillin, 10 µl/ml streptomycin and 1% (v/v) NEAA solution (100X)) and transferred into a cryovial. These vials were kept at -80°C in cryopods for approximately 48 hours before transferring to a liquid nitrogen storage facility for long term storage.

2.2.5 Revival of cryopreserved cells

Cryovials containing preserved cells were removed from liquid nitrogen storage and thawed in a 37°C water bath before being transferred dropwise to a sterile tube containing growth media to dilute the DMSO. The cells were subsequently centrifuged at 300*g* for 5 minutes. The supernatant

was then discarded, and the pellet was re-suspended in 1 ml of growth media before being transferred to a 6-well plate containing appropriate levels of pre-warmed growth media. Cells were then maintained appropriately as described in section 2.2.1.

2.2.6 Mycoplasma testing

Once revived and cells reached 70-80% confluence, 1 ml of cell supernatant was briefly centrifuged at 250*g* to pellet cellular debris prior to testing for mycoplasma using an EZ-PCR mycoplasma test kit (Biological Industries, Staffordshire, UK). The supernatant was subsequently transferred to a fresh sterile tube and centrifuged at 15000*g* for 10 minutes to sediment mycoplasma. The supernatant was carefully decanted, and the pellet was re-suspended thoroughly with 50 µl buffer solution supplied with the kit. The mixture was then heated to 95°C for 3 minutes before storing at -20°C. A reaction mixture was then prepared as follows for polymerase chain reaction (PCR) amplification:

Table 2.3 Volume of reagents needed for polymerase chain reaction amplification.

Reagents	Volume (µl)
H_2O	35
Reaction mix	10
Test Sample	5

All samples including a positive and negative mycoplasma DNA sample were then transferred to a thermal cycler with the following parameters:

Table 2.4 PCR cycle temperatures and time.

Temperature (°C)	Time (secs)	
94	30	35 Cycles
94	30	
60	120	
72	60	
94	30	
60	120	
72	300	

During PCR amplification 50 ml of a 2% agarose (w/v) gel was cast in Tris-acetate-EDTA (TAE) buffer (40 mM Tris, 20 mM acetic acid, 1 mM ethylenediamineetetraacetic acid, EDTA) with 10% (v/v)

SYBR safe (ThermoFisher Scientific, Loughborough, UK) into a mould whereupon a comb was immediately positioned within the gel to form wells to load the PCR samples. The gel was allowed to polymerise for approximately 30 minutes prior to comb removal and placement in an agarose gel tank containing TAE buffer. Subsequent to PCR amplification, 5 µl of blue/orange loading dye was added to the PCR samples prior to loading onto the gel. The gel was then subjected to a constant 90V for 30 minutes before the gel was visualised using U:Genius3 (Syngene, Cambridge, UK).

2.2.7 Differentiation

Cells were seeded at 6900 cells/cm^2 and incubated overnight at 37°C in a humidified atmosphere at 5% CO_2 in 10% full growth medium. Following overnight growth, media was removed and replaced with differentiation media containing 0.5% (v/v) heat inactivated foetal bovine serum, 1% (v/v) MEM non-essential amino acids, 200 units/ml penicillin and 200 µg/ml streptomycin and 10 µM all trans-retinoic acid (Sigma Aldrich, Dorset, UK) in DMEM/F12 media. Differentiation media was replaced with fresh media every 2 days. Cells were grown for a period of 5 days in retinoic acid containing differentiation media or grown with retinoic acid for 5 days followed by 50 ng/ml BDNF for 3 days. Following differentiation, cells were ready to be used in experiments.

2.2.8 Coating plates

Plates were coated with poly-L-lysine (Sigma Aldrich, Dorset, UK) overnight at 4°C with gentle agitation. Poly-L-lysine was subsequently removed, and plates were washed three times with double distilled water. Plates were then incubated with laminin (5 µg/ml) for 2 hours at room temperature. The plates were again washed 3 times with double distilled water prior to cell seeding.

2.2.9 Embryonic rat neuronal cultures

Timed pregnant CD Sprague Dawley rats (Charles River, Margate, UK) were killed in accordance with the UK Animals (Scientific Procedures) Act 1986 by overdose with inhaled isoflurane (Merial Animal Health, Harlow, UK) and confirmed with cervical dislocation at embryonic day 18. Embryos were then rapidly removed and decerebrated on ice. Cortical tissue was micro-dissected under sterile conditions and subjected to papain (2 mg/ml) digestion for 10 minutes at 37°C with inversion after 5 minutes. Papain was subsequently removed, and media was added to the tissue. Using a salinized glass pipette, tissue was mechanically triturated, and any debris allowed to settle for 1 minute. Supernatant was then centrifuged at 300g for 2 minutes. Supernatant was discarded, and pellet was resuspended in fresh growth media. Cells were counted using a 1:1 ratio of Trypan blue to determine cell viability using the Bio-Rad cell counter. Cells were plated at density of 25000

cells/cm2 on poly-L-lysine and laminin (5 μg/ml) coated plates in NeurobasalTM medium supplemented with B-27TM supplement (1X; Thermofisher Scientific, Loughborough, UK), 100 units/ml penicillin and 10 μl/ml streptomycin, at 37°C in a humidified atmosphere of 5% CO2. Cells were cultured for 5 days prior to treatment. Cells were seeded at 25000 cells/cm2 on poly-L-lysine and laminin (5 μg/ml) coated plates.

2.2.10 Quantification of axon, process and branching growth

Neurite outgrowth was studied using the IncuCyte S3 live-cell analysis system from Essen Biosceince (Ann Arbor, MI, USA). During the differnetiation process neurite outgrowth was tracked using the neurotracker software, which quantified neurite length and branch points.

Following masking, using the neurotracker software, the number of neuronal branches was quantified. Since branching varies with distance from the cell body, we used a Sholl analysis plugin in Fiji (Ferreira et al., 2014). Sholl analysis created a series of concentric circles from the centre of the cell body. The network of circles radii increased at regular steps of 0.05 μm for 150 μm. The number of intersections of branches was calculated and plotted against distance from the centre. This approach allowed multiple image quantification.

We also used the Skeleton analysis plugin (Lee and Kashyap, 1994) in Fiji to determine the length of branches in the same area used for the Sholl analysis. A total of 5 random neurons were analysed from 3 fields of view.

2.2.11 2,2'-Azobis(2-methylpropionamidine) dihydrochloride treatment

Cells were seeded in appropriate tissue culture vessels and then incubated at 37°C in a humidified atmosphere of 95% (v/v) air and 5% (v/v) CO_2 for approximately 48 hours. Cells were subsequently treated with growth media containing different concentrations of 2,2'-azobis(2-methylpropionamidine) dihydrochloride (AAPH; Sigma Aldrich, Dorset, UK; 0.1, 0.25, 0.5, 0.75, 1, 2.5, and 5 mM) for 24 or 48 hours.

2.2.12 Rotenone treatment

Cells were seeded in appropriate tissue culture vessels and then incubated at 37°C in a humidified atmosphere of 95% (v/v) air and 5% (v/v) CO_2 for approximately 48 hours. Cells were subsequently treated with growth media containing different concentrations of rotenone (Sigma-Aldrich, Dorset, UK; 0, 0.01, 0.05, 0.1, 0.5, 1 and 2.5 μM) for 24 or 48 hours.

2.2.13 Antioxidant treatment

Cells were seeded in appropriate tissue culture vessels and then incubated at 37°C in a humidified atmosphere of 95% (v/v) air and 5% (v/v) CO_2 for approximately 48 hours. Cells were subsequently treated with growth media containing different concentrations of rotenone (0, 0.1, 0.5 and 2.5 µM), AAPH (0, 0.25, 1, 5 mM) concurrently with 200 µM α-tocopherol (Sigma-Aldrich, Dorset, UK) or 1 mM ascorbic acid (Sigma-Aldrich, Dorset, UK).

2.3 Cell viability measurements

2.3.1 MTT reduction assay

The reduction of MTT (3-(4,5-dimethylthiazol-2-yl)-2,5-diphenyltetrazolium bromide to formazan via mitochondrial dehydrogenase provides a colorimetric assay to assess cell viability, particularly mitochondrial status, which is an early indicator of redox changes. Cells were seeded at the cell density mentioned previously and treated with their respective compounds (rotenone or AAPH) for up to 24 or 48 hours where they were treated with MTT to a final concentration of 0.5 mg/ml for 1 hour. The supernatant was removed, and the resultant formazan product was solubilised using 100 µl of DMSO. Absorbance was measured at 570 nm in a plate reader (BMG Labtech CLARIOSTAR). Cells not treated with MTT were used as blanks. Experiments were performed in triplicate where data was expressed as the mean ± SEM.

2.3.2 Luminometric ATP reduction assay

Total ATP reduction was estimated using the Vialight ® Plus Cell proliferation and cytotoxicity bioassay kit (Lonza, Slough, UK) luminescence assay according to the manufacturer's instructions. Briefly, cells were seeded as described previously and treated with their respective compounds for 24 or 48 hours. Cells were then washed with 100 µl serum free media prior to the addition of 50 µl of serum free media and 25 µl of lysing reagent (1:2 dilution) for 10 minutes. Aliquots of 50 µl of each cell lysate were transferred to a fresh white walled luminescence plate where 50 µl of ATP monitoring reagent PLUS was added to generate luminescence. Luminescence was read after a 2-minute incubation using a plate reader (BMG Labtech CLARIOSTAR). Results were expressed as a percentage change in ATP reduction against the control which was set to 100% and compared to known ATP standards. Each sample and standard were performed in triplicate where data is expressed as the mean ± SEM.

2.3.3 Lactate dehydrogenase assay

Lactate dehydrogenase is a soluble cytosolic enzyme found in most eukaryotic cells that is released into culture medium when cells lyse due to cellular membrane damage. Therefore, the increase in LDH activity is approximately proportional to the amount cell death and can be used to indirectly measure cytotoxicity. LDH release was estimated using Pierce LDH cytotoxicity assay kit (ThermoFisher, Scientific, Loughborough, UK). Extracellular LDH can be quantified by a coupled enzymatic reaction where LDH catalyses the dehydrogenation of lactate to pyruvate while NAD^+ is reduced to NADH. Next diaphorase also known as NADH dehydrogenase then reduces tetrazolium salt to a red formazan product which can be measured at 490 nm.

Cells were seeded in 96-well plates and treated with different concentrations of various treatments as described previously. Cells were incubated with treatments for 24 or 48 hours, prior to transferring a 50 µl aliquot of the cell supernatant to a fresh 96-well plate containing 50 µl of reconstituted reaction mix. After 45 minutes, the reaction was terminated with 50 µl of stop solution and the absorbance was measured at 490 nm using a plate reader (BMG Labtech CLARIOSTAR). Results are expressed as a percentage of control LDH release which was set to 100%. Experiments were performed in triplicate where data is expressed as the mean ± SEM.

2.3.4 Cellular impedance assay using the iCELLigence system

The real-time cell analysis system (RTCA) iCELLigence™ (ACEA Biosceinces, San Diego, CA, USA) was used to monitor cellular impedance to measure neural cytotoxicity according to the manufacturer's instructions. Briefly, 150 µl of growth media was added to each of the E-plate L8 and a calibration measurement was taken. Subsequently, each well was seeded with 17000 cells/cm^2 in 300 µl. Plates were left at room temperature for 20 minutes allowing cell adherence prior to plate insertion into the iCELLigence station. The system was set to take measurements every 15 minutes for 8 hours and then every hour for 40 hours. After 48 hours, plates were removed from the station and media was replaced with 350 µl of fresh media containing different concentrations of treatments (rotenone: 0, 0.1, 0.5, 2.5 µM and AAPH: 0, 0.25, 1, 5 mM with or without antioxidant). The plate was returned to the station and the system was set to take measurements every hour for 48 hours. Data analysis was initially performed using iCELLigence software where cell index was automatically calculated from the change in electrical impedance. The Cell Index was normalised at 48 hours when treatment was added to determine the cytotoxicity of the compounds. Experiments were performed in triplicate where data was expressed as the mean ± SEM.

2.3.5 Cytotoxicity analyses with the incucyte system

Differentiated neural cytotoxicity was assessed using the incucyte S3 live-cell analysis system. Neuronal SH-SY5Y and glial U-87MG were cultured in 96-well plates and differentiated as mentioned in section 2.2.9. Cells were subsequently treated with AAPH (0, 0.25, 1 and 5 mM) or rotenone (0, 0.1, 0.5 and 2.5 µM) with or without antioxidants (200 µM tocopherol or 1 mM ascorbic acid). Phase contrast images were automatically taken every hour for 48 hours using the incucyte S3 live-cell analysis system (Sartorius, Goettingen, Germany). The images were analysed by the incucyte software package (Sartorius).

2.4 Measuring reactive species

2.4.1 Real-time RS levels

The non-fluorescent probe 2',7'-dichlorofluorescin diacetate (DCFDA; Sigma Aldrich, Dorset, UK) is a cell permeable chemical which is de-esterified intracellularly. Subsequent oxidation via RS forms fluorescent 2',7'-dichlorofluorescein (DCF). This method was used to estimate the levels of endogenous ROS in control and experimental cells in a time-dependent manner. Cells were seeded as mentioned above and grown to 60-70% confluence. Media was subsequently replaced with 100 µl of phenol red free DMEM-F12 growth media containing 10 µM DCFDA. Cells were incubated with the dye at 37°C for 30 minutes. The dye was carefully removed and replaced with phenol red free growth media containing the treatments mentioned previously. Fluorescence intensity (representative of RS levels) was measured in a plate reader using an excitation wavelength 485 nm and emission wavelength of 535 nm which was read every hour for 12 hours at 37°C with 5% CO_2. RS levels were expressed as fluorescence intensity (arbitrary units) at each corresponding time point.

2.4.2 Endpoint RS levels

The non-fluorescent probe 2',7'-dichlorofluorescin diacetate (DCDFA) was also used to measure endpoint RS levels due to difficulty in sensitivity with rotenone. Cells were seeded as mentioned above and grown to 60-70% confluence. Cells were treated with rotenone treatment (0, 0.1, 0.5 and 2.5 µM) with or without antioxidant for the desired time. Following treatment media was removed and replaced with phenol red free DMEM-F12 growth media containing 10 µM DCFDA. Cells were incubated with the dye at 37°C for 30 minutes. The dye was carefully removed and replaced with phenol red free growth media and fluorescence was measured in a plate reader using an excitation wavelength 485 nm and emission wavelength of 535 nm or the S3 incucyte live-cell

analysis system to normalise fluorescence against cell phase contrast confluence. Experiments were performed in triplicate where data is expressed as the mean ± SEM.

2.4.3 Live imaging

The fluorescent dye DCDFA was also used to obtain live images of cellular RS levels. Cells were seeded in 8-well chamber slides at 7000 cells/cm^2 and incubated until 60-70% confluent. Media was subsequently replaced with rotenone (0, 0.1, 0.5 and 2.5 µM) or AAPH (0, 0.25, 1 and 5 mM) treatments and incubated for 24 hours. Following treatment, cells were washed with Dulbecco's phosphate buffered cells (DPBS) and incubated with growth media containing 100 µM DCDFA for 30 minutes. Slides were then washed with DPBS and incubated with fresh DPBS for visualisation. Images of cells were taken using a 20X objective. Following RS imaging, slides were washed with DPBS and fixed with ice-cold 90% (v/v) methanol/tris buffer saline (TBS) for 30 minutes at -20°C. Chambers were then removed and coverslips were mounted with anti-fade mountant vectorshield® containing DAPI nuclear stain. The coverslip was sealed with clear nail vanish and viewed using a Leica CLSM laser confocal microscope. Images were captured using a 20X objective.

2.5 Fluorogenic total glutathione assay

Total cellular glutathione levels were estimated using a commercially available glutathione fluorometric kit (Sigma, Dorset, UK). Both SH-SY5Y and U-87MG cells were seeded into two T25 flask at 17000 cells/cm^2. Cells were allowed to proliferate for the appropriate amount of time prior to treatment with AAPH and rotenone. Following treatment cells were mechanically detached, centrifuged at 300*g* for 5 minutes and then washed with PBS. The resulting pellet was subsequently incubated with lysis buffer for 15 minutes on ice. The resultant lysate was then centrifuged at 16000*g* for 5 minutes and the supernatant was collected. A range of standards (1.3-10 nM) and samples were then pipetted into a 96-well plate with 82.5 µl of assay buffer followed by the addition of 5 µl of glutathione S-transferase and 2.5 µl substrate solution to initiate the reaction. The plate was then incubated at 37°C for 1 hour prior to recording fluorescence levels on a BMGLabtech CLARIOSTAR using an excitation wavelength of 390 nm and emission wavelength 480 nm. The bicinchoninic acid (BCA) assay was then used to quantify the protein content of samples as described in section 2.7.5.2. Experiments were performed in quadruplicate and the results were expressed as mean % glutathione levels after calculating change in fluorescence/µg of protein ± SEM for control samples.

2.6 Preparation of cell lysates

2.6.1 Total protein extraction

Whole cell lysates were prepared by mechanically detaching cells into the growth medium which were then harvested by centrifugation at 300*g* for 5 minutes. The supernatant was discarded, and the pellet was re-suspended in ice-cold DPBS. Pellet was harvested by centrifugation at 300*g* at 4°C for 5 minutes. The supernatant was decanted carefully, and the pellet was washed two more times by re-suspending the pellet in ice-cold DPBS and harvesting at 300*g* at 4°C for 5 minutes. The pellet was extracted by re-suspension in 120 µl of boiling total extraction buffer (50 mM Tris, pH 6.8; 5 mM EDTA; 1% w/v SDS; 1% (v/v) protease cocktail inhibitor) and further boiled at 100°C for 5 minutes. Lysates were then cooled on ice. Samples were quantified using the Lowry assay described in section 2.7.5.1 and then stored at -20°C until needed.

2.6.2 RIPA extraction

Whole cell lysates were prepared by mechanically detaching cells into the growth medium which were then harvested by centrifugation at 300*g* for 5 minutes. The supernatant was discarded, and the pellet was re-suspended in ice-cold DPBS prior to harvesting by centrifugation at 300*g* at 4°C for 5 minutes. Pellet was then resuspended in 120 µl RIPA buffer with 0.1% protease inhibitor cocktail. Lysates were incubated on ice for 15 minutes and then centrifuged at 13000*g* for 5 minutes at 4°C. Supernatant was then collected and the pellet was discarded. Protein concentration was determined by the BCA protein estimation described in section 2.7.5.2. Lysates were stored at -20°C until needed.

2.6.3 Subcellular fractionation

Whole cell lysates were prepared by mechanically detaching cells into growth media which was then harvested by centrifugation at 300*g* for 5 minutes at 4°C. The supernatant was discarded, and the pellet was re-suspended in ice-cold DPBS. Pellet was harvested by centrifugation at 300*g* at 4°C for 5 minutes. The pellet was then resuspended in in 100 µl extraction buffer (10 mM HEPES, pH 7.5, 200 mM mannitol, 70 mM sucrose, 1 mM EGTA and 0.1% protease inhibitor cocktail) and transferred to a handheld homogeniser. Using the loose pestle 10 movements followed by 10 movements with the tight pestle to homogenise at room temperature. The sample was then removed from the handheld homogeniser and centrifuged at 1000*g* for 10 minutes at 4°C. The cytosolic supernatant fraction was collected, and the pellet nuclear fraction was resuspended in 50 µl of extraction buffer. The protein concentration of both cytosolic and nuclear fractions was

determined using the BCA protein estimation described in section 2.7.5.2. Lysates were stored at -20°C until needed.

2.6.4 Proteasome extraction

Lysates were prepared by mechanically detaching cells into growth media and harvested by centrifugation at 300*g* for 5 minutes. The supernatant was discarded, and pellets were frozen until all lysates were obtained. Pellet was re-suspended in ice-cold DPBS at 300*g* at 4°C for 5 minutes prior to resuspension in 100 µl ice-cold homogenisation buffer (20 mM Tris/HCl, pH 7.2, 0.1 mM EDTA, 1 mM 2-mercaptoethanol, 5 mM ATP, 20% (v/v) glycerol, 0.4% (v/v) Igepal CA-630). Samples were vortexed thoroughly for 2 minutes followed by centrifugation at 13000*g* for 2 minutes at 4°C. The resultant supernatant was transferred to a fresh Eppendorf tube and kept on ice ready for the fluorogenic assay described in section 2.8. Samples were quantified using the Bio-Rad estimation as described in section 2.7.5.3.

2.6.5 Protein quantification

2.6.5.1 Lowry protein estimation

The Lowry estimation is a colorimetric assay used to quantify the total protein content of lysates. A standard curve was generated by diluting 5-40 µg of 1 mg/ml bovine serum albumin (BSA) to a final volume of 100 µl with distilled water and total extraction buffer while samples were diluted with water, all of which were done in triplicate. 1 ml of working Lowry solution (containing 2% Na_2CO_3 and 0.1 M NaOH in distilled water with 1% (w/v) $CuSO_4$ and 2.7% NaK-tartrate) was added to both standards and samples, which were mixed by inversion. Samples were then incubated at room temperature for 15 minutes before adding 100 µl of Folin-Ciocalteu phenol reagent (1:1 with distilled water) to both standards and samples. Subsequently, all were vortex mixed and incubated at room temperature for 30 minutes. Finally, 100 µl of each standard and sample was transferred to a 96-well plate that was read at 750 nm using a plate reader. BSA standards were used to construct a standard curve to then calculate the protein content of lysates (figure 2.1).

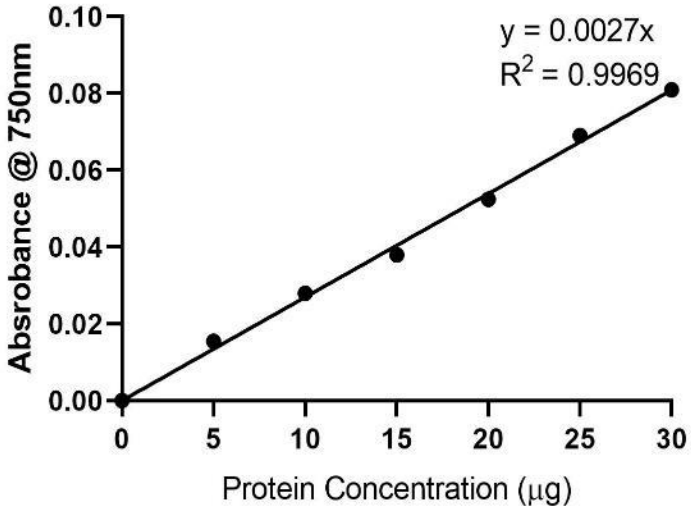

Figure 2.1 Standard calibration curve for Lowry protein estimation measured at 750 nm. *The protein content of the samples (unknowns) was calculated using the equation for the line of best fit.*

2.6.5.2 Bicinchoninic acid protein estimation

Protein content was assessed using a commercially available bicinchoninic acid (BCA) kit (Sigma Aldrich, Dorset, UK) where dilutions of BSA was used to create a linear standard curve with concentrations ranging from 0-1 mg/ml to which extraction or RIPA buffer was also added. 20 µl of samples and standards was added to a 96-well plate in triplicate. A 200 µl aliquot of working BCA reagent (BCA: copper II sulphate at 50:1) was added to each well and the plate was incubated at 37°C for 30 minutes. Absorbance was read at 540 nm using a Labtech BMG CLARIOSTAR plate reader.

2.6.5.3 Bio-Rad protein estimation

The Bio-Rad microassay was performed as per the manufacturer's instructions to assay the protein content of cell lysates prepared for the fluorogenic proteasome activity assay. A standard curve was generated by diluting 0-25 µg/ml of 1 mg/ml bovine serum albumin (BSA) in a volume of 800 µl. A 10 µl aliquot of each sample was prepared in a volume of 800 µl. Both samples and standards were assayed in triplicate. A 200 µl aliquot of Bio-Rad dye reagent concentrate (Coomassie Brilliant Blue G-250, phosphoric acid, methanol) was added to both standards and samples prior to vortex mixing. A 100 µl aliquot of both standards and samples was then transferred to a 96-well plate and the absorbance was measured at 595 nm. Standards were used to construct a graph to then calculate the protein content.

2.7 Proteasome activity assay using a fluorogenic peptide assay

10 µl aliquots of lysates were incubated at 37°C with 5 µl of 1 mM fluorogenic substrate for chymotrypsin-like activity (CLA), for the 20S proteasome (N-Succinyl-Leu-Leu-Val-Tyr-AMC) in assay buffer (50 mM HEPES, pH 8.0, 5 mM EGTA) in a total reaction volume of 100 µl to give a final 50 µM CLA working concentration. Using the CLARIOSTAR plate reader, readings were taken every 5 minutes for 1 hour at excitation and emission wavelengths of 360 nm and 465 nm, respectively (figure 2.2). Protein estimation was determined by the Bio-Rad protein assay described in section 2.7.5.3. The LINEST function was used to determine the line of best fit to calculate the change in fluorescence. Experiment was performed in triplicate and results were expressed as change in fluorescence units/min/µg protein mean ± SEM.

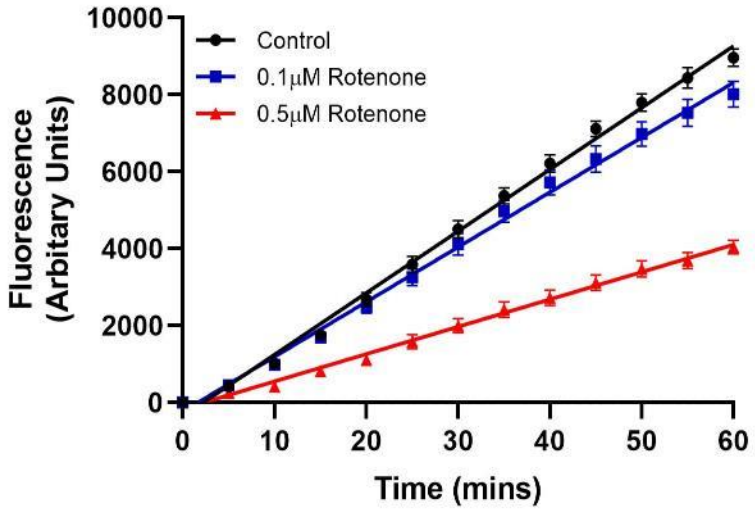

Figure 2.2 Example plot of fluorescence (arbitrary units) versus time (minutes) used to determine the proteasome activity. *The activity of the proteasome was determined using the LINEST function to determine the line of best fit for the data using the least squares method for the linear part of the curve where readings were taken every 5 minutes for 60 minutes. The rate in change of reaction was expressed as rate in change of fluorescence per µg protein calculated using the bio-rad protein estimation.*

2.8 Sodium dodecyl sulphate-polyacrylamide gel electrophoresis (SDS-PAGE)

Once the protein concentration was estimated and the volume needed was calculated this was dissolved in a 1:1 ratio with 2X reducing Laemmli buffer (Sigma Aldrich, Dorset, UK) and boiled at 100°C for 5 minutes, allowing denaturation. Prior to the preparation of the separating gel the Bio-Rad mini-PROTEAN® tetra vertical electrophoresis cell was assembled as per the manufacturer's guidelines. For each gel, 10 ml of resolving gel was prepared described in table 2.5. To initiate the polymerisation 50 µl of 10% (w/v) ammonium persulfate (APS; Sigma Aldrich, Dorset, UK) and 10 µl

of N,N,N',N'- tetramethylethylenediamine (TEMED; Sigma Aldrich, Dorset, UK) was added before casting 7 ml between two glass plates leaving the appropriate amount of space for the stacking gel. Distilled water was then added to the surface to create a smooth gel interface and allow polymerisation. The gel was left to polymerise at room temperature for approximately 30 minutes to an hour. Once the gel had polymerised the water was removed by blotting. Subsequently, 5 ml of 4% (w/v) acrylamide stacking gel was prepared for each gel. A 50 ml stock of stacking gel was prepared as described in table 2.6. When needed 10 µl of TEMED and 25 µl of APS was added to 5 ml of the stacking gel to initiate polymerisation. 3-4ml of stacking gel was cast onto the resolving gel and a plastic comb was immediately inserted to form wells. The stacking gel was left to polymerise for approximately 20-30 minutes at room temperature. Once polymerised the comb was removed and the gel was placed in the electrophoretic tank and submerged in SDS-running buffer (25 mM Tris, 192 mM Glycine and 0.1% (w/v) SDS, pH 8.5). The protein samples (20-50 µg/well) were loaded alongside 1 µl of the protein ladder (Bio-Rad Laboratories Ltd, Hertfordshire). Initially, the gel was run at 90V for approximately 20-30 minutes to allow the samples to enter the resolving gel. Subsequently, voltage was increased to 140V for approximately 40 minutes to separate the proteins.

Different percentages resulted is different protein separations where table 2.5 lists the various resolving gel compositions.

Table 2.5 Preparation of different percentage acrylamide resolving gels for SDS-PAGE.

Reagent	**7.5% (w/v) gel**	**10% (w/v) gel**	**12.5% (w/v) gel**	**15% (w/v) gel**
40% acrylamide solution (29:1)	1.9 ml	2.5 ml	3.0 ml	3.75 ml
1.5 M Tris buffer pH 8.8	2.5 ml	2.5 ml	2.5 ml	2.5 ml
10% (w/v) SDS	100 µl	100 µl	100 µl	100 µl
Distilled water	5.5 ml	4.9 ml	4.4 ml	3.65 ml

2.9 Western Blotting

Western blotting involves the transfer of proteins from a gel to a nitrocellulose membrane which is subsequently immunoprobed for the protein or protein modification of interest.

2.9.1 Wet blotting

Following electrophoresis, separated proteins were transferred to a nitrocellulose membrane (0.22 µM pore) by wet blotting. Briefly, the blotting sandwich was prepared as follows: sponge, filter paper, nitrocellulose membrane, gel, filter paper and sponge, all of which were initially soaked in ice-cold transfer buffer (25 mM Tris, 192 mM glycine, pH 8.3 and 20% (v/v) methanol). Bubbles were removed by submerging the sandwich in transfer buffer and use of a roller. The sandwich was clamped together in a western blotting cassette and transferred to the electrophoretic tank with the nitrocellulose facing the anode. The cassette was then submerged in transfer buffer and transferred at a constant 40V for 16 hours. Transfer success was evaluated by staining with 0.05% (w/v) copper phthalocyanine 3,4',4'',4''' tetrasuphonic acid terasodium salt in 12 mM HCl (Sigma Aldrich, Dorset, UK). The stain was then captured using an ImageQuant™ Las 4000 (GE healthcare, Buckinghamshire, UK) camera and the membrane was de-stained with 12 mM NaOH with gentle agitation.

2.9.2 Protein immunoprobing

Following destaining the nitrocellulose membrane was blocked in 3% (w/v) BSA in TBS-Tween for 1 hour at room temperature with gentle agitation. The blot was then immersed in primary antibody diluted in 3% (w/v) BSA in TBS-Tween at the relevant concentrations specified in table 2.1 on a roller at 4°C, overnight. Blots were then washed 3X with TBS-Tween for 15 minutes each on a roller at room temperature. Following this, blots were immersed in the appropriate HRP-conjugated secondary antibody diluted in 3% (w/v) marvel milk in TBS-tween at the dilutions mentioned in table 2.2 on a roller at room temperature for 2 hours. After this, blots were again washed 3X with TBS-tween for 15 minutes each on a roller at room temperature. Finally, blots were developed by adding Pierce ECL Western blotting substrate (ThermoFisher Scientific, Loughborough, UK) as described by the manufacturer for the appropriate time and chemiluminescence images captured by an ImageQuant™ Las 4000 (GE healthcare, Buckinghamshire, UK). Image development was terminated by extensive washing in distilled water.

2.9.3 Stripping and reprobing

Following termination of blot development, previous immunoprobed blots were incubated with 0.5 M NaOH for 8 minutes with gentle agitation. Blots were then washed 3X with distilled water for 5 minutes each and then 3X with TBS-tween for 5 minutes each. Finally, blots were blocked for 1 hour in 3% (w/v) BSA in TBS-Tween at room temperature with gentle agitation followed by the method described in section 2.11.2.

2.9.4 Western blot quantification

Western blot and copper stained images were quantified using the Aida Image Analyser v4.03, following the manufacturer's guidelines. Pixel intensity for equal sized areas around each band was obtained and quantified based on the number and intensity of the pixels in the area. Changes in protein loading were corrected against the control (using copper stains or B512 Tubulin respective lane pixel intensity). Corrected protein bands were expressed as % against control.

2.10 Mitochondrial staining

For morphological analyses mitochondria were stained with Mitotracker™ Red CMXRos as per the manufacturer's instructions prior to fixation. Briefly, cells were seeded as described previously and treated with rotenone (0, 0.1, 0.5 and 2.5 μM) or AAPH (0, 0.25, 1, 5 mM) with or without an antioxidant for 24-48 hours. Cells were subsequently washed with serum-free media and incubated with 300 nM Mitotracker™ Red CMXRos in serum-free media for 1 hour at 37°C. Cells were then washed with serum-free media and PBS and subsequently fixed with 3.7% (w/v) paraformaldehyde in PBS at room temperature for 30 minutes. Images were captured at 20X magnification on an EVOS FLOID cell imaging station (ThermoFisher Scientific, Loughborough, UK) and edited using Fiji software.

2.11 JC-1 staining

JC-1 (5',6,6'-tetrachloro-1,1',3,3'-tetraethylbenzimidazolylcarbocyanine iodide; Cambridge bioscience, Cambridge, UK) was used to visualise and quantify changes in mitochondrial membrane potential. SH-SY5Y and U-87MG cells were treated with AAPH or rotenone for 24 hours and then incubated with 30 μM JC-1 in phenol red free media for 30 minutes. Cells were then washed twice with PBS and imaged in both red and green using the incucyte S3 live cell analysis system.

2.12 Seahorse ATP live assay

To measure the rate of ATP production from mitochondria and glycolysis in live cells, a Seahorse XFe24 extracellular flux analyser was used. Cells were seeded at 17000 cells/cm^2 for undifferentiated experiments and 10000 cells/cm^2 for differentiation experiments in the XF24 cell culture microplate (Agilent, Santa Claret, US). Once cells were sufficiently confluent, they were treated with 1 mM AAPH or 0.5 μM rotenone for 24 hours. The Seahorse XFe24 extracellular flux analyser was then used to assess ATP production from mitochondrial respiration and glycolysis by sequentially injecting oligomycin (1.5 μM) and then rotenone/antimycin A (0.5 μM). The Seahorse XF analyser simultaneously measures the flux of protons resulting in extracellular acidification

(ECAR) and O_2 consumption (OCR) under basal conditions and after serial addition of mitochondrial inhibitors allowing mitochondrial and glycolytic rates of ATP production to be calculated. OCR and ECAR was calculated using the Wave software (Agilent, Santa Claret, US) and the Seahorse XF-real time ATP rate assay report generator.

2.13 Immunofluorescence microscopy

2.13.1 Methanol fixation

SH-SY5Y neuroblastoma and U-87MG glioblastoma cells were seeded in 8 well chamber slides at a density of 17000 cells/cm^2. Following treatment, cells were washed with PBS once and then fixed with ice-cold 90% (v/v) methanol/TBS for 20 minutes at -20°C.

2.13.2 Paraformaldehyde fixation

SH-SY5Y neuroblastoma and U-87MG glioblastoma cells were seeded in 8 well chamber slides at a density of 17000 cells/cm^2. Following treatment, cells were washed with PBS once and then fixed with 3.7% paraformaldehyde solution in PBS for 20 minutes at room temperature.

2.13.3 Immunofluorescence antibody staining

Previously fixed cells were permeabilised with 0.5% triton-X100 (v/v) in TBS for 15 minutes at room temperature. Cells were then washed with PBS 3X for 15 minutes each prior to block with 3% (w/v) BSA in PBS for 1 hour at room temperature. Cells were then incubated overnight at 4°C with primary antibody in blocking buffer at the dilutions stated in table 2.1. Following incubation cells were washed 3X with PBS for 5 minutes each. Cells were subsequently incubated with secondary antibodies in blocking buffer as described in table 2.2 for 2 hours at room temperature. After incubation with secondary antibody cells were washed 3X with PBS for 5 minutes each and nuclei was counter stained using DAPI in Vectorshield ® mounting medium. Slides were then sealed with glass coverslips and secured using transparent nail vanish. Slides were stored at 4°C until required. Images were acquired using Leica TCS SP5 II confocal microscope (Leica Microsystems, GmbH, Manheim, Germany).

2.14 Quantitative reverse transcription real time PCR

2.14.1 RNA extraction using Qiagen RNeasy columns

Following treatment, cells were washed with DPBS. RNA was extracted as per the manufacturer's instructions (Qiagen Ltd, UK). Briefly, cells were resuspended in RLT buffer (500 µl RLT buffer + 10 µl 2-mercaptoethanol) and 1 volume of 70% ethanol. A 700 µl aliquot of the sample was transferred

to a RNeasy Mini spin column and placed in a 2 ml collection tube. Samples were subsequently centrifuged at 10000*g* for 15 seconds. The sample flow-through was discarded and 700 µl of RW1 buffer was added to the RNeasy spin column and centrifuged at 10000*g* for 15 seconds. The sample flow-through was discarded and 500 µl of RPE buffer (1 volume RPE buffer + 4 volumes of 100% ethanol) was added to the column prior to centrifugation at 10000*g* for 15 seconds. The flow-through was discarded and 500 µl RPE buffer was added to column and centrifuged at 10000*g* for 2 minutes. The column was then transferred to fresh 1.5 ml collection tube. Finally, 20 µl of 60°C RNase-free water was added to the column and centrifuged at 10000*g* for 1 minute to elute the RNA. RNA samples were quantified using Nanodrop 8000 spectrophotometer (ThermoFisher, Scientific, Loughborough, UK), using the modified Beer-lambert law:

$$c = A\varepsilon/l$$

Where c: concentration, A: absorbance, ε: wavelength-dependent extinction coefficient and l: pathway length. Samples were used immediately to synthesise cDNA or stored at -80°C until required.

2.14.2 DNA extraction using PureLink™ Genomic DNA Mini Kit

Cells were washed with DPBS and DNA was extracted as per the manufacturer's instructions (ThermoFisher Scientific, Loughborough, UK). Cells were resuspended in 200 µl of DPBS and added to 20 µl Proteinase K. 20 µl of RNase A was added to the sample prior to vortexing and incubating at room temperature for 2 minutes. 200 µl of PureLink® Genomic lysis/binding buffer was added, and samples were made homogenous by vortexing. Samples were then incubated for 10 minutes at 55°C promoting protein digestion. A 200 µl aliquot of 100% ethanol was added to each sample and mixed by vortexing prior to adding the sample to a PureLink® spin column. Columns were centrifuged at 10000*g* for 1 minute at room temperature. The flow-through was discarded and DNA was washed with 500 µl of wash buffer 1 and the column was centrifuged at 10000*g* for 1 minute at room temperature. Flow-through was discarded and 500 µl of wash buffer 2 was added to the column before centrifuging at 20000*g* for 3 minutes at room temperature. DNA was eluted by adding 26 µl of PureLink® genomic elution buffer and incubating the columns at room temperature for 1 minute and transferred to a fresh 1.5 ml collection tube and then centrifuged at 20000*g* for 1 minute. DNA samples were quantified using Nanodrop 8000 spectrophotometer (ThermoFisher, Scientific, Loughborough, UK). Samples were stored at -20°C.

2.14.3 cDNA synthesis using iScript™ cDNA synthesis kit

Prior to quantitative real-time PCR RNA was reverse transcribed to cDNA using the mixture described in table 2.6 below.

Table 2.6 Component compositions for cDNA synthesis from RNA templates using iScript™ cDNA synthesis kit.

Reagents	Volume (µl)
5X iScript Reaction mix	4
iScript Reverse Transcriptase	1
Nuclease-free water	Variable
RNA template (100 ng)	Variable
Total volume	20

The complete reaction was then put in a Bio-Rad T100 thermal cycler (Bio-Rad, Hertfordshire, UK) using the following protocol (table 2.7).

Table 2.7 Reaction protocol for reverse transcribing cDNA using a thermal cycler.

Step	Time (min)	Temperature (°C)
Priming	5	25
Reverse transcription	20	46
Reverse transcriptase inactivation	1	95

Newly synthesised cDNA was stored at -20°C until needed.

2.14.4 Quantitative real-time PCR

The iTaq™ universal SYBR® green supermix reaction mix was prepared as per the manufacturer's instructions (Bio-Rad, Hertfordshire, UK) mentioned in table 2.8 in Rotogene® PCR tubes.

Table 2.8 Component compositions for quantitative real-time PCR using a thermal cycler.

Reagents	Volume (µl)
iTaq™ universal SYBR® green supermix (2x)	5
Forward and reverse primers	0.5 (10 µM)
DNA template (100 ng)	Variable
H_2O	Variable
Total volume	10

Tubes were transferred to Rotor-gene 6000 real-time PCR machine (ThermoFisher, Loughborough, UK). The thermocycler was set for the following protocol in table 2.9.

Table 2.9 Reaction protocol for quantitative real-time PCR using a real-time PCR machine.

Step	Time (sec)	Temperature (°C)	
Initial denaturation	600	95	
Denaturation	30	95	40 Cycles
Annealing	30	Described in table 2.11	
Extension	30	72	

A melt curve was generated by ramping the temperature from the annealing temperature to 95°C. the results were analysed using the $2^{-\Delta\Delta Ct}$ method. Results were performed in triplicate and expressed as percentage change in gene expression compared to the control ± SEM.

Table 2.10 Primer sequences and related information for quantitative real-time PCR.

Primer name	NCBI accession number	Sequence (5'-3')	Annealing temperature (°C)
NRF2 forward	NM_006164	AACCAGTGGATCTGCCAACTACTC	61
NRF2 reverse		CTGCGCCAAAAGCTGCAT	
KEAP1 forward	NM_012289	CCTVCTGGCCGGGTAATAGG	61
KEAP1 reverse		CCCCTCCCAGGTATCCAAGA	
GCLM forward	NM_002061	ACAGGTAAAACCAAATAGTAACAAAGTTAA	61
GCLM reverse		TGTTTAGCAAATGCAGTCAAATCTG	
HPRT forward	NM_000194	TGACACTGGCAAAACAATGCA	61
HPRT reverse		GGTCCTTTTCACCAGCAAGCT	
TBP forward	NM_001172085	TGCACAGGAGCCAAGAGTGAA	61
TBP reverse		CACATCACAGCTCCCCACCA	
SDH 1 forward	SY140405458-092-3	TGGGAACAAGAGGGCATCTG	60
SDH 1 reverse		CCACCACTGCATCAAATTCATG	
SDH 2 forward	SY140305473-087--088	CCAGCAAAATGGAATTATCTTGT	60
SDH 2 reverse		TCTCCTTCAATAGCTGGCTT	
MIT A forward	SY140305458—089-090	CACCATTAGCACCCAAAGCT	60
MIT A reverse		TACTTGACCACCTGTACTAC	
MIT B forward	SY140305458-091-094	GAGGATGGTGGTCAAGGGAC	60
MIT B reverse		TTTGATGTGGATTGGGTTT	

2.14.5 Agarose gel electrophoresis

A 1.5% (w/v) agarose gel was cast in Tris-acetate-EDTA (TAE) buffer (40 mM Tris, 20 mM acetic acid, 1 mM EDTA) supplemented with SYBR safe DNA gel stain (1:10000). Subsequent to PCR amplification, 5 µl of blue/orange loading dye was added to the PCR samples prior to loading onto the gel. A 2 µl aliquot of 100 bp DNA ladder (Promega®, Southampton, UK) was loaded alongside 20 µl of sample. The gel was then subjected to a constant 90V for 30 minutes before visualisation using U:Genius3 (Syngene, Cambridge, UK).

2.14.6 PCR array

Following RNA extraction using the Qiagen RNeasy columns and nanodrop 8000 spectrometer quantification (Thermo Scientific, Waltham, MA USA) gene expression changes induced by treatments following differentiation were analysed utilising 1 µg of total RNA using the RT^2 first strand kit and the human oxidative stress plus RT^2 profiler PCR array (Qiagen, Hilden, Germany) on the StepOnePlus™ real-time PCR system (Applied biosystems, Foster City, CA, USA). Data was normalised to B2M and HPRT. Relative gene expression was obtained using the ΔCt calculation (Livak and Schmittgen, 2001).

2.15 Small interference RNA (siRNA) analysis

SH-SY5Y and U-87MG cells were transfected with scramble, GAPDH or NRF2 siRNA. Briefly, cells were seeded with DMEM: F12 in plates at 7500 cells/cm^2. Non-selective or selective (NRF2 or GAPDH) knock-down was achieved using 15 pmol of scrambled (Santa Cruz biotechnology, USA), GAPDH (ThermoFisher Scientific, Loughborough, UK) or NRF2 (ThermoFisher Scientific, Loughborough, UK) siRNA, respectively utilising Lipofectamine 3000 transfection reagent (ThermoFisher Scientific, Loughborough, UK), according to the manufacturer's instructions. The transfection procedure was carried out 24 hours after seeding.

2.16 Lipid peroxidation

2.16.1 Click-iT lipid peroxidation imaging kit

To evaluate lipid peroxidation of differentiated neural cells in response to AAPH and rotenone the click-iT lipid peroxidation kit was used as per the manufacturer's instructions (ThermoFisher Scientific, Loughborough, UK). Briefly, SH-SY5Y and U-87MG cells were seeded and differentiated over 5 days with 10 µM retinoic acid as mentioned before in section 2.2.9. Cells were subsequently treated with 1 mM AAPH or 0.5 µM rotenone with and without tocopherol (200 µM) or ascorbic acid (1 mM) in the presence of 5 µM linoleamide alkyne (LAA) for 48 hours. 2 hours prior to the end

of treatment for a positive control cells were treated with 100 µM cumene hydroperoxide. Cells were then washed twice with PBS and incubated with 3.7% (w/v) paraformaldehyde in PBS for 20 minutes. Fixed cells were subsequently washed with PBS twice and incubated at room temperature with 0.5% (v/v) triton X-100 in PBS for 20 minutes. Cells were then blocked by adding 1% (w/v) BSA in PBS for 30 minutes at room temperature. The Click-iT reaction cocktail was then prepared as mentioned in table 2.11 in the order listed in the table.

Table 2.11 Click-iT reaction cocktail

Reaction components	96-well plate
1X Click-iT reaction buffer	5.15 ml
$CuSO_4$	240 µl
Alexa Fluor 488 azide	15 µl
1X Click-iT buffer additive	600 µl
Total volume	6005 µl

The blocking solution was removed, and cells were washed twice with PBS and 50 µl of Click-iT reaction cocktail was added to each sample and incubated at room temperature in the dark with agitation. Cells were then washed once with 1% (w/v) BSA/PBS and then twice with PBS alone. Fresh PBS was added to each well prior to imaging and quantification using the incucyte S3 live-cell analysis system.

2.16.2 TBARs assay

Screening for thiobarbituric acid reactive substances (TBARS) is a commonly used method to monitor lipid peroxidation (Armstrong and Browne, 1994). Therefore, the TBARS assay kit (Cambridge bioscience, Cambridge, UK) was used as per the manufacturer's instructions to assess lipid peroxidation in differentiated neural cells treated with AAPH or rotenone. Briefly, SH-SY5Y and U-87MG cells were seeded and differentiated over 5 days with 10 µM retinoic acid as mentioned before in section 2.2.9. Cells were subsequently treated with 1 mM AAPH or 0.5 µM rotenone with and without tocopherol (200 µM) or ascorbic acid (1 mM) for 48 hours. Cells were then mechanically detached and centrifuged at 300*g* for 5 minutes. Pellets were washed twice with PBS and harvested at 600*g* for 5 minutes at 4°C. Lysates were then extracted using RIPA buffer as mentioned in section 2.7.2. Standards were made up using the provided MDA standard (500 µM) as described in table 2.12.

Table 2.12 MDA standards preparation for TBARS fluorometric assay.

MDA (µl)	Water (µl)	MDA concentration (µM)
0	1000	0
5	995	0.625
10	990	1.25
20	980	2.5
40	960	5
80	920	10
200	800	25
400	600	50

50 µl of sample and standards was added to 50 µl SDS solution and mixed with inversion. 2 ml of colour reagent was then added to all samples and standards and vortex mixed. Vials were subsequently incubated in a 100°C water bath for 1 hour before incubating on ice for 10 minutes. Vials were then centrifuged at 1600*g* at 4°C for 10 minutes. 100 µl of each sample and standard was added in duplicate to a plate and fluorescence was read at 530 nm excitation and 550 nm emission. Finally, protein content was estimated using the BCA protein estimation described in section 2.7.5.2. Data was presented as MDA concentration per protein concentration (µM MDA/µg protein) where experiments were performed in triplicate and data is expressed as mean ± SEM.

2.17 Oxidative stress induced post-translational modifications

2.17.1 S-nitrosylation protein detection assay

Reactive nitrogen species can undergo reactions with thiol groups known as S-nitrosylation, which is a reversible post-translational modification. To monitor nitrosylation in differentiated neural cells the S-nitrosylation protein detection kit was used with some modifications to the manufacturer's instructions. Briefly, SH-SY5Y and U-87MG cells were seeded and differentiated over 5 days with 10 µM retinoic acid as mentioned before in section 2.2.9. Cells were subsequently treated with 1 mM AAPH or 0.5 µM rotenone with and without tocopherol (200 µM) or ascorbic acid (1 mM) for 48 hours. Cells were then washed twice with PBS and incubated with 3.7% paraformaldehyde in PBS for 20 minutes. Fixed cells were subsequently washed with PBS twice and incubated at room temperature with 0.5% triton X-100 in PBS for 20 minutes. Cells were then blocked with the blocking reagent in the kit in 0.1% triton X-100 in PBS for 30 minutes at 4°C. Cells were then washed with 0.1% triton X-100 in PBS twice. Subsequently cell were incubated with S-nitrosylation reducing

reagent in 1 ml of 0.1% triton X-100 mixed with S-nitrosylation labelling reagent which was dissolved in 100 µl DMF and 900 µl 0.1% triton X-100 in PBS made up to 10 ml with 0.1% triton X-100 in PBS for 1 hour at room temperature. Cells were then washed twice again with 0.1% triton X-100 in PBS prior to incubating with detection reagent II (Fluorescein) at a 1:20 dilution in 0.1% triton X-100 in PBS for 1 hour in a humidified chamber protected from light. Finally, cells were washed twice with PBS and fresh PBS was added to wells prior to imaging and quantification using the incucyte S3 live-cell analysis system.

2.17.2 Protein Carbonylation colorimetric assay

Reactive oxygen species are a common occurrence in neurodegenerative diseases and involved in oxidation of lipids, proteins and DNA. The most common post-translational modification of reactive oxygen species is carbonylation of proteins. Therefore, the carbonyl colorimetric kit (Cambridge bioscience, Cambridge, UK) was used to detect carbonyl content using 2,4-dinitrophenylhydrazine (DNPH) which reacts with protein carbonyls producing a Schiff base then the corresponding hydrazine which can be analysed spectrophotometrically as per the manufacturer's instructions. Briefly, SH-SY5Y and U-87MG cells were seeded and differentiated over 5 days with 10 µM retinoic acid as mentioned before in section 2.2.9. Cells were subsequently treated with 1 mM AAPH or 0.5 µM rotenone with and without tocopherol (200 µM) or ascorbic acid (1 mM) for 48 hours. Cells were then mechanically detached and centrifuged at 300*g* for 5 minutes. Pellets were then washed twice with PBS and harvested at 600*g* for 5 minutes at 4°C. Lysates were then extracted using RIPA buffer as mentioned in section 2.7.2. A 25 µl aliquot of each sample was transferred into two Eppendorf's where one tube was the sample and one the control. 200 µl of DNPH was added to the samples, whereas 200 µl of 2.5 M HCl was added to the control tubes. All samples were then incubated at room temperature for 1 hour with a vortex mix every 15 minutes. 250 µl of 20% trichloroacetic acid (TCA) was added to all tubes and the incubated-on ice for 5 minutes prior to centrifugation at 10000*g* at 4°C for 10 minutes. The supernatant was discarded, and the pellet was resuspended in 250 µl of 10% TCA and again incubated on ice for 5 minutes. Tubes were then centrifuged at 10000*g* for 10 minutes at 4°C. Again, the supernatant was discarded, and the pellet was resuspended in 1:1 ethanol/ethyl acetate, vortexed thoroughly and centrifuged at 4°C for 10 minutes. This step was repeated once more, and the pellet was then resuspended in 250 µl of guanidine hydrochloride by vortexing. Tubes were then centrifuged at 10000*g* at 4°C for 10 minutes. Finally, 100 µl of both sample and control were transferred to a 96-well plate in duplicate and absorbance was measured at 385 nm. Protein content of the pellets was then estimated using the BCA protein estimation described in section 2.7.5.2. Carbonyl content (nmol) was calculated by subtracting the corresponding average control from the average sample to obtain the corrected

absorbance (CA) Protein carbonyl content was then determined via the following equations where protein (mg/ml) was calculated using the BCA protein estimation:

$$Protein\ carbonyl\ \left(\frac{nmol}{ml}\right) = [\left(\frac{CA}{0.011\ \mu M^{-1}}\right)\left(\frac{250}{100}\right)]$$

$$Carbonyl\ content\ \left(\frac{nmol}{mg}\right) = (Protein\ carbonyl\left(\frac{nmol}{ml}\right))(protein\ \left(\frac{mg}{ml}\right))$$

Data is presented as carbonyl content (nmol/mg) where experiments were performed in triplicate and data is expressed as the mean ± SEM.

2.18 Mass spectrometry and pathway enrichment

2.18.1 Protein extraction and trypsinisation

Proteins were extracted by RIPA as described in section 2.6.2. The concentration of each supernatant was determined using the BCA assay described in section 2.6.5.2 before storage of the protein at -20°C.

Cell lysate/secretome (50 µg) were diluted in 50 mM tri-ethyl ammonium bicarbonate (TEAB, Sigma Aldrich UK) before reduction (5 mM DTT, 56°C, 20 min), alkylation (15 mM iodoacetamide , room temperature, 15 min in the dark) and digestion for 16 hours using Trypsin (Promega, UK) at 37°C at a 25:1 protein:protease ratio (w/w) in a thermomixer (650*rpm*). Samples were concentrated and de-salted using HyperSep C18 spin tips (10-200 µL size; ThermoFisher Scientific, Loughborough, UK) using the manufacturers protocol. The samples were concentrated using a vacuum concentrator before resuspension in 5% acetonitrile + 0.1% formic acid.

2.18.2 Mass Spectrometry

Each sample was analysed on a Sciex TripleTOF 6600 mass spectrometer coupled in line with a eksigent ekspert nano LC 425 system running in micro flow. Samples (4 µL) were injected and trapped onto a YMC Triart-C_{18} pre-column (0.3 x 5 mm, 300 µm ID) (mobile phase A; 0.1% formic acid, B; acetonitrile with 0.1% formic acid) at a flow rate of 10 µL/min mobile phase A for 2 min before gradient elution onto the YMC Triart-C_{18} analytical column (15 cm, 3 µm, 300 µm ID) in line to a Sciex TripleTOF 6600 Duospray Source using a 50 µm electrode, positive mode +5500V. Samples were analysed in both IDA (Information Dependent Acquisition, for the generation of a spectral library) and SWATH (Data Independent Acquisition, to generate quantitative data) modes. The following linear gradients were used: for IDA, mobile phase B increasing from 3-30% over 68 min; 40% B at 73 min followed by column wash at 80% B and re-equilibration (87 min total run time).

For SWATH, 3-30% B over 38 min; 40% B at 43 min followed by wash and re-equilibration as before (57 min total run time). IDA acquisition mode was used with a top 30 ion fragmentation (TOFMS *m/z* 400-1250; product ion 100-1500) followed by 15 sec exclusion using rolling collision energy, 50 ms accumulation time; 1.8 s cycle. SWATH acquisition was performed using 100 variable windows, 25 ms accumulation time, 2.6 s cycle (*m/z* 400-1250) (Mele et al., 2018). IDA data was searched together using ProteinPilot 5.0.2, iodoacetamide alkylation, thorough search with emphasis on biological modifications (Swissprot human database October 2018). SWATH data was analysed using Sciex OneOmics software (Lambert et al., 2013) extracted against the locally generated library (false discovery rate filtering of 1% and excluding shared peptides) with the parameters 12 peptides per protein, 6 transitions per peptide, XIC width 30 ppm, 6 min retention time window. The IDA data was also searched using PEAKS X software (Bioinformatics Solutions Inc. Canada) to identify any sites of post translational modifications (Swissprot human database March 2018, search with 313 built-in modifications) with the parameters precursor mass tolerance 25ppm, peptides -10lgP ≥ 15, proteins -10lgP ≥ 20, A-score ≥ 20.

2.18.3 Enriched pathway analysis

To identify enriched pathways between AAPH and rotenone treated U-87MG lysates and secretomes was loaded into Metacore, version 6.34 (https://portal.genego.com/), which enriched network, molecular functions, gene ontology processes, gene ontology functions, gene ontology localisations, pathways and diseases associated with the list of differentially expressed genes. Enrichment was calculated with mass spectrometry differentially identified proteins greater than 50% confidence. Pathways were considered significant if more than one of the given pathway were present in the data than would be expected by chance, based on the total number of genes associated with the pathway.

2.18.4 Validation of mass spectrometry identified proteins

Samples used for mass spectrometry were also used for western blots to validate differentially identified proteins as described in section 2.8 and 2.9 using antibodies against proteins differentially identified including HSP70 (1:1000) and HSP27 (1:1000).

2.18.5 String analysis for protein clusters among identified protein

Understanding what groups of proteins are impacted from treatments in both lysates and secretomes is important for understanding what biological processes and functions are altered. To understand what identified proteins interactions and how they link to cellular processes, a bioinformatics approach was used. STRING analysis utilises a biological database to predict protein-

protein interactions including physical and functional interactions. Using STRING 11.0 software to predict and associate the interactions between protein identified through mass spectrometry protein clusters were generated, where proteins related to specific functions were identified for U-87MG lysates and secretomes treated with AAPH or rotenone. These diagrams (chapter 5) help demonstrate the different responses to AAPH and rotenone.

2.19 iCelligence washes

Wells/inserts were submerged with 70% ethanol for 20 minutes on a shaker. Ethanol was aspirated, and wells/inserts were washed with a thorough flow of water. Wells/inserts were then submerged with 5% (v/v) Hellmanex III (Sigma Aldrich, Dorset, UK) for 1 hour on a shaker prior to aspiration and washing with a thorough flow of 70% (v/v) ethanol followed by water. Wells/inserts were left to dry overnight and exposed to UV light for approximately 20 minutes prior to cell seeding.

2.20 Statistical analysis

All results are represented as mean ± S.E.M and converted to % against control where appropriate, where the number of replicates (n) for each experiment is noted in the figure legend. Multiple statistical analyses were conducted using GraphPad Prism 8 software (GraphPad, Inc, USA). One-way ANOVA test were used for statistical analysis using the when with Dunnett's post-hoc test to compare treatment means to control mean. Two-way ANOVA multiple comparison test followed by Tukey or Sidak post hoc tests as appropriate were used to compare means of individual groups (i.e with or without tocopherol for the same concentrations). Results where p values <0.05 were considered statistically significant.

CHAPTER 3

MODELLING THE NEURODEGENERATIVE BERMUDA TRIANGLE

3.1 INTRODUCTION

Multiple studies with animal models have and are still providing information into the possible mechanisms underlying neuronal degeneration. Some of these factors include mitochondrial dysfunction, impaired protein degradation and oxidative stress, which may be interconnected in the so-called 'Neurodegenerative Bermuda triangle' (NBT; figure 3.1). However, animal models make it difficult to understand the feedback mechanisms between neurons and glia, increasing the complexity in understanding this disease pathology. The use of *in vitro* studies allows the investigation of specific pathways within monocultures to be understood, while controlling environmental factors. This allows primary investigations to be conducted to understand individual cell mechanisms before probing a more complex co-culture.

3.1.1 Use of the neuronal SH-SY5Y and glial U-87MG cell line to model neurodegeneration

3.1.1.1 SH-SY5Y neuroblastoma cell line

SH-SY5Y cells are derived from the SK-N-SH cell line which was obtained from a human metastatic bone tumour biopsy from a 4-year old patient in 1970. SK-N-SH cells can be divided into 2 cell types with distinct morphologies: neuroblastic cell type (N-type) that exhibit small areas of cytoplasm and cell processes with various lengths. The other cell type is a larger epithelial cell referred to as the substrate adherent type (S-type) (Kovalevich and Langford, 2013; Ross et al., 1983).

SH-SY5Y are suitable for *in vitro* investigations into neurodegeneration as characterisation reveals neuronal properties such as moderate dopamine-β-hydroxylase activity with minimal levels of choline acetyl transferase (Kovalevich and Langford, 2013), in addition to noradrenaline release and tyrosine hydroxylase activity (Cheung et al., 2009; Presgraves et al., 2003; Xicoy et al., 2017). SH-SY5Y cells can also display a catecholaminergic phenotype with enzymes that synthesise both dopamine and noradrenaline. Therefore, SH-SY5Y cells may not be purely dopaminergic but are still widely used for modelling neurodegeneration. This is further highlighted as the SH-SY5Y cell line has been used to study AD, neurotoxicity and ischemia through different differentiation methods to obtain a neuronal phenotype (Kovalevich and Langford, 2013; Krishna et al., 2014).

Alternative options are available but also have their own disadvantages including limited sample size, cost and ethical problems. For high throughput screening, phenotypically homogenous cells with identical genetic backgrounds, such as SH-SY5Y cells are required. Furthermore, SH-SY5Y

cells have high differentiation efficiency providing an advantage over other neuronal models such as primary neurons and induced pluripotent stem cells (J I Forster et al., 2016).

3.1.1.2 U-87MG glioblastoma cell line

The CNS is composed of two major cell types: neurons and glia where glia are the most abundant cell within the brain. Initially, glia were believed to serve as the connective tissue between neurons. Studies have revealed glia to be essential for neuronal development and cell-cell communication (Oswald et al., 2018; Seifert et al., 2006; Wilton et al., 2019). There are three types of glial cells: astrocytes, oligodendrocytes and microglia where astrocytes are the most numerous (Sauvageot, 2002; Sun et al., 2003). It is important to note that nigrostriatal dopaminergic neurons have the lowest glia/neuron ratio in the brain (von Bartheld et al., 2016), which may explain why glial dysfunction has a more critical effect in the substantia nigra relative to other areas of the brain (Mena and García de Yébenes, 2008). Indeed, the importance of astrocytes is highlighted with their high expression levels of detoxifying compounds such as ascorbic acid (AA), glutathione (GSH) and glutathione precursors, in addition to high levels of the NRF2 transcription factor responsible for regulating antioxidant defence mechanisms (Allaman et al., 2011; Oswald et al., 2018).

U-87MG, is a long established cell line from a grade IV glioblastoma, the most common aggressive brain tumour in adults (Ohgaki and Kleihues, 2005; Pontén, 1975). U-87MG cells have been chosen for these experiments to create a suitable model system as they display astrocyte-like morphology, functional similarity to normal astrocytes (Nishiguchi et al., 2003; Saeed et al., 2015; Yoshida et al., 2011) and can produce and release neurotrophic growth and brain derived neurotrophic factor, supporting these studies (Laganiere et al., 2010; Zabłocka et al., 2015). Furthermore, like SH-SY5Y cells, U-87MG cells can be differentiated with similar concentrations of all-trans retinoic acid that downregulates telomerase activity and increases glial fibrillary associated protein (GFAP), inducing morphological changes associated with a differentiated astrocyte phenotype (Das et al., 2008; Haque et al., 2007). As both SH-SY5Y and U-87MG cell lines can be differentiated with all-trans retinoic acid this will allow future co-culture experiments to have the same conditions.

However, it is important to note that like the SH-SY5Y cell line using U-87MG cells also has its limitations. For example, studies show that the U-87MG line differs from the originally supplied line possibly due to contamination or because of the cancerous nature of the cell line (Allen et al., 2016). Additionally, cancer cells produce higher levels of reactive species (RS) due to the increased metabolic stress and proliferative capacity (Schumacker, 2006; Trachootham et al., 2006; Waris and Ahsan, 2006). Furthermore, Jelluma *et al.* show the U-87MG glioblastoma line is susceptible to

apoptosis upon glucose withdrawal, leading to OS but not ATP depletion that is not observed in normal astrocytes (Jelluma, 2006). Further supporting this, glioblastoma's exhibit a 3-fold increase in glycolysis relative to their normal astrocytic counterparts (Fu et al., 2019). However, despite these limitations more studies are using SH-SY5Y and U-87MG cell lines in co-culture to investigate diseases (Olson et al., 2012; Saeed et al., 2015; Wang et al., 2015, Wang et al., 2014). They provide an adequate model of neurons and astrocytes that can be differentiated under similar conditions and allow high-throughput experiments, which are more difficult to perform with limited stem cells or ethically demanding primary cells.

3.1.2 Neurodegenerative Bermuda triangle

The brain has a high energy demand utilising mitochondria to provide ATP via oxidative phosphorylation (Franco-Iborra et al., 2016). Multiple studies suggest mitochondrial dysfunction is involved in dopaminergic neuronal degeneration in the pathogenesis of PD (Islam, 2017). In both familial and sporadic PD patients several gene mutations and defects in proteins linked to mitochondrial activity, protein degradation and antioxidant capacity have been implicated and are associated with OS (Müftüoglu et al., 2004).

In SH-SY5Y cells, down regulation of PINK1 leads to mitochondrial dysfunction and increased OS (van der Merwe et al., 2017). Similarly, dopaminergic neurons from post mortem brains from patients with idiopathic PD exhibit PINK1 deficiency and mitochondrial complex I dysfunction (Azkona et al., 2018; Hattingen et al., 2009). In addition, mitochondrial inhibitors are commonly used to model PD.

Astrocytes are important contributors to the pathology of PD (Maragakis and Rothstein, 2006), with astrocyte dysfunction preceding neuronal death (Abramov, 2004; Booth et al., 2017). For example, astrocytes bearing a SOD1 mutation displayed impaired mitochondrial function resulting in increased OS, which affected neuronal viability (Cassina et al., 2008). Furthermore, a study has identified astrocytes to be able to improve synaptogenesis of neurons treated with mitochondrial inhibitors (Du et al., 2018), further highlighting the importance of astrocytes in regulating the neurodegenerative process.

Increased RS levels are mainly attributed to mitochondrial dysfunction (Islam, 2017), though dopamine oxidation, xanthine oxidase and NADPH oxidase (NOX) also contribute (Gandhi and Abramov, 2012). Under normal homeostasis the redox balance is regulated by detoxifying proteins and peptides such as superoxide dismutase (SOD), DJ-1 and glutathione whose temporal production are regulated by RS involving a transcriptional level mechanism (Ighodaro and Akinloye,

2018). Genes encoding for proteins involved in detoxification of RS share a common promoter element referred to as the antioxidant response element (ARE).

Activation of ARE via RS involves NRF2 (a transcription factor), which is negatively regulated by KEAP1 in the cytoplasm. However NRF2 is also negatively regulated in the nucleus by a complex of Cul3/Rbx1 that degrades NRF2 under basal conditions (Schmidlin et al., 2019). In addition, in the nucleus there is Src subfamily A member including Fyn, Src, Yes and Fgr which phosphorylates Tyr568 in NRF2 resulting in nuclear export and degradation (Niture et al., 2011). Furthermore, within the nucleus Bach1 also competes with NRF2 for binding to the ARE suppressing antioxidant gene transcription (Dhakshinamoorthy et al., 2005). Upon exposure to RS, NRF2 translocates to the nucleus, where it binds to the ARE upregulating antioxidant enzymes such as Mn-SOD and glutathione peroxidase (Holley et al., 2010; Itoh et al., 2003; Kobayashi and Yamamoto, 2006; Motohashi and Yamamoto, 2004; R. Zhang et al., 2017). NRF2 has also been associated with mitochondrial function and different cell dynamics (Dinkova-Kostova et al., 2015; Dinkova-Kostova and Abramov, 2015). Furthermore, NRF2 has been reported to be unstable without the well-known redox regulating protein, DJ-1 (Taira et al., 2004; van Horssen et al., 2010). More recently dietary vitamins with antioxidant properties have also been implicated in the NRF2-ARE pathway (Hegazy et al., 2019), stressing the importance in regulating RS levels.

These RS can cause post-translational modifications impairing protein degradation and altering protein homeostasis. Impaired protein handling has been suggested in sporadic cases of PD, from increased oxidatively damaged proteins, protein aggregation and accumulation of poorly degraded proteins within inclusions (Lopiano et al., 2000). Studies show increased levels of carbonyls and 4-hydroxynonenal (HNE) protein adducts in the SN of PD brains (Shahmoradian et al., 2019; Zhao et al., 2017), alongside accumulation of both ubiquitinated and non-ubiquitinated proteins (Walden and Muqit, 2017). Furthermore, in sporadic PD a decrease in chymotrypsin, trypsin and postacidic-like activities have been observed. Proteasomal activity has also been shown to be reduced in rotenone treated SH-SY5Y cells with oxidative modification to the proteasome (Caneda-Ferrón et al., 2008; Shamoto-Nagai et al., 2003). Furthermore, in a recent study proteasome inhibition of LUHMES cells in monoculture led to proteotoxic and OS, which was alleviated by astrocyte-derived glutathione and NRF2 upregulation (Gutbier et al., 2018). Together, this evidence suggests impaired protein degradation or uncontrolled production of abnormal proteins plays a role in PD.

Therefore, mitochondrial dysfunction, RS and impaired protein degradation each contribute to neurodegeneration. Though these factors also appear to be interconnected, possibly

resulting in feed forward loops, where one could lead or contribute to another factor in what is known as the 'Neurodegenerative Bermuda triangle'.

3.1.3 Chemical induction of oxidative stress

Modelling neurodegenerative diseases *in vitro* and *in vivo* is challenging as it is difficult to reproduce all features of the disease. As such chemical toxins have been used to induce the pathological hallmarks of neurodegenerative diseases such PD. PD has been linked with both genetic and environmental contributions (Cannon and Greenamyre, 2013; Marchetti et al., 2011; Twelves et al., 2003). Epidemiological studies suggest exposure to environmental agents such as pesticides increase PD risk (Delamarre and Meissner, 2017). Rotenone is a naturally occurring organic pesticide used in lakes and reservoirs to kill unwanted fish and associated with an increased risk of PD (Betarbet et al., 2006).

Rotenone was initially used in 1985 to model PD where direct injection into the brain resulted in dopaminergic neuronal death (Heikkila et al., 1985). Rotenone was experimented with further as PD became associated with mitochondiral defects, whereby rotenone toxicity depends on its interaction with complex I in the ETC with an affinity of 10-20 nM (Higgins and Greenamyre, 1996). Rotenone binds downstream of an electron leak site in complex I (Dunham-Snary et al., 2019; Feng, 2006), resulting in more free electrons being released to react with intracellular oxygen producing superoxide, which can further damage complex I and other complexes within the ETC leading to more free electrons and RS (García-García et al., 2005).

Rotenone models demonstrate the importance of RS as they exhibit increased lipid peroxidation (Hasan et al., 2020), as well as increased protein carbonyl levels in neuroblastoma cell lines (Chiaradia et al., 2019). In addition to protein modifications, rotenone leads to DNA damage including oxidation of DNA bases and DNA strand breaks (Shokolenko et al., 2009; Swarnkar et al., 2012). Furthermore, *in vitro* studies show chronic rotenone treatment results in accumulation and aggregation of both α-synuclein and ubiquitin (Hao et al., 2017). Rotenone has also been linked with decreased proteasomal activity and associated with PD (Chen et al., 2017; Shamoto-Nagai et al., 2003). In addition, rotenone can also disrupt microtubules leading to tubulin polymerisation that may account for neuron toxicity (Passmore et al., 2017). As rotenone affects the ETC this leads to decreased ATP synthesis (Caneda-Ferrón et al., 2008; Sherer et al., 2003) however, it seems toxicity is primarily induced via OS. Indeed, the importance of rotenone's interaction with complex I leading to RS is highlighted, by replacement of complex I with the single subunit NADH dehydrogenase from *Saccharomyces cerevisiae* blocking mitochondrial impairment, oxidative

damage and cell death suggesting rotenone's specific interaction with complex I causes neurodegeneration primarily via OS (Chernivec et al., 2018).

Whilst rotenone is commonly used to replicate the pathological hallmarks of PD, it is difficult to use to examine the effect of specific types of RS. Using different oxidants with different structures allows specific RS to be generated (Piga et al., 2007). Therefore 2,2'-azobis(2-amidinopropane) dihydrochloride (AAPH), a hydrophilic azo compound may be used as this thermally degrades at a defined rate. AAPH degrades to carbon radicals via the loss of nitrogen whereupon these radicals can react with intracellular oxygen generating predominantly peroxyl radicals (Bassett et al., 1999; Ben Othman et al., 2016; Werber et al., 2011). Peroxyl radicals can react with membrane lipids, forming highly reactive lipid peroxyl radicals. These radicals can repeatedly attack other lipids generating lipid hydroperoxides; a known hallmark of neurodegeneration and Parkinson's disease (Angelova et al., 2015; Reed, 2011; Sultana et al., 2013b).

AAPH induced OS is also demonstrated by increased protein carbonyl, protein-bound HNE, 3-NT and HSP70 levels (Joshi et al., 2006; Razack et al., 2015). These results support AAPH's use as a toxin to model neurodegeneration as increased lipid peroxidation, HNE and acrolein levels are observed in neurodegenerative disorders (Simpson et al., 2004; Taso et al., 2019). However, unlike rotenone AAPH generates more specific types of RS rather than a cascade, allowing more investigations into how specific types of RS initiate different pathways which has yet to be investigated in neurodegenerative models.

3.1.4 Countering reactive species with antioxidants

Aerobic organisms have elaborate defences to cope with and protect against OS (Lemire et al., 2017). Initially antioxidants will attempt to prevent RS production by sequestering metal ions or reducing RS such as H_2O_2 to water. The second line of defence involves antioxidants scavenging and removing RS before damage can occur. Vitamin E and C as well as carotenoids are the major radical scavengers *in vivo,* where vitamin E (tocopherol) and C (ascorbic acid) are essential for lipophilic and hydrophilic radical removal, respectively (Niki, 2014; Traber and Atkinson, 2007; Zakharova et al., 2017).

Tocopherol is predominantly reported as an effective peroxyl and related alkyl peroxyl radical scavenger (Angeli et al., 2017; Fukuzawa et al., 1997). As a result, tocopherol reduces lipid peroxidation, which is aided by the localisation of tocopherol to membranes (Niki, 2014). Whereas ascorbic acid unlike tocopherol is reported to be an effective scavenger of superoxide radicals,

hydrogen peroxide and singlet oxygen (Buettner, 1993; Cabelli and Bielski, 1983; Tu et al., 2017). Patra *et al.* and others highlight the ability of tocopherol to reduce lipid peroxidation levels more than ascorbic acid when rat brains are exposed to lead, suggesting this is due to tocopherol being able to react with peroxyl radicals faster (Gotoh and Niki, 1992; Patra et al., 2001).

Antioxidants such as tocopherol and ascorbic acid are known to reduce OS and, in some part, this is done by NRF2. Antioxidants are strong activators of NRF2, as upon antioxidant metabolism a small amount of OS is produced stimulating NRF2 activation. There are multiple stages to antioxidant NRF2 activation: preinduction, induction and postinduction (Niture et al., 2014). During the preinduction phase, antioxidants initially lead to negative regulators being exported from the nucleus via tyrosine kinase phosphorylation of Cul3/Rbx1 complex, Fyn and Bach1, ultimately leading to their removal via ubiquitination and degradation (Kaspar and Jaiswal, 2011, 2010a, 2010b). This allows NRF2 to move into the nucleus unhindered, where it heterodimerises with small Maf or c-Jun protein resulting in subsequent binding to the ARE and activation of cytoprotective genes (Kaspar et al., 2009; Shelton and Jaiswal, 2013). As a result, these cytoprotective genes aid in decreasing RS, supporting the observed lowered fluorescence. Following this induction NRF2 is switched off, where GSK3β activation phosphorylates Fyn leading to nuclear localisation (Jain and Jaiswal, 2007) leading to NRF2 phosphorylation, followed by nuclear export and degradation (Jain and Jaiswal, 2006). In addition, during this induction de novo synthesis of Cul3/Rbx1, Fyn and Bach1 occurs and these are imported into the nucleus switching off NRF2, leading to cytoprotective gene levels returning to basal levels (Dhakshinamoorthy et al., 2005).

3.1.5 Aims of the chapter

While it is theorised that mitochondrial dysfunction, OS and impaired protein degradation are interconnected and influence neuronal death, few have shown this experimentally in both neurons and glia. Rotenone, known to inhibit complex I provoking mitochondrial dysfunction increases superoxide radicals, which subsequently generates a cascade of other RS. Thus, rotenone has been used extensively to investigate OS and model neurodegeneration. More recent studies have additionally investigated how rotenone also effects proteasome activity, though few have investigated the link between these factors. Furthermore, the effect of different RS has yet to be fully understood, which may be important in understanding how OS effects neurodegeneration and therefore using different chemicals may aid this.

To assess how OS effects different neural cells neuronal SH-SY5Y and glial U-87MG cells were exposed to mitochondrial complex I inhibitor, rotenone and RS generating agent, AAPH.

Rotenone was used as a complex I inhibitor resulting in mitochondrial dysfunction increasing RS levels linked with the occurrence of PD, whereas AAPH generates primarily peroxy radicals by thermal degradation. The ability of these agents to influence RS levels and cell death was investigated alongside the ability of known antioxidants, α-tocopherol (vitamin E) and ascorbic acid (vitamin C), to potentially attenuate these effects. This approach will characterise the differing responses of neural cell types to different RS and help to establish suitable pathological co-culture conditions. The ability of sub-lethal RS levels to alter mitochondrial and proteasomal function will evaluate how RS impact the NBT and alter levels of antioxidant response proteins, providing insight into how different RS influence both mitochondrial function and protein degradation. Understanding the pathways underlying the 'Neurodegenerative Bermuda Triangle' and how different RS effect this will improve our understanding of their role in neurodegeneration so novel therapies can be produced.

3.2 RESULTS

3.2.1 Differences in reactive species levels between neurons and glia

RS are a pathological hallmark of PD and can be generated in a few ways. AAPH can increase RS via thermal degradation into carboxyl radicals, which can react with intracellular oxygen mainly generating peroxy radicals that target cell membranes. Both neuronal SH-SY5Y and glial U-87MG cells were exposed to the same concentration range of AAPH, to compare how different neural cell types react to this paradigm. RS accumulation in neural cells following AAPH exposure was measured using the fluorescent probe 2',7'-dichlorofluorescin diacetate (DCFDA).

Live fluorescence microscopy showed a dose-dependent increase in RS-mediated fluorescence within neural cells exposed to increasing AAPH concentrations (figure 3.1A, B and 3.3A, B). Similarly, AAPH treatment showed a dose- and time-dependent increase in RS-mediated fluorescence when quantified temporally (figure 3.2A, B). The rate of RS generated was calculated (figure 3.2 and 3.4, table 1 and 2), which showed glial cells had a lower rate of fluorescence change relative to neuronal cells, although not significant.

Both antioxidants, α-tocopherol (figure 3.2) and ascorbic acid (figure 3.4), lowered AAPH-induced neural RS levels demonstrated by reduced fluorescence (figure 3.1A, B and figure 3.3A, B, respectively). This was supported with temporal measurements that showed a significant decrease in the rate of RS-mediated fluorescence generation for 1 mM AAPH, for both neural cell types and antioxidants (figure 3.2C, D and figure 3.4C, D). This supports the change in fluorescence is due to RS generated by AAPH, which can be attenuated with antioxidants α-tocopherol and ascorbic acid.

Rotenone was used to generate RS through mitochondrial dysfunction. Unfortunately, due to the fast nature of the RS generated by rotenone, experiments were restricted and thus, we relied on endpoint measurements to understand how rotenone affected RS levels in neural cells. For comparison, endpoints assays were also run with AAPH.

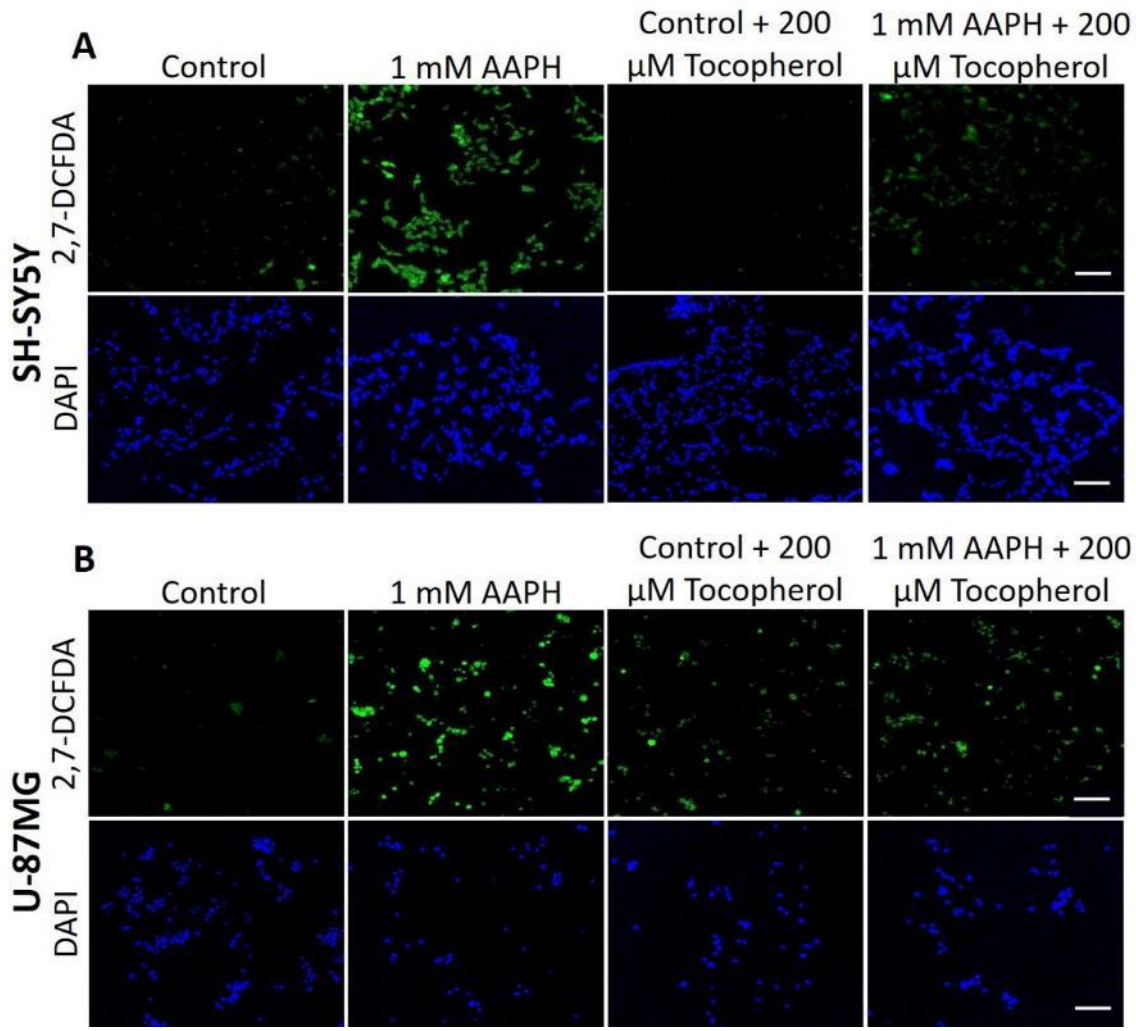

Figure 3.1 AAPH-induced RS levels are attenuated by α-tocopherol in neural cells using the fluorescent dye DCFDA. *Neuronal (A) and glial (B) RS levels measured using DCFDA (green) and nuclei stained with DAPI (blue) with and without 200 µM α-tocopherol. Scale bar = 100 µm.*

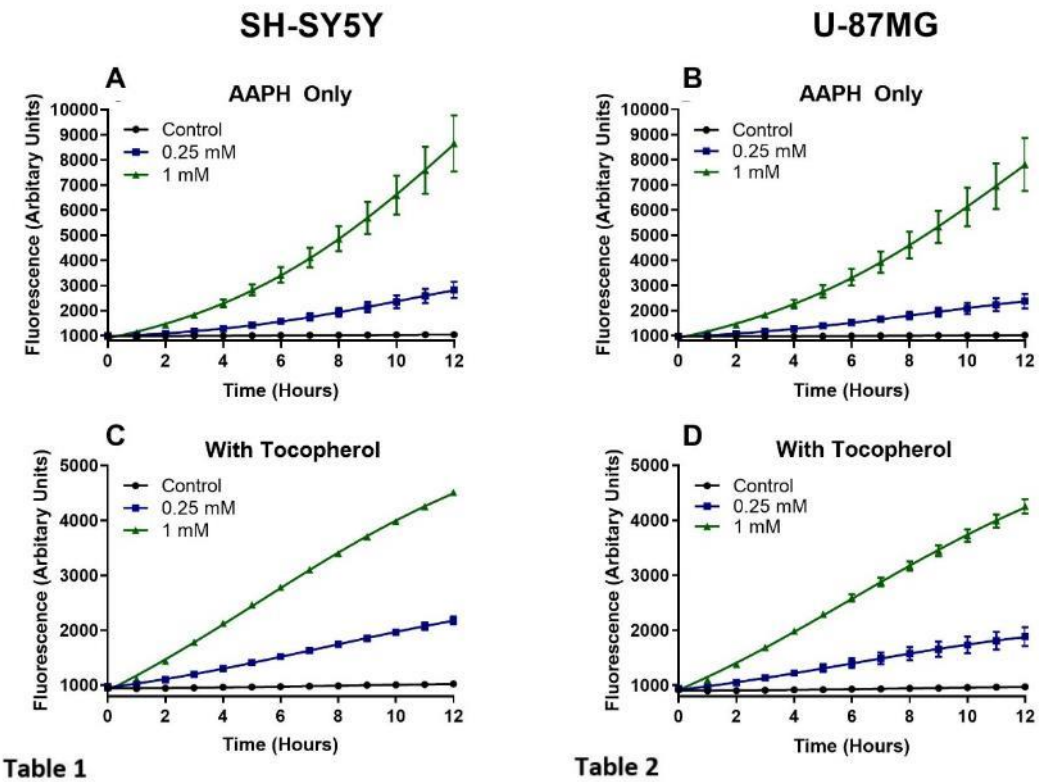

Table 1

Neuronal SH-SY5Y	Rate of change of fluorescence (ΔFl/Hour)	
Concentration (mM)	AAPH Only	200 µM Tocopherol
0	5.28 ± 0.209	6.80 ± 0.407
0.25	156 ± 29.5	105 ± 4.45
1	644 ± 91.3	309 ± 2.21***

Table 2

Glial U-87MG	Rate of change of fluorescence (ΔFl/Hour)	
Concentration (mM)	AAPH Only	200 µM Tocopherol
0	4.49 ± 0.456	5.76 ± 0.198
0.25	123 ± 27.9	83.1 ± 17.3
1	578 ± 90.8	285 ± 11.0***

Figure 3.2 AAPH-induced RS levels are attenuated by α-tocopherol in neural cells. *Temporal measurement of RS using DCDFA (Fluorescence ± SEM) in cells treated with AAPH alone (A, B) or AAPH + α-tocopherol (C, D). Neuronal (Table 1) and glial (Table 2) rates of change of fluorescence for AAPH only or AAPH + 200 µM α-tocopherol. Statistical analysis was performed using two-way ANOVA with Sidak's post-hoc test where n=3 for all experiments. Statistical significance was recorded as *p<0.05, **p<0.01 and ***p<0.001.*

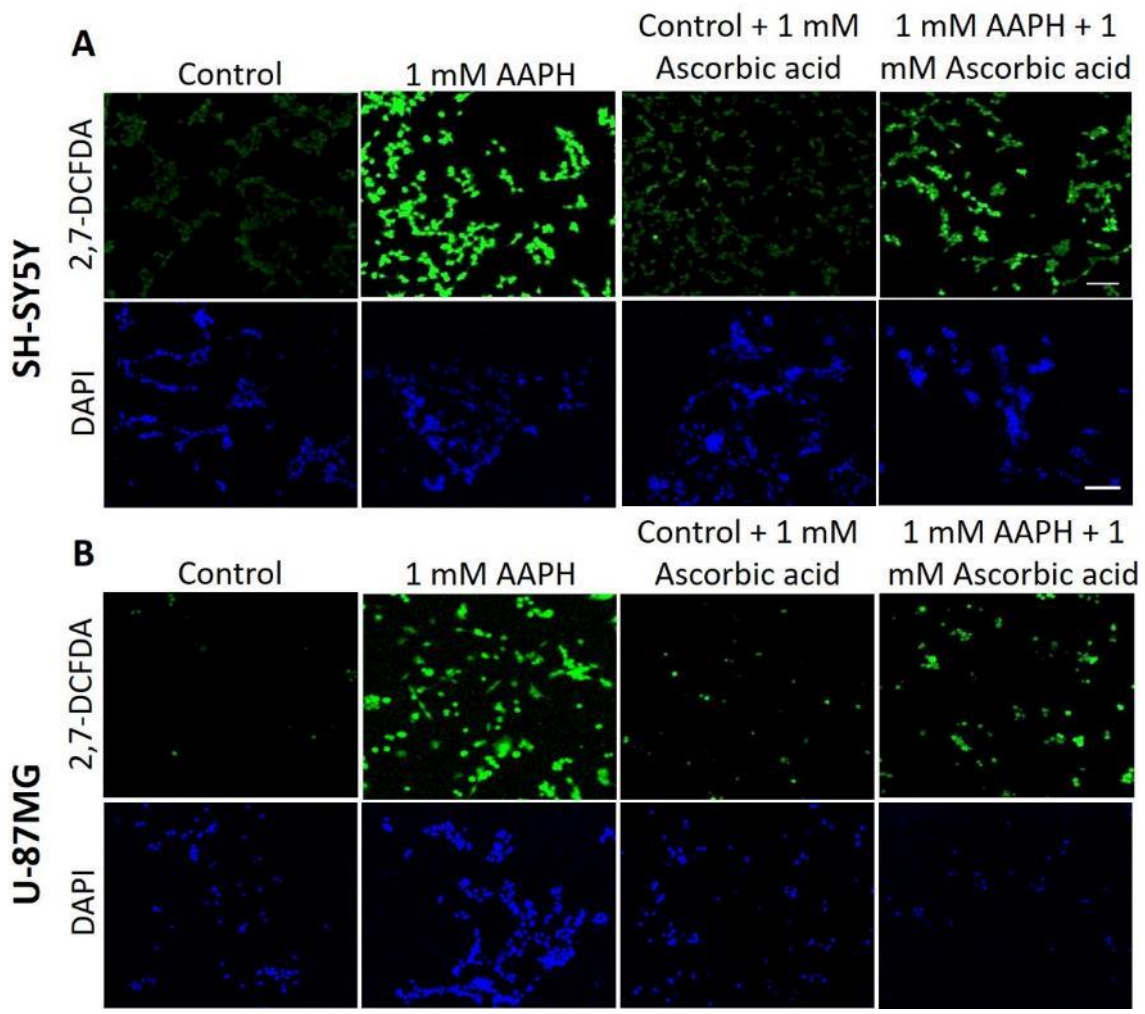

Figure 3.3 AAPH-induced RS levels are attenuated by ascorbic acid in neural cells using the fluorescent dye DCFDA. *Neuronal (A) and glial (B) RS levels measured using DCFDA (green) and nuclei stained with DAPI (blue) with and without 1 mM ascorbic acid. Scale bar = 100 µm.*

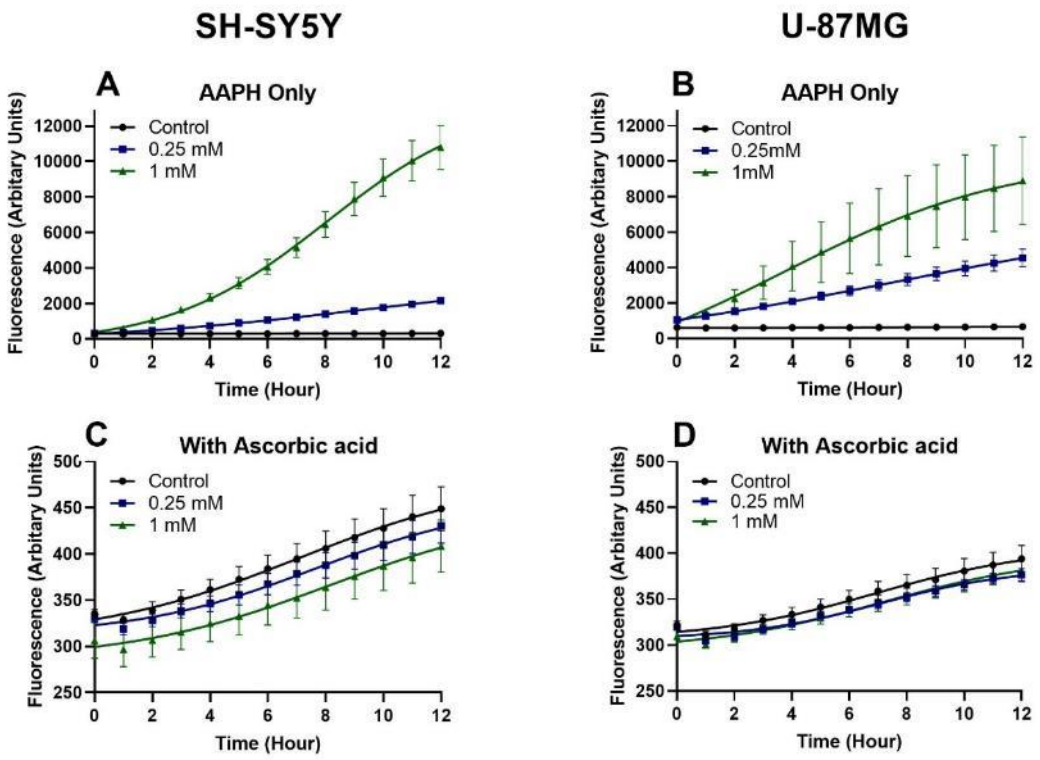

Table 1

Neuronal SH-SY5Y	Rate of change of fluorescence (ΔFl/Hour)	
Concentration (mM)	AAPH Only	1 mM Ascorbic acid
0	1.34 ± 0.579	8.13 ± 0.455
0.25	158 ± 14.2	9.36 ± 1.21
1	939 ± 111	9.40 ± 1.08****

Table 2

Glial U-87MG	Rate of change of fluorescence (ΔFl/Hour)	
Concentration (mM)	AAPH Only	1 mM Ascorbic acid
0	2.52 ± 0.454	7.03 ± 0.952
0.25	159 ± 17.9	6.05 ± 0.428
1	343 ± 109	6.62 ± 0.784****

Figure 3.4 AAPH-induced RS levels are attenuated by ascorbic acid in neural cells. *Temporal measurement of RS using DCDFA (Fluorescence ± SEM) in cells treated with AAPH alone (A, B) or AAPH + ascorbic acid (C, D). Neuronal (Table 1) and glial (Table 2) rates of change of fluorescence for AAPH only or AAPH + 1 mM ascorbic acid. Statistical analysis was performed using two-way ANOVA with Sidak's post-hoc test where n=3 for all experiments. Statistical significance was recorded as *p<0.05, **p<0.01, ***p<0.001 and ****p<0.0001.*

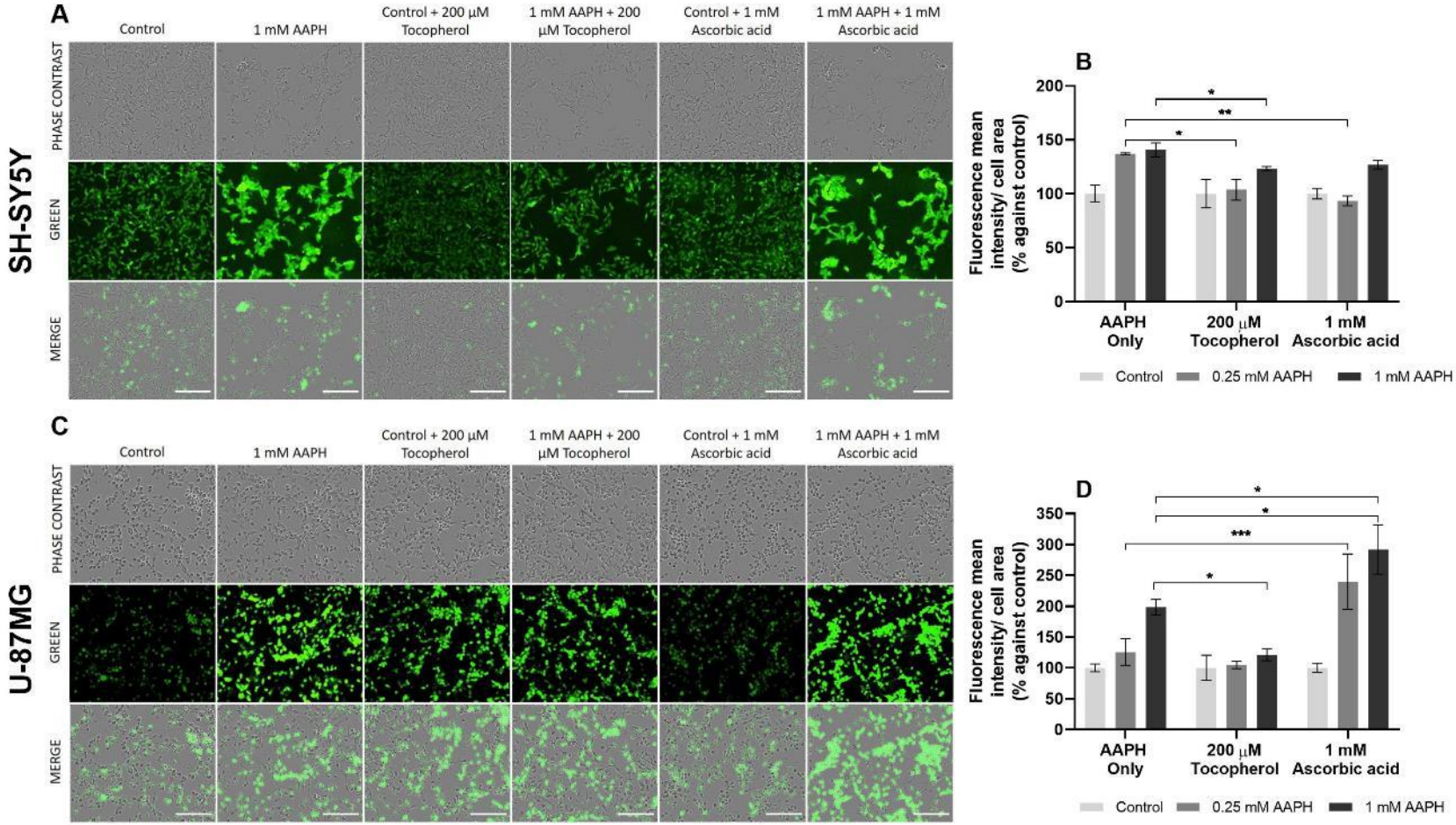

Figure 3.5 AAPH-induced RS levels are affected by α-tocopherol and ascorbic acid in neural cells. *AAPH induced neuronal (A) and glial (C) reactive species levels measured using DCFDA (green) with and without 200 µM α-tocopherol or 1 mM ascorbic acid. Images taken using incucyte S3 live-cell analysis system. Scale bar = 200 µm. Endpoint measurement of fluorescence was quantified using the incucyte S3 live-cell analysis system (Fluorescent intensity/cell area ± SEM) in neurons (B) and glia (D) where results are presented as % against control. Statistical analysis was performed using two-way ANOVA with Dunnett's post-hoc test relative to the control of each condition when n=4 for all experiments. Statistical significance was recorded as *p<0.05, **p<0.01 and *p<0.001.*

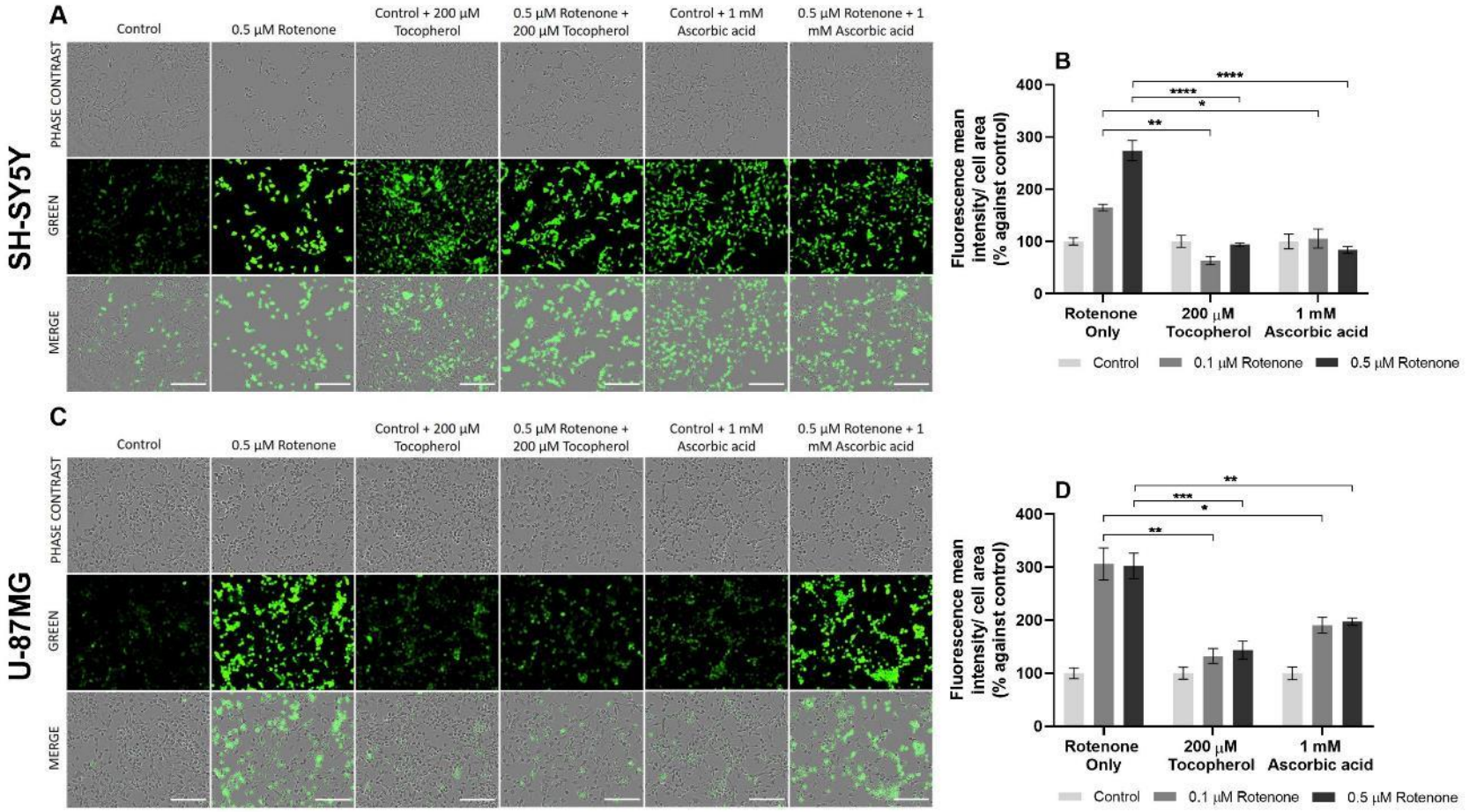

Figure 3.6 Rotenone-induced RS levels are affected by α-tocopherol and ascorbic acid in neural cells. *Rotenone induced neuronal (A) and glial (C) reactive species levels measured using DCFDA (green) with and without 200 µM α-tocopherol or 1 mM ascorbic acid. Images taken using incucyte S3 live-cell analysis system. Scale bar = 200 µm. Endpoint measurement of fluorescence was quantified using the incucyte S3 live-cell analysis system (Fluorescent intensity/cell area ± SEM) in neurons (B) and glia (D) presented as % against control. Statistical analysis was performed using two-way ANOVA with Dunnett's post-hoc test relative to the control of each condition when n=4 for all experiments. Statistical significance was recorded as *p<0.05, **p<0.01, ***p<0.001 and ****p<0.0001.*

Neural cells were treated with AAPH (figure 3.5) or rotenone (figure 3.6) for 48 hours with and without antioxidants, prior to the addition of DCFDA, then subsequently imaged and quantified using the incucyte S3-live cell analysis system. Again, AAPH showed a dose-dependent increase in fluorescence in both neuronal (figure 3.5A, B) and glial (figure 3.5C, D) cells, suggesting AAPH mediated RS generation. Furthermore, α-tocopherol was successfully able to attenuate fluorescence for 0.25 mM AAPH, suggesting the antioxidant was able to scavenge and reduce RS levels. Interestingly, ascorbic acid that previously at 12 hours showed reduced fluorescent levels did not show lower fluorescent levels for 1 mM AAPH in neurons and for all AAPH concentrations in glia. This suggests that α-tocopherol can continuously scavenge RS and thus, lower the fluorescent levels whereas ascorbic acid loses capacity to do so over time becoming less effective.

Rotenone, like AAPH, showed a dose-dependent increase in fluorescence for both neuronal (figure 3.6A, B) and glial (figure 3.6C, D) cells, suggesting rotenone could generate quantifiable levels of RS. The addition of α-tocopherol attenuated fluorescent levels for both neurons and glia suggesting α-tocopherol could scavenge the RS generated by rotenone. Ascorbic acid successfully lowered rotenone-induced RS in neuronal cells but was less successful than α-tocopherol within glial cells, suggesting ascorbic acid displays different effects in neurons and glia. In addition, in neuronal cells ascorbic acid was successfully able to reduce fluorescence induced by rotenone but not for higher concentrations of AAPH, highlighting differences between the RS generators and distinct scavenging capabilities of different antioxidants.

As temporal measurements with AAPH suggested a lower rate of change of fluorescence for glia relative to neurons, the antioxidant capacity of the different neural cells was investigated. One common antioxidant peptide that literature suggests is greater in glia than neurons is glutathione. Using a commercially available fluorometric kit, glutathione levels were measured (figure 3.7). Interestingly, U-87MG glial cells showed higher glutathione levels per μg protein relative to SH-SY5Y neuronal cells at 24 and 48 hours (figure 3.7A), suggesting glia have greater levels of glutathione. Additionally, when neurons and glia were treated with AAPH for 48 hours only neurons showed significantly higher levels of glutathione for 5 mM AAPH (figure 3.7B). This may be due to glia possessing greater basal levels of glutathione and as such can scavenge the RS generated by AAPH more effectively. Following 48-hour treatment with rotenone, both neurons and glia exhibited higher levels of glutathione (figure 3.7C). Together, this supports differences between the RS generators and activation of antioxidant mechanisms in the two neural cell types.

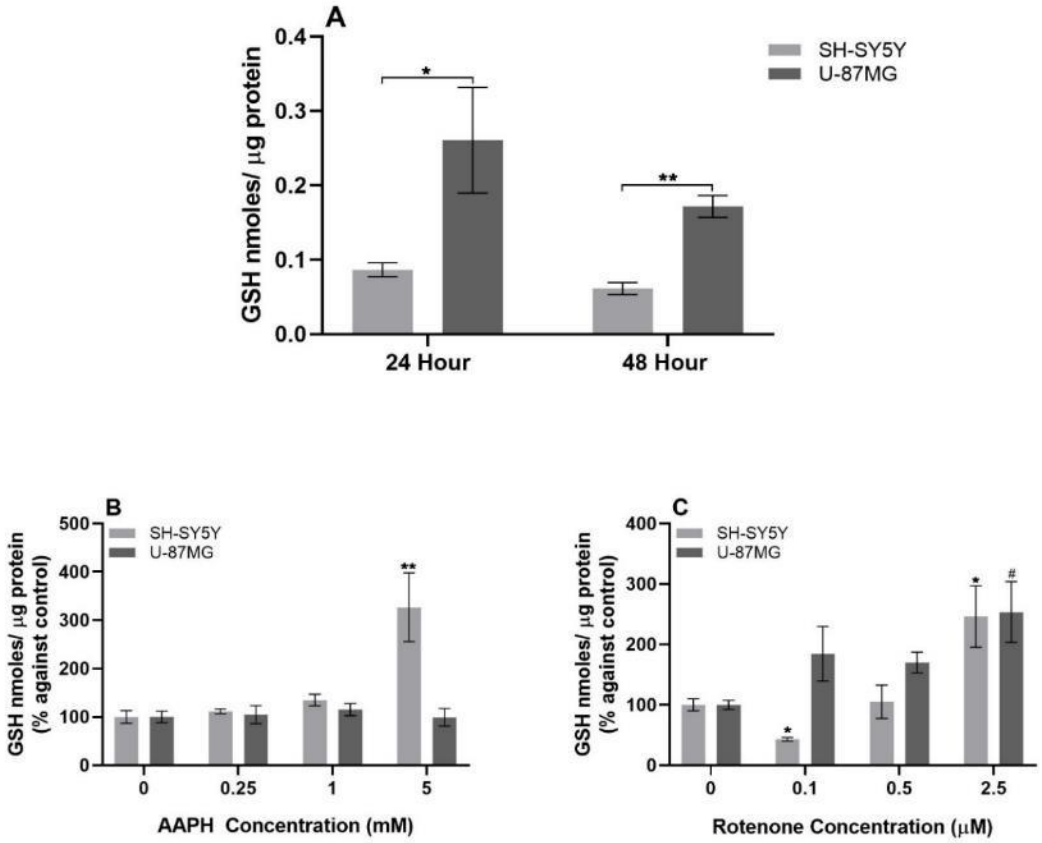

Figure 3.7 AAPH and rotenone alter glutathione levels in neural cells. *(A) Total glutathione levels were measured after 24 and 48 hours of growth for both SH-SY5Y and U-87MG cells. Both SH-SY5Y and U-87MG cells were treated with AAPH (B) or rotenone (C) for 48 hours and total glutathione levels were measured. Results are presented as % glutathione levels (GSH nmoles/µg protein) ± SEM against untreated control. Statistical analysis was performed using one-way ANOVA with Dunnett's post-hoc test where n=4 in all experiments. Statistical analysis was performed using one-way ANOVA with Dunnett's post-hoc test where n=4 for all experiments. Statistical significance was recorded as *p<0.05 and **p<0.01.*

3.2.2 Oxidative stress mediated changes in the cellular antioxidant response

To confirm sub-lethal levels of RS and possible pathways involved, antioxidant response element binding proteins and downstream antioxidant protein levels were investigated.

Western blot results show AAPH and rotenone treatment in both neural cells showed no significant change in levels of the antioxidant response binding protein, NRF2 (figure 3.8A and B). DJ-1 levels showed a dose-dependent decrease in SH-SY5Y cells treated with both AAPH and rotenone (figure 3.8C and D), whereas no significant change was observed in U-87MG cells. Both neural cells showed a significant decrease in peroxiredoxin 6 (PRDX6) levels when treated with AAPH (figure 3.8E). Whereas rotenone caused opposing effects on PRDX6 levels in both neural cells (figure 3.8F), where there was a significant decrease in SH-SY5Y cells but a significant increase in glial U-87MG cells.

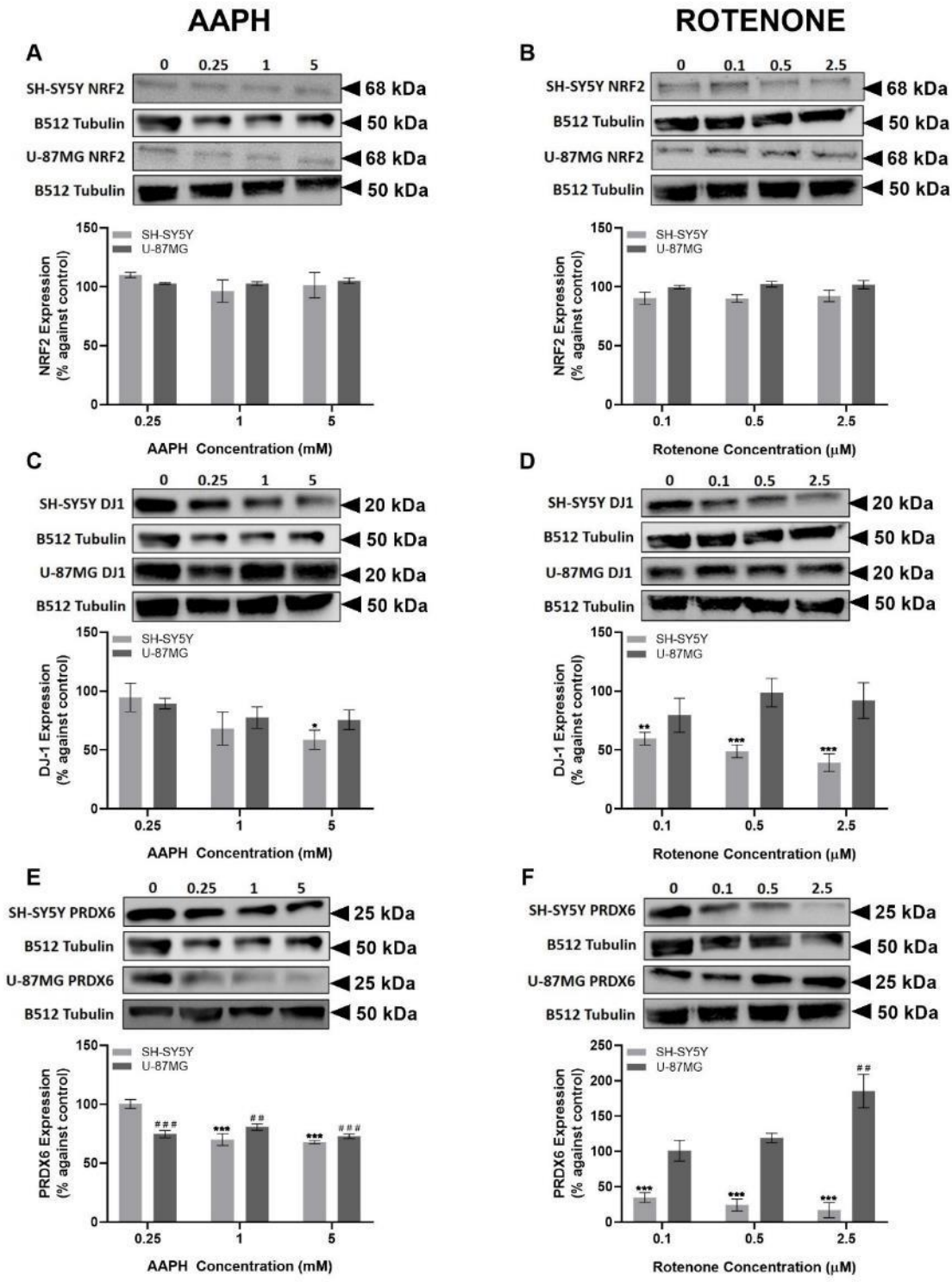

Figure 3.8 AAPH and rotenone-induced oxidative stress effects antioxidant response element proteins in neural cells. *Representative Western blots of neuronal SH-SY5Y and glial U-87MG total cell extracts were probed with (A, B) NRF2 (1:1000), (C, D) DJ-1 (1:10000) and (E, F) peroxiredoxin 6 (PRDX6; 1:1000). Each Western blot is accompanied by a plot summarising densitometric analyses of Western blots using AIDA software. Results are presents as % against control ± SEM. Statistical analysis was performed using one-way ANOVA with Dunnett's post-hoc test where n=4 for all experiments. Statistical significance was recorded as *p<0.05, **p<0.01 and ***p<0.001.*

Together, these results suggest RS in neural cells resulted in no significant change in NRF2 levels. However, neurons showed decreased levels of subsequent downstream antioxidant response proteins, while glial cells exhibited either no significant change or an increase in downstream antioxidant protein PRDX6 following rotenone treatment. Furthermore, these results suggest specific RS generated by rotenone or AAPH treatment results in different neural cell responses, where proteins downstream of the antioxidant response element protein are affected. Therefore, even though there is no significant change in total NRF2 levels the transcription factor may change cellular localisation affecting downstream protein levels.

As such, NRF2 subcellular localisation following AAPH and rotenone treatment was investigated. AAPH and rotenone treatment of SH-SY5Y cells (figure 3.9A and C) resulted in a dose-dependent increase in NRF2 co-localisation within the nucleus. Successful subcellular fractionation of total cell lysates also revealed that both rotenone and AAPH increased NRF2 nuclear expression relative to the control (figure 3.9D), supporting immunofluorescence images. Additionally, the antioxidant α-tocopherol successfully attenuated NRF2 nuclear colocalisation for both treatments, suggesting OS resulted in this translocalisation. However, while ascorbic acid was able to prevent nuclear localisation in rotenone treated cells the antioxidant was not able to do this in AAPH treated cells, which subcellular fractionation also exhibited (figure 3.9D). These results supported previous DCFDA fluorescence studies that ascorbic acid is not able to successfully scavenge the RS generated by AAPH.

The RS generated by AAPH and rotenone resulted in a similar effect in U-87MG glial cells where there was dose-dependent increase in nuclear localisation (figure 3.10A, C). Furthermore, subcellular fractionation revealed a significant increase in nuclear expression of NRF2 in both AAPH and rotenone treated U-87MG cells (figure 3.10D). Similarly, α-tocopherol was able to prevent nuclear localisation for both treatments. In contrast, ascorbic acid did not prevent NRF2 nuclear localisation. Subcellular fractionation Western blot results contravene this (figure 3.10D). However, immunofluorescence images suggest nuclear localisation in control ascorbic acid U-87MG cells suggesting ascorbic acid itself stresses U-87MG cells.

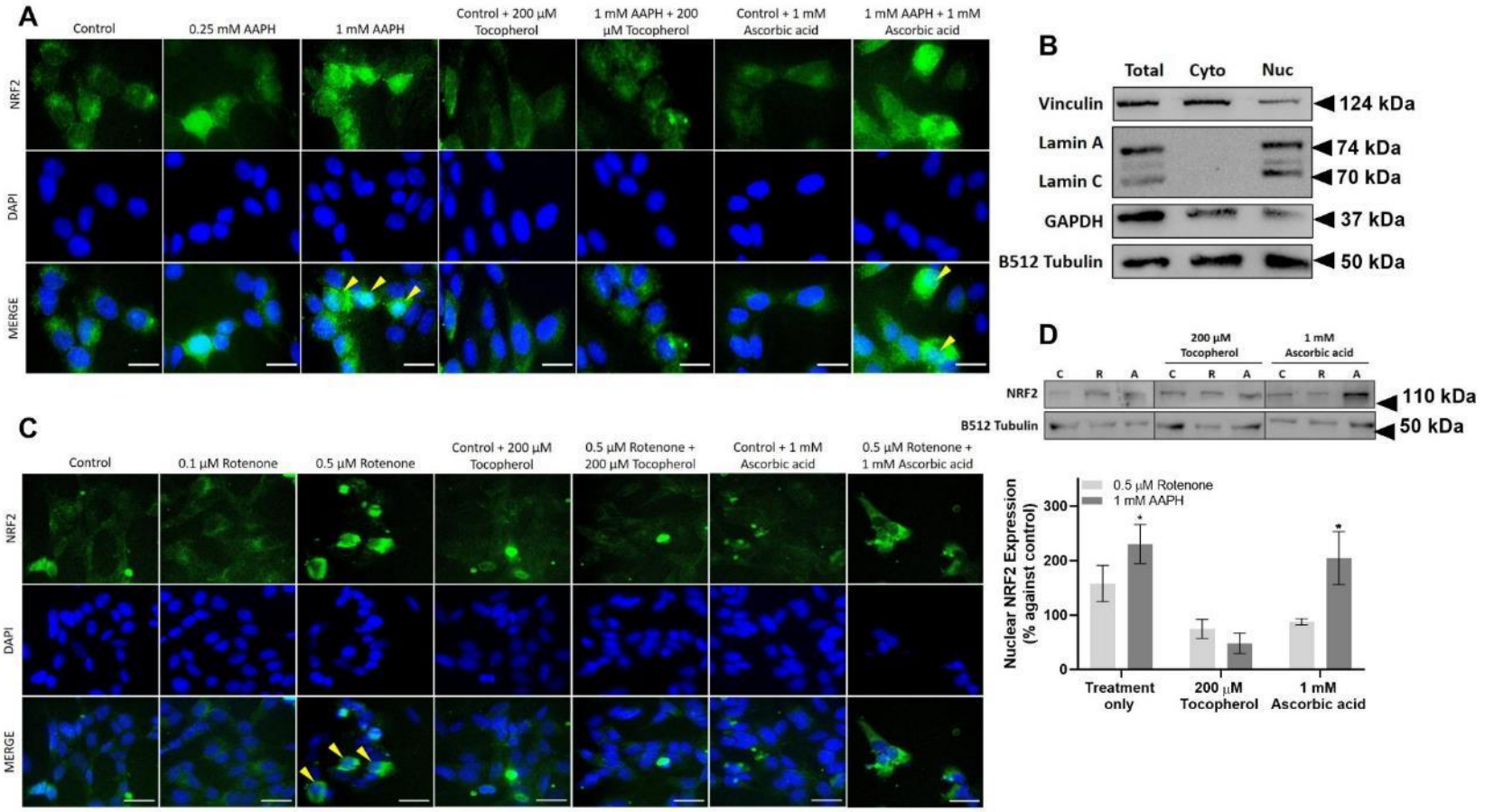

Figure 3.9 AAPH and rotenone induces NRF2 nuclear localisation in neuronal SH-SY5Y cells which is affected by antioxidants. *Immunofluorescence showed AAPH (A) and rotenone (C) induced nuclear localisation of NRF2 (green) where 200 µM α-tocopherol prevented this localisation but 1 mM ascorbic acid only prevented nuclear localisation in rotenone treated SH-SY5Y cells. Scale bar = 25 µm. (B) Localisation of NRF2 was confirmed in subcellular fractions (Total; Cyto-cytoplasmic; Nuc-nuclear) using SDS-PAGE and Western blots using subcellular markers vinculin (cytoplasmic), lamin a/c (nuclear) and GAPDH (cytoplasmic). (D) Representative Western blot of nuclear subcellular fraction of NRF2 expression where SH-SY5Y cells were treated with (R) 0.5 µM rotenone or (A) 1 mM AAPH with and without 200 µM α-tocopherol and 1 mM ascorbic acid. Western blot is accompanied by a plot summarising densitometric analyses of Western blots using AIDA software. Results are presents as % against control ± SEM. Statistical analysis was performed using two-way ANOVA with Dunnett's post-hoc test relative to the control of each condition when n=4 for all experiments. Statistical significance was recorded as *p<0.05 and **p<0.01.*

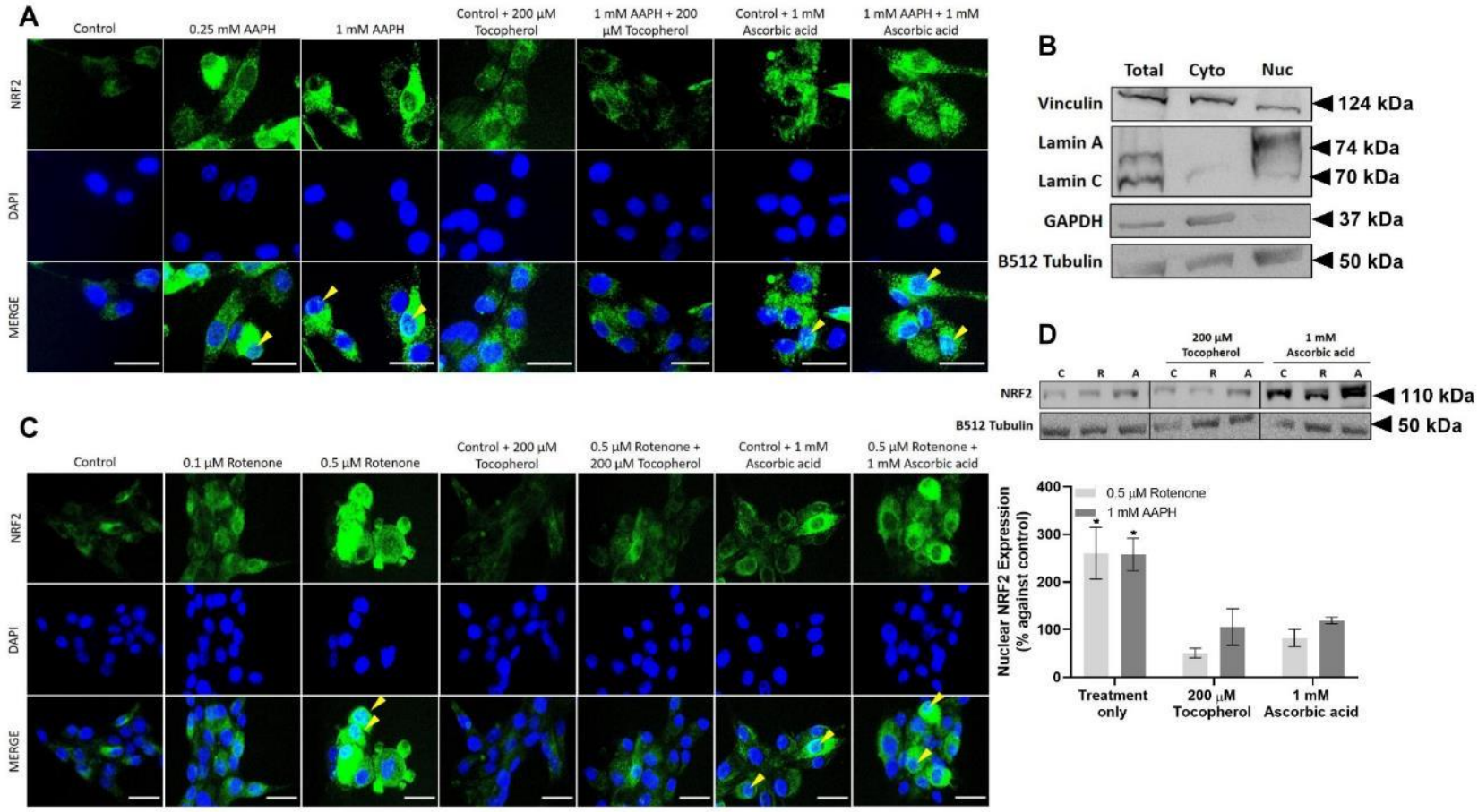

Figure 3.10 AAPH and rotenone induces NRF2 nuclear localisation in glial U-87MG cells which is affected by antioxidants. *Immunofluorescence showed AAPH (A) and rotenone (C) induced nuclear localisation of NRF2 (green) where 200 µM α-tocopherol prevented this localisation but 1 mM ascorbic acid doesn't. Scale bar = 25 µm. (B) Localisation of NRF2 was confirmed in subcellular fractions (Total; Cyto-cytoplasmic; Nuc-nuclear) using SDS-PAGE and Western blots using subcellular markers vinculin (cytoplasmic), lamin a/c (nuclear) and GAPDH (cytoplasmic). (D) Representative Western blot of nuclear subcellular fraction of NRF2 expression where U-87MG cells were treated with (R) 0.5 µM rotenone or (A) 1 mM AAPH with and without 200 µM α-tocopherol and 1 mM ascorbic acid. Western blot is accompanied by a plot summarising densitometric analyses of Western blots using AIDA software. Results are presents as % against control ± SEM. Statistical analysis was performed using two-way ANOVA with Dunnett's post-hoc test relative to the control of each condition when n=4 for all experiments. Statistical significance was recorded as *p<0.05 and **p<0.01.*

Together, these results suggest AAPH and rotenone result in a dose-dependent nuclear localisation of NRF2, possibly leading to binding to the antioxidant response element (ARE) and subsequent transcription of OS response genes. This colocalisation was attenuated by α-tocopherol for both neural cells types and treatments, whereas ascorbic acid was only successful in preventing NRF2 nuclear localisation in SH-SY5Y cells treated with rotenone. This localisation mimicked changes in RS species seen in DCFDA fluorescence studies (figure 3.1-6), suggesting the RS generated by AAPH and rotenone influenced NRF2 nuclear localisation, indicating the ARE is activated in response to RS.

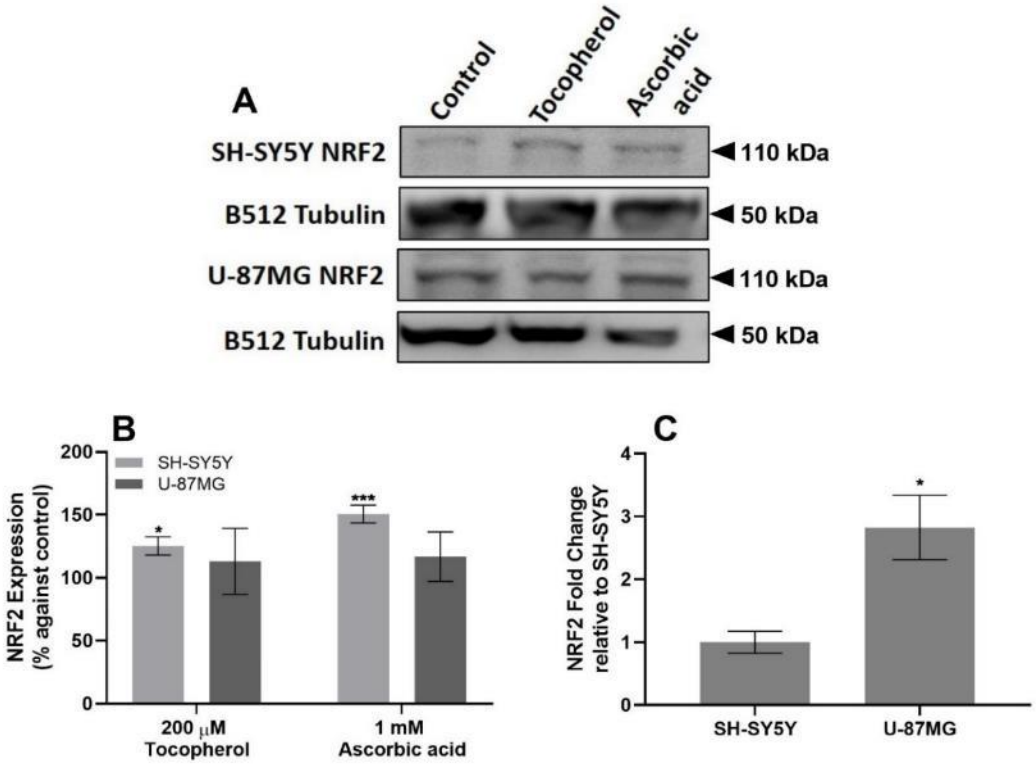

Figure 3.11 Antioxidants α-tocopherol and ascorbic acid effects NRF2 levels in neural cells. *(A) Representative Western blots of neuronal SH-SY5Y and glial U-87MG treated with 200 μM α-tocopherol and 1 mM ascorbic acid total cell extracts were probed with NRF2 (1:1000). (B)Western blot is accompanied by a plot summarising densitometric analyses of Western blots using AIDA software. (C) Western blots were also used to determine NRF2 levels in U-87MG cells relative to SH-SY5Y cells using AIDA software. NRF2 levels per unit protein for SH-SY5Y and U-87MG cells were 0.26 and 0.72, respectively. Results are presented as mean % against control ± SEM. Statistical analysis was performed using one-way ANOVA with Dunnett's post-hoc test where n=4 for all experiments. Statistical significance was recorded as *p<0.05, **p<0.01 and ***p<0.001.*

Furthermore, NRF2 immunofluorescent images appeared brighter with the addition of α-tocopherol and ascorbic acid relative to their control counterparts for both neural cells, as such NRF2 levels were investigated in both neurons and glia treated with antioxidants (figure 3.11). Western blot results show increased NRF2 levels in neurons treated with both antioxidants but did not significantly affect levels in glial cells (figure 3.11B), suggesting antioxidants may attenuate RS levels by increasing NRF2 levels in neurons but not in glia. This is possibly because glia rely on other antioxidant mechanisms or because glia have greater basal levels of NRF2 than neurons (figure 3.11C).

3.2.3 Oxidative stress influences neural viability

Following confirmation of RS generation neural cell viability was assessed via morphological changes, viability and functional activity assays. Neural cells were exposed to a range of AAPH concentrations (0.1- 5 mM) for up to 48 hours.

Phase contrast microscopy showed neuronal SH-SY5Y cells exhibited decreased processes and morphological rounding, alongside increased intercellular distance in a dose-dependent manner at 24 hours (figure 3.12A), which was exacerbated at 48 hours (figure 3.14A) relative to the control, consistent with loss of cell viability. However, glial U-87MG cells showed no significant change in morphology and intercellular distance as the concentration of AAPH increased at 24 hours (figure 3.12B), but higher concentrations resulted in decreased intercellular distances and extended processes at 48 hours (figure 3.14B). Furthermore, mitochondria of treated cells labelled with Mitotracker Red® (figure 3.12A, B and 3.14A, B) showed more diffuse staining indicating loss of mitochondrial integrity in SH-SY5Y neuronal and glial U-87MG cells.

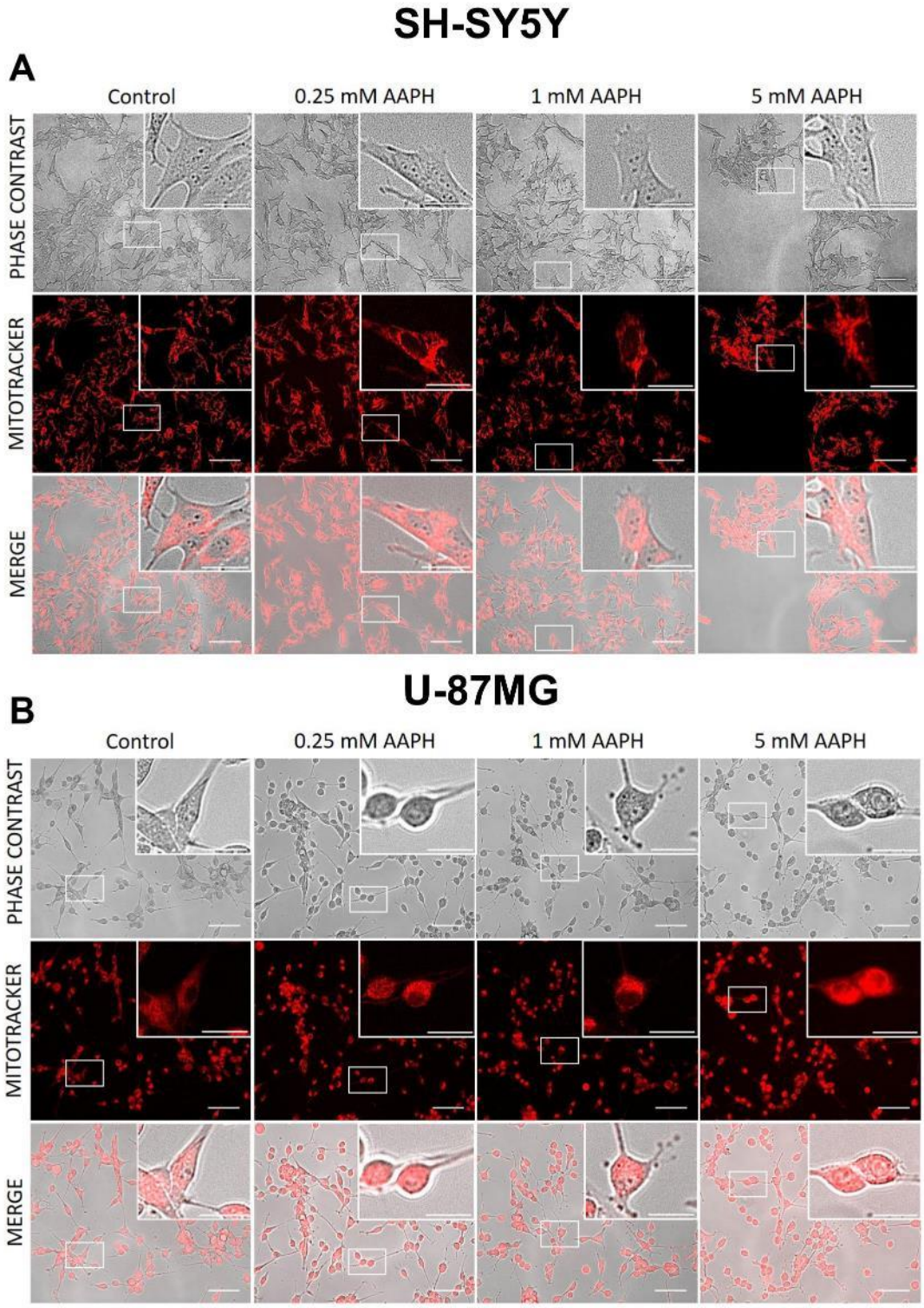

Figure 3.12 Neuronal SH-SY5Y and glial U-87MG morphology after 24-hour AAPH exposure. *Phase contrast microscopy and mitotracker staining (red) of (A) SH-SY5Y and (B) U-87MG monocultures after 24-hour AAPH exposure. Scale bar = 100 µm. Inset scale bar = 30 µm.*

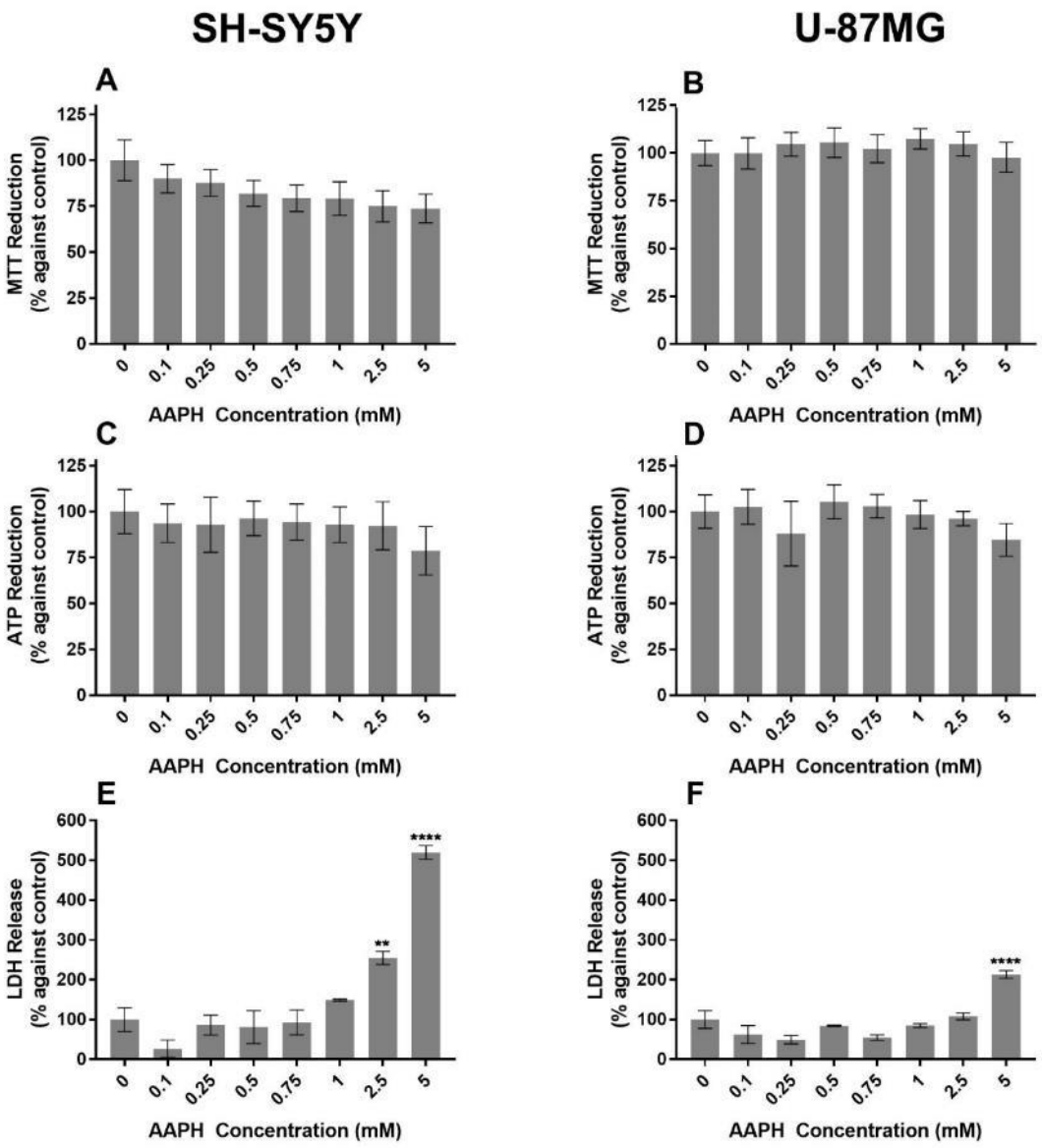

Figure 3.13 Neuronal SH-SY5Y and glial U-87MG cell viability after 24-hour AAPH exposure. *MTT reduction assay of (A) SH-SY5Y and (B) U-87MG cells treated with AAPH. Total ATP levels of (C) SH-SY5Y and (D) U-87MG monocultures treated with AAPH for 24 hours. LDH release of (E) SH-SY5Y and (F) U-87MG monocultures treated with AAPH for 24 hours. All viability assays are presented as mean % against control ± SEM. Statistical analysis was performed using one-way ANOVA with Dunnett's post-hoc test where n=3 for all experiments. Statistical significance was recorded as *p<0.05, **p<0.01, ***p<0.001 and ****p<0.0001.*

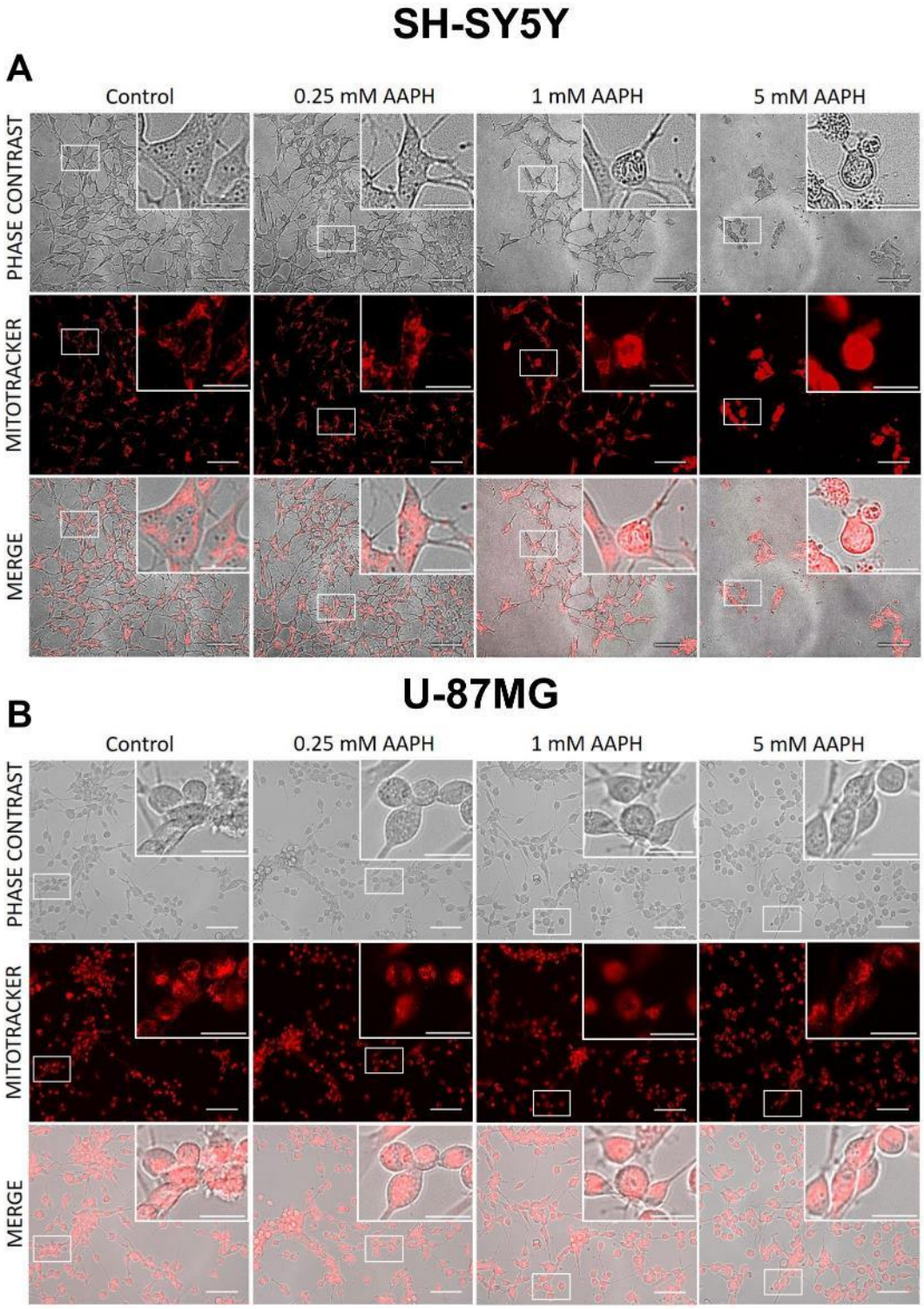

Figure 3.14 Neuronal SH-SY5Y and glial U-87MG morphology after 48-hour AAPH exposure. *Phase contrast microscopy and mitotracker staining (red) of (A) SH-SY5Y and (B) U-87MG monocultures after 48-hour AAPH exposure. Scale bar = 100 µm. Inset scale bar = 30 µm.*

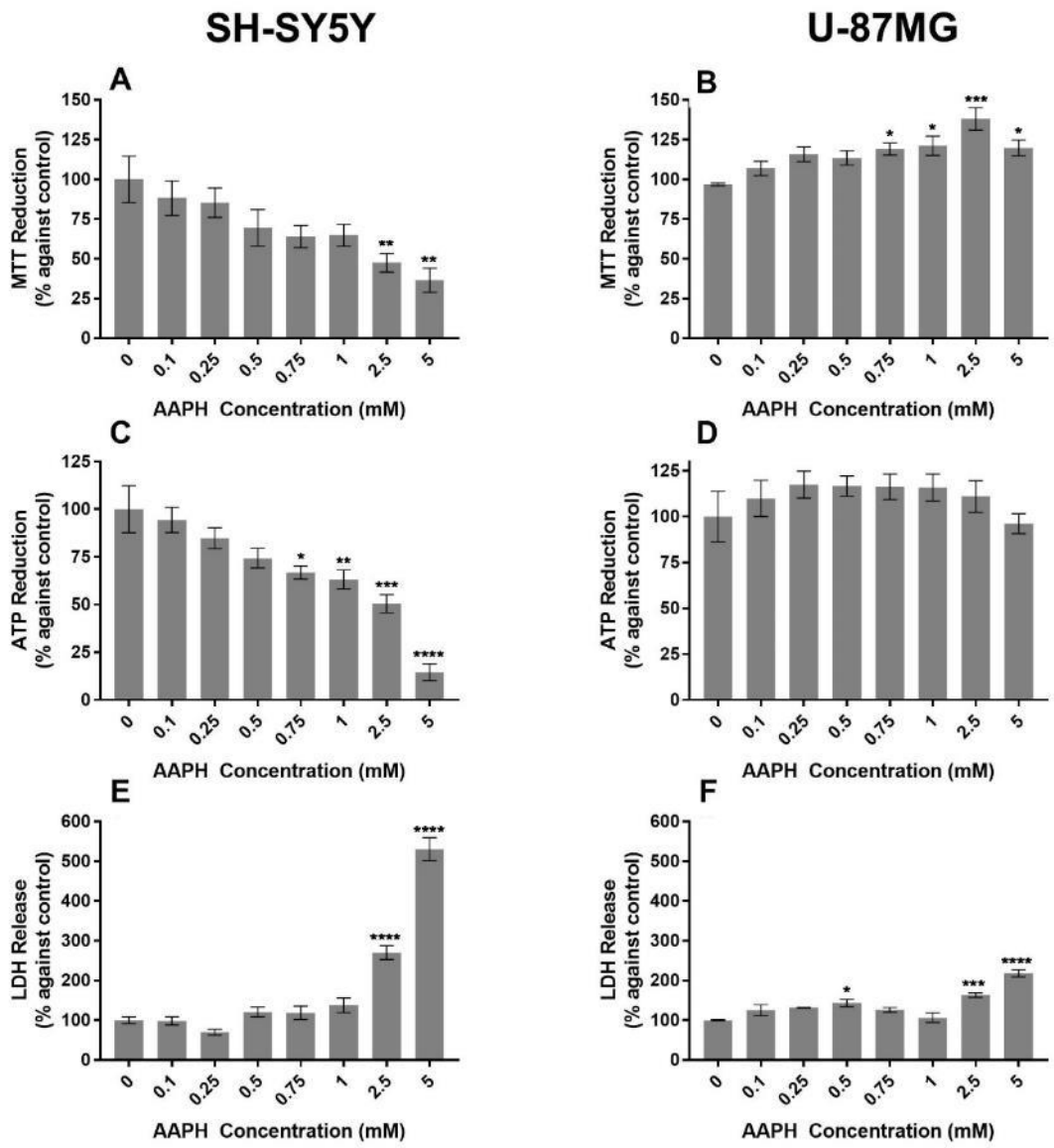

Figure 3.15 Neuronal SH-SY5Y and glial U-87MG cell viability after 48-hour AAPH exposure. *MTT reduction assay of (A) SH-SY5Y and (B) U-87MG cells treated with AAPH. Total ATP levels of (C) SH-SY5Y and (D) U-87MG monocultures treated with AAPH for 48 hours. LDH release of (E) SH-SY5Y and (F) U-87MG monocultures treated with AAPH for 48 hours. All viability assays are presented as mean % against control ± SEM. Statistical analysis was performed using one-way ANOVA with Dunnett's post-hoc test where n=3 for all experiments. Statistical significance was recorded as *p<0.05, **p<0.01, ***p<0.001 and ****p<0.0001.*

SH-SY5Y and U-87MG cells showed no significant change in metabolic function (MTT reduction and ATP levels; figure 3.13A, B, C, D) following 24-hour AAPH treatment. However, concentrations ≥2.5 mM AAPH resulted in increased LDH release (figure 3.13E and F), relating to reduced membrane integrity. Following 48-hour AAPH treatment, a dose-dependent effect on SH-SY5Y cell viability was observed with MTT reduction significantly decreased for ≥2.5 mM AAPH (figure 3.15A). In contrast, glial U-87MG cells showed a significant increase in MTT reduction for ≥0.75 mM AAPH following 48-hour treatment, suggesting a potential proliferative response (figure 3.15B). Cellular energy levels for neuronal SH-SY5Y cells showed a similar profile to the MTT reduction assays, where higher AAPH concentrations resulted in significantly decreased ATP levels (figure 3.15C). However, glial U-87MG cells showed no significant change in ATP levels for all concentrations of AAPH (figure 3.15D). Furthermore, at 48 hours LDH assays were exacerbated, where higher concentrations of AAPH (≥2.5 mM) resulted in significant LDH release (figure 3.15E, F), suggesting AAPH generated RS that may affect membrane integrity. In addition, glial cells showed lower LDH release with AAPH treatment than neurons for both 24- and 48-hours suggesting glia are less susceptible to loss of membrane integrity.

Neural cell viability was also investigated with rotenone induced RS assessed via morphological changes, viability and functional activity assays. Neural cells were exposed to a range of rotenone concentrations (0.01- 2.5 µM) for up to 48 hours.

Phase contrast microscopy of both neural cells (figure 3.16A, B) showed a dose-dependent decrease in cell density with greater intercellular distance observed, alongside a more rounded morphology consistent with loss of viability, further exacerbated at 48 hours (figure 3.18A, B). In addition, accumulation of cellular debris was observed at higher concentrations of rotenone. Furthermore U-87MG glia also showed aggregation and clustering with higher rotenone concentrations. Untreated cells labelled with MitoTracker Red® CMXRos (figure 3.16 and 3.18A, B) showed defined mitochondrial foci, whilst rotenone treatment of both neural cell types resulted in diffuse staining, indicative of loss of mitochondrial membrane integrity. Higher concentrations showed significantly reduced MTT (figure 3.17A, B), and ATP levels (figure 3.17C, D) with a corresponding increase in LDH release (figure 3.17E, F).

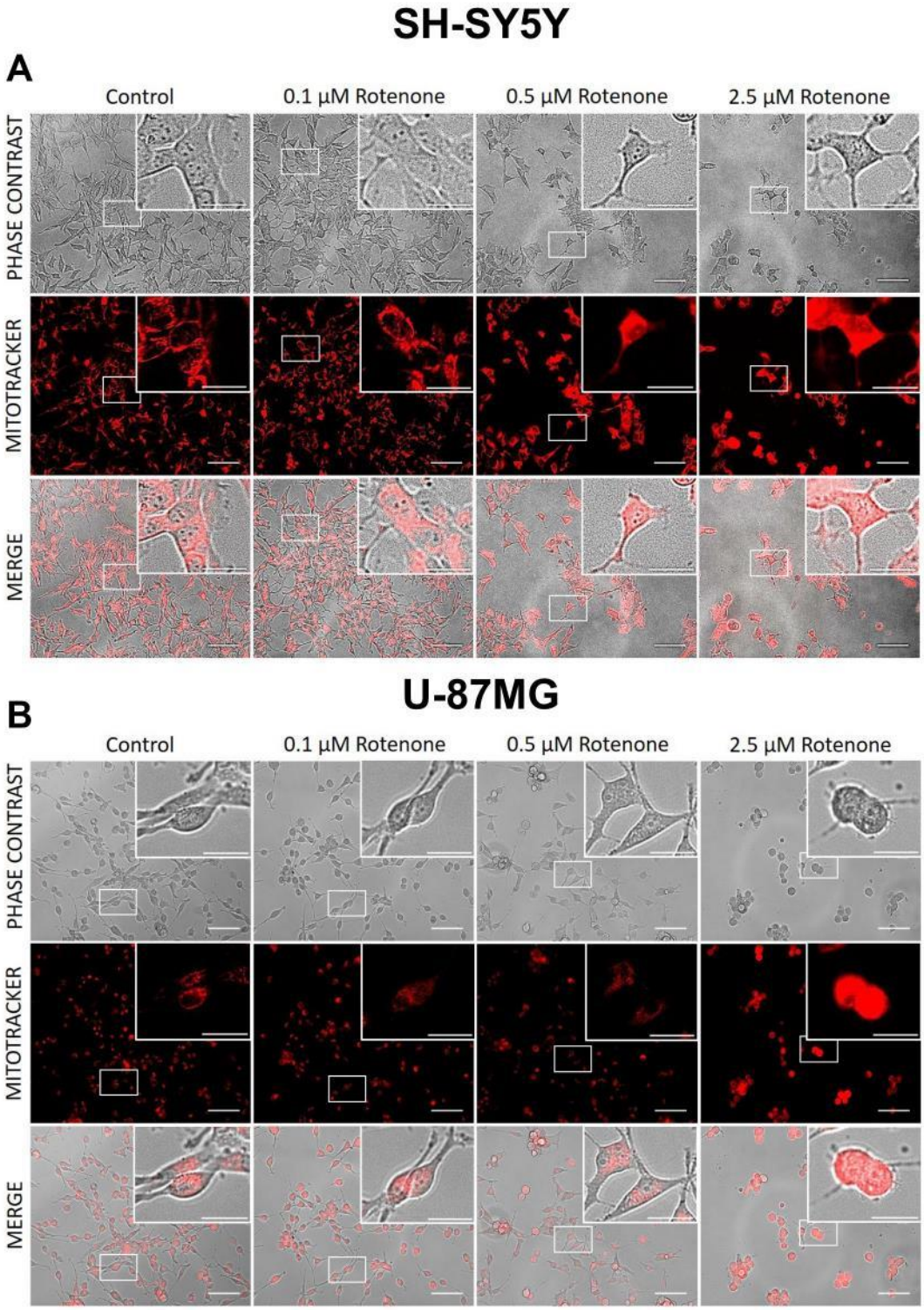

Figure 3.16 Neuronal SH-SY5Y and glial U-87MG cell morphology after 24-hour rotenone exposure. *Phase contrast microscopy and mitotracker staining (red) of (A) SH-SY5Y and (B) U-87MG monocultures after 24-hours rotenone exposure. Scale bar = 100 µm. Inset scale bar = 30 µm.*

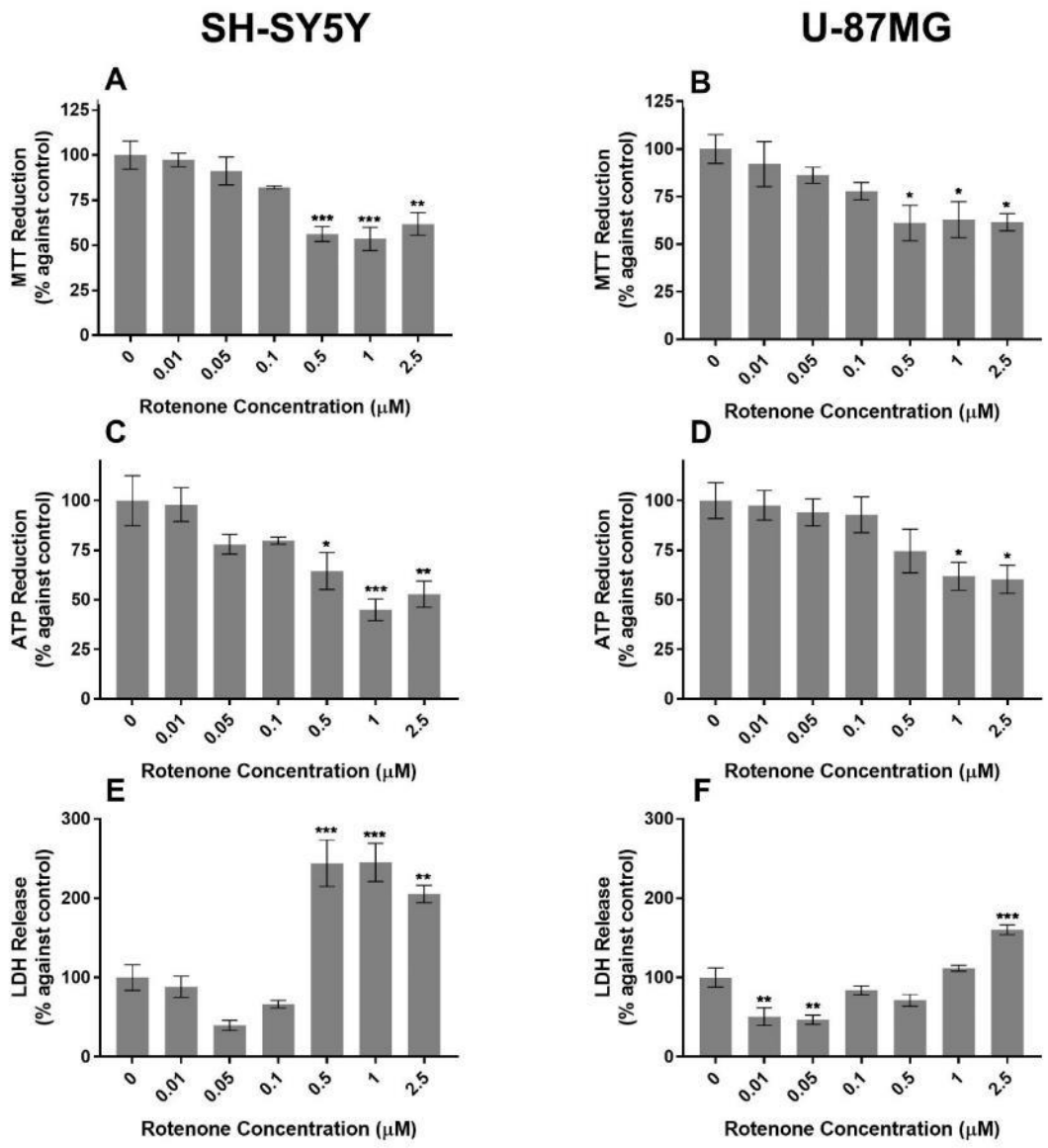

Figure 3.17 Neuronal SH-SY5Y and glial U-87MG cell viability after 24-hour rotenone exposure. *MTT reduction assay of (A) SH-SY5Y and (B) U-87MG cells treated with rotenone. Total ATP levels of (C) SH-SY5Y and (D) U-87MG monocultures treated with rotenone for 24 hours. LDH release of (E) SH-SY5Y and (F) U-87MG monocultures treated with rotenone for 24 hours. All viability assays are presented as mean % against control ± SEM. Statistical analysis was performed using one-way ANOVA with Dunnett's post-hoc test where n=3 for all experiments. Statistical significance was recorded as *p<0.05, **p<0.01 and ***p<0.001.*

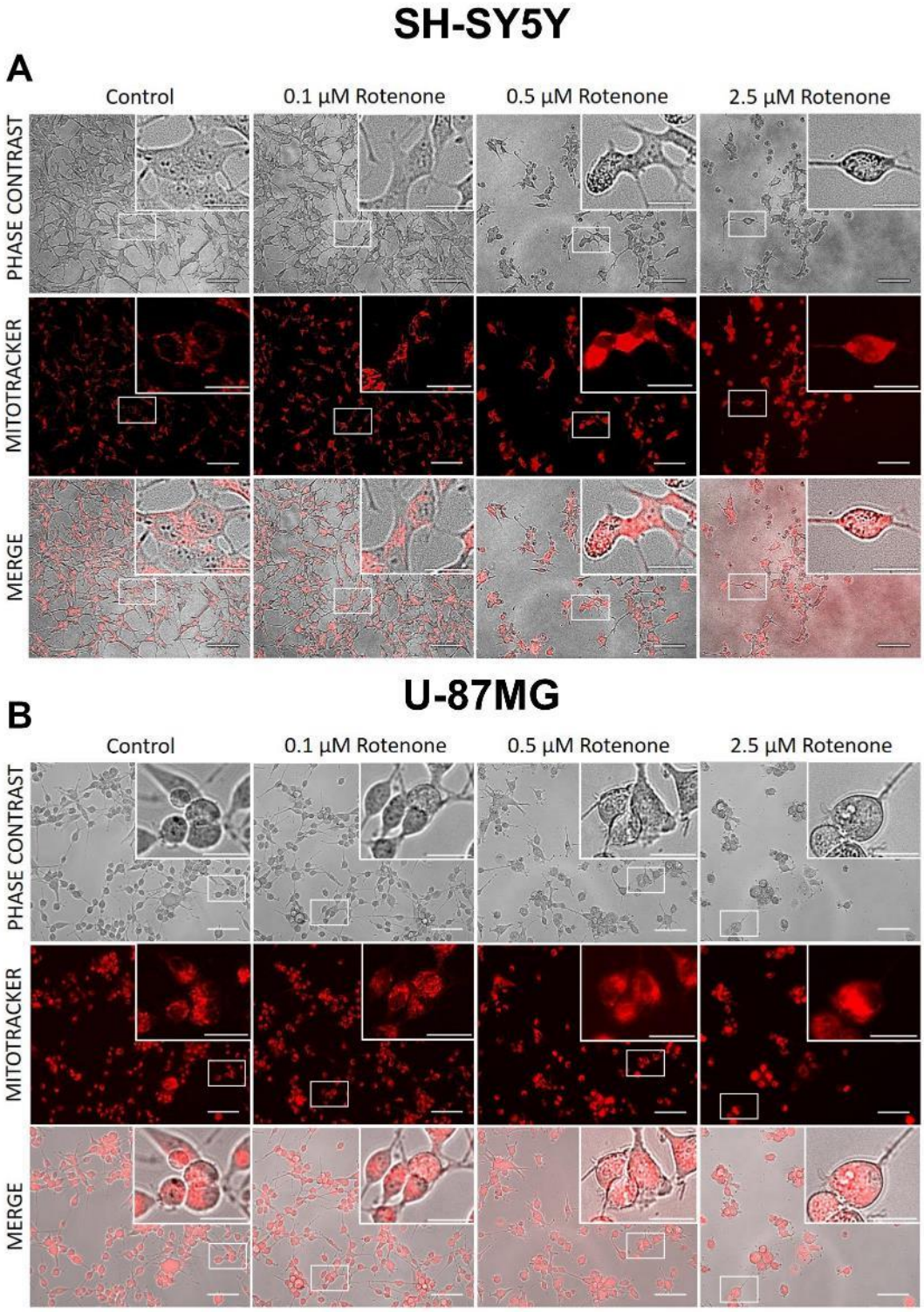

Figure 3.18 Neuronal SH-SY5Y and glial U-87MG cell morphology after 48-hour rotenone exposure. *Phase contrast microscopy and mitotracker staining (red) of (A) SH-SY5Y and (B) U-87MG monocultures after 48-hours rotenone exposure. Scale bar = 100 µm. Inset scale bar = 30 µm.*

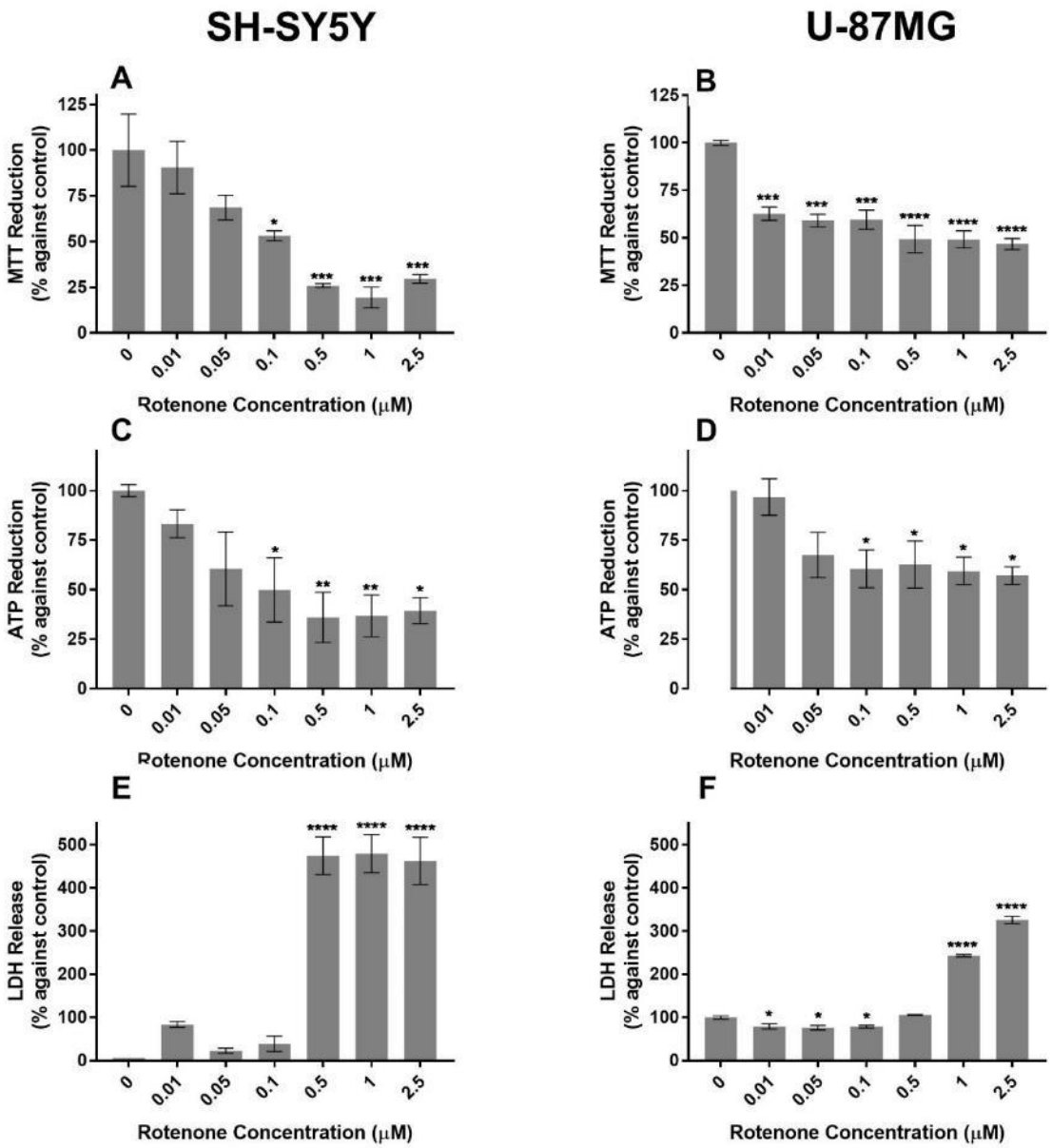

Figure 3.19 Neuronal SH-SY5Y and glial U-87MG cell viability after 48-hour rotenone exposure. *MTT reduction assay of (A) SH-SY5Y and (B) U-87MG cells treated with rotenone. Total ATP levels of (C) SH-SY5Y and (D) U-87MG monocultures treated with rotenone for 48 hours. LDH release of (E) SH-SY5Y and (F) U-87MG monocultures treated with rotenone for 48 hours. All viability assays are presented as mean % against control ± SEM. Statistical analysis was performed using one-way ANOVA with Dunnett's post-hoc test where n=3 for all experiments. Statistical significance was recorded as *p<0.05, **p<0.01, ***p<0.001 and ****p<0.0001.*

Following 48-hour rotenone treatment, cells showed an exacerbated dose-dependent loss of viability. MTT reduction assays showed concentrations of ≥0.1 μM significantly decreased viable SH-SY5Y cells (figure 3.19A), whereas all rotenone concentrations significantly decreased U-87MG cell viability (figure 3.19B); these results suggest glial cells are more susceptible to the cytotoxic effect of rotenone. Both neural cells exhibited significantly lower ATP levels at ≥0.1 μM rotenone (figure 3.19C, D) showing a concentration-dependent decrease in cellular energy levels for both neural cell types. Furthermore, LDH assays support decreased SH-SY5Y cell viability for ≥0.5 μM as a significant increase in LDH release was observed (Figure 3.19E). However, for glial cells only ≥1 μM rotenone showed a significant increase in LDH release (Figure 3.19F), further suggesting glia as less susceptible to loss of membrane integrity via RS induction.

3.2.4 Antioxidants attenuate neural death caused by oxidative stress

To confirm RS levels affected cell viability the antioxidants α-tocopherol (200 μM) and ascorbic acid (1 mM) were added concurrently with treatment (figure 3.20-7). Neural viability was again assessed by morphological changes, viability and functional activity assays. In addition, real-time analysis using the iCelligence system was used to track cell viability in a temporal manner.

Following 48-hour AAPH and rotenone treatment in the presence of α-tocopherol, cell death was attenuated (figure 3.20-3.21 and 3.22-3.23, respectively). Morphologically, both neural cells showed reduced intercellular distance and less rounding (figure 3.20 and 3.22A, B) when treated with AAPH and α-tocopherol, indicating improved neural viability. Neural viability improvement was also indicated by greater % MTT reduction (figure 3.21 and 3.23A, B) and reduced % LDH release (figure 3.21 and 3.23C, D) for both neural cell types, with both RS inducers. In addition, real-time analysis showed greater normalised cell index for both neural cell types treated with α-tocopherol (figure 3.21 and 3.23E, F) supporting viability assay data. Interestingly, U-87MG cells treated with AAPH and α-tocopherol showed greater % MTT reduction suggesting lowering the RS increases metabolic activity (figure 3.21B).

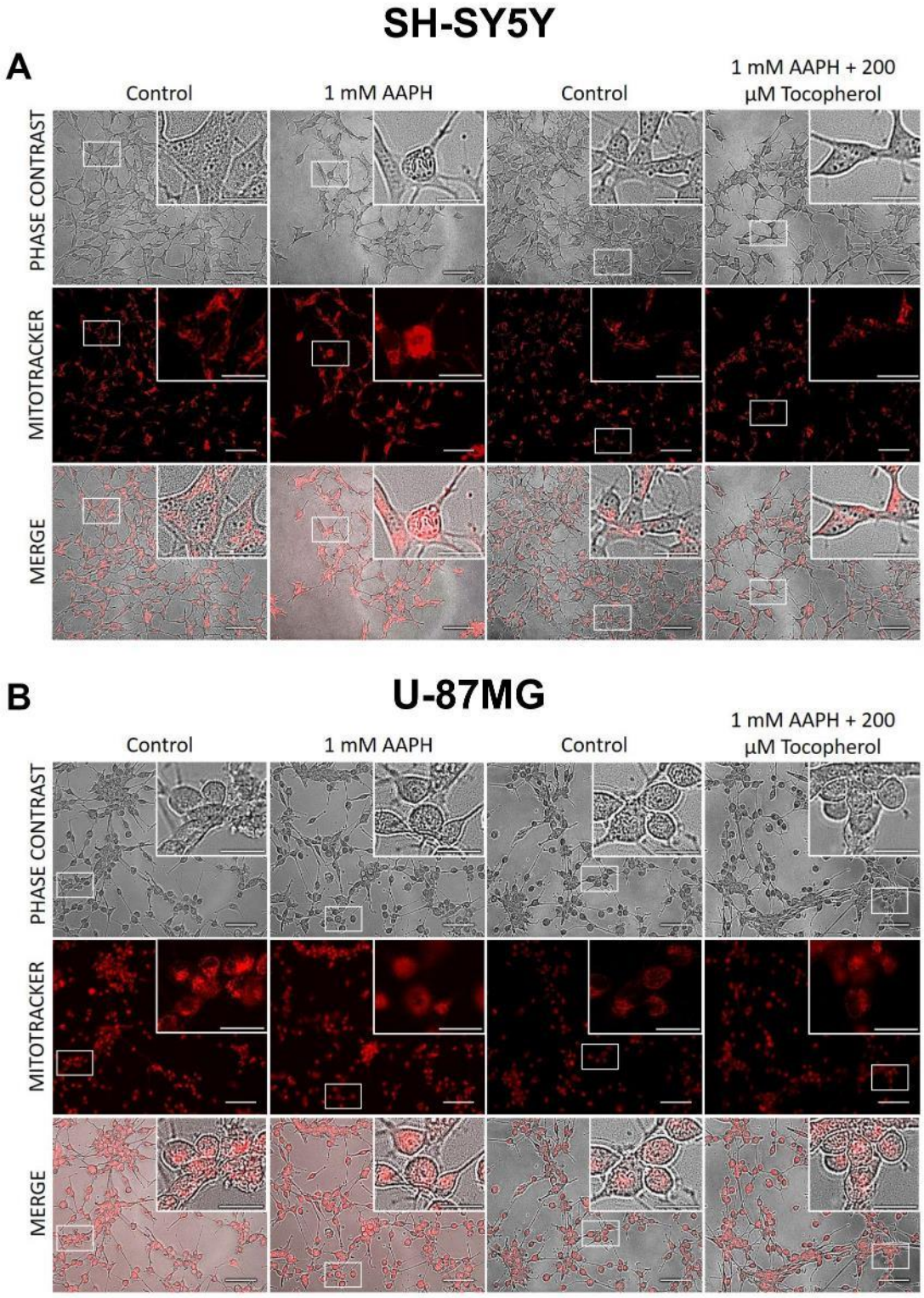

Figure 3.20 Neuronal SH-SY5Y and glial U-87MG cell morphology after 48-hour AAPH and α-tocopherol. *Viability assays were conducted on SH-SY5Y or U-87MG cells treated with AAPH for 48 hours with and without 200 µM α-tocopherol. Phase contrast microscopy and mitotracker staining (red) of (A) SH-SY5Y or (B) U-87MG monocultures. Scale bar = 100 µm. Inset scale bar = 30 µm.*

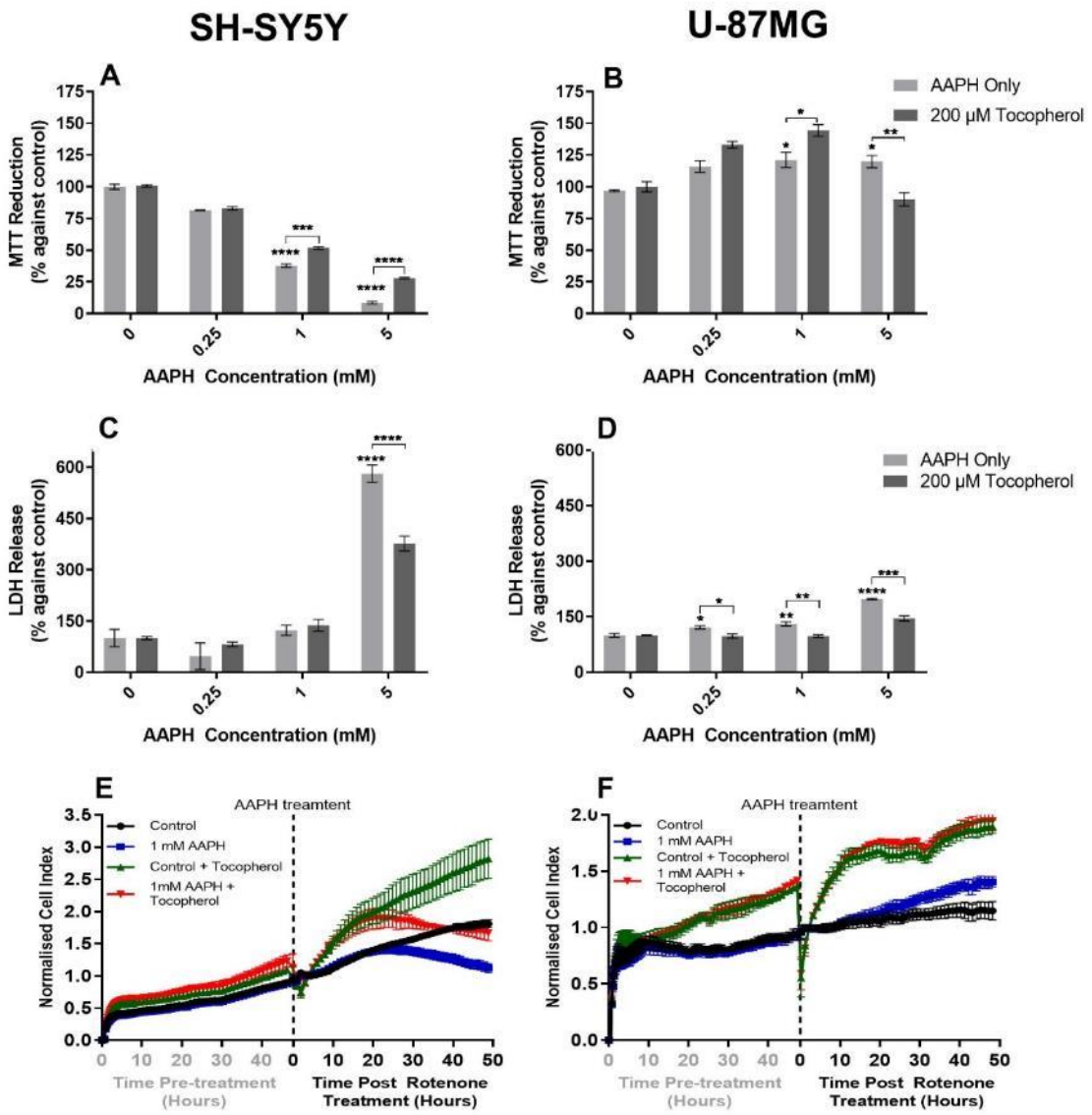

Figure 3.21 Neuronal SH-SY5Y and glial U-87MG cell viability after 48-hour AAPH and α-tocopherol. *Viability assays were conducted on SH-SY5Y or U-87MG cells treated with AAPH for 48 hours with and without 200 µM α-tocopherol. MTT reduction assay for (A) SH-SY5Y or (B) U-87MG monocultures. LDH release for (C) SH-SY5Y or (D) U-87MG monocultures. Real-time analysis with iCelligence for (E) SH-SY5Y or (F) U-87MG monocultures. Statistical analysis was performed using one-way ANOVA with Dunnett's post-hoc test where n=3 for all experiments. Statistical significance was recorded as *p<0.05, **p<0.01, ***p<0.001 and ****p<0.0001, where *'s above individual bars are relative to the control.*

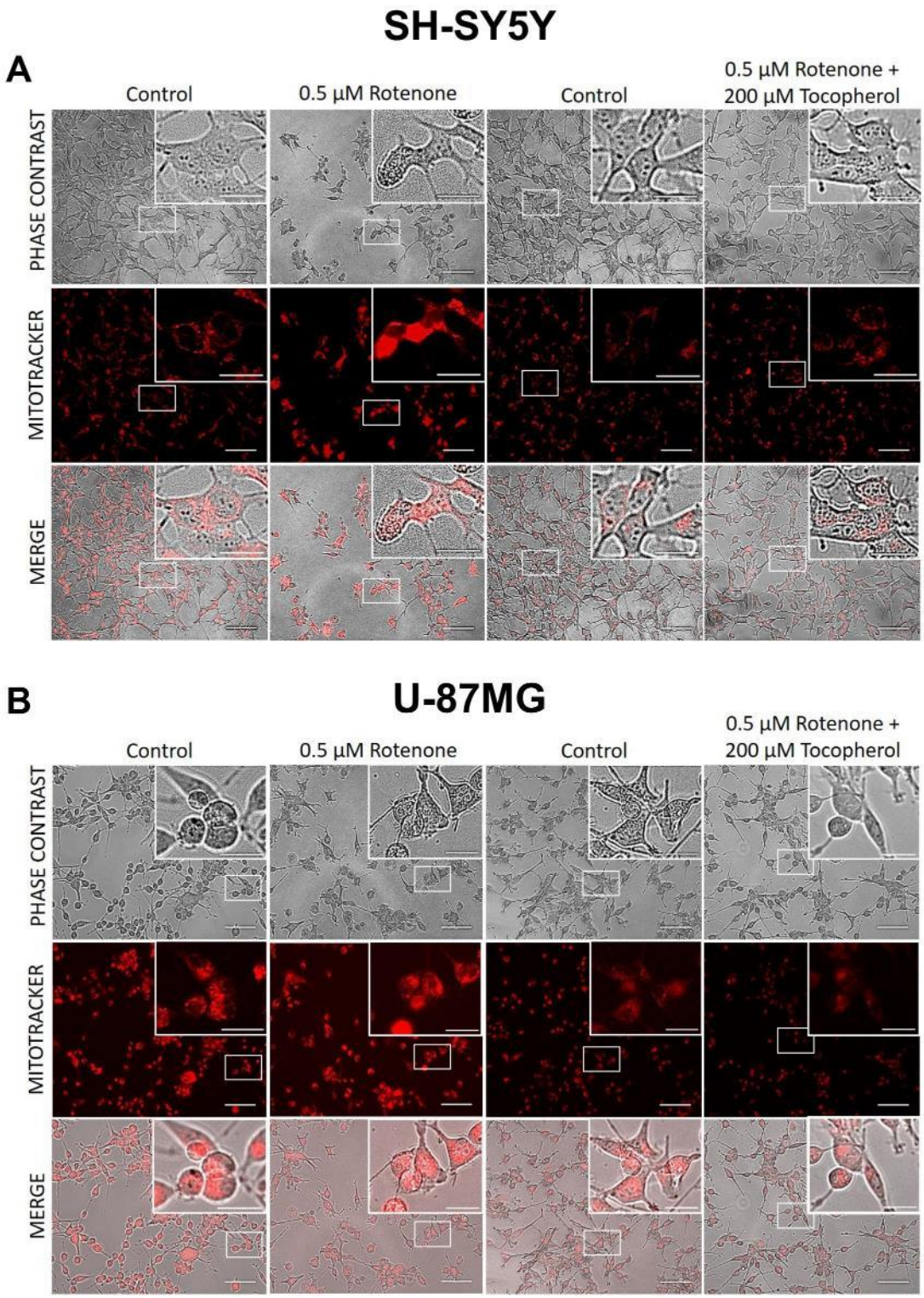

Figure 3.22 Neuronal SH-SY5Y and glial U-87MG cell morphology after 48-hour rotenone and α-tocopherol. *Viability assays were conducted on SH-SY5Y or U-87MG cells were treated with rotenone for 48 hours with and without 200 µM α-tocopherol. Phase contrast microscopy and mitotracker staining (red) of (A) SH-SY5Y or (B) U-87MG monocultures. Scale bar = 100 µm. Inset scale bar = 30 µm.*

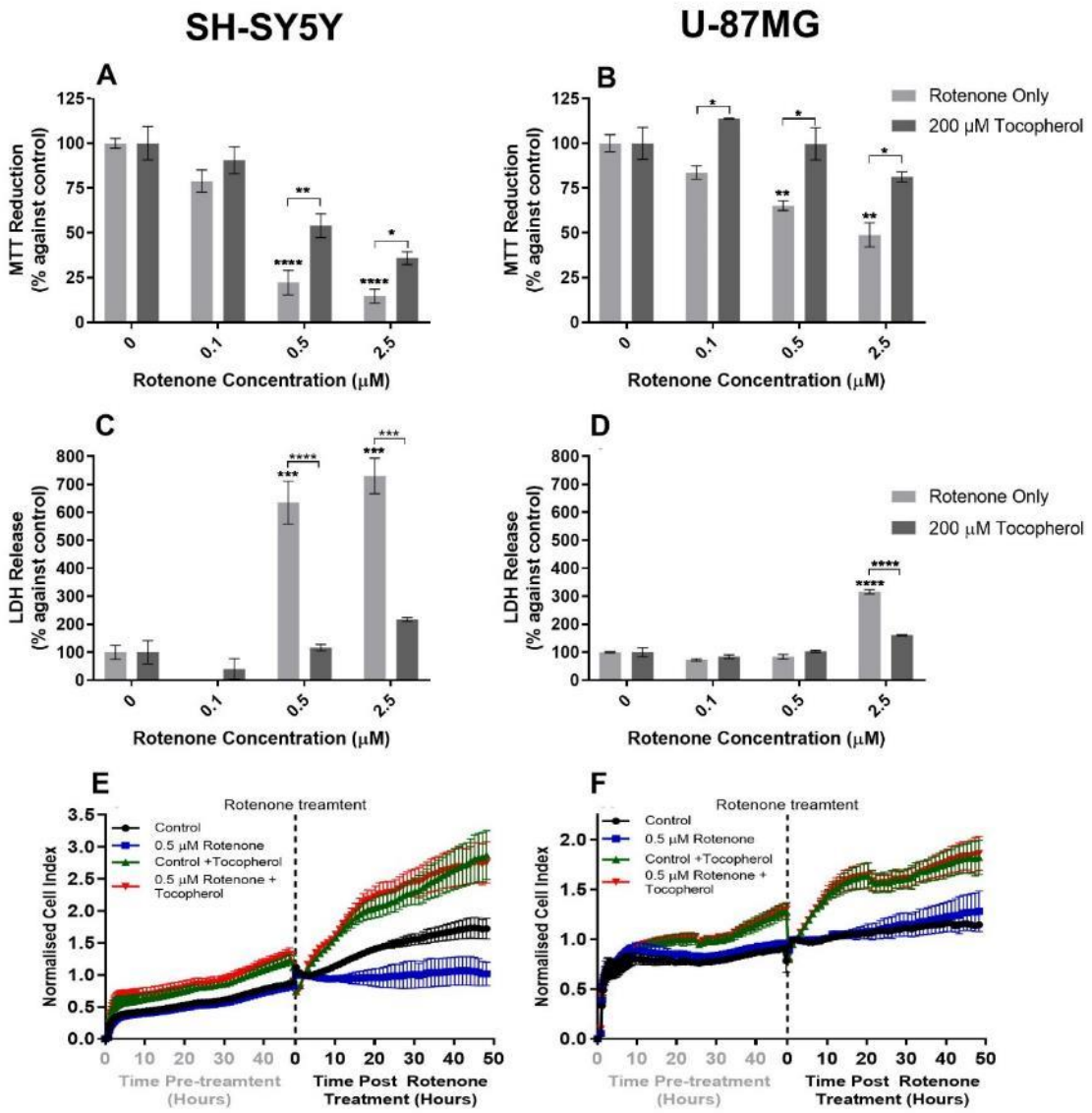

Figure 3.23 Neuronal SH-SY5Y and glial U-87MG cell viability after 48-hour rotenone and α-tocopherol. *Viability assays were conducted on SH-SY5Y or U-87MG cells were treated with rotenone for 48 hours with and without 200 μM α-tocopherol. MTT reduction assay for (A) SH-SY5Y or (B) U-87MG monocultures. LDH release for (C) SH-SY5Y or (D) U-87MG monocultures. Real-time analysis with iCelligence for (E) SH-SY5Y or (F) U-87MG monocultures. Statistical analysis was performed using one-way ANOVA with Dunnett's post-hoc test where n=3 for all experiments. Statistical significance was recorded as *p<0.05, **p<0.01, ***p<0.001 and ****p<0.0001, where *'s above individual bars are relative to the control.*

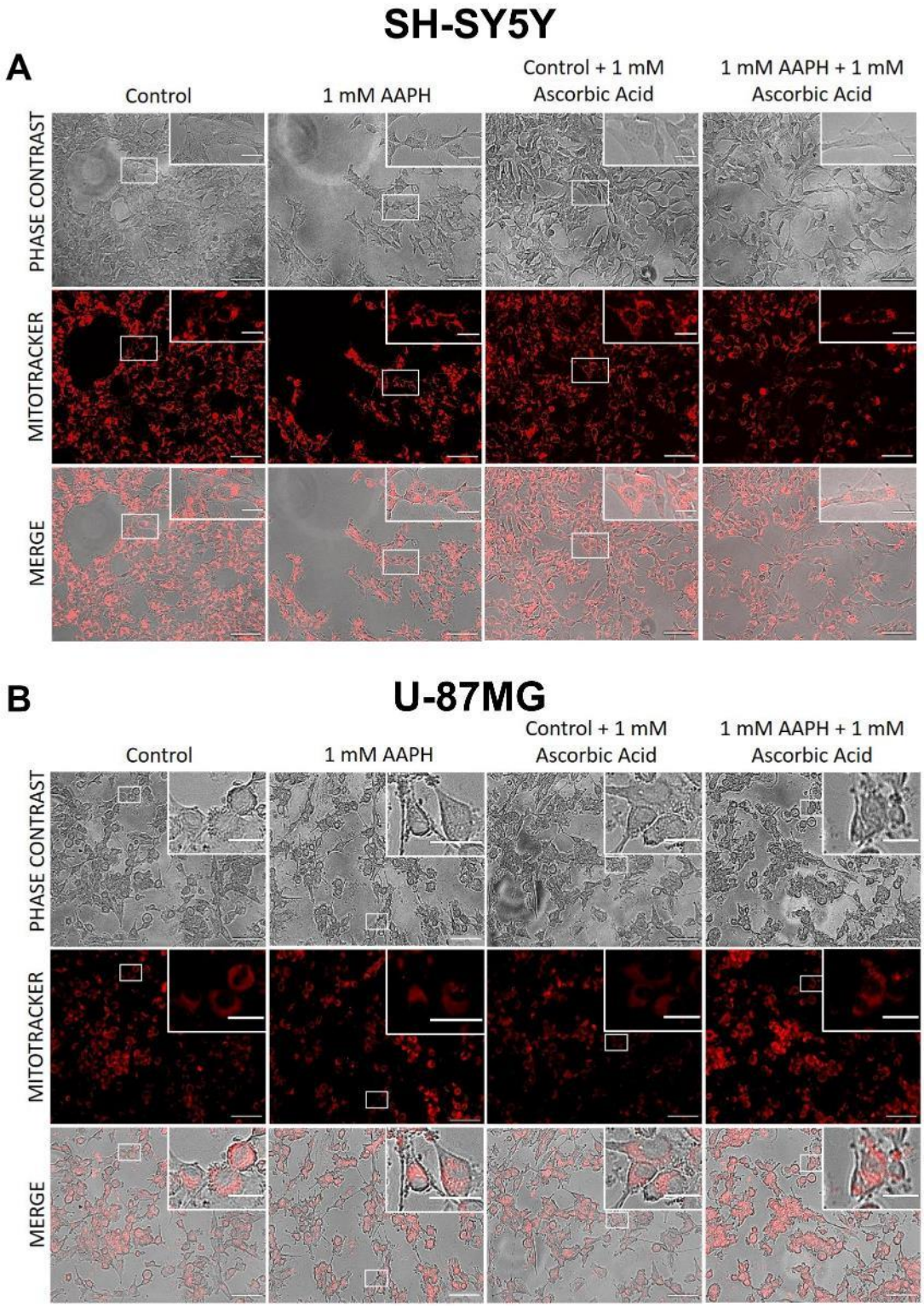

Figure 3.24 Neuronal SH-SY5Y and glial U-87MG cell morphology after 48-hour AAPH and ascorbic acid. *Viability assays were conducted on SH-SY5Y or U-87MG cells were treated with AAPH for 48 hours with and without 1 mM ascorbic acid. Phase contrast microscopy and mitotracker staining (red) of (A) SH-SY5Y or (B) U-87MG monocultures. Scale bar = 100 µm. Inset scale bar = 30 µm.*

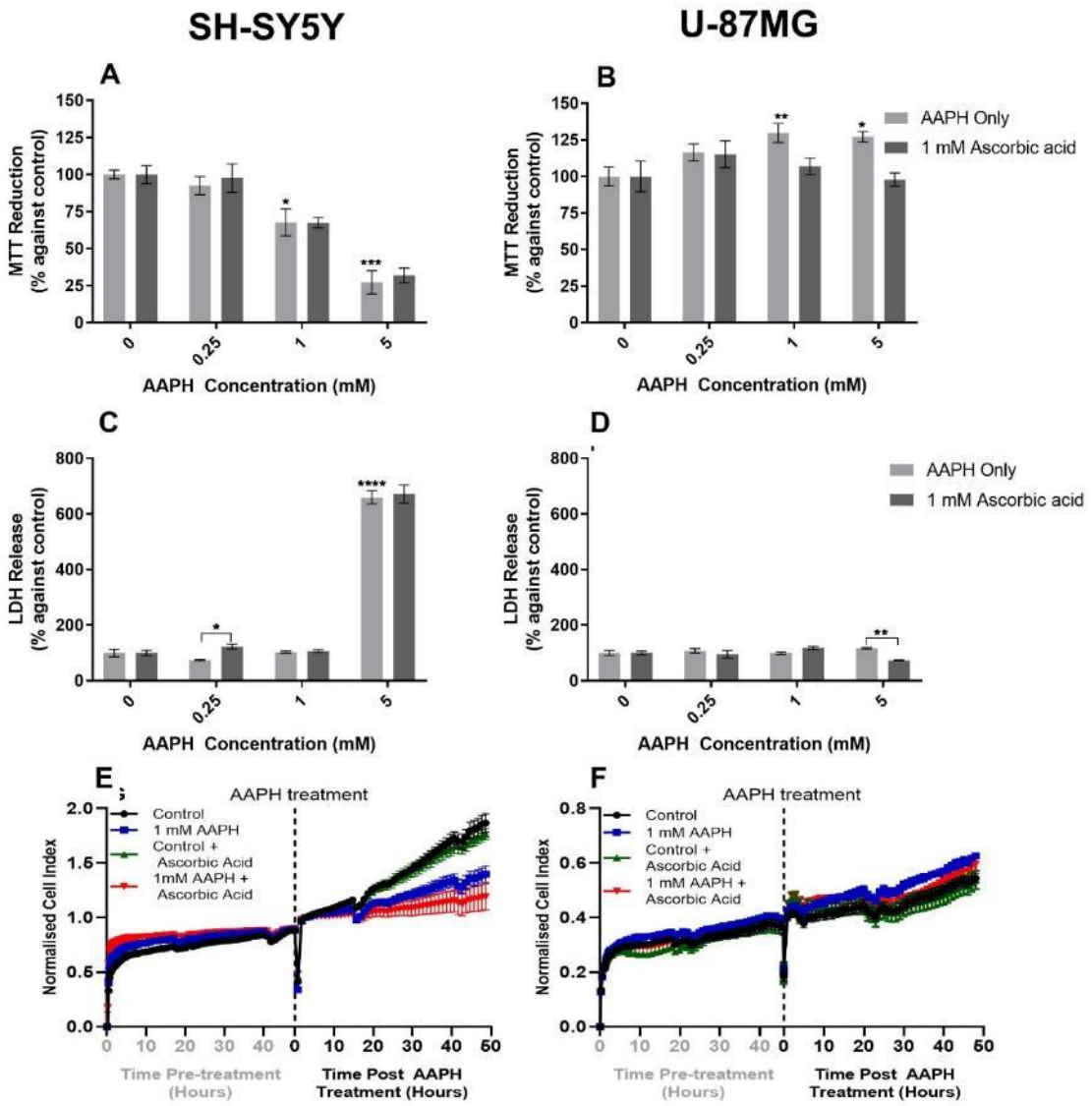

Figure 3.25 Neuronal SH-SY5Y and glial U-87MG cell viability after 48-hour AAPH and ascorbic acid. *Viability assays were conducted on SH-SY5Y or U-87MG cells were treated with AAPH for 48 hours with and without 1 mM ascorbic acid. MTT reduction assay for (A) SH-SY5Y or (B) U-87MG monocultures. LDH release for (C) SH-SY5Y or (D) U-87MG monocultures. Real-time analysis with iCelligence for (E) SH-SY5Y or (F) U-87MG monocultures. Statistical analysis was performed using one-way ANOVA with Dunnett's post-hoc test where n=3 for all experiments. Statistical significance was recorded as * or # - *p<0.05, **p<0.01, ***p<0.001 and ****p<0.0001, where *'s above individual bars are relative to the control.*

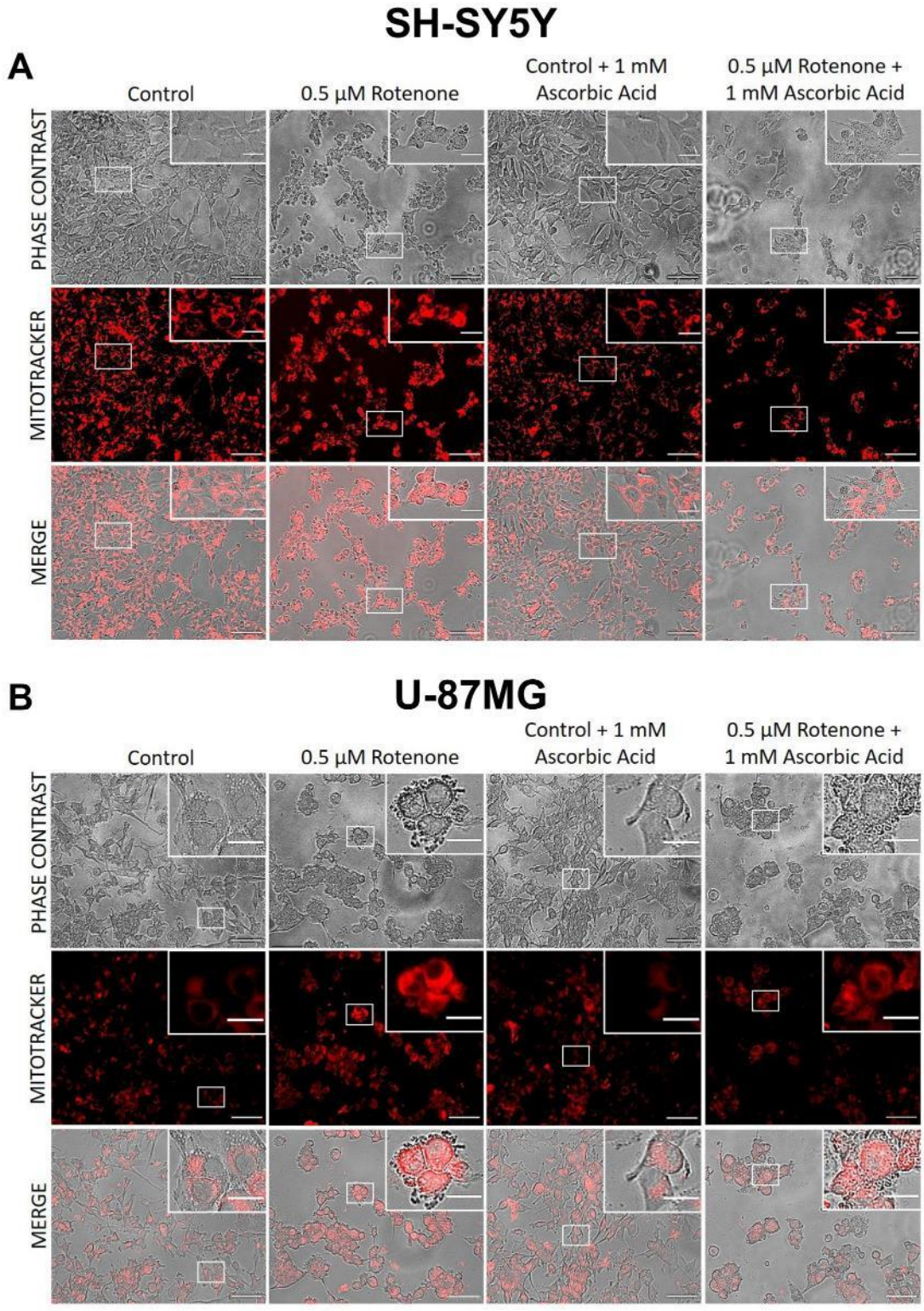

Figure 3.26 Neuronal SH-SY5Y and glial U-87MG cell morphology after 48-hour rotenone and ascorbic acid. *Viability assays were conducted on SH-SY5Y or U-87MG cells were treated with rotenone for 48 hours with and without 1 mM ascorbic acid. Phase contrast microscopy and mitotracker staining (red) of (A) SH-SY5Y or (B) U-87MG monocultures. Scale bar = 100 µm. Inset scale bar = 30 µm.*

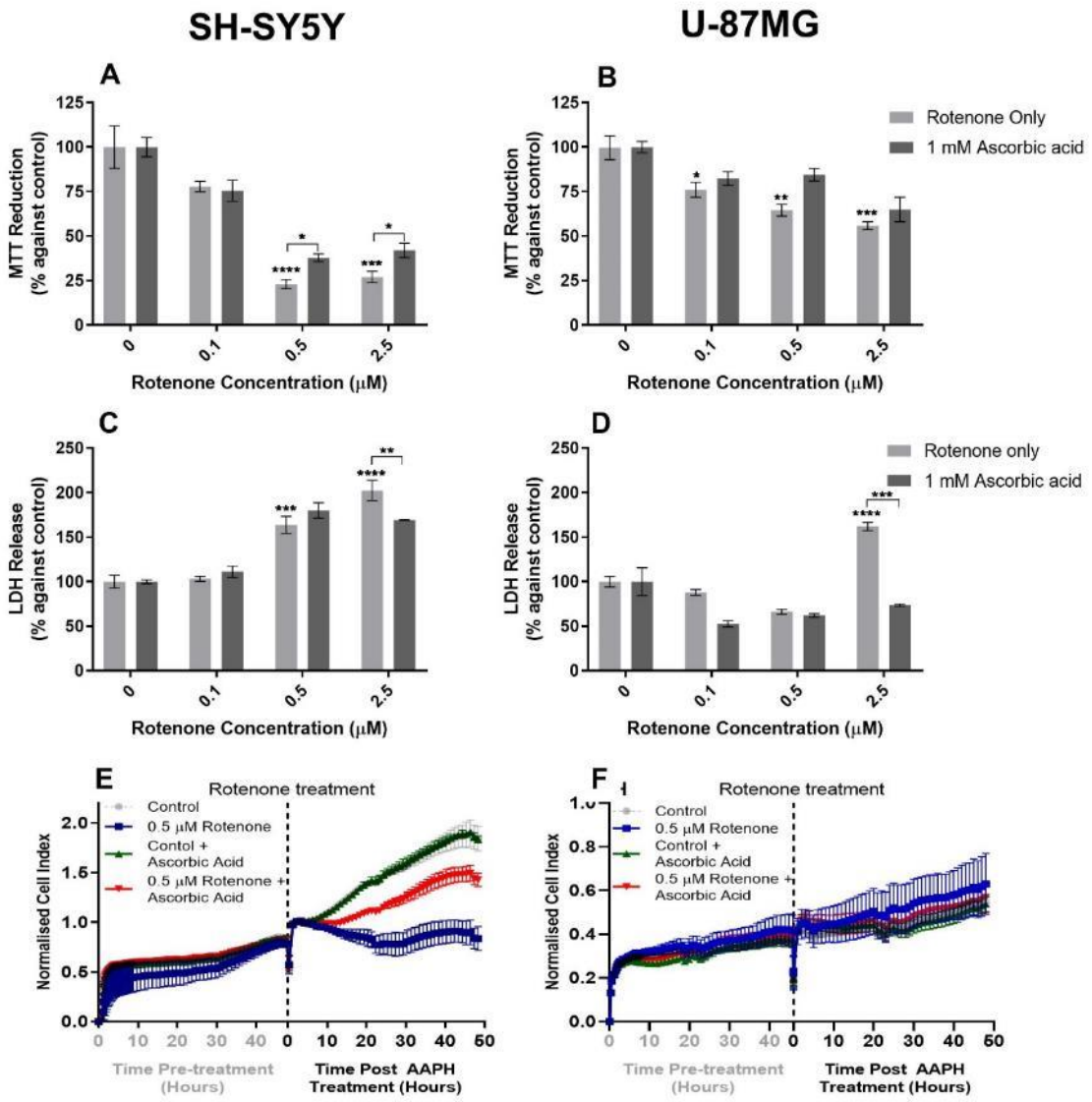

Figure 3.27 Neuronal SH-SY5Y and glial U-87MG cell viability after 48-hour rotenone and ascorbic acid. *Viability assays were conducted on SH-SY5Y or U-87MG cells were treated with rotenone for 48 hours with and without 1 mM ascorbic acid. MTT reduction assay for (A) SH-SY5Y or (B) U-87MG monocultures. LDH release for (C) SH-SY5Y or (D) U-87MG monocultures. Real-time analysis with iCelligence for (E) SH-SY5Y or (F) U-87MG monocultures. Statistical analysis was performed using one-way ANOVA with Dunnett's post-hoc test where n=3 for all experiments. Statistical significance was recorded as * or # - *p<0.05, **p<0.01, ***p<0.001 and ****p<0.0001.*

Ascorbic acid treatment showed different effects on rotenone- or AAPH-induced cell death (figure 3.24-3.25 and figure 3.26-3.27, respectively). For both neural cells treated with ascorbic acid, morphological changes induced by AAPH were unchanged (figure 3.24A, B). In addition, MTT reduction (figure 3.25A, B) and LDH release were unchanged (figure 3.25C, D). Real-time analysis with the iCelligence showed a comparable normalised cell index (figure 3.25E, F), indicating no improvement in cell viability from ascorbic acid treatment. In contrast, ascorbic acid improved rotenone-induced neuronal cell death as shown by the increased % MTT reduction (figure 3.27A), reduced LDH release (figure 3.27C) and a higher normalised cell index (figure 3.27E). However, glial U-87MG cells treated with rotenone and ascorbic acid still retained greater intercellular distances, as well as rounding and clustering (figure 3.26B), indicative of cell death and apoptosis. Viability assays also suggested ascorbic acid did not improve glial viability with no improvements seen in % MTT reduction (figure 3.27B), LDH release (figure 3.27D), or normalised cell index (figure 3.27F).

Together, these results suggest that α-tocopherol, a known scavenger of peroxy radicals can rescue both neurons and glia exposed to AAPH and rotenone. Whereas ascorbic acid, a predominantly superoxide scavenger was only able to increase the viability of neurons treated with rotenone but had no effect on AAPH treated neural cells or rotenone treated glial cells. This supports previous measurements of RS with DCF, suggesting OS generated by AAPH and rotenone affect neural cell viability through distinct RS production, which are attenuated by specific antioxidants.

3.2.5 Oxidative stress effects mitochondrial function

As mitochondrial dysfunction is another pathological hallmark of neurodegeneration the effect of the RS-inducers on mitochondrial function was investigated. Furthermore, as viability assays suggested U-87MG glia cells were more sensitive to rotenone induced RS (figure 3.19), it was important to examine the effect of RS on mitochondrial pathways in the different neural cell types.

Initially, mitochondrial DNA content was determined using quantitative real-time polymerase chain reactions (qRT-PCR) for both SH-SY5Y neuronal and U-87MG glial cells (figure 3.28). qRT-PCR revealed U-87MG glial cells exhibited significantly lower expression of mitochondrial genes relative to SH-SY5Y neuronal cells.

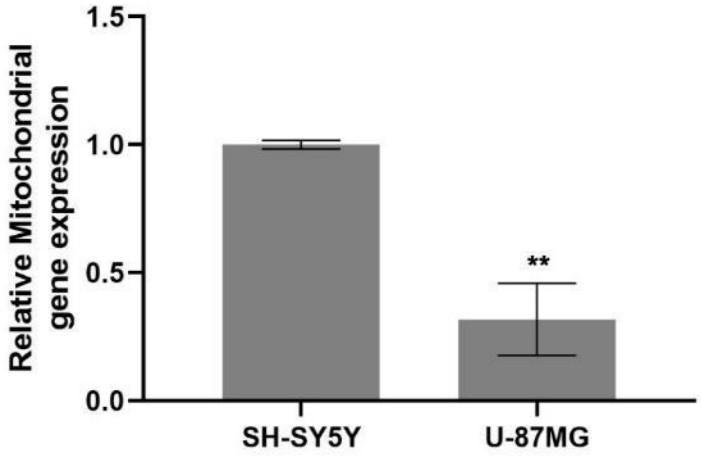

Figure 3.28 Glial U-87MG cells express lower levels of mitochondrial DNA than neuronal SH-SY5Y cells. *Cells were grown to 70-80% confluence before DNA was extracted using the PureLink® genomic DNA kit as per the manufacturer's instructions. 50 ng of DNA was subsequently used for qRT-PCR. Statistical analysis was performed using an unpaired t-test where n=3 for all experiments. Statistical significance was recorded as *p<0.05 and **p<0.01.*

Further supporting U-87MG glial possibly having lower mitochondrial levels than SH-SY5Y neuronal cells, oxygen consumption rate (OCR) and extracellular acidification rate (ECAR) was measured using the Seahorse XFe real-time cell analyser (figure 3.29A, B). Analysis showed that overall U-87MG cells had a greater ATP production (figure 3.29D) and ECAR (figure 3.29B) than SH-SY5Y neuronal cells. Specifically, control U-87MG glial cells exhibited a higher rate of ATP production from glycolysis than control SH-SY5Y neuronal cells; the latter relying more on mitochondrial ATP production (figure 3.29C, E). Therefore, qRT-PCR and Seahorse analysis highlighted the differences in mitochondrial function for distinct neural cell types.

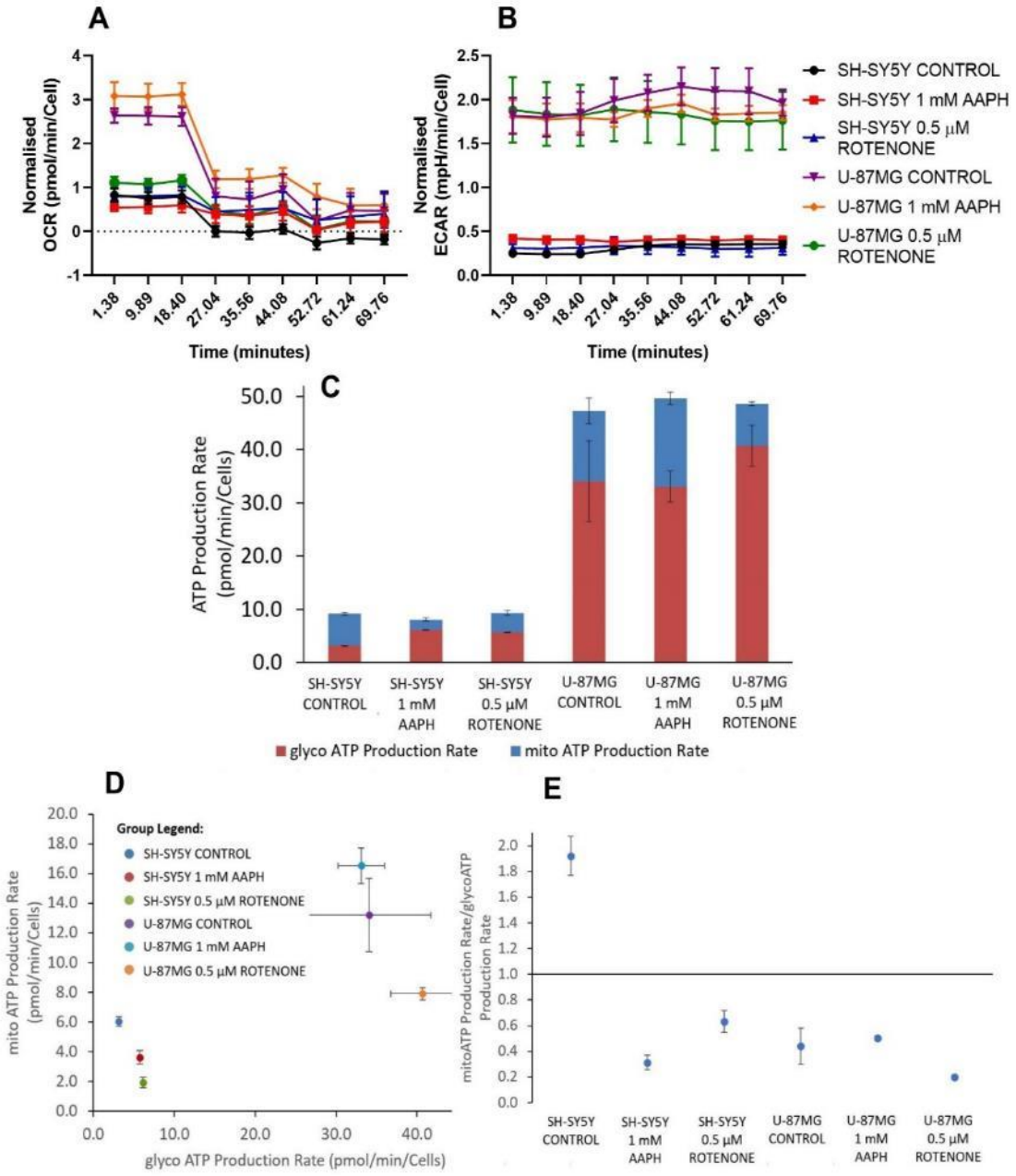

Figure 3.29 AAPH and rotenone increases glycolytic respiration in neuronal and glial cells. *(A) Oxygen consumption rate (OCR) and (B) extracellular acidification rate (ECAR) were concomitantly measured after 24 hours of 1 mM AAPH or 0.5 µM rotenone treatment for both SH-SY5Y neuronal and U-87MG glial cells. Using the Seahorse ATP report generator (C) glycolytic and mitochondrial basal ATP production rate was calculated. (D) An energetic map was also generated to show if cells or treatments resulted in a more glycolytic or mitochondrial ATP production which is further demonstrated in the (E) XF ATP rate index.*

To investigate the effect of RS inducers on cellular respiration both SH-SY5Y and U-87MG cells were incubated with 1 mM AAPH and 0.5 µM rotenone for 24 hours, prior to Seahorse analysis. Mammalian cells mainly generate ATP via glycolysis and oxidative phosphorylation (OXPHOS) utilising mitochondria. Both pathways contribute to media acidification (ECAR), either by glucose conversion to lactate during glycolysis accompanied by proton efflux, or OXPHOS, which consumes oxygen (OCR) while producing CO_2. Using the Seahorse basal ECAR and OCR were simultaneously measured for each cell line and treatment. Oligomycin and a combination of rotenone/antimycin A were added sequentially, where oligomycin inhibits ATP synthase decreasing OCR allowing mitochondrial ATP rate to be calculated. The addition of rotenone and antimycin A completely inhibits the electron transport chain so only the proton efflux from glycolysis occurs allowing glycolysis ATP production to be calculated. Both AAPH and rotenone treated SH-SY5Y cells exhibited higher ECAR and reduced OCR, suggesting a more glycolytic ATP production rate relative to control SH-SY5Y cells (figure 3.29C, D, and E). Rotenone but not AAPH increased ECAR and decreased OCR, suggesting a greater glycolytic ATP production rate in U-87MG glial cells (figure 3.29C, D and E). This suggests rotenone affects mitochondrial function as both cell lines show an increase in ECAR and drop in OCR, suggesting these cells increased their use of glycolysis to compensate for their loss of OXPHOS for ATP production. Whereas AAPH only appears to affect SH-SY5Y neuronal cell respiration and not glial, which suggests specific neural cell types respond differently to RS.

As RS generated by AAPH and rotenone affected respiration and mitochondrial damage is often associated with loss of membrane potential, the dual wavelength fluorescent probe, JC-1 was used to assess mitochondrial membrane potential. Both 24-hour AAPH and rotenone treated SH-SY5Y neuronal cells exhibited reduced membrane potential as a lower ratio of red aggregates to green monomers was observed (figure 3.30A, C, G, and E). Interestingly, while U-87MG glial cells treated with rotenone showed reduced membrane potential (figure 3.31C and D), AAPH increased membrane potential for the highest concentration of AAPH, suggesting AAPH initially improved mitochondrial function in glia (figure 3.31A and B). Therefore, rotenone appears to decrease both neural cells mitochondrial membrane potential, whereas AAPH decreases SH-SY5Y while increasing U-87MG membrane potential suggesting RS effect mitochondrial function in different ways.

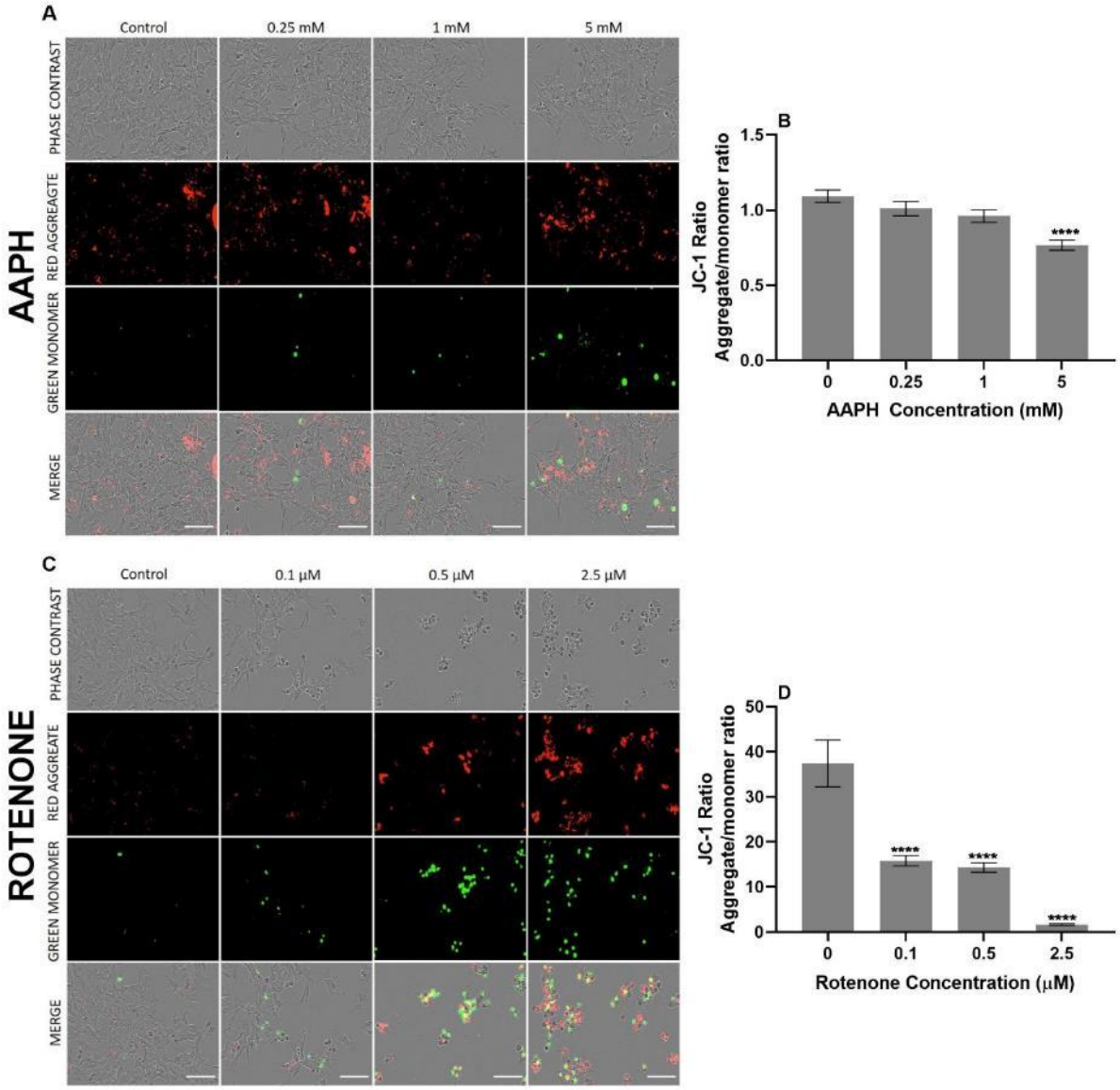

Figure 3.30 Mitochondrial membrane assessment in neuronal SH-SY5Y cells in response to 24-hour AAPH and rotenone treatment. *JC-1 was used to assess neuronal membrane potential of SH-SY5Y cells treated with AAPH (A, B) or rotenone (C, D) after 24-hour treatment. Scale bar = 200 µm. Phase, green and red images were taken and quantified using the incucyte S3 live-cell analysis system. Red to green ratio was calculated and statistical analysis was performed using one-way ANOVA with Dunnett's post-hoc test where n=4 for all experiments. Statistical significance was recorded as *p<0.05, **p<0.01, ***p<0.001 and ****p<0.0001.*

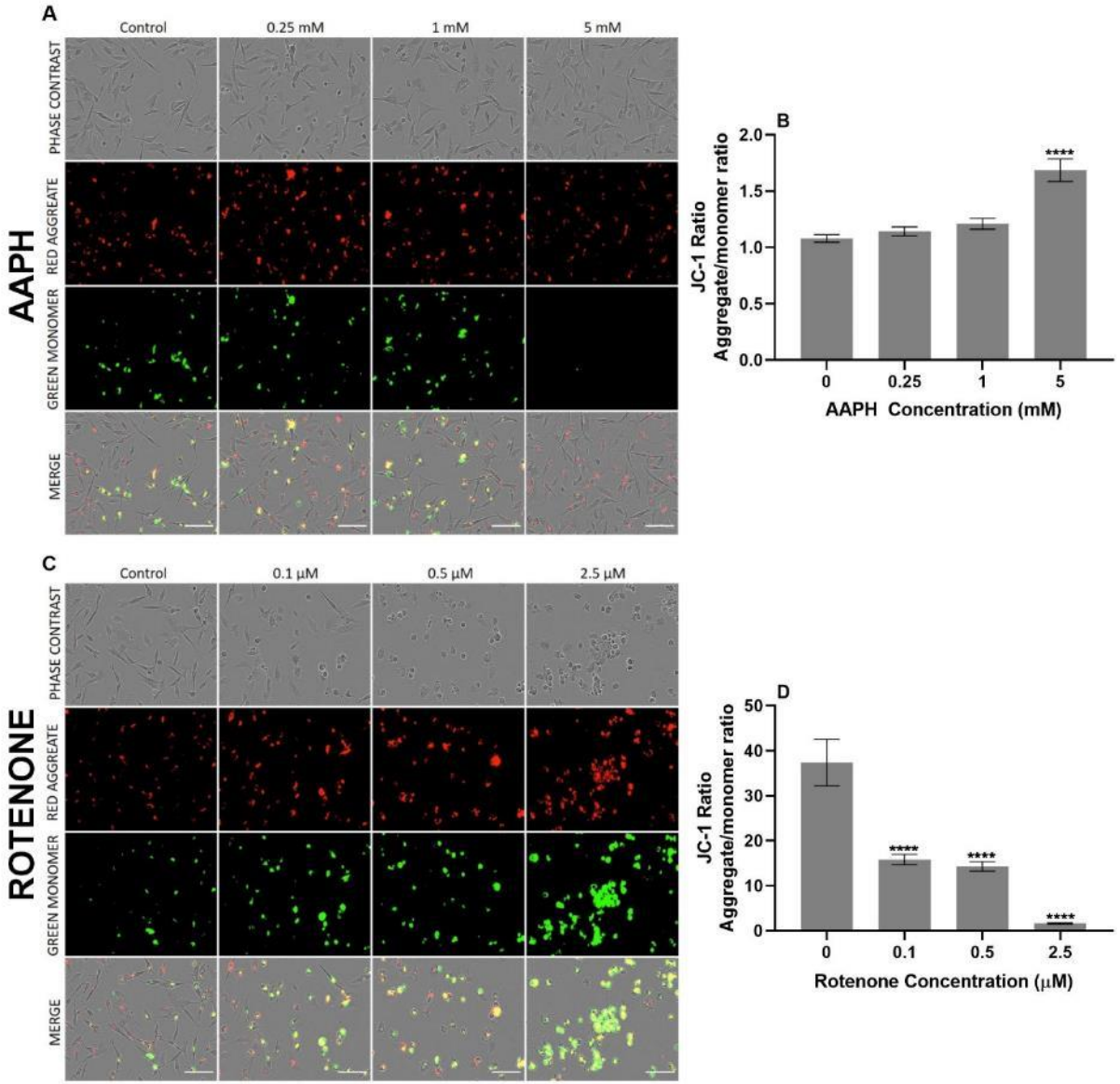

Figure 3.31 Mitochondrial membrane assessment in glial U-87MG cells in response to 24-hour AAPH and rotenone treatment. *JC-1 was used to assess glial membrane potential of U-87MG cells treated with AAPH (A, B) or rotenone (C, D) after 24-hour treatment. Scale bar = 200 µm. Phase, green and red images were taken and quantified using the incucyte S3 live-cell analysis system. Red to green ratio was calculated and statistical analysis was performed using one-way ANOVA with Dunnett's post-hoc test where n=4 for all experiments. Statistical significance was recorded as *p<0.05, **p<0.01, ***p<0.001 and ****p<0.0001.*

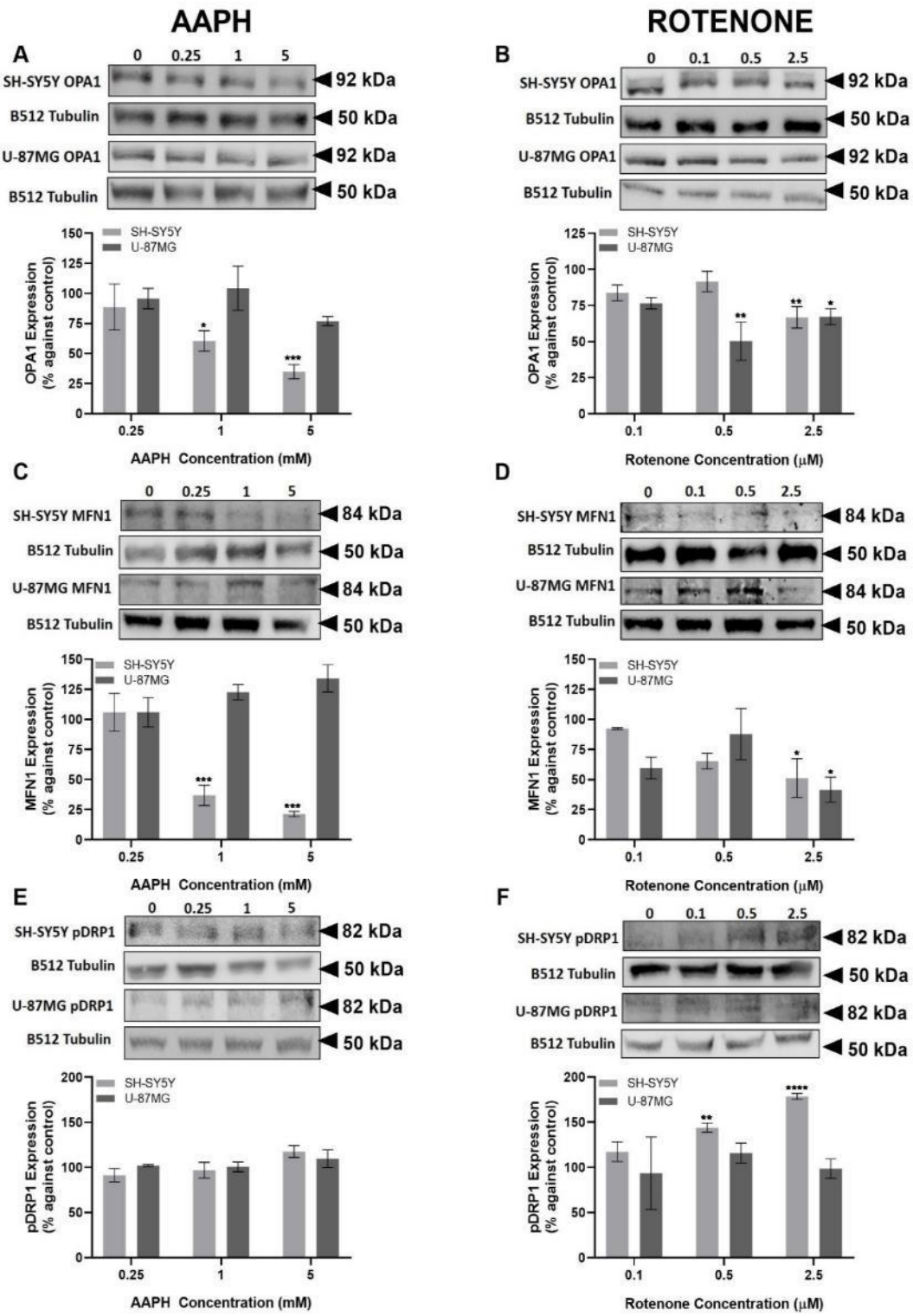

Figure 3.32 AAPH and rotenone-induced oxidative stress affects mitochondrial fission and fusion protein levels. *Representative Western blots of neuronal SH-SY5Y and glial U-87MG cells were treated with AAPH or rotenone for 24 hours and total cell extracts were probed with (A,B) optic atrophy 1(OPA1; 1:1000), (C,D) mitofusin-1 (MFN1; 1:500) and (E,F) phosphorylated dynamin-1-like protein (pDRP1; 1:500). Each Western blot is accompanied by a plot summarising densitometric analyses of Western blots using AIDA software. Results are presents as % against control ± SEM. Statistical analysis was performed using one-way ANOVA with Dunnett's post-hoc test where n=4 for all experiments. Statistical significance was recorded as *p<0.05, **p<0.01, ***p<0.001 and ****p<0.0001.*

To determine the molecular mechanisms responsible for the change in ATP production and the effect of mitochondrial dysfunction, mitochondrial fission and fusion proteins were examined following 24-hour treatment. Various protein responsible for the fission/fusion balance including optic atrophy 1 (OPA1), mitofusion-1 (MFN1) and phosphorylated-dynamin 1-like protein (pDRP1) were investigated. Western blot analyses showed AAPH resulted in a dose-dependent decrease in fusion associated protein OPA1 (figure 3.32A) and MFN1 (figure 3.32C), while the level of pDRP1 was unchanged in SH-SY5Y neuronal cells. Whereas AAPH treated U-87MG glial cells showed no significant change in mitochondrial biogenesis proteins OPA1, MFN1 and pDRP1 (figure 3.32A, C, and E). Rotenone treated SH-SY5Y and U-87MG cells exhibited a dose-dependent decrease in OPA1 and MFN1 levels (figure 3.32B, D). Furthermore, SH-SY5Y neurons treated with rotenone exhibited significantly increased pDRP1 levels, whereas U-87MG glial cells showed no significant change in pDRP1. Therefore, AAPH decreased mitochondrial fusion associated proteins in neurons whilst having no significant effect in U-87MG glial cells. In contrast, rotenone decreased mitochondrial fusion associated proteins in both neural cell types while increasing fusion associated protein pDRP1 in neurons but not glial.

Together, these results suggest basal mitochondrial function differs between neuronal SH-SY5Y and glial U-87MG cells. Furthermore, AAPH and rotenone affect mitochondrial function and associated molecular mechanisms differently in neurons and glia. This highlights the differences in neuronal and glial mitochondrial function and their response to RS.

3.2.6 Oxidative stress decreases neural proteome function

With oxidative and mitochondrial stress generated by AAPH and rotenone the effect on the neural proteome was investigated. Neural cells were treated with AAPH and rotenone for 24 hours and the proteasome activity of the collected lysates was assessed. The chymotrypsin-like activity of the 20S subunit of the proteasome was measured using N-Succinyl-Leu-Leu-Val-Tyr-AMC with exogenously added ATP (figure 3.33A, B). Both neuronal SH-SY5Y and glial U-87MG cells treated with AAPH for 24 hours showed a dose-dependent decrease in proteasome activity where the highest concentration was significant (figure 3.33A). Like AAPH, rotenone also resulted in decreased proteasome activity in both neural cells (figure 3.33B). Interestingly, both neural cells and treatments showed similar significant decreases in proteasome activity, suggesting that despite different RS downstream pathways were affected in similar ways.

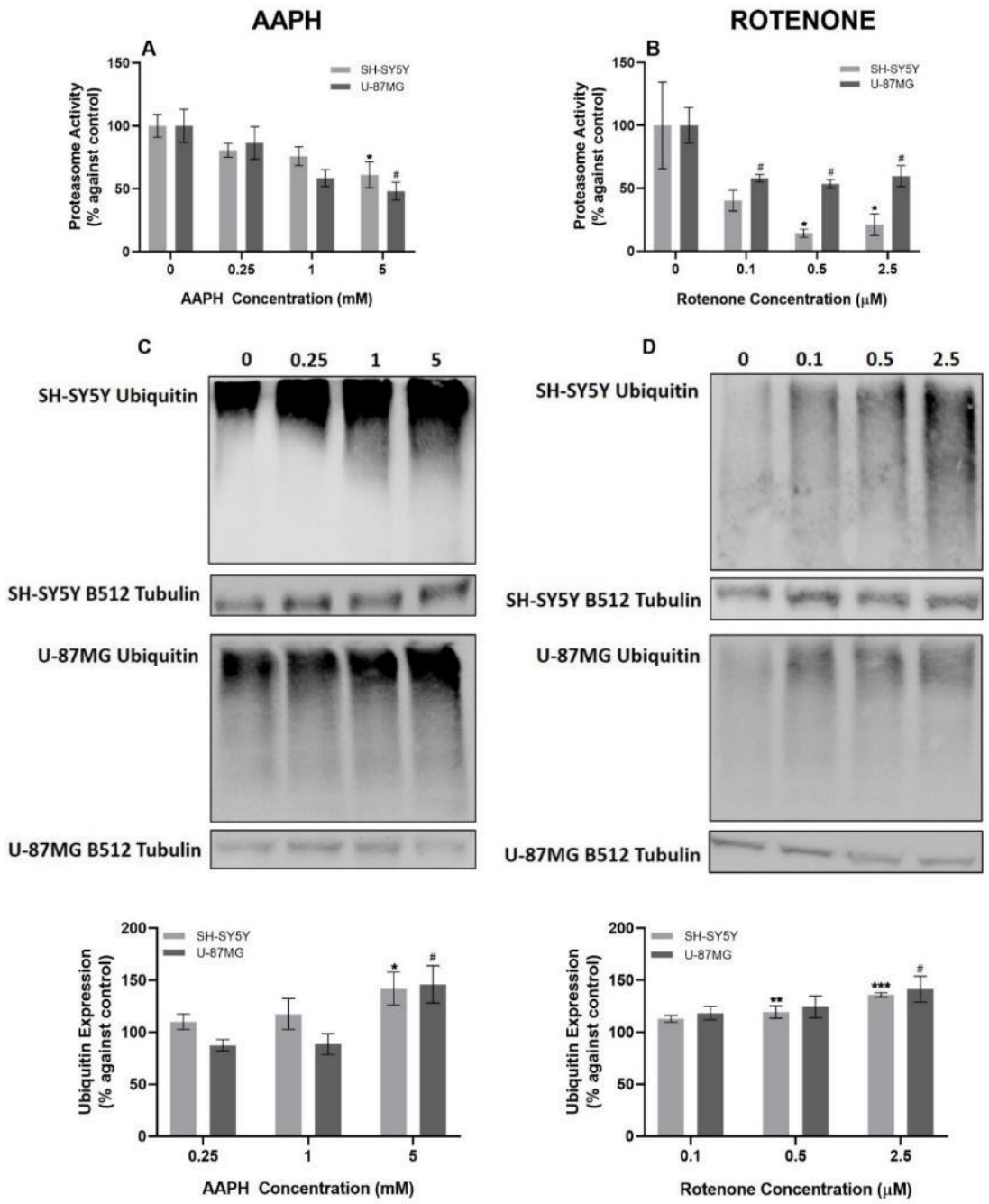

Figure 3.33 AAPH and rotenone-induced oxidative stress affects proteasome activity and subsequent ubiquitination levels. *Neuronal SH-SY5Y and glial U-87MG cells were treated with (A) AAPH or (B) rotenone for 24 hours and then proteasome activity was measured in the presence of ATP. Results are expressed as mean % against control ± SEM. (C, D) Following 48-hour treatment with AAPH and rotenone SH-SY5Y and U-87MG total cell extracts were probed with ubiquitin (1:1000) to examine levels of ubiquitinated proteins. Each Western blot is accompanied by a plot summarising densitometric analyses of Western blots using AIDA software. Results are presents as % against control ± SEM. Statistical analysis was performed using one-way ANOVA with Dunnett's post-hoc test where n=4 for all experiments. Statistical significance was recorded as *p<0.05, **p<0.01 and ***p<0.001.*

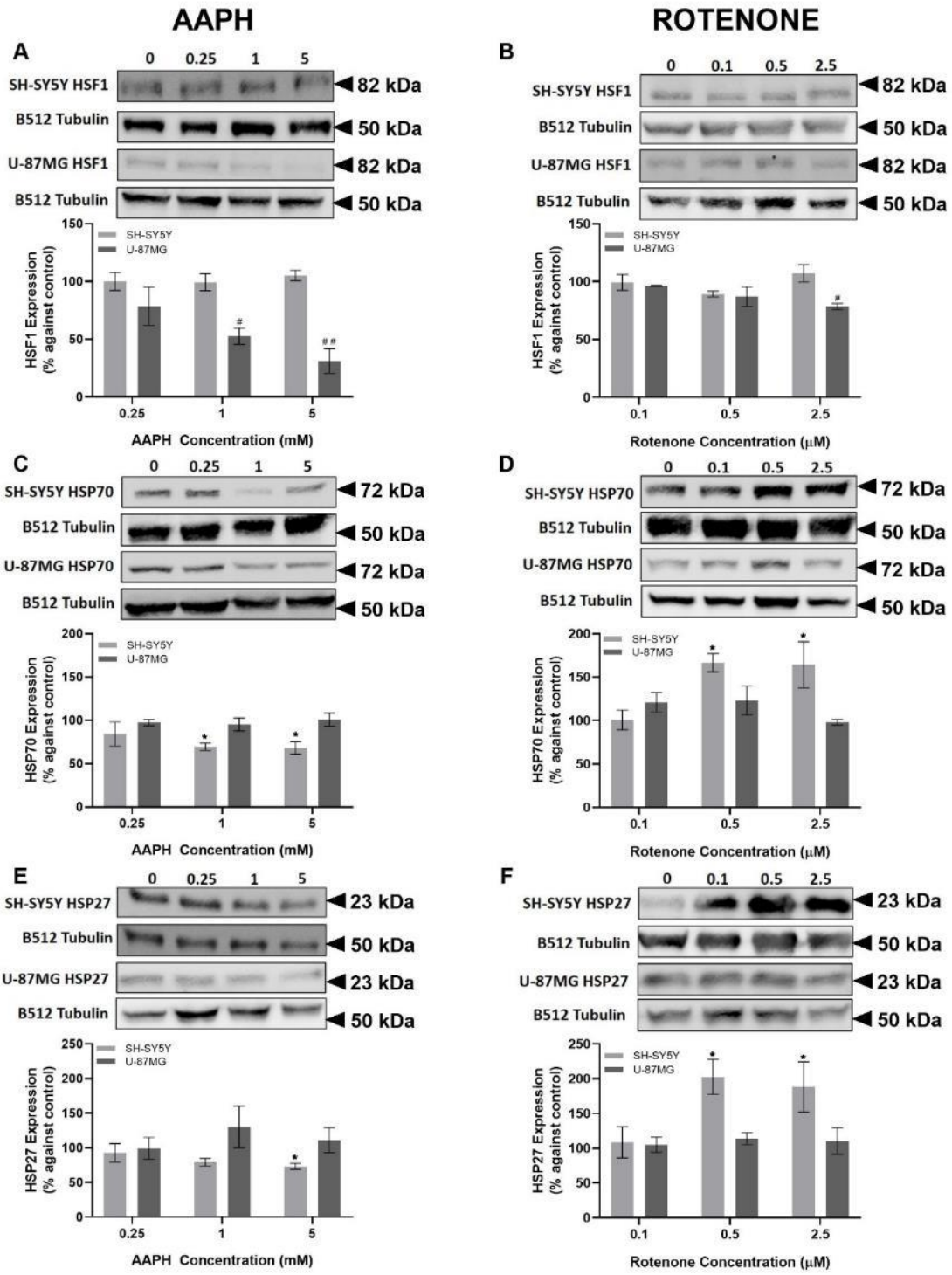

Figure 3.34 AAPH and rotenone-induced oxidative stress affects heat shock and chaperone protein levels. *Representative Western blots of neuronal SH-SY5Y and glial U-87MG cells were treated with AAPH or rotenone for 48 hours and total cell extracts were probed with (A,B) heat shock factor 1 (HSF1; 1:1000), (C,D) heat shock protein 70 (HSP70; 1:1000) and (E,F) heat shock protein 27 (HSP27; 1:1000). Each Western blot is accompanied by a plot summarising densitometric analyses of Western blots using AIDA software. Results are presents as % against control ± SEM. Statistical analysis was performed using one-way ANOVA with Dunnett's post-hoc test where n=4 for all experiments. Statistical significance was recorded as *p<0.05, **p<0.01 and ***p<0.001.*

To confirm proteasome dysfunction protein ubiquitination levels were measured. Western blots confirmed protein degradation was impaired, as levels of ubiquitinated proteins increased in a dose-dependent manner for both neural cells treated with AAPH and rotenone (figure 3.33C, D). Furthermore, as neural cells are dependent on the proteome for maintaining cell health, chaperones, which also help bind and refold misfolded proteins or target them for degradation were investigated to determine how OS affects these mechanisms. Heat shock factor 1 (HSF1) a master transcription factor of proteostasis did not change levels in neurons treated with either AAPH or rotenone (figure 3.34A, B). However, glial U-87MG cells showed a dose-dependent decrease in HSF1 levels following AAPH (figure 3.34A) and rotenone (figure 3.34B) exposure, where the decrease was more significant in AAPH treated cells. Heat shock protein 70 (HSP70; figure 3.34C), an OS modulated chaperone and the smaller heat shock protein 27 (HSP27; figure 3.34E) decreased in neurons treated with AAPH, while levels did not significantly change in U-87MG glial cells. However, in rotenone treated SH-SY5Y neuronal cells there was significant dose-dependent increase in both HSP70 (figure 3.34D) and HSP27 (figure 3.34F), while like AAPH there was no significant change in U-87MG glial cell levels.

Together, these results suggest pathways downstream of RS involved in neural proteostasis are affected including proteasome activity, protein ubiquitination and chaperone proteins levels supporting the idea that these pathological hallmarks of neurodegeneration are linked.

3.3 DISCUSSION

There is increasing evidence to suggest OS plays an important role in the pathology associated with neurodegenerative diseases such as PD (Puspita et al., 2017). In the present study we investigated the effect of OS on the antioxidant response, mitochondrial and proteasomal function in both neurons and glia *in vitro,* to gain a better understanding of the mechanisms underlying neurodegeneration in different neural cell types. Various oxidants with different structures and reactivity can cause different types of OS and RS (Piga et al., 2007). Two compounds were investigated: AAPH; a peroxyl radical generator that targets membranes and rotenone; a mitochondrial complex I inhibitor, which primarily generates superoxide.

AAPH, a hydrophilic azo compound that thermally degrades at physiological temperature producing free radicals at a defined rate (Werber et al., 2011) was used in this study to determine the effect of radicals in neural cells. AAPH resulted in a dose- and time-dependent increase in RS levels (figure 3.1-3.8). Due to dye sensitivity primarily measuring peroxy radicals (Kalyanaraman et al., 2012; Winterbourn, 2008), fluorescence was measured temporally allowing the rate of change of fluorescence and hence the rate of RS generation to be calculated. Previous studies with renal tubular epithelial cells (Yokozawa et al., 2000) and synaptosomes (Joshi et al., 2006) treated with AAPH showed increased lipid peroxidation and protein carbonyl levels. Furthermore SH-SY5Y cells labelled with diphenyl-1-pyrenylphosphine subsequently treated with 10 mM AAPH resulted in increased fluorescence, suggesting lipid peroxidation of the cell surface (Othman et al., 2016). This effect is not restricted to neurons as C6 rat glial cells treated with AAPH also show increased TBARS levels indicative of increased lipid peroxidation suggesting AAPH increases RS in glia (Sun et al., 2001). Similar to these results others show AAPH treated retinal ganglion cells (Yokoyama et al., 2014) and hippocampal neurons (Kanski et al., 2002) induced higher levels of RS, indicated with fluorescent probes, demonstrating RS generation across multiple cell types.

Antioxidants, α-tocopherol and ascorbic acid exhibited different effects in neural cells in response to oxidising agents AAPH and rotenone, where α-tocopherol efficiently attenuated RS levels against both RS inducers in neural cells (figure 3.1-3.6). In contrast, ascorbic acid was not as effective attenuating RS levels in neural cells treated with AAPH, but also glial cells treated with rotenone, suggesting different RS scavenging abilities.

Supporting the observed attenuation of RS fluorescence in this study, α-tocopherol is reported to be effective at removing lipid peroxyl and related alkyl peroxyl radicals (Angeli et al., 2017; Fukuzawa et al., 1997), which are believed to be the primary RS generated by AAPH (Bassett

et al., 1999; Ben Othman et al., 2016; Werber et al., 2011). Similar to Zhang *et al.,* this study shows rotenone treatment of neural cells resulted in a dose-dependent increase in fluorescence indicating increased levels of RS (Zhang et al., 2017). As rotenone can generate other RS downstream due to the cascade of reactions following superoxide production, it is not surprising that α-tocopherol also lowers RS levels in neural cells treated with rotenone (figure 3.6). Supporting these findings, SH-SY5Y cells treated with AAPH and α-tocopherol by Ben Othman *et al.* and others showed attenuation of RS levels and reduced fatty acid peroxidation (Ben Othman et al., 2016; Rehncrona et al., 1980; Tappel, 1972). Other studies also highlight the ability of tocopherol to reduce RS levels not just in neurons but also in astrocytes (Mannelli et al., 2013; Yu et al., 2015).

The observed decrease in RS fluorescence with neurons treated with rotenone and ascorbic acid is supported by Wenzel *et al.,* who demonstrate camptothecin that significantly increased mitochondrial superoxide levels in tumour cells was attenuated by ascorbic acid (Wenzel, 2003). This suggests ascorbic acid can scavenge superoxide radicals, which is the predominant RS generated by rotenone. Further supporting ascorbic acid as a superoxide scavenger is SMP30/GNL knockout mice with vitamin C depletion show increased superoxide levels in the brain (Kondo et al., 2008).

However, in U-87MG cells treated with rotenone ascorbic acid was not as effective at attenuating rotenone induced RS fluorescence relative to α-tocopherol. The reason for this is unclear but may possibly be due to the U-87MG cell line's high glycolytic rate (Kim et al., 2015; Oudard et al., 1996), resulting in media acidification. This is corroborated by the Seahorse findings herein, which show U-87MG glia mainly produce ATP via glycolysis and have a higher ECAR than neurons (figure 3.29). Cheng *et al.*'s findings also support this as they reported L-ascorbic acid inhibits astrocytic growth of both normal and tumour cells due to media acidification (Cheng et al., 1988). Together, with other studies the observed change in fluorescence and hence RS for neural cells when treated with AAPH and rotenone suggests these two chemicals generate different RS in neural cells, attenuated by distinct antioxidants.

In addition to RS, AAPH treatment resulted in a lower rate of the change in fluorescence in glial U-87MG cells relative to neuronal SH-SY5Y cells (figure 3.2 and 3.4), which suggests neural cells behave differently and possibly have different antioxidant capacity. It is generally proposed that astrocytes possess greater levels of glutathione than neurons (Dringen and Hamprecht, 1997), though this does vary depending on the brain region (Asanuma et al., 2019; Langeveld et al., 1996). Furthermore, glia are believed to be important in the brains antioxidant defence system as glial resistance to OS induced by hydrogen peroxide or peroxynitrite is greater than neuronal (Baxter

and Hardingham, 2016; Ben-Yoseph et al., 1996; Bolaños et al., 1995). Others also show incubation of glia with 6-OHDA or hydrogen peroxide for 6 and 24 hours showed no significant change in cell viability, but increased total glutathione levels with lower lipid peroxidation levels relative to neurons (Asanuma et al., 2019; Iwata-Ichikawa et al., 1999). Therefore, we investigated glutathione levels in neural cells using a commercially available fluorometric glutathione assay kit. Like others, we showed that glial U-87MG cells had greater basal levels of glutathione (figure 3.7A), potentially explaining why there was no change in glutathione levels in U-87MG cells treated with AAPH but was for neurons (figure 3.7B). Furthermore, glutathione assays further support the possibility of these two chemicals producing different RS, as rotenone induced higher glutathione expression in both neural cells (figure 3.7C); whereas AAPH only effected neuronal cells (figure 3.7B) highlighting the possibility of different antioxidant pathway activation in neural cells.

Neural cells in an effort to restore redox balance respond to RS by activating signalling pathways such as the NRF2-ARE, known to play a part in cell protection via an antioxidant and anti-inflammatory role (Lee et al., 2003b; Shih et al., 2005; Tufekci et al., 2011). Under basal conditions NRF2 is cytoplasmic due to KEAP1 binding, resulting in ubiquitination and proteasomal degradation of NRF2 (Zhang et al., 2017). Upon OS NRF2 dissociates from KEAP1 becoming stable, translocating to the nucleus (Chen and Kong, 2004), where it forms heterodimers with other regulators inducing and driving the expression of antioxidant genes (Itoh et al., 1997; Kovac et al., 2015; Tonelli et al., 2018). Therefore, with different RS generated in neural cells from AAPH and rotenone treatment we evaluated NRF2 and downstream OS related protein levels, to see how these pathways were affected. Western blot analysis showed no significant change in NRF2 levels following AAPH and rotenone exposure. However, like others we showed OS resulted in a concentration-dependent NRF2 activation where NRF2 translocates to the nucleus in neural cells as shown by immunofluorescent and subcellular fractionation studies (figure 3.9-3.10; Liddell et al., 2016; Malone and Hernandez, 2007; Quesada et al., 2011; Rizzi et al., 2018; Zagoura et al., 2017).

Antioxidants can activate NRF2 leading to pre-induction, induction and post-induction (Niture et al., 2014). Therefore, the lack of NRF2 localisation in α-tocopherol treated neural cells and ascorbic acid treated neurons is possibly due to the constitutively active ARE, scavenging RS. Indeed, α-tocopherol and ascorbic acid have been shown to protect against OS via NRF2 (Joshi and A. Johnson, 2012; Mostafavi-Pour et al., 2017; Vineetha et al., 2018). In this study, ascorbic acid did not prevent NRF2 nuclear localisation in AAPH treated neural cells and rotenone treated glia, perhaps because RS levels were not shown to be lower, as such OS is still present and as a result NRF2 is still active and located to the nucleus. It is also important to note that immunofluorescence showed NRF2 localised to the nucleus in U-87MG cells treated with ascorbic acid, likely because of

the increased media acidification relative to the control resulting in stress and hence, nuclear localisation. Furthermore, both ascorbic acid and α-tocopherol significantly upregulated NRF2 levels in neuronal cells but not glial cells (figure 3.11). This suggests antioxidants in neurons may combat OS by increasing NRF2 levels leading to ARE binding, increasing cytoprotective gene transcription allowing the return to basal conditions more quickly. Whereas antioxidants did not significantly change NRF2 levels in glia, possibly because glial cells have greater basal levels of NRF2 (figure 3.11C) relative to neurons, as some report glia protect neurons via NRF2 dependent mechanisms (Baxter and Hardingham, 2016; Jimenez-Blasco et al., 2015; Shih et al., 2003; Vargas et al., 2006). Additionally, glial cells have other mechanisms for removal of RS such as glutathione so they may not predominantly rely on the NRF2-ARE pathway for the activation of antioxidant proteins (Dringen et al., 2005; Dringen and Hamprecht, 1997).

NRF2 translocation to the nucleus induces and drives the expression of antioxidant genes and detoxification enzymes (Alam et al., 1999; Chen and Kong, 2004; Venugopal and Jaiswal, 1996). Neurons treated with both AAPH and rotenone exhibited decreased DJ-1 levels contravening other studies that show enhanced levels of DJ-1 in Parkinson's patients (Hong et al., 2010; Waragai et al., 2006), possibly due to high levels of oxidation inactivating DJ-1 leading to its degradation (Choi et al., 2006). In contrast, glial cells exhibited no significant change in DJ-1 levels for both RS inducers. This is potentially because glia are suggested to have a high antioxidant capacity and protect neurons via DJ-1 against OS inducers such as 6-hydroxydopamine (Lev et al., 2013). Furthermore, OS is reported to cause DJ-1 to co-localise with mitochondria or nuclei to enhance neuroprotection (Junn et al., 2009; Kim et al., 2012; Li et al., 2005; Zhang et al., 2005) and therefore localisation rather than total levels are key. Finally, peroxiredoxin 6 (PRDX6) levels decreased in both neural cells upon AAPH treatment, which may be due to PRDX6 being able to scavenge H_2O_2 and phospholipid hydroperoxides (Fisher, 2011; Manevich et al., 2009). As a result of high levels of RS generated by AAPH neural cells may have insufficient levels of glutathione to reduce PRDX6 disulphide binds resulting in its degradation (Poole et al., 2011a; Turner-Ivey et al., 2013). In contrast, PRDX6 levels in neurons and glia exhibited opposite reactions to rotenone where PRDX6 decreased in neurons and increased in glia (figure 3.8). This may be because antioxidant defence systems are overwhelmed in neurons, whereas in glia they remain active.

Together, these results suggest different RS from AAPH, and rotenone activate the antioxidant system via NRF2 nuclear translocation. This is supported by α-tocopherol attenuating this localisation possibly by reducing RS levels and thus, returning neural cells to redox balance. Whereas ascorbic acid did not prevent NRF2 localisation in AAPH treated neural cells and rotenone treated glia, possibly due to ascorbic acid not scavenging RS effectively in these models resulting in

activation of the NRF2-ARE pathway. Further downstream NRF2 levels are unchanged by treatment but are increased by antioxidants in neurons but not in glia. This suggests antioxidants increase basal NRF2 levels in neurons, enhancing RS removal via the NRF2-ARE pathway. In contrast, glial cells rely on other antioxidant pathways to reduce RS levels. Additionally, downstream proteins associated with OS such as DJ-1 and PRDX6 levels appeared to be differentially affected by specific RS in different neural cells. Therefore, AAPH and rotenone induce OS in neural cells but generate different types of RS resulting in divergent effects on protein levels and localisation.

With OS stimulated neural toxicity was investigated. The results herein show as AAPH concentration increases neuronal viability decreases with cellular morphology being affected (figure 3.10-3.15). This is supported by previous studies where SH-SY5Y exposed to 35mM AAPH for 6 hours showed 65% reduced viability (Othman et al., 2016). AAPH studies show decreased cellular viability in neuronal cells via OS (Ben Othman et al., 2016; Kanski et al., 2002; Rapin et al., 1998), with only higher concentrations having a significant effect on glial cells (Guo et al., 2016; Sun et al., 2001), which can be attenuated with antioxidants (Dooley et al., 1990; Terao and Niki, 1986). In contrast, glial cells showed no change in viability after 24-hour (figure 3.13) AAPH exposure but showed increased viability and maintenance of mitochondrial function as demonstrated by Mitotracker staining and ATP level stability after 48 hours (figure 3.14). Like our results, studies with astrocytes cultured from Sprague-Dawley rats showed increased astrocyte viability when they were incubated for short periods of time with low concentrations of AAPH. Whereas higher concentrations of AAPH (>20 mM) resulted in astrocyte viability decreasing (Guo et al., 2016). Furthermore C6 rat glial cultures showed low concentrations of AAPH had no significant effect on cell viability and only slightly increased levels of lipid peroxidation (Sun et al., 2001). In addition, concurrent treatment of both neuronal and glial cells with AAPH in the presence of α-tocopherol increased cell viability (figure 3.21), suggesting RS induced cell toxicity. This is supported by previous studies that indicate decreased neural cell viability when treated with OS inducers (Othman et al., 2016; Guo et al., 2016), while cells treated with α-tocopherol reduced levels of lipid peroxidation (Foret et al., 2019; Palozza and Krinsky, 1992). However, ascorbic acid was not successful in attenuating cell death induced by AAPH (figure 3.25). This could be related to the fact that ascorbic acid did not decrease RS levels as it predominantly scavenges superoxide (Patra et al., 2001; Wenzel, 2003), whereas AAPH primarily produces peroxyl radicals (Bassett et al., 1999; Werber et al., 2011).

This suggests that AAPH generates peroxy radicals, which may result in lipid peroxidation that is observed in neurodegenerative disorders possibly resulting in cellular apoptosis or ferroptosis, a regulated form of non-apoptotic death via altering lipid membrane assembly,

composition, structure and dynamics (Gaschler and Stockwell, 2017; Simpson et al., 2004; Zarkovic, 2003). This is supported by the LDH assays in this study that show for higher concentrations of AAPH both neural cells showed significant increases in LDH release, which has also been shown in renal-tubular epithelial cells (Yokozawa et al., 2000), and α-tocopherol (figure 3.21) but not ascorbic acid (figure 3.25) is able to attenuate.

With increasing rotenone concentrations and exposure time, loss of neural processes, morphological rounding, loss of cell viability and reduced cellular energy levels was observed (figure 3.16-3.19). Rotenone, a lipophilic organic pesticide is a complex I inhibitor used to model PD as both early and advanced PD patients have displayed reduced complex I activity (Dexter et al., 1994; Hattingen et al., 2009). This is supported by previous studies where neuronal and glial exposure to rotenone resulted in decreased number and process length (Goswami et al., 2015; Voronkov et al., 2016). This is possibly via apoptosis as suggested by previous rotenone research with SH-SY5Y cells (Fitzgerald et al., 2014; Newhouse et al., 2004; Ryter et al., 2007). However, it was also noted that there was a decrease in cellular energy for both cell types shown by the dose-dependent decrease in ATP levels, which may also contribute to cell death, supported by previous studies (Caneda-Ferrón et al., 2008; Sherer et al., 2003). This reduction in cellular energy may explain why all rotenone concentrations significantly decreased U-87MG cell viability, as *in vivo* studies suggest mitochondria isolated from neurons have greater complex IV activity, while mitochondria isolated from glia have higher ATPase activity (Hamberger, 1970; Hertz and Chen, 2016). Furthermore, qRT-PCR showed U-87MG glial cells exhibited lower mitochondrial gene expression relative to SH-SY5Y neuronal cells (figure 3.29), suggesting U-87MG cells possess less mitochondria than neurons. Indeed, this is not surprising as neurons are reported to rely exclusively on mitochondria for ATP (Franco-Iborra et al., 2016), while astrocytes depend on glycolysis for their high energy demands (Hertz et al., 2007). Therefore, the same rotenone concentration possibly results in saturation of glia mitochondria further affecting the ATP demand from glycolysis, whereas neurons still possess mitochondria that have not been inhibited by rotenone. Reduced ATP levels also suggests impaired mitochondrial function, which is supported by the more diffuse Mitotracker staining (figure 3.16-3.18), decreased red: green JC-1 ratio (figure 3.31-3.32) and a higher glycolytic rate of ATP production (figure 3.29) that has also been shown by others (Sarafian et al., 2010; Veenman et al., 2010). This suggests OS induces mitochondrial dysfunction as demonstrated previously (Cobb and Cole, 2015; Lin and Beal, 2006; Navarro and Boveris, 2004).

Further supporting rotenone induces cell death via RS, concurrent antioxidant α-tocopherol treatment attenuated rotenone induced death (figure 3.23), suggesting like others that rotenone causes cell death via OS (Filomeni et al., 2012; Testa et al., 2005). Furthermore, in neurons

ascorbic acid like α-tocopherol attenuated cell death (figure 3.27), possibly via reduced RS levels (figure 3.6) as shown previously (Gomez-Lazaro et al., 2008; Hongo et al., 2012). However, this was not the case for glia treated with rotenone and ascorbic acid possibly due to the acidification of the media (Cheng et al., 1988) and the lack of reduced RS levels (figure 3.6), as cells still showed rounding and clustering.

Considering both AAPH and rotenone treatment it is also important to note glial cells showed less LDH release with the same concentrations relative to neurons suggesting glia are less susceptible to loss of membrane stability (figure 3.14-3.27). This is possibly due to the higher levels of antioxidants such as glutathione and glutathione peroxidase in glia relative to neurons (figure 3.6; Dringen et al., 2005; Dringen and Hamprecht, 1997), which are responsible for the removal of hydrogen peroxide and lipid peroxides (Dasuri et al., 2013; Gandhi and Abramov, 2012). Furthermore, glia may also be more resistant to RS due to the accelerated glutathione synthesis under stress relative to neurons (McBean, 2017).

With RS species generated via AAPH and rotenone another pathological hallmark of neurodegeneration is mitochondrial dysfunction (Hattingen et al., 2009; Lou et al., 2020; Swerdlow, 2009). The importance of mitochondria as an important source of ATP for neurons is highlighted by the brain's high consumption of oxygen, leading to the idea that oxidative phosphorylation is the main source of energy (Franco-Iborra et al., 2016). The importance of aerobic glycolysis for fuelling nerve terminal activities and providing energy for other neural cells such as astrocytes (Pellerin and Magistretti, 1996; Vaishnavi et al., 2010). Our investigations support these and others findings that astrocytes utilise glycolysis as their main source of energy, as U-87MG glial cells showed a higher ECAR than SH-SY5Y neuronal cells (figure 3.29; Jády et al., 2016; Juaristi et al., 2019). This suggests glia rely on glycolysis as their source of ATP, while neurons rely more on mitochondria. Like Giordano *et al.* rotenone as expected, lowered ECAR for both neural cells proposing rotenone had a significant effect on mitochondrial function consistent with complex I inhibition, and as a result cells reverted to glycolysis to meet the cells energy demand (Giordano et al., 2014). However, the effect of AAPH on respiration has yet to be investigated in neural cells and while AAPH has been confirmed as a radical generator (Bassett et al., 1999; Terao and Niki, 1986; Werber et al., 2011), downstream effects on mitochondria has not been investigated. As such, it was interesting to see that AAPH induced a similar effect to rotenone in SH-SY5Y neuronal cells, where ECAR increased and OCR decreased suggesting AAPH resulted in a greater glycolytic ATP production but had no effects on U-87MG glial respiration. This may be because AAPH generates peroxyl radicals leading to lipid peroxidation of the mitochondrial membrane and dysfunction (Fuentes-Lemus et al., 2016; Niki, 1990; Werber et al., 2011). This was observed in SH-SY5Y neurons, but not in U-87MG glial

cells, possibly due glia being able to cope with the RS generated by AAPH due to their greater antioxidant capacity (Dringen and Hamprecht, 1997).

Indeed, mitochondria dysfunction is associated with loss of mitochondrial membrane potential associated with RS, leading to cytochrome C release into the cytosol resulting in caspase-9 and caspase 3 activation potentiating apoptosis in neural cells (Ikeda et al., 2008; Kugler et al., 2008; Veenman et al., 2008). Our studies using the fluorescent probe, JC-1 support this and other studies, as complex I inhibition by rotenone resulted in a dose-dependent decrease in aggregate to monomer ratio (figure 3.30-3.31; Dadakhujaev et al., 2010; De Pedro et al., 2016; Deng et al., 2013). Whereas AAPH only resulted in membrane depolarisation in SH-SY5Y but not U-87MG cells, supporting ATP studies suggesting AAPH may cause mitochondrial depolarisation in SH-SY5Y neurons resulting in cells resorting to glycolysis to meet the cells energy demands, while U-87MG glia may have a greater antioxidant system to cope with AAPH generated RS (Dringen and Hamprecht, 1997).

To adapt to the cells energy demands mitochondrial biogenesis is very important where mitochondria can undergo fission (division) and fusion (fuse) to maintain a homogeneous mitochondrial population (Chan, 2012; Grimm and Eckert, 2017), with reptitive cycles regulating morphology and dynamics (Sharma et al., 2014) to adapt to stress (Kowald and Kirkwood, 2011). As RS are implicated in mitochondrial dysfunction, fission/fusion proteins that determine mitochondrial motility and function were measured. OPA1 and MFN1 are pro-fission proteins, where MFN1 facilitates outer mitochondrial membrane fusion, while OPA1 promotes inner membrane fusion (Campello and Scorrano, 2010; Friedman and Nunnari, 2014; Hudson et al., 2008; Ishihara, 2004). In addition, cellular models of sporadic PD have been found to have altered expression of OPA1 and DRP1 (Santos et al., 2015). Like Peng *et al.* we observed a decrease in OPA1 expression while observing an increase in pDPR1 with rotenone treated neurons, which has been implicated in mitochondrial fragmentation (Guo et al., 2015; Peng et al., 2017). Rotenone treated glia showed similar changes in fission protein levels while fusion proteins were unchanged, potentially because they scavenge more RS in the early stages of treatment. Indeed, changes in mitochondrial fission/fusion induced by rotenone was not surprising due to the direct inhibition of complex I leading to mitochondrial dysfunction. Similarly, AAPH treatment showed a decrease in fusion proteins OPA1 and MFN1 without changing pDRP1 levels in neurons but had no effect on levels in glial cells. This suggests RS generated by rotenone and AAPH results in mitochondrial fusion rather than fission leading to disruption in mitochondrial biogenesis and cell death.

Together, this study along with others suggests different RS disrupt mitochondrial biogenesis, respiration and membrane permeability in neural cells linking these pathological hallmarks of neurodegeneration. However, as little is known about how AAPH effects mitochondrial dysfunction further research is needed to determine if cell apoptosis like rotenone, is linked to release of cytochrome C and caspase activation in neural cells.

In addition to mitochondrial dysfunction proteome dysfunction is also associated with ageing. All proteins exist in a dynamic state between synthesis and degradation known as turnover, which contribute to cellular development, differentiation and ageing. Protein degradation is important for the removal of aberrant proteins such as those post-translationally modified by RS that can accumulate, aggregate and compromise cellular function and viability (Douglas and Dillin, 2010; Gidalevitz, 2006; Lopiano et al., 2000). Neurons are particularly susceptible to proteotoxic stress due to being post-mitotic cells that are not replaced and axons regenerate poorly (Liu et al., 2011). Protein homeostasis involves three stages: protein synthesis and folding, conformational stability and degradation.

Under OS, degradation pathways such as the UPS can be directly or indirectly impaired resulting in toxic protein accumulation, leading to neuronal dysfunction and cellular apoptosis (Betarbet et al., 2005). Our results show like Shamoto-Nagai *et al.* that rotenone and AAPH results in a dose-dependent decrease in 20S proteasomal function in both neural cell types (figure 3.33; Shamoto-Nagai et al., 2003b). This is possibly because the 26S proteasome is susceptible to OS (Raynes et al., 2016; Reinheckel et al., 2000), where the 20S unit is responsible for the degradation of oxidised proteins via ubiquitination and ATP dependent degradation (Shringarpure et al., 2003), suggesting RS lead to proteasome dysfunction. Further supporting this, impaired protein degradation was demonstrated by increased ubiquitination levels, which has been shown in dopaminergic neurons of rotenone treated rats (Betarbet et al., 2006), as well as in Lewy bodies of PD patients (Giasson, 2000; Luk, 2019). This may be due to proteasomal posttranslational modifications by RS that has also been reported by others (Chou et al., 2010; Shamoto-Nagai et al., 2003). Alternatively, RS can post translationally modify proteins leading to high levels of aberrant proteins overwhelming the proteasome, leading to a feed-forward cycle resulting in cell cytotoxicity.

Aberrant protein accumulation can lead to aggregates and upregulation of chaperones aiding in refolding misfolded proteins or sending damaged protein for degradation (Ciechanover and Brundin, 2003; Esser et al., 2004). The possible role of chaperone heat shock proteins is highlighted by the presence of HSP70 and HSP27 in aggregates in neurodegenerative patients (Ito

et al., 2002; Rideout and Stefanis, 2002). This is further supported by studies showing upregulation of HSP27 and HSP70 attenuated cell death caused by MPP^+ or MPTP in cellular models of PD (Donaire et al., 2005; Fan et al., 2005; Quigney et al., 2003). Heat shock factor 1 (HSF1) is a master transcription factor of heat shock proteins, where under basal conditions it resides in the cytosol in a non-phosphorylated state. Upon stress such as RS, for example hydrogen peroxide, HSF1 is phosphorylated and dissociates from inhibiting chaperones exposing the nuclear localisation signal resulting in nuclear translocation (Katschinski et al., 2000; Morimoto, 2002; Raychaudhuri et al., 2014). Once in the nucleus HSF1 can bind to heat shock element promoting initiation of transcription of chaperones, upregulating their levels which can negatively regulate HSF1 (Pirkkala et al., 2001). Both AAPH and rotenone significantly lowered HSF1 levels in U-87MG cells but had no effect on SH-SY5Y neuronal cells (figure 3.34). The lack of change in SH-SY5Y cells may be similar to NRF2, in that RS results in its translocation to the nucleus leading to upregulation of heat shock proteins. HSP70 and HSP27 are two well-known heat shock proteins known to be cytoprotective against apoptosis and regulated by HSF1 (Au et al., 2008; Ekimova et al., 2018; Manzerra et al., 1997).

Chaperones are a major first line of defence against aberrant proteins and known to induced by RS, particularly in neural cells (Franklin et al., 2005; Gorman et al., 1999; Voth and Jakob, 2017). HSP70 is an ATP-dependent chaperone, which has little or no constitutive expression in the brain with particularly low levels detected in neurons (Khalouei et al., 2014; Manzerra et al., 1997). However stress induces HSP70, increasing its levels to help cells cope with increased misfolded, denatured or oxidatively modified proteins (Kabiraj et al., 2015; Nollen et al., 1999; Wang et al., 2002; Yoon et al., 2010). Therefore, HSP70 is possibly upregulated under OS to help refold denatured proteins or send them to the proteasome for degradation, if they are irreversibly damaged (Garrido et al., 2012). Whereas HSP27 is an ATP-independent chaperone responsible for preventing protein aggregation (Ehrnsperger, 1997) and is also protective against OS (Behdarvandy et al., 2020; Rogalla et al., 1999). Additionally, HSP27 is reported to increase antioxidant defences by increasing glutathione levels (Abaspour et al., 2019; Mehlen et al., 1996). Both HSP70 and HSP27 are also reported to have antiapoptotic activity as they can block caspase induced apoptosis (Bruey et al., 2000; Buzzard et al., 1998) by interacting with cytochrome c, or preventing recruitment of procapase-9 to the apoptosome (Beere et al., 2000; Bruey et al., 2000; Concannon et al., 2001).

Therefore, in response to RS these chaperones may have been upregulated in rotenone treated SH-SY5Y neuronal cells to counteract RS induced mitochondrial dysfunction, possibly leading to cytochrome C induced apoptosis. No change in HSP70 and HSP27 levels was observed in U-87MG glial cells treated with either AAPH or rotenone, potentially because they scavenge the RS

levels needed to induce activation of chaperones. While rotenone and AAPH effected proteasome activity and ubiquitination levels in similar ways, SH-SY5Y cells treated with AAPH showed decreased HSP70 and HSP27 levels, suggesting that despite both chemicals inducing RS, they resulted in different effects on neuronal chaperone levels. Therefore, the RS generated appear to have a different effect on chaperone levels within neural cells but this requires further investigation to determine which apoptotic pathways have been induced by these specific RS.

Table 3.1 Table summarising experimental findings of this study suggesting how AAPH and rotenone lead to the pathological hallmark of the 'neurodegenerative Bermuda triangle'.

RESULTS	SH-SY5Y			U-87MG		
	AAPH	**Rotenone**	**Infers**	**AAPH**	**Rotenone**	**Infers**
RS Levels	↑	↑	Rotenone and AAPH increases RS levels where antioxidants suggest specific RS generated	↑	↑	Rotenone and AAPH increase RS levels but ascorbic acid not effective
RS levels + tocopherol	↓	↓		↓	↓	
RS levels + ascorbic acid	↑	↓		↑	↑	
NRF2 colocalisation	Nuclear	Nuclear	RS induce activation of the NRF-ARE pathway where localisation reflects RS levels suggesting antioxidants help scavenge RS via the NRF-ARE pathway	Nuclear	Nuclear	RS induce activation of the NRF-ARE pathway where localisation reflects RS levels but ascorbic acid stresses glia as control with ascorbic acid also exhibits nuclear localisation possibly due to media acidification
NRF2 colocalisation + tocopherol	Cytoplasmic	Cytoplasmic		Cytoplasmic	Cytoplasmic	
NRF2 colocalisation + ascorbic acid	Nuclear	Cytoplasmic		Nuclear	Nuclear	
DJ-1 levels	↓	↓	Antioxidant protein levels decrease suggesting antioxidant defences have been overwhelmed	-	-	Glia have greater antioxidant capacity as levels differ from neurons
PRDX6 levels	↓	↓		↓	↑	
Viability	↓	↓	Antioxidant viability assays reflect RS levels suggesting RS result in cytotoxicity	↑	↓	Glia exhibit different viability for AAPH and rotenone suggesting specific RS cause different effects
Viability + tocopherol	↑	↑		↑	↑	
Viability + ascorbic acid	↓	↑		↓	↓	
Main source of ATP	Glycolytic	Glycolytic	RS generated by AAPH and rotenone effect downstream mitochondrial function and biogenesis. Suggests mitochondria susceptible to RS.	Glycolytic	Glycolytic	RS generated by AAPH and rotenone effect downstream mitochondrial function and biogenesis. Suggests mitochondria susceptible to RS.
JC-1 mitochondrial membrane potential	↓	↓		↑	↓	
Fusion protein OPA1 and MFN1 levels	↓	↓		-	↓	
pDRP1 levels	-	↑		-	-	
Proteasome activity	↓	↓	RS generated effect downstream protein degradation by UPS	↓	↓	RS generated effect downstream protein degradation by UPS
Ubiquitination levels	↑	↑		↑	↑	
HSF1 Levels	-	-	Chaperones activation depends of the RS generated	↓	↓	Glia have greater antioxidant capacity as no change in chaperone levels observed
HSP70 Levels	↓	↑		-	-	
HSP27 Levels	↓	↑		-	-	

In conclusion, this study shows AAPH and rotenone result in a multitude of changes to biochemical pathways in both SH-SY5Y neuronal and U-87MG glial cells as summarised in table 3.1 where differences appear to be due to the specific RS generated and neural cell type. This suggests neural cells react to RS differently. Furthermore, viability assays suggest that both RS inducers resulted in cytotoxicity, but glia are less susceptible. OS also results in mitochondrial dysfunction as suggested by increased glycolytic respiration, changes in mitochondria membrane permeability and biogenesis. Finally, proteomic activity in both neural cells was reduced by both treatments while also increasing ubiquitination levels but interestingly effecting chaperone levels in different ways, suggesting types of RS may affect the neural proteome differently.

Neurodegeneration is an incredibly complex multifaceted disease with multiple pathways being affected including OS, mitochondrial and proteomic function being affected where the only universal factor is aging (Ehrnhoefer et al., 2011). However, currently most research and treatments target one of these hallmarks. However, the work herein proposes these pathways are linked, where specific RS cause different responses depending on the type of neural cells. Future use of this model will help identify common factors that underlie these pathways and how different RS affect them in the hope of generating novel therapies.

CHAPTER 4

REACTIVE SPECIES

IN A DIFFERENTIATED MODEL

4.1 INTRODUCTION

4.1.1 Differentiation of neural cells

Neurodegenerative diseases are characterised by multiple hallmarks however, cellular models do not always recapture these. This is possibly due to immortalised neuronal cell lines lacking some of the features that define neurons such as long neurites, lack of cell division and expression of selected neuron specific markers (Carolindah et al., 2013). While alternatives are available, including human stem and primary cells, they have their own limitations. Human stem cells have are expensive, while primary cells from rats do not express some of the human proteins most closely associated with neurodegeneration (Kovalevich and Langford, 2013). Therefore, differentiation of immortalised cells lines into a neuronal phenotype is preferred for initially investigating neurodegenerative mechanisms.

The neuroblastoma SH-SY5Y cell line is commonly used for neurodegenerative studies. SH-SY5Y cells can produce both substrate adherent (S-type) and neuroblastic (N-type) cells that can undergo transdifferentiation (Ross et al., 1983; Teppola et al., 2016). There are multiple methods and protocols for SH-SY5Y differentiation leading to a more mature neuronal like phenotype (Påhlman et al., 1995; Shipley et al., 2016). Most common protocols involve serum reduction and retinoic acid (RA), which improves neurite outgrowth but also neuronal marker expression (Lopes et al., 2010; Xicoy et al., 2017). RA is a metabolite of vitamin A, derived from retinol in a 2-step enzymatic process via a retinaldehyde intermediate (Pavlovic et al., 2014). RA, as a neurotrophic factor, binds to nuclear receptors activating transcription and regulating physiological features at a genomic level (Khatib et al., 2019; Mey and Mccaffery, 2004). RA can also help neuronal differentiation independent of the genome, where RA can activate ERK1/2 which plays a role in cytoskeletal rearrangement and neurite outgrowth (Bruck et al., 2009; Cañón et al., 2004; Khatib et al., 2019; Pan et al., 2005). Therefore, the dual potency of RA makes it a good differentiating agent to enhance neurite outgrowth.

Furthermore, while RA promotes neuronal differentiation of SH-SY5Y N-type cells, S-type cells do not undergo any morphological changes over 5 days (Mario Encinas et al., 2002). Whereas longer time periods with RA can result in S-type cells overgrowing the culture due to their continuous proliferation, while N-type cell proliferation is attenuated leading to an imbalanced population (Mario Encinas et al., 2002; Påhlman et al., 1984). Though others contravene RA's ability to attenuate cell proliferation (Teppola et al., 2016). Consequently, RA is not suitable for long term differentiation due to the generation of a non-homogenous population.

Alternatively, RA can be combined with 12-o-tetradecanoyl-phorbol-13-acetate (TPA) to improve SH-SY5Y neuronal processes and increase membrane potential (Åkerman et al., 1984; P.-C. Wei et al., 2019). Furthermore RA/TPA differentiation increased expression of tyrosine hydroxylase and dopamine transporter, favouring differentiation towards a dopaminergic phenotype (Presgraves et al., 2003).

Other methods exploit RA's induction of neurotrophic tyrosine kinase receptor B (NTrkB), enabling cells to become responsive to brain derived neurotrophic factor (BDNF; Arcangeli et al., 1999; M. Encinas et al., 2002; Xicoy et al., 2017). NTrkB is part of a neurotrophin family of receptors, composed of multiple receptors with preferences to specific neurotrophins (Huang and Reichardt, 2003). NTrkB specifically binds BDNF activating intracellular kinase signalling cascades, increasing the selective pressure against S-type cells and enhancing RA induced differentiation, giving rise to a homogenous neuronal population with increased neurite outgrowth and attenuated proliferation (Constantinescu et al., 2007; de Medeiros et al., 2019).

These methods of differentiation in addition to improving neurite outgrowth, also increase neuronal protein markers such as dopaminergic cell markers (Cheung et al., 2009), while others report induction of cholinergic neuronal phenotypes (de Medeiros et al., 2019; Edsjö et al., 2003; Zimmermann et al., 2004). Some markers of neuronal differentiation include βIII tubulin, an exclusive neuronal marker (Katsetos et al., 2003); synaptophysin, a marker of synapse generation at the end of neurites and tyrosine hydroxylase, an enzyme required for dopamine synthesis (Cheung et al., 2009). Thus, while multiple studies use these methods for SH-SY5Y differentiation it remains controversial as to what neuronal phenotypes are generated. As many key features of neurons are generated through differentiation there is still a preference for use of these methods to study neurodegenerative diseases, due to their low cost and high-throughput nature.

RA is also used for U-87MG differentiation to produce a more astrocytic phenotype, upregulating GFAP expression (Das et al., 2009; Karmakar et al., 2008). Indeed, RA is used in combination with other drugs to combat glioblastomas through attenuating growth (Burton and Prados, 1999; Dreyfus et al., 2018). RA suppresses U-87MG proliferation through downregulation of telomerase activity leading to telomere shortening (Das et al., 2008; Haque et al., 2007; Pendino et al., 2001). Furthermore, RA is associated with the phosphorylation and inactivation of the anti-apoptotic bcl-2 protein (Neviackas and Kerstein, 1976; Papi et al., 2007; Xia et al., 2006). Hence, RA is not only used to differentiate SH-SY5Y cells but also U-87MG glial cells into an astrocytic phenotype.

Astrocytes have neuroprotective effects possibly via secreted factors (Jha et al., 2018; Werber et al., 2011). This is supported by *in vitro* studies that show differentiation of dopaminergic neurons from primary cultures can be manipulated by region specific glial cells (O'Malley et al., 1992) and striatal derived factors (Tomozawa and Appel, 1986). Furthermore, Engele *et al.* demonstrated conditioned media from multiple glial cell lines enhanced survival and differentiation of dopaminergic neurons, although the exact underlying mechanism is not fully understood (Caldwell et al., 2020; Engele et al., 1991). Glial cell lines are known to release a number of neurotrophins such as nerve growth factor, BDNF, ciliary neurotrophic factor and neurotrophin-3 effecting proliferation, differentiation and migration of neuronal cells (Coutinho-Budd et al., 2017; Maisonpierre et al., 1990; Popova et al., 2017; Rosewater and Sontheimer, 1994). Indeed, BDNF has been demonstrated to enhance differentiation of neurons (Wang and Kisaalita, 2011) and was shown to be present in higher levels in astrocyte conditioned media (Liu et al., 2012; Y. et al., 2016).

Mature neurons are post-mitotic and as such depend on OXPHOS for their energy demands whereas immortalised cell lines mainly rely on glycolysis (Choi et al., 2009). This is further supported by the Warburg hypothesis, which suggests rapidly dividing undifferentiated cells rely on glycolysis for cell division (Kaczanowski et al., 2018; Warburg, 1956, 2010). Furthermore, differentiation of SH-SY5Y neuronal cells has resulted in some controversy over susceptibility to RS. Some report differentiated SH-SY5Y cells are more resistant to RS induced by 6-hydroxydopamine, dopamine and MPP^+ (Cheung et al., 2009; Ferreira et al., 2013; Lopes et al., 2017). While others report differentiation results in greater vulnerability to RS induced by MPP^+ and 6-hydroxydopamine (Beck et al., 2006; J. I. Forster et al., 2016; Lopes et al., 2010). Others demonstrate differentiation also effects mitochondrial function (Gerencser et al., 2009; Schneider et al., 2011). This suggests other changes take place under differentiation including alteration to cellular metabolism and function.

4.1.2 Axonal degeneration

Neurodegenerative diseases are characterised by progressive neuronal death and loss of synapses. Axonal degeneration is a consequence of aging (Neukomm and Freeman, 2014), but also occurs in the early stages of neurodegeneration, preceding cell death and clinical symptoms in PD (Tagliaferro and Burke, 2016) and AD (Adalbert and Coleman, 2013). This suggests delaying axonal degeneration could provide a therapeutic potential for neurodegenerative disease.

During development, neurons generate more axons then necessary but later connections are fine-tuned where redundant connections are lost, this is referred to as neurite pruning which maximises network efficiency (Neukomm and Freeman, 2014; Raff, 2002). After development, axons can undergo degeneration through traumatic injury, chemical insults or general aging

(Salvadores et al., 2017). These different conditions can alter axonal morphology via multiple mechanisms (summarised in figure 4.1) including: retraction, local degeneration and Wallerian degeneration.

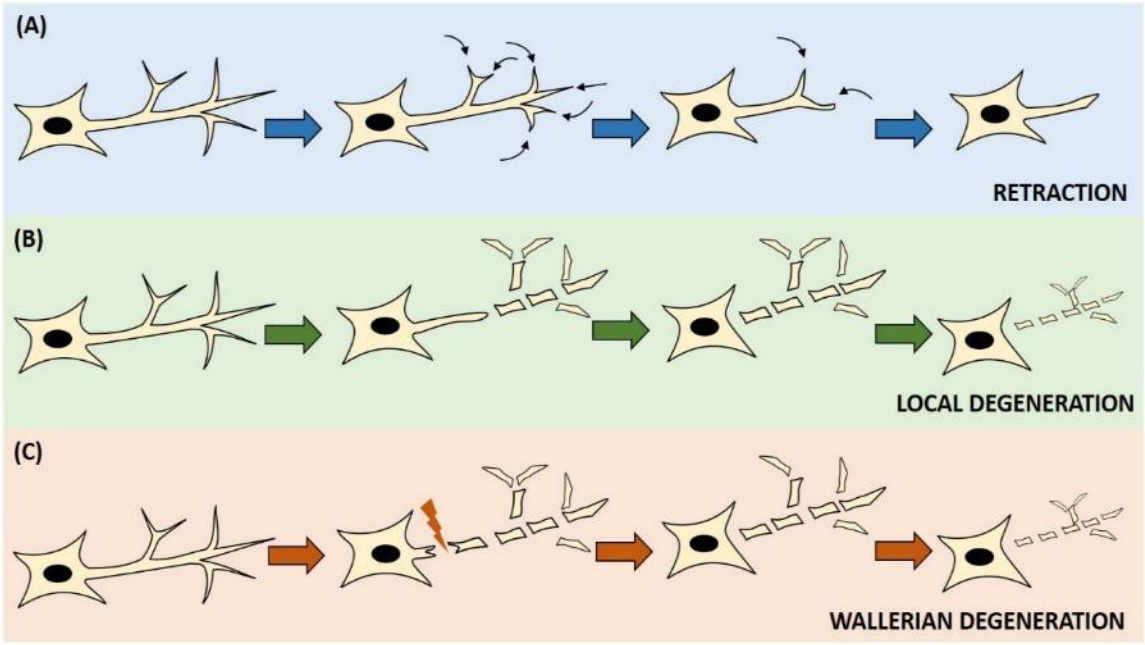

Figure 4.1 Distinct morphological methods of axon degeneration. *Schematic representation of neurons where soma and nucleus are on left with branched axons and dendrites. The axon and undergoes different methods of degeneration as shown in (A) – (C). (A) During axon retraction dendrites and axons retract in a retrograde manner without loss of integrity. (B) Local degeneration results in axons undergoing fragmentation in a synchronous manner where debris is subsequently removed by surrounding glia. (C) Wallerian degeneration is similar to local degeneration where axons undergo fragmentation due to axotomy but axons and dendrites fragment in an asynchronous manner fragmenting distal to the sight of injury. Adapted from Neukomm and Freeman et al., 2014.*

Retraction, unlike the other methods of degeneration, does not show morphological signs of fragmentation but involves axons retracting in a distal to proximal manner (Bagri et al., 2003). Axonal tips involute their membranes resulting in bulbous vesicle filled terminals at the end of axonal shafts referred to as retraction bulbs (Kao et al., 2019; Riley, 1981). The axon continues to involute in a retrograde manner until it is reabsorbed into the parent arbour where this degeneration preferentially occurs with shorter neurites to maximise energy efficiency and return contents to the cell body (Blanquie and Bradke, 2018; Portera-Cailliau et al., 2005).

Local axon degeneration primarily occurs with longer neurites and involves axon granulation and subsequent degradation by other cells (Portera-Cailliau et al., 2005). Initially, axons undergo blebbing where microtubules disassemble while axons swell. Finally, neurofilament

proteins fragment and the axon shaft degenerates in a synchronous manner (Kneynsberg et al., 2016; Saxena and Caroni, 2007).

Wallerian degeneration similar to local degeneration also results in axonal fragmentation but is as a result of axotomy (Coleman and Höke, 2020; Lee, 1963; Thomas, 1964). This involves 3 phases; initially acute degeneration effects both the proximal and distal stumps of the axons upon injury (Kerschensteiner et al., 2005). There is a brief latency period where these axons remain morphological intact and electrically active (Tsao et al., 1994). Finally, granular degeneration occurs where rapid asynchronous fragmentation of the axonal cytoskeleton occurs distal to the injury site (Coleman and Höke, 2020; Lubińska, 1982) within 24-48 hours *in vivo* (George and Griffin, 1994; Lubińska, 1977) and 12-24 hours *in vitro* (Araki et al., 2004; Coleman and Höke, 2020; Glass et al., 1993).

4.1.3 Antioxidant defences

There are multiple studies highlighting how RS are important for signalling including cellular growth and differentiation (Esposito et al., 2004; Paul D Ray et al., 2012), but when redox homeostasis becomes imbalanced cells become dysfunctional. As neural cells are susceptible to RS, they have multiple antioxidant defences to protect cells against specific RS including catalase, peroxiredoxin (PRDX), glutathione peroxidase (GPX), glutathione and superoxide dismutase (SOD).

Hydrogen peroxide is one of the few more stable RS able to cross membranes (De Grey, 2002), but cells contain multiple enzymes responsible for its removal. Catalase, is one enzyme present in numerous compartments including the cytosol, mitochondria and peroxisomes, playing a role in the removal of high levels of hydrogen peroxide (Gandhi and Abramov, 2012). Alternatively PRDX's are also important for hydrogen peroxide removal where there are a range of isoforms; PRDX1-6 (Fisher, 2011; Park et al., 2016). These isoforms localise to various compartments where PRDX1, 2, 5 and 6 are present in the cytosol where PRDX5 has also been shown in peroxisomes (Oberley et al., 2001). Whereas PRDX3 localises to mitochondria (Cox et al., 2010; Drechsel and Patel, 2010) while PRDX4 is present in the endoplasmic reticulum but is also secreted (Klichko et al., 2016; Rhee et al., 2005).

GPX's like PRDX's have multiple isoforms that are responsible for reducing hydrogen peroxide but also lipid peroxides (Dasuri et al., 2013; Gandhi and Abramov, 2012). These isoforms again have different cellular localisations such as the cytosol and mitochondria (Conrad and Friedmann Angeli, 2018). While detoxifying peroxides, GPX's also oxidise reduced glutathione (Dasuri et al., 2013; Gandhi and Abramov, 2012). Therefore, glutathione can protect against RS in

both a direct and indirect way, indirectly by becoming oxidised during GPX's reactions and directly through oxidation by RS themselves (Dringen et al., 2000; Maher, 2018). The difference in the glutathione defence system between different neural cell types is more understood, where glia are reported to have higher glutathione levels relative to neurons (Dringen et al., 2005; Dringen and Hamprecht, 1997), and synthesis is accelerated under stress more so in glia than neurons (Gleixner et al., 2016; Halliwell, 2003).

Other RS include superoxide where various isoforms of catalase are present in neural cells to combat this including cytosolic SOD1, mitochondrial SOD2, and extracellular SOD3. These enzymes are one of first defences against superoxide, catalysing its dismutation to hydrogen peroxide and oxygen (Dasuri et al., 2013; Donnelly et al., 1989; Fridovich, 1995).

Other enzymes are responsible for reducing oxidised proteins to allow recycling of PRDXs. For example, thioredoxin (TXN) that is responsible for reducing the disulphide bonds in PRDX's 1-5 (Poole et al., 2011b; Turner-Ivey et al., 2013). However, if there is not enough PRDX to cope with higher levels of RS, PRDX can be hyperoxidised to sulfinic or sulfonic acid, inactivating peroxidase activity as this cannot be reduced by thioredoxin (Rhee et al., 2007). This hyperoxidation has been associated with OS induced neuronal death *in vitro* (Bettegazzi et al., 2019; Papadia et al., 2008), and previously thought to be irreversible. However it is now known that sulfiredoxin, an ATP-dependent reductase is responsible for restoring inactive PRDX's back to the thioredoxin cycle, preventing permanent inactivation (Jönsson et al., 2008; Rhee et al., 2007; Shi et al., 2017).

Thus, antioxidant expression is essential to return cells to a balanced redox homeostasis. One of the major regulators of this antioxidant response is the NRF2/ARE pathway. NRF2 is a member of the leucine zipper transcription factor family playing a key role in cytoprotection and detoxification related to OS. NRF2 is regulated at multiple levels including transcription, translation, degradation, translocation and post-translational modifications (Dodson et al., 2019; Kong et al., 2001; Zhang and Hannink, 2003). Under physiological conditions NRF2 is maintained in the cytosol through binding with kelch-like ECH-associated protein (KEAP1), facilitating its degradation via the ubiquitin proteasome system (Dhakshinamoorthy and Jaiswal, 2001; Schmidlin et al., 2019; Suzuki and Yamamoto, 2015). Once redox becomes imbalanced RS result in NRF2 releasing from KEAP1 allowing translocation to the nucleus, binding to the ARE leading to upregulation of genes involved in redox balance (Chen and Kong, 2004; Dinkova-Kostova et al., 2018; Nguyen et al., 2005). NRF2 controls upregulation of various genes including those involved in glutathione synthesis (Lu, 2013; Nguyen et al., 2009), SOD (Holley et al., 2010), PRDX's, GPX's, TXN's and sulfiredoxin (reviewed more thoroughly in Korovila et al., 2017; Kwak et al., 2003).

4.1.4 Reactive species induce post-translational modifications

The plethora of RS including both ROS and RNS can react with multiple cellular components leading to cellular dysfunction. These can include a variety of changes such as lipid peroxidation, carbonylation and nitrosylation.

RS can attack lipid membranes initiating the self-propagating lipid peroxidation (Darley-usmar et al., 1992; Taso et al., 2019). Lipid peroxidation can subsequently result in a loss of membrane fluidity, affecting membrane permeability and slowing lateral diffusion (Borst et al., 2000b; Saleh et al., 2010). This process can also result in lipid peroxidation by-products such as 4-hydroxynonenal (4-HNE) and malondialdehyde (MDA), which are highly reactive toxic molecules due to their ability to interact with a variety of cellular components and proteins (Esterbauer et al., 1991; Gaschler and Stockwell, 2017). By covalently binding with proteins these molecules can alter function and can only be removed via degradation (Higdon et al., 2012). If not removed these proteins accumulate resulting in toxicity as interactions with mitochondrial subunits can overwhelm autophagy, contributing to mitochondrial dysfunction in neurons (Dodson et al., 2017; S. Zhang et al., 2017).

Carbonylation is a post-translational modification (PTM) commonly observed as a marker of OS in neurons where aldehyde, ketone or lactam groups are added to proteins (Møller et al., 2011; Reed and Butterfield, 2017). Multiple residues can by carbonylated where higher levels of carbonylated proteins have been reported in neurodegenerative diseases (Alam et al., 1997; Reed and Butterfield, 2017). Carbonylation is an irreversible PTM but other PTM's such as nitration and S-nitrosylation are reversible. While carbonylation is due to ROS, nitration is due to RNS that effect tyrosine residues (Nakamura and Lipton, 2017; Sadowska-Bartosz et al., 2014). Dinitrase enzymes are responsible for reversing this PTM (Deeb et al., 2013) but if not regulated this PTM contributes to neurodegeneration (Ljubuncic et al., 2010; Nakamura and Lipton, 2017). This is further highlighted by nitration of complex I in SH-SY5Y cells leading to ETC inhibition, enhancing apoptosis (Davis et al., 2010; Murray et al., 2003; van Horssen et al., 2019). S-nitrosylation is another reversible PTM that specifically effects thiol groups on cysteine and methionine residues. Like nitration, S-nitrosylation can inhibit ETC components (Di Giacomo et al., 2012; Foley et al., 2017) but also effect mitochondria via DRP1 enhancing oligomerisation resulting in mitochondrial fragmentation (Cho et al., 2009; Z. Zhang et al., 2016).

Therefore, while RS can induce signalling pathways that alter gene expression, they also affect cellular components and proteins via PTM's. Thus, understanding which PTM's RS induce will

aid in deciphering what pathways are activated during OS and hopefully provide more therapeutic potentials for neurodegenerative diseases.

4.1.5 Aims of the chapter

While immortalised cell lines are good for investigating neurodegenerative diseases due to their low-cost and high-throughput nature, they do not fully recapitulate all neurodegenerative hallmarks. Furthermore, there is controversy in the literature as to how differentiation effects susceptibility to RS. Therefore, different methods of SH-SY5Y differentiation were investigated while considering conditions would also have to be applicable to U-87MG glial cells for future co-culture work. Differentiation also allows this cellular model to better represent *in vivo* like conditions, improving investigations into the neuropathological hallmarks of neurodegeneration.

Once differentiation was established, neural cells were exposed to mitochondrial inhibitor rotenone and RS generating agent AAPH to assess how differentiation effects neural cell susceptibility to OS. This will provide a better model for investigating changes in gene expression and post-translational modifications in response to RS, allowing investigations into neural cell biochemical pathways underlying neurodegeneration. Furthermore, to determine if these cellular models are more representative of neurodegeneration, embryonic rat primary cortical neurons were also used to compare findings.

4.2 RESULTS

4.2.1 Differentiating SH-SY5Y neuronal and U-87MG glial cells

While mitotic cells are practical and effective for high throughput experiments, they have limitations. Therefore, to mimic an *in vivo* model we investigated differentiation methods for SH-SY5Y neuronal and U-87MG glial cells.

As complete differentiation of a mitotic line is difficult, we investigated optimal density for differentiation to ensure cells did not overgrow prior to treatment. Both SH-SY5Y (figure 4.2) and U-87MG (figure 4.3) neural cells were plated at 3450, 5180, 6900 and 10360 cells/cm^2 and differentiated over 5 days with 0.1, 0.5 and 1% (v/v) FBS in the presence of 10 µM retinoic acid (RA). Phase contrast microscopy images of SH-SY5Y neuronal cells (figure 4.2A) at 10360 cells/cm^2 appeared to have the greatest confluence with 1% (v/v) FBS, while 3450 cells/cm^2 showed fewer cells. SH-SY5Y cells differentiated with 0.1% (v/v) FBS showed large intercellular distances, some cell shrinkage and rounding with reduced neurites indicative of poor cell health. This was supported by confluence quantification using the incucyte S3 live-cell analysis system (figure 4.2B) and MTT reduction assays which showed the lowest absorbance values for 1% (v/v) FBS when compared to other FBS concentrations with the same cell density (figure 4.2E). 0.5 and 1% (v/v) FBS still showed pyramidal morphology and process development following 5-day differentiation instead of the usual cuboidal epithelial-like morphology observed with mitotic SH-SY5Y cells. Furthermore, incucyte proliferation quantification showed 0.5% (v/v) FBS had lower phase confluence (cell density) than 1% (v/v) FBS as growth plateaued at approximately 80 hours except with 10360 cells/cm^2 (figure 4.2C). Whereas SH-SY5Y cells differentiated with 1% (v/v) FBS, did not appear to plateau until approximately 100 hours (figure 4.2D). This suggests 0.5% (v/v) FBS was more successful in arresting cell division.

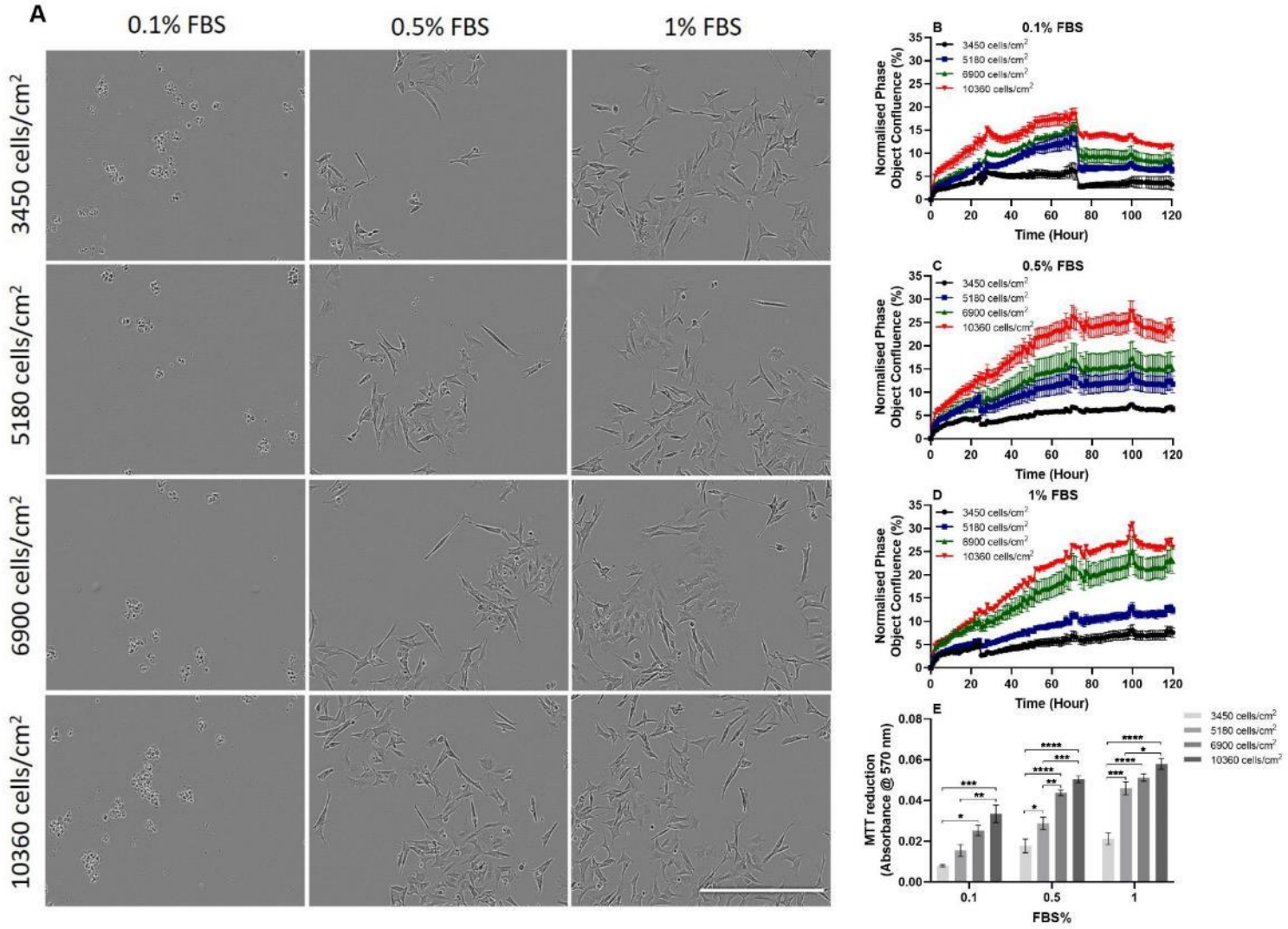

Figure 4.2 Minimal plating density for SH-SY5Y neuronal differentiation. *SH-SY5Y cells were plated at various densities and differentiated with 0.1, 0.5 and 1% (v/v) FBS with 10 µM retinoic acid over 5 days where media was changed every other day. (A) Day 5 images were taken using the incucyte S3 live-cell analysis system. Scale bar = 200 µm. Cell growth for 0.1% (B), 0.5% (C) and 1% (D) was monitored and quantified using the incucyte S3 live-cell analysis system. Viability on day 5 was quantified using the MTT reduction assay (E). Viability assay results are presented as % against control. Statistical analysis was performed using one-way ANOVA with Dunnett's post-hoc test where n=8 for all experiments. Statistical significance was recorded as * where *p<0.05, **p<0.01, ***p<0.001 and ****p<0.0001.*

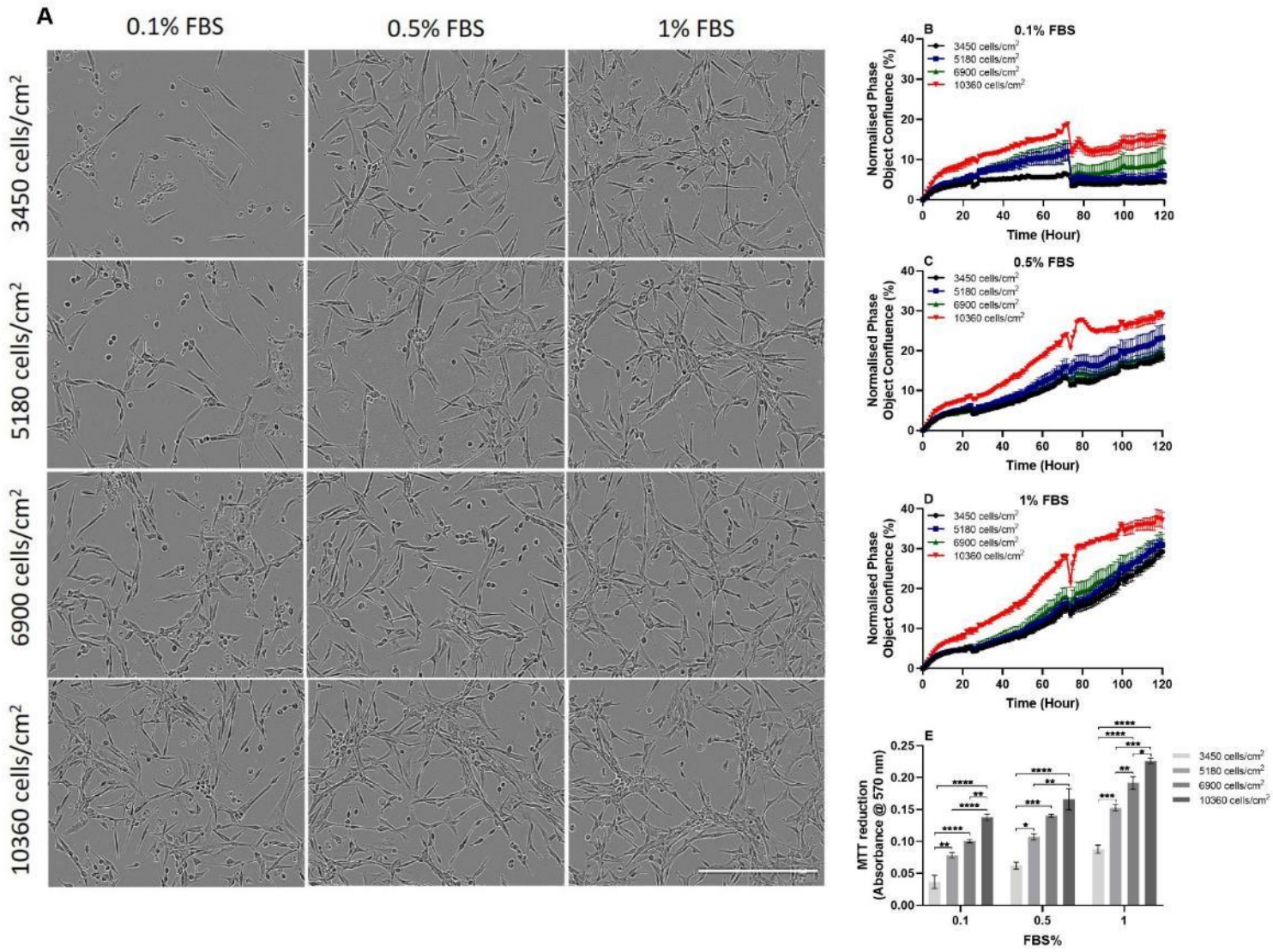

Figure 4.3 Minimal plating density for U-87MG glial differentiation. *U-87MG cells were plated at various densities and differentiated with 0.1, 0.5 and 1 % (v/v) FBS with 10 µM retinoic acid over 5 days where media was changed every other day. (A) Day 5 images were taken using the incucyte S3 live-cell analysis system. Scale bar = 200 µm. Cell growth for 0.1% (B), 0.5% (C) and 1% (D) was monitored and quantified using the incucyte S3 live-cell analysis system. Viability on day 5 was quantified using the MTT reduction assay (E). Viability assay results are presented as % against control. Statistical analysis was performed using one-way ANOVA with Dunnett's post-hoc test when n=8 for all experiments. Statistical significance was recorded as * where *p<0.05, **p<0.01, ***p<0.001 and ****p<0.0001.*

Unlike SH-SY5Y cells, U-87MG glial cells were less affected by plating density as all but 10360 cell/cm^2 showed similar growth curves for each FBS concentration (figure 4.3B, C and D), despite changes in MTT reduction (figure 4.3E). At 0.1% (v/v) FBS U-87MG cells showed few cell processes (figure 4.3A). Additionally, 0.5 and 1% (v/v) FBS showed cell body clustering with processes extended between clusters creating a network (figure 4.3A). As with SH-SY5Y cells, 1% (v/v) FBS showed the greatest U-87MG proliferation rate compared to 0.1 and 0.5% (v/v) FBS. Furthermore, 0.1% (v/v) FBS resulted in U-87MG glial cells exhibiting proliferation arrest at approximately 80 hours (figure 4.3B).

As axons and cell processes are characteristic of neurons *in vivo*, we also investigated which conditions improved neurite outgrowth and the influence of glia on this. One condition involved glia grown and differentiated over 5 days, prior to decellularisation to leave an extracellular matrix (ECM) scaffold. Debris was washed away prior to SH-SY5Y seeding. SH-SY5Y cells were subsequently incubated overnight in complete 10% (v/v) FBS media, whereupon media was replaced with differentiation media (0.5 or 1% (v/v) FBS with 10 μM RA). The second glia condition involved U-87MG glia being differentiated over 5 days where media was then collected and used to create conditioned media. This involved mixing the collected media 1:1 with fresh differentiation media, which was then added to the SH-SY5Y cells on the first day of differentiation, following overnight growth. Media was changed every other day where proliferation and neurite length was monitored using the incucyte S3 live-cell analysis system.

0.5% (v/v) FBS resulted in less proliferation during differentiation (figure 4.4C). However, SH-SY5Y seeded on decellularised U-87MG ECM showed the lowest increase in phase confluence/cell density (figure 4.4C), as supported by greater intercellular distance and cell rounding (figure 4.4B). In contrast, glial conditioned media increased proliferation relative to FBS/RA alone, suggesting U-87MG conditioned media supported SH-SY5Y growth. However, 0.5% (v/v) FBS with U-87MG conditioned media while increasing phase confluence arrested cell proliferation earlier, as growth plateaued at approximately 80 hours contrary to 1% (v/v), which plateaued at approximately 130 hours (figure 4.4C). Neurite growth mimicked phase confluence, where decellularised glia showed the lowest neurite growth over time as opposed to U-87MG conditioned media that showed the greatest (figure 4.4D). However, it is important to note 0.5% and 1% (v/v) FBS/RA with glia conditioned media showed similar neurite growth. Therefore, together this suggests that decellularised glia were not successful in improving neurite growth relative to FBS/RA differentiation, while U-87MG conditioned media aided neurite outgrowth.

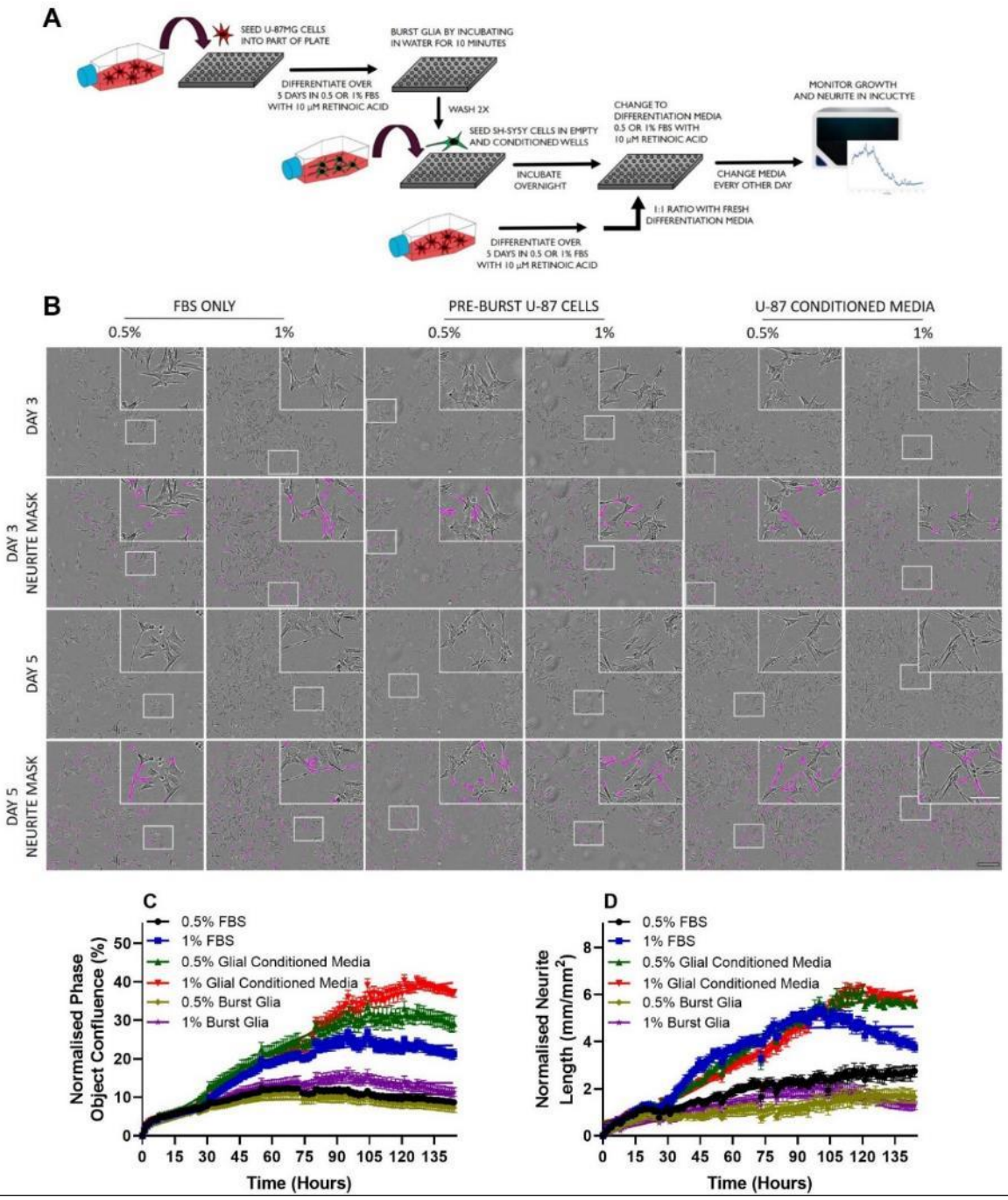

Figure 4.4 Optimising neurite outgrowth during differentiation. *Various conditions were used to determine the optimum conditions for neurite outgrowth during SH-SY5Y differentiation. (A) 3 conditions were used, each with 0.5 and 1% (v/v) FBS: where glia were grown and differentiated over 5 days prior to decellularising and washing prior to seeding. Following overnight incubation in complete 10% (v/v) FBS media fresh differentiation media (0.5 or 1% (v/v) FBS with 10 µM retinoic acid) was added to previous U-87MG wells. SH-SY5Y cells seeded in untouched wells were used as controls and the other condition had a 1:1 mixture of fresh differentiation media and U-87MG conditioned media taken from U-87MG cells differentiated over 5 days. (B) Images were taken using the incucyte S3 live-cell analysis system, and neurites were masked using the neurotracker software (purple). Scale bar = 200 µm. Inset scale bar = 100 µm. (C) Cell growth for each condition was monitored and quantified using the incucyte S3 live-cell analysis system. (D) Neurite outgrowth for each condition was monitored and quantified using the incucyte S3 live-cell analysis system.*

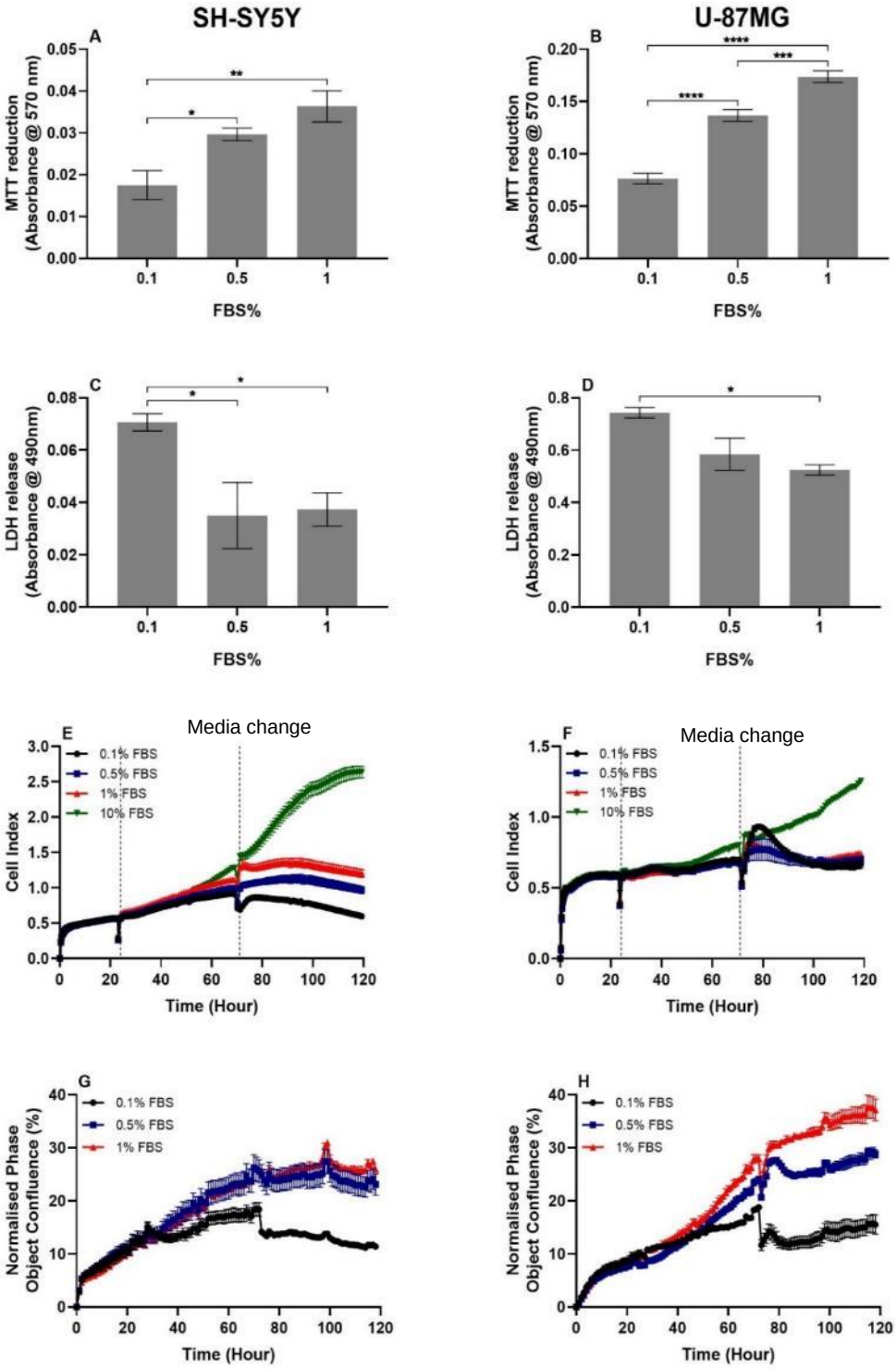

Figure 4.5 Evaluating the incucyte phase mask for monitoring cell proliferation and cytotoxicity studies. *Viability assays were conducted on SH-SY5Y and U-87MG cells differentiated at various FBS concentrations and 10 µM retinoic acid. MTT reduction assay for SH-SY5Y (A) and (B) U-87MG cells following 5 days of differentiation. LDH reduction assay for (C) SH-SY5Y and (D) U-87MG cells following 5 days of differentiation. Real-time analysis with iCelligence for (E) SH-SY5Y or (F) U-87MG differentiation. Real-time analysis using the incucyte S3 live-cell analysis system for (G) SH-SY5Y or (H) U-87MG differentiation. Statistical analysis was performed using one-way ANOVA with Dunnett's post-hoc test where n=4 for all experiments. Statistical significance was recorded as * where *p<0.05, **p<0.01, ***p<0.001 and ****p<0.0001.*

To confirm proliferation results quantified by the incucyte were accurate, we also investigated differentiation viability with other assays. MTT reduction assays of SH-SY5Y and U-87MG differentiation (figure 4.5A and B, respectively) showed a dose-dependent increase in MTT reduction with increasing FBS concentration. This was supported by LDH release assays that showed lower LDH release for higher FBS percentages for both SH-SY5Y and U-87MG neural cells (figure 4.5C and D, respectively). Furthermore, real-time cell analysis with the iCelligence showed similar patterns for growth as incucyte quantification for SH-SY5Y cells (figure 4.5E), where a plateau was observed at approximately 80 hours. Whereas differences were observed between iCelligence (figure 4.5F) and incucyte (figure 4.5H) results for U-87MG glial cells, possibly due to the clustering and network like formation observed with differentiation (figure 4.3A), as clustering would result in less iCelligence plate surface being covered, lowering cellular impedance while not impacting incucyte quantification.

BDNF, is a commonly used neurotrophic factor used to induce SH-SY5Y differentiation and neurite outgrowth. As such, we investigated the effect of BDNF on SH-SY5Y proliferation and neurite outgrowth following RA differentiation with and without U-87MG conditioned media. SH-SY5Y neuronal cells differentiated over 5 days with retinoic acid exhibited pyramidal morphology with some processes, where U-87MG conditioned media improved the length of these processes (figure 4.6A). Cells treated with BDNF alone and cells treated with BDNF and U-87MG conditioned media for a further 3 days showed less proliferation, where U-87MG conditioned media resulted in almost no proliferation (figure 4.6B). Additionally, following BDNF treatment cells showed a more flattened and elongated morphology but showed little change in neurite length (figure 4.6C), which is supported by the increased average cell diameter and process length summarised in table 4.1. Therefore, while BDNF improved neurite length for SH-SY5Y cells differentiated with FBS/RA alone it did not improve neurite length when compared to differentiation with FBS/RA and U-87MG conditioned media. However, BDNF did arrest proliferation more effectively than FBS/RA with or without U-87MG conditioned media alone. It is also interesting to note that there is an initial increase in neurite length upon addition of U-87MG conditioned media and BDNF (figure 4.6C). This is potentially due to the fresh U-87MG conditioned media promoting neurite outgrowth through secreted factors, but these are used up quickly and thus, not able to maintain this growth. Together, this suggests U-87MG cells secrete factors that aid neurite outgrowth and help arrest proliferation suggesting a more differentiated state but BDNF attenuates further cell proliferation.

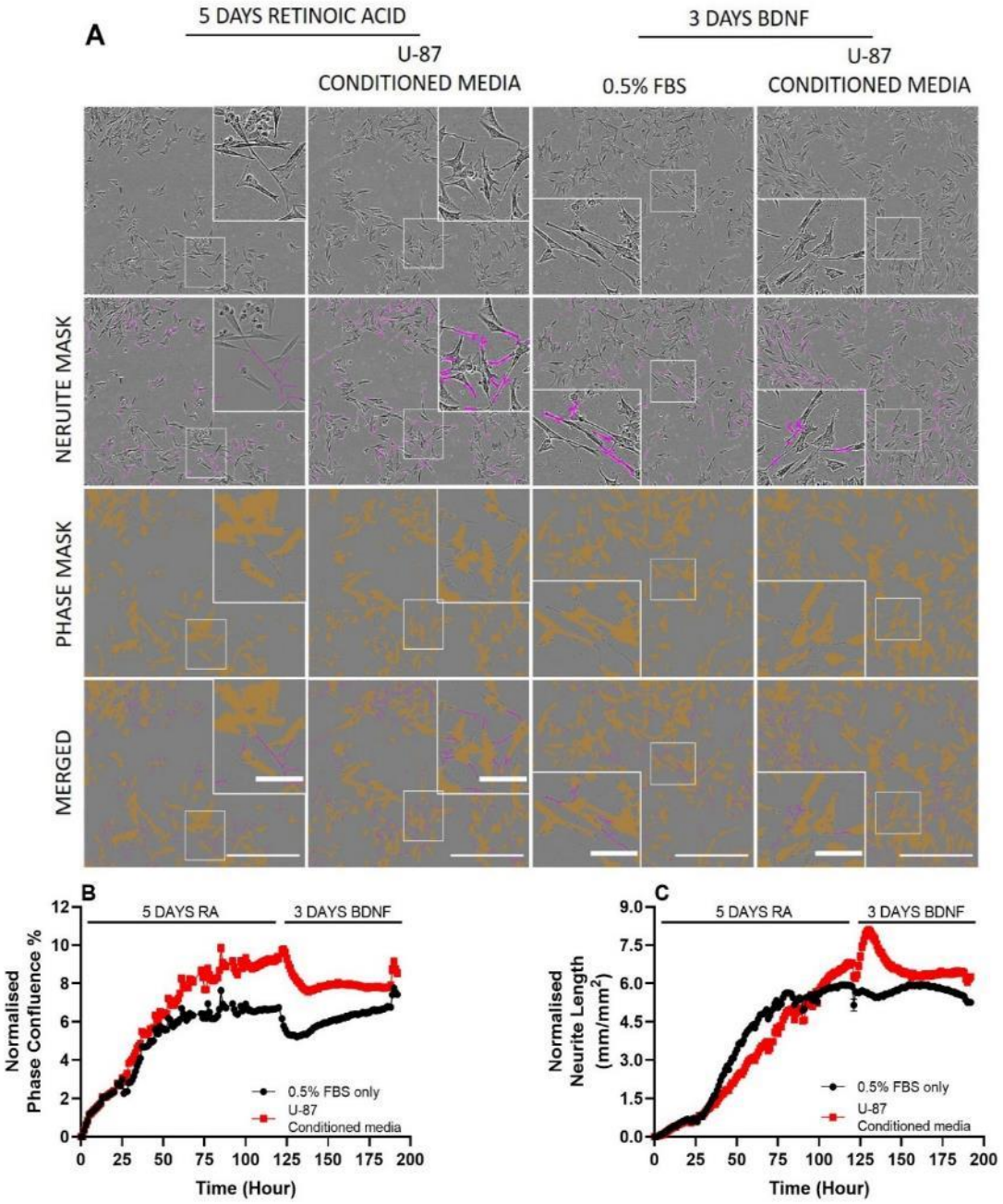

Figure 4.6 Effect of BDNF and U-87MG conditioned media on neurite outgrowth. *Following 5-day differentiation with 0.5% (v/v) FBS and 10 µM retinoic acid with and without U-87MG conditioned media 50 ng/ml of BDNF was added to cells in 0.5% (v/v) FBS for 3 days to investigate the effect on neurite outgrowth. (A) Images were taken every hour using the incucyte S3 live-cell analysis system, where the neurite mask is shown in purple and the cell bodies are masked in yellow. Scale bar = 200 µm. Inset scale bar = 100 µm. (B) Cell growth was monitored and quantified using the incucyte S3 live-cell analysis system. (C) Neurite outgrowth for each condition was monitored and quantified using the incucyte S3 live-cell analysis system neurotracker software.*

Table 4.1 Comparing morphological changes induced by different methods of differentiation. *Cell diameter and process length was assessed where 10 random neurons were selected per image, averaged and repeated in triplicate to calculate standard deviation where values were determined to be significant by t-tests relative to mitotic cells.*

	Average cell diameter (µm)	Standard deviation	P (t-test against mitotic)	Average process length (µm)	Standard deviation	P (t-test against mitotic)
Mitotic cells	33.1	3.06		38.4	9.44	
5 days retinoic acid	46.6	2.21	0.00148	73.2	8.09	0.00381
5 days retinoic acid/ U-87 conditioned media	64.5	1.80	0.00751	108	10.6	0.0119
5 days retinoic acid/ 3 days BDNF	62	3.29	0.0000250	85.5	17.2	0.0862
5 days retinoic acid/ 3 days BDNF/ U-87 conditioned media	63.4	8.20	0.019366	99.3	15.8	0.00462

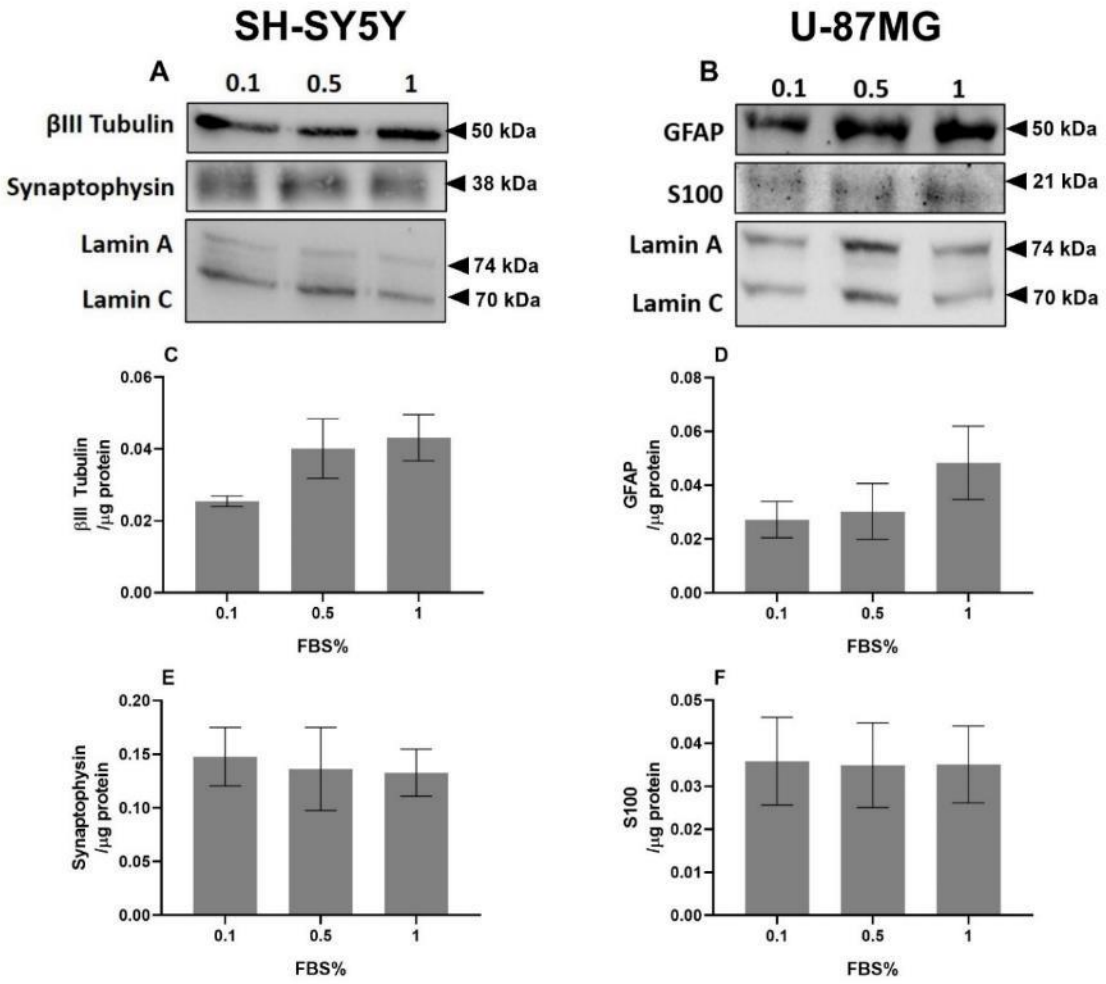

Figure 4.7 SH-SY5Y and U-87MG cells express markers of differentiation following reduced serum and retinoic acid exposure. *SH-SY5Y and U-87MG glial cells were differentiated with 0.1, 0.5 and 1% (v/v) FBS and 10 µM retinoic acid over 5 days were probed for neuronal and astrocyte markers, respectively. Representative Western blots of (A) neuronal SH-SY5Y total cell extracts were probed with (C) βIII tubulin (1:1000) and (E) synaptophysin (1:1000). (B) Glial U-87MG total cell extracts were probed with (D) GFAP (1:1000) and S100 (1:500). Each Western blot is accompanied by a plot summarising densitometric analyses of Western blots using AIDA software. Results are presented per µg of protein. Statistical analysis was performed using one-way ANOVA with Tukey's post-hoc test where n=3 for all experiments. Statistical significance was set at *p<0.05.*

To confirm differentiation, neural marker expression was investigated using Western blotting. All FBS/RA differentiated SH-SY5Y cells expressed both βIII tubulin and synaptophysin (figure 4.7A, C and E). Similarly, FBS/RA differentiated U-87MG glial cells expressed astrocytic markers GFAP and S100 (figure 4.7B, D and F). For both SH-SY5Y and U-87MG cells FBS concentration did not significantly affect the expression of these neural markers.

Creating a co-culture with SH-SY5Y and U-87MG was a project objective. Therefore, we opted to differentiate both SH-SY5Y and U-87MG cells with 0.5% (v/v) FBS with a density of 5180 cells/cm^2.

To determine whether differentiation with RA influences cellular respiration we assessed ATP levels in both mitotic and differentiated SH-SY5Y and U-87MG neural cells (figure 4.8). By measuring extracellular acidification rate (ECAR) and oxygen consumption rate (OCR) simultaneously with the Seahorse XFe24 analyser, ATP generation through glycolysis and OXPHOS was calculated. The basal OCR of differentiated SH-SY5Y and U-87MG cells was greater than their mitotic counterparts (figure 4.8A and B, respectively), while ECAR remained similar for SH-SY5Y and U-87MG cells (figure 4.8C and D). Following the addition of mitochondrial inhibitors (oligomycin and a mixture of rotenone/antimycin A) the rate of ATP production from glycolysis and mitochondria was calculated. Basal rates of both mitotic and differentiated SH-SY5Y cells showed comparable total ATP levels (figure 4.8E and F). However, the rate of ATP production by glycolysis decreased in differentiated SH-SY5Y neuronal cells, which was further supported by the change in energetic maps, where no glycolytic ATP production was observed in differentiated SH-SY5Y cells (figure 4.8G and H). In contrast, U-87MG cells showed greater ATP production following differentiation alongside a greater mitochondrial ATP production rate (figure 4.8E and F). Together, these results suggest differentiation with FBS/RA results in SH-SY5Y and U-87MG neural cells relying on mitochondria more for their ATP demand.

To confirm the greater rate of ATP production from mitochondria was not a result of increased mitochondrial numbers in differentiated cells, we investigated mitochondrial DNA content using quantitative real-time polymerase chain reactions. Cell lysates were collected after 5 days of FBS/RA differentiation to assess potential changes in mitochondrial number. Mitochondrial DNA copy number normalised to nuclear DNA copy number showed comparable values between differentiated and mitotic SH-SY5Y (figure 4.9B) and U-87MG (figure 4.9C) cells. In addition, as with previous mitotic investigations, SH-SY5Y cells showed a significantly greater number of mitochondria than U-87MG glial cells even when differentiated (figure 4.9A) suggesting U-87MG glial cells possibly rely more on glycolysis than SH-SY5Y cells.

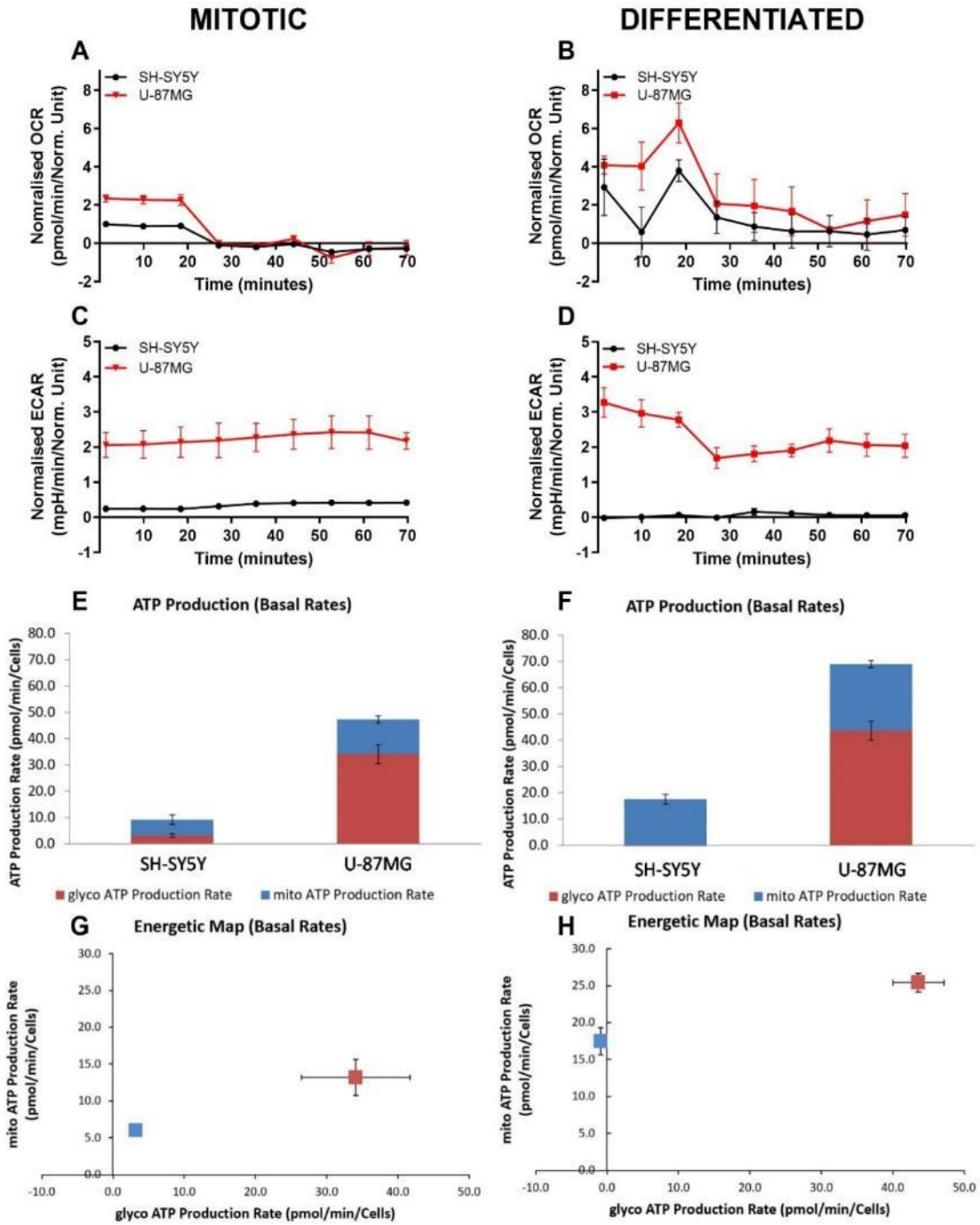

Figure 4.8 Changes to respiration following differentiation in neuronal and glial cells. *Following 5-day differentiation of SH-SY5Y and U-87MG cells with 0.5% (v/v) FBS and 10 µM retinoic acid respiration was measured using the Seahorse XFe24 analyser and compared to corresponding mitotic cells. To determine the cells main source of ATP, (A, C) oxygen consumption rate (OCR) and (B, D) extracellular acidification rate (ECAR) were concomitantly measured. Using the Seahorse ATP report generator glycolytic and mitochondrial basal ATP production rate was calculated for (E) mitotic and (F) differentiated neural cells. An energetic map was also generated to show how differentiation altered glycolytic or mitochondrial ATP production.*

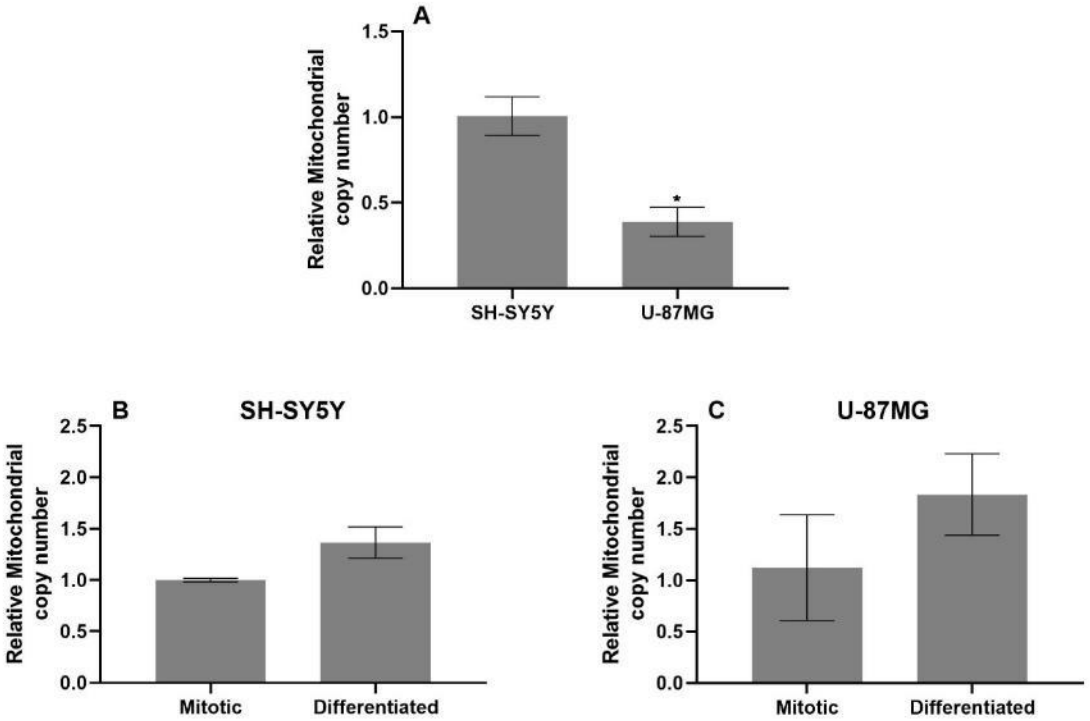

Figure 4.9 Differentiation does not affect mitochondrial DNA copy number. *DNA was extracted from mitotic or differentiated cells (5 days with 0.5% (v/v) FBS and 10 µM retinoic acid) using the PureLink® genomic DNA kit, as per the manufacturer's instructions. 50 ng of DNA was subsequently used for qRT-PCR. (A) Mitochondrial DNA expression of differentiated SH-SY5Y and U-87MG neural cells where results are expressed relative to SH-SY5Y expression. Expression between mitotic and differentiated (B) SH-SY5Y and (C) U-87MG cells where results are expressed relative to mitotic expression. Statistical analysis was performed using an unpaired t-test where n=3 for all experiments. Statistical significance was set at *p<0.05.*

4.2.2 The effect of reactive species on differentiated neural cell viability

Following differentiation of neural cells, we examined their susceptibility to RS generated by AAPH and rotenone following 48-hour treatment. Neural cell viability was assessed via morphological changes, viability and functional activity assays.

Phase contrast microscopy showed increased intercellular distance as well as cellular shrinkage and rounding for differentiated SH-SY5Y neuronal cells treated with AAPH suggesting reduced cell viability (figure 4.10A). In contrast, U-87MG cells treated with 1 mM AAPH show decreased intercellular distance and a more elongated morphology (figure 4.10A). However, with 5 mM AAPH U-87MG glial cells showed greater intercellular distance and cellular rounding like SH-SY5Y cells. This was supported by viability assays that showed MTT reduction significantly decreased in a dose-dependent manner for AAPH treated SH-SY5Y cells relative to the control (figure 4.11A).

Whereas U-87MG glial cells showed a significant increase in MTT reduction with 1 mM AAPH but significantly decreased at 5 mM AAPH (figure 4.11A). SH-SY5Y LDH assays showed LDH release significantly increased for ≥1 mM AAPH supporting MTT reduction assays (figure 4.11C). In contrast, U-87MG glial cells only showed significant LDH release for 5 mM AAPH (figure 4.11C), suggesting like the MTT reduction assays, 5 mM AAPH resulted in reduced cell viability. Phase contrast images at 48 hours reinforced these observations as there was a dose-dependent decrease in SH-SY5Y phase confluence, while U-87MG glia increased for 1 mM AAPH but decreased for 5 mM (figure 4.10A).

Following 48-hour rotenone treatment, phase contrast microscopy showed both differentiated SH-SY5Y and U-87MG exhibited characteristics of poor cell health (i.e. increased intercellular distance, loss of processes, cellular shrinkage and rounding; figure 4.10B). Interestingly, U-87MG glial cells also exhibited increased clustering in a dose dependent manner, alongside release of cellular debris. Further supporting this, viability assays show significantly decreased MTT reduction in a dose-dependent manner for both SH-SY5Y and U-87MG cells (figure 4.11B). LDH assays also showed that ≥0.5 µM rotenone treatment resulted in a significant release of LDH (figure 4.11D) and a decrease in phase confluence (figure 4.11F) in both cell types.

Interesting to note is that differentiated SH-SY5Y neuronal cells appear to have greater resistance to rotenone, as MTT reduction for mitotic SH-SY5Y cells shows a more significant reduction for ≥0.5 µM (figure 3.23A and 3.27A). This is supported by LDH assays, where mitotic SH-SY5Y cells show a greater significant increase in LDH release for 0.5 µM rotenone (figure 3.23C and 3.27C) than differentiated SH-SY5Y neuronal cells (figure 4.11D). In contrast, differentiated U-87MG glial cells appear to be more susceptible to rotenone than mitotic cells, as the latter only show significant LDH release at 2.5 µM rotenone (figure 3.23D and 3.27D). Rotenone treatment (≥0.5 µM) results in a significant LDH release for differentiated U-87MG cells (figure 4.11D). Additionally, differentiated SH-SY5Y neuronal cells appear to be more susceptible to AAPH as there is a significant increase in LDH release for 1 mM AAPH (figure 4.11C) that was not observed with mitotic SH-SY5Y cells (figure 3.21C and 3.25C). Both mitotic and differentiated U-87MG cells showed increased MTT reduction for 1 mM AAPH. However, mitotic U-87MG glial cells still showed increased MTT reduction with 5 mM AAPH (figure 3.21D and 3.25D), while differentiated U-87MG cells showed reduced MTT levels (figure 4.11C). Together, this suggests that reduced FBS and RA differentiation of SH-SY5Y and U-87MG neural cells results in changes in RS susceptibility.

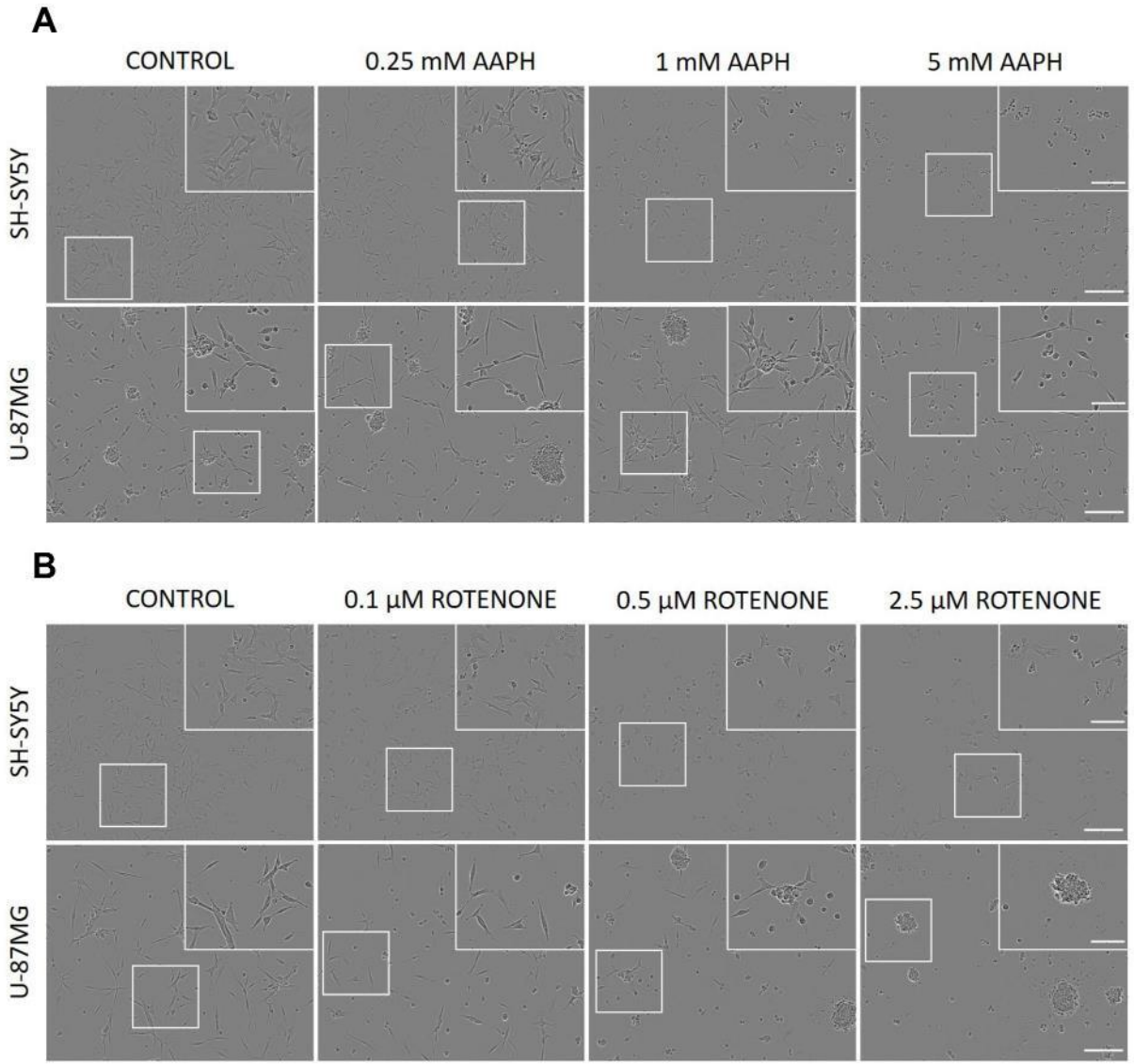

Figure 4.10 Differentiated neuronal SH-SY5Y and glial U-87MG cell morphology following 48-hour AAPH or rotenone exposure. *Morphology was examined following 5-day differentiated SH-SY5Y or U-87MG cells treated with AAPH or rotenone for 48 hours. Phase contrast microscopy of (A) SH-SY5Y or (B) U-87MG monocultures. Scale bar = 200 µm. Inset scale bar = 100 µm.*

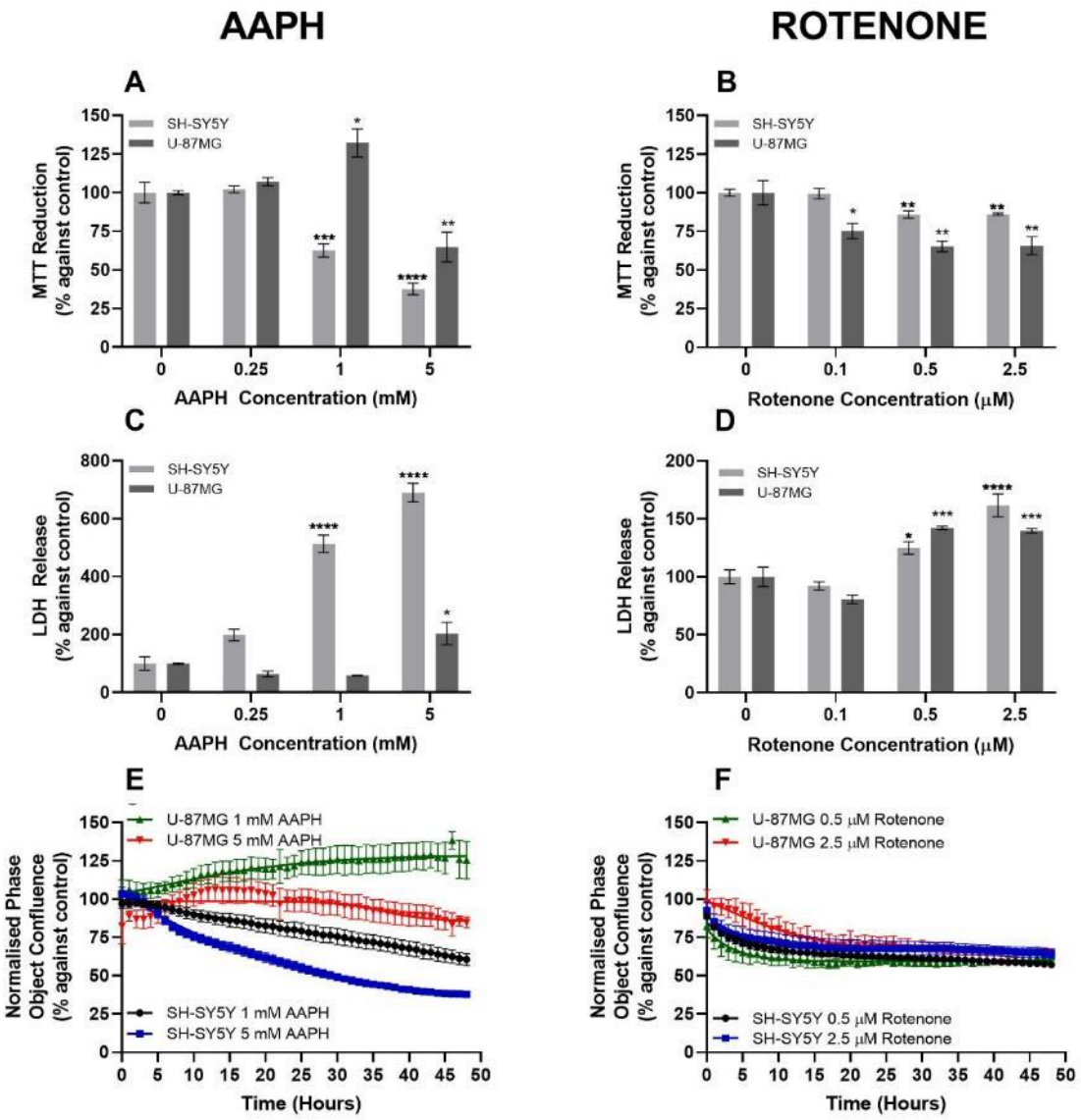

Figure 4.11 Differentiated neuronal SH-SY5Y and glial U-87MG cell viability following 48-hour AAPH or rotenone exposure. *Viability assays were conducted on 5-day differentiated SH-SY5Y or U-87MG cells treated with AAPH or rotenone for 48 hours. MTT reduction assay for (A) SH-SY5Y or (B) U-87MG monocultures. LDH release for (C) SH-SY5Y or (D) U-87MG monocultures. Real-time analysis using the incucyte S3 live-cell analysis system for (E) SH-SY5Y or (F) U-87MG monocultures. Viability assay results are presented as % against control. Statistical analysis was performed using one-way ANOVA with Dunnett's post-hoc test where n=3 for all experiments. Statistical significance was recorded as *p<0.05, **p<0.01, ***p<0.001 and ****p<0.0001, relative to each respective control.*

To confirm the changes in viability were due to RS, antioxidants α-tocopherol (200 μM) and ascorbic acid (1 mM) were added concurrently with treatment (figure 4.12-4.15). Differentiated neural viability was assessed by morphological changes, viability assays and real-time analysis using to incucyte S3 live-cell analysis system.

Following 48-hour treatment with 1 mM AAPH and α-tocopherol, differentiated SH-SY5Y cell death was attenuated. However, α-tocopherol was ineffective against 5 mM AAPH. In contrast, ascorbic acid was unable to attenuate AAPH-induced cell death (figure 4.12-4.13) at all concentrations tested. Phase contrast microscopy showed α-tocopherol attenuated the loss of cellular processes and improved cellular morphology for 1 mM AAPH. In contrast, ascorbic acid treated SH-SY5Y cells showed cellular rounding and shrinkage for all AAPH concentrations (figure 4.12A). Improved neuronal viability with α-tocopherol was also indicated by significantly increased MTT reduction for 1 mM but not for 5 mM AAPH, while ascorbic acid did not significantly change MTT reduction levels for all AAPH concentrations tested (figure 4.13A). LDH assays showed both antioxidants significantly improved membrane integrity for 1 mM AAPH treatment. However, both α-tocopherol and ascorbic acid were not able to reduce LDH levels for 5 mM AAPH where ascorbic acid exacerbated LDH release (figure 4.13C). Live-cell analysis showed concurrent treatment with α-tocopherol, but not ascorbic acid resulted in a higher phase confluence/cell density (figure 4.13E).

Differentiated U-87MG glial exhibited increased proliferation with 1 mM AAPH treatment which was attenuated by both antioxidants (figure 4.12-4.13). Phase contrast microscopy for both α-tocopherol and ascorbic acid showed greater intercellular distance, and less cellular elongation than 1 mM AAPH treated differentiated U-87MG glial cells alone (figure 4.12B). However, both antioxidants still showed cellular rounding and loss of processes for 5 mM AAPH (figure 4.12B). MTT reduction assays supported this, as both antioxidants significantly reduced MTT reduction levels relative to 1 mM AAPH alone, while having no significant effect on 5 mM AAPH treated cells (figure 4.13B). However, while MTT levels showed no significant change for 5 mM AAPH, LDH assays showed both antioxidants significantly decreased LDH release (figure 4.13D). Live-cell analysis supported MTT reduction and phase microscopy results as both antioxidants reduced differentiated U-87MG glia phase confluence (figure 4.13F).

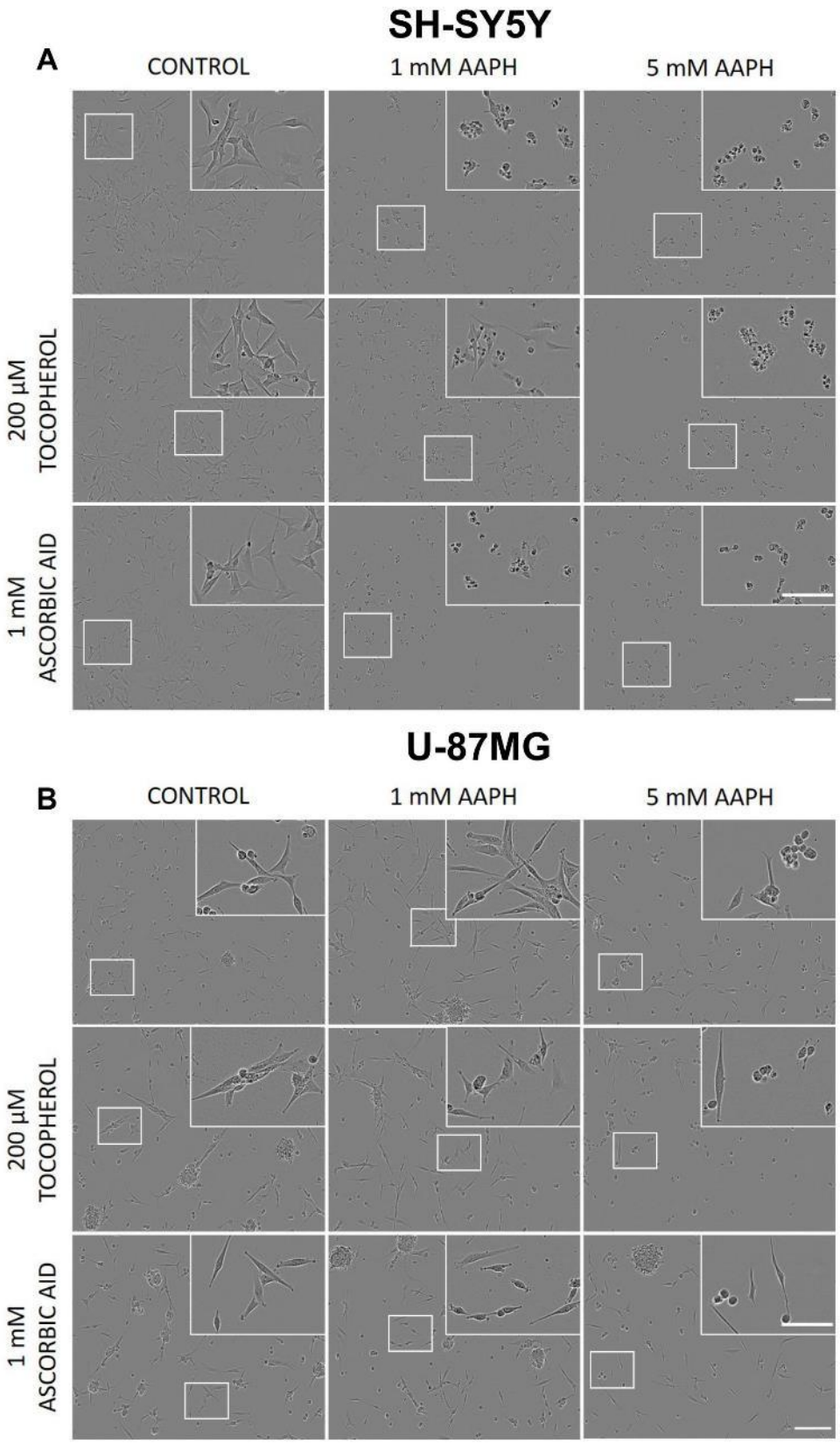

Figure 4.12 Differentiated neuronal SH-SY5Y and glial U-87MG cell morphology following 48-hour AAPH in the presence of antioxidants. *Morphology investigations were conducted on 5-day differentiated SH-SY5Y or U-87MG cells treated with AAPH, with or without 200 µM α-tocopherol or 1 mM ascorbic acid for 48 hours. Phase contrast microscopy of (A) SH-SY5Y or (B) U-87MG monocultures. Scale bar = 200 µm. Inset scale bar = 100 µm.*

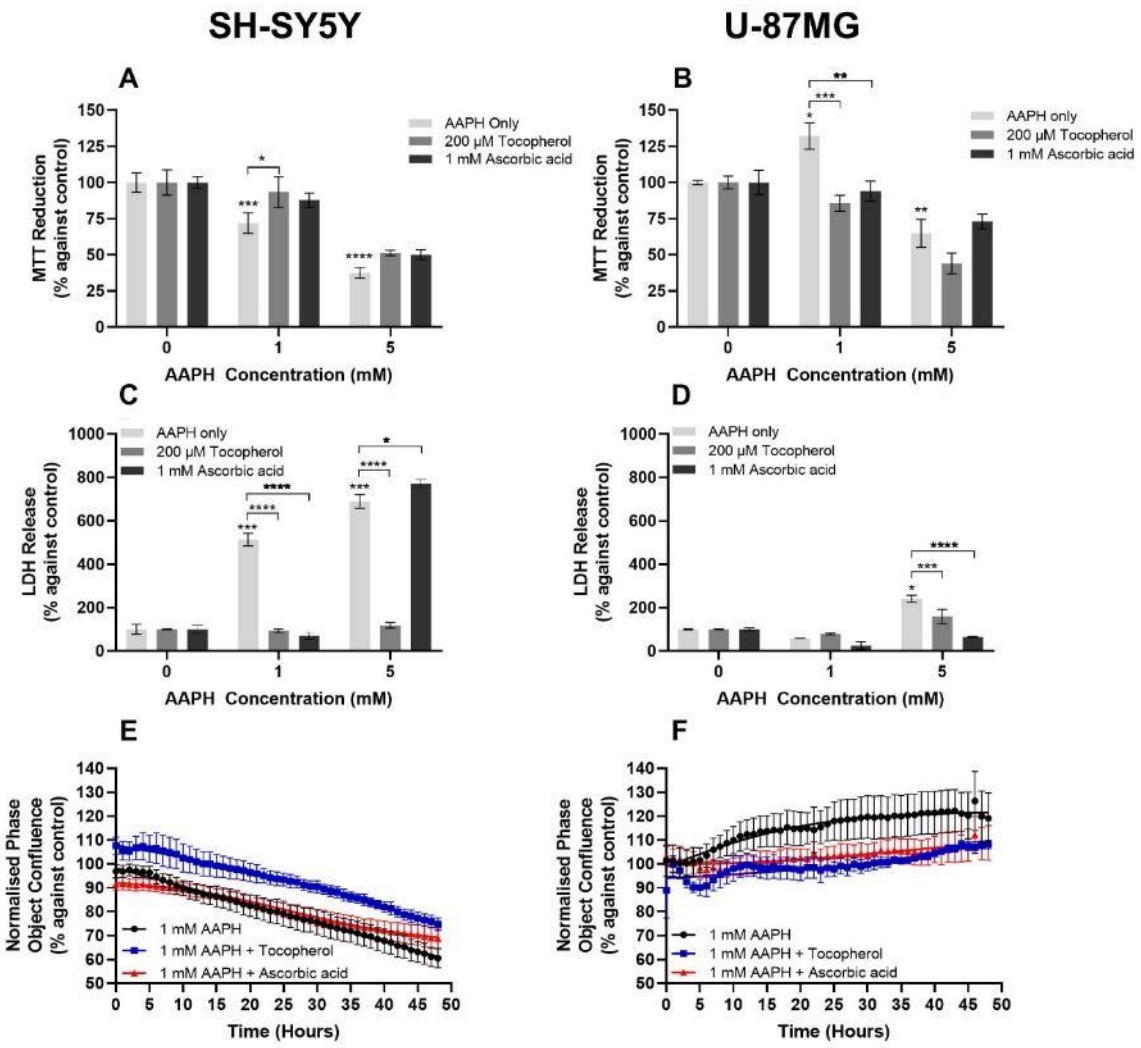

Figure 4.13 Differentiated neuronal SH-SY5Y and glial U-87MG cell viability following 48-hour AAPH in the presence of antioxidants. *Viability assays were conducted on 5-day differentiated SH-SY5Y or U-87MG cells treated with AAPH with or without 200 µM α-tocopherol or 1 mM ascorbic acid for 48 hours. MTT reduction assay for (A) SH-SY5Y or (B) U-87MG monocultures. LDH release for (C) SH-SY5Y or (D) U-87MG monocultures. Real-time analysis using the incucyte S3 live-cell analysis system for (E) SH-SY5Y or (F) U-87MG monocultures. Viability assay results are presented as % against control. Statistical analysis was performed using one-way ANOVA with Dunnett's post-hoc test where n=3 for all experiments. Statistical significance was recorded as *p<0.05, **p<0.01, ***p<0.001 and ****p<0.0001, where if not indicated this is relative to the appropriate cell control.*

Antioxidant treatments were also investigated with rotenone exposure. Unlike AAPH exposure, both α-tocopherol and ascorbic acid were able to attenuate differentiated SH-SY5Y rotenone induced cell death. Phase contrast microscopy showed each antioxidant was able to reduce intercellular distance, while attenuating cellular shrinkage and rounding suggesting improved viability (figure 4.14). This was supported by MTT reduction assays, which showed MTT reduction significantly increased when rotenone exposed cells were treated with either α-tocopherol or ascorbic acid (figure 4.15A). LDH assays also confirmed these findings as both antioxidants significantly reduced LDH release for both rotenone concentrations (figure 4.15C). Live-cell analysis also showed this as both α-tocopherol and ascorbic resulted in greater phase confluence compared to 0.5 µM rotenone alone (figure 4.15E).

Similar results were observed for differentiated U-87MG glial cells concurrently treated with α-tocopherol and ascorbic acid, where rotenone induced death was attenuated (figure 4.14-4.15). Antioxidants attenuated loss of processes and cell shrinkage observed with rotenone alone (figure 4.14B). Viability assays supported these findings as MTT reduction was significantly increased for 0.5 µM rotenone when concurrently treated with both antioxidants (figure 4.15B). Additionally, LDH release was significantly reduced for 0.5 µM rotenone when treated with either antioxidant (figure 4.15D). Live-cell analysis also confirmed improved viability as quantified phase confluence was greater for antioxidant treated differentiated U-87MG glial cells (figure 4.15F).

Together, these results suggest AAPH and rotenone damage differentiated SH-SY5Y and U-87MG viability via RS, which can be attenuated with antioxidants. Whilst ascorbic acid was not effective in attenuating cell death in mitotic U-87MG glial cells (figure 3.24-3.27), the antioxidant was able to attenuate cell death in differentiated U-87MG cells. This suggests differentiation results in some changes to cell metabolism, susceptibility to cellular stress and antioxidant capacity.

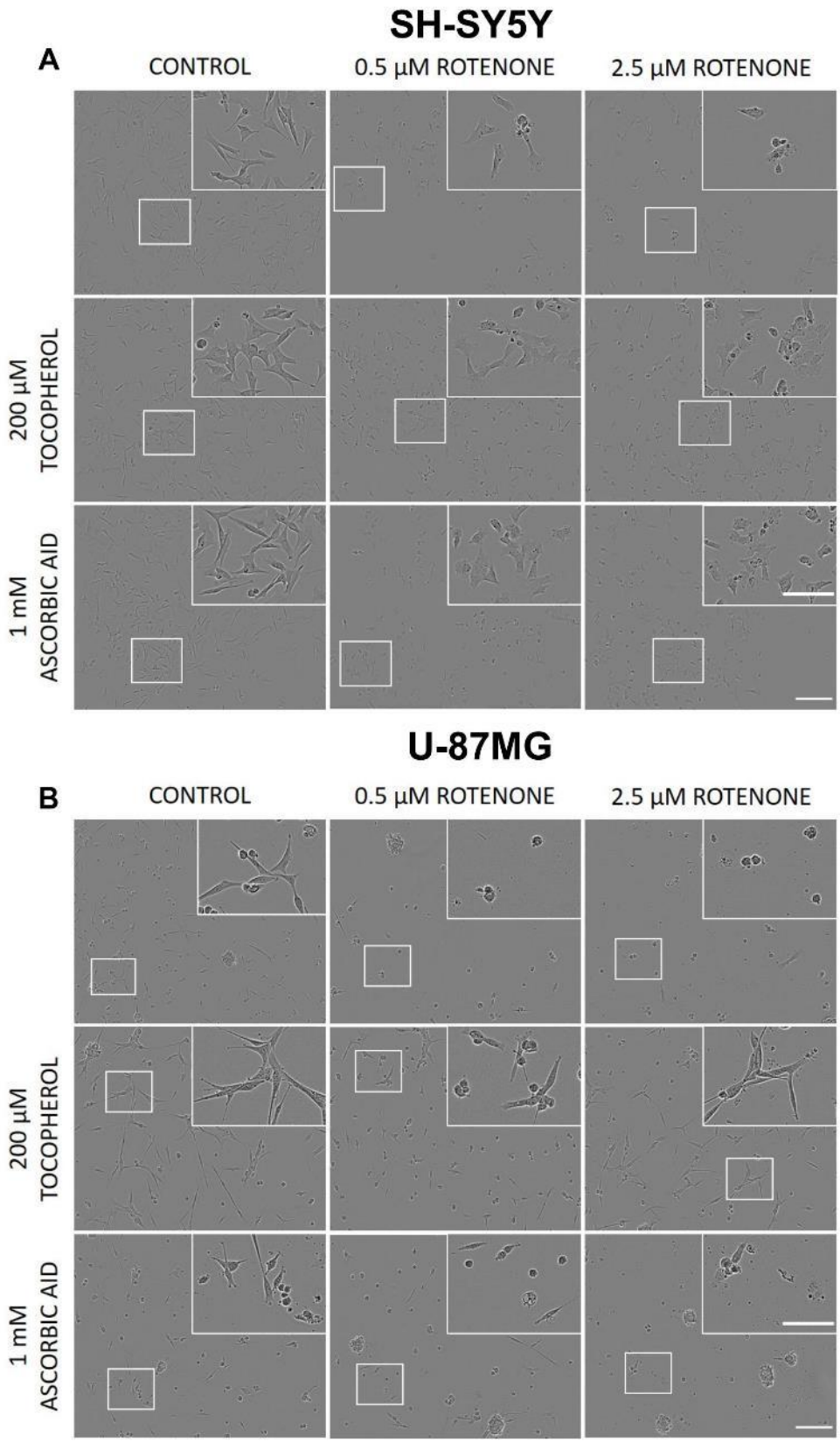

Figure 4.14 Differentiated neuronal SH-SY5Y and glial U-87MG cell morphology following 48-hour rotenone in the presence of antioxidants. *Morphology investigations were conducted on 5-day differentiated SH-SY5Y or U-87MG cells treated with rotenone with or without 200 µM α-tocopherol or 1 mM ascorbic acid for 48 hours. Phase contrast microscopy of (A) SH-SY5Y or (B) U-87MG monocultures. Scale bar = 200 µm. Inset scale bar = 100 µm.*

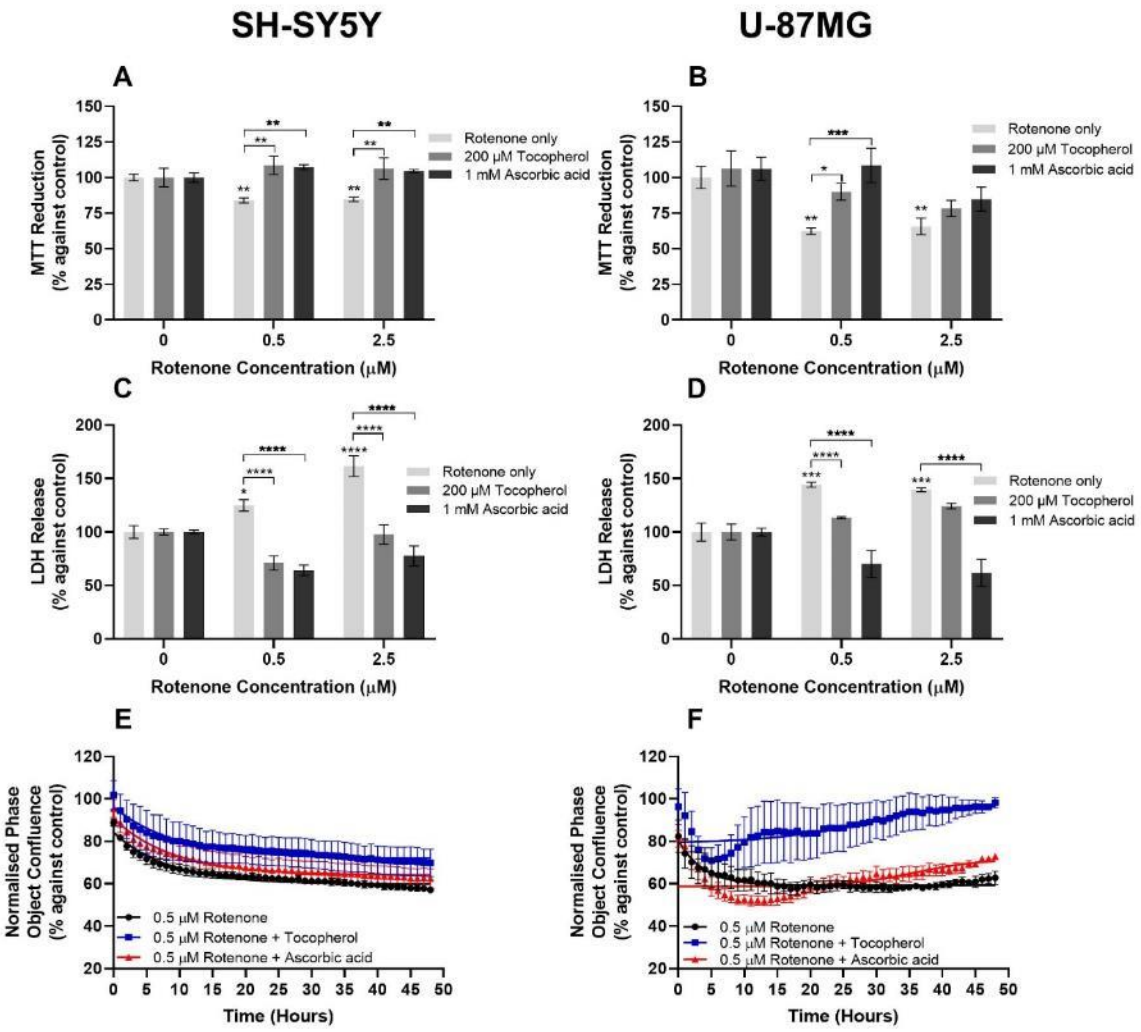

Figure 4.15 Differentiated neuronal SH-SY5Y and glial U-87MG cell viability following 48-hour rotenone in the presence of antioxidants. *Viability assays were conducted on 5-day differentiated SH-SY5Y or U-87MG cells treated with rotenone with or without 200 μM α-tocopherol or 1 mM ascorbic acid for 48 hours. MTT reduction assay for (A) SH-SY5Y or (B) U-87MG monocultures. LDH release for (C) SH-SY5Y or (D) U-87MG monocultures. Real-time analysis using the incucyte S3 live-cell analysis system for (E) SH-SY5Y or (F) U-87MG monocultures. Viability assay results are presented as % against control. Statistical analysis was performed using one-way ANOVA with Dunnett's post-hoc test where n=3 for all experiments. Statistical significance was recorded as *p<0.05, **p<0.01, ***p<0.001 and ****p<0.0001, where if not indicated this is relative to the appropriate cell control.*

The effect of AAPH and rotenone on cells differentiated with conditioned media/BDNF was also investigated. Like FBS/RA differentiated SH-SY5Y neuronal cells, both BDNF alone and in combination with U-87MG conditioned media showed a dose-dependent decrease in cell viability for both AAPH and rotenone treatment (figure 4.16-4.17). Phase contrast morphology showed similar effects where higher concentrations of AAPH (figure 4.16A) and rotenone (figure 4.16B) resulted in greater intercellular distances, and loss of processes accompanied by cellular rounding, suggesting poor cell health. BDNF differentiation resulted in SH-SY5Y cells being less susceptible to AAPH induced death as only 5 mM AAPH resulted in a significant decrease in MTT reduction (figure 4.17A) and a significant increase in LDH release (figure 4.17C), while ≥1 mM AAPH had this effect on FBS/RA differentiated SH-SY5Y cells (figure 4.16). In contrast, BDNF differentiated SH-SY5Y cells appeared more susceptible to rotenone induced cell death as all concentrations of rotenone significantly decreased MTT reduction relative to the control (figure 4.17B).

U-87MG conditioned media further increased resistance to AAPH as there was significantly greater MTT reduction at 1 mM AAPH, although LDH release was only significantly decreased for 5 mM AAPH (figure 4.17A and B). However, phase confluence results suggested this change in susceptibility was minor (figure 4.17E). In contrast, U-87MG conditioned media appeared to have a greater effect in conferring resistance to rotenone induced death as there was significantly greater MTT reduction for U-87MG conditioned media with 0.1 and 0.5 µM rotenone (figure 4.17B), which is further highlighted by the greater phase confluence (figure 4.17F).

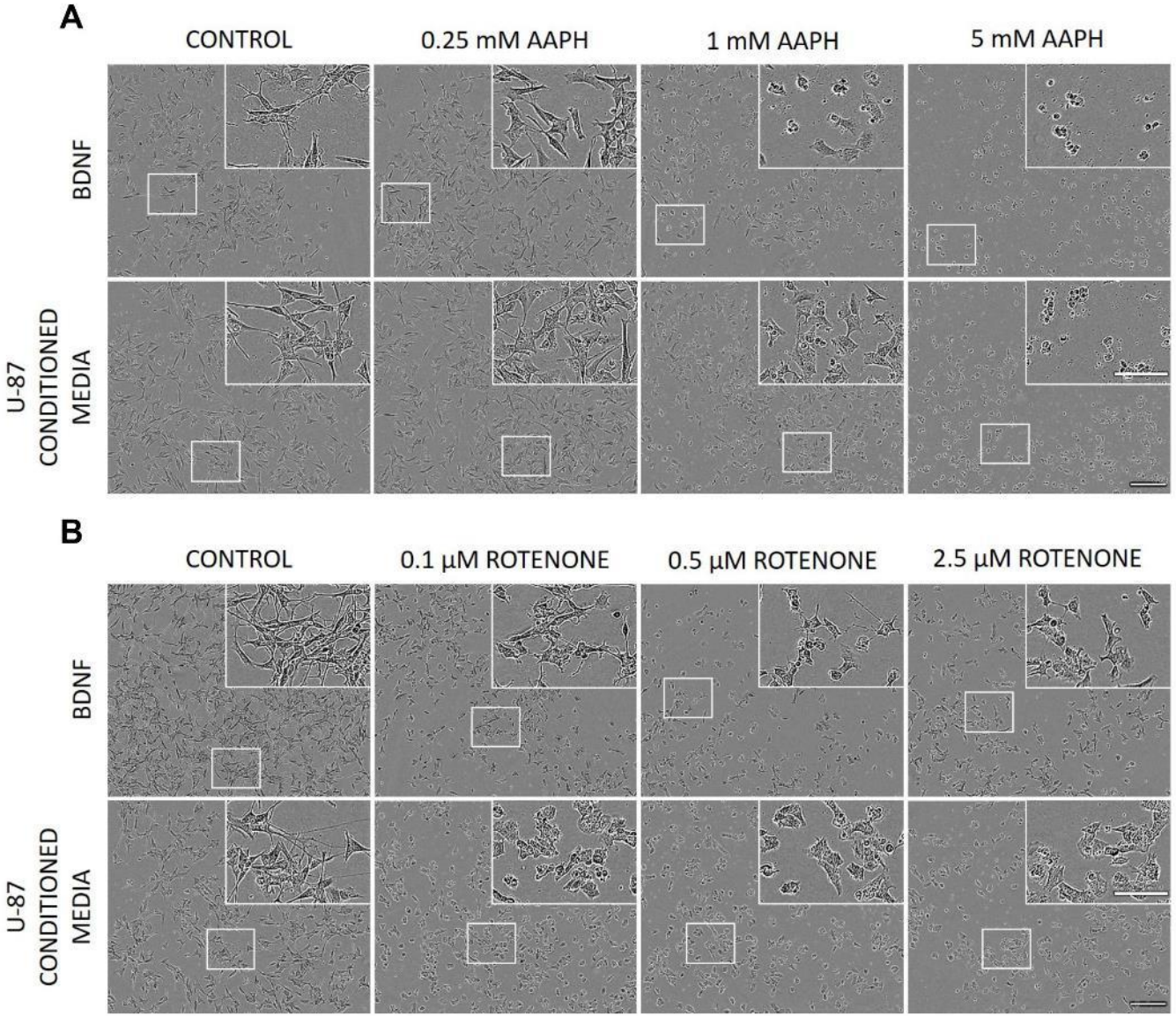

Figure 4.16 Differentiated neuronal SH-SY5Y cell morphology following retinoic acid and BDNF differentiation with or without U-87MG conditioned media and 48-hour AAPH and rotenone exposure. *Morphology investigations were conducted on 5-day retinoic acid, 3 days BDNF differentiated SH-SY5Y cells with or without differentiated U-87MG conditioned media. Phase contrast microscopy of (A) AAPH or (B) rotenone treated differentiated SH-SY5Y monocultures. Scale bar = 200 µm. Inset scale bar = 100 µm.*

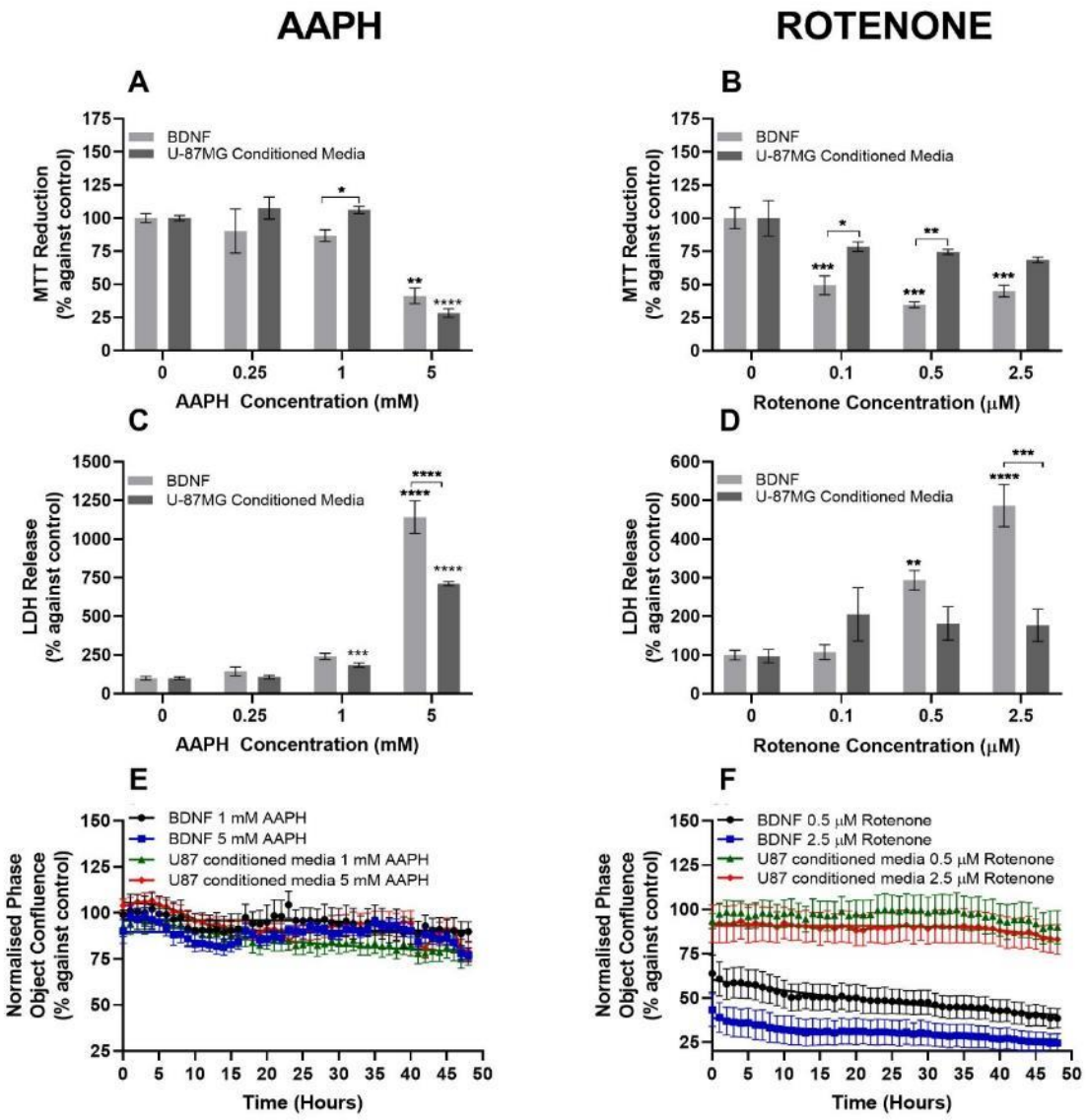

Figure 4.17 Differentiated neuronal SH-SY5Y cell viability following retinoic acid and BDNF differentiation with or without U-87MG conditioned media and 48-hour AAPH and rotenone exposure. *Viability assays were conducted on 5-day retinoic acid, 3 days BDNF differentiated SH-SY5Y cells with or without differentiated U-87MG conditioned media. MTT reduction assay for (A) AAPH or (B) rotenone treated differentiated cells. LDH release for (C) AAPH or (D) rotenone treated differentiated cells. Real-time analysis using the incucyte S3 live-cell analysis system for (E) AAPH or (F) rotenone treated monocultures. Viability assay results are presented as % against control. Statistical analysis was performed using one-way ANOVA with Dunnett's post-hoc test where n=4 for all experiments. Statistical significance was recorded as *p<0.05, **p<0.01, ***p<0.001 and ****p<0.0001, where if not indicated this is relative to the appropriate cell control.*

4.2.3 Reactive species effect on primary cortical neurons

Following dissection and plating of primary cortical neurons, we monitored growth to determine an optimal toxicity regimen to compare with the differentiation models. Images were taken every hour using the incucyte S3 live-cell analysis system to monitor cell morphology and neurite growth.

In the initial 24-hours after seeding, primary cortical neurons already showed signs of neurite outgrowth from multiple cell bodies (figure 4.18A). These neurites continued to exhibit linear growth up to day 4 (figure 4.18B), accompanied by multiple branch points (figure 4.18C). Furthermore, it is interesting to note after 48 hours, neuronal cell bodies appear to cluster as they use their neurites to pull each other together. After 4 days both neurite length and branch points appear to plateau, suggesting primary cortical neurons extend neurites over the first 4 days and then possibly reach a stable state. This suggests day 5 would be suitable for cytotoxicity assays similar to the SH-SY5Y cell differentiation time frame with FBS/RA.

Following 5-day growth, primary cells were treated with AAPH or rotenone for 24 hours, as morphological changes were visible for all concentrations as early as 24 hours (figure 4.19A and B). Interestingly, AAPH and rotenone appeared to have different effects on primary cortical neuron morphology. AAPH resulted in axon/neurite fragmentation producing punctate axon/neurite remnants, whereas rotenone treatment resulted in a reduced number of axons with fewer branches compared to untreated controls. This loss of axonal processes suggests both AAPH and rotenone treatment resulted in degenerating cortical neuron structure and viability, which was supported by viability assays. MTT reduction assays were significantly lower suggesting loss of viability for all concentrations of AAPH and rotenone (figure 4.20A and B, respectively). These results were supported by LDH assays, which showed significantly greater LDH release for AAPH and rotenone treatment (figure 4.20C and D, respectively). Furthermore, LDH assays showed greater levels of LDH release for AAPH treated primary cortical neurons compared to rotenone. Live-cell analysis showed a linear decrease in normalised phase confluence over 24 hours, with AAPH (figure 4.20E) and rotenone treatment (figure 4.20F).

Concurrent treatment with α-tocopherol was unable to improve MTT reduction of cortical neurons treated with AAPH (figure 4.20A) and was only able to significantly protect against 2.5 µM rotenone treatment (figure 4.20B). However, α-tocopherol treatment reduced LDH release for both AAPH and rotenone treatments (figure 4.20C and D, respectively). This may be due to the nature of the assays, where the MTT assay measures mitochondrial function. Mitochondria are known to be located to neurites and as α-tocopherol did not affect neurite loss (figure 4.14A and B), which may explain why MTT levels were unaffected. However, live-cell analysis showed α-tocopherol initially

attenuated AAPH induced death but was not able to keep protecting primary cortical neurons over time (figure 4.20E). In contrast, α-tocopherol was able to alleviate the effect of rotenone over 24-hours as measured by phase confluence (figure 4.20F).

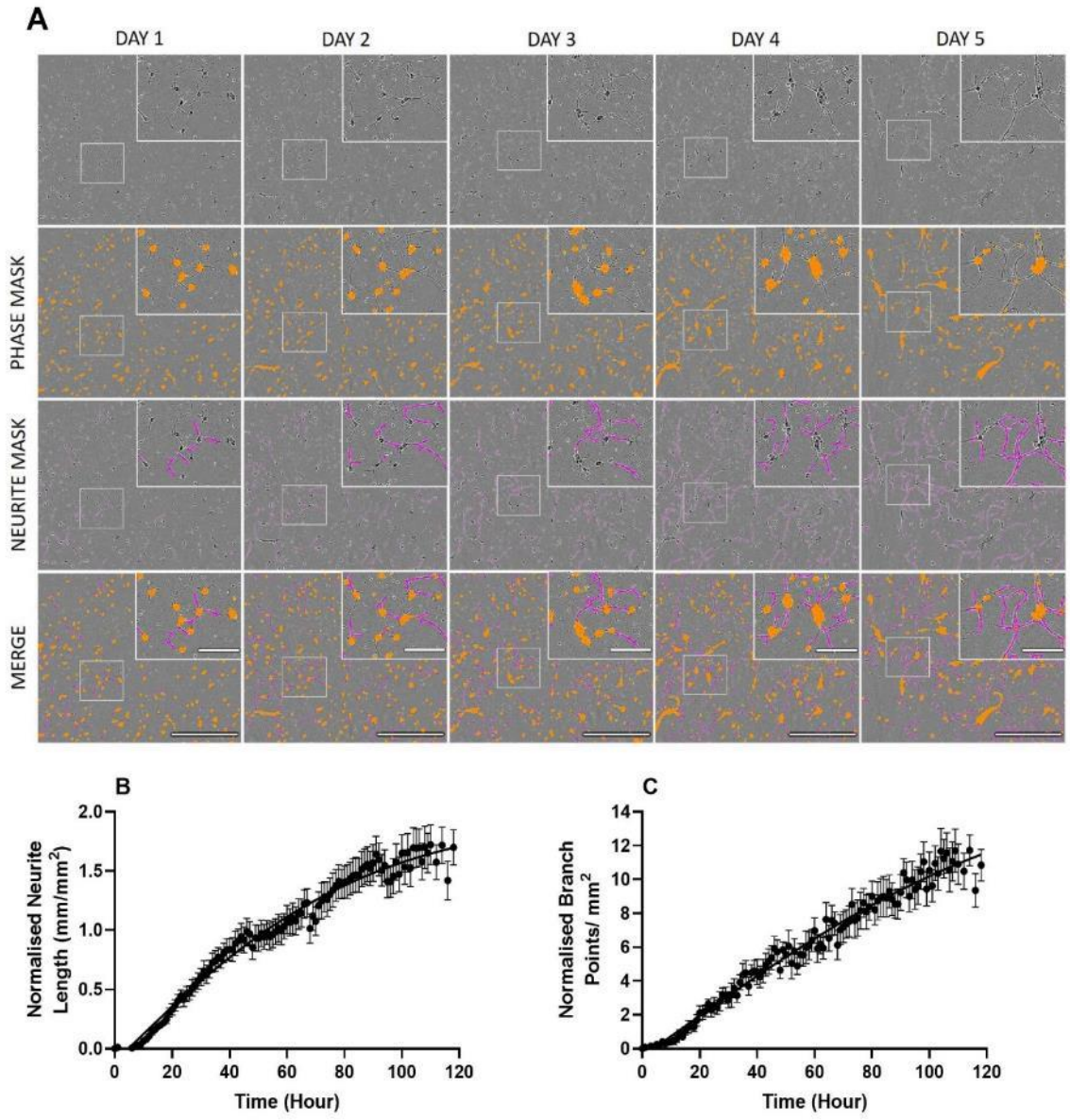

Figure 4.18 Primary embryonic rat cortical neuronal growth. *Once dissected and seeded on poly-L-lysine and laminin coated plates primary cortical neuron growth was monitored using the incucyte S3 live-cell analysis system. (A) Phase contrast images were taken every hour for 5 days and quantified using the incucyte neurotracker software to mask neurites (purple) and cell bodies (yellow). Scale bar = 200 µm. Inset scale bar = 100 µm. (B) Neurite length and (C) branch points were quantified over 5 days.*

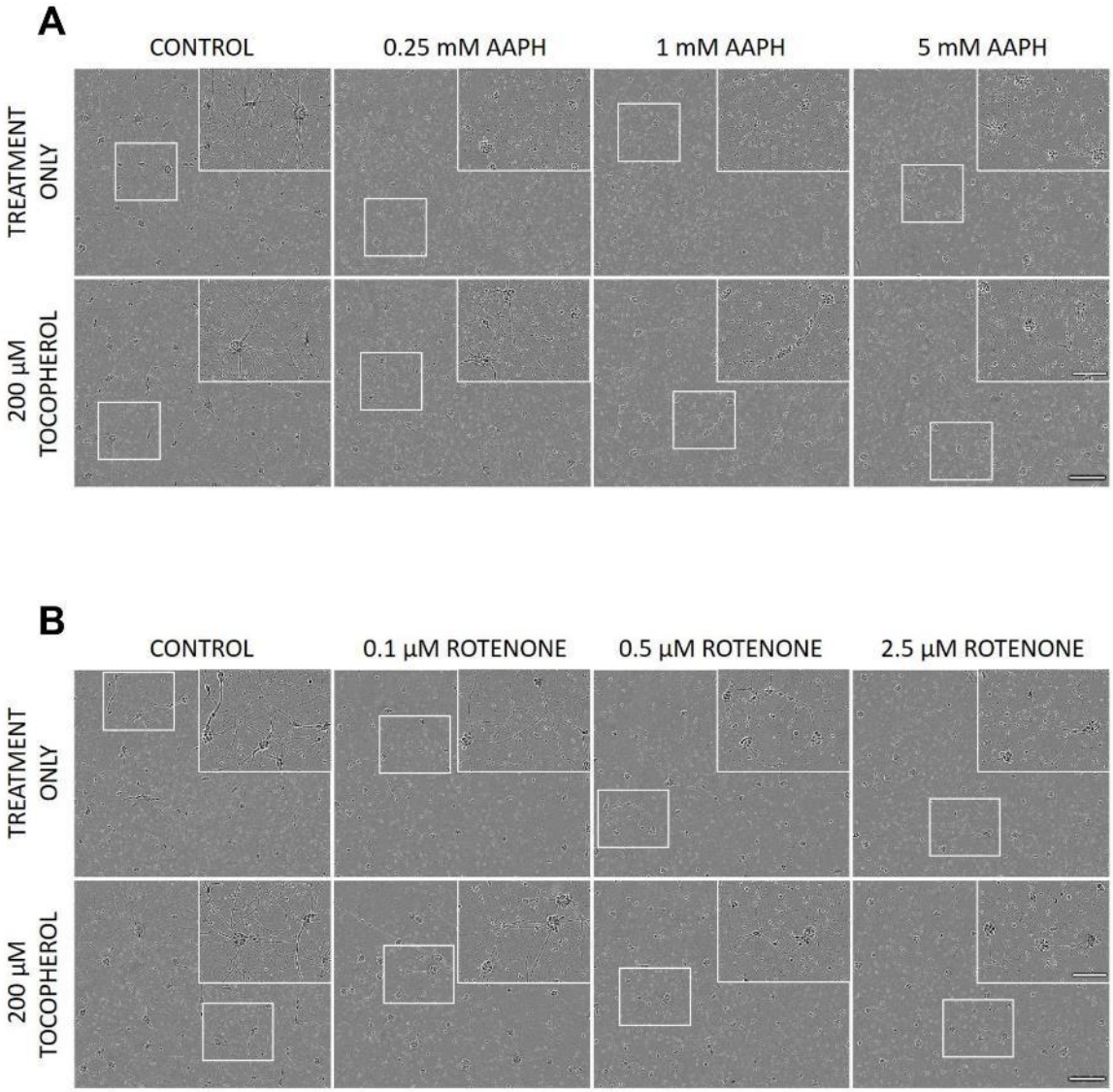

Figure 4.19 The effect of reactive species on primary cortical neuronal morphology with and without α-tocopherol. *Primary cortical neurons were grown for 5 days and then treated with AAPH or rotenone for 24 hours prior to morphology investigations. Phase contrast microscopy of 24-hour (A) AAPH or (B) rotenone treated primary neurons. Scale bar = 200 µm. Inset scale bar = 100 µm.*

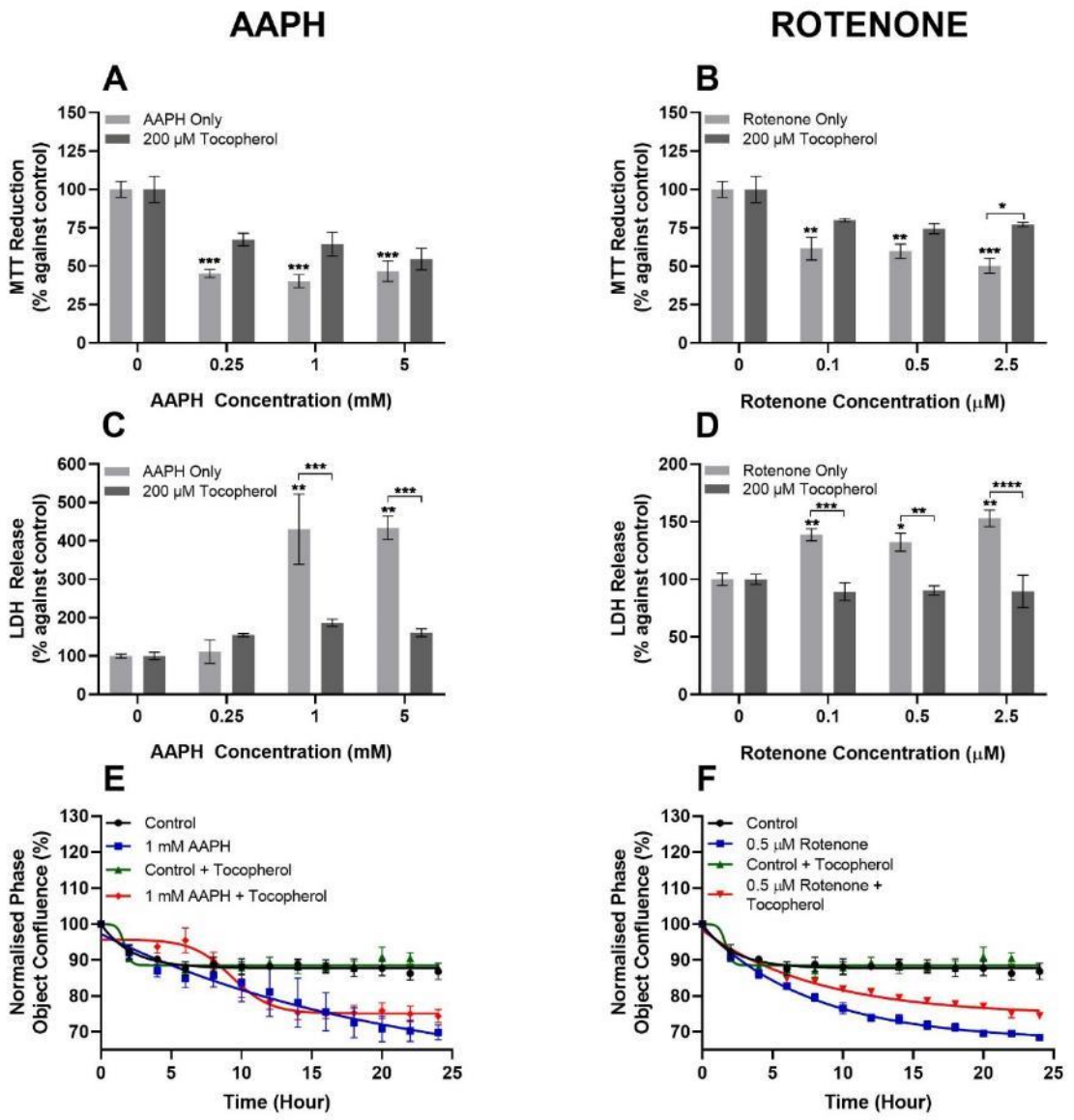

Figure 4.20 The effect of reactive species on primary cortical neuronal viability with and without α-tocopherol. *Primary cortical neurons were grown for 5 days and then treated with AAPH or rotenone for 24 hours prior to viability assays. MTT reduction assay of 24-hour (A) AAPH or (B) rotenone treated primary neurons. LDH release of 24-hour (C) AAPH or (D) rotenone treated primary neurons. Real-time analysis using the incucyte S3 live-cell analysis system for (E) AAPH or (F) rotenone treated primary neurons. Viability assay results are presented as % against control. Statistical analysis was performed using one-way ANOVA with Dunnett's post-hoc test where n=4 for all experiments. Statistical significance was recorded as *p<0.05, **p<0.01, ***p<0.001 and ****p<0.0001.*

Due to the interesting morphological differences observed with AAPH and rotenone, we quantified neurite length and branch points in real time using the incucyte S3 live-cell analysis system. Quantification was normalised to account for different starting neurite lengths. Phase contrast microscopy showed AAPH resulted in a dose-dependent decrease in neurite length over 24-hours (figure 4.21A). Furthermore, over time axons appeared to fragment in a retrograde manner towards the neuronal cell soma (figure 4.22A). This was supported by axon/neurite quantification, which showed that as the concentration of AAPH increased, the neurite length and branch points showed a similar time- and dose-dependent decline (figure 4.22C and E, respectively). In contrast, rotenone treatment resulted in a less significant decrease in neurite length and branch points (figure 4.22D and F, respectively). Furthermore, phase contrast microscopy showed different changes in axonal morphology as rotenone appeared to reduce the number of branch points over time, while not effecting axon length as prominently as AAPH and did not result in fragmentation (figure 4.22B).

α-tocopherol treatment was unable to attenuate AAPH or rotenone induced reduction of neurite length (figure 4.23). This is possibly due to primary cortical neurons being more sensitive to RS and further titration of α-tocopherol was needed. However, due to the different sensitivities of cell batches it was difficult to investigate this.

As neurite length quantification by the incucyte S3 live-cell analysis system also considers the branches in the overall length of neurites, the impact on branch length was unclear. Therefore, to investigate if AAPH and rotenone affect primary neuron branching the Sholl analysis (Ferreira et al., 2014) and Skeleton plugin (Lee and Kashyap, 1994) in ImageJ/Fiji were used. Sholl analysis works on the principle of measuring the number of intersections in contact with the sampling shells, which expand out from the centre of a neuronal arbour (figure 4.24A). Steps for Sholl analysis are described in figure 4.24B, where phase contrast images were initially masked using the neurotracker software from the incucyte S3 live-cell analysis system, which was then converted to a binary image and thresholded for Sholl analysis. Sholl analysis shows a dose-dependent decrease in the number of interactions for AAPH (figure 4.25A and B) and rotenone (Figure 4.25D and E), demonstrated by the Sholl heat maps and corresponding plots. Skeleton analysis also supported a dose-dependent decrease in average branch length for primary neurons treated with AAPH (figure 4.25C) or rotenone (figure 4.25F) for 24 hours.

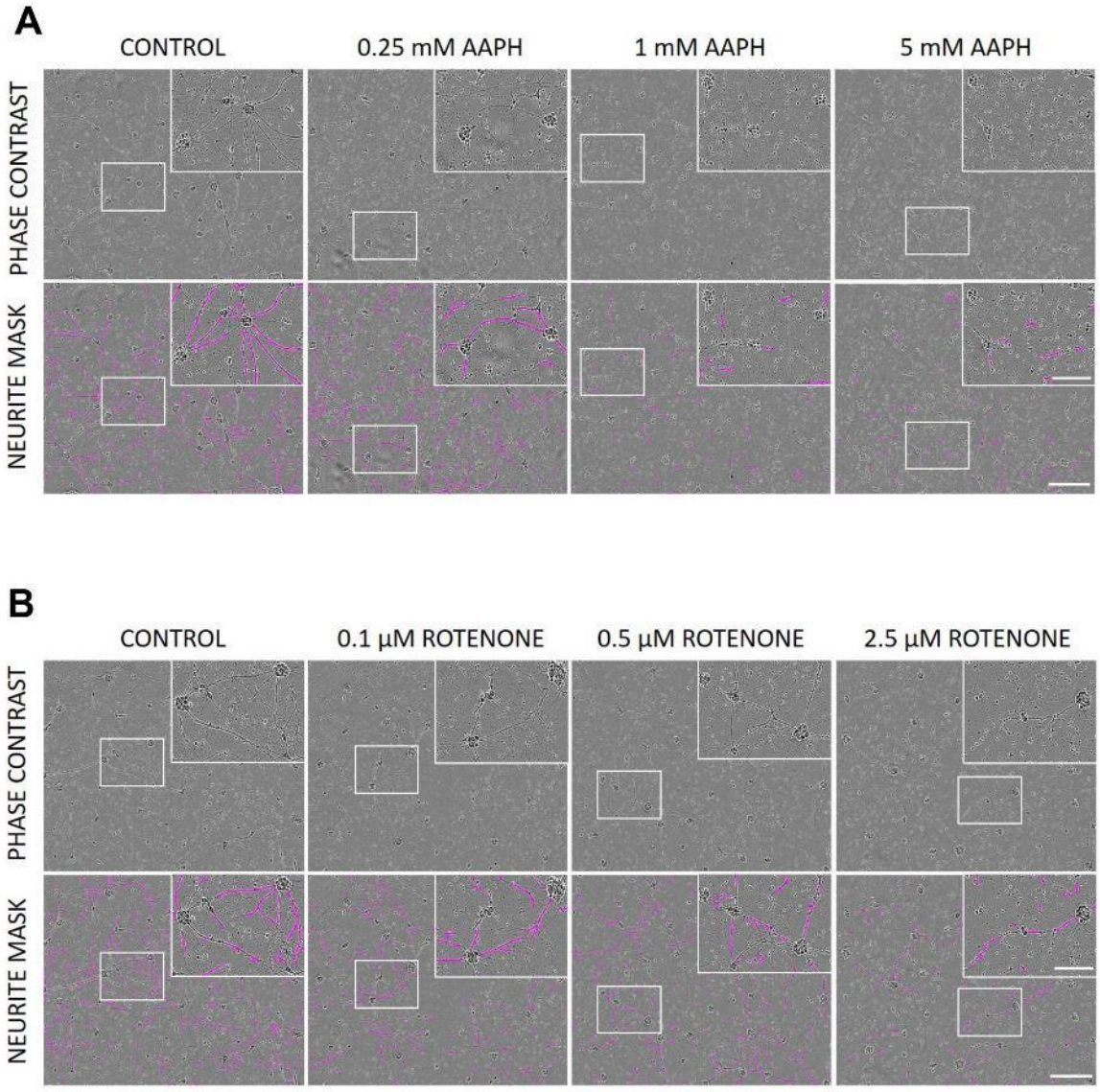

Figure 4.21 The effect of reactive species on primary cortical neurite morphology. *Following 5 days of growth primary neurons were treated with AAPH or rotenone for 24 hours and neurite outgrowth was monitored using the incucyte S3 live-cell analysis system. Scale bar = 200 µm. Inset scale bar = 100 µm. Phase contrast images of 24-hour (A) AAPH and (B) rotenone treated neurons. Phase contrast images were taken every hour for 24-hours and quantified using the incucyte neurotracker software to mask neurites (purple).*

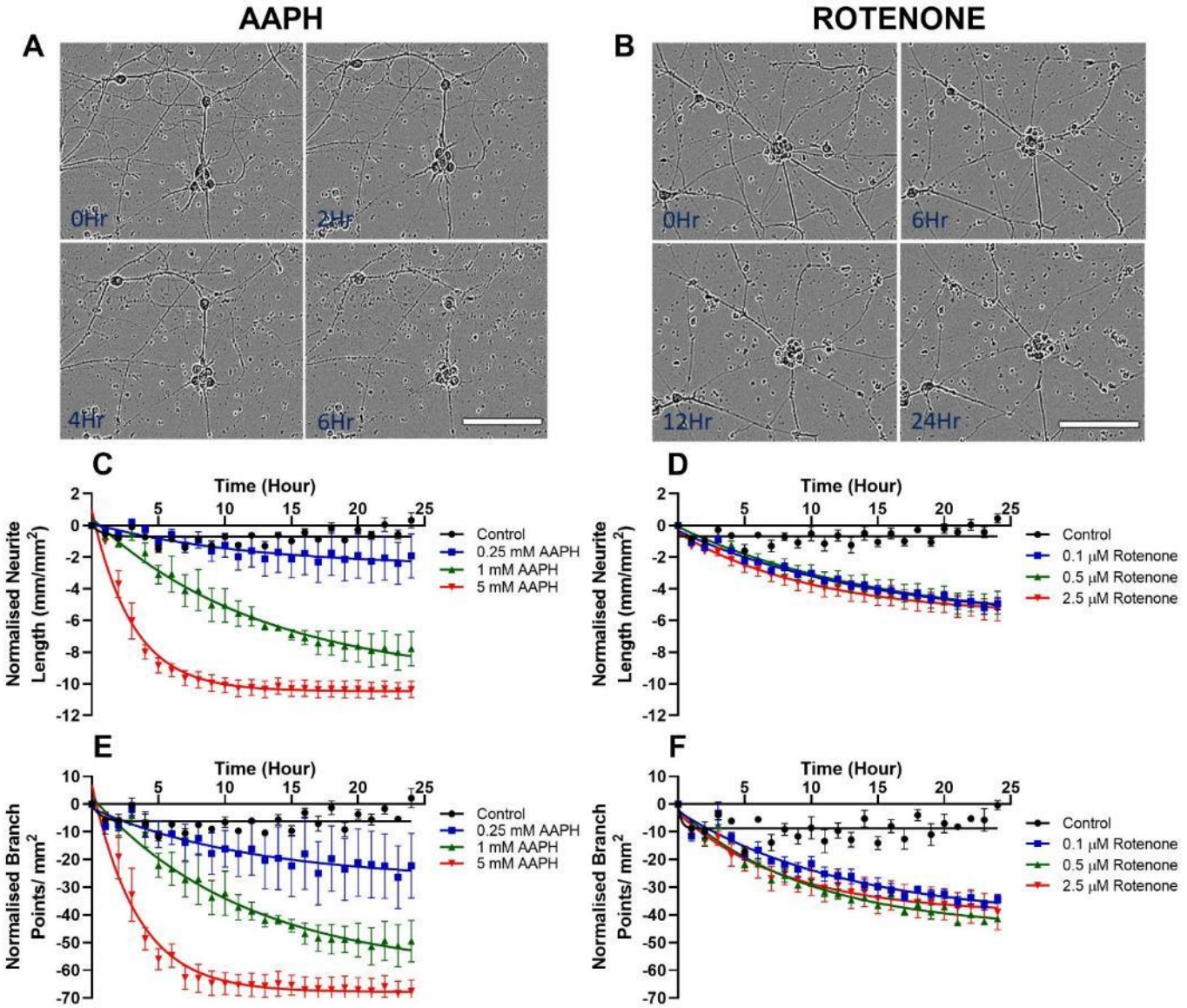

Figure 4.22 The effect of reactive species on primary cortical neurite outgrowth. *Following 5 days of growth primary neurons were treated with AAPH or rotenone for 24 hours and neurite outgrowth was monitored using the incucyte S3 live-cell analysis system. Scale bar = 100 µm. Phase contrast images monitoring neurites over time when treated with (A) AAPH or (B) rotenone. Live cell monitoring of neurite length of (C) AAPH and (D) rotenone treated primary neurons. Live cell monitoring of branch points of (E) AAPH and (F) rotenone treated primary neurons.*

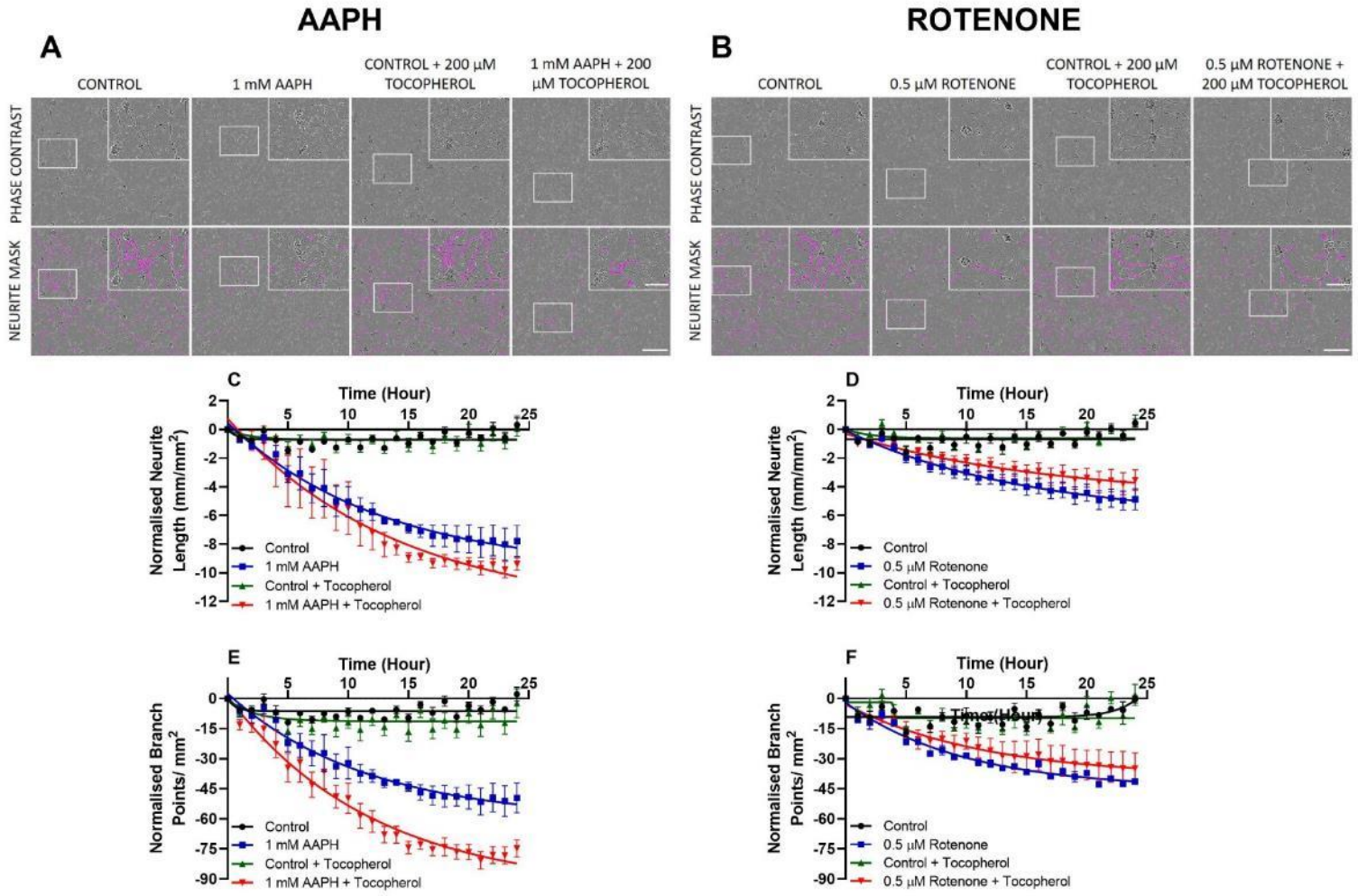

Figure 4.23 The effect of reactive species on primary cortical neurite outgrowth with α-tocopherol. *Following 5 days of growth primary neurons were treated with AAPH or rotenone with and without α-tocopherol for 24 hours and neurite outgrowth was monitored using the incucyte S3 live-cell analysis system. Scale bar = 200 µm. Inset scale bar = 100 µm. (A) Phase contrast images of 24-hour (A) AAPH and (B) rotenone treated neurons with and without α-tocopherol. Phase contrast images were taken every hour for 24-hours and quantified using the incucyte neurotracker software to mask neurites (purple). Live cell monitoring of neurite length of (C) AAPH and (D) rotenone treated primary neurons with and without α-tocopherol. Live cell monitoring of branch points of (E) AAPH and (F) rotenone treated primary neurons with and without α-tocopherol.*

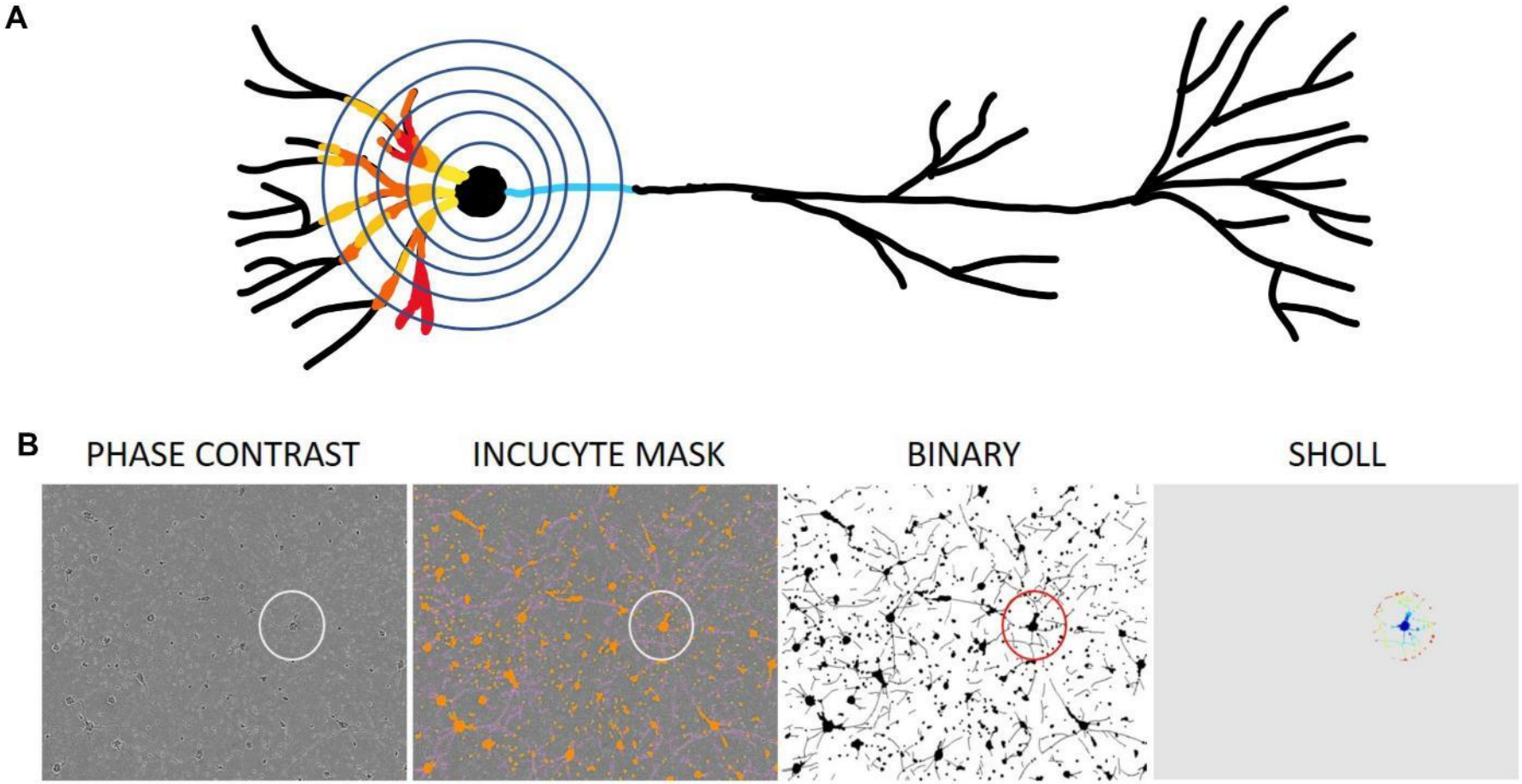

Figure 4.24 The steps involved in Sholl analysis. *(A) Diagrammatic representation of Sholl analysis, which involves creating a series of concentric shells around the focus of a neuronal arbour where the number of intersections is calculated from how neurits many intersect the sampling shells. (B) Stepwise imageJ processing of primary cortical neurons where phase contrast images were taken using the incucyte S3 live-cell analysis system and mask was generated using the neurotracker software. Mask was converted to a binary thresholded image and individual neurons were selected to generate a heat map according to the Sholl profile.*

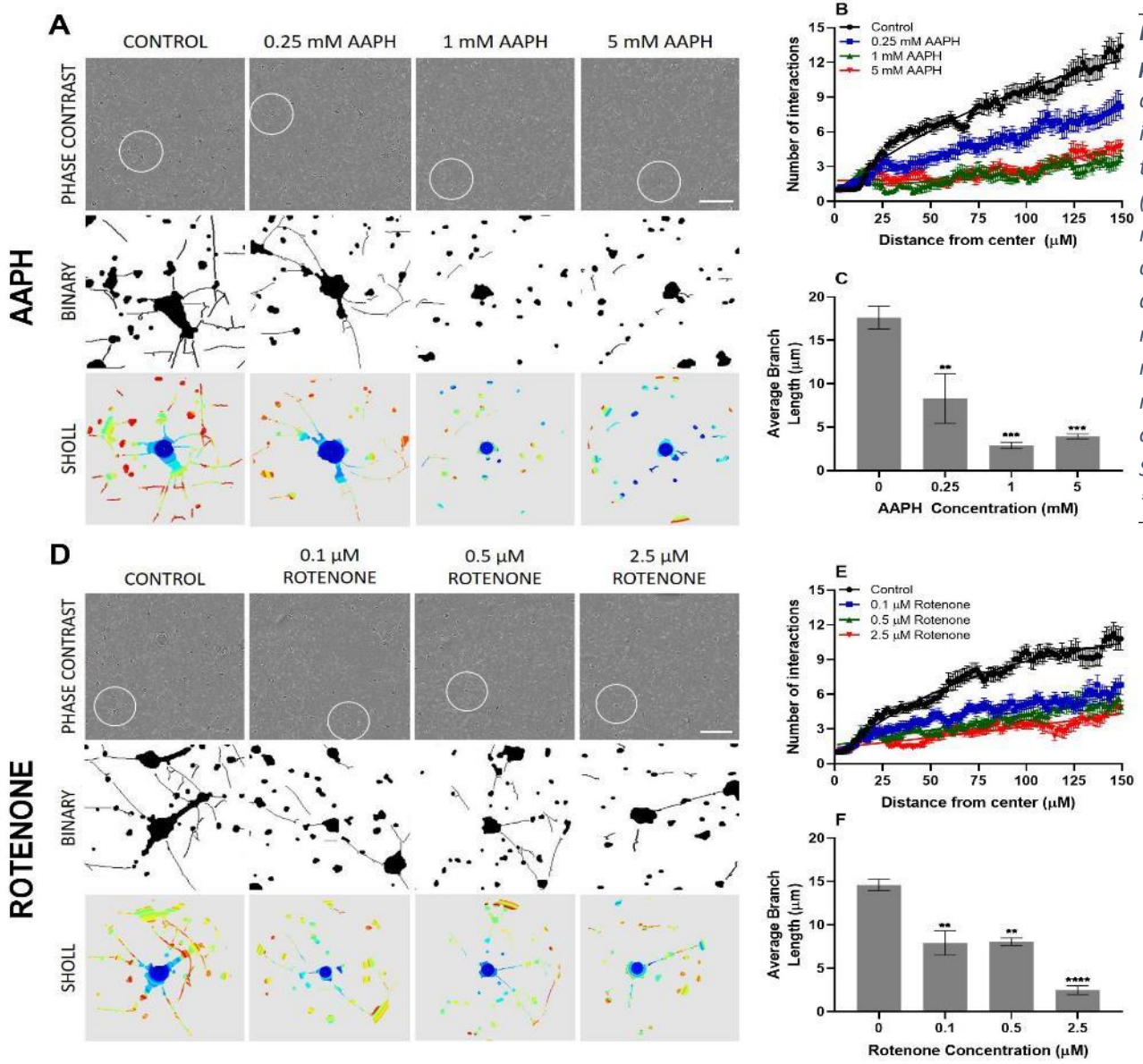

Figure 4.25 The effect of reactive species on primary cortical neurite complexity. *Phase contrast microscopy, binary and Sholl analysis images for 24-hour (A) AAPH and rotenone (D) treated neurons. Scale bar = 200 μm. Sholl plots of (B) AAPH and (E) rotenone treated primary neurons generated from images. Skeleton analysis in imageJ was also used to determine the average branch length for (C) AAPH and (F) rotenone treated neurons. Plots are representative of group means ± SEM where n=15. Statistical analysis was performed using one-way ANOVA with Dunnett's post-hoc test. Statistical significance was recorded as *p<0.05, **p<0.01, ***p<0.001 and ****p<0.0001.*

Together these results suggest neurite length, branch number and length are affected by AAPH and rotenone. Interesting to note though is lower rotenone concentrations effect branch number more than lower concentrations of AAPH suggesting rotenone possibly effects branching more than AAPH.

As branching appeared to be affected differently by AAPH and rotenone, we investigated the effect on synaptophysin (membrane glycoprotein) expression. Immunofluorescence staining showed a decrease in synaptophysin (green) expression with AAPH along neurites (figure 4.26A) whilst increasing with rotenone treatment (Figure 4.26B). Rotenone treated primary neurons showed more synaptophysin puncta along βIII tubulin stained processes (red) and within the cell soma as rotenone concentration increased. This suggests AAPH and rotenone affects synaptophysin in different ways. The distribution of synaptophysin expression corresponds with phase microscopy observations, where AAPH resulted in axonal process fragmentation while rotenone appeared to reduce branch length and interactions.

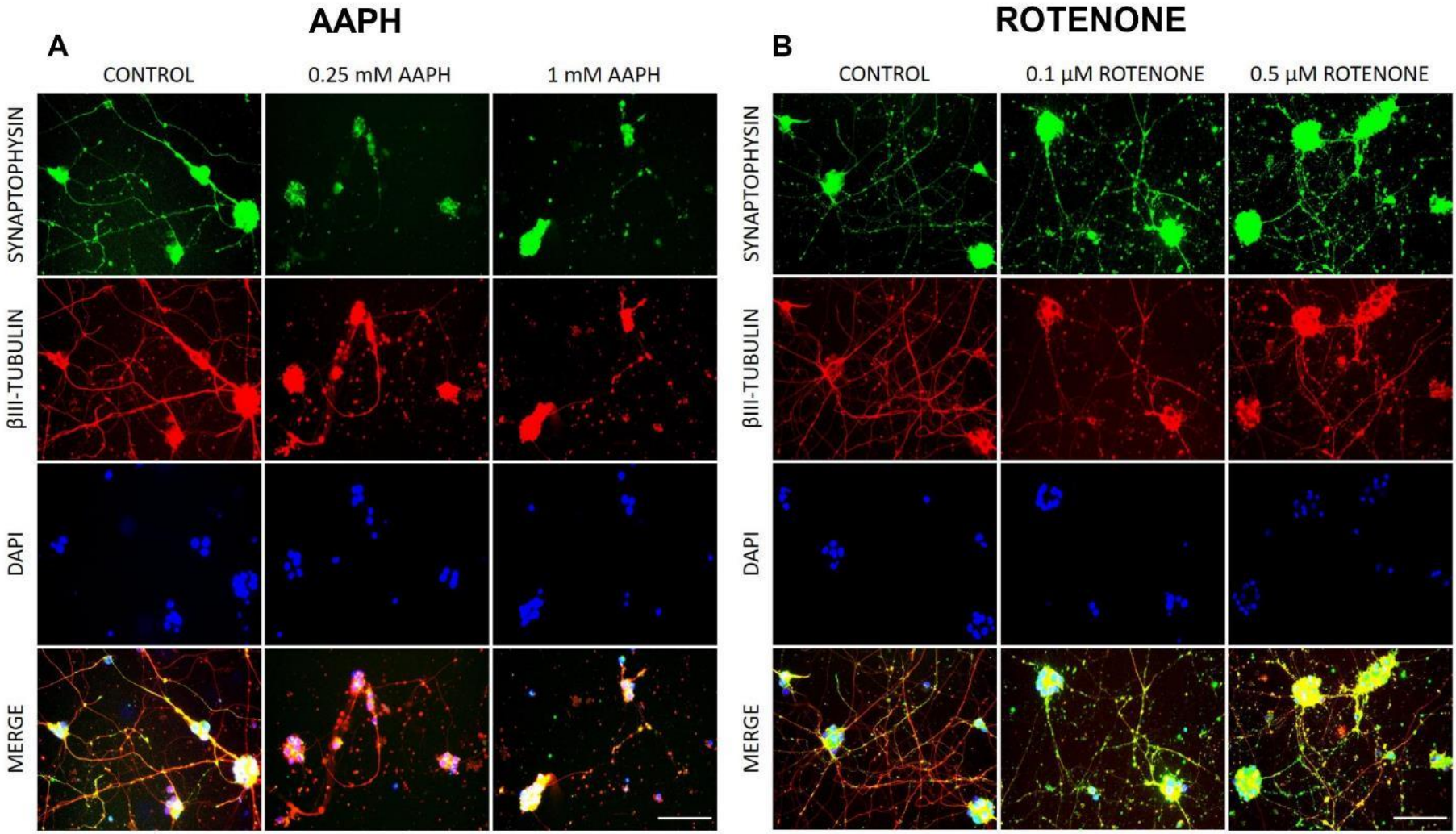

Figure 4.26 Toxicity of reactive species on primary cortical neuronal synaptophysin expression. *Primary cortical neurons were treated with increasing concentrations of (A) AAPH or (B) rotenone for 24 hours. Cells were co-stained with synaptophysin (green), βIII-tubulin (red) and DAPI (blue). Scale bar = 100 µm. AAPH resulted in decrease synaptophysin expression while rotenone increased expression.*

4.2.4 The effect of reactive species on differentiated neural processes

To investigate if our model of differentiation could replicate observations in primary cortical neurons, we investigated neurite outgrowth. BDNF with and without U-87MG conditioned media differentiation protocols were used, as they showed the greatest neurite network (figure 4.6).

As differentiated SH-SY5Y neurons showed similar viability at 48 hours to 24-hour treatment of primary cortical neurons we ran neurite outgrowth experiments for 48 hours. Similar to primary neurons, differentiated SH-SY5Y cells showed a dose-dependent decrease in neurite length for BDNF differentiated cells treated with AAPH or rotenone (figure 4.27A and B, respectively and quantified in figure 4.28A and B, respectively). Differentiation with U-87MG conditioned media showed AAPH treatment resulted in a neurite length decreasing at an earlier time point at an exponential rate (figure 4.28C) relative to BDNF differentiation (figure 4.28A). Rotenone treatment of differentiated cells using conditioned media resulted in a consistent reduction in neurite length (figure 4.29D); a phenomenon that was also observed with primary neurons (figure 4.22B). Indeed, the differentiation model mimicked some of the changes observed with primary neurons albeit with some differences in the extent of neurite retraction for rotenone and AAPH treatment (figure 4.28C and D, respectively).

To investigate if the observations were due to RS, we concurrently treated differentiated cells with AAPH or rotenone with and without α-tocopherol (figure 4.29-4.30). However, like primary neuronal cultures our differentiation models showed α-tocopherol had no significant effect on AAPH or rotenone induced neurite retraction (figure 4.30C).

Unfortunately, the differentiation models we used did not appear to show branching that was quantifiable and as such Sholl analysis was not conducted. As the mask was unable to quantify branching, we also investigated synaptophysin changes to compare with primary neurons. However, synaptophysin did not show punctate staining for either differentiation model (figure 4.31). Furthermore, while cells showed a dose-dependent decrease in viability and neurite loss in phase contrast microscopy, there was no obvious changes in synaptophysin staining between AAPH (figure 4.31A, C) or rotenone (Figure 4.31B, D) as was seen with primary neurons.

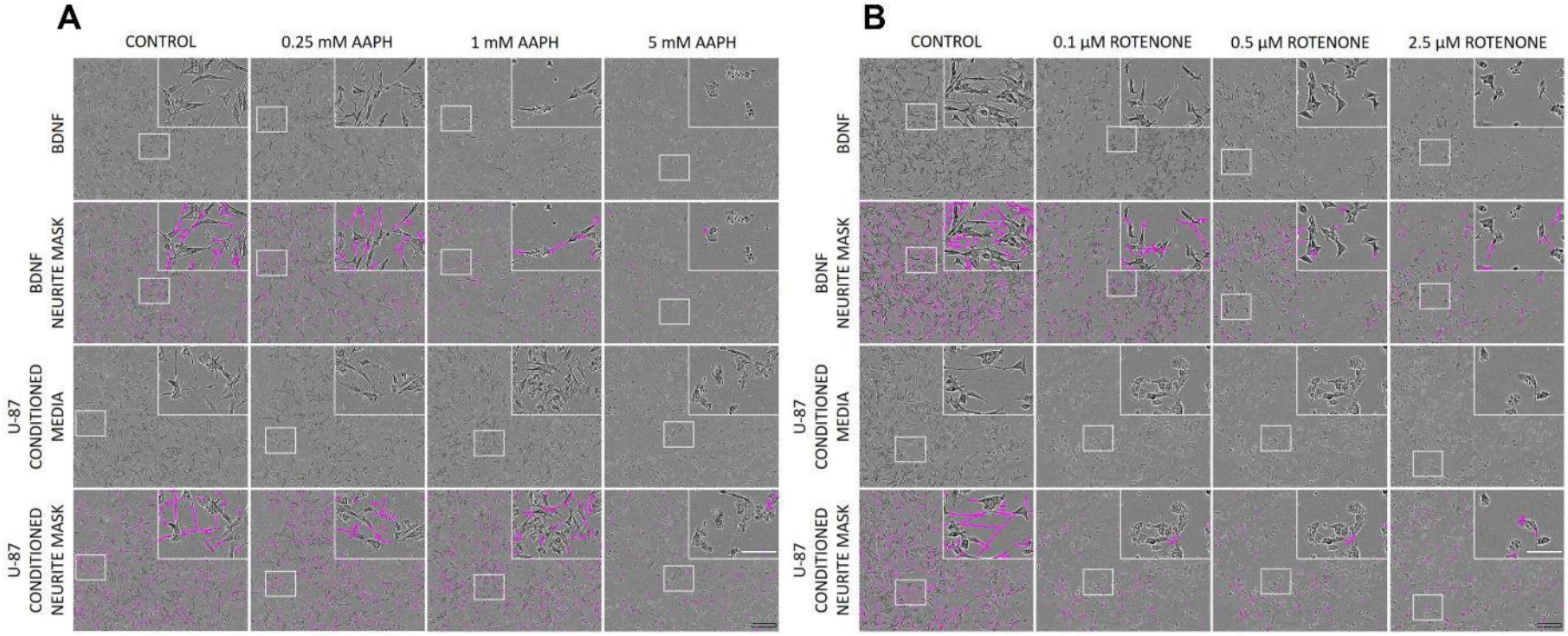

Figure 4.27 The effect of reactive species on differentiated SH-SY5Y neurite outgrowth morphology. *Following differentiation with FBS/RA and BDNF with and without U-87MG conditioned media SH-SY5Y cells were treated with AAPH or rotenone for 48 hours, where neurite outgrowth was monitored using the incucyte S3 live-cell analysis system. (A) Phase contrast images of 48-hour (A) AAPH and (B) rotenone treated neurons where neurotracker software from the incucyte S3 live-cell analysis system was used to mask neurites (purple). Scale bar = 200 µm. Inset scale bar = 100 µm.*

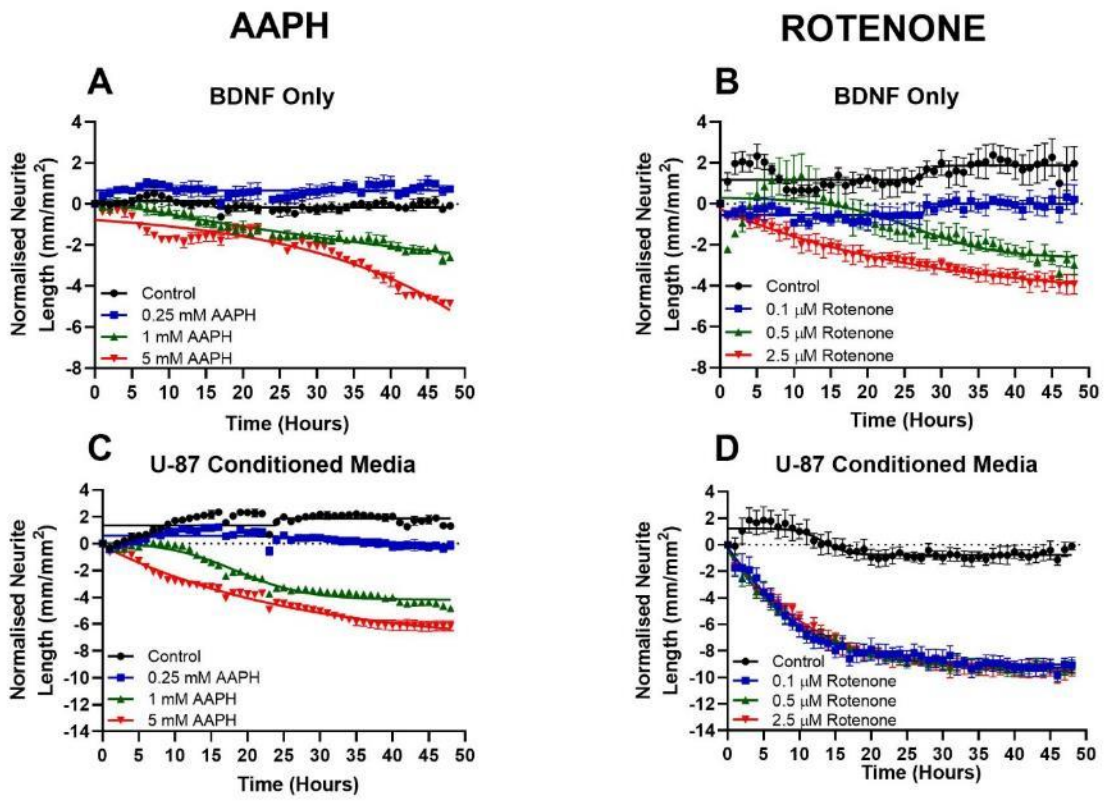

Figure 4.28 The effect of reactive species on differentiated SH-SY5Y neurite outgrowth. *Following differentiation with FBS/RA and BDNF with and without U-87MG conditioned media SH-SY5Y cells were treated with AAPH or rotenone for 48 hours, where neurite outgrowth was monitored using the incucyte S3 live-cell analysis system. Phase contrast images were taken every hour for 48-hours and quantified using the neurotracker software. Live cell monitoring of neurite length of (A) AAPH and (B) rotenone treated BDNF only differentiated SH-SY5Y cells. Live cell monitoring of neurite length of (C) AAPH and (D) rotenone treated U-87MG conditioned media differentiated SH-SY5Y cells.*

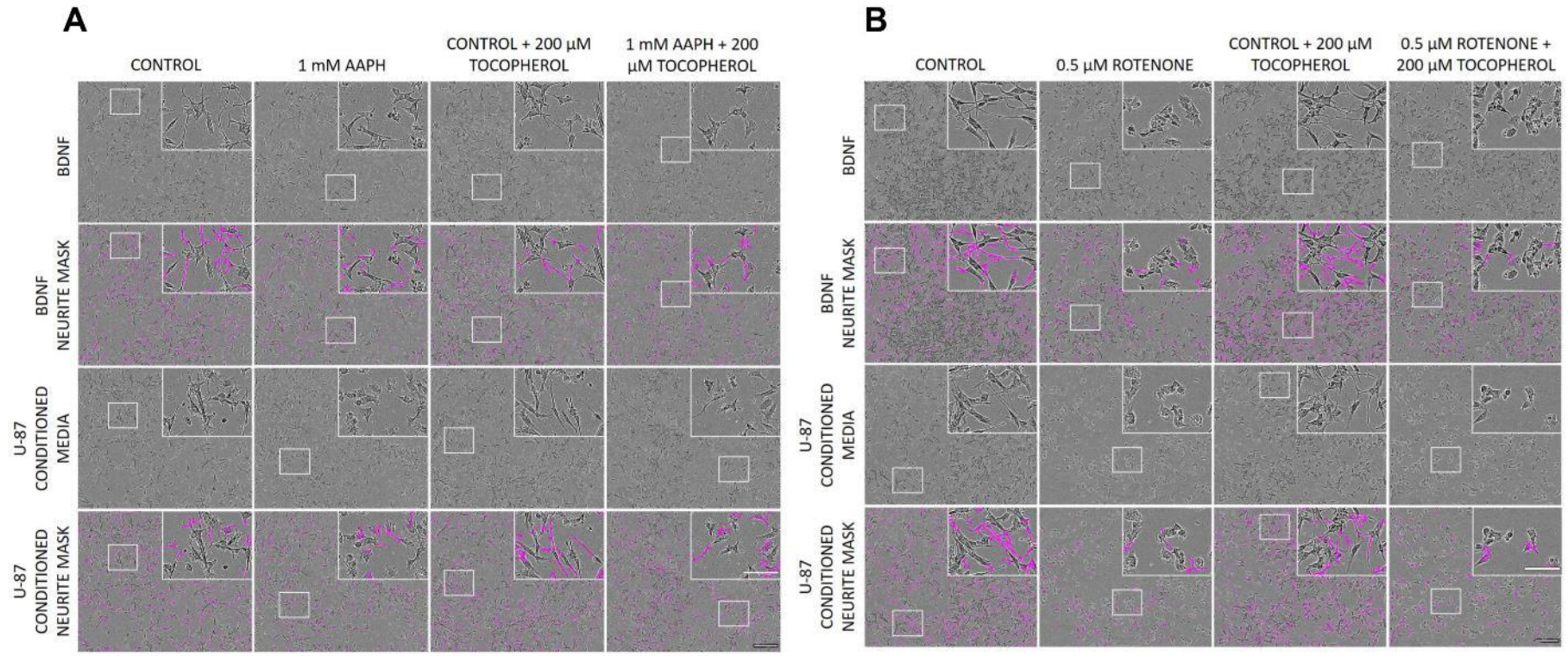

Figure 4.29 The effect of reactive species on differentiated SH-SY5Y neurite morphology with α-tocopherol. *Following differentiation with FBS/RA and BDNF with and without U-87MG conditioned media SH-SY5Y cells were treated with AAPH or rotenone for 48 hours with or without α-tocopherol, where neurite outgrowth was monitored using the incucyte S3 live-cell analysis system. (A) Phase contrast images of 48-hour (A) AAPH and (B) rotenone treated neurons where neurotracker software from the incucyte S3 live-cell analysis system was used to mask neurites (purple). Scale bar = 200 µm. Inset scale bar = 100 µm.*

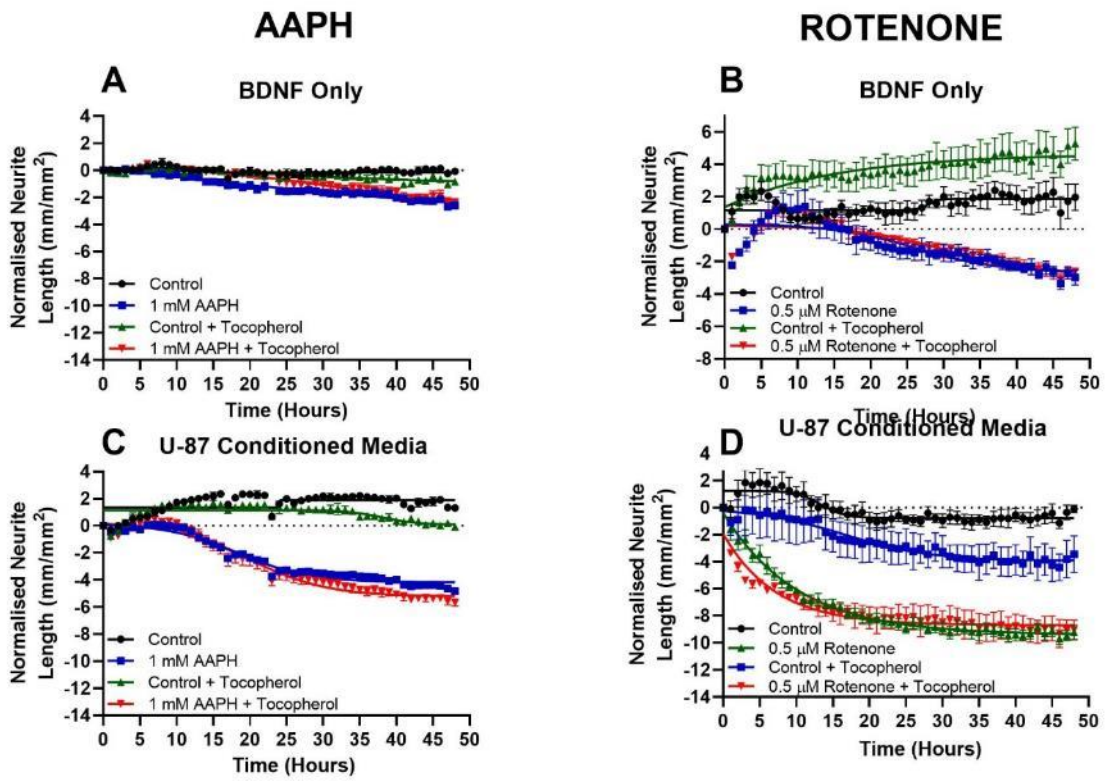

Figure 4.30 The effect of reactive species on differentiated SH-SY5Y neurite outgrowth with α-tocopherol. *Following differentiation with FBS/RA and BDNF with and without U-87MG conditioned media SH-SY5Y cells were treated with AAPH or rotenone for 48 hours with or without α-tocopherol, where neurite outgrowth was monitored using the incucyte S3 live-cell analysis system. Phase contrast images were taken every hour for 48-hours and quantified using the neurotracker software. Live cell monitoring of neurite length of (C) AAPH and (D) rotenone treated BDNF only differentiated SH-SY5Y cells. Live cell monitoring of neurite length of (E) AAPH and (F) rotenone treated U-87MG conditioned media differentiated SH-SY5Y cells.*

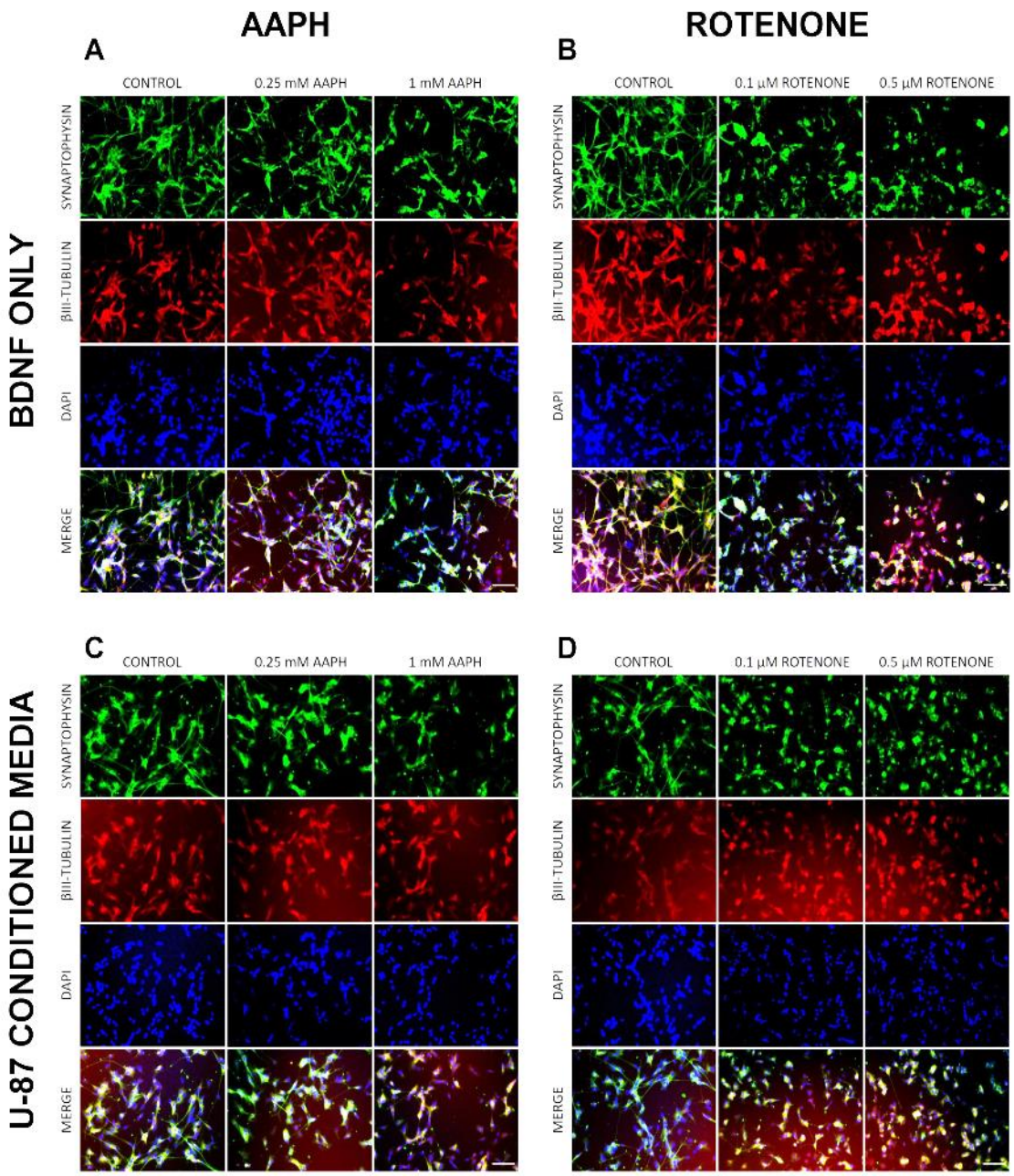

Figure 4.31 Toxicity of reactive species on differentiated SH-SY5Y neuronal cells. *SH-SY5Y neurons were differentiated over 5 days with retinoic acid followed by 3 days of BDNF with or without U-87MG conditioned media prior to 48-hour treatment with AAPH or rotenone. SH-SY5Y cells differentiated with BDNF alone were treated with (A) AAPH or (B) rotenone for 48 hours. SH-SY5Y differentiated in the presence of U-87MG conditioned media treated with (C) AAPH or (D) rotenone for 48 hours. Cells were co-stained with synaptophysin (green), βIII-tubulin (red) and DAPI (blue). Scale bar = 100 µm.*

Together, these neurite studies demonstrate the limitations of the differentiation models we are working with. While showing similar qualities in terms of viability, morphologically differentiated cells pose problems. Changes in neurite length for AAPH and rotenone were the opposite of those observed in primary cortical neurons with uncharacteristic synaptophysin staining or differences in distribution upon treatment. These problems may be due to the differentiated models lacking substantial neurite branching as was seen with primary cells and therefore require improved differentiation protocols.

We also used the incucyte S3 live-cell analysis neurotracker software to quantify glia processes. Phase contrast images showed 1 mM AAPH alongside increased cell number also resulted in U-87MG glial cells having longer processes (figure 4.32A and figure 4.32C). Rotenone treatment of U-87MG glial cells resulted in cellular rounding (figure 4.32B) and shortened processes (figure 4.32D). To investigate if this was as a result of RS, we treated U-87MG glial cells with α-tocopherol which attenuated process growth in 1 mM AAPH treated cells relative to the control (figure 4.33C). α-tocopherol improved processes observed in phase contrast images (figure 4.33B) in response to rotenone treatment (figure 4.33D). This suggests RS induced by AAPH and rotenone effect glial processes.

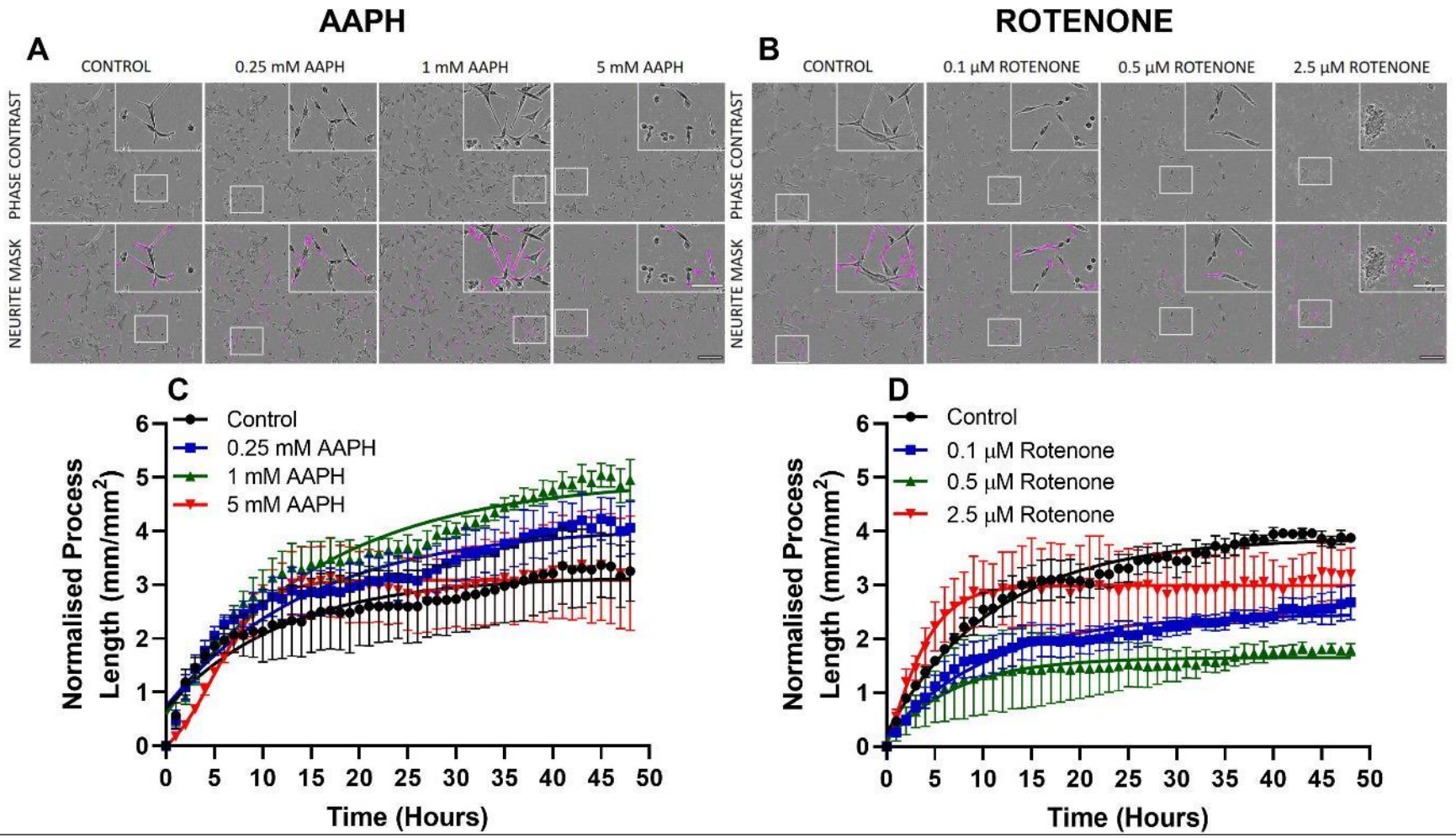

Figure 4.32 The effect of reactive species on glial processes. *Following differentiation with FBS/RA U-87MG glial cells were treated with AAPH or rotenone for 48 hours, where process outgrowth was monitored using the incucyte S3 live-cell analysis system. Phase contrast images of 48-hour (A) AAPH and (B) rotenone treated glia where neurotracker software from the incucyte S3 live-cell analysis system was used to mask processes (purple). Scale bar = 200 µm. Inset scale bar = 100 µm. Phase contrast images were taken every hour for 48-hours and quantified using the neurotracker software. Live cell monitoring of process length of (C) AAPH and (D) rotenone treated differentiated glial cells.*

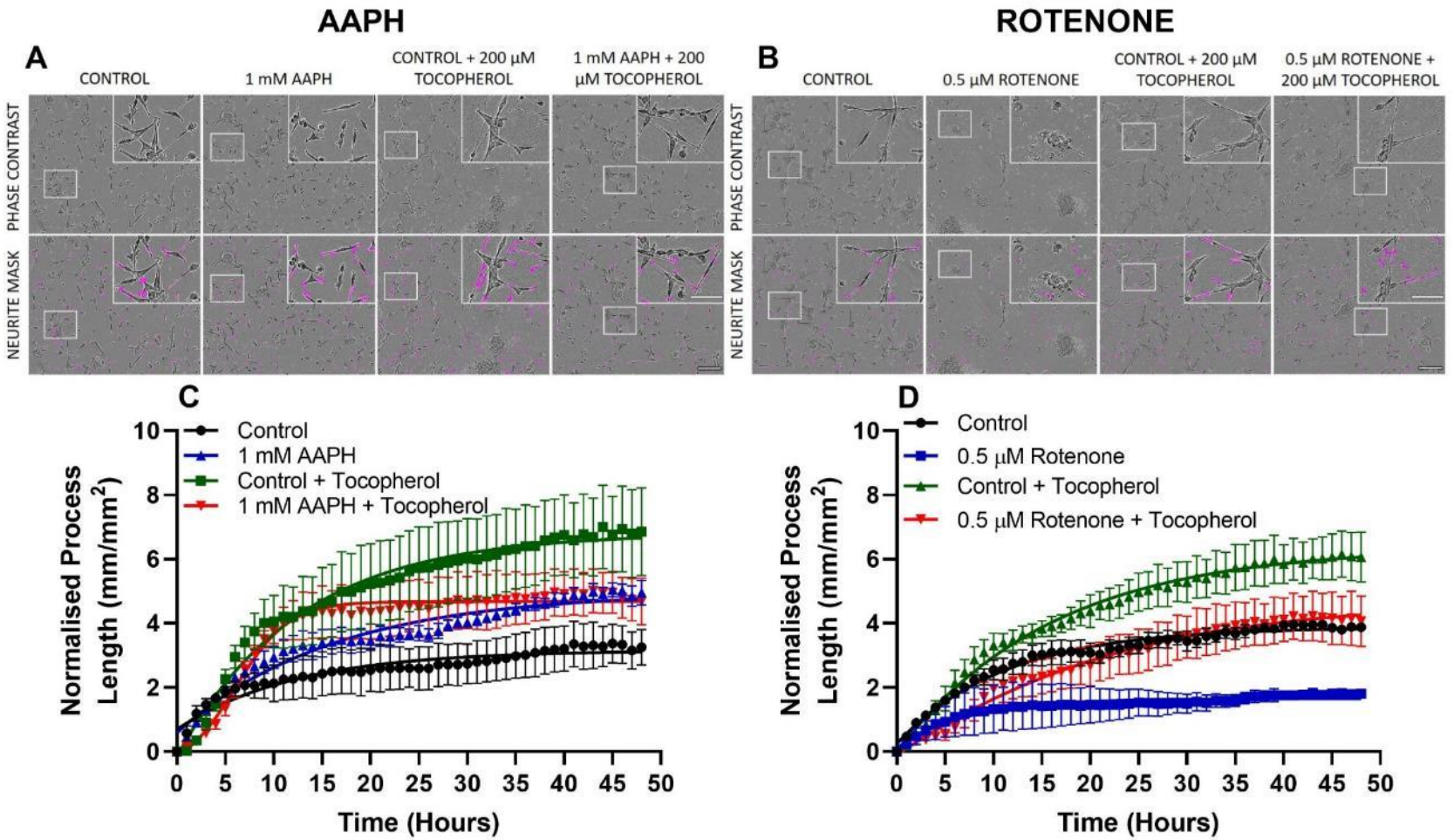

Figure 4.33 The effect of reactive species on glial processes in the presence of tocopherol. *Following differentiation with FBS/RA U-87MG glial cells were treated with AAPH or rotenone for 48 hours with or without α-tocopherol, where process outgrowth was monitored using the incucyte S3 live-cell analysis system. Phase contrast images of 48-hour (A) AAPH and (B) rotenone with and without α-tocopherol treated glia, where neurotracker software from the incucyte S3 live-cell analysis system was used to mask processes (purple). Scale bar = 200 µm. Inset scale bar = 100 µm. Phase contrast images were taken every hour for 48-hours and quantified using the neurotracker software. Live cell monitoring of process length of (C) AAPH and (D) rotenone treated differentiated glial cells with and without α-tocopherol.*

4.2.5 The effect of reactive species on gene expression in differentiated neural cells

With viability and morphology affected by RS inducers rotenone and AAPH we investigated the OS profile induced in both differentiated SH-SY5Y and U-87MG neural cells following 48-hour exposure. A RT^2 profiler PCR array focused on genes involved in OS was utilised.

SH-SY5Y and U-87MG profiles were compared to investigate the differences in basal gene expression between these different neural cell types. Genes significantly upregulated or downregulated in U-87MG glial cells relative to SH-SY5Y (figure 4.34A) were identified, and presented as a heatmap of differentially expressed OS related genes (figure 4.34B). Interestingly, U-87MG glial exhibited lower basal expression of most genes associated with glutathione synthesis, despite glia possessing greater levels of glutathione (figure 4.34C). Furthermore, peroxiredoxin (PRDX) and SOD levels appear to be expressed differently where some are upregulated while others are downregulated (figure 4.34B and 4.34D). Together, these results suggest differences in expression of OS associated genes in differentiated SH-SY5Y neuronal and U-87MG glial cells.

Next, we investigated differences in upregulated and downregulated genes from AAPH (figure 4.35A) or rotenone (figure 4.35B) treatment of differentiated SH-SY5Y cells. Heatmaps allowed significant differences in gene expression to be identified (figure 4.35C), where AAPH resulted in a greater proportion of genes being upregulated, while rotenone lead to more being downregulated. This was further demonstrated by fold changes in expression with rotenone inducing a decrease in glutathione related genes (figure 4.35D), PRDX genes (figure 4.35E) and thioredoxin related genes (figure 4.35F), whereas AAPH resulted in increased expression. This may be influenced by the treatment timeframe reaction of rotenone and AAPH.

Using Venny (an interactive tool; Oliveros, 2007), we compared differences in upregulated (figure 4.36A) and downregulated (figure 4.36B) genes following AAPH and rotenone treatment of SH-SY5Y cells. Only 6 genes were simultaneously upregulated, and 2 genes were downregulated in AAPH and rotenone treated SH-SY5Y cells, suggesting each RS stressor induced a unique gene profile. Pathway analyses showed AAPH treatment upregulated antioxidant genes (figure 4.36C), genes involved in the metabolism of RS (figure 4.36D) and OS responsive genes (figure 4.36E), while rotenone showed a decrease in genes linked to several of these pathways. This suggests the OS response is still active in AAPH treated SH-SY5Y cells while it is no longer active in rotenone treated SH-SY5Y neuronal cells at 48-hours.

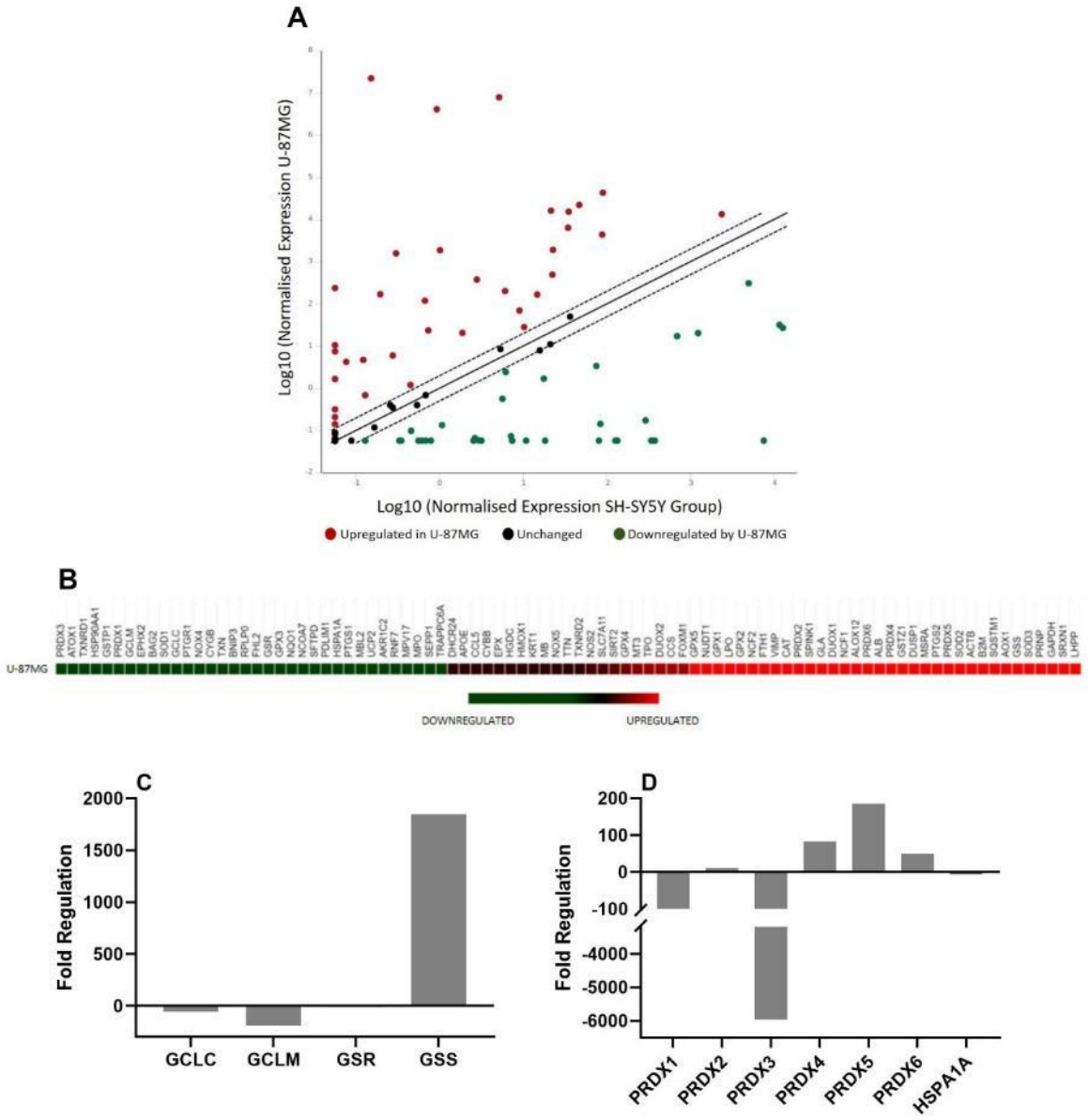

Figure 4.34 Oxidative stress related gene profile in U-87MG glial cells relative to SH-SY5Y neuronal cells using RT² profile array. *Comparisons among groups were analysed and normalised to mRNAs of DHCR24, SIRT2, GPX4, TRAPPC6A and SEPP1 as recommended. (A) Scatterplots comparing U-87MG glia against SH-SY5Y neuronal cells showing the normalised genes. Red: normalised expression of genes upregulated relative to SH-SY5Y neuronal cells. Green: normalised expression of genes downregulated relative to SH-SY5Y neuronal cells. Black: Normalised expression of unchanged genes. (B) Heatmap comparing genes significantly up- and downregulated in U-87MG glial cells relative to SH-SY5Y neuronal cells. (C) Fold change of glutathione related genes in U-87MG glia relative to SH-SY5Y neurons. (D) Fold change of peroxiredoxin and chaperone gene expression in U-87MG glial relative to neurons.*

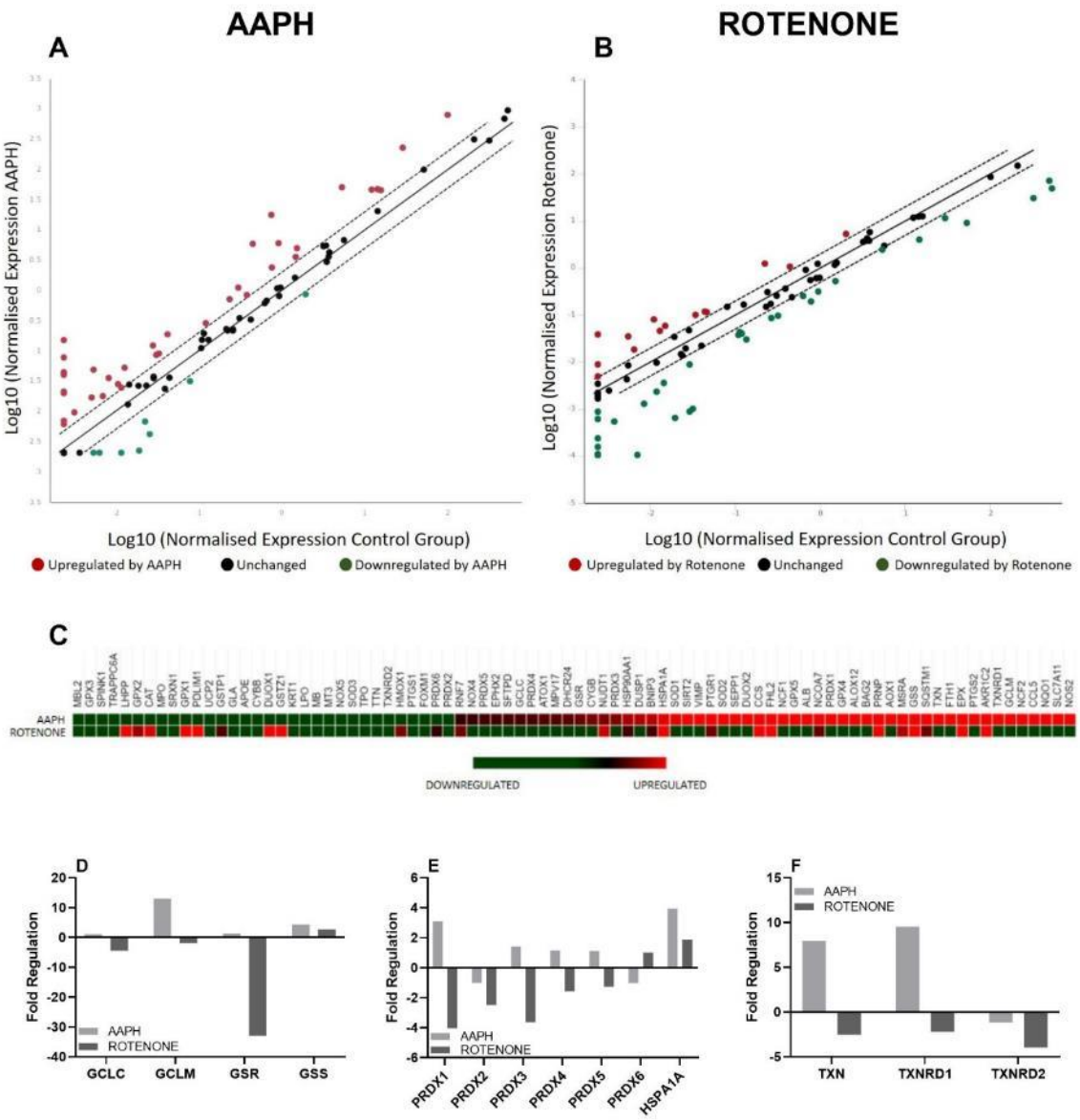

Figure 4.35 Oxidative stress related gene profile in SH-SY5Y neuronal cells in response to rotenone or AAPH using RT² profile array. *Cells were differentiated with FBS/RA over 5 days and then treated with AAPH or rotenone for 48-hours. Comparisons among treatments were analysed and normalised to mRNAs of B2M and HRPT1. Scatterplots comparing (A) AAPH and (B) rotenone treated SH-SY5Y neuronal cells showing the normalised expression. Red: normalised expression of genes upregulated by AAPH or rotenone relative to control neuronal cells. Green: normalised expression of genes downregulated by AAPH or rotenone relative to control neuronal cells. Black: Normalised expression of unchanged genes. (C) Heatmap comparing genes significantly up- and downregulated by AAPH or rotenone. (D) Fold change of glutathione related genes in response to AAPH or rotenone. (D) Fold change of peroxiredoxin and chaperone gene expression in response to AAPH or rotenone. (E) Fold change of thioredoxin related genes in response to AAPH or rotenone.*

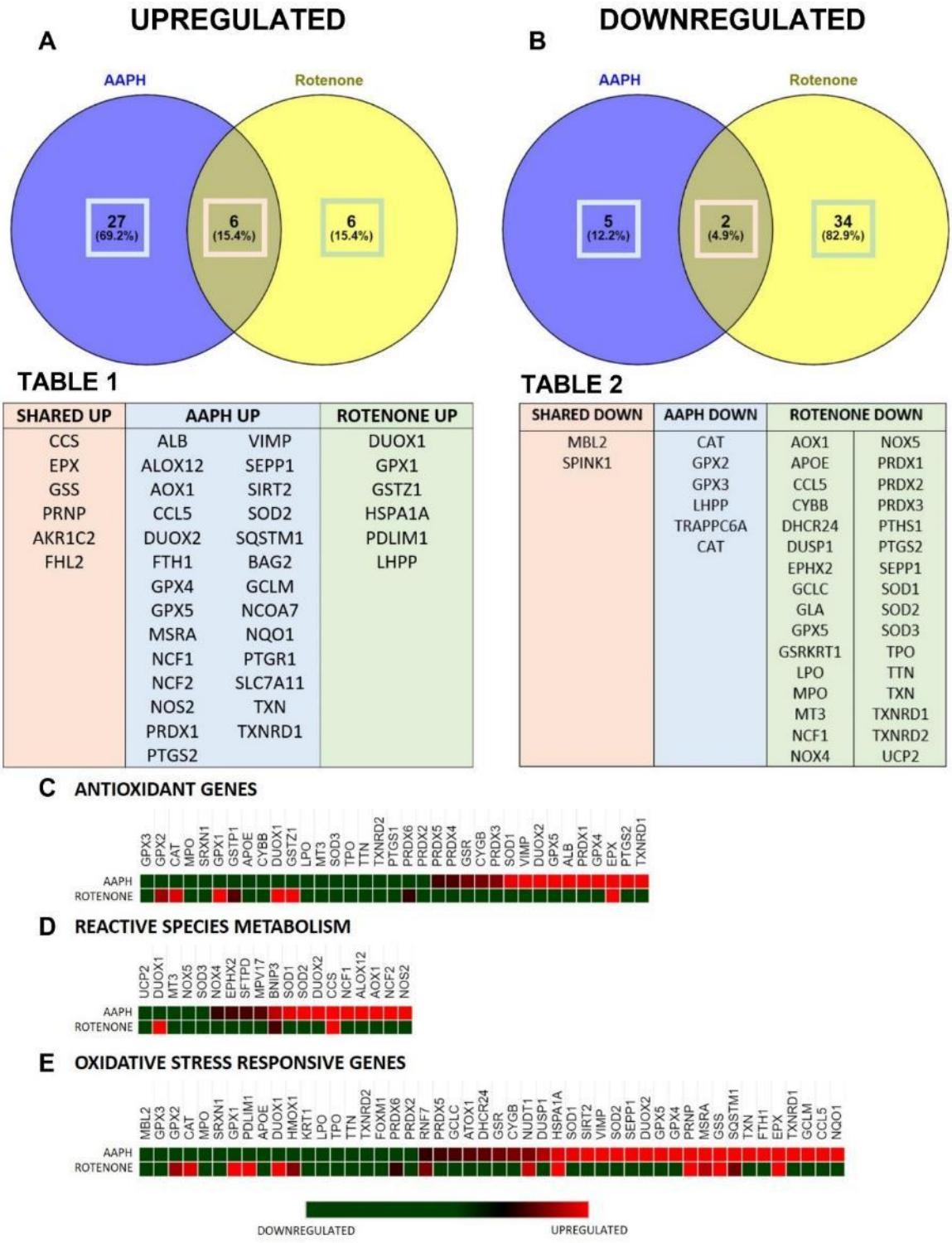

TABLE 1

SHARED UP	AAPH UP		ROTENONE UP
CCS	ALB	VIMP	DUOX1
EPX	ALOX12	SEPP1	GPX1
GSS	AOX1	SIRT2	GSTZ1
PRNP	CCL5	SOD2	HSPA1A
AKR1C2	DUOX2	SQSTM1	PDLIM1
FHL2	FTH1	BAG2	LHPP
	GPX4	GCLM	
	GPX5	NCOA7	
	MSRA	NQO1	
	NCF1	PTGR1	
	NCF2	SLC7A11	
	NOS2	TXN	
	PRDX1	TXNRD1	
	PTGS2		

TABLE 2

SHARED DOWN	AAPH DOWN	ROTENONE DOWN	
MBL2	CAT	AOX1	NOX5
SPINK1	GPX2	APOE	PRDX1
	GPX3	CCL5	PRDX2
	LHPP	CYBB	PRDX3
	TRAPPC6A	DHCR24	PTHS1
	CAT	DUSP1	PTGS2
		EPHX2	SEPP1
		GCLC	SOD1
		GLA	SOD2
		GPX5	SOD3
		GSRKRT1	TPO
		LPO	TTN
		MPO	TXN
		MT3	TXNRD1
		NCF1	TXNRD2
		NOX4	UCP2

Figure 4.36 Differences and similarities between AAPH and rotenone induced gene profile in SH-SY5Y neuronal cells. *Venn diagram illustrating the proteins (A) up- and (B) downregulated by AAPH or rotenone treatment in neuronal cells. Numbers represent the number of significantly altered proteins and percentages represent how many are unique or shared between each treatment. Respective genes are noted in table 1 and table 2. Heatmaps comparing genes significantly up- and downregulated by AAPH or rotenone grouped into (C) antioxidant genes, (D) genes involved in reactive species metabolism and (E) genes responsive to oxidative stress in neuronal cells.*

Differences in oxidative stress gene expression was also investigated in differentiated U-87MG glial cells treated with AAPH and rotenone. Both AAPH (figure 4.37A) and rotenone (figure 4.37B) resulted in a significant increase in several OS related genes. This is further highlighted by the heatmap, which shows similar clusters of genes upregulated by both AAPH and rotenone (figure 4.37C) including: glutathione related genes (figure 4.38D), PRDX's (figure 4.37E) and thioredoxin related genes (figure 4.37F).

The similarities in expression profiles in response to AAPH or rotenone treatment is visible in the Venn diagrams. A total of 61 genes are upregulated (figure 4.38A) and 10 genes downregulated (figure 4.38B) with both AAPH and rotenone treatment (87.1% and 55.6%, respectively). Groups of related genes appear to be regulated in similar ways for both AAPH and rotenone, for example glutathione peroxidases (GPX's) and thioredoxins (TXN's) are both upregulated. Of note, SOD isoform expression was different for AAPH or rotenone treatment as SOD1 was upregulated in both treatments but SOD2 was only upregulated in rotenone treated U-87MG glial cells.

Together, these findings suggest 48-hour AAPH or rotenone treatment of differentiated SH-SY5Y neuronal cells resulted in different gene expression profiles, suggesting divergent RS induce different gene expression responses. In contrast, AAPH or rotenone treatment of U-87MG glial cells showed similar gene expression profiles.

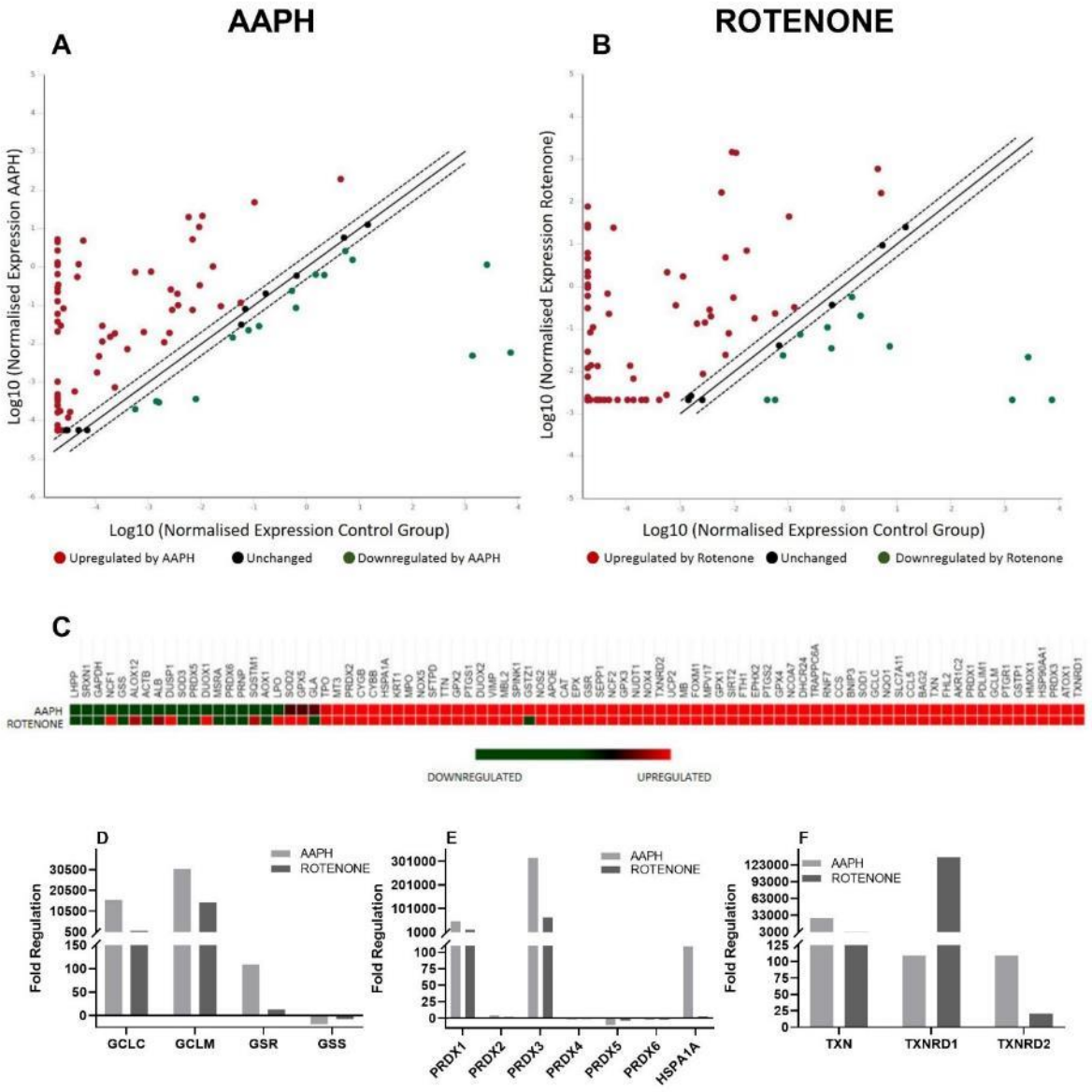

Figure 4.37 Oxidative stress related gene profile in U-87MG glial cells in response to rotenone or AAPH using RT² profile array. *Cells were differentiated with FBS/RA over 5 days and then treated with AAPH or rotenone for 48-hours. Comparisons among treatments were analysed and normalised to mRNAs of B2M and HRPT1. Scatterplots comparing (A) AAPH and (B) rotenone treated U-87MG glial cells showing the normalised expression. Red: normalised expression of genes upregulated by AAPH or rotenone relative to control glial cells. Green: normalised expression of genes downregulated by AAPH or rotenone relative to control glial cells. Black: Normalised expression of unchanged genes. (C) Heatmap comparing genes significantly up- and downregulated by AAPH or rotenone. (D) Fold change of glutathione related genes in response to AAPH or rotenone. (D) Fold change of peroxiredoxin and chaperone gene expression in response to AAPH or rotenone. (E) Fold change of thioredoxin related genes in response to AAPH or rotenone.*

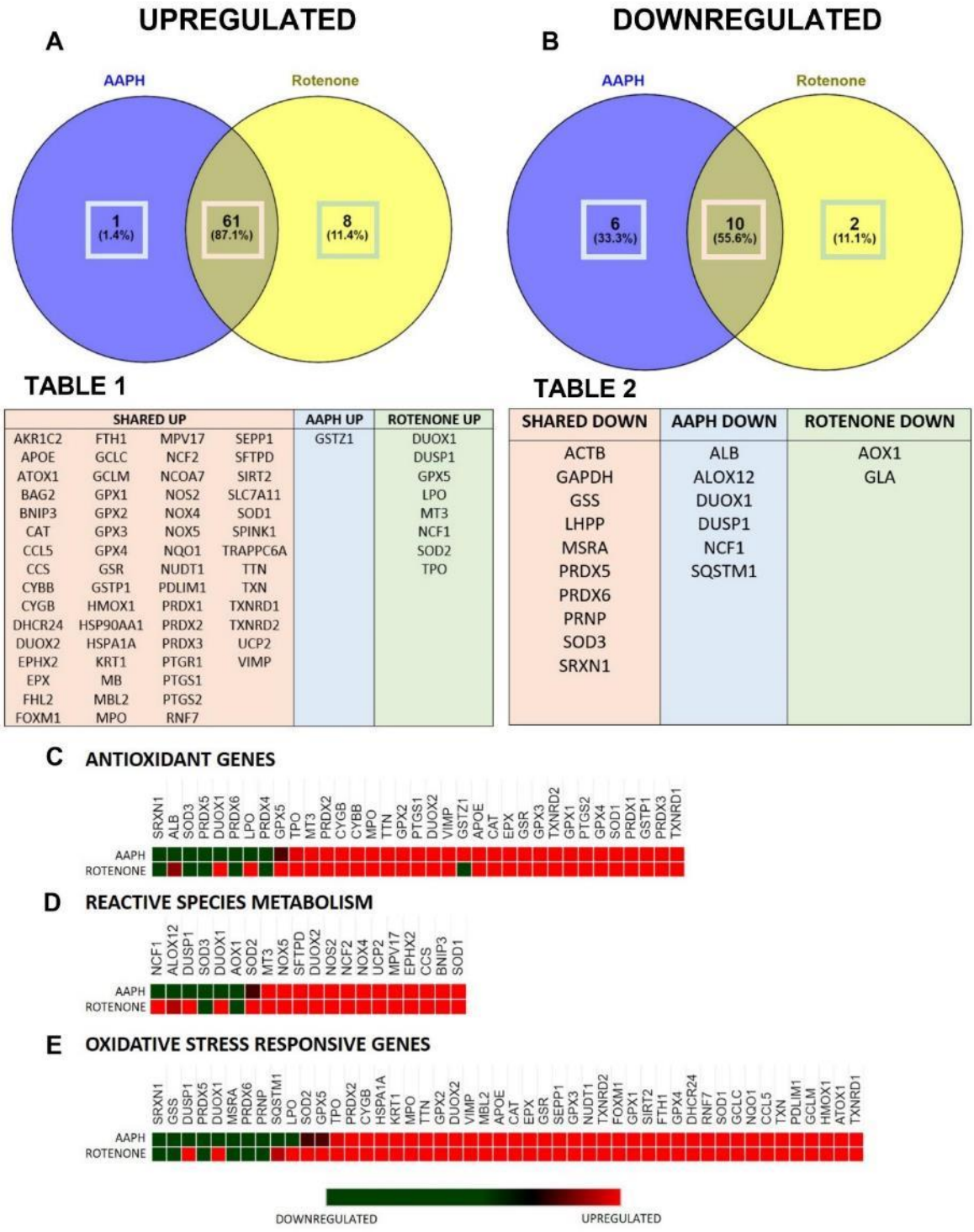

TABLE 1

SHARED UP				AAPH UP	ROTENONE UP
AKR1C2	FTH1	MPV17	SEPP1	GSTZ1	DUOX1
APOE	GCLC	NCF2	SFTPD		DUSP1
ATOX1	GCLM	NCOA7	SIRT2		GPX5
BAG2	GPX1	NOS2	SLC7A11		LPO
BNIP3	GPX2	NOX4	SOD1		MT3
CAT	GPX3	NOX5	SPINK1		NCF1
CCL5	GPX4	NQO1	TRAPPC6A		SOD2
CCS	GSR	NUDT1	TTN		TPO
CYBB	GSTP1	PDLIM1	TXN		
CYGB	HMOX1	PRDX1	TXNRD1		
DHCR24	HSP90AA1	PRDX2	TXNRD2		
DUOX2	HSPA1A	PRDX3	UCP2		
EPHX2	KRT1	PTGR1	VIMP		
EPX	MB	PTGS1			
FHL2	MBL2	PTGS2			
FOXM1	MPO	RNF7			

TABLE 2

SHARED DOWN	AAPH DOWN	ROTENONE DOWN
ACTB	ALB	AOX1
GAPDH	ALOX12	GLA
GSS	DUOX1	
LHPP	DUSP1	
MSRA	NCF1	
PRDX5	SQSTM1	
PRDX6		
PRNP		
SOD3		
SRXN1		

Figure 4.38 Differences and similarities between AAPH and rotenone induced gene profile in U-87MG glial cells. *Venn diagram illustrating the proteins (A) up- and (B) downregulated by AAPH or rotenone treatment in glial cells. Numbers represent the number of significantly altered proteins and percentages represent how many are unique or shared to each treatment. Respective genes are noted in table 1 and table 2. Heatmaps comparing genes significantly up- and downregulated by AAPH or rotenone grouped into (C) antioxidant genes, (D) genes involved in reactive species metabolism and (E) genes responsive to oxidative stress in glial cells.*

To validate some of these findings at the protein level, Western blots were performed. We demonstrated HSP70 (referred to as HSPA1A in the array) increased with both AAPH and rotenone treatment in differentiated SH-SY5Y cells (figure 4.39A), while only increasing for AAPH treatment in differentiated U-87MG glial cells (figure 4.39B) mimicking gene profile expression. In addition, PRDX6 protein levels of SH-SY5Y cells (figure 4.39B) remained stable in response to AAPH or rotenone treatment whilst being significantly reduced in U-87MG treated cells. These profiles were also observed with the gene expression data.

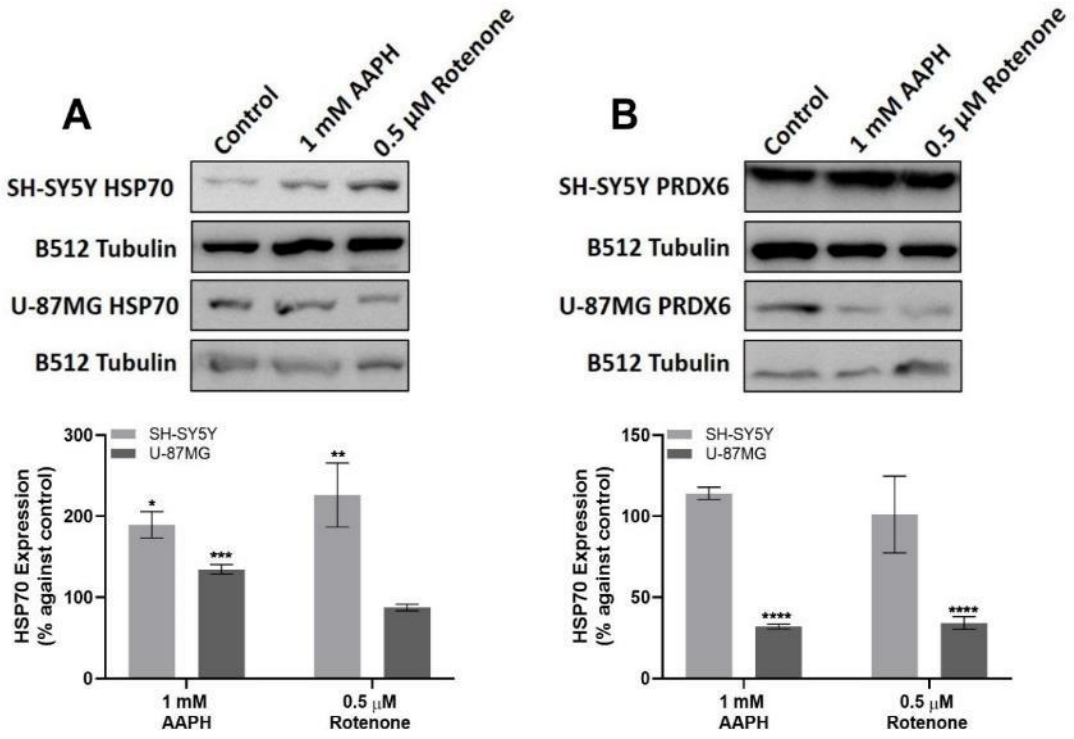

Figure 4.39 Western blot validation of PCR array. *Representative Western blots of differentiated neuronal SH-SY5Y and glial U-87MG total cell extracts were probed with (A) HSP70 (1:1000) or (B) PRDX6 (1:1000) following treatment with either 1 mM AAPH or 0.5 µM rotenone. Each Western blot is accompanied by a plot summarising densitometric analyses of Western blots using AIDA software. Results are presents as % against control ± SEM. Statistical analysis was performed using one-way ANOVA with Dunnett's post-hoc test where n=4 for all experiments. Statistical significance was recorded as *p<0.05, **p<0.01, ***p<0.001 and ****p<0.0001.*

OS gene profiles of SH-SY5Y and U-87MG treated cells was then analysed by MetaCore (Clavirate analytics) pathway analysis. Figure 4.40A summarises the significantly up- and downregulated pathways linked to differentially expressed genes. Further analysis revealed various upstream transcription factors summarised in 4.40 table 1. Of interest was NRF2, a transcription factor that regulates several genes altered by AAPH and rotenone treatment (circled on figure 4.40A). As previous studies with mitotic cells also showed nuclear translocation of NRF2 (figures 3.9 and 3.10), we investigated NRF2 and KEAP1, (an inhibitor of NRF2) gene expression via qRT-PCR. Both neural cells showed increased NRF2 expression upon treatment with AAPH or rotenone with significant changes being observed for AAPH treated SH-SY5Y neuronal cells and rotenone treated U-87MG glial cells (figure 4.40B). In contrast, only rotenone treated U-87MG glial cells showed significantly downregulated levels of KEAP1 (figure 4.40C). Together, with previous localisation studies, this suggests NRF2 may play a role in the antioxidant stress response in AAPH and rotenone treated neural cells.

A

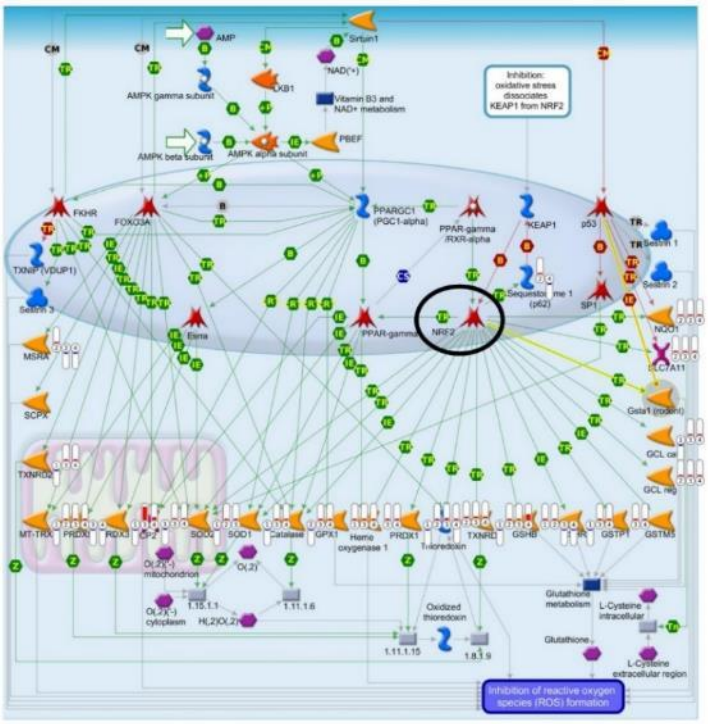

Table 1

Transcription factor	P-value	Transcription factor	P-value
SOX17	6.05E-248	HNF4-alpha	2.8E-132
GATA-1	1.27E-225	KLF4	2.8E-132
TAL1	6.3E-211	STAT3	8.82E-129
AML1	2.3E-196	SP3	8.82E-129
SP1	9.6E-193	c-Jun	8.82E-129
FOXP3	3.94E-189	C/EBPβ	2.74E-125
E2F1	3.94E-189	TCF8	2.74E-125
ETS1	2.45E-178	p53	8.38E-122
c-Myc	9.4E-175	HIF1A	8.38E-122
Oct-3/4	4.8E-164	ESR1	7.55E-115
SOX2	1.72E-160	FOXO3A	7.55E-115
RelA	4.63E-155	N-myc	2.22E-111
NRF2	2.47E-146	NRF1	1.85E-104
CREB1	2.71E-139	BMAL1	5.22E-101

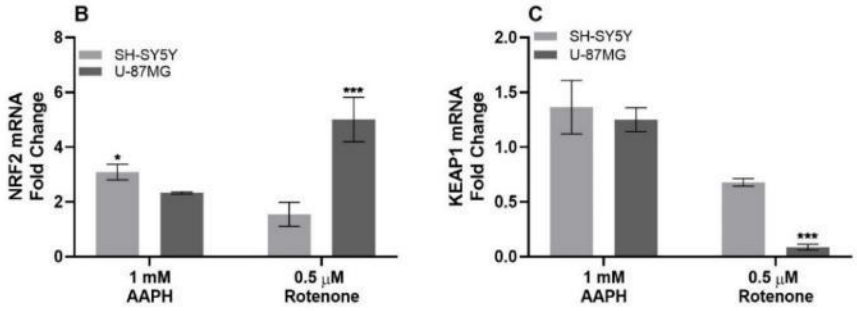

Figure 4.40 Pathways associated with oxidative stress gene profiles. *MetaCore from Clarivate analytics was used to analyse gene array data with SH-SY5Y neuronal and U-87MG glial cells treated with rotenone or AAPH. Symbols numbered 1-4 where 1: Rotenone treated SH-SY5Y neuronal cells, 2: AAPH treated SH-SY5Y neuronal cells, 3: Rotenone treated U-87MG glial cells and 4: AAPH treated U-87MG glial cells. Metacore was also used to identify upstream transcription factors summarised in table 1 and NRF2, an identified transcription factor is circled in the pathways diagram. qRT-PCR was used to determine (B) NRF2 and (C) KEAP1 gene expression in differentiated SH-SY5Y neuronal and U-87MG glial cells following 48-hour exposure to 1 mM AAPH or 0.5 μM rotenone, where results are expressed relative to control. Statistical analysis was performed using an unpaired t-test where n=3 for all experiments. Statistical significance was recorded as *p<0.05, **p<0.01 and ***p<0.001.*

4.2.6 The effect of NRF2 knockdown of neural cells

In order to investigate NRF2's potential role in neural cells in response to RS we knocked down NRF2 expression with siRNA in SH-SY5Y and U-87MG neural cells, prior to treatment with AAPH and rotenone.

Initially, the optimum concentration of lipofectamine for each cell line was determined using green fluorescent protein expression, where transfection was monitored and quantified using the incucyte S3 live-cell analysis system. Phase contrast and fluorescent microscopy at 48 hours showed green fluorescent protein in both 1.5 and 3% (v/v) lipofectamine transfected SH-SY5Y and U-87MG cells (figure 4.41A and D, respectively). SH-SY5Y cells showed greater green fluorescence protein expression with 3% (v/v) lipofectamine (figure 4.41A), whereas U-87MG glial cells showed greater green fluorescence for 1.5% (v/v) lipofectamine (figure 4.41D). This was supported by live-cell analysis, which showed fluorescence increased over the first 48 hours for SH-SY5Y cells with 3% (v/v) lipofectamine (figure 4.41C), while more green fluorescence was observed with 1.5% lipofectamine for U-87MG cells (figure 4.41F). To ensure lipofectamine was not toxic to cells we also investigated viability by quantifying phase confluence images and found that 1.5 and 3% (v/v) lipofectamine exhibited similar growth to control SH-SY5Y and U-87MG cells (figure 4.41B and E, respectively). Therefore, these results suggest the optimum lipofectamine concentration is 3% (v/v) for SH-SY5Y neuronal cells, whereas 1.5% (v/v) was optimal for U-87MG glial cells.

With optimum lipofectamine concentrations determined, we transfected both neural cells with NRF2 siRNA for up to 72 hours to determine the optimum transfection time to knockdown NRF2. Western blots of NRF2 levels showed the greatest knockdown of NRF2 at 72 hours for SH-SY5Y neuronal cells (figure 4.42E) while U-87MG glial cells showed the greatest knockdown at 24 hours (figure 4.42F). In addition, cell proliferation was monitored over 72 hours to determine if cell viability was affected by NRF2 knockdown. Live-cell analysis using the incucyte S3 live cell analysis showed no significant difference between control and NRF2 knockdown for both SH-SY5Y neuronal (figure 4.42C) and U-87MG glial cells (figure 4.42D), which was supported by phase contrast microscopy images (figure 4.42A and B). Together, these results suggest 72 hours was optimal for NRF2 knockdown in SH-SY5Y neuronal cells whereas 24 hours was suitable for U-87MG glial NRF2 knockdown.

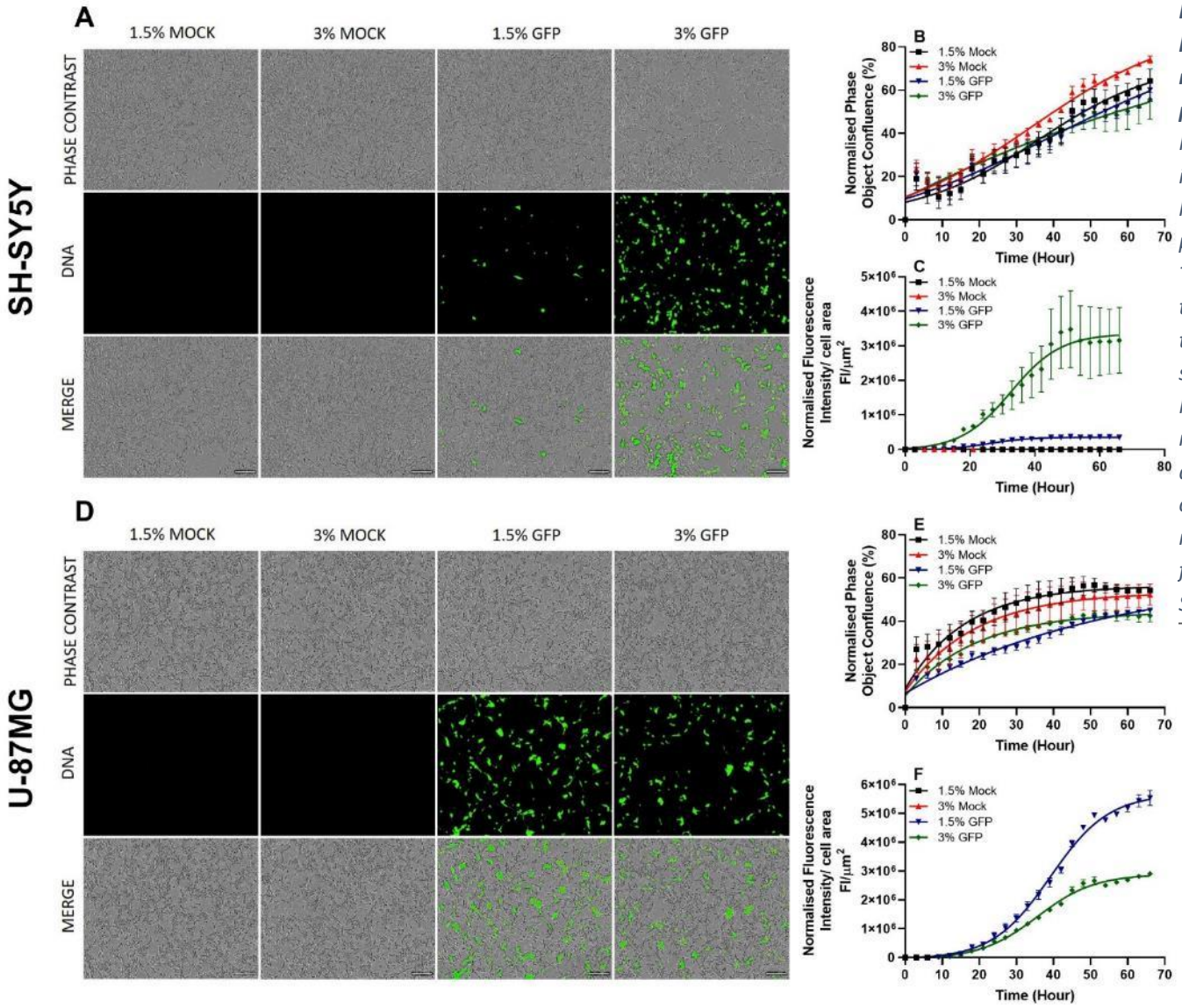

Figure 4.41 Optimising lipofectamine transfection in neural cells with green fluorescent protein. *48-hour images of Neuronal (A) and glial (D) cells were incubated with 1.5% or 3% (v/v) lipofectamine with or without 0.5 µg green fluorescent protein. Transfection was monitored over time and images were taken using the incucyte S3 live-cell analysis system. Scale bar = 200 µm. Normalised phase confluence of neurons (B) and glia (E) was quantified over time. Transfection of neurons (C) and glia (F) was monitored by measuring green fluorescence intensity/cell area ± SEM.*

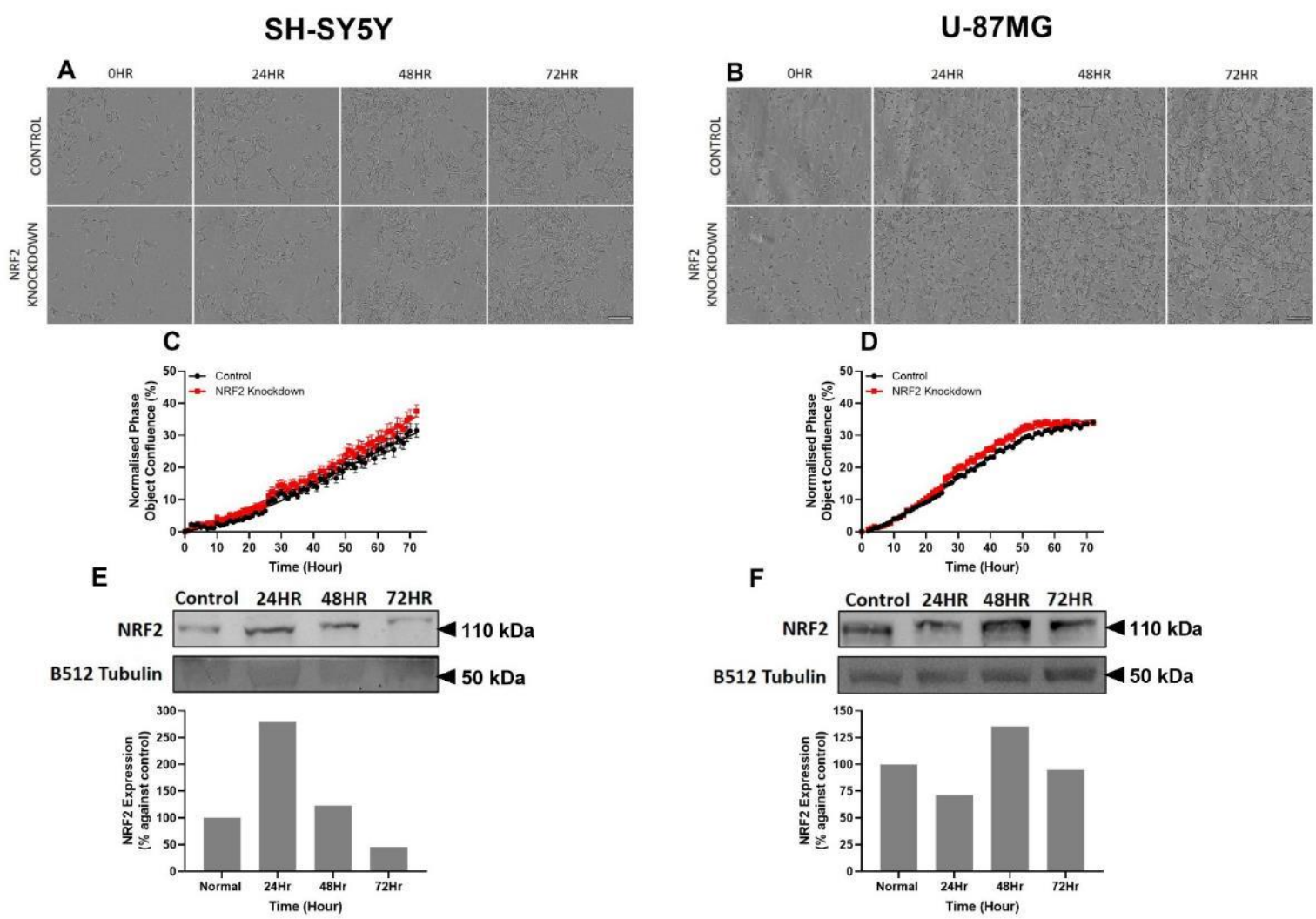

Figure 4.42 NRF2 knockdown in neural cells. *Neural cells were transfected with NRF2 siRNA for up to 72 hours, viability and successful knockdown was investigated. Phase contrast microscopy of (A) SH-SY5Y and (B) U-87MG cells with and without NRF2 siRNA. Scale Bar = 200 µm. Images were taken 2 hours using the incucyte S3 live-cell analysis system, which was then used to quantify phase confluence of (C) SH-SY5Y and (D) U-87MG with and without NRF2 siRNA ± SEM. Total cell lysates were collected at 24, 48 and 72h, and SDS-PAGE and Western blot was run to determine the optimum time for NRF2 knockdown in (E) SH-SY5Y neuronal and (F) U-87MG glial cells. Each Western blot is accompanied by a plot summarising densitometric analyses of Western blots using AIDA software.*

To investigate the potential role of NRF2 in response to RS both SH-SY5Y and U-87MG neural cells were transfected with scramble, GAPDH or NRF2 siRNA prior to treatment with AAPH or rotenone. Following 48-hour AAPH and rotenone treatment, neural viability was assessed via morphological changes, viability and functional activity assays.

Phase contrast microscopy of SH-SY5Y neuronal cells showed greater intercellular distance, cellular shrinkage and rounding for 1 mM AAPH treated NRF2 knockdown cells relative to scramble and GAPDH transfected cells (figure 4.43A). Whereas rotenone (0.5 μM) treated NRF2 knockdown SH-SY5Y cells showed little morphological differences from scramble and GAPDH transfected cells (figure 4.43A). Viability assessment showed NRF2 knockdown of SH-SY5Y cells treated with 1 mM AAPH had significantly lower viability (MTT reduction), relative to scramble and GAPDH transfected cells (figure 4.44A). In contrast, NRF2 knockdown did not significantly affect rotenone treated SH-SY5Y cells as viability (MTT reduction) was not significantly different from scramble, but was significantly greater than GAPDH transfected SH-SY5Y neuronal cells (figure 4.44A). LDH assays supported the SH-SY5Y AAPH findings where NRF2 knockdown showed significantly greater LDH release than scramble and GAPDH transfected cells (figure 4.44C). Phase confluence quantification with the incucyte S3 live-cell analysis system also confirmed MTT results, as NRF2 knockdown resulted in a significant decrease in phase confluence relative to scramble when treated with 1 mM AAPH, while rotenone treatment of NRF2 knockdown cells showed significantly greater phase confluence than GAPDH siRNA transfected cells (figure 4.44E). Together, these results suggest NRF2 knockdown increased SH-SY5Y susceptibility to AAPH but not rotenone induced cell death.

Interestingly, NRF2 knockdown in U-87MG glial cells resulted in attenuation of 1 mM AAPH induced proliferation, as phase contrast microscopy showed greater intercellular distances for NRF2 knockdown relative to scramble siRNA transfected cells (figure 4.43B), which was further supported by MTT assays showing a significant decrease in MTT reduction for NRF2 knockdown relative to scramble cells (figure 4.44B). LDH assays supported these findings as scramble transfected U-87MG cells showed significantly less LDH release than NRF2 knockdown glia, whereas GAPDH transfected glia showed significantly greater LDH release (figure 4.44D). Furthermore, glial NRF2 knockdown resulted in greater susceptibility to rotenone induced death as MTT reduction levels were significantly lower compared to scramble and GADPH transfected glia (figure 4.44B). Phase contrast images showed NRF2 knockdown glia exhibited greater cellular rounding and intercellular distance when treated with rotenone relative to scramble controls (figure 4.43B). LDH assays reinforced these findings as NRF2 knockdown in glia showed greater LDH release for 48-hour exposure to 1 mM AAPH or 0.5 μM rotenone relative to scramble controls (figure 4.44D). Quantification of images also suggested NRF2 knockdown in glia resulted in lower phase confluence relative to scramble when

treated for 48 hours with AAPH or rotenone (figure 4.44F). Together, these results suggest NRF2 knockdown in U-87MG glial cells attenuated AAPH induced proliferation and increased susceptibility to rotenone-induced death, suggesting NRF2 is an important response factor to RS in glia.

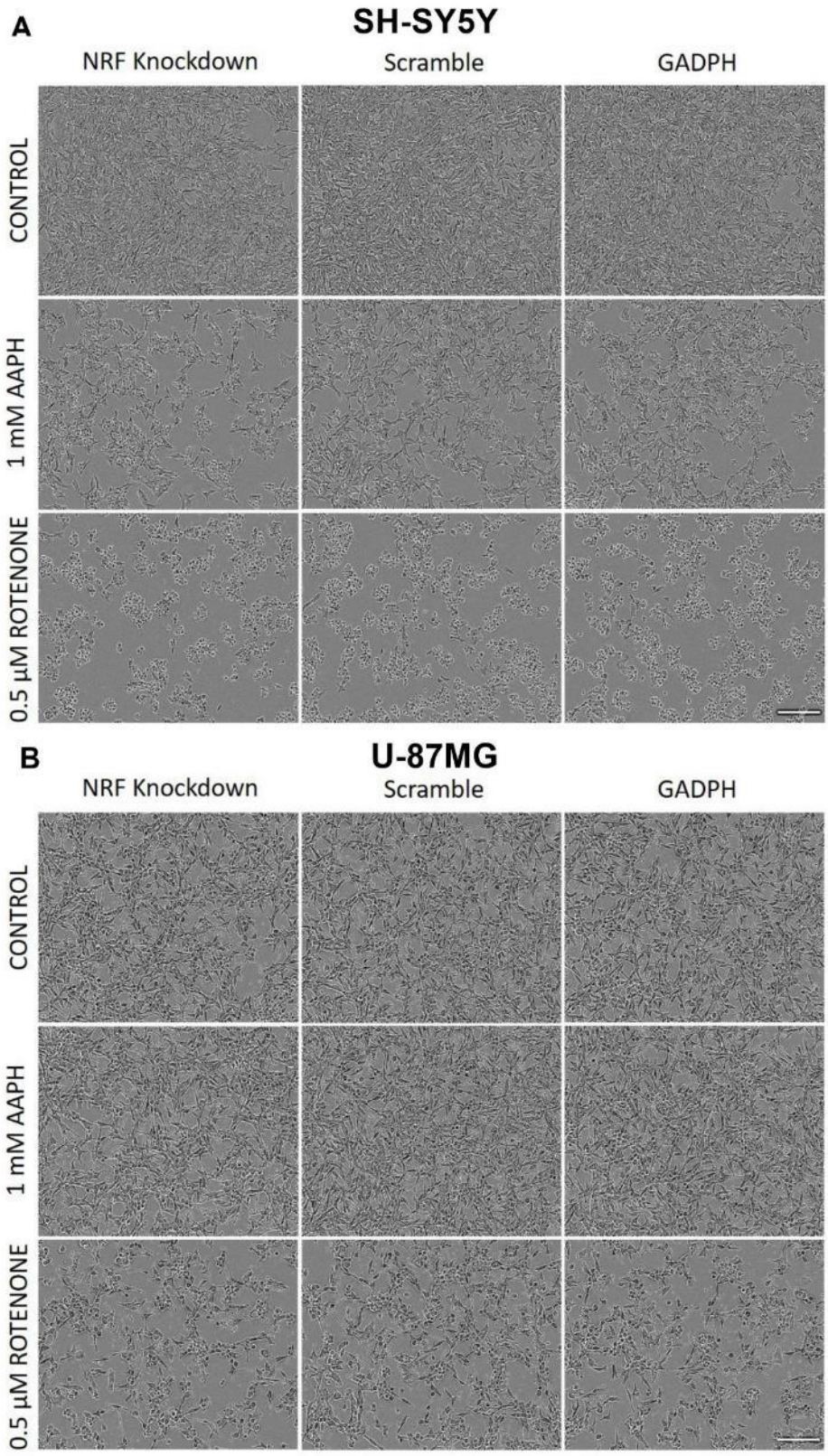

Figure 4.43 NRF2 knockdown effects neural morphology following treatment with AAPH or rotenone. *SH-SY5Y neuronal (A) and U-87MG glial (B) cells were incubated with lipofectamine with NRF2, scramble or GAPDH siRNA for the 3 days or 1 day, respectively. Following NRF2 knockdown cells were treated with 1 mM AAPH or 0.5 µM rotenone for 48 hours. 48-hour images were taken using the incucyte S3 live-cell analysis system. Scale bar = 200 µm.*

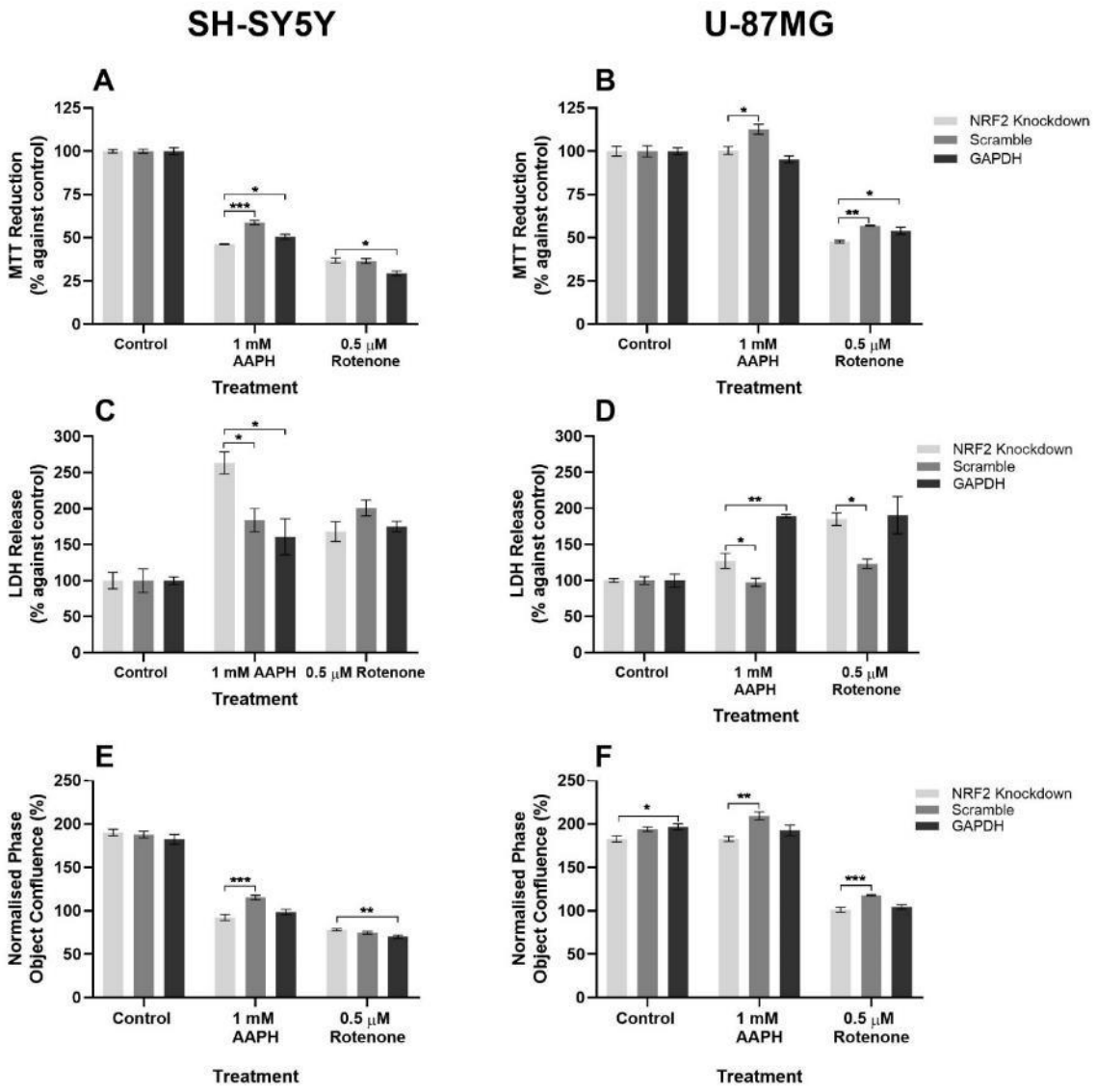

Figure 4.44 NRF2 knockdown exacerbates decreased neural cell viability in response to reactive species. *SH-SY5Y neuronal and U-87MG glial cells were incubated with lipofectamine with NRF2, scramble or GAPDH siRNA for the 3 days or 1 day, respectively. Following NRF2 knockdown cells were treated with 1 mM AAPH or 0.5 µM rotenone for 48 hours. MTT reduction assay of (A) SH-SY5Y and (B) U-87MG cells treated with AAPH and rotenone for 48 hours following transfection. LDH release of (C) SH-SY5Y and (D) U-87MG treated with AAPH or rotenone for 48 hours following transfection. Endpoint images of neurons (E) and glia (F) were quantified using the incucyte S3 live-cell analysis system where results were normalised prior to addition of treatments ± SEM. MTT and LDH viability assays are presented as mean % against control ± SEM. Statistical analysis was performed using one-way ANOVA with Dunnett's post-hoc test where n=3 for all experiments. Statistical significance was recorded as *p<0.05, **p<0.01 and ***p<0.001.*

4.2.7 Post-translational modifications induced by reactive species in differentiated neural cells

As previous studies with antioxidants and gene expression suggested differences in AAPH and rotenone mediated RS, we investigated downstream post-translational modifications in neural cells to define variation in OS. As AAPH is known to mainly generate peroxyl radicals, lipid peroxidation was investigated using a Click-iT lipid peroxidation kit. Click-iT allows detection of lipid peroxidation by cellular incorporation of linoleamide alkyne into membranes, which decompose to reactive aldehydes that can modify proteins. Alkyne modified proteins can subsequently be detected. Furthermore, as lipid peroxides are unstable compounds that can decompose to reactive carbonyl molecules such as malondialdehyde (MDA), we measured MDA levels using a colourimetric assay.

SH-SY5Y cells were differentiated over 5 days prior to 48-hour treatment with 1 mM AAPH or 0.5 μM rotenone to induce OS. Fluorescence quantification showed both AAPH and rotenone induced lipid peroxidation (figure 4.45A), where AAPH had a more significant effect on lipid peroxidation (figure 4.45B). Concurrent treatment with α-tocopherol or ascorbic acid attenuated fluorescence suggesting OS generated by these stressors resulted in lipid peroxidation. Preliminary investigations suggest AAPH significantly affected differentiated SH-SY5Y MDA levels, but rotenone did not, which was attenuated by both antioxidants (figure 4.45C).

U-87MG glial cells also showed significantly greater fluorescence levels when exposed to AAPH or rotenone for 48-hours following 5-day differentiation (figure 4.46A). Fluorescence quantification showed AAPH significantly increased lipid peroxidation more than rotenone, and this was attenuated by both α-tocopherol or ascorbic acid (Figure 4.46B). However, preliminary MDA quantification showed neither AAPH nor rotenone significantly affected MDA levels.

Therefore, these results show Click-iT immunofluorescence studies suggest AAPH significantly increased lipid peroxidation more than rotenone for both differentiated SH-SY5Y neuronal and U-87MG glial cells. This suggests AAPH generated RS that cause greater levels of lipid peroxidation than rotenone. Whereas MDA level quantification was controversial to these findings possibly due to limited replicates and kit sensitivity.

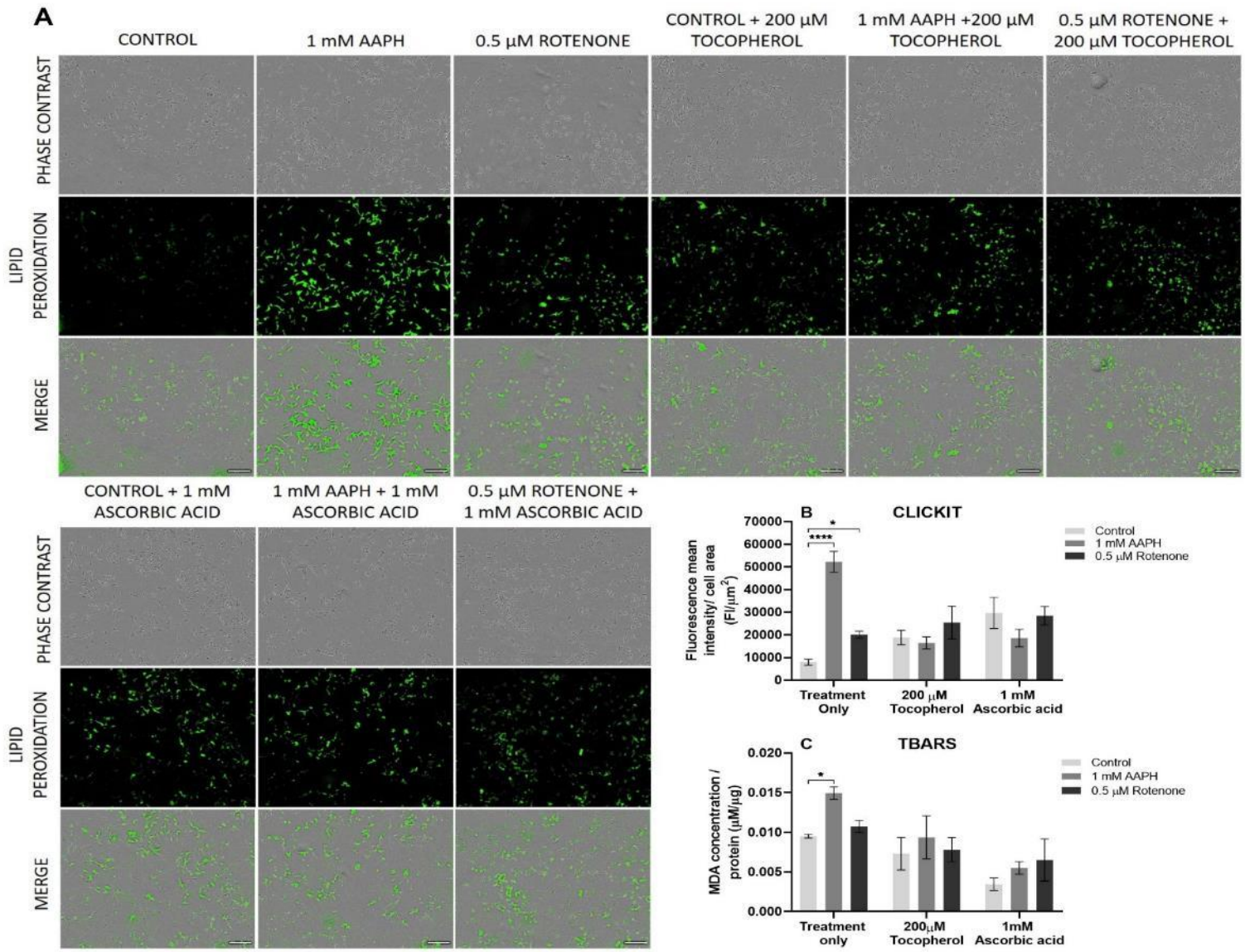

Figure 4.45 AAPH and rotenone increases lipid peroxidation in SH-SY5Y neuronal cells. *(A) Lipid peroxidation fluorescent levels (green) for neuronal cells treated with AAPH and rotenone, with and without 200 µM α-tocopherol or 1 mM ascorbic acid using Click-IT assay kit. Images taken using incucyte S3 live-cell analysis system. Scale bar = 200 µm. (B) Endpoint measurement of fluorescence was quantified using the incucyte S3 live-cell analysis system (Fluorescent intensity/cell area ± SEM). (C) Malondialdehyde levels (MDA), a by-product of lipid peroxidation were measured using a thiobarbituric acid reactive substances (TBARS) assay kit. Statistical analysis was performed using two-way ANOVA with Dunnett's post-hoc test relative to the control of each condition where n=3 for Click-iT but n=2 for TBARS experiments. Statistical significance was recorded as *p<0.05, **p<0.01, ***p<0.001 and ****p<0.0001.*

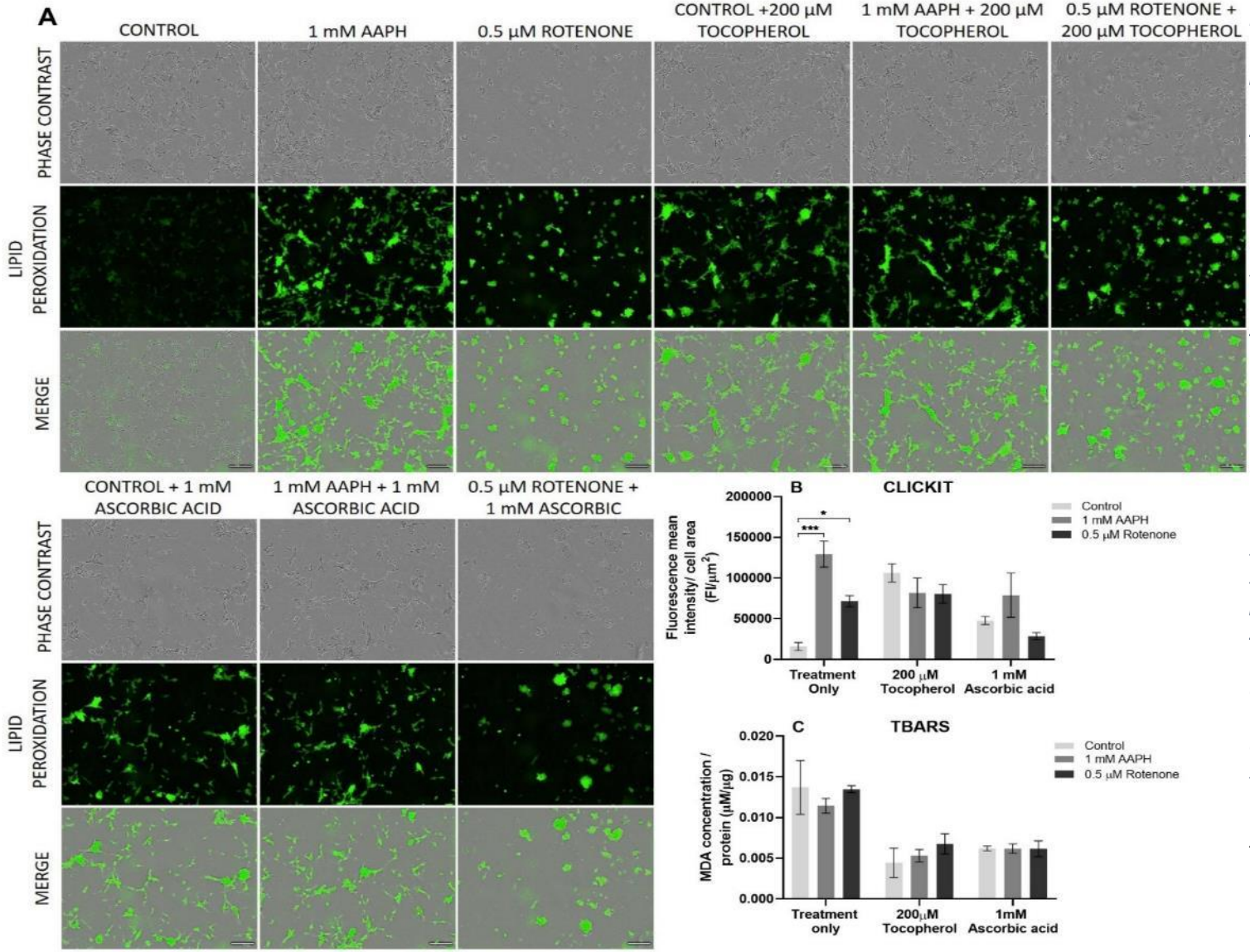

Figure 4.46 AAPH and rotenone increases lipid peroxidation in U-87MG glial cells. *(A) Lipid peroxidation fluorescent levels (green) for glial cells treated with AAPH and rotenone with and without 200 µM α-tocopherol or 1 mM ascorbic acid using Click-IT assay kit. Images taken using incucyte S3 live-cell analysis system. Scale bar = 200 µm. (B) Endpoint measurement of fluorescence was quantified using the incucyte S3 live-cell analysis system (Fluorescent intensity/cell area ± SEM). (C) Malondialdehyde levels (MDA), a by-product of lipid peroxidation were measured using a thiobarbituric acid reactive substances (TBARS) assay kit. Statistical analysis was performed using two-way ANOVA with Dunnett's post-hoc test relative to the control of each condition where n=3 for Click-iT but n=2 for TBARS experiments. Statistical significance was recorded as *p<0.05, **p<0.01 and ***p<0.001.*

Nitrosylation and carbonylation are other common markers of OS, which are propagated by different RS. Therefore, the biotin switch method of Jaffrey *et al.* was used to visualise S-nitrosylated proteins by fluorescent microscopy (Jaffrey et al., 2001). This method initially blocks free SH groups, then any S-NO bonds present are cleaved and substituted for a biotin group. The previously nitrosylated groups are then detected by tagging the biotin using and anti-biotin antibody that is fluorescently labelled for visualisation. Carbonylation levels were quantified by a colourimetric assay.

Differentiated SH-SY5Y neuronal cells showed higher levels of fluorescence when treated with AAPH or rotenone for 48-hours (figure 4.47A), suggesting greater levels of nitrosylation. This fluorescence was attenuated when SH-SY5Y neuronal cells were concurrently treated with antioxidants α-tocopherol or ascorbic acid (figure 4.47B). In addition, differentiated SH-SY5Y carbonyl content was significantly greater for 48-hour exposure to AAPH or rotenone (figure 4.47C). Carbonyl levels were attenuated by α-tocopherol, but ascorbic acid was only successful in attenuating rotenone induced carbonylation.

U-87MG glial cells showed 48-hour AAPH or rotenone exposure significantly increased fluorescence levels (figure 4.48A), suggesting increased nitrosylation that was attenuated by both antioxidants α-tocopherol and ascorbic acid (figure 4.49B). Whilst rotenone significantly increased carbonyl levels in U-87MG cells, AAPH showed no significant change (figure 4.48C). Both antioxidants successfully attenuated rotenone induced carbonyl levels.

Together, these results suggest AAPH and rotenone result in different PTM's dependent on the neural cell type. For example, rotenone resulted in more significant changes in nitrosylation levels in neuronal cells relative to glial cells. Whereas while AAPH and rotenone increase carbonyl levels in neuronal cells AAPH did not affect glial carbonyl levels. This highlights how specific RS affect downstream processes in cells and due to different cell characteristics responses between cells vary.

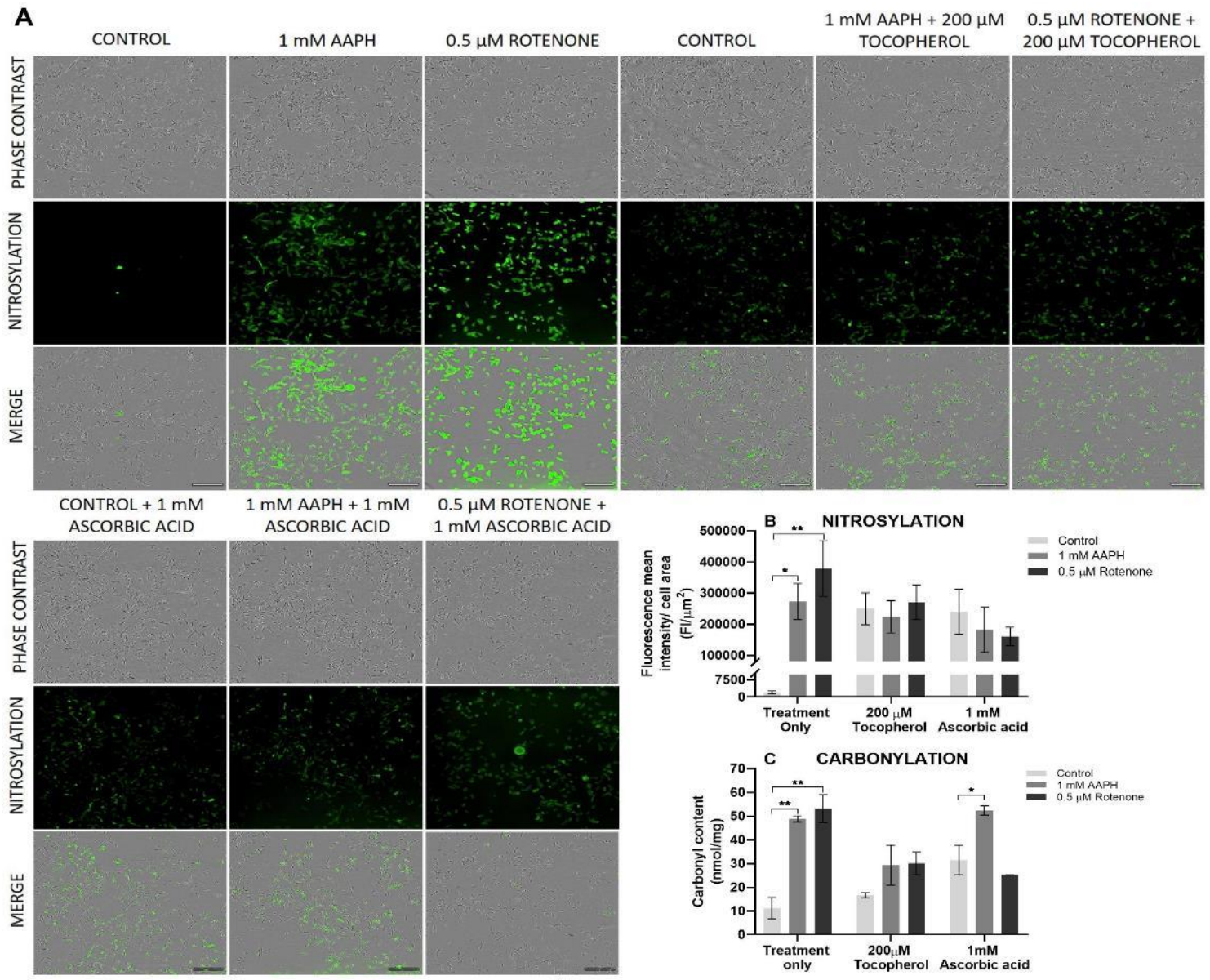

Figure 4.47 AAPH and rotenone increases post-translational modifications in neuronal cells. *(A) Nitrosylation fluorescent levels (green) for neuronal cells treated with AAPH and rotenone, with and without 200 µM α-tocopherol or 1 mM ascorbic acid using S-nitrosylation protein detection kit. Images taken using incucyte S3 live-cell analysis system. Scale bar = 200 µm. (B) Endpoint measurement of fluorescence was quantified using the incucyte S3 live-cell analysis system (Fluorescent intensity/cell area ± SEM). (C) Carbonylation levels were measured using a protein carbonyl colourimetric kit. Statistical analysis was performed using two-way ANOVA with Dunnett's post-hoc test relative to the control of each condition where n=3 for nitrosylation but n=2 for carbonylation experiments. Statistical significance was recorded as *p<0.05 and **p<0.01.*

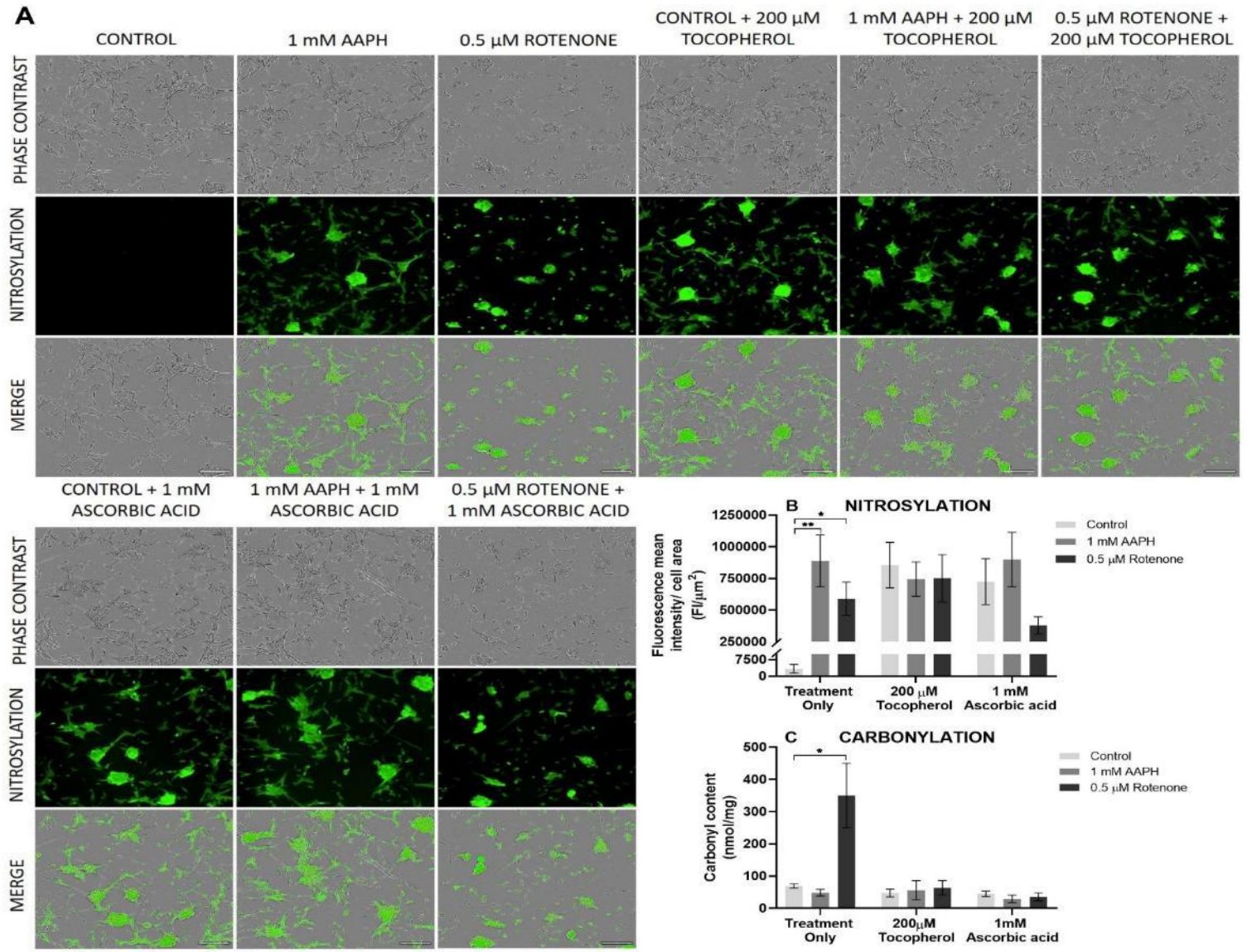

Figure 4.48 AAPH and rotenone increases post-translational modifications in glial cells. *(A) Nitrosylation fluorescent levels (green) for glial cells treated with AAPH and rotenone with and without 200 µM α-tocopherol or 1 mM ascorbic acid using S-nitrosylation protein detection kit. Images taken using incucyte S3 live-cell analysis system. Scale bar = 200 µm. (B) Endpoint measurement of fluorescence was quantified using the incucyte S3 live-cell analysis system (Fluorescent intensity/ cell area ± SEM). (C) Carbonylation levels were measured using a protein carbonyl colourimetric kit. Statistical analysis was performed using two-way ANOVA with Dunnett's post-hoc test relative to the control of each condition when n=3 for nitrosylation but n=2 for carbonylation experiments. Statistical significance was recorded as *p<0.05 and **p<0.01.*

4.3 DISCUSSION

To assess the response of neural cells in more *in vivo* like conditions we initially investigation differentiation methods. Morphological features of SH-SY5Y and U-87MG neural cell lines were assessed following reduced FBS and RA differentiation. Phase contrast images of FBS/RA differentiated SH-SY5Y cells showed neuronal soma were elongated, while neurite outgrowth increased creating an interconnected network consistent previous studies (Mario Encinas et al., 2002; Xicoy et al., 2017). However, our findings contravene some features described by Encinas *et al.*, as like Teppola *et al.* we found RA alone showed limited attenuation of SH-SY5Y cell proliferation (figure 4.2; Teppola et al., 2016). This is possibly due to the different cell types in the SH-SY5Y neuroblastoma cell line, which includes both S- and N-type cells (Xicoy et al., 2017). While N-type cells undergo morphological changes when differentiated with RA S-type cells remain unaffected and continue to proliferate (Mario Encinas et al., 2002). Encinas *et al.* also report how longer culture periods in the presence of BDNF enhance the N-type population. This is supported by findings herein that show upon RA removal and addition of BDNF cell proliferation was reduced (figure 4.5). RA initially induced NTrkB enabling N-type cells to become receptive to BDNF, which arrested them into G1 phase so they no longer proliferated (Mario Encinas et al., 2002). In addition to the arrest of cell proliferation, BDNF further improved neurite outgrowth like others who also demonstrated an improved neuronal phenotype and morphology (Constantinescu et al., 2007; de Medeiros et al., 2019; Mario Encinas et al., 2002).

While RA and subsequent BDNF is a universally accepted protocol for neuronal differentiation it is commonly known that astrocytes can aid neuronal survival, proliferation and differentiation (Kıray et al., 2016; Lin et al., 2016; Luo et al., 2017). In this study, we found U-87MG conditioned media improved neuronal survival and supported neurite outgrowth (figure 4.5). These results support others findings, where conditioned media from different glial cell lines enhanced neuronal survival and differntiation (Engele et al., 1991; Lo Furno et al., 2018). This may be due to U-87MG glial cells secreting neurotrophic factors such as BDNF (Fornaro et al., 2020; Liu et al., 2012), as upon addition of BDNF to SH-SY5Y cells with and without U-87MG conditioned media similar levels of proliferation and neurite outgrowth were observed. However, further work is needed to determine the factors secreted by U-87MG cells and how these influence SH-SY5Y neuronal differentiation.

While FBS/RA differentiation enhanced SH-SY5Y neuronal morphology and altered U-87MG proliferation, we also found that markers of differentiation were expressed. Differentiated SH-SY5Y neuronal cells expressed βIII tubulin, which is almost exclusively expressed by neurons and is

commonly used as a marker for differentiation (Katsetos et al., 2003). Synaptophysin expression was also evident suggesting mature neurite development (Cheung et al., 2009; Kumar et al., 2018). While differentiated U-87MG glial cells expressed GFAP and S100, common astrocytic markers (Das et al., 2009; Grundmann et al., 2019; Karmakar et al., 2008). Therefore, FBS/RA enhanced SH-SY5Y and U-87MG differentiation and thus, was used for subsequent experiments while select investigations were conducted with BDNF and U-87MG conditioned media due to cost and difficulty in obtaining large quantities of conditioned media.

In addition to morphological changes, we also investigated changes to bioenergetics as these would play a role in the response to OS. Herein, we found that RA induced differentiation altered the source of ATP in both SH-SY5Y neuronal and U-87MG glial cells. Differentiation of these neural cells resulted in ATP production shifting from glycolysis to OXPHOS, highlighting how undifferentiated cells rely more on glycolysis for cell division supporting the Warburg hypothesis (Kaczanowski et al., 2018; Warburg, 1956, 2010). From qRT-PCR studies, no increase in total mitochondrial number was seen between mitotic and differentiated cells (figure 4.7). This suggests the increase in ATP production from OXPHOS is not due to a greater quantity of mitochondria but due to a change in activity, consistent with other studies as Schneider *et al.* report RA induced differentiation altered SH-SY5Y mitochondrial function (Schneider et al., 2011). Additionally, mitochondrial membrane potential, cytochrome C oxidase and mitochondrial reserve capacity increased as a result of differentiation (Schneider et al., 2011; Xun et al., 2012). Primary neurons also demonstrate higher mitochondrial reserve capacity than mitotic neurons (Gerencser et al., 2009). This change may be as a result of differentiated cells no longer proliferating, and as such are more vulnerable to mitochondrial dysfunction as cells cannot divide, remove or dissipate damaged components. This would be especially detrimental for neurons as they possess lower levels of antioxidants than other neural cells such as glia. As a result, mitochondria may change their capacity upon differentiation to ensure they are not as susceptible to damage and therefore reduce cell vulnerability.

These changes in mitochondria may explain the susceptibility of differentiated SH-SY5Y neuronal cells to AAPH and rotenone. In this study, differentiated SH-SY5Y cells showed a dose-dependent decrease in cell viability when exposed to AAPH or rotenone, but AAPH had a more significant effect. In contrast, differentiated cells appeared to have a greater resistance to rotenone than their mitotic counterparts (figure 3.22-3.23 and 3.26-3.27). This is possibly due to differentiation increasing OXPHOS capacity and as a result differentiated SH-SY5Y cells have greater resistance to rotenone induced RS (Schneider et al., 2011; Xun et al., 2012). However, differentiation appeared to increase susceptibility to AAPH, possibly due to previous Seahorse

investigations suggesting AAPH resulted in greater glycolysis (figure 3.29) and thus, because differentiated cells rely more on OXPHOS for ATP, they fail to cope with the changes induced by AAPH. This is supported by Dodson *et al.* who show that inhibition of glycolysis increases apoptosis induced by 4-hydroxynonenal, a well-known lipid peroxidation product produced during OS (Dodson et al., 2013). Interestingly, differentiated U-87MG glial cells treated with 1 mM AAPH exhibited proliferation whilst 5 mM resulted in decreased cell viability contrary to previous mitotic findings. This suggests certain levels of AAPH are beneficial for astrocytes, possibly causing an acute anti-inflammatory response while high levels of RS result in cell death similar to chronic inflammation (Amor et al., 2014; Koudriavtseva and Mainero, 2016).

Further differentiation with BDNF appeared to have to opposite effect, where differentiated SH-SY5Y cells were more susceptible to rotenone but less to AAPH. This raises questions as to what changes differentiation induces. This is also highlighted when concurrent differentiation with U-87MG conditioned media improved resistance to these OS inducers. This suggests different differentiation methods may result in different biochemical changes and susceptibilities to specific RS. This may explain the controversies in the literature as to whether differentiation results in SH-SY5Y cells becoming more or less susceptible to different RS inducing toxins. More investigations into what changes each differentiation protocol generates are needed to understand why the observed changes are seen. Furthermore, these models need to be compared to more *in vivo* like conditions to generate a better *in vitro* model for high-throughput experiments with lower costs.

To compare clonal cell responses with primary cell responses, rat embryonic primary cortical neurons were exposed to AAPH and rotenone. One of the major neuronal morphological features of differentiation is the formation of axons. Axonal pathology has been implicated to precede cell body loss in neurodegenerative diseases such as Parkinson's, Alzheimer's and Huntington's disease (Coleman, 2013; De Vos et al., 2008; Tagliaferro and Burke, 2016). Multiple methods of axonal degeneration have been described (Salvadores et al., 2017; Wang et al., 2012). Herein, we observed a greater sensitivity with primary neurons to AAPH and rotenone alongside a decrease in neurite length for both stressors (Nesti et al., 2011; Virga et al., 2018). In addition, we observed two distinct methods of axonal degeneration induced by different RS inducers: fragmentation and retraction.

AAPH, a peroxyl radical generator resulted in fragmentation where processes appear to collapse compacting around areas of cytoplasm, which results in axons exhibiting a 'beads on a string appearance' (figure 4.19-4.20). This process was rapid, where fragmentation occurred within

4-6 hours of treatment progressing towards the cell soma in a retrograde manner. Whereas rotenone treatment appeared to result in process retraction, highlighted by Sholl analysis that occurred over a longer time period. Furthermore, fragmentation was quickly followed by cell death, whereas higher viability was observed with cells that exhibited retraction. These different timeframes and associated cell death with these unique degeneration methods suggests different molecular mechanisms underlie these changes.

The observed fragmentation with AAPH is similar to local axon and Wallerian degeneration, which is characterised by restricted granular disintegration of axons. Wallerian degeneration usually follows transection of axons resulting in axon fragmentation distal to the injury site (Coleman and Höke, 2020; Thomas, 1964). Similar fragmentation has been observed in both Parkinson's and Huntington's disease (Adalbert and Coleman, 2013). As our model did not involve axonal transection it is more likely these observations are due to local axon degeneration. Axons initially swelled before fragmenting, which has been observed in mammals where axons degrade in a synchronous manner *in vivo,* followed by glial cells removing this debris (Kneynsberg et al., 2016; Saxena and Caroni, 2007). This method of degeneration is thought to help remove longer axons while retraction is preferential for shorter axons as this is a more efficient use of energy (Blanquie and Bradke, 2018; Portera-Cailliau et al., 2005).

It is suggested that in order to survive neurons attempt to conserve energy and thus retract excessive or injured neurites (Blanquie and Bradke, 2018; Raff, 2002). This is consistent with previous studies alongside ours that show rotenone results in decreased ATP levels, and as a result neurons may retract neurites to conserve energy (Berbusse et al., 2016; Denton et al., 2018; Persson et al., 2013; Press and Milbrandt, 2008). However, others contravene this as treatment with Nicotinamide nucleotide adenylyltransferase 1 (Nmnat1) prevents neurite retraction and changes in ATP levels (Virga et al., 2018). Alternatively, RS produced by rotenone may play a role in neurite length as nitric oxide has been implicated in axonal retraction (He et al., 2002; Stroissnigg et al., 2007) and Nmnat1 is suggested to decrease OS induced by rotenone (Press and Milbrandt, 2008), which is also supported by antioxidants attenuating motor nerve degeneration (Hall, 1987). Furthermore, retraction may also allow recovery of subcellular components of neurites to aid cell survival. This is supported by Öztürk *et al.* who demonstrate retracted neurites allowed regeneration of other neurites (Öztürk et al., 2013).

Synaptophysin, a marker of presynaptic membrane protein is associated with recycling vesicles essential for neurotransmission and co-localises with axon terminals (Daly et al., 2000; Nithianantharajah, 2004; Riemann et al., 2018). In neurodegenerative conditions such as AD and

PD loss of synapses is observed (Henstridge et al., 2019; Schulz-Schaeffer, 2010). AAPH resulted in decreased synaptophysin expression whilst rotenone increased expression. The increased synaptophysin puncta along processes and in the cell soma of rotenone treated neurons may possibly be due to retraction. Retraction possibly results in vesicles transporting the cellular contents of the neurites back to the soma to be used elsewhere, as others have demonstrated transport between sister branches potentially aiding neurite regrowth (Nakata et al., 1998). This is supported by others who have observed increased localisation of synaptophysin within the cell soma following rotenone treatment, suggesting vesicle accumulation (Jiang et al., 2006; Ren and Feng, 2007). Furthermore, due to retraction axon terminals are closer together and thus, appear to be more abundant in neuronal processes as rotenone concentration increases. Together these results suggest AAPH and rotenone result in different axonal morphological changes. To determine if these effects are due to RS different concentrations of antioxidants in primary neurons need to be investigated to see if these changes can be attenuated.

Unfortunately, our differentiation models for SH-SY5Y cells with BDNF, or in combination with U-87MG conditioned media did not display significant neurite branching. Whilst it showed a decrease in neurite length, it did not display the morphological changes that were observed with primary neurons. This is possibly due to the models not developing fully formed axons and therefore shows the limitations of the differentiated models.

Neuroinflammation is another key feature of neurodegeneration that can effect neuronal viability (Segura-Aguilar et al., 2014). The results herein propose specific RS play a role in astrogliosis as AAPH increased process length while rotenone induced RS did not, both of which were attenuated by the antioxidant α-tocopherol. Others propose RS play a role in astrogliosis a common feature of neuroinflammation (Ferrer, 2017; Hirsch and Hunot, 2009; Teismann and Schulz, 2004). Together, these results suggest RS effect morphological feature of both neurons and astrocytes, where specific RS elicit different responses.

With morphological and viability changes induced by AAPH and rotenone it was not surprising to see changes in the OS gene profile. As expected, basal profiles of differentiated SH-SY5Y neuronal and U-87MG glial cells showed differences. Controversial to the literature we found that glutathione gene expression was lower in U-87MG relative to SH-SY5Y neuronal cells (Dringen and Hamprecht, 1997). However, while this study (figure 3.7) and many others suggest astrocytes possess greater levels of glutathione than neurons, none have investigated the effect of RA differentiation on U-87MG. There is increasing evidence that redox homeostasis and thus levels of antioxidants such as glutathione are important during this processes (Esposito et al., 2004; Paul D.

Ray et al., 2012; Sciarretta et al., 2019). In other cell lines such as HL-60 glutathione levels vary during differentiation where inhibition of glutathione increased differentiation (Krance et al., 2010). Furthermore, Xia *et al.* show RA differentiation in human carcinoma cells resulted in decreased glutathione S-transferase (Xia et al., 1993), which was also lower in our differentiated U-87MG glial cells relative to SH-SY5Y neuronal cells. Therefore, the lower glutathione gene expression in differentiated U-87MG glial cells may be due to RA induced differentiation.

Upon further examination some of the genes downregulated in differentiated U-87MG glial cells relative to differentiated SH-SY5Y neuronal cells appear to be localised to the mitochondria such as PRDX3 (De Armas et al., 2019; Drechsel and Patel, 2010), BNIP3 (Bellot et al., 2009; Glick et al., 2012), GPX3 (Kritsiligkou et al., 2017) and GSTP1 (Goto et al., 2009). Although some mitochondrial genes are upregulated relative to SH-SY5Y neuronal cells such as SOD2 (Gomez and Germain, 2019; Zelko et al., 2002) and GSTZ1 (Li et al., 2011), the majority are cytosolic. The lower expression of mitochondrial localised genes in U-87MG glial cells relative to SH-SY5Y neuronal cells may be due to glia having lower levels of mitochondria than neurons, which we have shown with qRT-PCR and others support, reporting a greater rate of glycolysis in astrocytes (Hertz et al., 2007). Whereas neurons rely almost exclusively on OXPHOS for their energy (Franco-Iborra et al., 2016). Therefore, as neurons have more mitochondria and rely on them more to meet their energy demand, they may have higher antioxidant gene expression to counteract susceptibility to RS that would diminish cellular function. In contrast, as glia rely more on glycolysis for their energy they prioritise antioxidants in the cytosol where glycolysis could be affected by RS.

RS generated by AAPH in differentiated SH-SY5Y neuronal cells resulted in upregulation of a variety of genes including those involved in glutathione synthesis, superoxide dismutation, and reducing oxidised enzymes (Dasuri et al., 2013; Gandhi and Abramov, 2012; Poole et al., 2011b; Turner-Ivey et al., 2013). Therefore, AAPH treated neurons exhibited upregulation of some antioxidant response genes to detoxify RS by increasing the amount of relative antioxidant enzymes (Korovila et al., 2017; Kwak et al., 2003). In contrast, many OS related genes were downregulated in rotenone treated neurons. This difference in response induced by these stressors may be due to the treatment timeframe, as viability assays showed at 48-hours rotenone treated SH-SY5Y cell death had plateaued while AAPH treated cell viability was still declining (figure 4.9). As rotenone viability had plateaued antioxidant systems may have already been switched off whereas AAPH treated cells are still dying and as a result, the OS response is still actively combatting this.

Whereas AAPH and rotenone treatment resulted in similar gene expression profiles in differentiated U-87MG glial cells. Antioxidant genes such as glutathione related genes (Dringen et

al., 2000), GPX's (Dasuri et al., 2013; Gandhi and Abramov, 2012), and PRDX's (Fisher, 2011) were upregulated to combat RS. Interestingly different isoforms of SOD appeared to be affected by AAPH or rotenone treatment as SOD1 was upregulated for both treatments, but SOD2 was only upregulated by rotenone. This is possibly due to difference in localisation of SOD1 (cytosolic) and SOD2 (mitochondrial; Dasuri et al., 2013, Y. Wang et al., 2018). As rotenone inhibits mitochondria and thus generates RS in its vicinity it is possible glia upregulate the mitochondrial isoform to combat superoxide generated (L. Wang et al., 2015). In contrast, AAPH degrades in the cytosol and therefore the cytosolic isoform of SOD would be a more appropriate antioxidant (Bassett et al., 1999; Sanz, 2016; Werber et al., 2011). These investigations highlight the possibility of RS localisation affecting the antioxidant response.

Several neurodegenerative diseases are characterised by increased OS and activation of antioxidant related genes. This OS is observed in various neural cultures exposed to different toxins including rotenone (Fitzgerald et al., 2014; Sherer et al., 2003) and less so AAPH (Niki, 1990; Werber et al., 2011). To restore redox homeostasis neural cultures upregulate pathways involved in cytoprotective, antioxidant and anti-inflammation via signalling pathways such as NRF2-ARE (Schmidlin et al., 2019; Shih et al., 2005; Tufekci et al., 2011). Upon OS the NRF2-KEAP1 interaction is interrupted alleviating degradation and facilitating nuclear translocation (Dhakshinamoorthy and Jaiswal, 2001; Itoh et al., 1999; Suzuki and Yamamoto, 2015). In the nucleus, NRF2 binds the ARE upregulating antioxidant gene expression (Korovila et al., 2017; Kwak et al., 2003).

Here we show for the first time that AAPH like rotenone results in activation of the NRF2 pathway in both neurons and astrocytes, as shown by the change in viability upon NRF2 knockdown. Additionally, our results suggest rotenone also effects KEAP1 gene expression in glia possibly enhancing activation of the NRF2 pathway as Zagoura *et al.* have also recently reported (Zagoura et al., 2017). This is further supported by RT^2 profiler array results that showed AAPH resulted in a variety of genes downstream of NRF2 (Korovila et al., 2017) being upregulated upon treatment in both differentiated SH-SY5Y neuronal and U-87MG glial cells. Presumably, AAPH generates RS, which results in NRF2 activation followed by upregulation of antioxidant genes to protect cells against possible oxidative damage to DNA, lipids and proteins. While activation and upregulation of other genes such as TXN (Poole et al., 2011b; Turner-Ivey et al., 2013) and sulfiredoxin (Biteau et al., 2003; Jönsson et al., 2008; Rhee et al., 2007) allows these downstream proteins to be reduced and thus, recycled continuously to combat OS. Although the list of NRF2 genes appears to vary between neural cell types as well as different toxins, NRF2 appears to be critical for cellular defence in the brain (Schmidlin et al., 2019).

Other than changes to gene expression, AAPH and rotenone also induced changes in PTM's such as lipid peroxidation, carbonylation and S-nitrosylation. We propose herein that AAPH induces RS that result in greater lipid peroxidation than rotenone in both SH-SY5Y neuronal and U-87MG glial cells. Lipid peroxidation is frequently associated with decreased membrane fluidity and increased permeability supported by the greater LDH release exhibited with AAPH than rotenone (figure 4.11). Primary neuronal cultures treated with AAPH also demonstrated greater LDH release (figure 4.20), supporting AAPH increases membrane permeability more as compared to rotenone. In addition to lipid peroxidation, we show AAPH and rotenone also increased nitrosylation and carbonylation levels in differentiated SH-SY5Y neuronal cells. Interestingly, while AAPH and rotenone increased nitrosylation levels in U-87MG glial cells, only rotenone resulted in carbonylation levels increasing. This suggests AAPH and rotenone induce RS that result in different PTM's where carbonylation possibly contributes to rotenone induced glial cell death. However, more research is needed to confirm if carbonylation is a detrimental PTM, as the other PTM's are also present in AAPH treated glia that exhibited increased proliferation.

In conclusion, understanding what changes unique differentiation protocols induce not only morphologically but also biochemically is important for understanding changes in RS susceptibility. The differentiation models we used herein are limited in terms of neurite branching, making comparisons to primary neurons more difficult. While primary neurons are more sensitive to RS inducers AAPH and rotenone, they affect neuronal axon morphology differently suggesting alternate mechanisms of action. In addition to altering neural viability RS induce antioxidant gene expression dependent on both the stressor and neural cell type. Indeed, this is also true for PTM's where each toxin effects PTM levels uniquely, but the responses also depend on the neural cell type. Further investigations into the changes in gene expression and PTM's specific RS induced within neural cells is needed to aid in understanding neurodegeneration and develop novel therapies.

CHAPTER 5
REACTIVE SPECIES IN A CO-CULTURE

5.1 INTRODUCTION

5.1.1 *In vitro* co-culture methods

Understanding both intracellular and intercellular mechanisms are crucial for understanding the formation, maintenance and repair of biological tissues as well as the disease pathogenesis and how drugs impact these. Initial studies to investigate these problems involve studying monocultures (de Oliveira et al., 2017; Park et al., 2011). Monocultures attempt to simplify and understand complex interactions *in vitro* by reducing cellular interactions while altering the environment to predict specific cell type behaviour *in vivo*. However, they also have their disadvantages, including if the observed phenotype has physiological relevance as various cell-cell connections are not present (Renaud and Martinoli, 2016). Additionally, because there is only a single cell type contributing to the environment intercellular signals are limited affecting some cellular functions (Volterra and Meldolesi, 2005). Therefore, to get a more representative model of what interactions occur *in vitro* co-cultures are needed to mimic more complex pathway interactions.

Co-cultures consist of more than one cell type grown with some degree of interaction/contact, either physical or via secreted factors. There are two main *in vitro* methods for co-cultures summarised in figure 5.1 including: contact and non-contact co-cultures (Bogdanowicz and Lu, 2013).

The simplest contact co-culture comprises of a monolayer of multiple cell types (figure 5.1A; Wang *et al.*, 2007; Proffen *et al.*, 2013). These are produced by combining cell suspensions after determining a desired ratio prior to seeding (Jiang et al., 2005). This system allows heterotypic and homotypic communication that can be altered with the seeding density ratios. However, mixed co-cultures result in dilution effects while growth and metabolic rates differ between cell types making it difficult to discern the contribution of each cell type (Herrero-Mendez et al., 2009; Lovatt et al., 2007; Vilchez et al., 2007). Furthermore, as growth rates of cells differ there is no guarantee the starting ratio is maintained. Attempts to understand the contribution of each cell type requires separation techniques, which can adversely affect the results.

Alternatively, physical barriers can be used to regulate cell contact to prevent the need for separation. Dividers can be removed at any time allowing migration and controlled cell contact (figure 5.1B; Wang *et al.*, 2007). Physical barriers provide the advantage of control over heterotypic and homotypic interactions via control of physical contact and soluble factor interactions. However,

creating a seal between cellular compartments is challenging and soluble factor interactions depend critically on the barrier material (Delsing et al., 2018; Leddy et al., 2004).

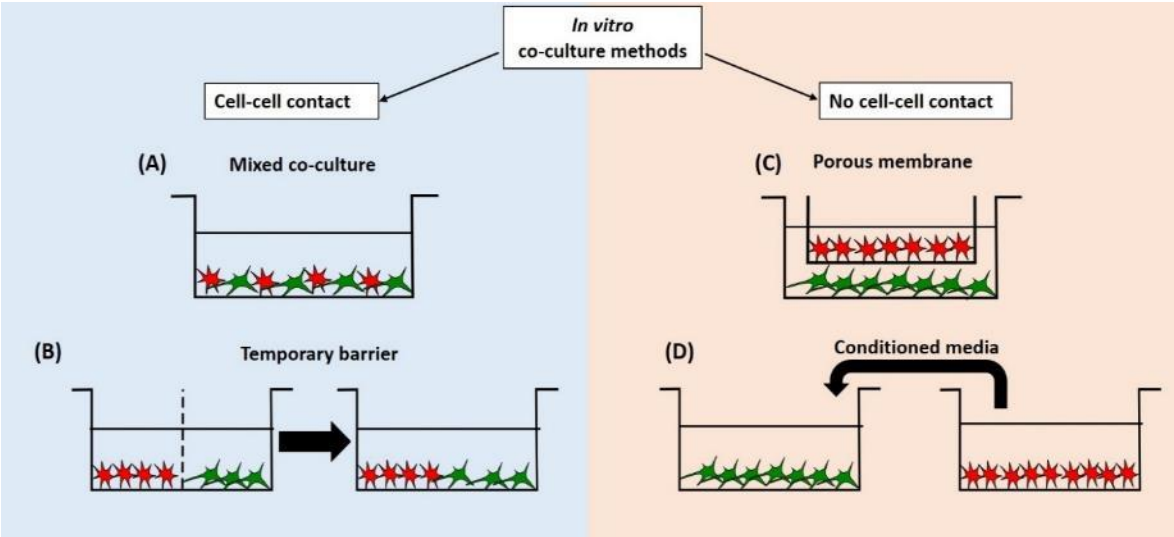

Figure 5.1 Schematic representation of different methods of co-cultures to investigate cell-cell interactions. *(A) Simplest co-culture consists of a full contact mixed co-culture. (B) Cell contact, and secreted factor affects can be controlled by a temporary barrier. (C) Insert co-culture system where the upper compartment consists of one cell type grown on an insert while the lower compartment consists of a well with the second cell type. The insert is designed to lie above the lower compartment so there is no cell-cell contact but the porous membrane allows bidirectional diffusion of secreted factors. (D) Unidirectional signalling of secreted factors can be investigated using conditioned media from one cell type on the other. Adapted from* Bogdanowicz and Lu, 2013.

While maintaining bidirectional signalling inserts allow individual cell lines to be grown separately and then co-cultured later in the same environment (figure 5.1C). The separation of specific types of cells allows investigations into the response of each subpopulation. However, physical contact between individual cell lines cannot be permanently prevented, and multistage seeding can provide its own difficulties. One such difficulty includes preventing cell-cell contact while being close enough to allow short- and long-lived factors to reach the other culture. Cell membrane inserts have presented a way to provide more reproducible models (Grobstein, 1953). Studies into inflammation in the CNS between glia and neurons has greatly benefited from inserts allowing bi-directional signalling in the absence of cell-cell contact and studying soluble factors (Bournival et al., 2012; Zhu et al., 2014). Furthermore, soluble factors have also been implicated in differentiation (Abouelfetouh et al., 2004; Pyka et al., 2011; Yu et al., 2016). Additionally, inserts have supported investigations into the protective effects of secreted factors from glia on neurons (Du et al., 2018; Roqué et al., 2016; ZHU et al., 2014).

Inserts can be made of various materials including polyester (PET), polycarbonate or collagen coated polytetrafluoroethylene with differing pore sizes. Over the last decade the importance of cellular mechanosensitivity has arisen as materials have been found to affect cellular functions including differentiation, growth, survival, motility, adhesion and contractility (Spencer et al., 2017; Wells, 2008). Cells usually require adhesion for survival through focal adhesion points, primarily using integrins that vary from cell-to-cell (Discher, 2005; Moeton et al., 2016). Young's modulus usually measured in pascals (Pa), is a common term used to determine resistance to deformation and thus, can be used to describe how hard a material is. Brains exhibit modulus in the magnitude of several hundred pascals whereas muscles demonstrate moduli of 12 kPa (Engler et al., 2004; Georges et al., 2006; Levental et al., 2007; Wellman et al., 2018). In contrast, plastics such as polystyrene and polyethylene terephthalate (PET), commonly used for tissue culture plastic and inserts exhibit a Young's modulus of 3.2 (Sultanova et al., 2009) and 1.7 (Li et al., 2001) GPa, respectively demonstrating the non-physiological mechanical environment employed in tissue culture.

The importance of the environment is further highlighted with different cell types within tissues showing a morphological dependence on substrate stiffness (Aregueta-Robles et al., 2019; Georges et al., 2006; Yeung et al., 2005). Even neuronal cells demonstrate a preference where dorsal root ganglion and motor neurons from the spine show increased neurite length and branching on soft materials (Balgude et al., 2001; Flanagan et al., 2002; Lantoine et al., 2016). Using hydrogels Georges *et al.* demonstrate astrocytes on soft surfaces show small rounded morphology while on harder surfaces they have a reactive morphology with highly extended processes; supported by greater F-actin staining and stress fibre expression on harder surfaces, which is absent on soft surfaces (Georges et al., 2006). In contrast, neurons showed branching and neurite growth on both soft and hard surfaces which was significantly greater on soft hydrogels consistent with previous findings that soft substrates enhance neurite branching (Balgude et al., 2001; Flanagan et al., 2002). As such, different materials can result in another variable being added to the system when using inserts and thus, needs to be considered when culturing different cell types together (Li et al., 2017).

Alternatively, conditioned media can be used to mimic parameters of a co-culture system. For example, conditioned media can be used to explore intercellular communication where cultured media from one cell type is introduced to the other without the direct culture of both cells together, preventing the need for a seal between different cell compartments (figure 5.1D; Saeed *et al.*, 2015). This provides a simpler strategy for identifying secreted factors and their effects. However, this produces its own challenges including nutrient deficiency and difficulty reproducing

optimal concentrations as well as temporal distribution of secreted factors (Lamarche et al., 2004). Furthermore, short-lived molecules are degraded over time limiting their identification and characterisation of their effects. Finally, only unidirectional signalling can take place as the other cell is not present, preventing feedback loops observed *in vivo* demonstrating the limitations of this method.

5.1.2 Glia in neuroprotection and neurotoxicity

While neurons have been the focus of neurodegenerative research due to their loss in various neurodegenerative diseases, glia are becoming key in solving possible underlying mechanisms. Glia, the most abundant cells within the brain can be separated into 3 types; oligodendrocytes, microglia and astrocytes, which are the most populous (Herculano-Houzel, 2009; Rasband, 2016; Verkhratsky et al., 2012). Microglia and astrocytes seem to play a role in neurodegeneration for example, microglia are primarily associated with neuroinflammation (Barcia et al., 2004; Piirainen et al., 2017). Whereas astrocytes undergo astrogliosis following neuronal death and inflammation (Colombo and Farina, 2016; Hirsch and Hunot, 2009; Teismann and Schulz, 2004). Astrocytes have also been found to provide neuroprotection, particularly against OS, by producing detoxifying enzymes including ascorbic acid, glutathione and its precursors (Allaman et al., 2011; Thorne et al., 2016; Vargas and Johnson, 2009), in addition to neurotrophic factors such as GNDF and BDNF (Skaper and Facci, 2018).

To determine the effect of astrocytes on neuron viability, investigations have utilised astrocyte rich and poor conditions (Desagher et al., 1996; Gritsenko et al., 2017; Lucius and Sievers, 1996). Several studies have highlighted the importance of astrocytic glutathione content in neuronal protection (Chen et al., 2001; Drukarch et al., 1998; McBean, 2017). The importance of astrocytic glutathione is further supported by their incubation with the gamma-glutamylcysteine synthetase inhibitor, buthionine sulfoximine. This reduces their ability to prevent neuronal death (Griffith and Meister, 1979). Indeed, astrocytes are reported to have greater levels of glutathione than neuronal cells (Makar et al., 2008; McBean, 2017) and thus, thought to be a key enzyme in reducing OS in neurons, in particular nitric oxide (Clancy et al., 1994; Hogg et al., 1996; Moriyama et al., 2016). Nitric oxide can damage cells by reacting with protein thiol groups and protein iron complexes leading to neuronal death and contributing to neurodegeneration (Dawson and Dawson, 2018; Moncada and Bolanos, 2006; Shukla, 2007). However, high levels of nitric oxide result in cellular glutathione being quickly oxidised resulting in cells losing this defence (Clancy et al., 1994; Padgett and Whorton, 1998).

In addition, to removing nitric oxide directly astrocytes may aid in reducing OS via oxidised vitamin C (also referred to as dehydroascorbic acid), which can be taken up by astrocytes, reduced back to ascorbate at the expense of glutathione and ascorbate is then released back into the extracellular fluid for neurons to utilise (Moretti et al., 2017; Wilson, 1997). While neurons cannot take up glutathione directly, astrocytes can secrete glutathione leading to its subsequent breakdown into γ-glutamyl and cysteinyl glycine via γ-glutamyl transferase. This is further broken down by ectopeptidases leading to cystine and glycine that can be taken up by neurons providing them with precursors for glutathione synthesis (Baxter and Hardingham, 2016; Dringen et al., 1999; Kranich et al., 1998). Additionally, glutathione synthesising enzyme glutamate cysteine ligase is controlled by NRF2, which is shown to have greater levels in astrocytes than neurons (Dowell and Johnson, 2013; Jimenez-Blasco et al., 2015; Lee et al., 2003a). Therefore, glutathione appears to play a critical role in neuroprotection.

5.1.3 Glial secretome

Astrocytes are no longer viewed to only have passive involvement in neuronal support but also play essential roles in neuronal development, extracellular maintenance and inflammatory responses and thus, it is important to investigate neuron-glial crosstalk. Furthermore, emerging evidence suggests astrocytes are secretory cells within the CNS (Verkhratsky et al., 2016). Currently, mass spectrometry-based proteomics has been employed to investigate both intracellular and secreted proteins within astrocytes (Delcourt et al., 2005; Samy et al., 2018; Yang et al., 2005). Astrocytes can secrete protective or neurotoxic proteins following injury or during diseased states. These can be detrimental via neuroinflammatory mediators or beneficial, where secreted neurotrophic factors can initiate repair processes, axon regeneration, angiogenesis and neural circuitry rewiring. Some secreted factors are believed to participate in neurodegenerative pathology (reviewed in Jha et al., 2018).

Over the last decade secretome analysis has become more in-depth with mass spectrometry and bioinformatic tools allowing insights into astrocyte status, function and possible diagnostic/prognostic agent identification for CNS diseases (Jha et al., 2013; Kim et al., 2020). The first secretome analysis involved primary astrocytes under proinflammatory conditions. This showed only a few protein identities (<40) to generate a network (Lafon-Cazal et al., 2003). Later, mass spectrometry with astrocytes of CD-1 mice with labelled amino acid isotopes allowed the identification of 516 secreted proteins, where some possessed the N-terminal signal for secretion such as apoE, SPARC and cathepsins while others did not, including vimentin: ferritins and histones (Greco et al., 2010). Han *et al.* identified over 6000 proteins from conditioned media from murine

astrocyte cultures using a combination of two-step digestion, filter-aided sample preparation, StageTip-based high pH fractionation, and high-resolution mass spectrometry (Han et al., 2014). Most secretome studies have used rodent models (Greco et al., 2010; Keene et al., 2009; Moore et al., 2009; Yin et al., 2012) but RNA sequencing analysis revealed human astrocytes differ from murine astrocytes (Kim et al., 2020; Y. Zhang et al., 2016). While samples from both healthy and neurodegenerative patients would be ideal to characterise secreted factors and possible biomarkers, this is challenging and thus the use of human clonal cell lines may provide a reproducible profile.

A recent systematic review by Jha *et al.* proposed the major functions of secreted factors including: regulation of the extracellular matrix (ECM), neuron regulation and homeostasis (Jha et al., 2018). Where regulation of the ECM involves cell adhesion, migration, metalloprotease activity, cell growth, synaptogenesis, neuronal differentiation and axonal guidance. Neuronal regulation and homeostasis include ion homeostasis, morphogenesis, redox homeostasis as well as cell growth, cell death and neuroinflammation.

Within the CNS oxidants are implicated in axonal damage, including degeneration, swelling and incomplete regeneration, where cytoskeletal alterations are believed to be an early event in cell death (Bellomo and Mirabelli, 1992; Compagnucci et al., 2016). Cytoskeleton filaments are important for cell shape, determining polarity, facilitating movement and membrane organization where the cytoskeletons is composed of 3 majors filaments including microfilaments such as actin, microtubules including tubulin and intermediate filaments for example vimentin (Allani et al., 2004). While not fully understood in neuronal cells, OS plays a role in cytoskeletal protein changes such as vimentin, tubulin and filamin A (Fratelli et al., 2002; Neely et al., 2002; Pierozan et al., 2017; Zhang et al., 2014). Additionally, lipid peroxidation product 4-HNE disrupted microtubules and modified tubulin inhibiting neurite outgrowth in N2a neuroblastoma cells (Neely et al., 2002). In PC12 cells tubulin depolymerization was observed under oxidative insult followed by cell death (Hinshaw et al., 1993). Furthermore, hippocampal neuronal cells showed OS altered vimentin (Choi et al., 2003). Thus, while not fully understood, together these studies suggest cytoskeletal proteins within the ECM appear to be altered in diseases.

Fibronectin alongside glycosaminoglycans and proteoglycans are secreted and accumulate in the ECM, regulating matrix organization (Hynes, 2009; Oláh et al., 2009). Fibronectin is produced and secreted by astrocytes and endothelial cells, which is subsequently assembled in the ECM (Rieske et al., 2009). While fibronectin interacts with integrins playing a critical role in adhesion, it is also important in extrasynaptic transmission (Andrews et al., 2018; Wang et al., 2013). This

process involves bidirectional communication where molecules diffuse through the ECM modulating neuronal activity (Araque, 2008). Whilst dopamine is transported through channels, it can also be delivered via diffusion through the ECM (Rice et al., 2011). Thus levels of fibronectin can affect the ECM and the diffusion of dopamine thereby disrupting intercellular signalling during aging (Allani et al., 2004; Brodski et al., 2019). This is supported by downregulated expression of fibronectin in the elderly effecting dopamine transmission (Fuxe et al., 2006; Syková, 2001). Furthermore, extrinsic administration of fibronectin protects against PD development (Fuxe et al., 2006; Hall et al., 2016; Nowak et al., 2006), suggesting its neuroprotective ability. This is supported by its anti-inflammatory properties highlighting the importance of the ECM (Lin et al., 2012; Tsuda et al., 2008).

Metalloproteinases are involved in the degradation of the ECM (Levin et al., 2017), where disruption of the ECM occurs during disease (Chaturvedi and Kaczmarek, 2014; Lau et al., 2013). Additionally, metalloproteinases also stimulate proinflammatory mediators such as chemokines (Gómez-Piña et al., 2012; Rosenberg, 2002). OS, thrombin and TNF-α can induce astrocytic metalloproteinases (Gottschall and Deb, 1996; Gottschall and Yu, 2002). Under normal conditions metalloproteinases are suppressed by metalloproteinase inhibitors preventing neuronal degeneration (Brkic et al., 2015; Cunningham et al., 2005; Sadeghian et al., 2012).

While the ECM can affect neuronal morphology and degeneration secreted proteins can also influence neurons. Wingless-type mouse mammary tumour proto-oncogene integration protein (WNT), is secreted by astrocytes and is involved in various signalling pathways including neurogenesis, neuronal survival, axonal extension, synapse formation and dopaminergic neuronal plasticity (Ciani and Salinas, 2005; F. L'Episcopo et al., 2011; Maiese et al., 2008; Marchetti et al., 2013). WNT ligands bind to the transmembrane receptor of the frizzled family leading to stabilisation of β-catenin, which binds to transcription activators leading to upregulation of genes involved in growth, development, adhesion and synapse dynamics (Gordon and Nusse, 2006; Taylor et al., 2013; Valenta et al., 2012). If WNT is absent, β-catenin is phosphorylated by glycogen synthase kinase-3β (GSK-3β) targeting β-catenin for ubiquitination and degradation by the proteasome (Aberle et al., 1997; Gordon and Nusse, 2006). Leucine rich repeat 2 (LRRK) encoded by PARK8 is proposed to have a role in canonical WNT signalling, as LRRK2 mutations are shown to reduce WNT signalling, suggesting WNT may be involved in PD pathogenesis (Berwick and Harvey, 2012). Frizzled receptor localisation reinforces WNT's role in neuronal morphology as receptors are localised to growth cones of regenerating neurons, playing a role in pre-synaptic differentiation and hippocampal neurons function (Chacón et al., 2008; Toledo et al., 2008). The importance in PD is also highlighted as 6-OHDA, rotenone and MPTP/MPP^+ induced neuronal apoptosis via GSK-3β in

SH-SY5Y, PC12 cell and primary mesencephalic neurons suggesting the importance of upstream WNT (Chen et al., 2004; Petit-Paitel et al., 2009; W. Wang et al., 2007). This is supported by siRNA studies of WNT in astrocytes, which resulted in decreased tyrosine hydroxylase positive neuron survival following 6-OHDA and MPP^+ treatment in co-cultures (L'Episcopo et al., 2011). Together, these studies suggest secreted factors from astrocytes also affect the ECM contributing to neurodegenerative process.

While astrocyte secretomes regulate the ECM and neuronal morphology they also coordinate neuronal homeostasis through heat shock proteins such as HSP70 and HSP90 (Lackie et al., 2017; Verkhratsky et al., 2016). HSP70 is an exosomal protein (Kowal et al., 2016) that regulates protein folding and is upregulated in various neurodegenerative diseases (reviewed in Turturici et al., 2011). Cells can secrete HSP70 into the extracellular space via exosomes. Extracellular HSP70 is reported to play a role in neuroprotection during aging (Houenou et al., 1996; Posimo et al., 2015). Recently, treatment of N2A neuronal cells with HSP70 attenuated amyloid-β peptide oligomerization, suggesting extracellular HSP70 may help prevent protein aggregation providing neuroprotection (Rivera et al., 2018).

Stressed glia can also secrete antioxidants as an initial neuroprotective strategy. These include peroxiredoxins, thioredoxins and extracellular SOD (Cásedas et al., 2019; Cruz-Garcia et al., 2019; Sandhu et al., 2009). Under chronic stress, glia become enlarged and overactive leading to cytokine and chemokine secretion resulting in neuroinflammation; characteristics observed in neurodegenerative diseases (Jung et al., 2020; Mena and García de Yébenes, 2008; Tambuyzer et al., 2009). Animal models treated with MPTP, 6-OHDA and rotenone exhibit glial activation prior to neuronal death (Bjarkam et al., 2008; Grünblatt et al., 2000; Meredith et al., 2008; Schneider and Denaro, 1988). This activation is characterised by the release of cytokines and chemokines that affect neighbouring cells. However, due to glia heterogeneity within different CNS regions it is difficult to determine the target cell response. Therefore, a simplified cell model is needed to probe the functional role of astrocytes during astrogliosis and inflammation (Imura et al., 2006; Yeh et al., 2009).

During neuroinflammation dendritic cells can present major histocompatibility complexes (MHC) I and II, where I is proinflammatory and II is anti-inflammatory (Arbore et al., 2017), facilitating communication with other cells such as macrophages. MHC-I presentation has been observed in both rodent and human dopaminergic neurons (Cebrián et al., 2014; Song et al., 2016). If not controlled, neuroinflammation can lead to neuronal degeneration highlighting the importance of understanding glia factor secretion and their downstream consequences.

5.1.4 Aims of the chapter

Previous chapters have established that AAPH and rotenone generate RS that lead to neurodegeneration in isolated mitotic and differentiated neural cell models. This chapter will investigate RS in a more *in vivo* like environment and will attempt to create a co-culture model using SH-SY5Y and U-87MG cells to represent neurons and astrocytes within the CNS.

To create a co-culture, we will investigate different methodologies to introduce these two cell lines together prior to investigating the effect of OS. This includes contact co-cultures by seeding cells together prior to exposure to RS stressors. An alternate method will utilise transwell inserts to determine the effect of secreted factors while maintaining feedback loops between SH-SY5Y neuronal and U-87MG glial cells. Transwell inserts will also allow the cells lines to be kept separate, preventing one cell type overgrowing the other.

Finally, the effect of the glial secretome on neuronal cell parameters will also be investigated. Proteomic analysis via mass spectrometry and subsequent enrichment will allow the identification of perturbed pathways in glial cells and link this to the secretome profile. This will help identify possibly biomarkers of OS and pathways associated with neuroprotection or neurotoxicity potentially aiding understanding of neurodegenerative pathologies.

5.2 RESULTS

5.2.1 Contact co-cultures

Initially the project attempted to create a contact co-culture, where cells were seeded at the same time at a 1:1 ratio, and then treated with AAPH or rotenone for up to 48 hours.

Following 48-hour growth mono- and co-cultures were treated with AAPH or rotenone for 24 hours (figure 5.2). Phase contrast microscopy showed similar intercellular distances and morphology for 0.25 and 1 mM AAPH treated mono- and co-cultures relative to the control (figure 5.2A). Whilst 5 mM AAPH appeared to have no significant effect on U-87MG monocultures, SH-SY5Y monocultures and co-cultures showed increased intercellular distances and less processes relative to the control. This was supported by viability assays (figure 5.2B) that showed significantly lower MTT reduction levels for SH-SY5Y monocultures and co-cultures but not for U-87MG monocultures. Additionally, LDH assays (figure 5.2C) showed the greatest LDH release for SH-SY5Y monocultures, while U-87MG monocultures and co-cultures were significantly increased relative to the control, but significantly less than SH-SY5Y monocultures. This suggests 5 mM AAPH reduced viability of SH-SY5Y cells but not U-87MG cells and the presence of the SH-SY5Y cells was enough to affect co-culture viability.

24-hour treatment with rotenone resulted in lower viability than AAPH as both SH-SY5Y and U-87MG monocultures, as well as co-cultures showed cellular rounding and increased intercellular distances (figure 5.2D). MTT assays supported this as they showed lower levels of MTT reduction for ≥0.5 µM rotenone (figure 5.2E). While MTT assays suggested no significant difference between mono- or co-cultures, LDH assays showed lower levels of LDH release for U-87MG monocultures and co-cultures (figure 5.2F). This suggests SH-SY5Y cells are more sensitive to membrane permeability induced by rotenone.

Following 48-hour treatment phase contrast microscopy of AAPH treated SH-SY5Y monocultures exhibited greater intercellular distances and cellular rounding in a dose-dependent manner (figure 5.3A). In contrast, U-87MG monocultures appeared to proliferate exhibiting more processes. In the co-culture, some cells displayed cellular rounding while others still showed processes. These observations were consistent with MTT results (figure 5.3B), which showed the lowest level of MTT reduction for SH-SY5Y monocultures. Whereas, MTT reduction levels for co-cultures were lower than U-87MG monocultures, yet not as low as SH-SY5Y monocultures. This was consistent with LDH assays that showed 5 mM AAPH resulted in the greatest LDH release for SH-SY5Y monocultures, while U-87MG monocultures exhibited the lowest, with co-cultures somewhere in between (figure 5.3C). This suggests that co-cultures display altered viability in response to AAPH treatment.

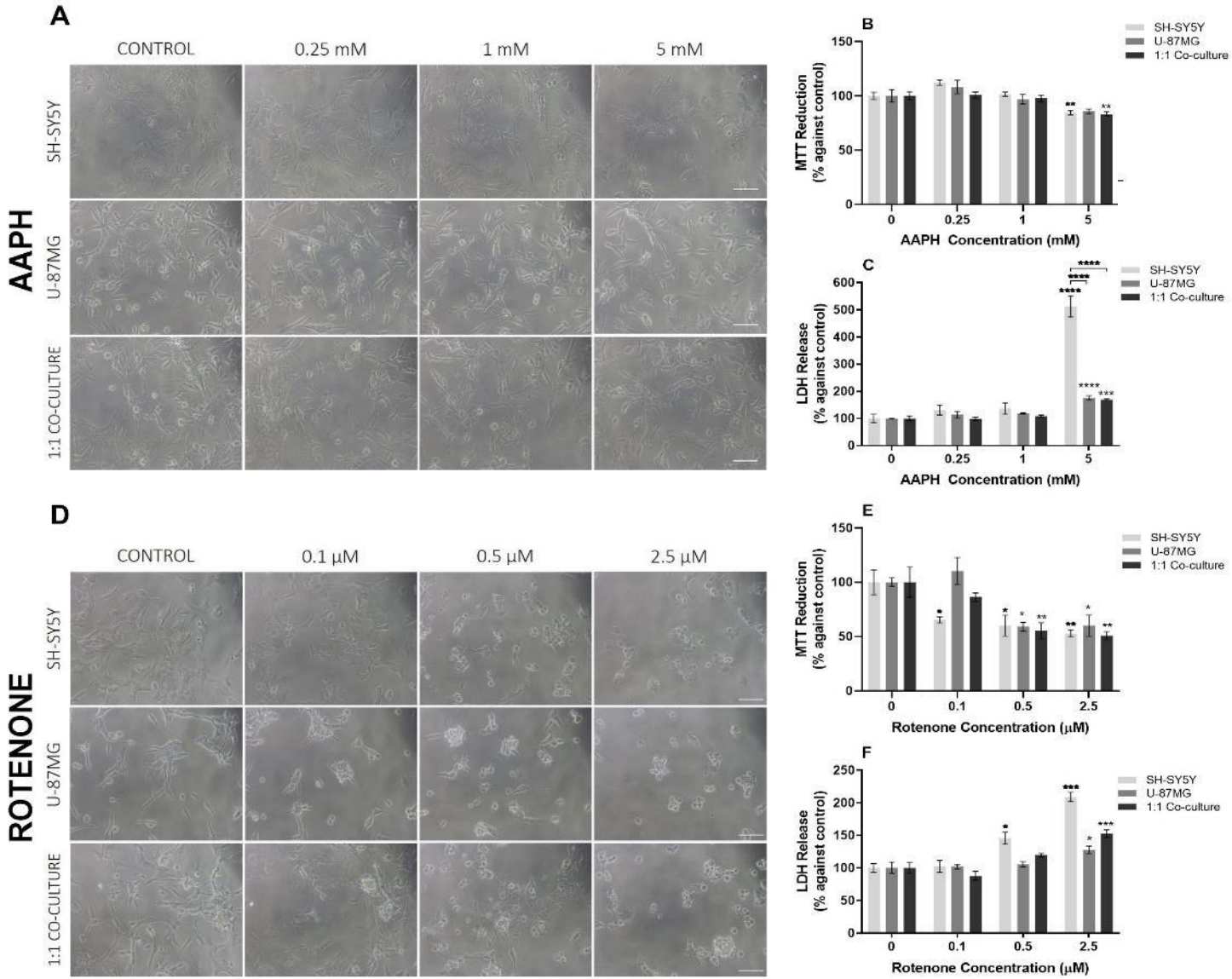

Figure 5.2 Neuronal SH-SY5Y and glial U-87MG contact co-culture cell viability after 24-hour AAPH or rotenone exposure. *Phase contrast microscopy of (A) AAPH and (D) rotenone treated mono- and co-cultures after 24-hour exposure. Scale bar = 100 µm. MTT reduction assay of (B) AAPH and (E) rotenone treated mono- and co-cultures following 24-hour exposure. LDH release of (C) AAPH and (F) rotenone treated mono- and co-cultures after 24-hours. All viability assays are presented as mean % against control ± SEM. Statistical analysis was performed using one-way ANOVA with Dunnett's post-hoc test where n=4 for all experiments. Statistical significance was recorded as *p<0.05, **p<0.01 and ***p<0.001, relative to the control unless otherwise demonstrated.*

In contrast, 48-hour rotenone treatment of both mono- and co-cultures of SH-SY5Y and U-87MG neural cells resulted in similar morphological changes, where cells exhibited increased intercellular distances and cellular rounding in a dose-dependent manner (figure 5.3D). This was consistent with MTT assays, which showed a dose-dependent decrease in MTT reduction for all cultures (figure 5.3E). These observations were supported with LDH assays, which showed similar LDH release for SH-SY5Y monocultures and co-cultures (figure 5.3F). In contrast, U-87MG monocultures demonstrated the lowest levels of LDH release. This suggests co-cultures had similar susceptibility to rotenone induced death as SH-SY5Y monocultures.

Changes in morphology and viability could be affected by the relative cell ratio. Maintenance of the seeding ratio of 1:1 could change as specific neural cells grow at different rates. Indeed, U-87MG cells proliferate with AAPH, possibly altering the ratio of neurons to glia. Thus, we investigated whether immunofluorescent staining of SH-SY5Y neuronal and U-87MG glial cells could be used to verify the neural cell ratio.

Initially, SH-SY5Y and U-87MG cells were seeded at increasing densities and then stained with βIII-tubulin and GFAP, respectively. Immunofluorescent microscopy showed an increase in fluorescence with increasing cell density for both SH-SY5Y and U-87MG cells (figure 5.4A and C, respectively). Fluorescent quantification using the incucyte S3 live-cell analysis system showed a linear increase in fluorescence with cell density (figure 5.4B and D). However, it is important to note that at higher densities of U-87MG cells clustering occurs increasing the standard error.

With immunofluorescent staining as a possible option 1:1 co-cultures of SH-SY5Y and U-87MG cells were grown for 48 hours prior to fixing and staining with βIII-tubulin (red) and GFAP (green; figure 5.5). However, a large majority of the βIII-tubulin and GFAP staining overlapped in the merge image suggesting the cells may express both markers. As such, monocultures were stained with both βIII-tubulin and GFAP where immunofluorescent microscopy showed U-87MG monocultures stained for both markers. This suggests immunofluorescent staining with these markers is not suitable for determining the ratio of the cells in co-culture posing a limitation for contact co-cultures.

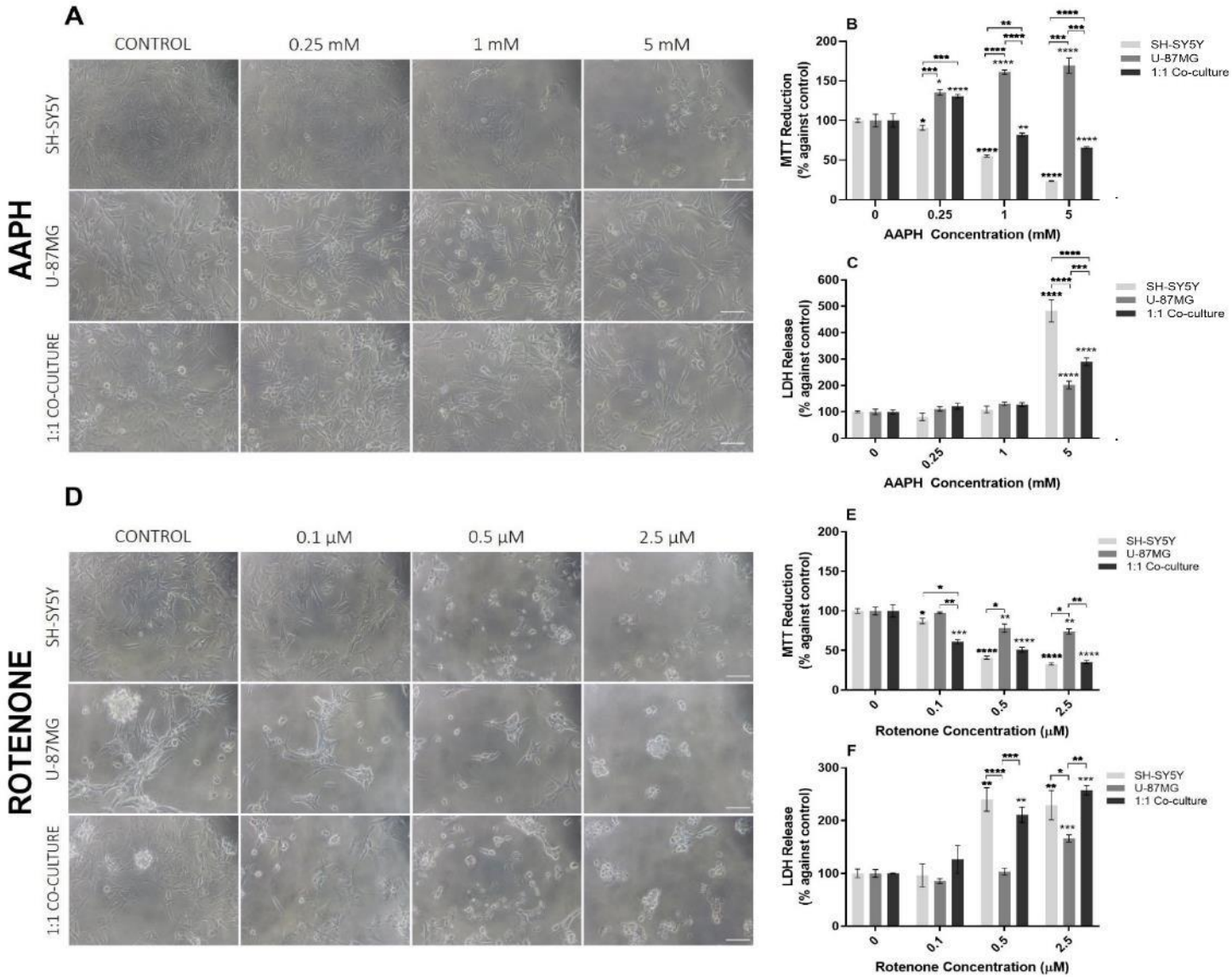

Figure 5.3 Neuronal SH-SY5Y and glial U-87MG contact co-culture cell viability after 48-hour AAPH or rotenone exposure. *Phase contrast microscopy of (A) AAPH and (D) rotenone treated mono- and co-cultures after 48-hour exposure. Scale bar = 100 µm. MTT reduction assay of (B) AAPH and (E) rotenone treated mono- and co-cultures following 48-hour exposure. LDH release of (C) AAPH and (F) rotenone treated mono- and co-cultures after 48-hours. All viability assays are presented as mean % against control ± SEM. Statistical analysis was performed using one-way ANOVA with Dunnett's post-hoc test where n=4 for all experiments. Statistical significance was recorded as *p<0.05, **p<0.01 and ***p<0.001, relative to the control unless otherwise demonstrated.*

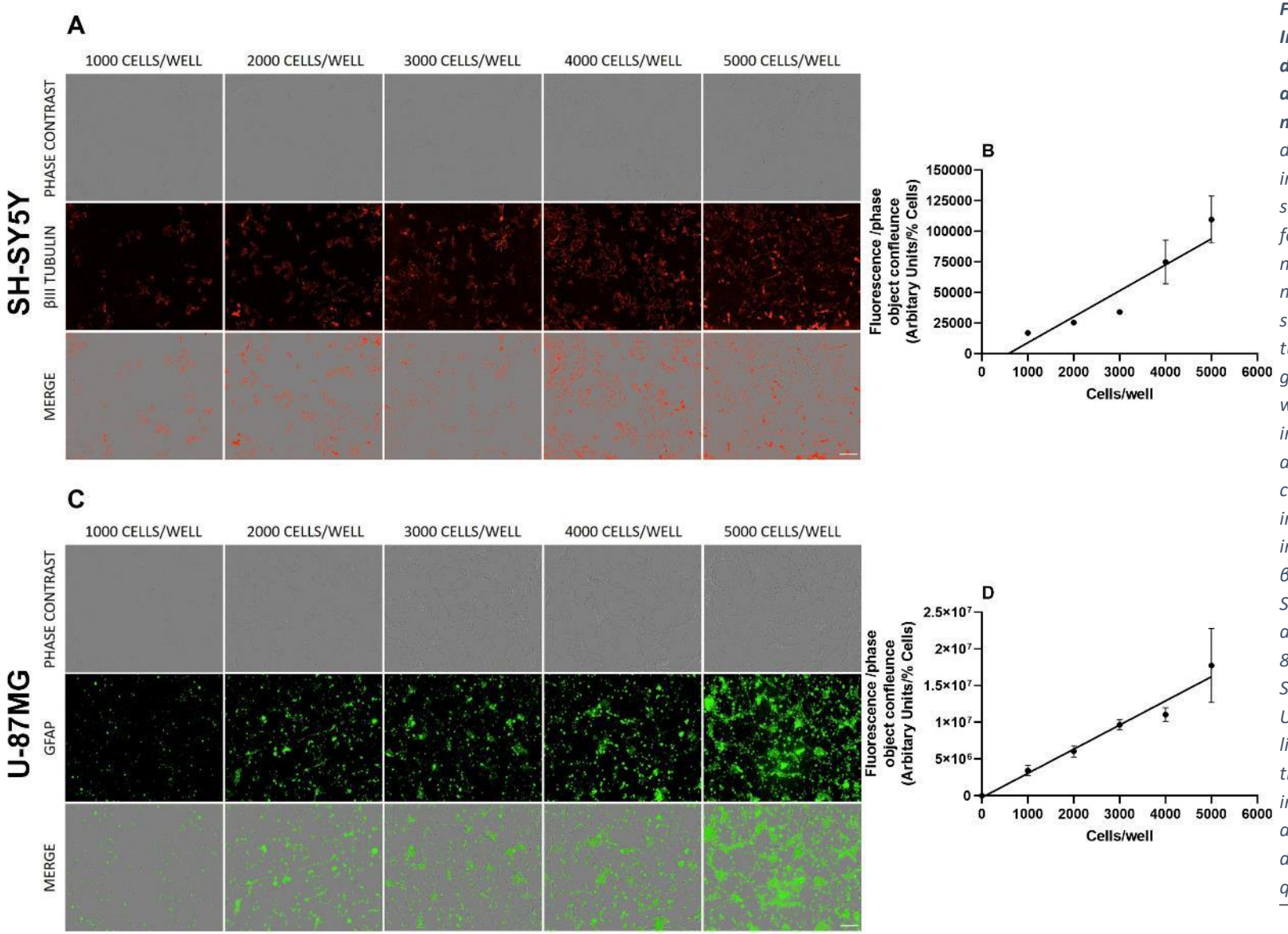

Figure 5.4 Immunofluorescence density of SH-SY5Y and U-87MG monocultures. *To determine if immunofluorescent staining was suitable for quantifying cell number, SH-SY5Y neuronal cells were stained with βIII-tubulin and U-87MG glial cells were stained with GFAP. Using the incucyte S3-live cell analysis system phase contrast and immunofluorescent images were taken of βIII-tubulin stained SH-SY5Y neuronal cells (A) and GFAP stained U-87MG glial cells (C). Scale bar = 200 µm. Using the incucyte S3-live analysis system the fluorescence of increasing SH-SY5Y (B) and U-87MG (D) cell density was quantified.*

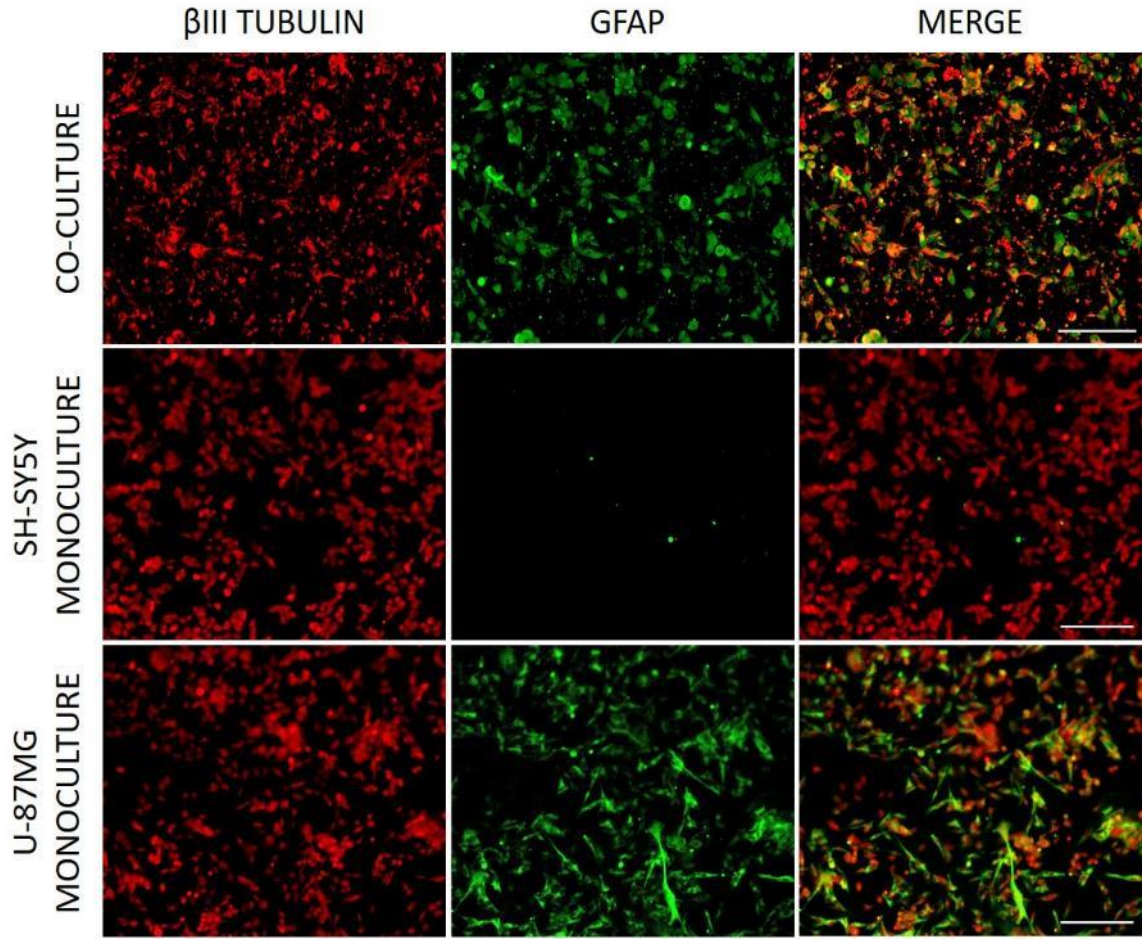

Figure 5.5 Immunofluorescence of SH-SY5Y neuronal and U-87MG glial co-cultures and monocultures. *Co-cultures of SH-SY5Y neuronal and U-87MG glial cells were stained with βIII-tubulin (Red) and GFAP (Green) to try to determine the ratio of the cells within the co-culture. Scale bar = 200 µm. SH-SY5Y neuronal and U-87MG glial monocultures were stained with with βIII-tubulin (Red) and GFAP (Green), which revealed U-87MG glial cells also express with βIII-tubulin.*

5.2.2 Non-contact cell cultures using transwell inserts

Due to difficulties encountered with contact co-cultures we employed transwell inserts to maintain communication between SH-SY5Y neuronal and U-87MG glial cells, but to avoid the problems of cell ratios altering through growth.

Herein SH-SY5Y and U-87MG cells were differentiated together in co-culture over 5 days initially to determine how co-cultures effect differentiation viability. To do this, SH-SY5Y neuronal cells were cultivated in 24-well plates, while U-87MG glial cells were seeded in inserts at the same cellular density. As neurons and glia are reported to have different mechanosensitivities this was also reversed, where U-87MG glial were cultivated in 24-well plates and SH-SY5Y neuronal cells were seeded on inserts, as represented in figure 5.6A. Following overnight growth, media was changed to differentiation media (0.1, 0.5 or 1% (v/v) FBS with 10 µM retinoic acid). After 5 days of differentiation, viability was assessed. As expected, higher FBS resulted in a greater absorbance/cell number at 570 nm for both neural cells (figure 5.6D and E), suggesting lower FBS resulted in attenuated cell proliferation. Phase contrast microscopy of SH-SY5Y neuronal cells showed similar confluence and morphology when seeded on either 24-well plates or inserts (figure 5.6B). These observations were supported by MTT reduction assays, which showed that 0.1 and 0.5% (v/v) FBS resulted in comparable levels of absorbance (figure 5.6D), while 1% (v/v) FBS inserts showed greater absorbance. In contrast, LDH reduction assays showed that all FBS percentages showed greater LDH release for SH-SY5Y differentiation in 24-well plates compared to inserts (figure 5.6F). Together, this suggests SH-SY5Y cells grow more efficiently with higher membrane integrity during differentiation on inserts than 24-well plates.

In contrast, U-87MG glial showed a more stellate morphology in 24-well plates in comparison to the rounded state observed on inserts (figure 5.6C). These observations were consistent with viability assays, where all FBS percentages showed greater absorbance for U-87MG glial cells differentiated in 24-well plates relative to inserts (figure 5.6E). This was consistent with LDH assays that demonstrated greater LDH release for U-87MG glial cells differentiated in inserts relative to 24-well plates (figure 5.6G). This suggests U-87MG viability during differentiation is improved when cultivated on 24-well plates compared to inserts.

Together, these results suggest SH-SY5Y neuronal cells have greater viability during differentiation on inserts whereas U-87MG glial cells grow more efficiently on 24-well plates. This is possibly due to 24-well plates being composed of polystyrene, whereas inserts are made of polyethylene terephthalate, which suggests neural cell growth is affected by cultivation material.

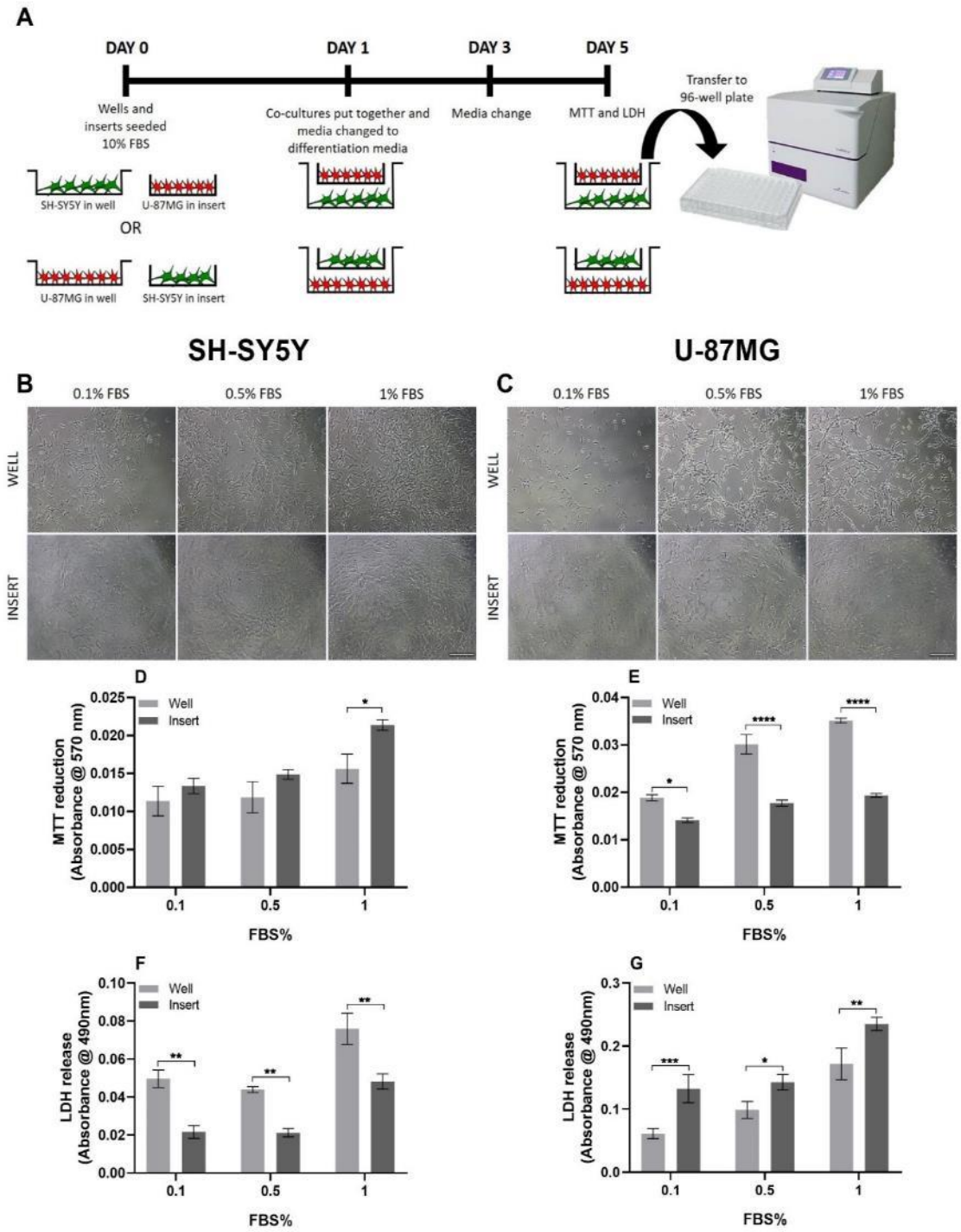

Figure 5.6 Insert material effects neural cell viability. *(A) Diagrammatic scheme of how co-cultures were constructed where SH-SY5Y and U-87MG cells were seeded to either wells or inserts and grown in full media overnight. On day 1 inserts were brought into contact with wells to create co-culture and media was changed to differentiation media (0.1, 0.5 or 1% (v/v) FBS with 10 µM retinoic acid). Media was refreshed on day 3 and then MTT and LDH assays were conducted on day 5 where solutions were transferred to a 96-well plate for the plate reader. Phase contrast microscopy of day 5 (B) SH-SY5Y cells or (C) U-87MG cells in wells or inserts. Scale bar = 200 µm. MTT reduction assay of 5-day differentiated (D) SH-SY5Y or (E) U-87MG cells in wells or inserts. LDH release of 5-day differentiated (F) SH-SY5Y or (G) U-87MG cells in wells or inserts.*

As material appeared to affect these neural cells, we performed 5-day co-culture differentiation under both circumstances, where SH-SY5Y neuronal cells were cultivated in 24-well plates and U-87MG glia in inserts (figure 5.7). Alternatively, U-87MG cells were cultivated in 24-well plates and SH-SY5Y neurons seeded on inserts (figure 5.8) to compare to monoculture differentiation.

SH-SY5Y differentiation showed decreased intercellular distances for both co-cultures of SH-SY5Y neuronal cells cultivated on 24-well plates or inserts relative to monocultured SH-SY5Y cells. Furthermore, all conditions appeared to show pyramidal morphology upon differentiation (figure 5.7A). MTT reduction assays showed significantly greater levels of absorbance for both conditions of co-cultures relative to monocultures at the same FBS concentration (figure 5.7B). For 0.1% (v/v) FBS, co-cultures showed significantly lower LDH release relative to monocultures (figure 5.7C). No significant differences were observed for 0.5% (v/v) FBS, while 1% (v/v) FBS in 24-well and insert co-cultures showed greater LDH release than monocultures, possibly because this concentration alongside glia increased proliferation resulting in culture overgrowth (figure 5.7C).

U-87MG monoculture differentiation showed greater cell clustering with higher FBS concentrations, while co-cultures in 24-well plates exhibited a flat, fibroblast-like morphology (figure 5.8A). Additionally, insert co-cultures with 0.1% (v/v) FBS showed greater intercellular distances and cellular rounding indicative of reduced viability, while 0.5 and 1% (v/v) FBS showed more stellate morphology but did not display the network like clusters observed in both the co-culture and monoculture in the 24-well plates (figure 5.8A). This suggests U-87MG differentiation on inserts was detrimental to cell viability even in co-culture, which was consistent with MTT reduction assays. All FBS concentrations showed lower levels of viability for U-87MG co-cultures cultivated on inserts (figure 5.8B). This supported by LDH release assays where 0.5 and 1% (v/v) FBS showed greater LDH release for U-87MG co-cultured on inserts (figure 5.8C). Furthermore, MTT reduction and LDH assays showed U-87MG co-cultured on 24-well plates showed greater cell proliferation, indicated by the higher MTT absorbance levels and lower LDH release levels.

Together, this suggests SH-SY5Y cells co-cultured on either plates or inserts showed increased viability relative to monocultures. Whereas U-87MG glial cells only showed increased viability for co-cultures on 24-well plates, supporting previous observations that insert material is detrimental to U-87MG viability. This suggests co-cultures improve neural cell viability during differentiation. Furthermore, to prevent overgrowth of the co-culture but not significantly increase cell death 0.5% (v/v) FBS was the most optimal differentiation condition.

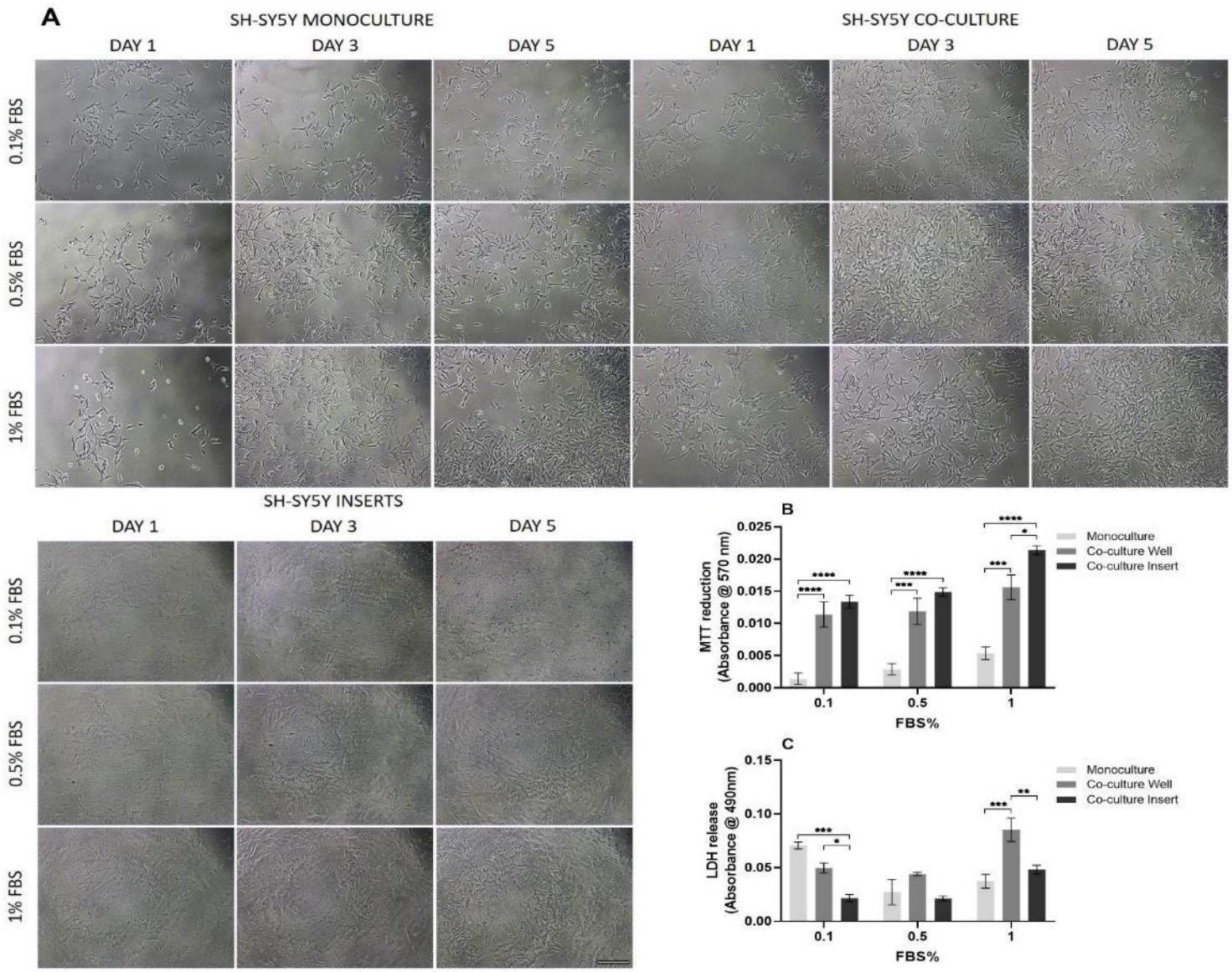

Figure 5.7 The effect of non-contact co-culture with U-87MG on SH-SY5Y differentiation viability. *Transwell inserts were used to culture SH-SY5Y neuronal cells and U-87MG glial cells together without contact. (A) Phase contrast microscopy of day 1, 3 and 5 of differentiated SH-SY5Y monoculture, co-cultured SH-SY5Y in wells and inserts. Scale bar = 200 µm. (B) MTT reduction assay of 5-day SH-SY5Y monoculture and SH-SY5Y well and insert co-cultures. (C) LDH release of 5-day SH-SY5Y monoculture and SH-SY5Y well and insert co-cultures. Statistical analysis was performed using two-way ANOVA with Tukey's post-hoc test where n=4 for all experiments. Statistical significance was recorded *p<0.05, **p<0.01, ***p<0.001 and ****p<0.0001.*

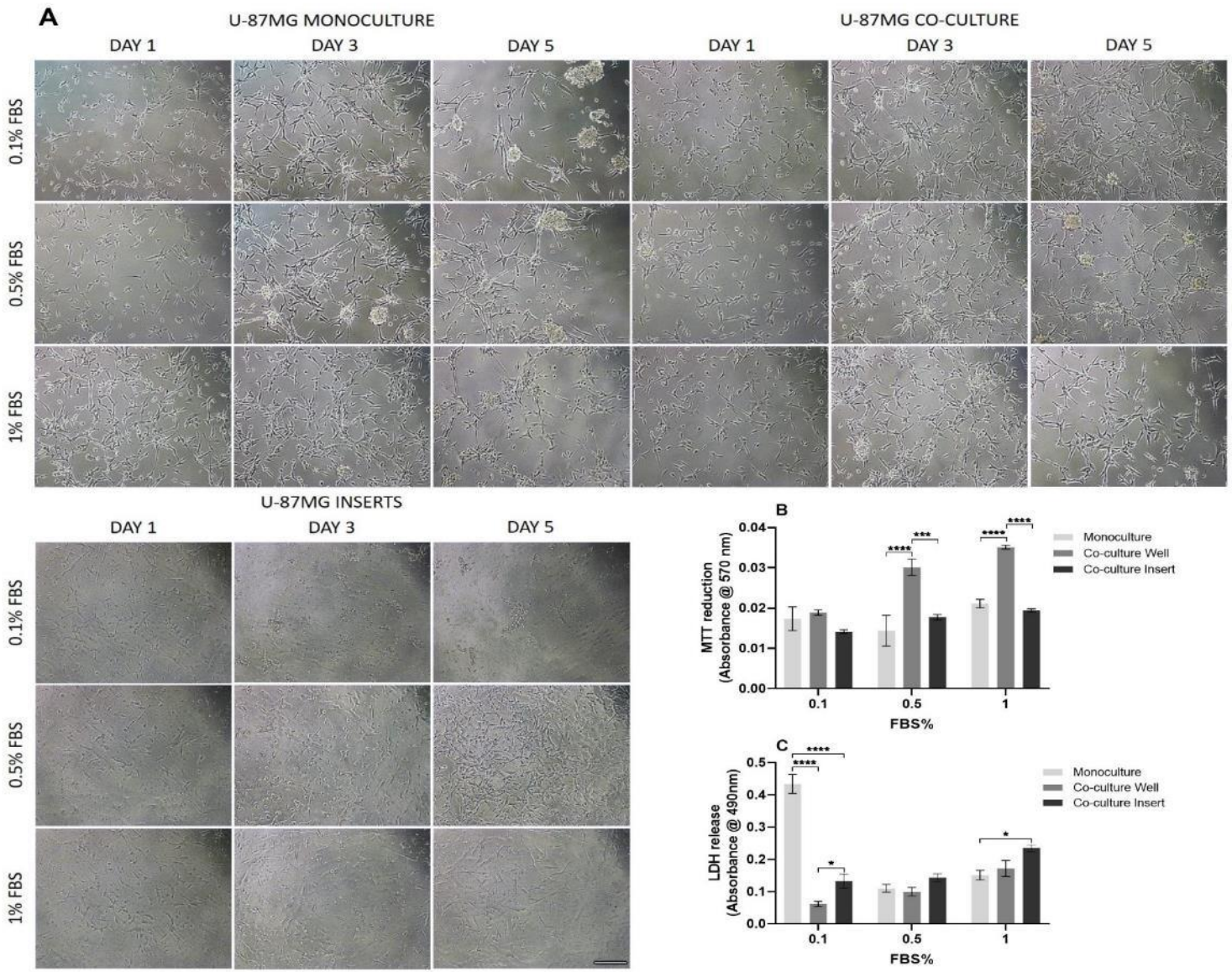

Figure 5.8 The effect of non-contact co-culture with SH-SY5Y on U-87MG differentiation viability. *Transwell inserts were used to culture SH-SY5Y neuronal cells and U-87MG glial cells together without contact. (A) Phase contrast microscopy of day 1, 3 and 5 of differentiated U-87MG monoculture and U-87MG well and insert co-cultures. Scale bar = 200µm. (B) MTT reduction assay of 5-day U-87MG monoculture and U-87MG well and insert co-cultures. (C) LDH release of 5-day U-87MG monoculture and U-87MG well and insert co-cultures. Statistical analysis was performed using two-way ANOVA with Tukey's post-hoc test where n=4 for all experiments. Statistical significance was recorded *p<0.05, **p<0.01, ***p<0.001 and ****p<0.0001.*

To investigate the effect of RS on co-cultures, SH-SY5Y and U-87MG cells were differentiated over 5 days (0.5% (v/v) FBS, 10 µM retinoic acid) in co-culture, prior to treatment with AAPH or rotenone. As shown before, SH-SY5Y co-cultures in both 24-well plates and inserts showed lower intercellular distances in control cells relative to monocultures (figure 5.9A), suggesting co-cultures with U-87MG glial cells improve SH-SY5Y viability. Both AAPH and rotenone resulted in increased intercellular distances, where rotenone also resulted in cell rounding. While AAPH resulted in similar observations with phase contrast microscopy for both mono- and co-cultures of SH-SY5Y cells, rotenone treated SH-SY5Y co-cultures appeared to have lower intercellular distances and more processes relative to SH-SY5Y monocultures (figure 5.9A). MTT assays were consistent with this as both SH-SY5Y well and insert co-cultures treated with rotenone had greater absorbance levels relative to monocultures (figure 5.9B). This was supported by LDH assays, which showed lower levels of LDH release for SH-SY5Y co-cultures relative to monocultures following rotenone exposure (figure 5.9C). This suggests co-cultures with U-87MG glial cells improved SH-SY5Y viability in response to rotenone, but not AAPH, suggesting specific RS result in different responses in neural cells.

As shown before U-87MG glial cells co-cultured with SH-SY5Y cells when cultivated on inserts showed a more rounded morphology (figure 5.10A), while showing lower absorbance levels for MTT reduction assays (figure 5.9B), suggesting insert material significantly effects viability. As observed previously, AAPH treated monocultures show increased proliferation as observed with phase microscopy (figure 5.10A) and MTT assays (figure 5.10B). In contrast, AAPH treated co-cultures exhibited lower cell number in phase microscopy images (figure 5.10A) and decreased absorbance levels for MTT assays (figure 5.10B), suggesting co-cultures prevented the usual proliferation. This suggests the presence of SH-SY5Y cells affects the normal response of glia to this RS inducer. Furthermore, while U-87MG cells in co-culture still showed cellular rounding with rotenone treatment as seen with monocultures, co-cultures showed greater cell numbers and clusters (figure 5.10A). These observations were consistent with MTT reduction assays that showed greater absorbance for U-87MG glial cells co-cultured with SH-SY5Y cells (figure 5.10B), while LDH release levels were lower for co-cultures relative to monocultures (figure 5.10C). This suggests that like with SH-SY5Y co-cultures, rotenone induced U-87MG glial death was attenuated relative to monocultures whereas AAPH treated co-cultures did not exhibit the previously observed proliferation.

Together this suggests co-cultures aid differentiated neural cell viability when treated with rotenone but not with AAPH. This strengthens that different RS species effect co-cultures in contrasting ways with feedback loops influencing viability in both a positive and negative ways.

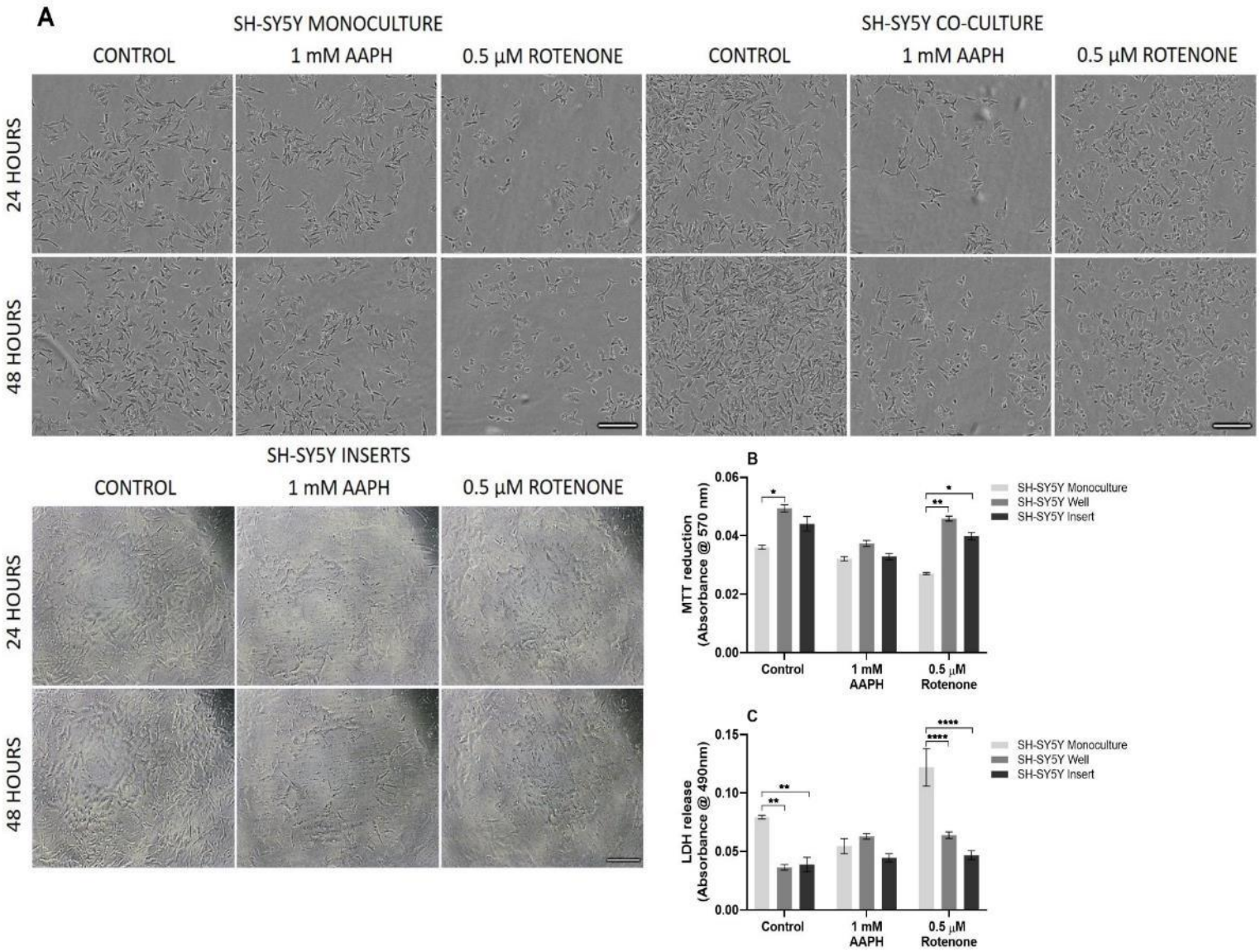

Figure 5.9 The effect of non-contact co-culture with U-87MG on SH-SY5Y viability following AAPH or rotenone treatment. *Transwell inserts were used to culture SH-SY5Y neuronal cells and U-87MG glial cells together without contact. (A) Phase contrast microscopy of 24 and 48-hour AAPH or rotenone exposure to SH-SY5Y monocultures and SH-SY5Y well and insert co-cultures. Scale bar = 200 µm. (B) MTT reduction assay of 48-hour 1 mM AAPH or 0.5 µM rotenone treatment of SH-SY5Y monoculture and SH-SY5Y well and insert co-cultures. (C) LDH release of 48-hour 1 mM AAPH or 0.5 µM rotenone treatment of SH-SY5Y monoculture and SH-SY5Y well and insert co-cultures. Statistical analysis was performed using two-way ANOVA with Tukey's post-hoc test where n=4 for all experiments. Statistical significance was recorded *p<0.05, **p<0.01, ***p<0.001 and ****p<0.0001.*

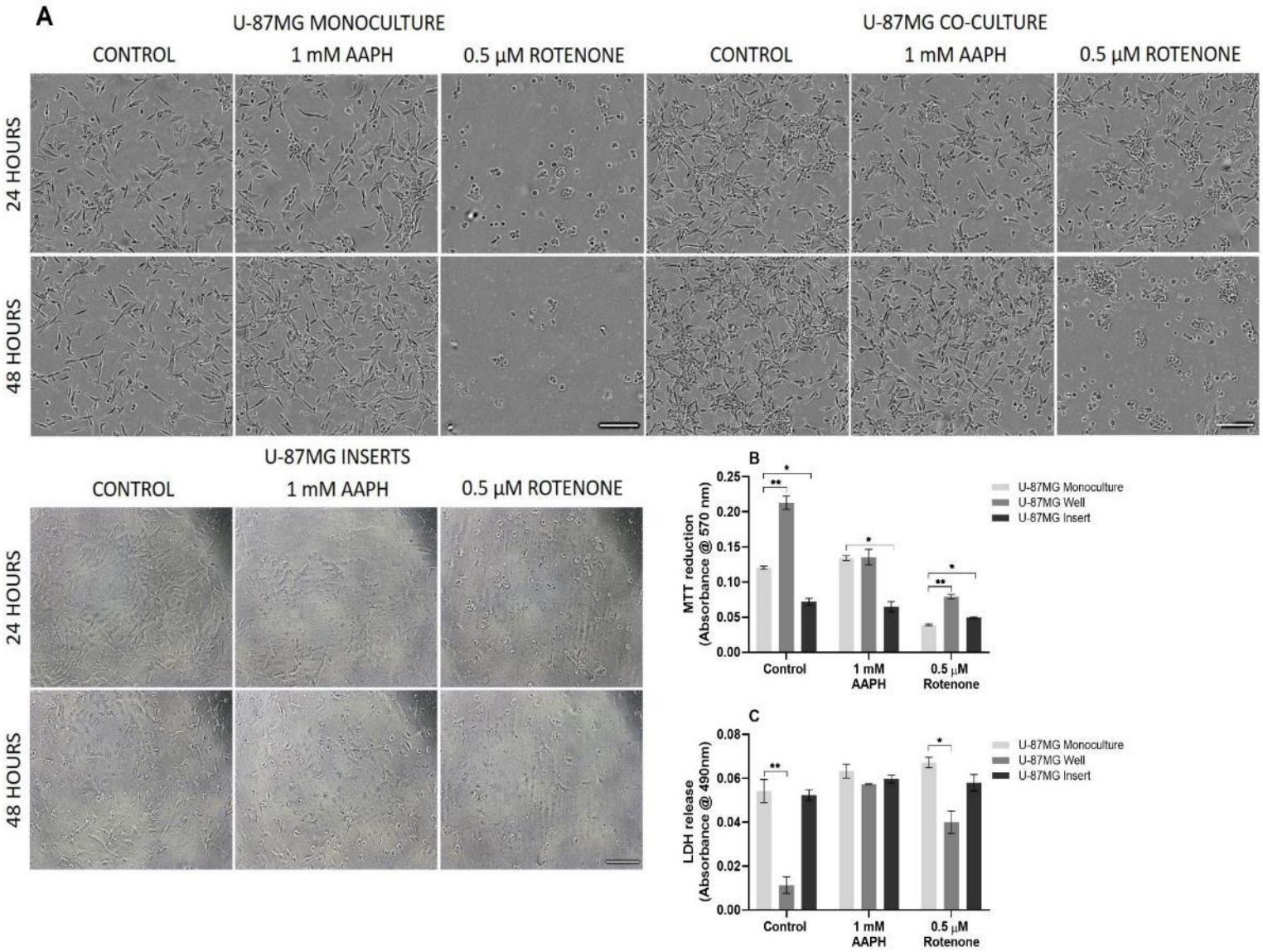

Figure 5.10 The effect of non-contact co-culture with SH-SY5Y on U-87MG viability following AAPH or rotenone treatment. *Transwell inserts were used to culture SH-SY5Y neuronal cells and U-87MG glial cells together without contact. (A) Phase contrast microscopy of 24 and 48-hour AAPH or rotenone exposure to U-87MG monocultures and U-87MG well and insert co-cultures. Scale bar = 200 µm. (B) MTT reduction assay of 48-hour 1 mM AAPH or 0.5 µM rotenone treatment of U-87MG monoculture and U-87MG well and insert co-cultures. (C) LDH release of 48-hour 1 mM AAPH or 0.5 µM rotenone treatment of U-87MG monoculture and U-87MG well and insert co-cultures. Statistical analysis was performed using two-way ANOVA with Tukey's post-hoc test where n=4 for all experiments. Statistical significance was recorded *p<0.05, **p<0.01, ***p<0.001 and ****p<0.0001.*

5.2.3 Different reactive species induce divergent effects on the U-87MG glial secretome

While inserts are one method, we utilised to create a co-culture of SH-SY5Y neuronal and U-87MG glial cells, they are difficult for high-throughput experiments. Thus, to determine if the effects are a consequence of secreted factors, conditioned media experiments were conducted.

As demonstrated in figure 5.11A, SH-SY5Y neuronal cells were plated in complete media for 24 hours prior to changing to differentiation media (0.5% (v/v) FBS, 10 µM retinoic acid). Cells were differentiated over 5 days, where media was refreshed on day 3. In parallel, U-87MG glial cells were differentiated over 5 days and then treated with 1 mM AAPH or 0.5 µM rotenone for 48 hours. On day 5, SH-SY5Y cells were subjected to 4 conditions: media only, U-87MG conditioned media, 1 mM AAPH U-87MG conditioned media or 0.5 µM rotenone U-87MG conditioned media. Each condition was also treated with 1 mM AAPH or 0.5 µM rotenone to determine if stressed U-87MG glial secrete factors that affect SH-SY5Y viability in response to OS. Cell growth and cytotoxicity was monitored over 48-hours using the incucyte S3 live-cell analysis system and viability was subsequently assessed using in-house viability assays.

Phase contrast microscopy at 24 hours showed AAPH and rotenone in all conditions resulted in greater intercellular distances and cell rounding, which was greater with rotenone as AAPH treated SH-SY5Y cells still showed processes (figure 5.11B). Furthermore, U-87MG and AAPH U-87MG conditioned media appeared to result in more cell processes relative to media alone. Interestingly, SH-SY5Y cells cultured with rotenone U-87MG conditioned media showed similar morphology to AAPH and rotenone treatment of media alone, displaying a more cuboidal morphology and lack of processes. This suggests that while U-87MG and AAPH U-87MG conditioned media improved processes rotenone U-87MG conditioned media was detrimental to SH-SY5Y morphology. Additionally, all media conditions seemed to show similar changes to morphology upon AAPH or rotenone treatment.

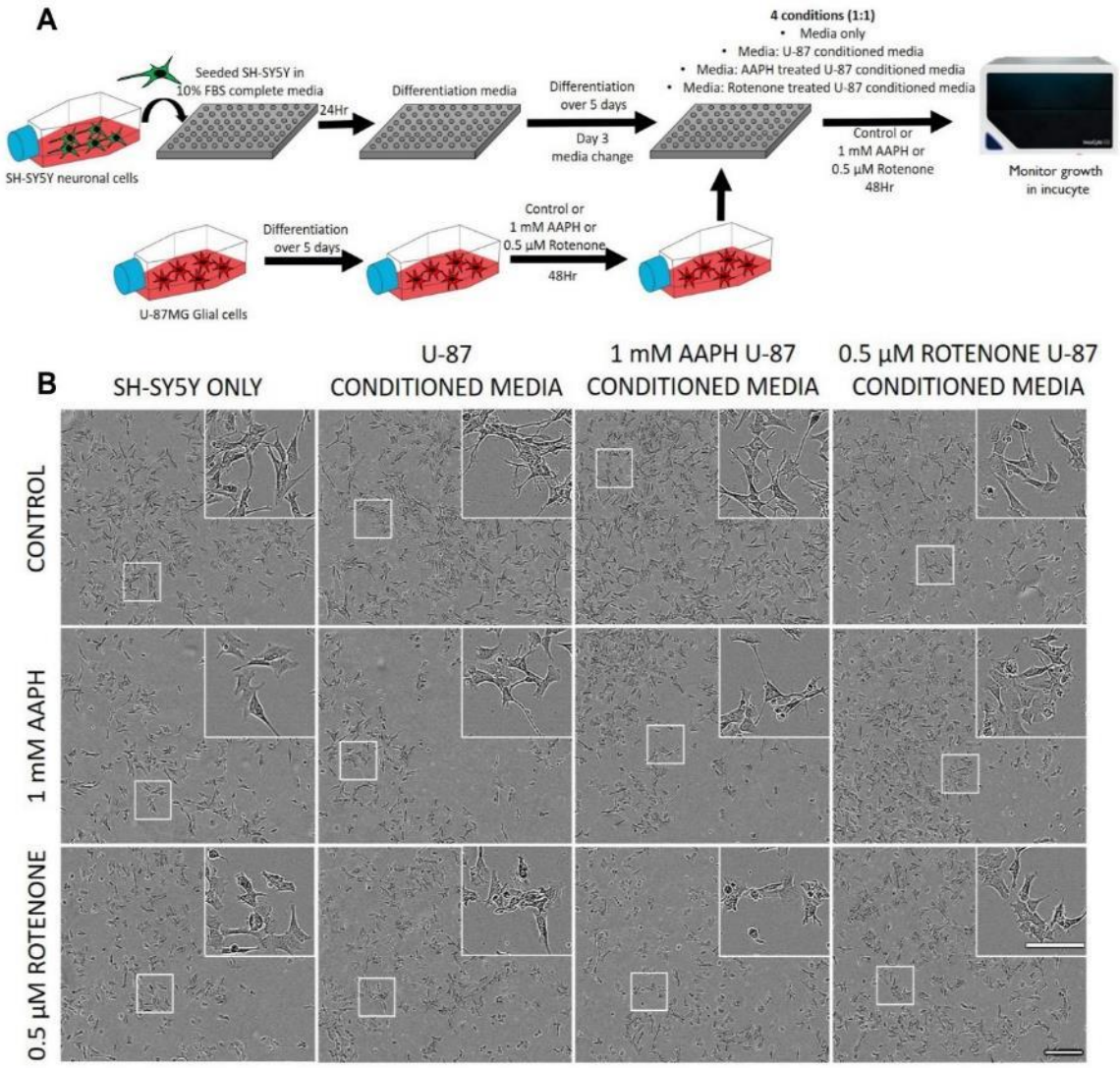

Figure 5.11 The effect of different U-87MG conditioned media on SH-SY5Y viability. *(A) Schematic representation of conditioned media cultures where SH-SY5Y cells grown overnight in complete media. SH-SY5Y cells were differentiated over 5 days with media replaced on day 3. In parallel, U-87MG glial cells were differentiated over 5 days and subsequently treated with 1 mM AAPH or 0.5 µM rotenone for 48 hours prior to addition in a 1:1 ratio with fresh media to differentiated SH-SY5Y neuronal cells. In addition, each condition was treated with 1 mM AAPH or 0.5 µM rotenone. Cells were monitored over 48 hours using the incucyte S3 live-cell analysis system. (B) 24-hour phase confluence microscopy of differentiated SH-SY5Y cells with different U-87MG conditioned media when treated with 1 mM AAPH or 0.5 µM rotenone. Scale bar 200 µm. Inset scale bar = 100 µm.*

Following 48-hour exposure to AAPH and rotenone, cells exhibited increased intercellular distance and greater cell rounding (figure 5.12A). However, control cells treated with U-87MG and AAPH U-87MG conditioned media showed improved parameters relative to SH-SY5Y media alone. SH-SY5Y cells cultured with rotenone U-87MG conditioned media demonstrated cuboidal shaped cells that lacked defined processes. Indeed, AAPH and rotenone treatment appeared to have a greater effect on SH-SY5Y morphology cultured with media alone, whilst U-87MG conditioned

media and AAPH U-87MG conditioned media improved neuronal viability. Cells still appeared elongated, with less rounding for U-87MG and AAPH U-87MG conditioned media cultivated cells treated with AAPH or rotenone, relative to media conditioned SH-SY5Y cells alone. As these two media conditions are where U-87MG cells are still growing, this suggests healthy U-87MG cells secrete factors that improve SH-SY5Y neuronal viability. In contrast, rotenone treated U-87MG glial cells show decreased viability, and this conditioned media resulted in SH-SY5Y cells showing morphological differences from other conditions, suggesting U-87MG cells undergoing cell death secrete different factors that are possibly neurotoxic.

MTT reduction assays showed that all U-87MG conditioned media increased absorbance levels relative to SH-SY5Y cultured with media alone (figure 5.12B). AAPH U-87MG conditioned media showed the greatest absorbance (viability), whereas rotenone U-87MG conditioned media showed the lowest viability levels supporting morphological observations. These observations were in contradiction to LDH assays as SH-SY5Y cells cultured with U-87MG conditioned media and treated with AAPH showed higher levels of LDH release relative to media alone (figure 5.12C). This may be due to AAPH specifically generating RS specific for lipid peroxidation, and thus increasing LDH release. Consistent with phase microscopy observations, LDH release levels were significantly higher for rotenone U-87MG conditioned media relative to media alone, suggesting reduced viability.

Live cell monitoring with the incucyte supported these findings in some parts where U-87MG conditioned media improved the phase confluence of rotenone treated SH-SY5Y cells relative to media alone (figure 5.12D-G). In contrast, AAPH U-87MG conditioned media did not improve susceptibility to AAPH or rotenone treatment relative to media alone (figure 5.12F). However, interestingly, both treatments of SH-SY5Y cells with rotenone U-87MG conditioned media showed similar viability (figure 5.12G), which was also observed with viability assays, suggesting the secreted factors from rotenone treated U-87MG result in a senescence, of sort. While U-87MG and AAPH U-87MG conditioned media improved control SH-SY5Y growth (figure 5.12E and F, respectively) relative to media alone, rotenone U-87MG conditioned media resulted in reduced phase confluence (figure 5.12G). Therefore viability, phase microscopy and live-cell monitoring suggests media from growing/healthy U-87MG cells improves SH-SY5Y neuronal viability but does not significantly affect susceptibility to AAPH or rotenone treatment. In contrast, stressed U-87MG glial cells release factors detrimental to SH-SY5Y viability. However, the factors released are likely to be a mixture of positive and negative regulators of cell death as viability was improved with subsequent rotenone and AAPH treatment.

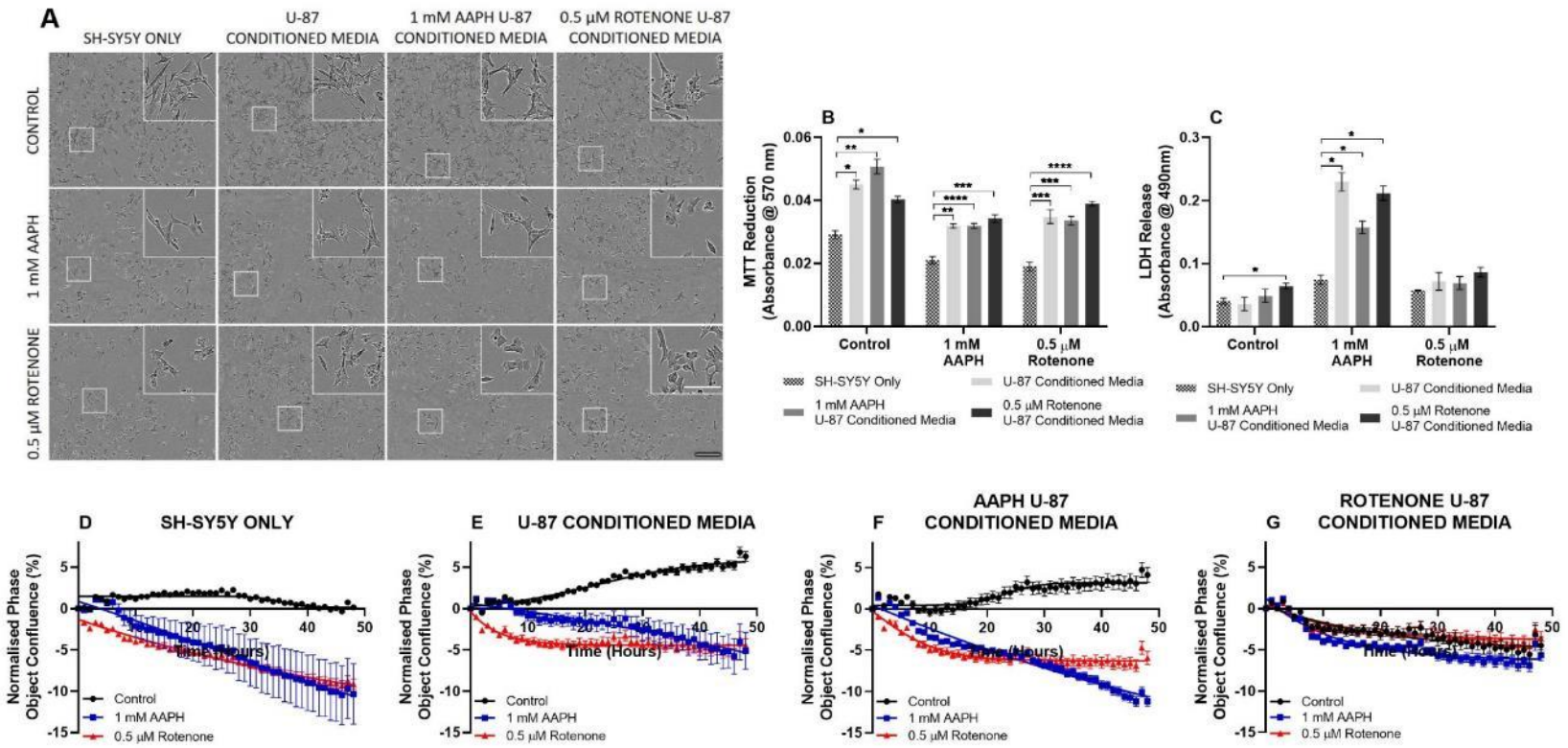

Figure 5.12 The effect of different U-87MG conditioned media on 48-hour SH-SY5Y viability in the presence of AAPH and rotenone. *SH-SY5Y cells were differentiated over 5 days and subsequently treated with 1 mM AAPH or 0.5 µM Rotenone in the presence of U-87MG conditioned media, 1 mM AAPH U-87MG conditioned media, and 0.5 µM rotenone U-87MG conditioned media. (A) 48-hour phase confluence microscopy of differentiated SH-SY5Y cells with different U-87MG conditioned media when treated with 1 mM AAPH or 0.5 µM rotenone. Scale bar = 200 µm. Inset scale bar = 100 µm. (B) 48-hour MTT reduction assay of 1 mM AAPH and 0.5 µM rotenone treated SH-SY5Y neuronal cells in the presence of different U-87MG conditioned media. (C) 48-hour LDH release assay of 1 mM AAPH and 0.5 µM rotenone treated SH-SY5Y neuronal cells in the presence of different U-87MG conditioned media. Incucyte S3 live-cell monitoring of phase confluence of (D) media alone, (E) U-87 conditioned media, (F) 1 mM AAPH U-87 conditioned media and (G) 0.5 µM rotenone U-87 conditioned media.*

To get a better understanding of the possible factors secreted by U-87MG glia and their impact of SH-SY5Y neuronal cells, mass spectrometry of the secretomes of U-87MG glia treated with AAPH or rotenone were performed (figure 5.13). Lysates were digested with trypsin and prepared for SWATH MS (Sequential Windowed Acquisition of all Theoretical Fragment ion Mass Spectra) analysis as described in section 2.18.1-2.18.2 of chapter 2. Initially, a spectral library was generated using data dependent acquisition (DDA), followed by SWATH data gathering via data independent acquisition (DIA). Due to the extensive nature of proteins identified via mass spectrometry tables for AAPH and rotenone treated U-87MG lysates and secretomes are provided in the supplementary data (table 8.1 and 8.2, respectively). Using differentially identified proteins with a 50% or greater confidence, pathway analysis was performed using MetaCore network enriched proteomic data analysis.

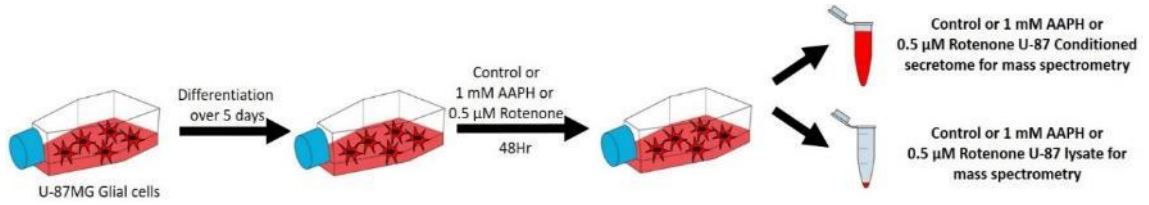

Figure 5.13 Schematic representation of how U-87MG lysates and secretomes were obtained for mass spectrometry. *U-87MG cells were differentiated over 5 days with media replaced on day 3. Cells were subsequently treated 1 mM AAPH or 0.5 µM for 48 hours where conditioned media and lysates were taken forward for mass spectrometry.*

Using Venny (Oliveros, 2007), an interactive tool we determined how many of these differentially identified proteins were up- or downregulated, but also unique and shared between AAPH and rotenone treated U-87MG lysates (figure 5.14A and C) and secretomes (figure 5.15A and C). In U-87MG lysates only 6 proteins were upregulated in both AAPH and rotenone treated cells, suggesting how specific RS effect different proteins relative to the control (figure 5.14A). Whereas a greater number of proteins (54) were downregulated in both AAPH and rotenone treated U-87MG cells (figure 5.14C). In both cases, rotenone resulted in a higher number of unique proteins identified, suggesting this treatment resulted in more proteins and possibly more pathways being affected. This is possibly due to rotenone effecting multiple cellular functions as it not only generates OS but also lowers ATP levels.

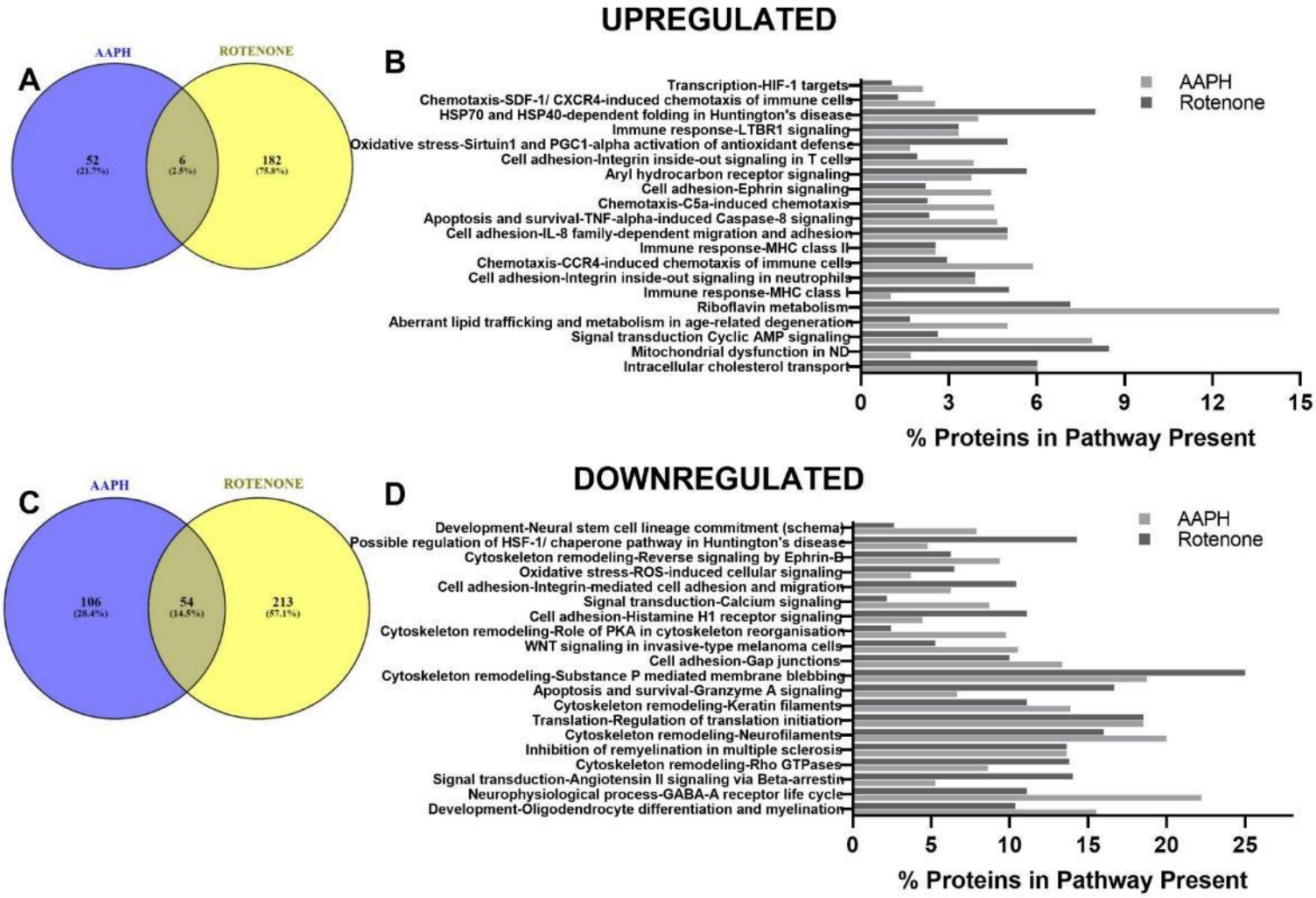

Figure 5.14 Mass spectrometry of differentially expressed proteins of AAPH and rotenone U-87MG treated cells and pathways identified using MetaCore. *U-87MG glial cells were differentiated over 5 days (0.5% (v/v) FBS, 10 µM retinoic acid) and then treated with 1 mM AAPH or 0.5 µM rotenone for 48 hours. Venn diagrams were used to illustrate how many differentially identified proteins were upregulated (A) and downregulated (C), and how many were common and unique to AAPH and rotenone treatment. MetaCore™ was used to determine upregulated (B) and downregulated (D) pathways and how many proteins in these were differentially expressed in AAPH and rotenone treated cells.*

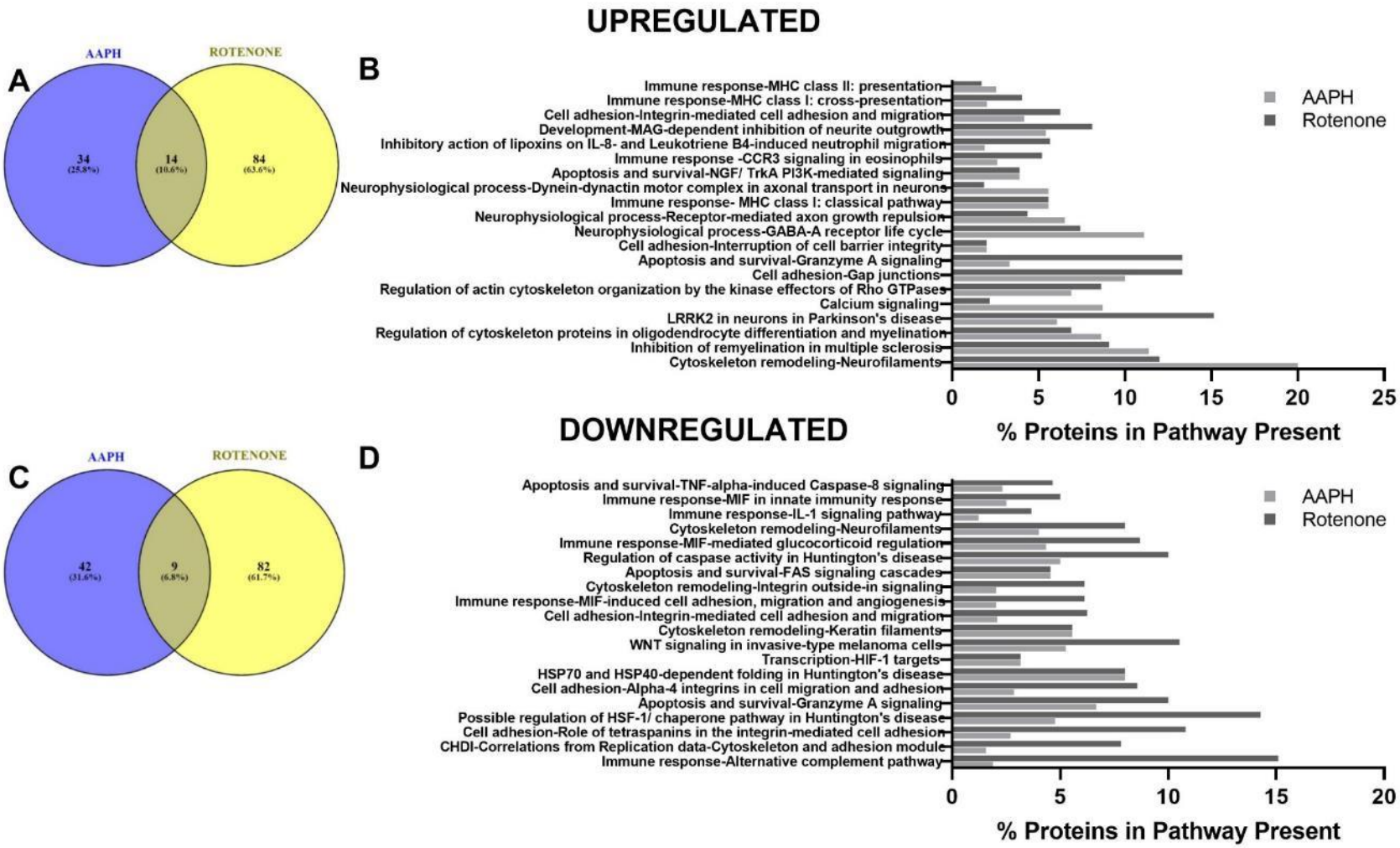

Figure 5.15 Mass spectrometry of differentially expressed proteins of AAPH and rotenone U-87MG treated secretomes and pathways identified using MetaCore. *U-87MG glial cells were differentiated over 5 days (0.5% (v/v) FBS, 10 µM retinoic acid) and then treated with 1 mM AAPH or 0.5 µM rotenone for 48 hours where the mass spectrometry was performed on the conditioned media. Venn diagrams were used to illustrate how many differentially identified proteins were upregulated (A) and downregulated (C), and how many were common and unique to AAPH and rotenone treatment. MetaCore™ was used to determine upregulated (B) and downregulated (D) pathways and how many proteins in these were differentially expressed in AAPH and rotenone treated cells.*

While less proteins were identified in the U-87MG secretome (figure 5.15), rotenone treated glia still presented a greater number of differentially identified proteins both up- and downregulated (figure 5.15A and C). However, it is important to consider that rotenone results in glial death and thus, it is hard to determine if these proteins are actively secreted or just released due to cell lysis. This is less of a problem with AAPH treated cells as AAPH induced proliferation and therefore, we can be more confident the identified proteins are secreted factors.

Metacore enrichment highlighted multiple pathways in U-87MG lysates (figure 5.14B, table 5.1), where some of the top 50 key upregulated pathways included activation of antioxidant defences including SOD and PRDX3, supporting previous findings in chapter 3. Other pathways included mitochondrial dysfunction, where more proteins were upregulated with rotenone including mitochondrial permeability transition pore complex and SOD2. In contrast, proteins associated with lipid trafficking and metabolism in age-related degeneration were upregulated more in AAPH treated U-87MG glial cells than rotenone. This suggests AAPH and rotenone both resulted in OS via different mechanisms as previously proposed. Rotenone primarily targeted mitochondria to a greater extent than AAPH; where the latter primarily affected lipids.

As we have previously proposed that OS can also lead to changes in protein degradation as well as mitochondrial dysfunction via the “neurodegenerative Bermuda triangle”, it was interesting to note that HSP70 was significantly upregulated and its involvement in protein folding was highlighted as an important pathway. Additionally, both the MHC I and MHC II class pathways were upregulated by both rotenone and AAPH, suggesting a neuroinflammatory response.

AAPH and rotenone secretomes showed similar pathway upregulation associated with neuroinflammation including MHC class I and II presentation (table 5.3), suggesting neuroinflammatory pathways are extracellular as well as intracellular. Unlike lysates though, HSP70 was downregulated in the secretome, possibly due HSP70 being retained to help cells cope with OS.

Enrichment analysis highlighted a large majority of the downregulated pathways (table 5.2) were involved in cell adhesion including: cytoskeleton remodelling, integrin mediated cell adhesions, gap junctions, WNT signalling, remodelling of keratin filaments and neurofilaments. Some of the proteins highlighted in these pathways included fibronectin, filamin A, vimentin and tubulin. Filamin A and fibronectin were also downregulated in U-87MG secretomes alongside metalloproteinase inhibitors (MMP), suggesting oxidatively stressed glia secrete factors that influence cellular adhesion and the ECM (table 5.4)

Table 5.1 Upregulated pathway maps enriched in AAPH and rotenone treated U-87MG cells. *U-87MG cells were treated with AAPH or rotenone for 48 hours and analysed using mass spectrometry. Using differentially identified proteins upregulated by AAPH or rotenone pathways were subsequently enriched using MetaCore.*

Lysate Pathway Map Enrichments	Proteins upregulated by AAPH in pathway	Proteins upregulated by rotenone in pathway
Transcription-HIF-1 targets	TGM2, Heme oxygenase 1	FGF2
Chemotaxis-SDF-1/CXCR4-induced chemotaxis of immune cells	RAP-1A, G-protein alpha-i family	RAP-1A
HSP70 and HSP40-dependent folding in Huntington's disease	Cathepsin D	HSP90, HSP70
Immune response – LTBR1 signalling	RAP-1A, G-protein alpha-i family	COX-2 (PTGS2), RAP-1A
Oxidative stress -Sirtuin1 and PGC1-α activation of antioxidant defence	Heme oxygenase 1	PBEF, SOD2, PRDX3
Cell adhesion-integrin inside out signalling in T-cells	RAP-1A, G-protein alpha-i family	RAP-1A
Aryl hydrocarbon receptor signalling	CYP1B1, Cathepsin D	COX-2 (PTGS2), IL-8, Epiregulin
Cell adhesion – Ephrin signalling	RAP-1A, G-protein alpha-i family	RAP-1A
Chemotaxis-C5a-induced chemotaxis	RAP-1A, G-protein alpha-i family	RAP-1A
Apoptosis and survival-TNF-α-induced chemotaxis	Acid sphingomyelinase, Cathepsin D	HSP90
Cell adhesion-IL-8 family dependent migration and adhesion	RAP-1A, G-protein alpha-i family	RAP-1A, IL-8
Immune response-MHC class II	MHC class II alpha chain, Rab-7, Itch	HSP90, Endoplasmin, Cathepsin L
Chemotaxis-CCR4-induced chemotaxis of immune cells	RAP-1A, G-protein alpha-i family	RAP-1A
Cell adhesion-Integrin inside-out signalling in neutrophils	RAP-1A, FPR, G-protein alpha-i family	CD44, RAP-1A, IL-8
Immune response-MHC class I	Rab-7	HSP90, Endoplasmin, Cathepsin L, HSP70, HSP60
Riboflavin metabolism	FLAD1, PPAL	PPAL
Aberrant lipid trafficking and metabolism in age-related degeneration	CD36L2, SR-BI, Cathepsin D	CD36L2
Signal transduction Cyclic AMP signalling	RAP-2A, RAP-1A, G-protein alpha-i family	RAP-1A
Mitochondrial dysfunction in neurodegeneration (ND)	TGM2	SDHA, MPTP complex, SOD2, VDAC 1, ANT
Intracellular cholesterol transport	NPC2, MENTHO, CD36L2, Rab-7, SR-BI	Rab-4, TIP47, PBR, CD36L2, Caveolin-1

Table 5.2 Downregulated pathway maps enriched in AAPH and rotenone treated U-87MG cells. *U-87MG cells were treated with AAPH or rotenone for 48 hours and analysed using mass spectrometry. Using differentially identified proteins downregulated by AAPH or rotenone pathways were subsequently enriched using MetaCore.*

Lysate Pathway Map Enrichments	Proteins Downregulated by AAPH in pathway	Proteins downregulated by rotenone in pathway
Development-neural stem cell lineage commitment (schema)	Tubulin beta 3, Vimentin, MAP-1B	Tubulin beta 3
Possible regulation of HSF1/chaperone pathway in huntington's disease	HSP27	HSP27, p23 co-chaperone, E2I
Cytoskeleton remodelling-reverse signalling by ephrin-b	Tubulin alpha, Ephrin-B, Tubulin (in microtubules)	Tubulin alpha, Tubulin (in microtubules)
Oxidative stress-ROS-induced cellular signalling	NF-kB, HSP27, RelA (p65 NF-kB subunit), IL-1 beta	HSP27, Cytochrome c, TfR1, SCD, FASN, DLC1 (Dynein LC8a), E2I
Cell adhesion-integrin-mediated cell adhesion and migration	MLCP (cat), MyHC, Zyxin	Alpha-actinin, MLCP (cat), Talin, MRLC, MyHC
Signal transduction-calcium signalling	CD44, IP3 receptor, IP3R1, PP1-cat	PP1-cat
Cell adhesion-histamine H1 receptor signalling	MLCP (cat), IP3 receptor	Alpha-actinin, MLCP (cat), Talin, MRLC, p120-catenin
Cytoskeleton remodelling-role of PKA in cytoskeleton reorganisation	MLCP (cat), LASP1, Fodrin (spectrin), IP3 receptor	MLCP (cat)
WNT signalling in invasive type melanoma cells	Filamin-A (CTF), CD44, Vimentin, Filamin A	Filamin A, Filamin-A (CTF)
Cell adhesion-gap junctions	Tubulin beta, Tubulin alpha, Tubulin (in microtubules), Caveolin-1	Tubulin beta, Tubulin alpha, Tubulin (in microtubules)
Cytoskeleton remodelling-substance p mediated membrane blebbing	MLCP (cat), Tubulin alpha, Tubulin (in microtubules)	MLCP (cat), Tubulin alpha, MRLC, Tubulin (in microtubules)
Apoptosis and survival-granzyme a signalling	Histone H1, Lamin A/C	Ku70/80, Ku80, Histone H2B, NDUFS3, Ku70
Cytoskeleton remodelling-keratin filaments	Plectin 1, Tubulin beta, Vimentin, Tubulin alpha, Tubulin (in microtubules)	Plectin 1, Tubulin beta, Tubulin alpha, Tubulin (in microtubules)
Translation-regulation of translation initiation	eIF4G1/3, PABPC1, PABPC4, eIF3S8, RPS6	eIF4A, eIF4G1/3, eIF4E, PABPC1, PABPC4
Cytoskeleton remodelling-neurofilaments	Plectin 1, Tubulin beta, Vimentin, Tubulin alpha, Tubulin (in microtubules)	Plectin 1, Tubulin beta, Tubulin alpha, Tubulin (in microtubules)
Inhibition of remyelination in multiple sclerosis	PCBP-1, hnRNP A2, MLCP (cat), Tubulin beta, Tubulin alpha, Tubulin (in microtubules)	MLCP (cat), Tubulin beta, Tubulin alpha, PCBP-1, MRLC, Tubulin (in microtubules)
Cytoskeleton remodelling -Rho GTPases	Cortactin, MLCP (cat), MyHC, Filamin A, Spectrin	Alpha-actinin, MLCP (cat), Talin, RhoC, RhoA-related, Filamin A, MRLC, MyHC
Signal transduction-angiotensin II signalling via β-arrestin	Clathrin heavy chain, MLCP (cat), Clathrin	Clathrin heavy chain, MLCP (cat), ARF6, p90Rsk, MRLC, eIF4E,

		p23 co-chaperone, 14-3-3
Neurophysiological process-GABA-a receptor life cycle	Clathrin heavy chain, Dynein 1, cytoplasmic, heavy chain, Clathrin light chain, Clathrin, Tubulin (in microtubules), PP1-cat	Clathrin heavy chain, Tubulin (in microtubules), PP1-cat
Development-oligodendrocyte differentiation and myelination	PCBP-1, hnRNP A2, Cortactin, MLCP (cat), MAP4, Tubulin beta, Tubulin alpha, Tubulin (in microtubules), MAP-1B	MLCP (cat), Tubulin beta, Tubulin alpha, PCBP-1, MRLC, Tubulin (in microtubules)

Table 5.3 Upregulated pathway maps enriched in AAPH and rotenone treated U-87MG secretomes. *U-87MG cells were treated with AAPH or rotenone for 24 hours, media was then collected and analysed using mass spectrometry. Using differentially identified proteins upregulated by AAPH or rotenone pathways were subsequently enriched using MetaCore*

secretome Pathway Map Enrichments	Proteins upregulated by AAPH in pathway	Proteins upregulated by rotenone in pathway
Immune response-MHC class II: presentation	Tubulin (in microtubules), Rab-7, RhoA	Cathepsin L, Tubulin (in microtubules)
Immune response-MHC class I: cross-presentation	HSP70, Rab-7	HSP70, HSP60, Cathepsin L, VCP
Cell adhesion-integrin-mediated cell adhesion and migration	MLCP (cat), RhoA	MRLC, Alpha-actinin, MyHC
Development-mag-dependent inhibition of neurite outgrowth	MLCP (cat), RhoA	MRLC, Reticulon 4, MyHC
Inhibitory action of lipoxins on IL-8- and leukotriene B4-induced neutrophil migration	MLCP (cat)	MRLC, Alpha-actinin, Actin
Immune response -CCR3 signalling in eosinophils	MLCP (cat), RhoA	MRLC, Profilin, Profilin I, MyHC
Apoptosis and survival-NGF/TRKA PI3K-mediated signalling	MLCP (cat), Tubulin (in microtubules), RhoA	MRLC, Tubulin (in microtubules), MSN (moesin)
Neurophysiological process-dynein-dynactin motor complex in axonal transport in neurons	Vimentin, Tubulin (in microtubules), Rab-7	Tubulin (in microtubules)
Immune response- MHC class I: classical pathway	GANAB, Beta-2-microglobulin, HSP70	GANAB, PDIA3, HSP70
Neurophysiological process-receptor mediated axon growth repulsion	CRMP2, Tubulin (in microtubules), RhoA	CRMP2, Tubulin (in microtubules)
Neurophysiological process-gaba-a receptor life cycle	Clathrin heavy chain, Tubulin (in microtubules), PP1-cat	Clathrin heavy chain, Tubulin (in microtubules)
Cell adhesion-interruption of cell barrier integrity	MLCP (cat), RhoA	MRLC, Alpha-actinin
Apoptosis and survival-granzyme a signalling	MLCP (cat), Tubulin (in microtubules), RhoA	MRLC, Tubulin (in microtubules), MSN (moesin)

Cell adhesion-gap junctions	Tubulin alpha, Tubulin beta, Tubulin (in microtubules)	Tubulin alpha, Tubulin beta, Tubulin (in microtubules), Actin
Regulation of actin cytoskeleton organization by kinase effectors of rho gtpases	MLCP (cat), RhoA-related, Spectrin, RhoA	MRLC, Alpha-actinin, ERM proteins, MyHC, MSN (moesin)
Calcium signalling	FKBP12, CD44, PP1-cat, RhoA	FKBP12
LRRK2 in neurons in parkinson's disease	Clathrin heavy chain, Tubulin (in microtubules)	eEF1A, Clathrin heavy chain, Tubulin (in microtubules), 14-3-3, MSN (moesin)
Regulation of cytoskeleton proteins in oligodendrocyte differentiation and myelination	MLCP (cat), Tubulin alpha, Tubulin beta, Tubulin (in microtubules), RhoA	MRLC, Tubulin alpha, Tubulin beta, Tubulin (in microtubules)
Inhibition of remyelination in multiple sclerosis	MLCP (cat), Tubulin alpha, Tubulin beta, Tubulin (in microtubules), RhoA	MRLC, Tubulin alpha, Tubulin beta, Tubulin (in microtubules)
Cytoskeleton remodelling-neurofilaments	Plectin 1, Tubulin alpha, Tubulin beta, Vimentin, Tubulin (in microtubules)	Tubulin alpha, Tubulin beta, Tubulin (in microtubules)

Table 5.4 Downregulated pathway maps enriched in AAPH and rotenone treated U-87MG secretomes. *U-87MG cells were treated with AAPH or rotenone for 24 hours, media was then collected and analysed using mass spectrometry. Using differentially identified proteins downregulated by AAPH or rotenone pathways were subsequently enriched using MetaCore*

Secretome Pathway Map Enrichments	Proteins Downregulated by AAPH in pathway	Proteins downregulated by rotenone in pathway
Apoptosis and survival-TNF-α-induced caspase-8 signalling	Cathepsin D	HSP90, Cathepsin B
Immune reponse-MIF in innate immunity response	MIF	MIF, IL-8
Immune response-IL-1 signalling pathway	HSP27	HSP27, CD44, IL-8
Cytoskelelton remodelling-neurofilaments	Tubulin beta	Plectin 1, Tubulin beta
Immune response-MIF-mediated glucocorticoid regulation	MIF	MIF, CD44, IL-8
Regulation of caspase activity in Huntington's disease	HSP27, HSP70	HSP90, HSP27, HSP70
Apoptosis and survival-FAS signalling cascades	Lamin A/C, HSP27	HSP27, Lamin A/C
Cytoskeleton remodelling-integrin outside-in signalling	Filamin A	Fibronectin, Talin, Filamin A
Immune response-MIF-induced cell adhesion, migration and angiogenesis	MIF	MIF, CD44, IL-8
Cell adhesion-integrin-mediated cell adhesion and migration	MyHC	Fibronectin, MLCP (cat), Talin
Cytoskelton remodelling-keratin filaments	Tubulin beta, Keratin 14	Plectin 1, Tubulin beta

WNT signalling in invasive-type melanoma cells	Filamin A, Filamin-A (CTF)	Filamin-A (CTF), CD44, MMP-2, Filamin A
Transcription-HIF1 targets	LDHA, ENO1, TGM2	LOXL2, PAI1, MMP-2
HSP70 and HSP40-dependent folding in Huntington's disease	HSP27, Cathepsin D HSP70	HSP90, HSP27 HSP70
Cell adhesion-α-4-integrins in cell migration and adhesion	Filamin A	Fibronectin, ITGB1, Filamin A
Apoptosis and survival-granzyme A signalling	Lamin A/C, Histone H1	Ku80, Lamin A/C, HMG2
Possible regulation of HSF1/ chaperone pathway in Huntington's disease	HSP27	HSP90, HSP27, p23 co-chaperone
Cell adhesion-role of tetraspanins in integrin-mediated cell adhesion	Filamin A	Fibronectin, ITGB1, Talin, Filamin A
CHDI-correlation from replication data-cytoskeleton and adhesion module	MyHC	Fibronectin, MLCP (cat), Plasminogen, Talin, Plasmin
Immune reponse-alternative complement pathway	Annexin II	C3b, C3dg, C3a, C3, Factor I, C3c, Clusterin, iC3b

A number of protein clusters were identified by STRING analysis from mass spectrometry data. Interestingly U-87MG lysates treated with both AAPH and rotenone resulted in downregulation of proteins associated with mRNA metabolic processing (figure 5.16 and 5.18). Furthermore, clusters identified cytoskeleton organisation was downregulated in both U-87MG lysates treated with AAPH or rotenone (figure 5.16 and 5.18), where different tubulins were affected. Of note, rotenone treatment resulted in mitochondrial gene associated proteins and those involved in mitochondrial organisation being downregulated (figure 5.18), which was not observed with AAP, suggesting specific RS have different effects. Further highlighting this AAPH resulted in proteins associated with lipid metabolism being upregulated potentially to combat lipid peroxidation induced by AAPH (figure 5.17). Both AAPH and rotenone treatment of U-87MG resulted in upregulated of secretion and vesicle mediated transport (figure 5.17 and 5.19), suggesting despite different RS there are some common processes affected. Furthermore, a greater number of proteins were downregulated by AAPH and rotenone than upregulated with more proteins identified from rotenone treatment (figure 5.16-5.19).

STRING analysis of proteins identified by mass spectrometry in AAPH and rotenone treated U-87MG secretomes demonstrates how less proteins were discovered. Of note from cluster analysis are that proteins associated with nitrogen processes were both downregulated and upregulated in U-87MG secretomes treated with AAPH (figure 5.20), potentially to combat nitrogen induced stress from AAPH. In contrast, rotenone resulted in more proteins associated with nitrogen processes only being upregulated in the secretome (figure 5.23), suggesting they can spare these and thus secrete them.

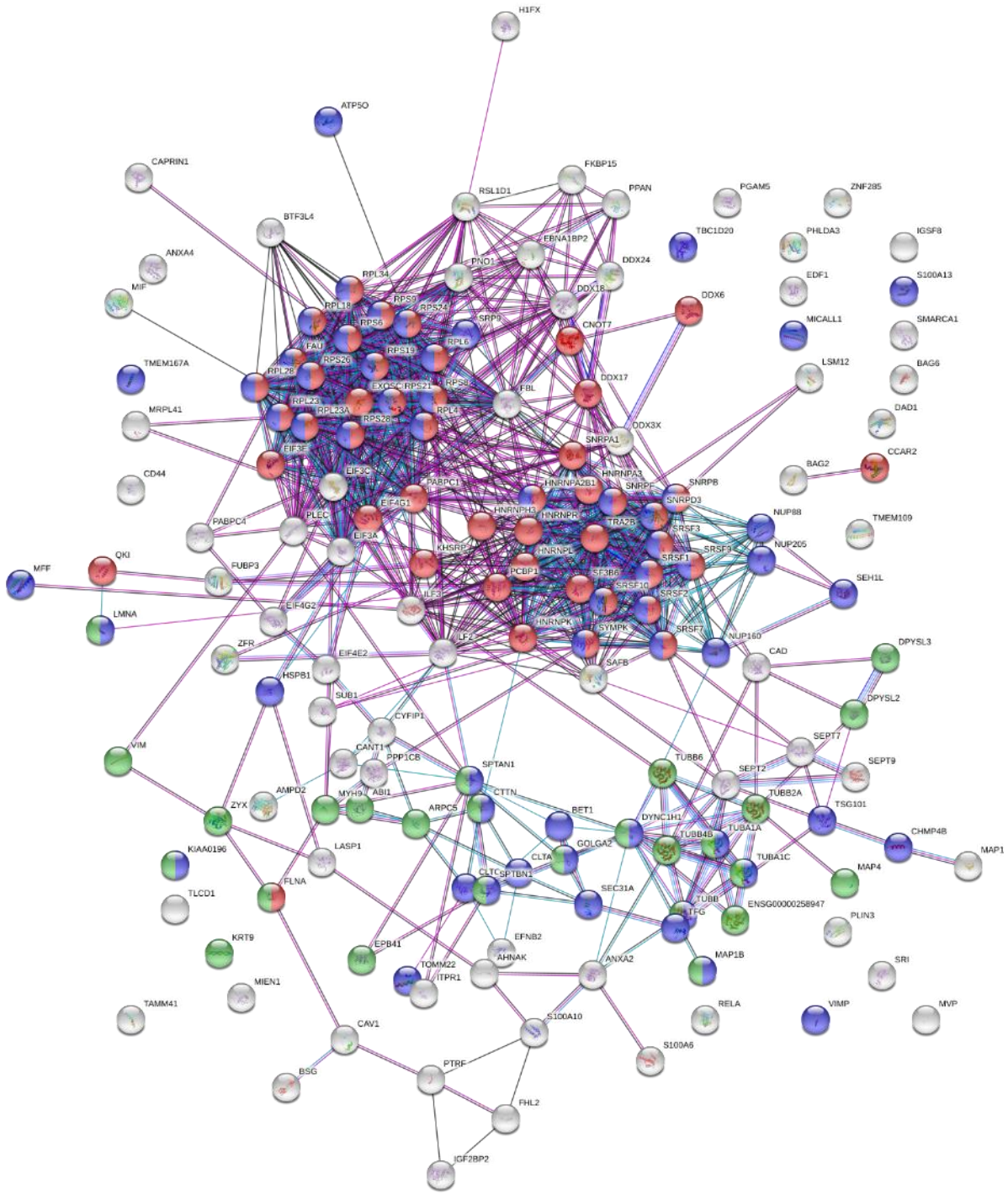

Figure 5.16 STRING analysis of downregulated proteins identified from mass spectrometry of U-87MG lysates treated with AAPH. *Proteins were clustered based on enrichment of GO biological processes. The nodes represent individual proteins, which are linked by coloured lines representing a category of interaction (purple: experiments, light blue: databases, dark blue: gene co-currence, black: co-expression). These interactions are based on the predicted and known protein information held within the database. Coloured nodes represent proteins associated with red: mRNA metabolic processing, blue: intercellular transport, and green: cytoskeleton organisation.*

Additionally from looking at the protein clusters rotenone treatment appears to result in downregulation of proteins associated with cell adhesion and process development (figure 5.22), which was not observed with AAPH treat U-87MG secretomes, where process development even increased in AAPH secretomes (figure 5.20).

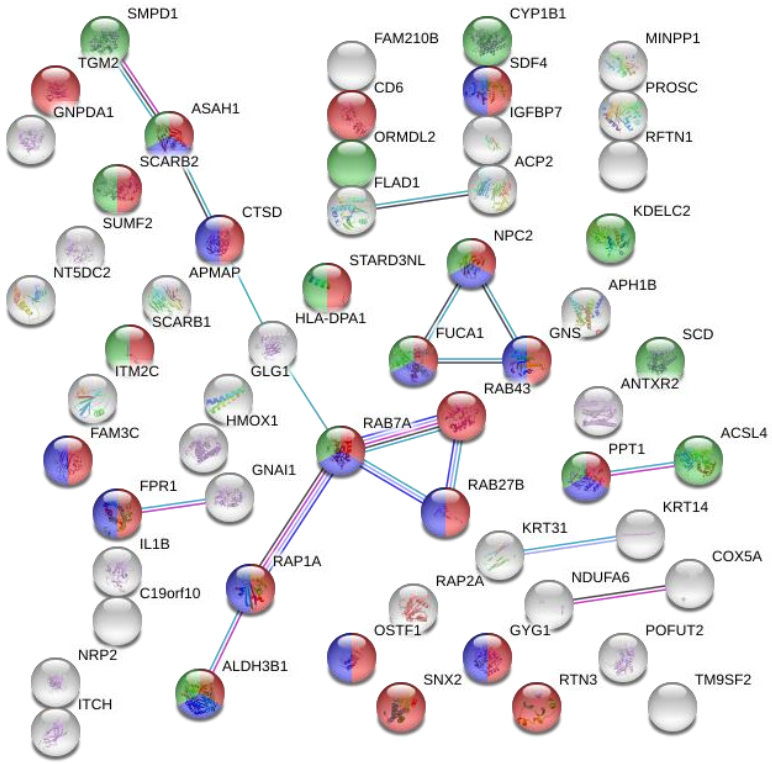

Figure 5.17 STRING analysis of upregulated proteins identified from mass spectrometry of U-87MG lysates treated with AAPH. *Proteins were clustered based on enrichment of GO biological processes. The nodes represent individual proteins, which are linked by coloured lines representing a category of interaction (purple: experiments, light blue: databases, dark blue: gene co-currence, black: co-expression). These interactions are based on the predicted and known protein information held within the database. Coloured nodes represent proteins associated with red: vesicle mediated transport, blue: secretion, and green: lipid metabolic processes.*

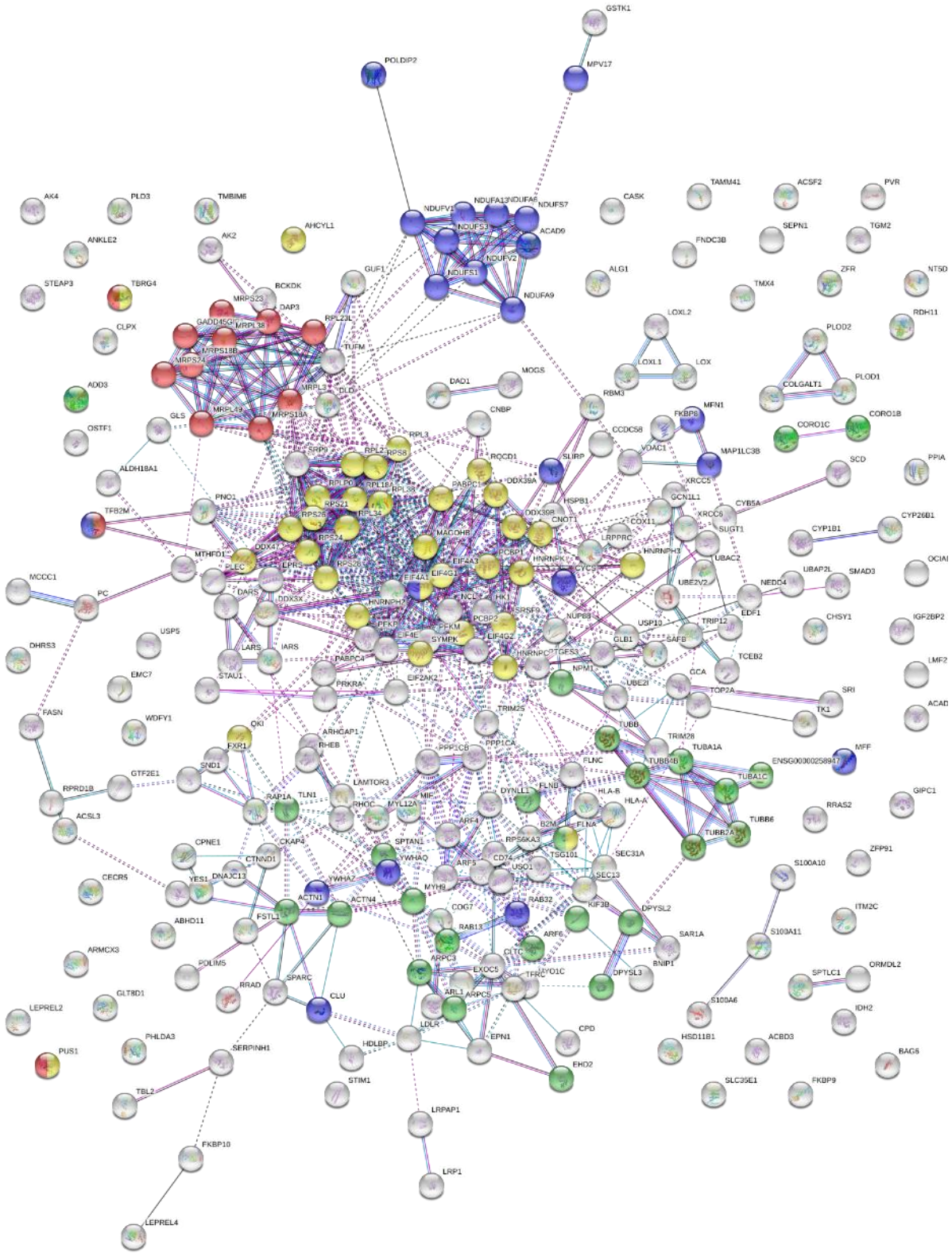

Figure 5.18 STRING analysis of downregulated proteins identified from mass spectrometry of U-87MG lysates treated with rotenone. *Proteins were clustered based on enrichment of GO biological processes. The nodes represent individual proteins, which are linked by coloured lines representing a category of interaction (purple: experiments, light blue: databases, dark blue: gene co-currence, black: co-expression). These interactions are based on the predicted and known protein information held within the database. Coloured nodes represent proteins associated with red: proteins associated with mitochondrial genes, blue: mitochondrial organisation, green: cytoskeleton organisation and yellow: mRNA metabolic processing.*

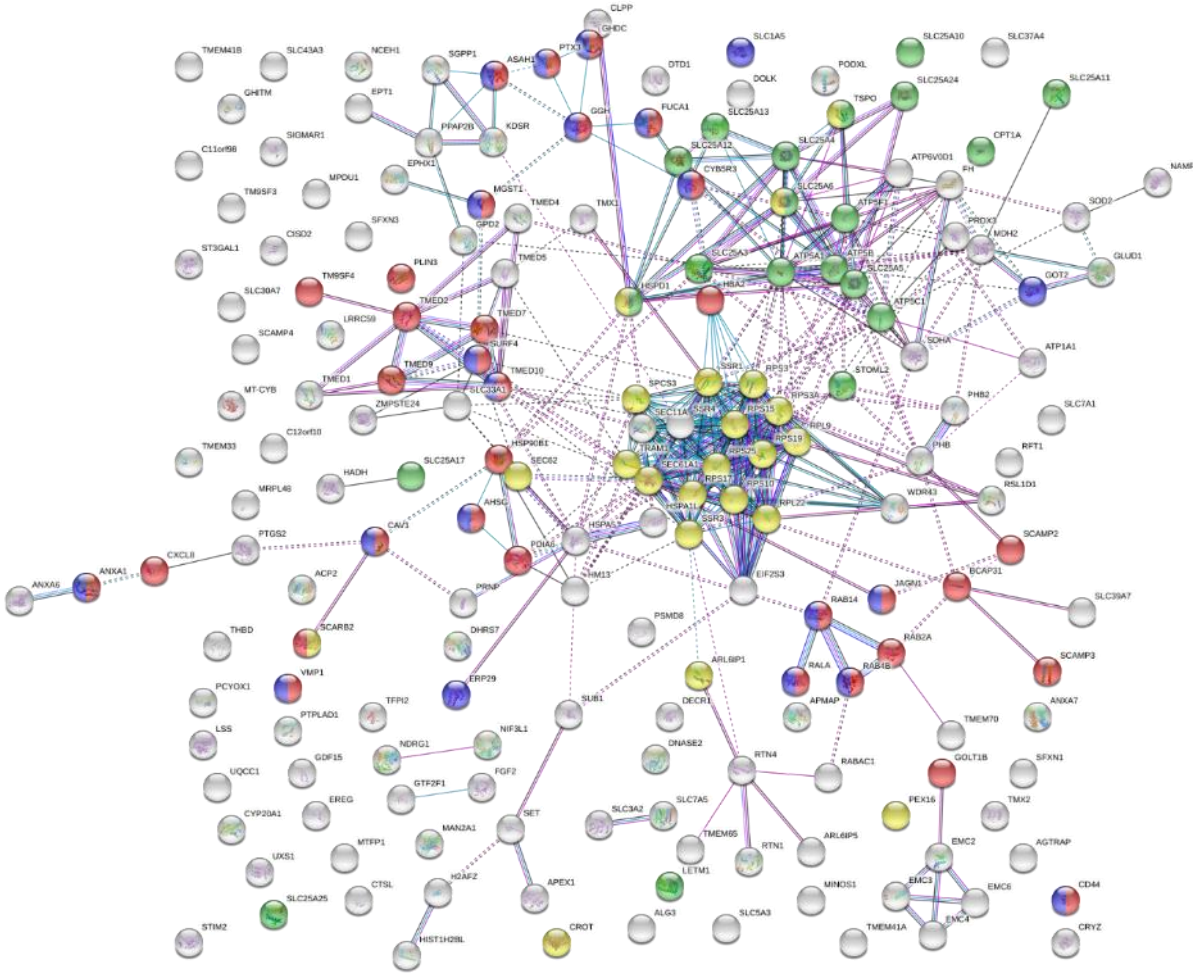

Figure 5.19 STRING analysis of upregulated proteins identified from mass spectrometry of U-87MG lysates treated with rotenone. *Proteins were clustered based on enrichment of GO biological processes. The nodes represent individual proteins, which are linked by coloured lines representing a category of interaction (purple: experiments, light blue: databases, dark blue: gene co-currence, black: co-expression). These interactions are based on the predicted and known protein information held within the database. Coloured nodes represent proteins associated with red: vesicle mediated transport, blue: secretion, green: mitochondrial transport and yellow: protein targeting.*

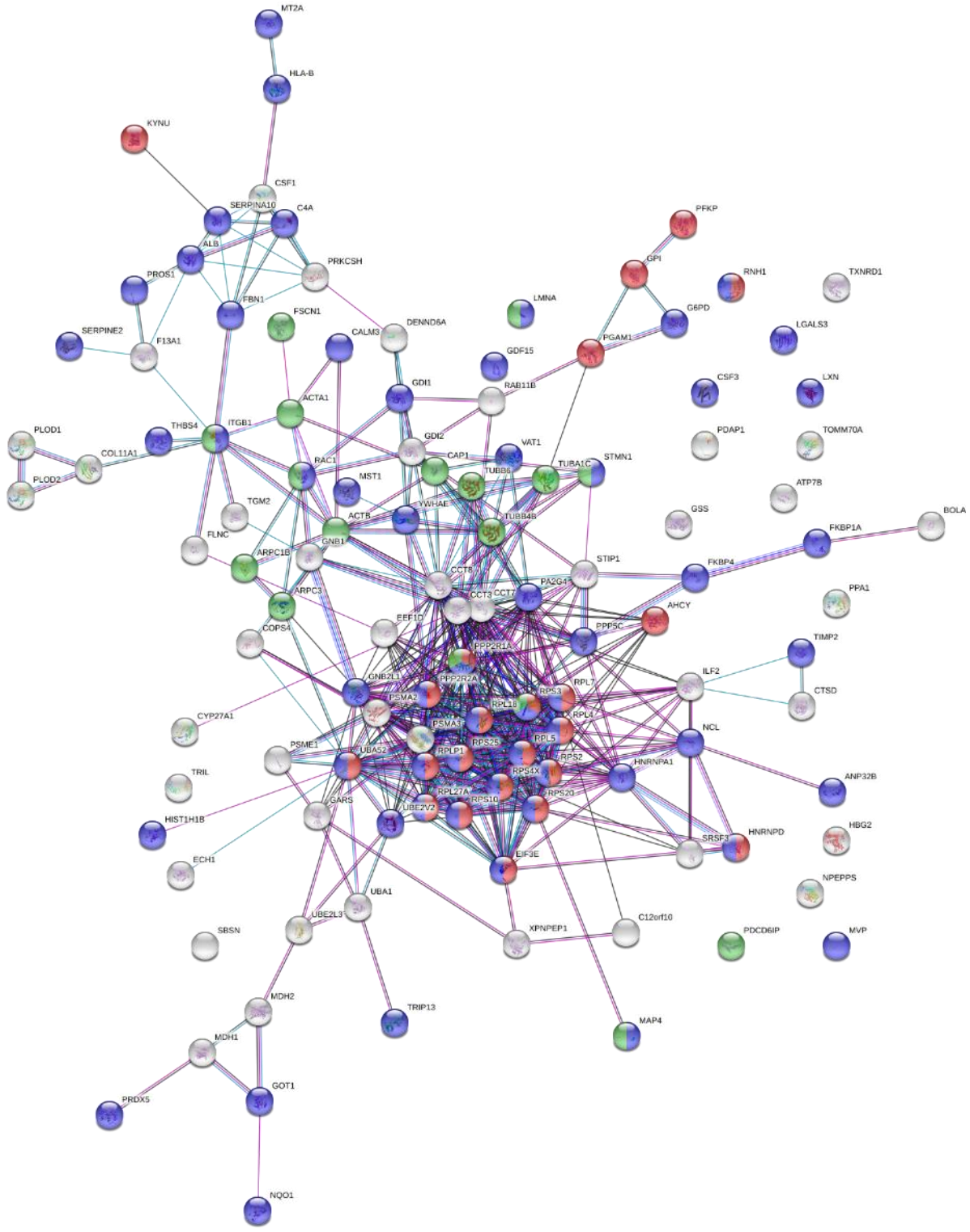

Figure 5.20 STRING analysis of downregulated proteins identified from mass spectrometry of U-87MG secretomes treated with AAPH. *Proteins were clustered based on enrichment of GO biological processes. The nodes represent individual proteins, which are linked by coloured lines representing a category of interaction (purple: experiments, light blue: databases, dark blue: gene co-currence, black: co-expression). These interactions are based on the predicted and known protein information held within the database. Coloured nodes represent proteins associated with red: nitrogen processes, blue: negative regulation of processes, green: cytoskeleton organisation.*

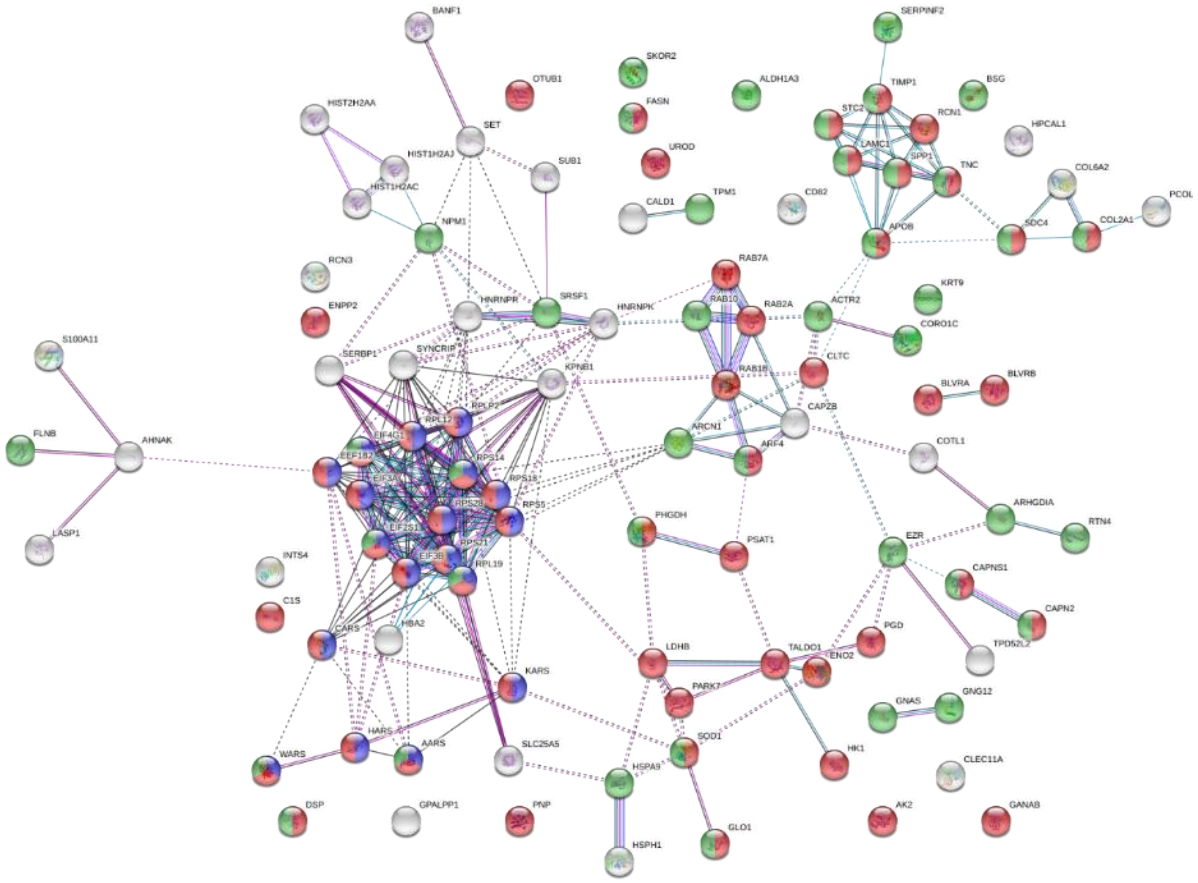

Figure 5.21 STRING analysis of upregulated proteins identified from mass spectrometry of U-87MG secretomes treated with AAPH. *Proteins were clustered based on enrichment of GO biological processes. The nodes represent individual proteins, which are linked by coloured lines representing a category of interaction (purple: experiments, light blue: databases, dark blue: gene co-currence, black: co-expression). These interactions are based on the predicted and known protein information held within the database. Coloured nodes represent proteins associated with red: nitrogen processes, blue: translation, green: process development.*

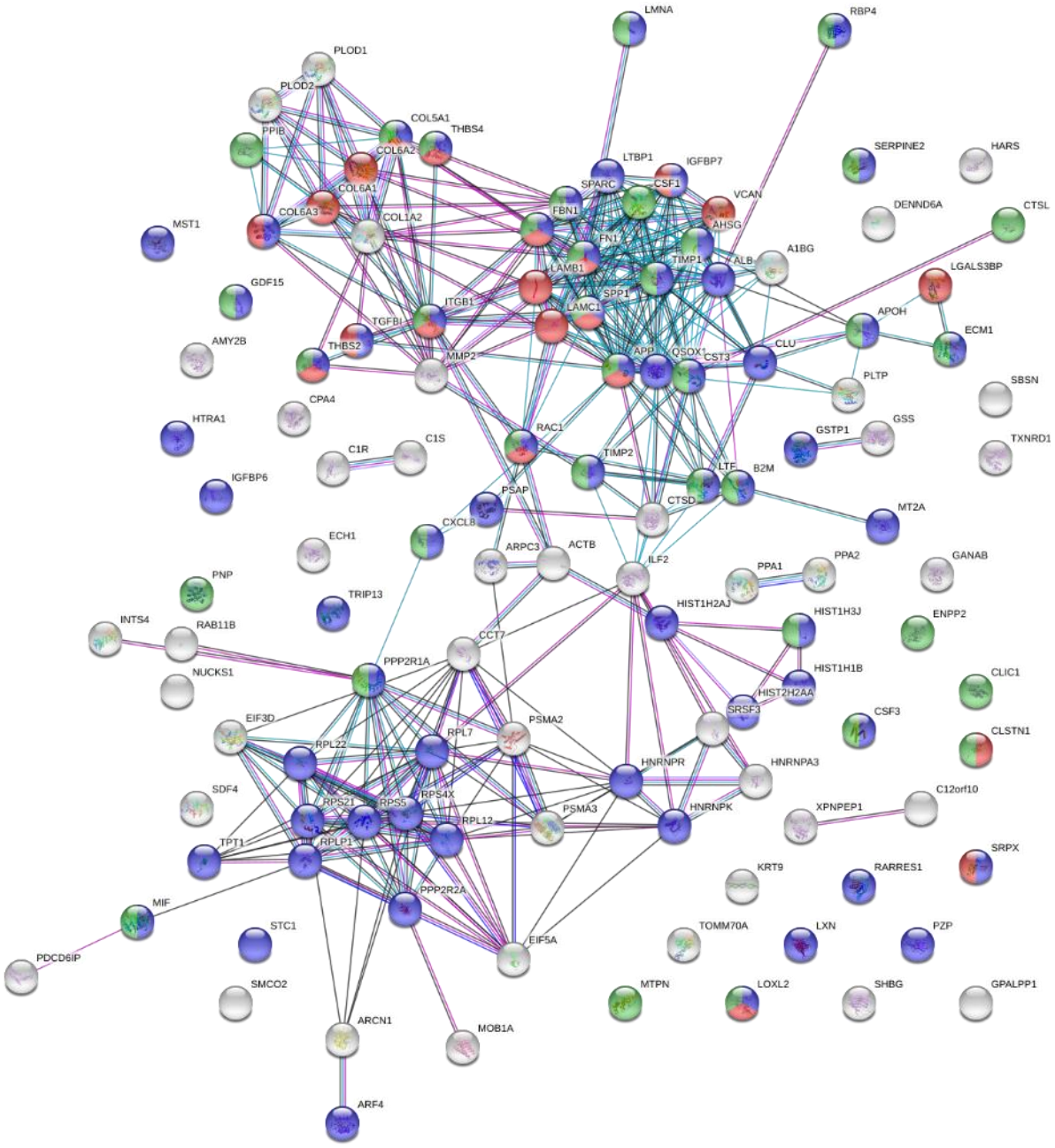

Figure 5.22 STRING analysis of downregulated proteins identified from mass spectrometry of U-87MG secretomes treated with rotenone. *Proteins were clustered based on enrichment of GO biological processes. The nodes represent individual proteins, which are linked by coloured lines representing a category of interaction (purple: experiments, light blue: databases, dark blue: gene co-currence, black: co-expression). These interactions are based on the predicted and known protein information held within the database. Coloured nodes represent proteins associated with red: cell adhesion, blue: process development, green: negative regulation of biological processes.*

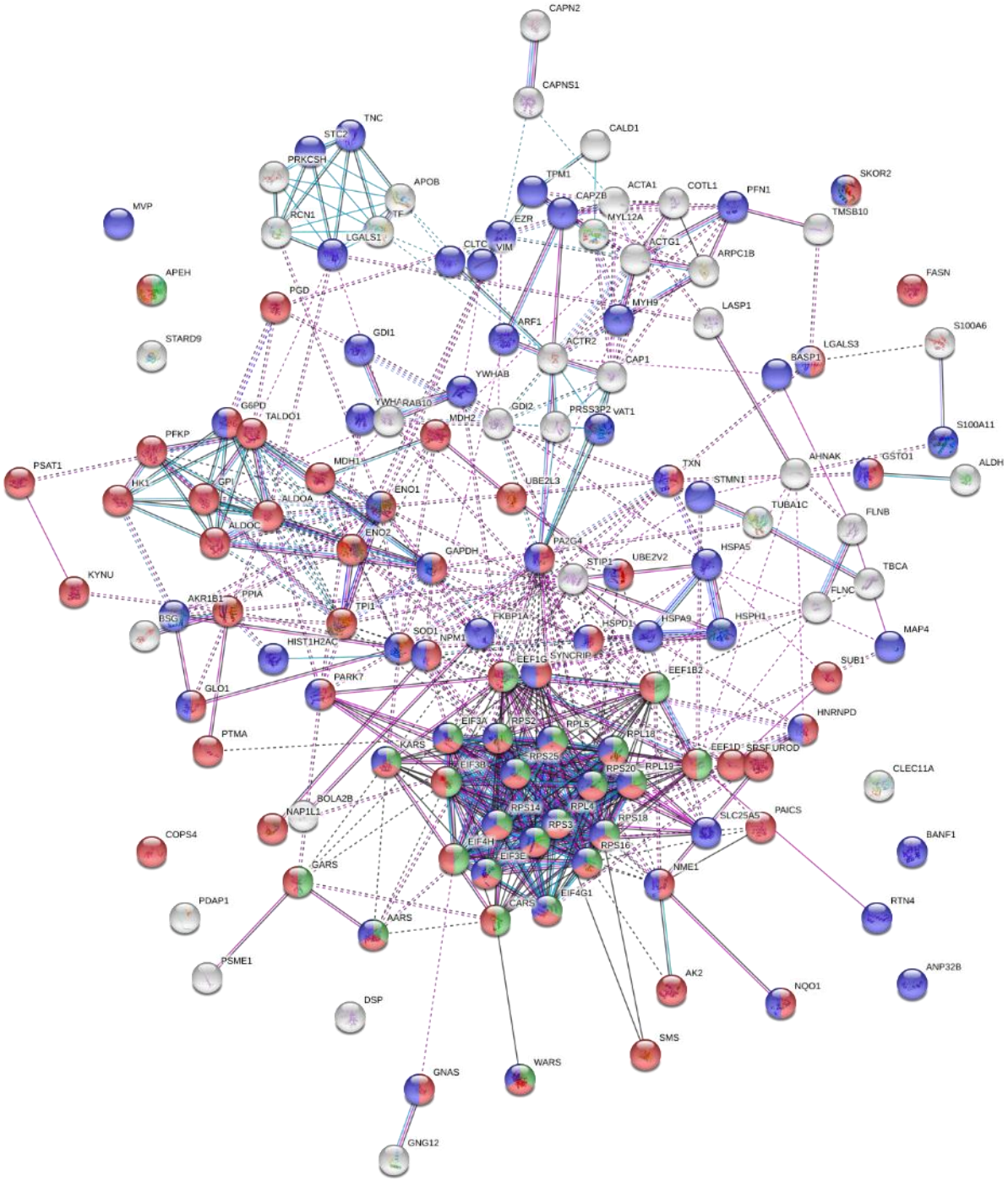

Figure 5.23 STRING analysis of upregulated proteins identified from mass spectrometry of U-87MG secretomes treated with rotenone. *Proteins were clustered based on enrichment of GO biological processes. The nodes represent individual proteins, which are linked by coloured lines representing a category of interaction (purple: experiments, light blue: databases, dark blue: gene co-currence, black: co-expression). These interactions are based on the predicted and known protein information held within the database. Coloured nodes represent proteins associated with red: nitrogen processes, blue: negative regulation of processes, green: translation.*

Western blot analysis confirmed mass spectrometry observations where HSP70 increased as a result of AAPH and rotenone treatment while HSP27 (referred to as heat shock protein β1 in mass spectrometry data) decreased (figure 5.24) and was used to validate the mass spectrometry findings.

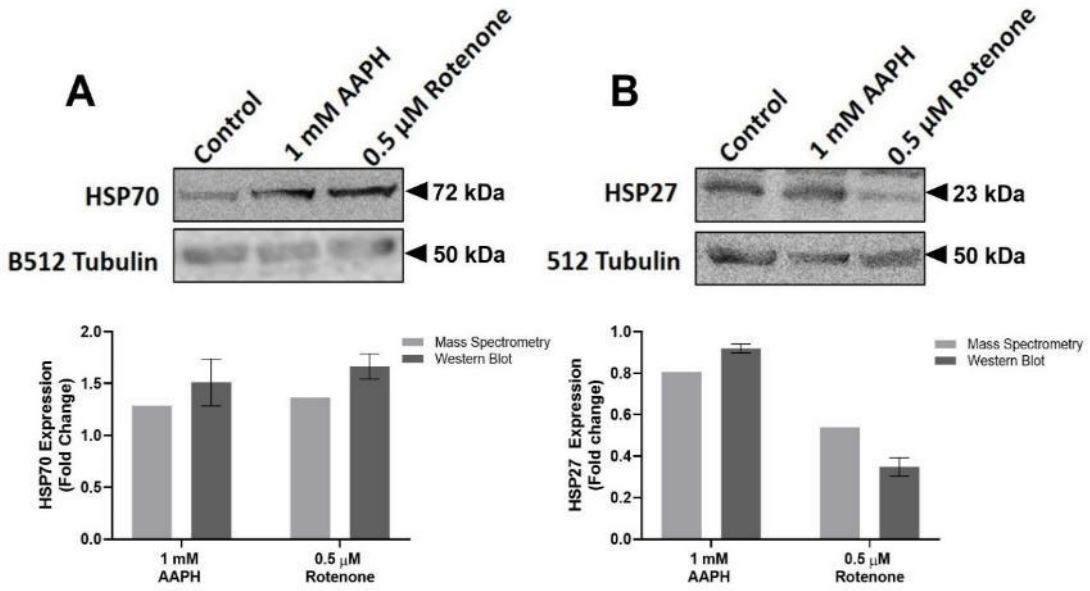

Figure 5.24 Western blot validation of mass spectrometry. *Representative Western blot of differentiated glial U-87MG total cell extracts were probed with (A) HSP70 (1:1000) or (B) HSP27 (1:1000) after treatment with either 1 mM AAPH or 0.5 µM rotenone for 48 hours following 5 day differentiation (0.5% (v/v) FBS, 10 µM retinoic acid). Each Western blot is accompanied by a plot summarising densitometric analyses of Western blots using AIDA software. Results are presents as fold change against control ± SEM.*

Furthermore, post-translational modification identification following mass spectrometry using the statistical software PEAKS via peptide fragmentation, demonstrates that AAPH and rotenone induced a significant number of oxidative modifications on differentially identified proteins for both U-87MG lysates and secretomes (figure 5.25A and B, respectively). Interestingly, the average number of oxidative modifications in lysates was greater with rotenone treatment. However, in the secretome AAPH showed the highest oxidative modifications. PEAKS analysis also highlighted a greater number of malondialdehyde (MDA) adducts, a by-product of lipid peroxidation for AAPH treatment in both U-87MG lysates and secretomes (figure 5.25C and D, respectively). Thus, supporting the idea that AAPH results in greater lipid peroxidation than rotenone. Together, these results suggest that while both AAPH and rotenone induce OS the RS they generate induce different pathways, which may explain the morphological differences observed when SH-SY5Y neuronal cells were treated with AAPH and rotenone conditioned U-87MG media.

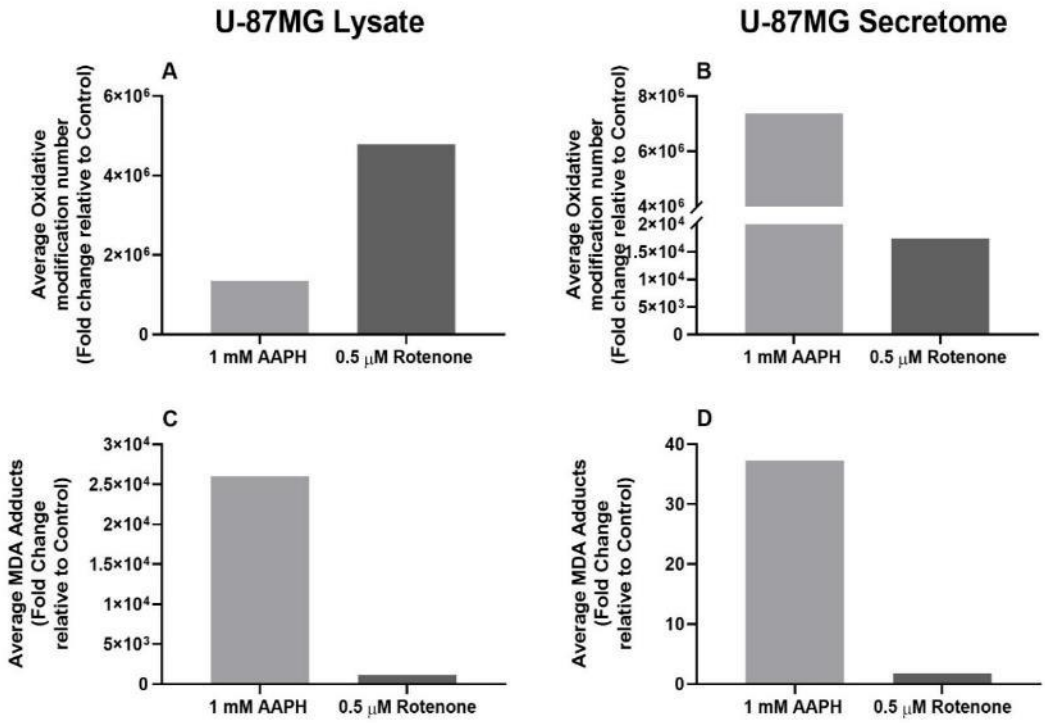

Figure 5.25 Post-translational modifications identified using the PEAKS software on both U-87MG lysates and secretomes that have been treated with AAPH or rotenone. *U-87MG glial cells were differentiated over 5 days (0.5% (v/v) FBS, 10 µM retinoic acid) and then treated with 1 mM AAPH or 0.5 µM rotenone for 48 hours where lysates and secretomes were analysed via mass spectrometry. Subsequently, the statistical search engine PEAKS was used to identify post-translational modifications. The average number of oxidative modifications was then calculated for both U-87MG lysates (A) and secretomes (B). The average number of malondialdehyde (MDA) adducts was also determined for U-87MG lysates (C) and secretomes (D).*

5.3 DISCUSSION

Over recent years intercellular communication has been receiving more attention to aid pathology understanding. However, the interactions between glia and neurons in neurodegenerative diseases still needs further investigation. Currently, generating co-cultures is difficult and involves cells brought together via contact or non-contact means. Initially, we attempted to create a 1:1 contact co-culture by combining cells suspensions prior to seeding (Jiang et al., 2005). While co-cultures of SH-SY5Y and U-87MG cells showed greater viability when treated with AAPH relative to SH-SY5Y monocultures, rotenone treatment resulted in similar viability. However, as previous viability studies show AAPH induced proliferation in U-87MG cells it is unknown whether the higher viability is because U-87MG cells within the co-culture proliferate, while SH-SY5Y cells underwent cell death. As such, we attempted to determine the ratio of neurons to glia using immunofluorescent staining. Unfortunately, this was unsuccessful due to the shared expression of βIII-tubulin by SH-SY5Y and U-87MG cells (Katsetos et al., 2007; Wang and Liu, 2019) and thus, co-staining was unsuccessful for determining cell ratios. As such, future experiments would require cells to be stably transfected with an immunofluorescent tag or other markers for immunofluorescence would be needed.

With difficulties encountered with contact co-cultures, transwell inserts were used to investigate non-contact co-cultures. When using transwell inserts it is important to consider which insert to use. As we wanted to investigate secreted factors and feedback loops 0.4 µm pore sizes that allow soluble factor diffusion while preventing cell migration were utilised. However, due to the porous nature required for inserts companies tend to use PET due to their transparent properties, allowing phase microscopy visibility while not being collagen coated, which can be problematic with adherent cells making them optimal for morphological studies. However, as inserts are a different material from the polystyrene 24-well tissue culture plates this needed to be considered. Different cell types exhibit different cellular functions on different substrates including growth, proliferation, differentiation and adhesion that could affect results (Ventre and Netti, 2016; Wells, 2008).

Thus, initially co-cultures of SH-SY5Y neuronal and U-87MG glial cells were investigated, where each cell line was grown on either polystyrene 24-well plates or PET inserts. Of note, polystyrene has a Young's modulus of 3.2 GPa (Sultanova et al., 2009) while PET is much lower with 1.7 GPa (Li et al., 2001), suggesting polystyrene plates are a much harder surface than the PET membranes of inserts. As others have demonstrated, the results herein suggest SH-SY5Y neuronal and U-87MG glial cells have a morphological dependence on the culture material (Chemmarappally et al., 2020; Georges et al., 2006; Morçimen et al., 2019; Yeung et al., 2005). Indeed, SH-SY5Y neuronal cells appear to be able to grow on both polystyrene and PET surfaces, where improved membrane integrity was observed for

the softer PET insert surface consistent with previous findings (Balgude et al., 2001; Flanagan et al., 2002; Georges et al., 2006). In contrast, U-87MG glial cells struggled to grow on PET inserts displaying a more rounded morphology compared to their stellate counterparts in the polystyrene plates, similar to results with astrocytes on softer hydrogels (Georges et al., 2006). Thus, when investigating a co-culture between SH-SY5Y neuronal and U-87MG glial cells in the future the insert material needs to be considered as these cells show morphological dependence on cultivation material.

Investigating neurodegeneration is not limited to neuronal cells, with research addressing other neural cells including oligodendrocytes, microglia and astrocytes (Cunningham et al., 2019; Hickman et al., 2018; Philips and Rothstein, 2017). Astrocytes in particular, are suggested to be involved in neuroprotection against OS (Allaman et al., 2011; Drukarch et al., 1998; Vargas and Johnson, 2009). One of the main astrocytic mechanisms proposed in neuroprotection involves glutathione, which is higher in astrocytes than neurons (Alsayyah et al., 2019; Li et al., 2019; Makar et al., 2008). The results herein propose U-87MG glial cells protect neurons against specific RS as co-cultures show greater viability than their respective monocultures when treated with rotenone but not with AAPH. Looking at previous data we observed that rotenone upregulated glutathione in both SH-SY5Y neuronal and U-87MG glial cells but AAPH only upregulated glutathione levels in SH-SY5Y neuronal cells (figure 3.7). Glutathione is the primary cellular antioxidant against the RS nitric oxide, which can cause S-nitrosylation (Deng et al., 2018; Hogg et al., 1996). The results in chapter 4 support this as AAPH generated significantly more S-nitrosylation in AAPH treated U-87MG glia than rotenone (figure 4.48). This suggests greater levels of nitric oxide that can result in glutathione oxidation, leading to reduced antioxidant defence (Deng et al., 2018; Padgett and Whorton, 1998). Therefore, AAPH treatment of U-87MG cells may result in glutathione levels not being sufficient to support neurons against OS. In contrast, rotenone treated U-87MG exhibit greater levels of glutathione, which can be secreted into the extracellular space, where ectopeptidases can break glutathione down into its precursors; glycine and cysteine to be taken up by neurons thus, improving glutathione synthesis in neurons to combat RS (McBean, 2017; Sedlak et al., 2019).

Alternatively, glutathione may be reducing oxidised vitamin C from neurons releasing ascorbate back into the extracellular fluid for neurons to utilise (García-Krauss et al., 2016; Wilson, 1997). This may explain why co-cultures are effective against rotenone as we have previously shown that ascorbic acid was not effective at improving the viability of AAPH treated SH-SY5Y neuronal cells but was with rotenone treated cells, highlighting how different antioxidants are more effective against specific RS.

Therefore, while the results herein suggest U-87MG co-cultures are able to protect SH-SY5Y neurons against specific RS, the underlying mechanism is still not understood. To determine if U-87MG cells improve SH-SY5Y neuronal viability in response to rotenone via glutathione future studies could involve incubating U-87MG glial cells with buthionine sulfoximine, prior to treatment with rotenone. However, as glia struggle to grow on the soft insert material SH-SY5Y neuronal cells may have to be cultivated on inserts in future investigations.

With difficulties in creating co-cultures, a lot of research over the past decade has involved investigations into the secretome, further enhanced due to possible identification of biomarkers as diagnostic tools to identify neurodegenerative diseases before clinical symptoms arise, symbolising irreversible damage. Astrocytes are believed to be secretory cells able to release factors that mediate either neurotoxic or neuroprotective effects (Jha et al., 2018; Verkhratsky et al., 2016). Currently, most secretome analyses have used rodent models (Greco et al., 2010; Keene et al., 2009; Moore et al., 2009; Yin et al., 2012), however, murine astrocytes differ from human astrocytes (Y. Zhang et al., 2016). As such, immortalised and cancer cell lines are now being investigated to generate a catalogue of potential secreted proteins. The mass spectrometry results of the U-87MG glial secretome herein hope to add to the catalogue of proteins identified previously, in the hope of generating a more detailed proteome to infer the potential functions and pathways of secreted proteins.

Consistent with previous studies, we observed differential expression of common astrocytic secreted proteins including, vimentin, thrombospondin, fibronectin, cystatin, apolipoprotein E, extracellular SOD, SPARC, and metalloproteinase inhibitors (supplementary table 8.2; Greco et al., 2010; Keene et al., 2009; Lafon-Cazal et al., 2003; Moore et al., 2009; Yin et al., 2012). This highlights that while the results herein are from a human glioblastoma cell line some secreted proteins are the same as those secreted by murine astrocytes, supporting the use of immortalised cell lines for secretome analysis.

Proteins secreted by astrocytes under OS could be grouped into proteins effecting the ECM and those effecting neuronal homeostasis including neuroinflammation (as also seen in Jha *et al,* 2018). From pathway enrichment analysis using MetaCore, the majority of the downregulated pathways in AAPH and rotenone treated U-87MG glial lysates and secretomes were involved in cell adhesion (figure 5.14 and 5.15). Fibronectin and metalloproteinase inhibitors were some of the proteins downregulated possibly contributing to decreased cell adhesion pathways being enriched. Fibronectin, an ECM protein is involved in adhesion but also in regulating intercellular diffusion signalling by modulating the ECM (Wang et al., 2013), alongside having anti-inflammatory properties (Lin et al., 2012; Tsuda et al., 2008). As others have demonstrated the results included here suggest

OS downregulates fibronectin as rotenone treated U-87MG conditioned media exhibited lower levels of fibronectin (Allani et al., 2004), but increased in AAPH treated U-87MG conditioned media relative to the control. This possibly leads to reduced cell adhesion that could explain the glial clustering, cell rounding, and apoptosis observed in rotenone treatment. Additionally, rotenone U-87MG conditioned media also resulted in reduced SH-SY5Y viability, possibly due to decreased fibronectin levels leading to the ECM preventing signalling between neurons, or the presence of less anti-inflammatory mediators. These results suggest specific RS effect U-87MG glial secretome protein levels altering the ECM.

Under normal conditions within the ECM metalloproteinases are inhibited however astrocytic metalloproteinases can be activated by OS (Gottschall and Deb, 1996; Gottschall and Yu, 2002; Latronico et al., 2018). Our results suggest RS from both AAPH and rotenone result in metalloproteinase inhibitors being downregulated in both the secretomes and lysates relative to controls. As metalloproteinases are involved in ECM degradation (Levin et al., 2017) downregulation of the inhibitors would lead to their activation and subsequent disruption of the ECM, possibly explaining the neuronal degeneration observed as others have reported (Brkic et al., 2015; Cunningham et al., 2005; Sadeghian et al., 2012).

The results within suggest not only do different RS induce secretome changes that affect neuronal viability but also morphology, as rotenone U-87MG conditioned media culture conditions exhibited cuboidal morphology and lack of processes. Filamin A is an actin cross-linker involved in dendrites, where stable filamin A regulates dendritic morphogenesis (Zhang et al., 2014), axonal growth cones (Zheng et al., 2011) and neuronal migration (Sarkisian et al., 2006). Thus, the downregulation of filamin A in rotenone treated U-87MG cells and secretomes may explain the lack of processes. Furthermore, enrichment analysis highlighted the WNT-signalling pathway was downregulated in both rotenone treated U-87MG lysates and secretomes. This supports previous studies who suggest the WNT-signalling pathway plays a role in neuronal survival, axonal extension and synapse formation; where astrocytes may be involved in this through the secretome (Ciani and Salinas, 2005; F. L'Episcopo et al., 2011; Maiese et al., 2008; Marchetti et al., 2013; Patapoutian and Reichardt, 2000). Lower levels of WNT-signalling may explain the decreased neuronal viability as neuronal apoptosis may be triggered by GSK-3β as has been shown with other neurotoxins such as 6-OHDA, rotenone and MPTP/MPP^+ in SH-SY5Y and PC12 *in vitro* studies (Petit-Paitel et al., 2009; W. Wang et al., 2007). Further reinforcing the astrocyte secretome may play a role in this behaviour is highlighted by L'Episcopo *et al.,* who show WNT knockdown in astrocytes resulted in decreased tyrosine hydroxylase positive neuronal viability relative to control astrocyte co-cultures (L'Episcopo et

al., 2011). Together, this suggests OS affects adhesion directly via the ECM and secreted factors that can also determine neuronal morphology.

The results herein also suggest homestasis was affected as AAPH and rotenone resulted in downregulation of HSP70 and HSP90 in the U-87MG secretome, which are primary chaperones involved in protein folding (supplementary table 8.2; Lackie et al., 2017; Verkhratsky et al., 2016). Recently, HSP70 has been reported to be secreted in glial media via exosomes (Kowal et al., 2016). However, as the glia within this study were subjected to OS they may have retained HSP70 and HSP90 in an attempt to combat OS. This suggests glia under OS do not provide as many supportive factors to neurons and thus, are not neuroprotective against stress and therefore may have a neurotoxic effect instead.

Further suggesting rotenone conditioned U-87MG media induced greater stress than AAPH conditioned U-87MG media relative to the control, neuroinflammation appeared to be induced. This was suggested by the enrichment analysis highlighting MHC-I and II pathways being in the top 50 (figure 5.14 and 5.15). This supports previous observations of MHC-1 presentation observed in astrocytes of neurodegenerative diseases (Hinkle et al., 2019; Höftberger et al., 2004; Sorrentino et al., 2019). This suggests pro-inflammatory and anti-inflammatory factors (Arbore et al., 2017) have been stimulated in the U-87MG cells and secretomes as a result of OS.

Mass spectrometry while highlighting new pathways such as inflammation, the ECM and chaperones as potential mechanisms that play a role in the secretome affecting neurons, also confirmed previous observations and hypotheses. As mentioned previously, we hypothesise the hallmarks of neurodegeneration: mitochondrial dysfunction, protein degradation and OS are not independent but are linked in what we refer to as the “neurodegenerative Bermuda triangle”. Pathways enrichment highlighted mitochondrial dysfunction and changes to chaperone proteins such as HSP70 and HSP90 accompanied by increased oxidative modifications, this supports our hypothesis. Furthermore, AAPH is recognised as a peroxyl generator (Bassett et al., 1999; Terao and Niki, 1986; Werber et al., 2011) and thus, we proposed it could be used as a more specific RS generator to investigate lipid peroxidation. PTM analysis using PEAKs further supported results in chapter 4, where AAPH generated a larger average of MDA adducts, a by-product of lipid peroxidation (Esterbauer et al., 1991; Gaschler and Stockwell, 2017), suggesting the RS generated by AAPH resulted in greater lipid peroxidation than rotenone.

In conclusion, co-cultures remain difficult to investigate with multiple methods being utilised herein. Contact co-cultures are one procedure that can be exploited but for future investigations, immunofluorescent tagging would aid in determining cell ratios as it is difficult to determine each

cell types contribution, and if the observations are due to cell ratio or feedback between the cells. Transwell inserts allow these problems to be countered but have their own problems. With the need for inserts to be transparent but also possess pores companies have employed the use of PET, which has a different hardness to the 24-well plates these inserts are suspended over. As such, the use of these needs to be considered as specific cell types can grow and react differently depending on the material they are grown on. This is particularly important to note when creating co-cultures between glia and neurons as they prefer hard and soft materials, respectively (Balgude et al., 2001; Engler et al., 2004; Georges et al., 2006; Yeung et al., 2005). Furthermore, with the inserts only having a small surface area which limits the well size that can be used it is difficult to obtain enough protein from cells to conduct experiments without using multiple plates, which can be costly. As such, transwell inserts while avoiding the problems encountered with contact co-cultures still host a series of problems and should be used for select experiments. Finally, conditioned media is posing an alternative way for investigating cellular interactions if only in one direction but could allow the identification of potential biomarkers that may aid in diagnosing neurodegenerative diseases before clinical symptoms arise. However, for this to occur a large amount of research is needed, exploiting the recent advances in mass spectrometry and bioinformatic analysis to help create a catalogue of secreted proteins in diseased and physiological conditions. Through collaborating and combining these findings pathways and potentially novels therapies can be generated to help treat or combat neurodegenerative diseases.

CHAPTER 6
CONCLUSIONS
AND FUTURE WORK

6.1 CONCLUSIONS

A worldwide increase in the aging population highlights neurodegeneration as a key disease that significantly impacts both lifestyle and the economy. Epidemiological predictions suggest the population affected by neurodegenerative disease will increase by 50% by 2030 (Dorsey et al., 2013). Alzheimer's and Parkinson's disease are the most common neurodegenerative diseases and while they affect different brain regions, they share progressive and irreversible loss of neuronal structure and function (Feitosa et al., 2018). Thus, understanding the individual underlying mechanisms and commonalities that contribute to these neurodegenerative processes will help pinpoint the molecular targets. Indeed, there are several common molecular features that characterise the diseases including: changes in protein degradation leading to protein aggregates, mitochondrial defects, neuroinflammation and OS (Chaturvedi and Flint Beal, 2013; Feitosa et al., 2018; Heneka et al., 2014; Jucker and Walker, 2013).

Currently, most if not all therapies treat the symptoms of neurodegenerative diseases and not the underlying cause. Multiple mechanisms have been implicated in neurodegenerative diseases, which highlights the need to develop novel therapies that target these pathways to prevent neuronal loss and prevent the manifestation of clinical symptoms (Nieoullon, 2011). OS is one of the primary hallmarks of neurodegeneration but is one of the least understood mechanisms as various RS can be generated. RS include reactive oxygen and nitrogen species. ROS include superoxide, hydrogen peroxide, peroxyl radicals, hydroxyl radicals and lipid hydroperoxides. While nitric oxide, nitrite, nitrogen dioxide and peroxynitrites are examples of RNS (Koskenkorva-Frank et al., 2013).

The ROS, superoxide is the main precursor that leads to a cascade of other RS, where superoxide is generated due to electrons leaking from the electron transport chain during the reduction of molecular oxygen in mitochondria but also nicotinamide adenine dinucleotide phosphate (NADPH) oxidase, within membranes and the non-membrane bound enzyme xanthine oxidase (Nita and Grzybowski, 2016; Winterbourn, 2015). As such, mitochondrial dysfunction is proposed to increase OS within cells. RNS instead, are generated from L-arginine, where the reaction is catalysed by nitric oxide synthase (NOS) enzymes within the cytosol including neuronal, endothelial and inducible NOS (Ghasemi and Fatemi, 2014). Furthermore the combination of nitric oxide with superoxide also forms the RNS peroxynitrite which can result in various cellular damage if not controlled (Steinert et al., 2010).

Under physiological conditions, various antioxidant systems function to counteract the damaged induced by RS. For example, SOD dismutates superoxide to hydrogen peroxide (Dasuri et al., 2013; Donnelly et al., 1989), which can be degraded to water via catalase (CAT), peroxiredoxins (PRDX) and glutathione peroxidase (GPX; Gandhi and Abramov, 2012; Sue et al., 2005) . However, if not degraded hydrogen peroxide can be converted to the highly reactive hydroxyl radical. Alternatively low molecular weight antioxidants such as vitamin C and E in addition to glutathione (GLUT) help scavenge RS within the CNS (Birben et al., 2012; Feitosa et al., 2018; Rice, 2000). Within the CNS, the antioxidant levels differ depending on the neural cell types, possibly explaining varying susceptibilities to OS (Hertz et al., 2007; Schönfeld and Reiser, 2013). If RS levels become uncontrolled both ROS and RNS can result in DNA damage, lipid peroxidation and protein modifications leading to aggregates that can impair protein degradation further promoting OS (summarised in figure 6.1). Thus, OS also appears to contribute and exacerbate other mechanisms involved in neurodegeneration including mitochondrial dysfunction and protein degradation; collectively referred to as the “Neurodegenerative Bermuda triangle”.

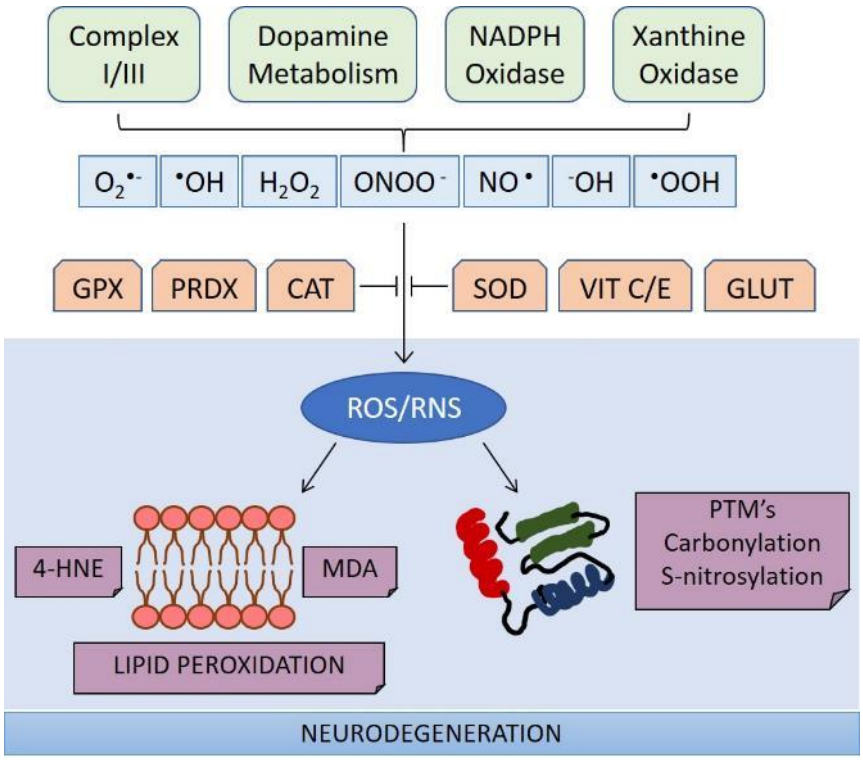

Figure 6.1 Diagrammatic representation of reactive species sources, antioxidants and changes induced by oxidative stress in neurodegeneration. *Under physiological conditions reactive species and controlled by antioxidants: glutathione peroxidase (GPX), peroxiredoxin (PRDX), catalase (CAT), superoxide dismutase (SOD), vitamin C and E (VIT C/E) and glutathione (GLUT). Common by-products of lipid peroxidation include 4-hydroxynonenal (4-HNE) and malondialdehyde (MDA). Other common post-translational modifications (PTM’s) observed include carbonylation and S-nitrosylation. Adapted from Feitosa et al., 2018*

The aim of this thesis was to investigate the role of RS in neural cell models and initiate the development of an *in vitro* co-culture to investigate OS. By using clonal SH-SY5Y and U-87MG cell lines we were able to mimic neurons and astrocytes within the CNS, respectively. OS was induced in SH-SY5Y and U-87MG monocultures, specifically peroxy radicals and superoxide radicals using 2,2'-Azobis(2-methylpropionamidine) dihydrochloride (AAPH; a ROS generating lipid peroxidation agent) and rotenone (a mitochondrial disruptor that inhibits complex I), respectively.

The initial treatment of monocultures showed that rotenone and AAPH could generate RS that could be fluorescently measured using DCFDA. These RS could be attenuated using antioxidants (Patra et al., 2001; Wenzel, 2003). The different responses of each cell line were first highlighted here, as the rate of fluorescence in response to AAPH was greater in SH-SY5Y cells than U-87MG cells. This suggested U-87MG glial cells could mitigate changes in RS levels more effectively than SH-SY5Y neuronal cells, suggesting glia possess greater antioxidant capacity (Dringen and Hamprecht, 1997). This was supported by higher levels of glutathione and NRF2 being observed in U-87MG cells relative to SH-SY5Y cells, where glutathione can directly reduce RS levels (Dringen et al., 2005; Dringen and Hamprecht, 1997) and NRF2 can upregulate antioxidant gene transcription via the ARE pathway (Lee et al., 2003b; Shih et al., 2005; Tufekci et al., 2011). Additionally, between glia and neurons the sources of cellular energy appeared to differ as U-87MG glial cells appeared to depend more on glycolysis for energy, while neurons relied more on mitochondria consistent with previous literature (Jády et al., 2016; Juaristi et al., 2019). The results herein propose this difference is in part due to U-87MG glial cells exhibiting lower mitochondrial gene expression, implying glia possess less mitochondria than SH-SY5Y neuronal cells, explaining their greater susceptibility to rotenone induced cellular death. Furthermore, despite both SH-SY5Y and U-87MG cells being treated with AAPH or rotenone they displayed different levels of carbonylation and S-nitrosylation, demonstrating different PTM's result from the same treatment in different cells. Together these results highlight how neuronal SH-SY5Y and glial U-87MG cells respond differently to OS, mimicking the differences reported in the CNS.

RS treatments also elicited different responses within the neural cells suggesting AAPH and rotenone affected specific pathways in glia and neurons. Viability assays showed rotenone resulted in a dose-dependent decrease in viability for both SH-SY5Y neuronal and U-87MG glial cells. In contrast, AAPH only decreased SH-SY5Y neuronal viability but appeared to increase U-87MG glial up to a threshold concentration. Furthermore, the antioxidant ascorbic acid (reported primarily to scavenge superoxide, Kondo et al., 2008; Wenzel et al., 2004) was not effective at attenuating RS levels or cell death in AAPH treated SH-SY5Y cells but was effective against rotenone. Additionally, PTM assays demonstrated that both SH-SY5Y neuronal and U-87MG glial cells treated with AAPH

exhibited higher levels of lipid peroxidation than rotenone treatment. These greater levels of lipid peroxidation are possibly due to AAPH mainly generating peroxyl radicals (Bassett et al., 1999; Terao and Niki, 1986; Werber et al., 2011), supporting other studies that demonstrate AAPH enhanced lipid peroxidation (Ben Othman et al., 2016; Sun et al., 2001). Indeed, AAPH altered cell membranes more so than rotenone. LDH assays showed greater LDH release for both SH-SY5Y and U-87MG cells treated with AAPH relative to control cells. Limited experiments with rat primary cortical neurons also suggest different pathways were induced by AAPH and rotenone as contrasting morphological changes in axon degradation was observed. Alongside OS induced changes in viability and PTM's, AAPH and rotenone also affected mitochondrial function as demonstrated by changes in the source of respiration, mitochondrial membrane potential and mitochondrial fission/fusion protein levels. Additionally, treatments also altered ubiquitination, proteasomal activity and chaperone levels, calling attention to changes in protein degradation. Together, the results herein suggest that while AAPH and rotenone appear to generate different RS, mitochondrial function and protein degradation pathways were also affected by OS, emphasising the "Neurodegenerative Bermuda triangle".

With OS being generated by both AAPH and rotenone we investigated changes in antioxidant gene expression using a specialised OS PCR array. This resulted in the upregulation of several target genes in glial cells following both AAPH and rotenone treatment. In contrast, neuronal exposure to rotenone resulted in the suppression of target gene expression. However, we believe the down regulation of gene expression in rotenone treated SH-SY5Y cells was due to the time of treatments. Upstream of these genes we identified NRF2 as a possible transcription factor. NRF2 has been recently proposed as a possible therapeutic target for neurodegeneration due to its major role as a regulator of antioxidant enzymes within neurons (Dinkova-Kostova et al., 2018). The results herein support NRF2's role in counteracting OS as both AAPH and rotenone increased nuclear NRF2 localisation, leading to target gene expression (Liddell et al., 2016; Rizzi et al., 2018). Additionally, antioxidants possibly help to regulate NRF2 expression and hence antioxidant enzyme levels to protect neurons (Kim et al., 2015; Mostafavi-Pour et al., 2017; Vineetha et al., 2018). NRF2 knockdown experiments with siRNA suggested for the first time that AAPH activated the NRF2 pathway, as knockdown exacerbated neuronal death and attenuated glial proliferation; parameters that the initial consequence of AAPH treatment. Therefore, while AAPH and rotenone generated different RS, both appeared to alter NRF2 localisation and downstream gene expression. Changes to NRF2 were significant in AAPH treated neural cells suggesting the NRF2-ARE pathway plays a protective role against lipid peroxidation.

The results herein also suggest different differentiation methods of mitotic SH-SY5Y neuronal cells effects susceptibility to OS, as some conditions made SH-SY5Y cells more susceptible to AAPH or rotenone treatment. This possibly explains why current literature shows conflicting evidence as to whether differentiation results in SH-SY5Y neuronal cells becoming more or less vulnerable to OS (Beck et al., 2006; Cheung et al., 2009; Ferreira et al., 2013; Lopes et al., 2010). Furthermore, differentiated SH-SY5Y cells still lack the lengthy neurites observed with primary neuronal cultures and thus, limits investigations into morphological and functional changes with synapses. Therefore, while SH-SY5Y neuroblastoma cells allow high-throughput investigations into OS in a cost-effective manner the results herein propose the limitations of these cells as a neural model, which needs further improvement.

One of the other limitations of *in vitro* cell models is that investigations are carried out using monocultures, which is not how cells function *in vivo.* With multiple cells present in the CNS including neurons, microglia, oligodendrocytes and astrocytes (Herculano-Houzel, 2009; Verkhratsky et al., 2012) the interaction between these cells may help identify possible therapeutic targets. Therefore, co-cultures have become more relevant over the last decade, where culture complexity has been increased in the hope of understanding cell-cell interactions and how these influence neurodegeneration (Renaud and Martinoli, 2016). With astrocytes being proposed to have neurotoxic and neuroprotective effects (Jha et al., 2018) we attempted to create a co-culture between SH-SY5Y neuronal and U-87MG glial cells. The results herein are the first to utilise transwell inserts with these mitotic cell lines, stressing the importance of culture material for future investigations. U-87MG glial cells exhibited reduced viability on PET inserts relative to polystyrene 24-well plates and thus, should be considered in future co-culture investigations. However, currently the maximum size of transwell inserts only allows 24-well plates to be used and investigations with inserts are still constrained due to difficulty in obtaining enough cell protein from lysates and creating sufficient replicates are economically demanding.

Due to the difficulties posed with transwell inserts we like others reverted to investigating the astrocytic secretome under conditions of OS using mass spectrometry. We demonstrated the U-87MG glioblastoma line expresses several proteins identified in previous research (Greco et al., 2010; Keene et al., 2009; Moore et al., 2009; Yin et al., 2012), which has primarily focused on rodent models. Our approach adds to the growing catalogue of secreted proteins in a human model and provides the first insights into the secretome mediated by OS (AAPH and rotenone). To probe the effects of these secreted factors differentiated SH-SY5Y neuronal cells were exposed to U-87MG conditioned media, with morphological alterations being noted. Through enrichment analysis using MetaCore, potential pathways involved in neurodegeneration have been identified. The results

herein highlight the importance of the ECM, neuroinflammation and protein degradation during OS.

In conclusion, this thesis identified the differences between SH-SY5Y neuronal and U-87MG glial cell lines, which could attribute to their differential responses to OS. While rotenone is commonly used to mimic Parkinson's disease in neuronal models (Blesa et al., 2015; Franco-Iborra et al., 2016; Schapira, 2008), we propose that specific RS effect different pathways in neural cells and suggest AAPH as a lipid peroxidising agent for future studies. Furthermore, we suggest like others, that NRF2 plays an important role in OS and may be a therapeutic target in the future (Dinkova-Kostova et al., 2018). Additionally, we provide the first insights into how rat primary cortical neurons respond to AAPH, where there appears to be a significant change in morphology that is dissimilar to rotenone, supporting the hypothesis that specific RS stimulate different pathways, which requires further investigations to understand their role in neurodegeneration. We have also taken the first steps to creating a co-culture between SH-SY5Y neuronal and U-87MG glial cells using transwell inserts, with the materials being an important consideration for the future. Finally, initial investigations into the U-87MG secretome under OS have yielded a catalogue of differentially identified proteins and pathways effected by conditioned media highlighting potential factors involved in neurodegeneration that require further investigations.

6.2 FUTURE WORK

With current treatment of neurodegenerative diseases confined to limiting the symptoms and not treating the underlying pathological conditions the diseases still progress, where neurons continue to degrade. Thus, there is a greater need to understand the pathological hallmarks including mitochondrial dysfunction, protein degradation and OS to generate novel therapies.

The current work herein suggests specific RS affect neural cells differently; however, current research into OS has not looked in depth at how these RS induce specific pathways or changes. AAPH provides a novel way to generate lipid peroxidation that is more specific than the currently used rotenone, which can have other effects due to complex I inhibition, including lower ATP levels (Caneda-Ferrón et al., 2008; Sherer et al., 2003). To confirm that AAPH primarily results in lipid peroxidation, the TBARS assays need to be repeated to obtain a representative set of data as not enough replicates were obtained. Additionally, detection of 4-hydroxynonenal via dinitrophenylhydrazine would allow the detection of another lipid peroxidation product to further confirm if AAPH results in greater lipid peroxidation than rotenone.

With NRF2 being a possible upstream transcription factor involved in the antioxidant response to AAPH and rotenone, future experiments should utilise siRNA to knockdown NRF2 and determine which proteins are affected (Lee et al., 2003b; Shih et al., 2005; Tufekci et al., 2011). Following this, specific knockdown of these proteins will help identify which ones have the greatest neuroprotective role and hence provide a therapeutic target. As mentioned in chapter 3 the hallmarks of neurodegeneration that make up the "Neurodegenerative Bermuda triangle" appear to be linked and more research needs to be done into how these factors are linked. Therefore, when conducting these investigations, one should also look at proteins that also effect mitochondrial dysfunction and protein degradation. This will allow a therapeutic target that effects all three mechanisms to be targeted, hopefully preventing neuronal degeneration as if only one hallmark is targeted others may overcompensate leading to their eventual failure as well. Furthermore, this may explain why current treatments only effect the symptoms of neurodegeneration but do not prevent its progression.

Future treatments also need investigating in a co-culture model as monocultures do not provide adequate *in vivo* like conditions. Therefore, the results herein regarding the effect of materials needs to be considered when using inserts with glia and neurons. Additionally, differentially identified proteins and the pathways enriched by MetaCore need further investigations to determine if secreted factors could provide an alternative therapeutic target. This will provide an advantage over intracellular proteins targets as these may be taken up more easily by cells making the treatment more effective. The initial results herein suggest OS alters the secretome highlighting the ECM, neuroinflammation and chaperones are possible targets to investigate. Recent studies demonstrate chaperones such as HSP70 are secreted by astrocytes possibly via exosomes, but this has yet to be confirmed (Lackie et al., 2017; Rivera et al., 2018; Verkhratsky et al., 2016). Therefore, further studies should aim to investigate exosomes from U-87MG glial cells to determine if they possess chaperones or other antioxidants that may be neuroprotective providing the basis for novel therapies.

CHAPTER 7

REFERENCE LIST

7.0 REFERENCES

Abaspour, A.R., Taghikhani, M., Parizadeh, S.M.R., Seyedi, S.M.R., Ghazizadeh, H., Kazemi, E., Moohebati, M., Ghafoori, F., Mardannik, M., Avan, A., Ferns, G.A., Ghayour-Mobarhan, M., 2019. HSP27 expression in the human peripheral blood mononuclear cells as an early prognostic biomarker in coronary artery disease patients. Diabetes Metab. Syndr. Clin. Res. Rev. 13, 1791–1795. https://doi.org/10.1016/j.dsx.2019.04.010

Aberle, H., Bauer, A., Stappert, J., Kispert, A., Kemler, R., 1997. β-catenin is a target for the ubiquitin-proteasome pathway. EMBO J. 16, 3797–804. https://doi.org/10.1093/emboj/16.13.3797

Abouelfetouh, A., Kondoh, T., Ehara, K., Kohmura, E., 2004. Morphological differentiation of bone marrow stromal cells into neuron-like cells after co-culture with hippocampal slice. Brain Res. 1029, 114–9. https://doi.org/10.1016/j.brainres.2004.07.092

Abramov, A.Y., 2004. β-Amyloid Peptides Induce Mitochondrial Dysfunction and Oxidative Stress in Astrocytes and Death of Neurons through Activation of NADPH Oxidase. J. Neurosci. 24, 565–75. https://doi.org/10.1523/jneurosci.4042-03.2004

Adalbert, R., Coleman, M.P., 2013. Review: Axon pathology in age-related neurodegenerative disorders. Neuropathol. Appl. Neurobiol. 39, 90–108. https://doi.org/10.1111/j.1365-2990.2012.01308.x

Ahn, S.G., Thiele, D.J., 2003. Redox regulation of mammalian heat shock factor 1 is essential for Hsp gene activation and protection from stress. Genes Dev. 17, 516–28. https://doi.org/10.1101/gad.1044503

Åkerfelt, M., Trouillet, D., Mezger, V., Sistonen, L., 2007. Heat shock factors at a crossroad between stress and development, in: Annals of the New York Academy of Sciences. pp. 15–27. https://doi.org/10.1196/annals.1391.005

Åkerman, K.E.O., Scott, I.G., Andersson, L.C., 1984. Functional differentiation of a human ganglion cell derived neuroblastoma cell line SH-SY5Y induced by a phorbol ester (TPA). Neurochem. Int. 6, 77–80. https://doi.org/10.1016/0197-0186(84)90029-9

Alam, J., Stewart, D., Touchard, C., Boinapally, S., Choi, a M., Cook, J.L., 1999. Nrf2, a Cap'n'Collar transcription factor, regulates induction of the heme oxygenase-1 gene. J. Biol. Chem. 274, 26071–26078. https://doi.org/10.1074/jbc.274.37.26071

Alam, Z.I., Daniel, S.E., Lees, A.J., Marsden, D.C., Jenner, P., Halliwell, B., 1997. A generalised increase in protein carbonyls in the brain in Parkinson's but not incidental Lewy body disease. J. Neurochem. 69, 1326–1329. https://doi.org/10.1046/j.1471-4159.1997.69031326.x

Allaman, I., Bélanger, M., Magistretti, P.J., 2011. Astrocyte-neuron metabolic relationships: For better and for worse. Trends Neurosci. https://doi.org/10.1016/j.tins.2010.12.001

Allani, P.K., Sum, T., Bhansali, S.G., Mukherjee, S.K., Sonee, M., 2004. A comparative study of the effect of oxidative stress on the cytoskeleton in human cortical neurons. Toxicol. Appl. Pharmacol. 196, 29–36. https://doi.org/10.1016/j.taap.2003.12.010

Allen, M., Bjerke, M., Edlund, H., Nelander, S., Westermark, B., 2016. Origin of the U87MG glioma cell line: Good news and bad news. Sci. Transl. Med. 8, 354–7. https://doi.org/10.1126/scitranslmed.aaf6853

Alsayyah, A., ElMazoudy, R., Al-Namshan, M., Al-Jafary, M., Alaqeel, N., 2019. Chronic neurodegeneration by aflatoxin B1 depends on alterations of brain enzyme activity and immunoexpression of astrocyte in male rats. Ecotoxicol. Environ. Saf. 182, 109407. https://doi.org/10.1016/j.ecoenv.2019.109407

Ambrogini, P., Torquato, P., Bartolini, D., Albertini, M.C., Lattanzi, D., Di Palma, M., Marinelli, R., Betti, M., Minelli, A., Cuppini, R., Galli, F., 2019. Excitotoxicity, neuroinflammation and oxidant stress as molecular bases of epileptogenesis and epilepsy-derived neurodegeneration: The role of vitamin E. Biochim. Biophys. Acta - Mol. Basis Dis. 1865, 1098–1112. https://doi.org/10.1016/j.bbadis.2019.01.026

Amor, S., Peferoen, L.A.N., Vogel, D.Y.S., Breur, M., van der Valk, P., Baker, D., van Noort, J.M., 2014. Inflammation in neurodegenerative diseases - an update. Immunology 142, 151–166. https://doi.org/10.1111/imm.12233

Anckar, J., Sistonen, L., 2011. Regulation of HSF 1 Function in the Heat Stress Response: Implications in Aging and Disease. Annu. Rev. Biochem. 80, 1089–115. https://doi.org/10.1146/annurev-biochem-060809-095203

Anckar, J., Sistonen, L., 2007. Heat shock factor 1 as a coordinator of stress and developmental pathways. Adv. Exp. Med. Biol. https://doi.org/10.1007/978-0-387-39975-1_8

Andreazza, A.C., Shao, L., Wang, J.-F., Young, L.T., 2010. Mitochondrial Complex I Activity and Oxidative Damage to Mitochondrial Proteins in the Prefrontal Cortex of Patients With Bipolar Disorder. Arch. Gen. Psychiatry 67, 360–8. https://doi.org/10.1001/archgenpsychiatry.2010.22

Andrews, R.N., Caudell, D.L., Metheny-Barlow, L.J., Peiffer, A.M., Tooze, J.A., Bourland, J.D., Hampson, R.E., Deadwyler, S.A., Cline, J.M., 2018. Fibronectin Produced by Cerebral Endothelial and Vascular Smooth Muscle Cells Contributes to Perivascular Extracellular Matrix in Late-Delayed Radiation-Induced Brain Injury. Radiat. Res. 190, 361. https://doi.org/10.1667/RR14961.1

Angeli, J.P.F., Shah, R., Pratt, D.A., Conrad, M., 2017. Ferroptosis Inhibition: Mechanisms and Opportunities. Trends Pharmacol. Sci. https://doi.org/10.1016/j.tips.2017.02.005

Angelova, P.R., Horrocks, M.H., Klenerman, D., Gandhi, S., Abramov, A.Y., Shchepinov, M.S., 2015. Lipid peroxidation is essential for α-synuclein-induced cell death. J. Neurochem. 133, 582–9. https://doi.org/10.1111/jnc.13024

Anglade, P., 1997. Apoptosis and autophagy in nigral neurons of patients with Parkinson's disease. Histol. Histopathol. 12, 25–31.

Aon, M.A., Cortassa, S., Juhaszova, M., Sollott, S.J., 2016. Mitochondrial health, the epigenome and healthspan. Clin. Sci. 130, 1285–305. https://doi.org/10.1042/CS20160002

Ara, J., Przedborski, S., Naini, a B., Jackson-Lewis, V., Trifiletti, R.R., Horwitz, J., Ischiropoulos, H., 1998. Inactivation of tyrosine hydroxylase by nitration following exposure to peroxynitrite and 1-methyl-4-phenyl-1,2,3,6-tetrahydropyridine (MPTP). Proc. Natl. Acad. Sci. U. S. A. 95, 7659–7663. https://doi.org/10.1073/pnas.95.13.7659

Araki, T., Sasaki, Y., Milbrandt, J., 2004. Increased nuclear NAD biosynthesis and SIRT1 activation prevent axonal degeneration. Science (80-.). 205, 1010–3. https://doi.org/10.1126/science.1098014

Araque, A., 2008. Astrocytes process synaptic information. Neuron Glia Biol. 4, 3–10. https://doi.org/10.1017/s1740925x09000064

Araque, A., Carmignoto, G., Haydon, P.G., Oliet, S.H.R., Robitaille, R., Volterra, A., 2014. Gliotransmitters travel in time and space. Neuron. https://doi.org/10.1016/j.neuron.2014.02.007

Arbore, G., Kemper, C., Kolev, M., 2017. Intracellular complement – the complosome – in immune cell regulation. Mol. Immunol. https://doi.org/10.1016/j.molimm.2017.05.012

Arcangeli, A., Rosati, B., Crociani, O., Cherubini, A., Fontana, L., Passani, B., Wanke, E., Olivotto, M., 1999. Modulation of HERG current and herg gene expression during retinoic acid treatment of human neuroblastoma cells: Potentiating effects of BDNF. J. Neurobiol. 40, 214–25. https://doi.org/10.1002/(SICI)1097-4695(199908)40:2<214::AID-NEU7>3.0.CO;2-0

Aregueta-Robles, U.A., Martens, P.J., Poole-Warren, L.A., Green, R.A., 2019. Tissue engineered hydrogels supporting 3D neural networks. Acta Biomater. 95, 269–284. https://doi.org/10.1016/j.actbio.2018.11.044

Armstrong, D., Browne, R., 1994. The Analysis of Free Radicals, Lipid Peroxides, Antioxidant Enzymes and Compounds Related to Oxidative Stress as Applied to the Clinical Chemistry Laboratory, in: 366. pp. 43–58. https://doi.org/10.1007/978-1-4615-1833-4_4

Asanuma, M., Okumura-Torigoe, N., Miyazaki, I., Murakami, S., Kitamura, Y., Sendo, T., 2019. Region-Specific Neuroprotective Features of Astrocytes against Oxidative Stress Induced by 6-Hydroxydopamine. Int. J. Mol. Sci. 20, 598. https://doi.org/10.3390/ijms20030598

Au, Q., Kanchanastit, P., Barber, J.R., Ng, S.C., Zhang, B., 2008. High-content image-based screening for small-molecule chaperone amplifiers in heat shock. J. Biomol. Screen. 13, 953–9. https://doi.org/10.1177/1087057108326538

Azkona, G., López de Maturana, R., del Rio, P., Sousa, A., Vazquez, N., Zubiarrain, A., Jimenez-Blasco, D.,

Bolaños, J.P., Morales, B., Auburger, G., Arbelo, J.M., Sánchez-Pernaute, R., 2018. LRRK2 Expression Is Deregulated in Fibroblasts and Neurons from Parkinson Patients with Mutations in PINK1. Mol. Neurobiol. 55, 506–516. https://doi.org/10.1007/s12035-016-0303-7

Bagri, A., Cheng, H.J., Yaron, A., Pleasure, S.J., Tessier-Lavigne, M., 2003. Stereotyped pruning of long hippocampal axon branches triggered by retraction inducers of the semaphorin family. Cell 113, 285–99. https://doi.org/10.1016/S0092-8674(03)00267-8

Balchin, D., Hayer-Hartl, M., Hartl, F.U., 2016. In vivo aspects of protein folding and quality control. Science (80-.). https://doi.org/10.1126/science.aac4354

Balgude, A.P., Yu, X., Szymanski, A., Bellamkonda, R. V, 2001. Agarose gel stiffness determines rate of DRG neurite extension in 3D cultures. Biomaterials 22, 1077–84.

Bandookwala, M., Sengupta, P., 2020. 3-Nitrotyrosine: a versatile oxidative stress biomarker for major neurodegenerative diseases. Int. J. Neurosci. 1–16. https://doi.org/10.1080/00207454.2020.1713776

Bantle, C.M., Phillips, A.T., Smeyne, R.J., Rocha, S.M., Olson, K.E., Tjalkens, R.B., 2019. Infection with mosquito-borne alphavirus induces selective loss of dopaminergic neurons, neuroinflammation and widespread protein aggregation. npj Park. Dis. 5, 20. https://doi.org/10.1038/s41531-019-0090-8

Barcia, C., Sánchez Bahillo, A., Fernández-Villalba, E., Bautista, V., Poza Y Poza, M., Fernández-Barreiro, A., Hirsch, E.C., Herrero, M.T., 2004. Evidence of active microglia in substantia nigra pars compacta of parkinsonian monkeys 1 year after MPTP exposure. Glia 46, 402–409. https://doi.org/10.1002/glia.20015

Barrera, G., Pizzimenti, S., Ciamporcero, E.S., Daga, M., Ullio, C., Arcaro, A., Cetrangolo, G.P., Ferretti, C., Dianzani, C., Lepore, A., Gentile, F., 2015. Role of 4-Hydroxynonenal-Protein Adducts in Human Diseases. Antioxid. Redox Signal. 22, 1681–702. https://doi.org/10.1089/ars.2014.6166

Barrera, G., Pizzimenti, S., Daga, M., Dianzani, C., Arcaro, A., Cetrangolo, G.P., Giordano, G., Cucci, M.A., Graf, M., Gentile, F., 2018. Lipid Peroxidation-Derived Aldehydes, 4-Hydroxynonenal and Malondialdehyde in Aging-Related Disorders. Antioxidants 7, 102. https://doi.org/10.3390/antiox7080102

Bassett, C.N., Neely, M.D., Sidell, K.R., Markesbery, W.R., Swift, L.L., Montine, T.J., 1999. Cerebrospinal fluid lipoproteins are more vulnerable to oxidation in Alzheimer's disease and are neurotoxic when oxidized ex vivo. Lipids 34, 1273–80. https://doi.org/10.1007/s11745-999-0478-1

Baxter, P.S., Hardingham, G.E., 2016. Adaptive regulation of the brain's antioxidant defences by neurons and astrocytes. Free Radic. Biol. Med. 100, 147–52. https://doi.org/10.1016/j.freeradbiomed.2016.06.027

Beal, M.F., 2003. Mitochondria, oxidative damage, and inflammation in Parkinson's disease. Ann. N. Y. Acad. Sci. 991, 120–31. https://doi.org/10.1111/j.1749-6632.2003.tb07470.x

Beck, K.E., De Girolamo, L.A., Griffin, M., Billett, E.E., 2006. The role of tissue transglutaminase in 1-methyl-4-

phenylpyridinium (MPP+)-induced toxicity in differentiated human SH-SY5Y neuroblastoma cells. Neurosci. Lett. 405, 46–51. https://doi.org/10.1016/j.neulet.2006.06.061

Beckwith, R., Estrin, E., Worden, E.J., Martin, A., 2013. Reconstitution of the 26S proteasome reveals functional asymmetries in its AAA+ unfoldase. Nat. Struct. Mol. Biol. 20, 1164–72. https://doi.org/10.1038/nsmb.2659

Bedford, L., Paine, S., Sheppard, P.W., Mayer, R.J., Roelofs, J., 2010. Assembly, structure, and function of the 26S proteasome. Trends Cell Biol. 20, 391–401. https://doi.org/10.1016/j.tcb.2010.03.007

Beere, H.M., Wolf, B.B., Cain, K., Mosser, D.D., Mahboubi, A., Kuwana, T., Tailor, P., Morimoto, R.I., Cohen, G.M., Green, D.R., 2000. Heat-shock protein 70 inhibits apoptosis by preventing recruitment of procaspase-9 to the Apaf-1 apoptosome. Nat. Cell Biol. 2, 469–75. https://doi.org/10.1038/35019501

Behdarvandy, M., Karimian, M., Atlasi, M.A., Azami Tameh, A., 2020. Heat shock protein 27 as a neuroprotective biomarker and a suitable target for stem cell therapy and pharmacotherapy in ischemic stroke. Cell Biol. Int. 44, 356–367. https://doi.org/10.1002/cbin.11237

Beilina, A., Van Der Brug, M., Ahmad, R., Kesavapany, S., Miller, D.W., Petsko, G. a, Cookson, M.R., 2005. Mutations in PTEN-induced putative kinase 1 associated with recessive parkinsonism have differential effects on protein stability. Proc. Natl. Acad. Sci. U. S. A. 102, 5703–5708. https://doi.org/10.1073/pnas.0500617102

Bellomo, G., Mirabelli, F., 1992. Oxidative Stress and Cytoskeletal Alterations. Ann. N. Y. Acad. Sci. 663, 97–109. https://doi.org/10.1111/j.1749-6632.1992.tb38653.x

Bellot, G., Garcia-Medina, R., Gounon, P., Chiche, J., Roux, D., Pouyssegur, J., Mazure, N.M., 2009. Hypoxia-Induced Autophagy Is Mediated through Hypoxia-Inducible Factor Induction of BNIP3 and BNIP3L via Their BH3 Domains. Mol. Cell. Biol. 29, 2570–81. https://doi.org/10.1128/MCB.00166-09

Ben-Yoseph, O., Boxer, P. a, Ross, B.D., 1996. Assessment of the role of the glutathione and pentose phosphate pathways in the protection of primary cerebrocortical cultures from oxidative stress. J. Neurochem. 66, 2329–37. https://doi.org/10.1046/j.1471-4159.1996.66062329.x

Ben Othman, S., Katsuno, N., Kitayama, A., Fujimura, M., Kitaguchi, K., Yabe, T., 2016. Water-soluble fractions from defatted sesame seeds protect human neuroblast cells against peroxyl radicals and hydrogen peroxide-induced oxidative stress. Free Radic. Res. 50, 949–958. https://doi.org/10.1080/10715762.2016.1207248

Benard, G., Karbowski, M., 2009. Mitochondrial fusion and division: Regulation and role in cell viability. Semin. Cell Dev. Biol. https://doi.org/10.1016/j.semcdb.2008.12.012

Benit, P., 2004. Mutant NDUFS3 subunit of mitochondrial complex I causes Leigh syndrome. J. Med. Genet. 41, 14–7. https://doi.org/10.1136/jmg.2003.014316

Bennett, M C, Bishop, J.F., Leng, Y., Chock, P.B., Chase, T.N., Mouradian, M.M., 1999. Degradation of alpha-synuclein by proteasome. J. Biol. Chem. 274, 33855–33858. https://doi.org/10.1074/jbc.274.48.33855

Bennett, M. Catherine, Bishop, J.F., Leng, Y., Chock, P.B., Chase, T.N., Mouradian, M.M., 1999. Degradation of a-synuclein by proteasome. J. Biol. Chem. 274, 33855–33858. https://doi.org/10.1074/jbc.274.48.33855

Berbusse, G.W., Woods, L.C., Vohra, B.P.S., Naylor, K., 2016. Mitochondrial Dynamics Decrease Prior to Axon Degeneration Induced by Vincristine and are Partially Rescued by Overexpressed cytNmnat1. Front. Cell. Neurosci. 10, 179. https://doi.org/10.3389/fncel.2016.00179

Berwick, D.C., Harvey, K., 2012. The importance of Wnt signalling for neurodegeneration in Parkinson's disease. Biochem. Soc. Trans. 40, 1123–8. https://doi.org/10.1042/bst20120122

Betarbet, R., Canet-Aviles, R.M., Sherer, T.B., Mastroberardino, P.G., McLendon, C., Kim, J.H., Lund, S., Na, H.M., Taylor, G., Bence, N.F., Kopito, R., Seo, B.B., Yagi, T., Yagi, A., Klinefelter, G., Cookson, M.R., Greenamyre, J.T., 2006. Intersecting pathways to neurodegeneration in Parkinson's disease: Effects of the pesticide rotenone on DJ-1, α-synuclein, and the ubiquitin-proteasome system. Neurobiol. Dis. 22, 404–20. https://doi.org/10.1016/j.nbd.2005.12.003

Betarbet, R., Sherer, T.B., Greenamyre, J.T., 2005. Ubiquitin–proteasome system and Parkinson's diseases. Exp. Neurol. 191, S17–S27. https://doi.org/10.1016/j.expneurol.2004.08.021

Betarbet, R., Sherer, T.B., Mackenzie, G., Garcia-osuna, M., Panov, A. V, Greenamyre, J.T., 2000. Chronic systemic pesticide exposure reproduces features of Parkinson's disease. Nat. Neurosci. 3, 1301–1306. https://doi.org/10.1038/81834

Bettegazzi, B., Pelizzoni, I., Scarzella, F.S., Restelli, L.M., Zacchetti, D., Maltecca, F., Casari, G., Grohovaz, F., Codazzi, F., 2019. Upregulation of Peroxiredoxin 3 Protects Afg3l 2-KO Cortical Neurons In Vitro from Oxidative Stress: A Paradigm for Neuronal Cell Survival under Neurodegenerative Conditions. Oxid. Med. Cell. Longev. 2019, 1–13. https://doi.org/10.1155/2019/4721950

Birben, E., Sahiner, U.M., Sackesen, C., Erzurum, S., Kalayci, O., 2012. Oxidative stress and antioxidant defense. World Allergy Organ. J. 5, 9–19. https://doi.org/10.1097/WOX.0b013e3182439613

Bishop, P., Rocca, D., Henley, J.M., 2016. Ubiquitin C-terminal hydrolase L1 (UCH-L1): structure, distribution and roles in brain function and dysfunction. Biochem. J. 473, 2453–2462. https://doi.org/10.1042/BCJ20160082

Biteau, B., Labarre, J., Toledano, M.B., 2003. ATP-dependent reduction of cysteine–sulphinic acid by S. cerevisiae sulphiredoxin. Nature 425, 980–984. https://doi.org/10.1038/nature02075

Bizzozero, O.A., 2009. Protein Carbonylation in Neurodegenerative and Demyelinating CNS Diseases, in: Handbook of Neurochemistry and Molecular Neurobiology. Springer US, Boston, MA, pp. 543–562.

https://doi.org/10.1007/978-0-387-30375-8_23

Bjarkam, C.R., Nielsen, M.S., Glud, A.N., Rosendal, F., Mogensen, P., Bender, D., Doudet, D., Møller, A., Sørensen, J.C., 2008. Neuromodulation in a minipig MPTP model of Parkinson disease. Br. J. Neurosurg. 22, S9–S12. https://doi.org/10.1080/02688690802448285

Blanquie, O., Bradke, F., 2018. Cytoskeleton dynamics in axon regeneration. Curr. Opin. Neurobiol. 51, 60–69. https://doi.org/10.1016/j.conb.2018.02.024

Blesa, J., Trigo-Damas, I., Quiroga-Varela, A., Jackson-Lewis, V.R., 2015. Oxidative stress and Parkinson's disease. Front. Neuroanat. 9, 91. https://doi.org/10.3389/fnana.2015.00091

Bogdanowicz, D.R., Lu, H.H., 2013. Studying cell-cell communication in co-culture. Biotechnol. J. 8, 395–396. https://doi.org/10.1002/biot.201300054

Boillée, S., Vande Velde, C., Cleveland, D.W., 2006. ALS: A Disease of Motor Neurons and Their Nonneuronal Neighbors. Neuron 52, 39–59. https://doi.org/10.1016/j.neuron.2006.09.018

Bolaños, J.P., 2016. Bioenergetics and redox adaptations of astrocytes to neuronal activity. J. Neurochem. 139, 115–125. https://doi.org/10.1111/jnc.13486

Bolaños, J.P., Heales, S.J.R., Land, J.M., Clark, J.B., 1995. Effect of Peroxynitrite on the Mitochondrial Respiratory Chain: Differential Susceptibility of Neurones and Astrocytes in Primary Culture. J. Neurochem. 64, 1965–1972. https://doi.org/10.1046/j.1471-4159.1995.64051965.x

Bonifati, V, Rizzu, P., Van Baren, M.J., Schaap, O., Breedveld, G.J., Krieger, E., Dekker, M.C., Squitieri, F., Ibanez, P., Joosse, M., Van Dongen, J.W., Vanacore, N., Van Swieten, J.C., Brice, A., Meco, G., Van Duijn, C.M., Oostra, B.A., Heutink, P., 2003. Mutations in the DJ-1 Gene Associated with Autosomal Recessive Early- Onset Parkinsonism. Science (80-.). 299, 256–259. https://doi.org/10.1126/science.1077209

Bonifati, Vincenzo, Rizzu, P., van Baren, M.J., Schaap, O., Breedveld, G.J., Krieger, E., Dekker, M.C.J., Squitieri, F., Ibanez, P., Joosse, M., van Dongen, J.W., Vanacore, N., van Swieten, J.C., Brice, A., Meco, G., van Duijn, C.M., Oostra, B. a, Heutink, P., 2003. Mutations in the DJ-1 gene associated with autosomal recessive early-onset parkinsonism. Science 299, 256–259. https://doi.org/10.1126/science.1077209

Booth, H.D.E., Hirst, W.D., Wade-Martins, R., 2017. The Role of Astrocyte Dysfunction in Parkinson's Disease Pathogenesis. Trends Neurosci. 40, 358–370. https://doi.org/10.1016/j.tins.2017.04.001

Borisov, V.B., 2002. Defects in mitochondrial respiratory complexes III and IV, and human pathologies. Mol. Aspects Med. 23, 385–412. https://doi.org/10.1016/S0098-2997(02)00013-4

Borrás, C., Gambini, J., López-Grueso, R., Pallardó, F. V., Viña, J., 2010. Direct antioxidant and protective effect of estradiol on isolated mitochondria. Biochim. Biophys. Acta - Mol. Basis Dis. 1802, 205–211. https://doi.org/10.1016/j.bbadis.2009.09.007

Borrás, C., Sastre, J., García-Sala, D., Lloret, A., Pallardó, F. V., Viña, J., 2003. Mitochondria from females exhibit higher antioxidant gene expression and lower oxidative damage than males. Free Radic. Biol. Med. 34, 546–552. https://doi.org/10.1016/S0891-5849(02)01356-4

Borst, J.W., Visser, N. V., Kouptsova, O., Visser, A.J.W.G., 2000a. Oxidation of unsaturated phospholipids in membrane bilayer mixtures is accompanied by membrane fluidity changes. Biochim. Biophys. Acta - Mol. Cell Biol. Lipids. https://doi.org/10.1016/S1388-1981(00)00084-6

Borst, J.W., Visser, N. V, Kouptsova, O., Visser, A.J.W.G., 2000b. Oxidation of unsaturated phospholipids in membrane bilayer mixtures is accompanied by membrane fluidity changes. Biochim. Biophys. Acta - Mol. Cell Biol. Lipids 1487, 61–73. https://doi.org/10.1016/S1388-1981(00)00084-6

Bournival, J., Plouffe, M., Renaud, J., Provencher, C., Martinoli, M.-G., 2012. Quercetin and Sesamin Protect Dopaminergic Cells from MPP + -Induced Neuroinflammation in a Microglial (N9)-Neuronal (PC12) Coculture System. Oxid. Med. Cell. Longev. 2012, 1–11. https://doi.org/10.1155/2012/921941

Braak, H., Braak, E., Yilmazer, D., Schultz, C., de Vos, R.A., Jansen, E.N., 1995. Nigral and extranigral pathology in Parkinson's disease. J. Neural Transm. Suppl. 46, 15–31.

Braak, H., Del Tredici, K., Rüb, U., De Vos, R.A.I., Jansen Steur, E.N.H., Braak, E., 2003. Staging of brain pathology related to sporadic Parkinson's disease. Neurobiol. Aging 24, 197–211. https://doi.org/10.1016/S0197-4580(02)00065-9

Bradshaw, T.Y., Romano, L.E.L., Duncan, E.J., Nethisinghe, S., Abeti, R., Michael, G.J., Giunti, P., Vermeer, S., Chapple, J.P., 2016. A reduction in Drp1-mediated fission compromises mitochondrial health in autosomal recessive spastic ataxia of Charlevoix Saguenay. Hum. Mol. Genet. 25, 3232–3244. https://doi.org/10.1093/hmg/ddw173

Breitzig, M., Bhimineni, C., Lockey, R., Kolliputi, N., 2016. 4-Hydroxy-2-nonenal: a critical target in oxidative stress? Am. J. Physiol. Physiol. 311, C537–C543. https://doi.org/10.1152/ajpcell.00101.2016

Brkic, M., Balusu, S., Libert, C., Vandenbroucke, R.E., 2015. Friends or Foes: Matrix Metalloproteinases and Their Multifaceted Roles in Neurodegenerative Diseases. Mediators Inflamm. 2015, 1–27. https://doi.org/10.1155/2015/620581

Brodski, C., Blaess, S., Partanen, J., Prakash, N., 2019. Crosstalk of Intercellular Signaling Pathways in the Generation of Midbrain Dopaminergic Neurons In Vivo and from Stem Cells. J. Dev. Biol. 7, 3. https://doi.org/10.3390/jdb7010003

Bruck, N., Vitoux, D., Ferry, C., Duong, V., Bauer, A., de Thé, H., Rochette-Egly, C., 2009. A coordinated phosphorylation cascade initiated by p38MAPK/MSK1 directs RARα to target promoters. EMBO J. 28, 34–47. https://doi.org/10.1038/emboj.2008.256

Bruey, J.-M., Ducasse, C., Bonniaud, P., Ravagnan, L., Susin, S.A., Diaz-Latoud, C., Gurbuxani, S., Arrigo, A.-P.,

Kroemer, G., Solary, E., Garrido, C., 2000. Hsp27 negatively regulates cell death by interacting with cytochrome c. Nat. Cell Biol. 2, 645–652. https://doi.org/10.1038/35023595

Bryan, H.K., Olayanju, A., Goldring, C.E., Park, B.K., 2013. The Nrf2 cell defence pathway: Keap1-dependent and -independent mechanisms of regulation. Biochem. Pharmacol. 85, 705–717. https://doi.org/10.1016/j.bcp.2012.11.016

Buettner, G.R., 1993. The Pecking Order of Free Radicals and Antioxidants: Lipid Peroxidation, α-Tocopherol, and Ascorbate. Arch. Biochem. Biophys. 300, 535–543. https://doi.org/10.1006/abbi.1993.1074

Bukau, B., Weissman, J., Horwich, A., 2006. Molecular Chaperones and Protein Quality Control. Cell 125, 443–451. https://doi.org/10.1016/j.cell.2006.04.014

Burbulla, L.F., Song, P., Mazzulli, J.R., Zampese, E., Wong, Y.C., Jeon, S., Santos, D.P., Blanz, J., Obermaier, C.D., Strojny, C., Savas, J.N., Kiskinis, E., Zhuang, X., Krüger, R., Surmeier, D.J., Krainc, D., 2017. Dopamine oxidation mediates mitochondrial and lysosomal dysfunction in Parkinson's disease. Science (80-.). 357, 1255–1261. https://doi.org/10.1126/science.aam9080

Burns, L.H., Wang, H.-Y., 2017. Altered filamin A enables amyloid beta-induced tau hyperphosphorylation and neuroinflammation in Alzheimer's disease. Neuroimmunol. Neuroinflammation 4, 263. https://doi.org/10.20517/2347-8659.2017.50

Burton, E., Prados, M., 1999. New chemotherapy options for the treatment of malignant gliomas. Curr. Opin. Oncol. 11, 157–61.

Burton, G.W., Ingold, K.U., 1986. Vitamin E: application of the principles of physical organic chemistry to the exploration of its structure and function. Acc. Chem. Res. 19, 194–201. https://doi.org/10.1021/ar00127a001

Bushong, E.A., Martone, M.E., Jones, Y.Z., Ellisman, M.H., 2002. Protoplasmic astrocytes in CA1 stratum radiatum occupy separate anatomical domains. J. Neurosci. 22, 183–92. https://doi.org/10.1023/A:1011172915691

Buzzard, K.A., Giaccia, A.J., Killender, M., Anderson, R.L., 1998. Heat Shock Protein 72 Modulates Pathways of Stress-induced Apoptosis. J. Biol. Chem. 273, 17147–17153. https://doi.org/10.1074/jbc.273.27.17147

Cabelli, D.E., Bielski, B.H.J., 1983. Kinetics and mechanism for the oxidation of ascorbic acid/ascorbate by HO2/O2- (hydroperoxyl/superoxide) radicals. A pulse radiolysis and stopped-flow photolysis study. J. Phys. Chem. 87, 1809–1812. https://doi.org/10.1021/j100233a031

Caldwell, A.L., Diedrich, J.K., Shokhirev, M.N., Allen, N.J., 2020. Aberrant astrocyte protein secretion contributes to altered neuronal development in diverse disorders. bioRxiv. https://doi.org/10.1101/2020.02.17.939991

Calkins, M.J., Reddy, P.H., 2011. Assessment of newly synthesized mitochondrial DNA using BrdU labeling in

primary neurons from Alzheimer's disease mice: Implications for impaired mitochondrial biogenesis and synaptic damage. Biochim. Biophys. Acta - Mol. Basis Dis. 1812, 1182–1189. https://doi.org/10.1016/j.bbadis.2011.04.006

Całyniuk, B., Grochowska-Niedworok, E., Walkiewicz, K., Kawecka, S., Popiołek, E., Fatyga, E., 2016. Malondialdehyde (MDA) – product of lipid peroxidation as marker of homeostasis disorders and aging. Ann. Acad. Medicae Silesiensis 70, 224–228. https://doi.org/10.18794/aams/65697

Campello, S., Scorrano, L., 2010. Mitochondrial shape changes: orchestrating cell pathophysiology. EMBO Rep. 11, 678–684. https://doi.org/10.1038/embor.2010.115

Caneda-Ferrón, B., De Girolamo, L.A., Costa, T., Beck, K.E., Layfield, R., Billett, E.E., 2008. Assessment of the direct and indirect effects of MPP+ and dopamine on the human proteasome: implications for Parkinson's disease aetiology. J. Neurochem. 105, 225–38. https://doi.org/10.1111/j.1471-4159.2007.05130.x

Cannon, J.R., Greenamyre, J.T., 2013. Gene-environment interactions in Parkinson's disease: specific evidence in humans and mammalian models. Neurobiol. Dis. 57, 38–46. https://doi.org/10.1016/j.nbd.2012.06.025

Cañón, E., Cosgaya, J.M., Scsucova, S., Aranda, A., 2004. Rapid Effects of Retinoic Acid on CREB and ERK Phosphorylation in Neuronal Cells. Mol. Biol. Cell 15, 5583–5592. https://doi.org/10.1091/mbc.e04-05-0439

Carelli, V., Maresca, A., Caporali, L., Trifunov, S., Zanna, C., Rugolo, M., 2015. Mitochondria: Biogenesis and mitophagy balance in segregation and clonal expansion of mitochondrial DNA mutations. Int. J. Biochem. Cell Biol. 63, 21–24. https://doi.org/10.1016/j.biocel.2015.01.023

Carolindah, M.N., Rosli, R., Adam, A., Nordin, N., 2013. An Overview of in Vitro Research Models for Alzheimer'S Disease. Regen. Res. 2, 8–13.

Carta, M., Hirsch, E., 2018. Dyskinesia in Parkinson's disease: a clinical complication and an open scientific question. J. Neural Transm. 125, 1107–1107. https://doi.org/10.1007/s00702-018-1907-z

Cásedas, G., Bennett, A.C., González-Burgos, E., Gómez-Serranillos, M.P., López, V., Smith, C., 2019. Polyphenol-associated oxidative stress and inflammation in a model of LPS-induced inflammation in glial cells: do we know enough for responsible compounding? Inflammopharmacology 27, 189–197. https://doi.org/10.1007/s10787-018-0549-y

Cassina, P., Cassina, A., Pehar, M., Castellanos, R., Gandelman, M., de Leon, A., Robinson, K.M., Mason, R.P., Beckman, J.S., Barbeito, L., Radi, R., 2008. Mitochondrial Dysfunction in SOD1G93A-Bearing Astrocytes Promotes Motor Neuron Degeneration: Prevention by Mitochondrial-Targeted Antioxidants. J. Neurosci. 28, 4115–4122. https://doi.org/10.1523/JNEUROSCI.5308-07.2008

Cavaliere, F., Cerf, L., Dehay, B., Ramos-Gonzalez, P., De Giorgi, F., Bourdenx, M., Bessede, A., Obeso, J.A., Matute, C., Ichas, F., Bezard, E., 2017. In vitro α-synuclein neurotoxicity and spreading among neurons and astrocytes using Lewy body extracts from Parkinson disease brains. Neurobiol. Dis. 103, 101–112. https://doi.org/10.1016/j.nbd.2017.04.011

Cebrián, C., Zucca, F.A., Mauri, P., Steinbeck, J.A., Studer, L., Scherzer, C.R., Kanter, E., Budhu, S., Mandelbaum, J., Vonsattel, J.P., Zecca, L., Loike, J.D., Sulzer, D., 2014. MHC-I expression renders catecholaminergic neurons susceptible to T-cell-mediated degeneration. Nat. Commun. 5, 3633. https://doi.org/10.1038/ncomms4633

Chacón, M.A., Varela-Nallar, L., Inestrosa, N.C., 2008. Frizzled-1 is involved in the neuroprotective effect of Wnt3a against Aβ oligomers. J. Cell. Physiol. 217, 215–227. https://doi.org/10.1002/jcp.21497

Chan, D.C., 2012. Fusion and Fission: Interlinked Processes Critical for Mitochondrial Health. Annu. Rev. Genet. 46, 265–287. https://doi.org/10.1146/annurev-genet-110410-132529

Chan, D.C., 2006. Mitochondria: Dynamic Organelles in Disease, Aging, and Development. Cell 125, 1241–1252. https://doi.org/10.1016/j.cell.2006.06.010

Chan, N.C., Salazar, A.M., Pham, A.H., Sweredoski, M.J., Kolawa, N.J., Graham, R.L.J., Hess, S., Chan, D.C., 2011. Broad activation of the ubiquitin–proteasome system by Parkin is critical for mitophagy. Hum. Mol. Genet. 20, 1726–1737. https://doi.org/10.1093/hmg/ddr048

Chang, K.-H., Cheng, M.-L., Chiang, M.-C., Chen, C.-M., 2018. Lipophilic antioxidants in neurodegenerative diseases. Clin. Chim. Acta 485, 79–87. https://doi.org/10.1016/j.cca.2018.06.031

Chaturvedi, M., Kaczmarek, L., 2014. MMP-9 Inhibition: a Therapeutic Strategy in Ischemic Stroke. Mol. Neurobiol. 49, 563–573. https://doi.org/10.1007/s12035-013-8538-z

Chaturvedi, R.K., Flint Beal, M., 2013. Mitochondrial Diseases of the Brain. Free Radic. Biol. Med. 63, 1–29. https://doi.org/10.1016/j.freeradbiomed.2013.03.018

Chemmarappally, J.M., Pegram, H.C.N., Abeywickrama, N., Fornari, E., Hargreaves, A.J., De Girolamo, L.A., Stevens, B., 2020. A co-culture nanofibre scaffold model of neural cell degeneration in relevance to Parkinson's disease. Sci. Rep. 10, 2767. https://doi.org/10.1038/s41598-020-59310-x

Chen, C., Kong, A.-N.T., 2004. Dietary chemopreventive compounds and ARE/EpRE signaling. Free Radic. Biol. Med. 36, 1505–1516. https://doi.org/10.1016/j.freeradbiomed.2004.03.015

CHEN, G., BOWER, K.A., MA, C., FANG, S., THIELE, C.J., LUO, J., 2004. Glycogen synthase kinase 3β (GSK3β) mediates 6-hydroxydopamine-induced neuronal death. FASEB J. 18, 1162–1164. https://doi.org/10.1096/fj.04-1551fje

Chen, H., Chan, D.C., 2009. Mitochondrial dynamics-fusion, fission, movement, and mitophagy-in neurodegenerative diseases. Hum. Mol. Genet. 18, R169–R176. https://doi.org/10.1093/hmg/ddp326

Chen, J., Zhang, Z., Cai, L., 2014. Diabetic Cardiomyopathy and Its Prevention by Nrf2: Current Status. Diabetes Metab. J. 38, 337. https://doi.org/10.4093/dmj.2014.38.5.337

Chen, T., Tan, J., Wan, Z., Zou, Y., Kessete Afewerky, H., Zhang, Z., Zhang, T., 2017. Effects of Commonly Used Pesticides in China on the Mitochondria and Ubiquitin-Proteasome System in Parkinson's Disease. Int. J. Mol. Sci. 18, 2507. https://doi.org/10.3390/ijms18122507

Chen, Y., Vartiainen, N.E., Ying, W., Chan, P.H., Koistinaho, J., Swanson, R.A., 2001. Astrocytes protect neurons from nitric oxide toxicity by a glutathione-dependent mechanism. J. Neurochem. 77, 1601–1610. https://doi.org/10.1046/j.1471-4159.2001.00374.x

Chen, Z.J., Sun, L.J., 2009. Nonproteolytic Functions of Ubiquitin in Cell Signaling. Mol. Cell 33, 275–286. https://doi.org/10.1016/j.molcel.2009.01.014

Cheng, J.T., Yang, C.F., Jou, T.C., 1988. Inhibitory effect of l-ascorbic acid on the growth of astrocytes in cell culture. Neuropharmacology 27, 1179–82. https://doi.org/10.1016/0028-3908(88)90014-7

Chernivec, E., Cooper, J., Naylor, K., 2018. Exploring the Effect of Rotenone—A Known Inducer of Parkinson's Disease—On Mitochondrial Dynamics in Dictyostelium discoideum. Cells 7, 201. https://doi.org/10.3390/cells7110201

Cheung, Y.-T., Lau, W.K.-W., Yu, M.-S., Lai, C.S.-W., Yeung, S.-C., So, K.-F., Chang, R.C.-C., 2009. Effects of all-trans-retinoic acid on human SH-SY5Y neuroblastoma as in vitro model in neurotoxicity research. Neurotoxicology 30, 127–135. https://doi.org/10.1016/j.neuro.2008.11.001

Chiaradia, E., Renzone, G., Scaloni, A., Caputo, M., Costanzi, E., Gambelunghe, A., Muzi, G., Avellini, L., Emiliani, C., Buratta, S., 2019. Protein carbonylation in dopaminergic cells exposed to rotenone. Toxicol. Lett. 309, 20–32. https://doi.org/10.1016/j.toxlet.2019.04.002

Cho, D.-H., Nakamura, T., Fang, J., Cieplak, P., Godzik, A., Gu, Z., Lipton, S.A., 2009. S-Nitrosylation of Drp1 Mediates β-Amyloid-Related Mitochondrial Fission and Neuronal Injury. Science (80-.). 324, 102–105. https://doi.org/10.1126/science.1171091

Cho, H.-Y., Reddy, S.P., Kleeberger, S.R., 2006. Nrf2 Defends the Lung from Oxidative Stress. Antioxid. Redox Signal. 8, 76–87. https://doi.org/10.1089/ars.2006.8.76

Choi, J., Conrad, C.C., Dai, R., Malakowsky, C.A., Talent, J.M., Carroll, C.A., Weintraub, S.T., Gracy, R.W., 2003. Vitamin E prevents oxidation of antiapoptotic proteins in neuronal cells. Proteomics 3, 73–77. https://doi.org/10.1002/pmic.200390011

Choi, J., Sullards, M.C., Olzmann, J.A., Rees, H.D., Weintraub, S.T., Bostwick, D.E., Gearing, M., Levey, A.I., Chin, L.-S., Li, L., 2006. Oxidative Damage of DJ-1 Is Linked to Sporadic Parkinson and Alzheimer Diseases. J. Biol. Chem. 281, 10816–10824. https://doi.org/10.1074/jbc.M509079200

Choi, S.W., Gerencser, A.A., Nicholls, D.G., 2009. Bioenergetic analysis of isolated cerebrocortical nerve

terminals on a microgram scale: spare respiratory capacity and stochastic mitochondrial failure. J. Neurochem. 109, 1179–1191. https://doi.org/10.1111/j.1471-4159.2009.06055.x

Chou, A.P., Li, S., Fitzmaurice, A.G., Bronstein, J.M., 2010. Mechanisms of rotenone-induced proteasome inhibition. Neurotoxicology 31, 367–372. https://doi.org/10.1016/j.neuro.2010.04.006

Chouchani, E.T., Methner, C., Nadtochiy, S.M., Logan, A., Pell, V.R., Ding, S., James, A.M., Cochemé, H.M., Reinhold, J., Lilley, K.S., Partridge, L., Fearnley, I.M., Robinson, A.J., Hartley, R.C., Smith, R.A.J., Krieg, T., Brookes, P.S., Murphy, M.P., 2013. Cardioprotection by S-nitrosation of a cysteine switch on mitochondrial complex I. Nat. Med. 19, 753–759. https://doi.org/10.1038/nm.3212

Choudhury, G.R., Daadi, M.M., 2018. Charting the onset of Parkinson-like motor and non-motor symptoms in nonhuman primate model of Parkinson's disease. PLoS One 13, e0202770. https://doi.org/10.1371/journal.pone.0202770

Chu, C.T., 2010. A pivotal role for PINK1 and autophagy in mitochondrial quality control: implications for Parkinson disease. Hum. Mol. Genet. 19, R28–R37. https://doi.org/10.1093/hmg/ddq143

Ciani, L., Salinas, P.C., 2005. WNTS in the vertebrate nervous system: from patterning to neuronal connectivity. Nat. Rev. Neurosci. 6, 351–362. https://doi.org/10.1038/nrn1665

Ciechanover, A., Brundin, P., 2003. The ubiquitin proteasome system in neurodegenerative diseases: Sometimes the chicken, sometimes the egg. Neuron 40, 427–446. https://doi.org/10.1016/S0896-6273(03)00606-8

Clancy, R.M., Levartovsky, D., Leszczynska-Piziak, J., Yegudin, J., Abramson, S.B., 1994. Nitric oxide reacts with intracellular glutathione and activates the hexose monophosphate shunt in human neutrophils: evidence for S-nitrosoglutathione as a bioactive intermediary. Proc. Natl. Acad. Sci. 91, 3680–3684. https://doi.org/10.1073/pnas.91.9.3680

Clark, I.E., Dodson, M.W., Jiang, C., Cao, J.H., Huh, J.R., Seol, J.H., Yoo, S.J., Hay, B. a, Guo, M., 2006. Drosophila pink1 is required for mitochondrial function and interacts genetically with parkin. Nature 441, 1162–1166. https://doi.org/10.1038/nature04779

Clements, C.M., McNally, R.S., Conti, B.J., Mak, T.W., Ting, J.P., 2006. DJ-1, a cancer- and Parkinson's disease-associated protein, stabilizes the antioxidant transcriptional master regulator Nrf2. Proc Natl Acad Sci U S A 103, 15091–15096. https://doi.org/10.1073/pnas.0607260103

Clements, R.T., Sodha, N.R., Feng, J., Mieno, S., Boodhwani, M., Ramlawi, B., Bianchi, C., Sellke, F.W., 2007. Phosphorylation and translocation of heat shock protein 27 and αB-crystallin in human myocardium after cardioplegia and cardiopulmonary bypass. J. Thorac. Cardiovasc. Surg. 134, 1461-1470.e3. https://doi.org/10.1016/j.jtcvs.2007.06.026

Cloos, P.A.C., Christgau, S., 2004. Post-translational modifications of proteins: Implications for aging, antigen

recognition, and autoimmunity. Biogerontology. https://doi.org/10.1023/B:BGEN.0000031152.31352.8b

Cobb, C.A., Cole, M.P., 2015. Oxidative and nitrative stress in neurodegeneration. Neurobiol. Dis. 84, 4–21. https://doi.org/10.1016/j.nbd.2015.04.020

Coleman, M.P., 2013. The challenges of axon survival: Introduction to the special issue on axonal degeneration. Exp. Neurol. 246, 1–5. https://doi.org/10.1016/j.expneurol.2013.06.007

Coleman, M.P., Höke, A., 2020. Programmed axon degeneration: from mouse to mechanism to medicine. Nat. Rev. Neurosci. 1–14. https://doi.org/10.1038/s41583-020-0269-3

Collier, T.J., Kanaan, N.M., Kordower, J.H., 2017. Aging and Parkinson's disease: Different sides of the same coin? Mov. Disord. 32, 983–990. https://doi.org/10.1002/mds.27037

Colombo, E., Farina, C., 2016. Astrocytes: Key Regulators of Neuroinflammation. Trends Immunol. 37, 608–620. https://doi.org/10.1016/j.it.2016.06.006

Compagnucci, C., Piemonte, F., Sferra, A., Piermarini, E., Bertini, E., 2016. The cytoskeletal arrangements necessary to neurogenesis. Oncotarget 7. https://doi.org/10.18632/oncotarget.6838

Concannon, C.G., Orrenius, S., Samali, A., 2001. Hsp27 Inhibits Cytochrome c -Mediated Caspase Activation by Sequestering Both Pro-caspase-3 and Cytochrome c. Gene Expr. 9, 195–201. https://doi.org/10.3727/000000001783992605

Conrad, M., Friedmann Angeli, J.P., 2018. Glutathione Peroxidases, in: Comprehensive Toxicology. Elsevier, pp. 260–276. https://doi.org/10.1016/B978-0-12-801238-3.95621-6

Constantinescu, R., Constantinescu, A.T., Reichmann, H., Janetzky, B., 2007. Neuronal differentiation and long-term culture of the human neuroblastoma line SH-SY5Y. J. Neural Transm. Suppl. 72, 17–28. https://doi.org/10.1007/978-3-211-73574-9-3

Coutinho-Budd, J.C., Sheehan, A.E., Freeman, M.R., 2017. The secreted neurotrophin Spätzle 3 promotes glial morphogenesis and supports neuronal survival and function. Genes Dev. 31, 2023–2038. https://doi.org/10.1101/gad.305888.117

Cox, A.G., Winterbourn, C.C., Hampton, M.B., 2010. Mitochondrial peroxiredoxin involvement in antioxidant defence and redox signalling. Biochem. J. 425, 313–325. https://doi.org/10.1042/BJ20091541

Coyle, J., Puttfarcken, P., 1993. Oxidative stress, glutamate, and neurodegenerative disorders. Science (80-.). 262, 689–695. https://doi.org/10.1126/science.7901908

Cronin-Furman, E.N., Borland, M.K., Bergquist, K.E., Bennett, J.P., Trimmer, P.A., 2013. Mitochondrial quality, dynamics and functional capacity in Parkinson's disease cybrid cell lines selected for Lewy body expression. Mol. Neurodegener. 8, 6. https://doi.org/10.1186/1750-1326-8-6

Cruz-Garcia, D., Brouwers, N., Malhotra, V., Curwin, A.J., 2019. Reactive oxygen species (ROS) production triggers unconventional secretion of antioxidant enzymes. bioRxiv 628321. https://doi.org/10.1101/628321

Cuervo, A.M., Wong, E., 2014. Chaperone-mediated autophagy: roles in disease and aging. Cell Res. 24, 92–104. https://doi.org/10.1038/cr.2013.153

Cunningham, C., Dunne, A., Lopez-Rodriguez, A.B., 2019. Astrocytes: Heterogeneous and Dynamic Phenotypes in Neurodegeneration and Innate Immunity. Neurosci. 25, 455–474. https://doi.org/10.1177/1073858418809941

Cunningham, L.A., Wetzel, M., Rosenberg, G.A., 2005. Multiple roles for MMPs and TIMPs in cerebral ischemia. Glia 50, 329–339. https://doi.org/10.1002/glia.20169

D'Autréaux, B., Toledano, M.B., 2007. ROS as signalling molecules: mechanisms that generate specificity in ROS homeostasis. Nat. Rev. Mol. Cell Biol. 8, 813–824. https://doi.org/10.1038/nrm2256

Dadakhujaev, S., Noh, H.S., Jung, E.J., Cha, J.Y., Baek, S.M., Ha, J.H., Kim, D.R., 2010. Autophagy protects the rotenone-induced cell death in α-synuclein overexpressing SH-SY5Y cells. Neurosci. Lett. 472, 47–52. https://doi.org/10.1016/j.neulet.2010.01.053

Daly, C., Sugimori, M., Moreira, J.E., Ziff, E.B., Llinas, R., 2000. Synaptophysin regulates clathrin-independent endocytosis of synaptic vesicles. Proc. Natl. Acad. Sci. 97, 6120–6125. https://doi.org/10.1073/pnas.97.11.6120

Danial, N.N., Korsmeyer, S.J., 2004. Cell Death. Cell 116, 205–219. https://doi.org/10.1016/S0092-8674(04)00046-7

Darios, F., Corti, O., Lücking, C.B., Hampe, C., Muriel, M.P., Abbas, N., Gu, W.J., Hirsch, E.C., Rooney, T., Ruberg, M., Brice, A., 2003. Parkin prevents mitochondrial swelling and cytochrome c release in mitochondria-dependent cell death. Hum. Mol. Genet. 12, 517–526. https://doi.org/10.1093/hmg/ddg044

Darley-usmar, V.M., Hogg, N., O'leary, V.J., Wilson, M.T., Moncada, S., 1992. The Simultaneous Generation of Superoxide and Nitric Oxide Can Initiate Lipid Peroxidation in Human Low Density Lipoprotein. Free Radic. Res. Commun. 17, 9–20. https://doi.org/10.3109/10715769209061085

Das, A., Banik, N.L., Ray, S.K., 2009. Molecular Mechanisms of the Combination of Retinoid and Interferon-gamma for Inducing Differentiation and Increasing Apoptosis in Human Glioblastoma T98G and U87MG Cells. Neurochem. Res. 34, 87–101. https://doi.org/10.1007/s11064-008-9669-x

Das, A., Banik, N.L., Ray, S.K., 2008. Retinoids induced astrocytic differentiation with down regulation of telomerase activity and enhanced sensitivity to taxol for apoptosis in human glioblastoma T98G and U87MG cells. J. Neurooncol. 87, 9–22. https://doi.org/10.1007/s11060-007-9485-1

Das, A., Sarwar, M.S., Hossain, M.S., Karmakar, P., Islam, M.S., Hussain, M.E., Banik, S., 2019. Elevated Serum Lipid Peroxidation and Reduced Vitamin C and Trace Element Concentrations Are Correlated With Epilepsy. Clin. EEG Neurosci. 50, 63–72. https://doi.org/10.1177/1550059418772755

Dasuri, K., Zhang, L., Keller, J.N., 2013. Oxidative stress, neurodegeneration, and the balance of protein degradation and protein synthesis. Free Radic. Biol. Med. 62, 170–185. https://doi.org/10.1016/j.freeradbiomed.2012.09.016

Davis, C.W., Hawkins, B.J., Ramasamy, S., Irrinki, K.M., Cameron, B.A., Islam, K., Daswani, V.P., Doonan, P.J., Manevich, Y., Madesh, M., 2010. Nitration of the mitochondrial complex I subunit NDUFB8 elicits RIP1- and RIP3-mediated necrosis. Free Radic. Biol. Med. 48, 306–317. https://doi.org/10.1016/j.freeradbiomed.2009.11.001

Dawson, T.M., Dawson, V.L., 2018. Nitric Oxide Signaling in Neurodegeneration and Cell Death, in: Advances in Pharmacology. pp. 57–83. https://doi.org/10.1016/bs.apha.2017.09.003

De Armas, M.I., Esteves, R., Viera, N., Reyes, A.M., Mastrogiovanni, M., Alegria, T.G.P., Netto, L.E.S., Tórtora, V., Radi, R., Trujillo, M., 2019. Rapid peroxynitrite reduction by human peroxiredoxin 3: Implications for the fate of oxidants in mitochondria. Free Radic. Biol. Med. 130, 369–378. https://doi.org/10.1016/j.freeradbiomed.2018.10.451

de Farias, C.C., Maes, M., Bonifácio, K.L., Bortolasci, C.C., de Souza Nogueira, A., Brinholi, F.F., Matsumoto, A.K., do Nascimento, M.A., de Melo, L.B., Nixdorf, S.L., Lavado, E.L., Moreira, E.G., Barbosa, D.S., 2016. Highly specific changes in antioxidant levels and lipid peroxidation in Parkinson's disease and its progression: Disease and staging biomarkers and new drug targets. Neurosci. Lett. 617, 66–71. https://doi.org/10.1016/j.neulet.2016.02.011

De Grey, A.D.N.J., 2002. HO2•: The Forgotten Radical. DNA Cell Biol. 21, 251–257. https://doi.org/10.1089/104454902753759672

de Medeiros, L.M., De Bastiani, M.A., Rico, E.P., Schonhofen, P., Pfaffenseller, B., Wollenhaupt-Aguiar, B., Grun, L., Barbé-Tuana, F., Zimmer, E.R., Castro, M.A.A., Parsons, R.B., Klamt, F., 2019. Cholinergic Differentiation of Human Neuroblastoma SH-SY5Y Cell Line and Its Potential Use as an In vitro Model for Alzheimer's Disease Studies. Mol. Neurobiol. 1605–19. https://doi.org/10.1007/s12035-019-1605-3

de Oliveira, M.R., Brasil, F.B., Andrade, C.M.B., 2017. Naringenin Attenuates H2O2-Induced Mitochondrial Dysfunction by an Nrf2-Dependent Mechanism in SH-SY5Y Cells. Neurochem. Res. 42, 3341–3350. https://doi.org/10.1007/s11064-017-2376-8

de Pablo, Y., Chen, M., Möllerström, E., Pekna, M., Pekny, M., 2018. Drugs targeting intermediate filaments can improve neurosupportive properties of astrocytes. Brain Res. Bull. 136, 130–138. https://doi.org/10.1016/j.brainresbull.2017.01.021

de Pedro, N., Cantizani, J., Ortiz-López, F.J., González-Menéndez, V., Cautain, B., Rodríguez, L., Bills, G.F.,

Reyes, F., Genilloud, O., Vicente, F., 2016. Protective effects of isolecanoric acid on neurodegenerative in vitro models. Neuropharmacology 101, 538–548. https://doi.org/10.1016/j.neuropharm.2015.09.029

De Vos, K.J., Grierson, A.J., Ackerley, S., Miller, C.C.J., 2008. Role of Axonal Transport in Neurodegenerative Diseases. Annu. Rev. Neurosci. 31, 151–173. https://doi.org/10.1146/annurev.neuro.31.061307.090711

Deakin, M.R., Kovach, P.M., Stutts, K.J., Wightman, R.M., 1986. Heterogeneous mechanisms of the oxidation of catechols and ascorbic acid at carbon electrodes. Anal. Chem. 58, 1474–1480. https://doi.org/10.1021/ac00298a046

DeBalsi, K.L., Hoff, K.E., Copeland, W.C., 2017. Role of the mitochondrial DNA replication machinery in mitochondrial DNA mutagenesis, aging and age-related diseases. Ageing Res. Rev. 33, 89–104. https://doi.org/10.1016/j.arr.2016.04.006

Deeb, R.S., Nuriel, T., Cheung, C., Summers, B., Lamon, B.D., Gross, S.S., Hajjar, D.P., 2013. Characterization of a cellular denitrase activity that reverses nitration of cyclooxygenase. Am. J. Physiol. Circ. Physiol. 305, H687–H698. https://doi.org/10.1152/ajpheart.00876.2012

Delamarre, A., Meissner, W.G., 2017. Epidemiology, environmental risk factors and genetics of Parkinson's disease. Presse Med. 46, 175–181. https://doi.org/10.1016/j.lpm.2017.01.001

Delcourt, N., Jouin, P., Poncet, J., Demey, E., Mauger, E., Bockaert, J., Marin, P., Galéotti, N., 2005. Difference in Mass Analysis Using Labeled Lysines (DIMAL-K). Mol. Cell. Proteomics 4, 1085–1094. https://doi.org/10.1074/mcp.M500040-MCP200

Delsing, L., Dönnes, P., Sánchez, J., Clausen, M., Voulgaris, D., Falk, A., Herland, A., Brolén, G., Zetterberg, H., Hicks, R., Synnergren, J., 2018. Barrier Properties and Transcriptome Expression in Human iPSC-Derived Models of the Blood-Brain Barrier. Stem Cells 36, 1816–1827. https://doi.org/10.1002/stem.2908

Demasi, M., Davies, K.J.A., 2003. Proteasome inhibitors induce intracellular protein aggregation and cell death by an oxygen-dependent mechanism. FEBS Lett. 542, 89–94. https://doi.org/10.1016/S0014-5793(03)00353-3

Deng, Y.-N., Shi, J., Liu, J., Qu, Q.-M., 2013. Celastrol protects human neuroblastoma SH-SY5Y cells from rotenone-induced injury through induction of autophagy. Neurochem. Int. 63, 1–9. https://doi.org/10.1016/j.neuint.2013.04.005

Deng, Y., Jia, F., Chen, S., Shen, Z., Jin, Q., Fu, G., Ji, J., 2018. Nitric oxide as an all-rounder for enhanced photodynamic therapy: Hypoxia relief, glutathione depletion and reactive nitrogen species generation. Biomaterials 187, 55–65. https://doi.org/10.1016/j.biomaterials.2018.09.043

Denton, K., Mou, Y., Xu, C.-C., Shah, D., Chang, J., Blackstone, C., Li, X.-J., 2018. Impaired mitochondrial

dynamics underlie axonal defects in hereditary spastic paraplegias. Hum. Mol. Genet. 27, 2517–2530. https://doi.org/10.1093/hmg/ddy156

Desagher, S., Glowinski, J., Premont, J., 1996. Astrocytes protect neurons from hydrogen peroxide toxicity. J. Neurosci. 16, 2553–62.

Deshmukh, F., Yaffe, D., Olshina, M.A., Ben-Nissan, G., Sharon, M., 2019. The Contribution of the 20S Proteasome to Proteostasis. Biomolecules 9, 190. https://doi.org/10.3390/biom9050190

Dexter, D.T., Sian, J., Rose, S., Hindmarsh, J.G., Mann, V.M., Cooper, J.M., Wells, F.R., Daniel, S.E., Lees, a J., Schapira, a H., 1994. Indices of oxidative stress and mitochondrial function in individuals with incidental Lewy body disease. Ann. Neurol. 35, 38–44. https://doi.org/10.1002/ana.410350107

Dhakshinamoorthy, S., Jain, A.K., Bloom, D.A., Jaiswal, A.K., 2005. Bach1 Competes with Nrf2 Leading to Negative Regulation of the Antioxidant Response Element (ARE)-mediated NAD(P)H:Quinone Oxidoreductase 1 Gene Expression and Induction in Response to Antioxidants. J. Biol. Chem. 280, 16891–16900. https://doi.org/10.1074/jbc.M500166200

Dhakshinamoorthy, S., Jaiswal, a K., 2001. Functional characterization and role of INrf2 in antioxidant response element-mediated expression and antioxidant induction of NAD(P)H:quinone oxidoreductase1 gene. Oncogene 20, 3906–3917. https://doi.org/10.1038/sj.onc.1204506

Di Cesare Mannelli, L., Zanardelli, M., Failli, P., Ghelardini, C., 2013. Oxaliplatin-induced oxidative stress in nervous system-derived cellular models: Could it correlate with in vivo neuropathy? Free Radic. Biol. Med. 61, 143–150. https://doi.org/10.1016/j.freeradbiomed.2013.03.019

Di Giacomo, G., Rizza, S., Montagna, C., Filomeni, G., 2012. Established Principles and Emerging Concepts on the Interplay between Mitochondrial Physiology and S -(De)nitrosylation: Implications in Cancer and Neurodegeneration. Int. J. Cell Biol. 2012, 1–20. https://doi.org/10.1155/2012/361872

Di Nottia, M., Masciullo, M., Verrigni, D., Petrillo, S., Modoni, A., Rizzo, V., Di Giuda, D., Rizza, T., Niceta, M., Torraco, A., Bianchi, M., Santoro, M., Bentivoglio, A.R., Bertini, E., Piemonte, F., Carrozzo, R., Silvestri, G., 2017. DJ-1 modulates mitochondrial response to oxidative stress: clues from a novel diagnosis of PARK7. Clin. Genet. 92, 18–25. https://doi.org/10.1111/cge.12841

Diaz, F., Fukui, H., Garcia, S., Moraes, C.T., 2006. Cytochrome c Oxidase Is Required for the Assembly/Stability of Respiratory Complex I in Mouse Fibroblasts. Mol. Cell. Biol. 26, 4872–4881. https://doi.org/10.1128/MCB.01767-05

Didonna, A., Benetti, F., 2015. Post-translational modifications in neurodegeneration. AIMS Biophys. 3, 27–49. https://doi.org/10.3934/biophy.2016.1.27

Ding, Q., Dimayuga, E., Martin, S., Bruce-Keller, A.J., Nukala, V., Cuervo, A.M., Keller, J.N., 2004. Characterization of chronic low-level proteasome inhibition on neural homeostasis. J. Neurochem. 86,

489–497. https://doi.org/10.1046/j.1471-4159.2003.01885.x

Dinkova-Kostova, A.T., Abramov, A.Y., 2015. The emerging role of Nrf2 in mitochondrial function. Free Radic. Biol. Med. 88, 179–188. https://doi.org/10.1016/j.freeradbiomed.2015.04.036

Dinkova-Kostova, A.T., Baird, L., Holmström, K.M., Meyer, C.J., Abramov, A.Y., 2015. The spatiotemporal regulation of the Keap1–Nrf2 pathway and its importance in cellular bioenergetics. Biochem. Soc. Trans. 43, 602–610. https://doi.org/10.1042/BST20150003

Dinkova-Kostova, A.T., Kostov, R. V., Kazantsev, A.G., 2018. The role of Nrf2 signaling in counteracting neurodegenerative diseases. FEBS J. 285, 3576–3590. https://doi.org/10.1111/febs.14379

Diot, A., Morten, K., Poulton, J., 2016. Mitophagy plays a central role in mitochondrial ageing. Mamm. Genome 27, 381–395. https://doi.org/10.1007/s00335-016-9651-x

Discher, D.E., 2005. Tissue Cells Feel and Respond to the Stiffness of Their Substrate. Science (80-.). 310, 1139–1143. https://doi.org/10.1126/science.1116995

Dodson, M., Castro-Portuguez, R., Zhang, D.D., 2019. NRF2 plays a critical role in mitigating lipid peroxidation and ferroptosis. Redox Biol. https://doi.org/10.1016/j.redox.2019.101107

Dodson, M., Liang, Q., Johnson, M.S., Redmann, M., Fineberg, N., Darley-Usmar, V.M., Zhang, J., 2013. Inhibition of glycolysis attenuates 4-hydroxynonenal-dependent autophagy and exacerbates apoptosis in differentiated SH-SY5Y neuroblastoma cells. Autophagy 9, 1996–2008. https://doi.org/10.4161/auto.26094

Dodson, M., Wani, W.Y., Redmann, M., Benavides, G.A., Johnson, M.S., Ouyang, X., Cofield, S.S., Mitra, K., Darley-Usmar, V., Zhang, J., 2017. Regulation of autophagy, mitochondrial dynamics, and cellular bioenergetics by 4-hydroxynonenal in primary neurons. Autophagy 13, 1828–1840. https://doi.org/10.1080/15548627.2017.1356948

Donaire, V., Niso, M., Morán, J.M., García, L., González-Polo, R.A., Soler, G., Fuentes, J.M., 2005. Heat shock proteins protect both MPP+ and paraquat neurotoxicity. Brain Res. Bull. 67, 509–514. https://doi.org/10.1016/j.brainresbull.2005.08.002

Donnelly, J.K., McLellan, K.M., Walker, J.L., Robinson, D.S., 1989. Superoxide dismutases in foods. A review. Food Chem. 33, 243–270. https://doi.org/10.1016/0308-8146(89)90036-8

Dooley, M.M., Sano, N., Kawashima, H., Nakamura, T., 1990. Effects of 2,2′-azobis (2-amidinopropane) hydrochloride in vivo and protection by vitamin E. Free Radic. Biol. Med. 9, 199–204. https://doi.org/10.1016/0891-5849(90)90028-H

Dorsey, E.R., George, B.P., Leff, B., Willis, A.W., 2013. The coming crisis: Obtaining care for the growing burden of neurodegenerative conditions. Neurology 80, 1989–1996. https://doi.org/10.1212/WNL.0b013e318293e2ce

Dou, F., Netzer, W.J., Tanemura, K., Li, F., Hartl, F.U., Takashima, A., Gouras, G.K., Greengard, P., Xu, H., 2003. Chaperones increase association of tau protein with microtubules. Proc. Natl. Acad. Sci. 100, 721–726. https://doi.org/10.1073/pnas.242720499

Douglas, P.M., Dillin, A., 2010. Protein homeostasis and aging in neurodegeneration. J. Cell Biol. 190, 719–729. https://doi.org/10.1083/jcb.201005144

Dowell, J.A., Johnson, J.A., 2013. Mechanisms of Nrf2 Protection in Astrocytes as Identified by Quantitative Proteomics and siRNA Screening. PLoS One 8, e70163. https://doi.org/10.1371/journal.pone.0070163

Drechsel, D.A., Patel, M., 2010. Respiration-dependent H 2 O 2 Removal in Brain Mitochondria via the Thioredoxin/Peroxiredoxin System. J. Biol. Chem. 285, 27850–27858. https://doi.org/10.1074/jbc.M110.101196

Dreyfus, M., El-Atifi, M., Court, M., Bidart, M., Coutton, C., Leclech, C., Ballester, B., Garcion, E., Bouamrani, A., Berger, F., Wion, D., 2018. Reprogramming glioma cell cultures with retinoic acid: Additional arguments for reappraising the potential of retinoic acid in the context of personalized glioma therapy. Glioma 1, 66. https://doi.org/10.4103/glioma.glioma_3_18

Dringen, R., Gutterer, J.M., Hirrlinger, J., 2000. Glutathione metabolism in brain. Eur. J. Biochem. 267, 4912–4916. https://doi.org/10.1046/j.1432-1327.2000.01597.x

Dringen, R., Hamprecht, B., 1997. Involvement of glutathione peroxidase and catalase in the disposal of exogenous hydrogen peroxide by cultured astroglial cells. Brain Res. 759, 67–75. https://doi.org/10.1016/S0006-8993(97)00233-3

Dringen, R., Hirrlinger, J., 2003. Glutathione pathways in the brain. Biol. Chem. 384, 505–16. https://doi.org/10.1515/BC.2003.059

Dringen, R., Pawlowski, P.G., Hirrlinger, J., 2005. Peroxide detoxification by brain cells. J. Neurosci. Res. 79, 157–65. https://doi.org/10.1002/jnr.20280

Dringen, R., Pfeiffer, B., Hamprecht, B., 1999. Synthesis of the antioxidant glutathione in neurons: supply by astrocytes of CysGly as precursor for neuronal glutathione. J. Neurosci. 19, 562–9. https://doi.org/10.1523/JNEUROSCI.19-02-00562.1999

Dröge, W., 2002. Free radicals in the physiological control of cell function. Physiol. Rev. 82, 47–95. https://doi.org/10.1152/physrev.00018.2001

Drukarch, B., Schepens, E., Stoof, J.C., Langeveld, C.H., Van Muiswinkel, F.L., 1998. Astrocyte-enhanced neuronal survival is mediated by scavenging of extracellular reactive oxygen species. Free Radic. Biol. Med. 25, 217–220. https://doi.org/10.1016/S0891-5849(98)00050-1

Du, F., Yu, Q., Chen, A., Chen, D., Yan, S.S., 2018. Astrocytes Attenuate Mitochondrial Dysfunctions in Human Dopaminergic Neurons Derived from iPSC. Stem Cell Reports 10, 366–374.

https://doi.org/10.1016/j.stemcr.2017.12.021

Du, J., Cullen, J.J., Buettner, G.R., 2012. Ascorbic acid: Chemistry, biology and the treatment of cancer. Biochim. Biophys. Acta - Rev. Cancer 1826, 443–457. https://doi.org/10.1016/j.bbcan.2012.06.003

Dunham-Snary, K.J., Wu, D., Potus, F., Sykes, E.A., Mewburn, J.D., Charles, R.L., Eaton, P., Sultanian, R.A., Archer, S.L., 2019. Ndufs2, a Core Subunit of Mitochondrial Complex I, Is Essential for Acute Oxygen-Sensing and Hypoxic Pulmonary Vasoconstriction. Circ. Res. 124, 1727–1746. https://doi.org/10.1161/CIRCRESAHA.118.314284

Echtay, K.S., Murphy, M.P., Smith, R.A.J., Talbot, D.A., Brand, M.D., 2002. Superoxide Activates Mitochondrial Uncoupling Protein 2 from the Matrix Side. J. Biol. Chem. 277, 47129–47135. https://doi.org/10.1074/jbc.M208262200

Edsjö, A., Lavenius, E., Nilsson, H., Hoehner, J.C., Simonsson, P., Culp, L.A., Martinsson, T., Larsson, C., Påhlman, S., 2003. Expression of trkB in Human Neuroblastoma in Relation to MYCN Expression and Retinoic Acid Treatment. Lab. Investig. 83, 813–823. https://doi.org/10.1097/01.LAB.0000074895.48776.D8

Ehrnhoefer, D.E., Wong, B.K.Y., Hayden, M.R., 2011. Convergent pathogenic pathways in Alzheimer's and Huntington's diseases: shared targets for drug development. Nat. Rev. Drug Discov. 10, 853–867. https://doi.org/10.1038/nrd3556

Ehrnsperger, M., 1997. Binding of non-native protein to Hsp25 during heat shock creates a reservoir of folding intermediates for reactivation. EMBO J. 16, 221–229. https://doi.org/10.1093/emboj/16.2.221

Ekimova, I. V., Plaksina, D. V., Pastukhov, Y.F., Lapshina, K. V., Lazarev, V.F., Mikhaylova, E.R., Polonik, S.G., Pani, B., Margulis, B.A., Guzhova, I. V., Nudler, E., 2018. New HSF1 inducer as a therapeutic agent in a rodent model of Parkinson's disease. Exp. Neurol. 306, 199–208. https://doi.org/10.1016/j.expneurol.2018.04.012

El Massri, N., Johnstone, D.M., Peoples, C.L., Moro, C., Reinhart, F., Torres, N., Stone, J., Benabid, A.-L., Mitrofanis, J., 2016. The effect of different doses of near infrared light on dopaminergic cell survival and gliosis in MPTP-treated mice. Int. J. Neurosci. 126, 76–87. https://doi.org/10.3109/00207454.2014.994063

Encinas, Mario, Iglesias, M., Liu, Y., Wang, H., Muhaisen, A., Ceña, V., Gallego, C., Comella, J.X., 2002. Sequential Treatment of SH-SY5Y Cells with Retinoic Acid and Brain-Derived Neurotrophic Factor Gives Rise to Fully Differentiated, Neurotrophic Factor-Dependent, Human Neuron-Like Cells. J. Neurochem. 75, 991–1003. https://doi.org/10.1046/j.1471-4159.2000.0750991.x

Encinas, M., Iglesias, M., Llecha, N., Comella, J.X., 2002. Extracellular-Regulated Kinases and Phosphatidylinositol 3-Kinase Are Involved in Brain-Derived Neurotrophic Factor-Mediated Survival and neuritogenesis of the Neuroblastoma Cell Line SH-SY5Y. J. Neurochem. 73, 1409–1421.

https://doi.org/10.1046/j.1471-4159.1999.0731409.x

Engele, J., Schubert, D., Bohn, M.C., 1991. Conditioned media derived from glial cell lines promote survival and differentiation of dopaminergic neurons in vitro: Role of mesencephalic glia. J. Neurosci. Res. 30, 359–371. https://doi.org/10.1002/jnr.490300212

Engler, A.J., Griffin, M.A., Sen, S., Bönnemann, C.G., Sweeney, H.L., Discher, D.E., 2004. Myotubes differentiate optimally on substrates with tissue-like stiffness. J. Cell Biol. 166, 877–887. https://doi.org/10.1083/jcb.200405004

Eroglu, C., Barres, B.A., 2010. Regulation of synaptic connectivity by glia. Nature 468, 223–231. https://doi.org/10.1038/nature09612

Espay, A.J., Vizcarra, J.A., Marsili, L., Lang, A.E., Simon, D.K., Merola, A., Josephs, K.A., Fasano, A., Morgante, F., Savica, R., Greenamyre, J.T., Cambi, F., Yamasaki, T.R., Tanner, C.M., Gan-Or, Z., Litvan, I., Mata, I.F., Zabetian, C.P., Brundin, P., Fernandez, H.H., Standaert, D.G., Kauffman, M.A., Schwarzschild, M.A., Sardi, S.P., Sherer, T., Perry, G., Leverenz, J.B., 2019. Revisiting protein aggregation as pathogenic in sporadic Parkinson and Alzheimer diseases. Neurology 92, 329–337. https://doi.org/10.1212/WNL.0000000000006926

Espinosa-Diez, C., Miguel, V., Mennerich, D., Kietzmann, T., Sánchez-Pérez, P., Cadenas, S., Lamas, S., 2015. Antioxidant responses and cellular adjustments to oxidative stress. Redox Biol. 6, 183–197. https://doi.org/10.1016/j.redox.2015.07.008

Esposito, F., Ammendola, R., Faraonio, R., Russo, T., Cimino, F., 2004. Redox Control of Signal Transduction, Gene Expression and Cellular Senescence. Neurochem. Res. 29, 617–628. https://doi.org/10.1023/B:NERE.0000014832.78725.1a

Esser, C., Alberti, S., Höhfeld, J., 2004. Cooperation of molecular chaperones with the ubiquitin/proteasome system. Biochim. Biophys. Acta - Mol. Cell Res. 1695, 171–188. https://doi.org/10.1016/j.bbamcr.2004.09.020

Esterbauer, H., Schaur, R.J., Zollner, H., 1991. Chemistry and biochemistry of 4-hydroxynonenal, malonaldehyde and related aldehydes. Free Radic. Biol. Med. 11, 81–128. https://doi.org/10.1016/0891-5849(91)90192-6

Fan, G.-H., Qi, C., Chen, S.-D., 2005. Heat shock proteins reduce toxicity of 1-methyl-4-phenylpyridinium ion in SK-N-SH cells. J. Neurosci. Res. 82, 551–562. https://doi.org/10.1002/jnr.20656

Fariss, M.W., Chan, C.B., Patel, M., Van Houten, B., Orrenius, S., 2005. Role of mitochondria in toxic oxidative stress. Mol. Interv. 5, 94–111. https://doi.org/10.1124/mi.5.2.7

Feany, M.B., Bender, W.W., 2000. A Drosophila model of Parkinson's disease. Nature 404, 394–398. https://doi.org/10.1038/35006074

Feitosa, C.M., da Silva Oliveira, G.L., do Nascimento Cavalcante, A., Morais Chaves, S.K., Rai, M., 2018. Determination of Parameters of Oxidative Stress in vitro Models of Neurodegenerative Diseases-A Review. Curr. Clin. Pharmacol. 13, 100–109. https://doi.org/10.2174/1574884713666180301091612

Feng, J., 2006. Microtubule: A Common Target for Parkin and Parkinson's Disease Toxins. Neurosci. 12, 469–476. https://doi.org/10.1177/1073858406293853

Fernández-Fernández, M.R., Gragera, M., Ochoa-Ibarrola, L., Quintana-Gallardo, L., Valpuesta, J.M., 2017. Hsp70 - a master regulator in protein degradation. FEBS Lett. 591, 2648–2660. https://doi.org/10.1002/1873-3468.12751

Ferreira, M., Massano, J., 2017. An updated review of Parkinson's disease genetics and clinicopathological correlations. Acta Neurol. Scand. 135, 273–284. https://doi.org/10.1111/ane.12616

Ferreira, P.S., Nogueira, T.B., Costa, V.M., Branco, P.S., Ferreira, L.M., Fernandes, E., Bastos, M.L., Meisel, A., Carvalho, F., Capela, J.P., 2013. Neurotoxicity of "ecstasy" and its metabolites in human dopaminergic differentiated SH-SY5Y cells. Toxicol. Lett. 216, 159–170. https://doi.org/10.1016/j.toxlet.2012.11.015

Ferreira, T.A., Blackman, A. V, Oyrer, J., Jayabal, S., Chung, A.J., Watt, A.J., Sjöström, P.J., van Meyel, D.J., 2014. Neuronal morphometry directly from bitmap images. Nat. Methods 11, 982–984. https://doi.org/10.1038/nmeth.3125

Ferrer, I., 2017. Diversity of astroglial responses across human neurodegenerative disorders and brain aging. Brain Pathol. 27, 645–674. https://doi.org/10.1111/bpa.12538

Filomeni, G., Graziani, I., De Zio, D., Dini, L., Centonze, D., Rotilio, G., Ciriolo, M.R., 2012. Neuroprotection of kaempferol by autophagy in models of rotenone-mediated acute toxicity: possible implications for Parkinson's disease. Neurobiol. Aging 33, 767–785. https://doi.org/10.1016/j.neurobiolaging.2010.05.021

Filosto, M., Scarpelli, M., Cotelli, M.S., Vielmi, V., Todeschini, A., Gregorelli, V., Tonin, P., Tomelleri, G., Padovani, A., 2011. The role of mitochondria in neurodegenerative diseases. J. Neurol. 258, 1763–1774. https://doi.org/10.1007/s00415-011-6104-z

Finley, D., 2018. The proteasome and the Biology of Aging. Innov. Aging 2, 387–387. https://doi.org/10.1093/geroni/igy023.1444

Finley, D., 2009. Recognition and processing of ubiquitin-protein conjugates by the proteasome. Annu. Rev. Biochem. 78, 477–513. https://doi.org/10.1146/annurev.biochem.78.081507.101607

Fischer, F., Hamann, A., Osiewacz, H.D., 2012. Mitochondrial quality control: an integrated network of pathways. Trends Biochem. Sci. 37, 284–292. https://doi.org/10.1016/j.tibs.2012.02.004

Fisher, A.B., 2011. Peroxiredoxin 6: A Bifunctional Enzyme with Glutathione Peroxidase and Phospholipase A 2 Activities. Antioxid. Redox Signal. 15, 831–844. https://doi.org/10.1089/ars.2010.3412

Fitzgerald, J.C., Ugun-Klusek, A., Allen, G., De Girolamo, L.A., Hargreaves, I., Ufer, C., Abramov, A.Y., Billett, E.E., 2014. Monoamine oxidase-A knockdown in human neuroblastoma cells reveals protection against mitochondrial toxins. FASEB J. 28, 218–229. https://doi.org/10.1096/fj.13-235481

Flanagan, L.A., Ju, Y.-E., Marg, B., Osterfield, M., Janmey, P.A., 2002. Neurite branching on deformable substrates. Neuroreport 13, 2411–2415. https://doi.org/10.1097/00001756-200212200-00007

Foley, T.D., Koval, K.S., Olsen, S.H., Gallagher, A.G., Dennis, E.R., 2017. Protein S-Nitrosylation: Possible Links between Psychophysiological Stress and Neurodegeneration. Free Radic. Biol. Med. 112, 73–74. https://doi.org/10.1016/j.freeradbiomed.2017.10.106

Foret, M.K., Do Carmo, S., Lincoln, R., Greene, L.E., Zhang, W., Cuello, A.C., Cosa, G., 2019. Effect of antioxidant supplements on lipid peroxidation levels in primary cortical neuron cultures. Free Radic. Biol. Med. 130, 471–477. https://doi.org/10.1016/j.freeradbiomed.2018.11.019

Fornai, F., Schlüter, O.M., Lenzi, P., Gesi, M., Ruffoli, R., Ferrucci, M., Lazzeri, G., Busceti, C.L., Pontarelli, F., Battaglia, G., Pellegrini, A., Nicoletti, F., Ruggieri, S., Paparelli, A., Südhof, T.C., 2005. Parkinson-like syndrome induced by continuous MPTP infusion: convergent roles of the ubiquitin-proteasome system and alpha-synuclein. Proc. Natl. Acad. Sci. U. S. A. 102, 3413–3418. https://doi.org/10.1073/pnas.0409713102

Fornaro, M., Giovannelli, A., Foggetti, A., Muratori, L., Geuna, S., Novajra, G., Perroteau, I., 2020. Role of neurotrophic factors in enhancing linear axonal growth of ganglionic sensory neurons in vitro. Neural Regen. Res. 15, 1732. https://doi.org/10.4103/1673-5374.276338

Forster, J I, Köglsberger, S., Trefois, C., Boyd, O., Baumuratov, A.S., Buck, L., Balling, R., Antony, P.M.A., 2016. Characterization of Differentiated SH-SY5Y as Neuronal Screening Model Reveals Increased Oxidative Vulnerability. J. Biomol. Screen. 21, 496–509. https://doi.org/10.1177/1087057115625190

Forster, J. I., Köglsberger, S., Trefois, C., Boyd, O., Baumuratov, A.S., Buck, L., Balling, R., Antony, P.M.A., 2016. Characterization of Differentiated SH-SY5Y as Neuronal Screening Model Reveals Increased Oxidative Vulnerability. J. Biomol. Screen. 21, 496–509. https://doi.org/10.1177/1087057115625190

Franco-Iborra, S., Vila, M., Perier, C., 2016. The Parkinson Disease Mitochondrial Hypothesis. Neurosci. 22, 266–277. https://doi.org/10.1177/1073858415574600

Franco, R., Vargas, M.R., 2018. Redox Biology in Neurological Function, Dysfunction, and Aging. Antioxid. Redox Signal. 28, 1583–1586. https://doi.org/10.1089/ars.2018.7509

Franklin, T.B., Krueger-Naug, A.M., Clarke, D.B., Arrigo, A.-P., Currie, R.W., 2005. The role of heat shock proteins Hsp70 and Hsp27 in cellular protection of the central nervous system. Int. J. Hyperth. 21, 379–392. https://doi.org/10.1080/02656730500069955

Fratelli, M., Demol, H., Puype, M., Casagrande, S., Eberini, I., Salmona, M., Bonetto, V., Mengozzi, M.,

Duffieux, F., Miclet, E., Bachi, A., Vandekerckhove, J., Gianazza, E., Ghezzi, P., 2002. Identification by redox proteomics of glutathionylated proteins in oxidatively stressed human T lymphocytes. Proc. Natl. Acad. Sci. 99, 3505–3510. https://doi.org/10.1073/pnas.052592699

Fridovich, I., 1995. Superoxide Radical and Superoxide Dismutases. Annu. Rev. Biochem. 64, 97–112. https://doi.org/10.1146/annurev.bi.64.070195.000525

Friedman, J.R., Nunnari, J., 2014. Mitochondrial form and function. Nature 505, 335–343. https://doi.org/10.1038/nature12985

Frøyset, A.K., Edson, A.J., Gharbi, N., Khan, E.A., Dondorp, D., Bai, Q., Tiraboschi, E., Suster, M.L., Connolly, J.B., Burton, E.A., Fladmark, K.E., 2018. Astroglial DJ-1 over-expression up-regulates proteins involved in redox regulation and is neuroprotective in vivo. Redox Biol. 16, 237–247. https://doi.org/10.1016/j.redox.2018.02.010

Fu, Y., Wang, D., Wang, H., Cai, M., Li, C., Zhang, Xue, Chen, H., Hu, Y., Zhang, Xuan, Ying, M., He, W., Zhang, J., 2019. TSPO deficiency induces mitochondrial dysfunction, leading to hypoxia, angiogenesis, and a growth-promoting metabolic shift toward glycolysis in glioblastoma. Neuro. Oncol. 22, 240–252. https://doi.org/10.1093/neuonc/noz183

Fuentes-Lemus, E., Silva, E., Dorta, E., López-Alarcón, C., 2016. Oxidation of α- and β-Caseins Mediated by AAPH-Derived Free Radicals. Free Radic. Biol. Med. 100, S23. https://doi.org/10.1016/j.freeradbiomed.2016.10.053

Fukui, H., Moraes, C.T., 2007. Extended polyglutamine repeats trigger a feedback loop involving the mitochondrial complex III, the proteasome and huntingtin aggregates. Hum. Mol. Genet. 16, 783–797. https://doi.org/10.1093/hmg/ddm023

Fukuzawa, K., Matsuura, K., Tokumura, A., Suzuki, A., Terao, J., 1997. Kinetics and Dynamics of Singlet Oxygen Scavenging by α-Tocopherol in Phospholipid Model Membranes. Free Radic. Biol. Med. 22, 923–930. https://doi.org/10.1016/S0891-5849(96)00485-6

Fuxe, K., Manger, P., Genedani, S., Agnati, L., 2006. The nigrostriatal DA pathway and Parkinson's disease, in: Parkinson's Disease and Related Disorders. Springer Vienna, Vienna, pp. 71–83. https://doi.org/10.1007/978-3-211-45295-0_13

Gallo, E.F., Iadecola, C., 2011. Neuronal Nitric Oxide Contributes to Neuroplasticity-Associated Protein Expression through cGMP, Protein Kinase G, and Extracellular Signal-Regulated Kinase. J. Neurosci. 31, 6947–6955. https://doi.org/10.1523/JNEUROSCI.0374-11.2011

Gan, L., Vargas, M.R., Johnson, D.A., Johnson, J.A., 2012. Astrocyte-Specific Overexpression of Nrf2 Delays Motor Pathology and Synuclein Aggregation throughout the CNS in the Alpha-Synuclein Mutant (A53T) Mouse Model. J. Neurosci. 32, 17775–17787. https://doi.org/10.1523/JNEUROSCI.3049-12.2012

Ganapathy, K., Datta, I., Bhonde, R., 2019. Astrocyte-Like Cells Differentiated from Dental Pulp Stem Cells Protect Dopaminergic Neurons Against 6-Hydroxydopamine Toxicity. Mol. Neurobiol. 56, 4395–4413. https://doi.org/10.1007/s12035-018-1367-3

Gandhi, S., Abramov, A.Y., 2012. Mechanism of Oxidative Stress in Neurodegeneration. Oxid. Med. Cell. Longev. 2012, 1–11. https://doi.org/10.1155/2012/428010

Gandhi, S., Wood, N.W., 2005. Molecular pathogenesis of Parkinson's disease. Hum. Mol. Genet. 14, 2749–2755. https://doi.org/10.1093/hmg/ddi308

García-García, F., Ponce, S., Brown, R., Cussen, V., Krueger, J.M., 2005. Sleep disturbances in the rotenone animal model of Parkinson disease. Brain Res. 1042, 160–168. https://doi.org/10.1016/j.brainres.2005.02.036

García-Krauss, A., Ferrada, L., Astuya, A., Salazar, K., Cisternas, P., Martínez, F., Ramírez, E., Nualart, F., 2016. Dehydroascorbic Acid Promotes Cell Death in Neurons Under Oxidative Stress: a Protective Role for Astrocytes. Mol. Neurobiol. 53, 5847–5863. https://doi.org/10.1007/s12035-015-9497-3

Garrido, C., Paul, C., Seigneuric, R., Kampinga, H.H., 2012. The small heat shock proteins family: The long forgotten chaperones. Int. J. Biochem. Cell Biol. 44, 1588–1592. https://doi.org/10.1016/j.biocel.2012.02.022

Gaschler, M.M., Stockwell, B.R., 2017. Lipid peroxidation in cell death. Biochem. Biophys. Res. Commun. 482, 419–425. https://doi.org/10.1016/j.bbrc.2016.10.086

George, R., Griffin, J.W., 1994. Delayed Macrophage Responses and Myelin Clearance during Wallerian Degeneration in the Central Nervous System: The Dorsal Radiculotomy Model. Exp. Neurol. 129, 225–236. https://doi.org/10.1006/exnr.1994.1164

Georges, P.C., Miller, W.J., Meaney, D.F., Sawyer, E.S., Janmey, P.A., 2006. Matrices with Compliance Comparable to that of Brain Tissue Select Neuronal over Glial Growth in Mixed Cortical Cultures. Biophys. J. 90, 3012–3018. https://doi.org/10.1529/biophysj.105.073114

Georgiou, G., 2003. BIOCHEMISTRY: An Overoxidation Journey with a Return Ticket. Science (80-.). 300, 592–594. https://doi.org/10.1126/science.1084976

Gerencser, A.A., Neilson, A., Choi, S.W., Edman, U., Yadava, N., Oh, R.J., Ferrick, D.A., Nicholls, D.G., Brand, M.D., 2009. Quantitative Microplate-Based Respirometry with Correction for Oxygen Diffusion. Anal. Chem. 81, 6868–6878. https://doi.org/10.1021/ac900881z

Ghadery, C., Koshimori, Y., Coakeley, S., Harris, M., Rusjan, P., Kim, J., Houle, S., Strafella, A.P., 2017. Microglial activation in Parkinson's disease using [18F]-FEPPA. J. Neuroinflammation 14, 8. https://doi.org/10.1186/s12974-016-0778-1

Ghasemi, M., Fatemi, A., 2014. Pathologic role of glial nitric oxide in adult and pediatric neuroinflammatory

diseases. Neurosci. Biobehav. Rev. 45, 168–182. https://doi.org/10.1016/j.neubiorev.2014.06.002

Giasson, B.I., 2000. Oxidative Damage Linked to Neurodegeneration by Selective alpha -Synuclein Nitration in Synucleinopathy Lesions. Science (80-.). 290, 985–989. https://doi.org/10.1126/science.290.5493.985

Gidalevitz, T., 2006. Progressive Disruption of Cellular Protein Folding in Models of Polyglutamine Diseases. Science (80-.). 311, 1471–1474. https://doi.org/10.1126/science.1124514

Giordano, S., Dodson, M., Ravi, S., Redmann, M., Ouyang, X., Darley Usmar, V.M., Zhang, J., 2014. Bioenergetic adaptation in response to autophagy regulators during rotenone exposure. J. Neurochem. 131, 625–633. https://doi.org/10.1111/jnc.12844

Gitler, A.D., Dhillon, P., Shorter, J., 2017. Neurodegenerative disease: models, mechanisms, and a new hope. Dis. Model. Mech. 10, 499–502. https://doi.org/10.1242/dmm.030205

Glass, J.D., Brushart, T.M., George, E.B., Griffin, J.W., 1993. Prolonged survival of transected nerve fibres in C57BL/Ola mice is an intrinsic characteristic of the axon. J. Neurocytol. 22, 311–321. https://doi.org/10.1007/BF01195555

Gleixner, A.M., Posimo, J.M., Pant, D.B., Henderson, M.P., Leak, R.K., 2016. Astrocytes Surviving Severe Stress Can Still Protect Neighboring Neurons from Proteotoxic Injury. Mol. Neurobiol. 53, 4939–4960. https://doi.org/10.1007/s12035-015-9427-4

Glick, D., Zhang, W., Beaton, M., Marsboom, G., Gruber, M., Simon, M.C., Hart, J., Dorn, G.W., Brady, M.J., Macleod, K.F., 2012. BNip3 Regulates Mitochondrial Function and Lipid Metabolism in the Liver. Mol. Cell. Biol. 32, 2570–2584. https://doi.org/10.1128/MCB.00167-12

Glickman, M.H., Ciechanover, A., 2002. The Ubiquitin-Proteasome Proteolytic Pathway: Destruction for the Sake of Construction. Physiol. Rev. 82, 373–428. https://doi.org/10.1152/physrev.00027.2001

Glinka, Y.Y., Youdim, M.B.H., 1995. Inhibition of mitochondrial complexes I and IV by 6-hydroxydopamine. Eur. J. Pharmacol. Environ. Toxicol. Pharmacol. 292, 329–332. https://doi.org/10.1016/0926-6917(95)90040-3

Goedert, M., 2001. Alpha-synuclein and neurodegenerative diseases. Nat. Rev. Neurosci. 2, 492–501. https://doi.org/10.1038/35081564

Goedert, M., Jakes, R., Spillantini, M.G., 2017. The Synucleinopathies: Twenty Years On. J. Parkinsons. Dis. 7, S51–S69. https://doi.org/10.3233/JPD-179005

Gökçe Çokal, B., Yurtdaş, M., Keskin Güler, S., Güneş, H.N., Ataç Uçar, C., Aytaç, B., Durak, Z.E., Yoldaş, T.K., Durak, İ., Çubukçu, H.C., 2017. Serum glutathione peroxidase, xanthine oxidase, and superoxide dismutase activities and malondialdehyde levels in patients with Parkinson's disease. Neurol. Sci. 38, 425–431. https://doi.org/10.1007/s10072-016-2782-8

Goldbaum, O., Riedel, M., Stahnke, T., Richter-Landsberg, C., 2009. The small heat shock protein HSP25 protects astrocytes against stress induced by proteasomal inhibition. Glia 57, 1566–1577. https://doi.org/10.1002/glia.20870

Goldberg, M.S., Pisani, A., Haburcak, M., Vortherms, T.A., Kitada, T., Costa, C., Tong, Y., Martella, G., Tscherter, A., Martins, A., Bernardi, G., Roth, B.L., Pothos, E.N., Calabresi, P., Shen, J., 2005. Nigrostriatal dopaminergic deficits and hypokinesia caused by inactivation of the familial parkinsonism-linked gene DJ-1. Neuron 45, 489–496. https://doi.org/10.1016/j.neuron.2005.01.041

Gomez-Lazaro, M., Bonekamp, N.A., Galindo, M.F., Jordán, J., Schrader, M., 2008. 6-Hydroxydopamine (6-OHDA) induces Drp1-dependent mitochondrial fragmentation in SH-SY5Y cells. Free Radic. Biol. Med. 44, 1960–1969. https://doi.org/10.1016/j.freeradbiomed.2008.03.009

Gómez-Piña, V., Martínez, E., Fernández-Ruíz, I., del Fresno, C., Soares-Schanoski, A., Jurado, T., Siliceo, M., Toledano, V., Fernández-Palomares, R., García-Rio, F., Arnalich, F., Biswas, S.K., López-Collazo, E., 2012. Role of MMPs in orchestrating inflammatory response in human monocytes via a TREM-1-PI3K-NF-κB pathway. J. Leukoc. Biol. 91, 933–945. https://doi.org/10.1189/jlb.0711340

Gomez, M., Germain, D., 2019. Cross talk between SOD1 and the mitochondrial UPR in cancer and neurodegeneration. Mol. Cell. Neurosci. 98, 12–18. https://doi.org/10.1016/j.mcn.2019.04.003

Gordon, M.D., Nusse, R., 2006. Wnt Signaling: Multiple Pathways, Multiple Receptors, and Multiple Transcription Factors. J. Biol. Chem. 281, 22429–22433. https://doi.org/10.1074/jbc.R600015200

Gorenberg, E.L., Chandra, S.S., 2017. The Role of Co-chaperones in Synaptic Proteostasis and Neurodegenerative Disease. Front. Neurosci. 11. https://doi.org/10.3389/fnins.2017.00248

Gorisse, L., Pietrement, C., Vuiblet, V., Schmelzer, C.E.H., Köhler, M., Duca, L., Debelle, L., Fornès, P., Jaisson, S., Gillery, P., 2016. Protein carbamylation is a hallmark of aging. Proc. Natl. Acad. Sci. 113, 1191–1196. https://doi.org/10.1073/pnas.1517096113

Gorman, A.M., Heavey, B., Creagh, E., Cotter, T.G., Samali, A., 1999. Antioxidant-mediated inhibition of the heat shock response leads to apoptosis. FEBS Lett. 445, 98–102. https://doi.org/10.1016/S0014-5793(99)00094-0

Goswami, P., Gupta, S., Joshi, N., Sharma, S., Singh, S., 2015. Astrocyte activation and neurotoxicity: A study in different rat brain regions and in rat C6 astroglial cells. Environ. Toxicol. Pharmacol. 40, 122–139. https://doi.org/10.1016/j.etap.2015.06.001

Goto, S., Kawakatsu, M., Izumi, S., Urata, Y., Kageyama, K., Ihara, Y., Koji, T., Kondo, T., 2009. Glutathione S-transferase π localizes in mitochondria and protects against oxidative stress. Free Radic. Biol. Med. 46, 1392–1403. https://doi.org/10.1016/j.freeradbiomed.2009.02.025

Gotoh, N., Niki, E., 1992. Rates of interactions of superoxide with vitamin E, vitamin C and related

compounds as measured by chemiluminescence. Biochim. Biophys. Acta - Gen. Subj. 1115, 201–207. https://doi.org/10.1016/0304-4165(92)90054-X

Gottschall, P.E., Deb, S., 1996. Regulation of Matrix Metalloproteinase Expression in Astrocytes, Microglia and Neurons. Neuroimmunomodulation 3, 69–75. https://doi.org/10.1159/000097229

Gottschall, P.E., Yu, X., 2002. Cytokines Regulate Gelatinase A and B (Matrix Metalloproteinase 2 and 9) Activity in Cultured Rat Astrocytes. J. Neurochem. 64, 1513–1520. https://doi.org/10.1046/j.1471-4159.1995.64041513.x

Gracia, L., Lora, G., Jinwal, U.K., 2019. Role of Hsp90 Interacting Molecular Chaperones on Tau and Aß Processing in Alzheimer's Disease. pp. 131–145. https://doi.org/10.1007/978-3-030-24285-5_9

Greco, T.M., Seeholzer, S.H., Mak, A., Spruce, L., Ischiropoulos, H., 2010. Quantitative Mass Spectrometry-based Proteomics Reveals the Dynamic Range of Primary Mouse Astrocyte Protein Secretion. J. Proteome Res. 9, 2764–2774. https://doi.org/10.1021/pr100134n

Green, D.R., Van Houten, B., 2011. SnapShot: Mitochondrial Quality Control. Cell 147, 950-950.e1. https://doi.org/10.1016/j.cell.2011.10.036

Greene, J.C., Whitworth, A.J., Kuo, I., Andrews, L.A., Feany, M.B., Pallanck, L.J., 2003. Mitochondrial pathology and apoptotic muscle degeneration in Drosophila parkin mutants. Proc. Natl. Acad. Sci. U. S. A. 100, 4078–83. https://doi.org/10.1073/pnas.0737556100

Griffith, O.W., Meister, A., 1979. Potent and specific inhibition of glutathione synthesis by buthionine sulfoximine (S-n-butyl homocysteine sulfoximine). J. Biol. Chem. 254, 7558–60.

Grimm, A., Eckert, A., 2017. Brain aging and neurodegeneration: from a mitochondrial point of view. J. Neurochem. 143, 418–431. https://doi.org/10.1111/jnc.14037

Grimm, A., Friedland, K., Eckert, A., 2016. Mitochondrial dysfunction: the missing link between aging and sporadic Alzheimer's disease. Biogerontology 17, 281–296. https://doi.org/10.1007/s10522-015-9618-4

Gritsenko, P., Leenders, W., Friedl, P., 2017. Recapitulating in vivo-like plasticity of glioma cell invasion along blood vessels and in astrocyte-rich stroma. Histochem. Cell Biol. 148, 395–406. https://doi.org/10.1007/s00418-017-1604-2

GROBSTEIN, C., 1953. Morphogenetic Interaction between Embryonic Mouse Tissues separated by a Membrane Filter. Nature 172, 869–871. https://doi.org/10.1038/172869a0

Groll, M., Bajorek, M., Köhler, A., Moroder, L., Rubin, D.M., Huber, R., Glickman, M.H., Finley, D., 2000. A gated channel into the proteasome core particle. Nat. Struct. Biol. 7, 1062–1067. https://doi.org/10.1038/80992

Groll, M., Ditzel, L., Löwe, J., Stock, D., Bochtler, M., Bartunik, H.D., Huber, R., 1997. Structure of 20S proteasome from yeast at 2.4Å resolution. Nature 386, 463–471. https://doi.org/10.1038/386463a0

Grünblatt, E., Mandel, S., Youdim, M.B., 2000. MPTP and 6-hydroxydopamine-induced neurodegeneration as models for Parkinson's disease: neuroprotective strategies. J. Neurol. 247 Suppl, II95-102. https://doi.org/10.1007/pl00022909

Grünblatt, E., Ruder, J., Monoranu, C.M., Riederer, P., Youdim, M.B., Mandel, S.A., 2018. Differential Alterations in Metabolism and Proteolysis-Related Proteins in Human Parkinson's Disease Substantia Nigra. Neurotox. Res. 33, 560–568. https://doi.org/10.1007/s12640-017-9843-5

Grundmann, D., Loris, E., Maas-Omlor, S., Huang, W., Scheller, A., Kirchhoff, F., Schäfer, K., 2019. Enteric Glia: S100, GFAP, and Beyond. Anat. Rec. 302, 1333–1344. https://doi.org/10.1002/ar.24128

Grune, T., Catalgol, B., Licht, A., Ermak, G., Pickering, A.M., Ngo, J.K., Davies, K.J.A., 2011. HSP70 mediates dissociation and reassociation of the 26S proteasome during adaptation to oxidative stress. Free Radic. Biol. Med. 51, 1355–1364. https://doi.org/10.1016/j.freeradbiomed.2011.06.015

Guerra, F., Girolimetti, G., Beli, R., Mitruccio, M., Pacelli, C., Ferretta, A., Gasparre, G., Cocco, T., Bucci, C., 2019. Synergistic Effect of Mitochondrial and Lysosomal Dysfunction in Parkinson's Disease. Cells 8, 452. https://doi.org/10.3390/cells8050452

Guo, A., Zhao, Y., Wang, Y., Wang, Q., 2016. Cattle encephalon glycoside and ignotin injection promoted synthesis of glial cell line-derived neurotrophic factor by astrocytes that protected against neuronal damage induced by AAPH 9, 1794–1800.

Guo, K., Lu, J., Huang, Y., Wu, M., Zhang, L., Yu, H., Zhang, M., Bao, Y., He, J.C., Chen, H., Jia, W., 2015. Protective Role of PGC-1α in Diabetic Nephropathy Is Associated with the Inhibition of ROS through Mitochondrial Dynamic Remodeling. PLoS One 10, e0125176. https://doi.org/10.1371/journal.pone.0125176

Gutbier, S., Spreng, A.-S., Delp, J., Schildknecht, S., Karreman, C., Suciu, I., Brunner, T., Groettrup, M., Leist, M., 2018. Prevention of neuronal apoptosis by astrocytes through thiol-mediated stress response modulation and accelerated recovery from proteotoxic stress. Cell Death Differ. 25, 2101–2117. https://doi.org/10.1038/s41418-018-0229-x

Haim, L. Ben, Rowitch, D.H., 2017. Functional diversity of astrocytes in neural circuit regulation. Nat. Rev. Neurosci. 18, 31–41. https://doi.org/10.1038/nrn.2016.159

Hall, A., Nelson, K., Poole, L.B., Karplus, P.A., 2011. Structure-based Insights into the Catalytic Power and Conformational Dexterity of Peroxiredoxins. Antioxid. Redox Signal. 15, 795–815. https://doi.org/10.1089/ars.2010.3624

Hall, E.D., 1987. Intensive anti-oxidant pretreatment retards motor nerve degeneration. Brain Res. 413, 175–

178. https://doi.org/10.1016/0006-8993(87)90166-1

Hall, J., Prabhakar, S., Balaj, L., Lai, C.P., Cerione, R.A., Breakefield, X.O., 2016. Delivery of Therapeutic Proteins via Extracellular Vesicles: Review and Potential Treatments for Parkinson's Disease, Glioma, and Schwannoma. Cell. Mol. Neurobiol. 36, 417–427. https://doi.org/10.1007/s10571-015-0309-0

Halliwell, B., 2019. Making Sense of Neurodegeneration: A Unifying Hypothesis, in: Learning To Live Together: Promoting Social Harmony. Springer International Publishing, Cham, pp. 115–120. https://doi.org/10.1007/978-3-319-90659-1_13

Halliwell, B., 2003. Oxidative stress in cell culture: an under-appreciated problem? FEBS Lett. 540, 3–6. https://doi.org/10.1016/S0014-5793(03)00235-7

Halliwell, B., Gutteridge, J.M.C., 1991. Free radicals in biology and medicine, second edition. Free Radic. Biol. Med. 10, 449–450. https://doi.org/10.1016/0891-5849(91)90055-8

Hamazaki, J., Hirayama, S., Murata, S., 2015. Redundant Roles of Rpn10 and Rpn13 in Recognition of Ubiquitinated Proteins and Cellular Homeostasis. PLOS Genet. 11, e1005401. https://doi.org/10.1371/journal.pgen.1005401

Hamberger, A., 1970. COMPARATIVE STUDIES ON MITOCHONDRIA ISOLATED FROM NEURON-ENRICHED AND GLIA-ENRICHED FRACTIONS OF RABBIT AND BEEF BRAIN. J. Cell Biol. 45, 221–234. https://doi.org/10.1083/jcb.45.2.221

Han, D., Jin, J., Woo, J., Min, H., Kim, Y., 2014. Proteomic analysis of mouse astrocytes and their secretome by a combination of FASP and StageTip-based, high pH, reversed-phase fractionation. Proteomics 14, 1604–1609. https://doi.org/10.1002/pmic.201300495

Han, X.-J., Lu, Y.-F., Li, S.-A., Kaitsuka, T., Sato, Y., Tomizawa, K., Nairn, A.C., Takei, K., Matsui, H., Matsushita, M., 2008. CaM kinase Iα–induced phosphorylation of Drp1 regulates mitochondrial morphology. J. Cell Biol. 182, 573–585. https://doi.org/10.1083/jcb.200802164

Hao, X.-M., Li, L.-D., Duan, C.-L., Li, Y.-J., 2017. Neuroprotective effect of α-mangostin on mitochondrial dysfunction and α-synuclein aggregation in rotenone-induced model of Parkinson's disease in differentiated SH-SY5Y cells. J. Asian Nat. Prod. Res. 19, 833–845. https://doi.org/10.1080/10286020.2017.1339349

Haque, A., Das, A., Hajiaghamohseni, L.M., Younger, A., Banik, N.L., Ray, S.K., 2007. Induction of apoptosis and immune response by all-trans retinoic acid plus interferon-gamma in human malignant glioblastoma T98G and U87MG cells. Cancer Immunol. Immunother. 56, 615–625. https://doi.org/10.1007/s00262-006-0219-6

Haroon, S., Vermulst, M., 2016. Linking mitochondrial dynamics to mitochondrial protein quality control. Curr. Opin. Genet. Dev. 38, 68–74. https://doi.org/10.1016/j.gde.2016.04.004

Harris, J., Deen, N., Zamani, S., Hasnat, M.A., 2018. Mitophagy and the release of inflammatory cytokines. Mitochondrion 41, 2–8. https://doi.org/10.1016/j.mito.2017.10.009

Harris, P.S., Roy, S.R., Coughlan, C., Orlicky, D.J., Liang, Y., Shearn, C.T., Roede, J.R., Fritz, K.S., 2015. Chronic ethanol consumption induces mitochondrial protein acetylation and oxidative stress in the kidney. Redox Biol. 6, 33–40. https://doi.org/10.1016/j.redox.2015.06.021

Harrison, F.E., May, J.M., 2009. Vitamin C function in the brain: vital role of the ascorbate transporter SVCT2. Free Radic. Biol. Med. 46, 719–730. https://doi.org/10.1016/j.freeradbiomed.2008.12.018

Hartl, F.U., Bracher, A., Hayer-Hartl, M., 2011. Molecular chaperones in protein folding and proteostasis. Nature 475, 324–332. https://doi.org/10.1038/nature10317

Hasan, W., Kori, R.K., Jain, J., Yadav, R.S., Jat, D., 2020. Neuroprotective effects of mitochondria-targeted curcumin against rotenone-induced oxidative damage in cerebellum of mice. J. Biochem. Mol. Toxicol. 34. https://doi.org/10.1002/jbt.22416

Hattingen, E., Magerkurth, J., Pilatus, U., Mozer, A., Seifried, C., Steinmetz, H., Zanella, F., Hilker, R., 2009. Phosphorus and proton magnetic resonance spectroscopy demonstrates mitochondrial dysfunction in early and advanced Parkinson's disease. Brain 132, 3285–97. https://doi.org/10.1093/brain/awp293

Hauser, D.N., Hastings, T.G., 2013. Mitochondrial dysfunction and oxidative stress in Parkinson's disease and monogenic parkinsonism. Neurobiol. Dis. https://doi.org/10.1016/j.nbd.2012.10.011

Haut, S., Brivet, M., Touati, G., Rustin, P., Lebon, S., Garcia-Cazorla, A., Saudubray, J.M., Boutron, A., Legrand, A., Slama, A., 2003. A deletion in the human QP-C gene causes a complex III deficiency resulting in hypoglycaemia and lactic acidosis. Hum. Genet. 113, 118–22. https://doi.org/10.1007/s00439-003-0946-0

He, F., Zuo, L., 2015. Redox Roles of Reactive Oxygen Species in Cardiovascular Diseases. Int. J. Mol. Sci. 16, 27770–27780. https://doi.org/10.3390/ijms161126059

He, Y., Yu, W., Baas, P.W., 2002. Microtubule reconfiguration during axonal retraction induced by nitric oxide. J. Neurosci. 22, 5982–91. https://doi.org/20026604

He, Y., Yu, Z., Chen, S., 2019. Alpha-Synuclein Nitration and Its Implications in Parkinson's Disease. ACS Chem. Neurosci. 10, 777–782. https://doi.org/10.1021/acschemneuro.8b00288

Hegazy, A.M., El-Sayed, E.M., Ibrahim, K.S., Abdel-Azeem, A.S., 2019. Dietary antioxidant for disease prevention corroborated by the Nrf2 pathway. J. Complement. Integr. Med. https://doi.org/10.1515/jcim-2018-0161

Heikkila, R.E., Cohen, G., 1973. 6-Hydroxydopamine: Evidence for Superoxide Radical as an Oxidative Intermediate. Science (80-.). 181, 456–457. https://doi.org/10.1126/science.181.4098.456

Heikkila, R.E., Nicklas, W.J., Vyas, I., Duvoisin, R.C., 1985. Dopaminergic toxicity of rotenone and the 1-methyl-4-phenylpyridinium ion after their stereotaxic administration to rats: Implication for the mechanism of 1-methyl-4-phenyl-1,2,3,6-tetrahydropyridine toxicity. Neurosci. Lett. 62, 389–394. https://doi.org/10.1016/0304-3940(85)90580-4

Heneka, M.T., Kummer, M.P., Latz, E., 2014. Innate immune activation in neurodegenerative disease. Nat. Rev. Immunol. 14, 463–477. https://doi.org/10.1038/nri3705

Henstridge, C.M., Tzioras, M., Paolicelli, R.C., 2019. Glial Contribution to Excitatory and Inhibitory Synapse Loss in Neurodegeneration. Front. Cell. Neurosci. 13. https://doi.org/10.3389/fncel.2019.00063

Herculano-Houzel, S., 2009. The human brain in numbers: a linearly scaled-up primate brain. Front. Hum. Neurosci. 3, 31. https://doi.org/10.3389/neuro.09.031.2009

Herrero-Mendez, A., Almeida, A., Fernández, E., Maestre, C., Moncada, S., Bolaños, J.P., 2009. The bioenergetic and antioxidant status of neurons is controlled by continuous degradation of a key glycolytic enzyme by APC/C–Cdh1. Nat. Cell Biol. 11, 747–752. https://doi.org/10.1038/ncb1881

Hertz, L., Chen, Y., 2016. Importance of astrocytes for potassium ion (K+) homeostasis in brain and glial effects of K+ and its transporters on learning. Neurosci. Biobehav. Rev. 71, 484–505. https://doi.org/10.1016/j.neubiorev.2016.09.018

Hertz, L., Peng, L., Dienel, G.A., 2007. Energy Metabolism in Astrocytes: High Rate of Oxidative Metabolism and Spatiotemporal Dependence on Glycolysis/Glycogenolysis. J. Cereb. Blood Flow Metab. 27, 219–249. https://doi.org/10.1038/sj.jcbfm.9600343

Hickman, S., Izzy, S., Sen, P., Morsett, L., El Khoury, J., 2018. Microglia in neurodegeneration. Nat. Neurosci. 21, 1359–1369. https://doi.org/10.1038/s41593-018-0242-x

Higdon, A., Diers, A.R., Oh, J.Y., Landar, A., Darley-Usmar, V.M., 2012. Cell signalling by reactive lipid species: new concepts and molecular mechanisms. Biochem. J. 442, 453–64. https://doi.org/10.1042/BJ20111752

Higgins, D.S., Greenamyre, J.T., 1996. [3H]dihydrorotenone binding to NADH: ubiquinone reductase (complex I) of the electron transport chain: an autoradiographic study. J. Neurosci. 16, 3807–16.

Hinkle, J.T., Dawson, V.L., Dawson, T.M., 2019. The A1 astrocyte paradigm: New avenues for pharmacological intervention in neurodegeneration. Mov. Disord. 34, 959–969. https://doi.org/10.1002/mds.27718

Hinshaw, D.B., Miller, M.T., Omann, G.M., Beals, T.F., Hyslop, P.A., 1993. A cellular model of oxidant-mediated neuronal injury. Brain Res. 615, 13–26. https://doi.org/10.1016/0006-8993(93)91110-E

Hirsch, E.C., Hunot, S., 2009. Neuroinflammation in Parkinson's disease: a target for neuroprotection? Lancet Neurol. 8, 382–397. https://doi.org/10.1016/S1474-4422(09)70062-6

Hod, Y., Pentyala, S.N., Whyard, T.C., El-Maghrabi, M.R., 1999. Identification and characterization of a novel protein that regulates RNA-protein interaction. J. Cell. Biochem. 72, 435–444. https://doi.org/10.1002/(SICI)1097-4644(19990301)72:3<435::AID-JCB12>3.0.CO;2-H [pii]

Höftberger, R., Aboul-Enein, F., Brueck, W., Lucchinetti, C., Rodriguez, M., Schmidbauer, M., Jellinger, K., Lassmann, H., 2004. Expression of Major Histocompatibility Complex class I Molecules on the Different Cell Types in Multiple Sclerosis Lesions. Brain Pathol. 14, 43–50. https://doi.org/10.1111/j.1750-3639.2004.tb00496.x

Hogg, N., Kalyanaraman, B., 1999. Nitric Oxide and Lipid Peroxidation. Biochim. Biophys. Acta - Bioenerg. 1411, 378–384. https://doi.org/10.1016/S0005-2728(99)00027-4

Hogg, N., Singh, R.J., Kalyanaraman, B., 1996. The role of glutathione in the transport and catabolism of nitric oxide. FEBS Lett. 382, 223–228. https://doi.org/10.1016/0014-5793(96)00086-5

Holley, A.K., Dhar, S.K., St. Clair, D.K., 2010. Manganese superoxide dismutase vs. p53: Regulation of mitochondrial ROS. Mitochondrion 10, 649–661. https://doi.org/10.1016/j.mito.2010.06.003

Hong, Z., Shi, M., Chung, K.A., Quinn, J.F., Peskind, E.R., Galasko, D., Jankovic, J., Zabetian, C.P., Leverenz, J.B., Baird, G., Montine, T.J., Hancock, A.M., Hwang, H., Pan, C., Bradner, J., Kang, U.J., Jensen, P.H., Zhang, J., 2010. DJ-1 and α-synuclein in human cerebrospinal fluid as biomarkers of Parkinson's disease. Brain 133, 713–726. https://doi.org/10.1093/brain/awq008

Hongo, H., Kihara, T., Kume, T., Izumi, Y., Niidome, T., Sugimoto, H., Akaike, A., 2012. Glycogen synthase kinase-3β activation mediates rotenone-induced cytotoxicity with the involvement of microtubule destabilization. Biochem. Biophys. Res. Commun. 426, 94–99. https://doi.org/10.1016/j.bbrc.2012.08.042

Hosomi, A., Goto, K., Kondo, H., Iwatsubo, T., Yokota, T., Ogawa, M., Arita, M., Aoki, J., Arai, H., Inoue, K., 1998. Localization of α-tocopherol transfer protein in rat brain. Neurosci. Lett. 256, 159–162. https://doi.org/10.1016/S0304-3940(98)00785-X

Houenou, L.J., Li, L., Lei, M., Kent, C.R., Tytell, M., 1996. Exogenous heat shock cognate protein Hsc 70 prevents axotomy-induced death of spinal sensory neurons. Cell Stress Chaperones 1, 161–6. https://doi.org/10.1379/1466-1268(1996)001<0161:ehscph>2.3.co;2

Hough, R., Pratt, G., Rechsteiner, M., 1986. Ubiquitin-lysozyme conjugates. Identification and characterization of an ATP-dependent protease from rabbit reticulocyte lysates. J. Biol. Chem. 261, 2400–2408.

Huang, E.J., Reichardt, L.F., 2003. Trk Receptors: Roles in Neuronal Signal Transduction. Annu. Rev. Biochem. 72, 609–642. https://doi.org/10.1146/annurev.biochem.72.121801.161629

Huang, Y., Li, W., Su, Z., Kong, A.-N.T., 2015. The complexity of the Nrf2 pathway: beyond the antioxidant

response. J. Nutr. Biochem. 26, 1401–1413. https://doi.org/10.1016/j.jnutbio.2015.08.001

Hudson, G., Amati-Bonneau, P., Blakely, E.L., Stewart, J.D., He, L., Schaefer, A.M., Griffiths, P.G., Ahlqvist, K., Suomalainen, A., Reynier, P., McFarland, R., Turnbull, D.M., Chinnery, P.F., Taylor, R.W., 2008. Mutation of OPA1 causes dominant optic atrophy with external ophthalmoplegia, ataxia, deafness and multiple mitochondrial DNA deletions: a novel disorder of mtDNA maintenance. Brain 131, 329–337. https://doi.org/10.1093/brain/awm272

Hung, C.H.-L., Cheng, S.S.-Y., Cheung, Y.-T., Wuwongse, S., Zhang, N.Q., Ho, Y.-S., Lee, S.M.-Y., Chang, R.C.-C., 2018. A reciprocal relationship between reactive oxygen species and mitochondrial dynamics in neurodegeneration. Redox Biol. 14, 7–19. https://doi.org/10.1016/j.redox.2017.08.010

Husnjak, K., Elsasser, S., Zhang, N., Chen, X., Randles, L., Shi, Y., Hofmann, K., Walters, K.J., Finley, D., Dikic, I., 2008. Proteasome subunit Rpn13 is a novel ubiquitin receptor. Nature 453, 481–488. https://doi.org/10.1038/nature06926

Hynes, R.O., 2009. The Extracellular Matrix: Not Just Pretty Fibrils. Science (80-.). 326, 1216–1219. https://doi.org/10.1126/science.1176009

Hyun, D.H., Lee, M.H., Hattori, N., Kubo, S.I., Mizuno, Y., Halliwell, B., Jenner, P., 2002. Effect of wild-type or mutant parkin on oxidative damage, nitric oxide, antioxidant defenses, and the proteasome. J. Biol. Chem. 277, 28572–28577. https://doi.org/10.1074/jbc.M200666200

Ighodaro, O.M., Akinloye, O.A., 2018. First line defence antioxidants-superoxide dismutase (SOD), catalase (CAT) and glutathione peroxidase (GPX): Their fundamental role in the entire antioxidant defence grid. Alexandria J. Med. 54, 287–293. https://doi.org/10.1016/j.ajme.2017.09.001

Ikeda, Y., Tsuji, S., Satoh, A., Ishikura, M., Shirasawa, T., Shimizu, T., 2008. Protective effects of astaxanthin on 6-hydroxydopamine-induced apoptosis in human neuroblastoma SH-SY5Y cells. J. Neurochem. 107, 1730–1740. https://doi.org/10.1111/j.1471-4159.2008.05743.x

Imai, Y., Soda, M., Takahashi, R., 2000. Parkin suppresses unfolded protein stress-induced cell death through its E3 ubiquitin-protein ligase activity. J. Biol. Chem. 275, 35661–35664. https://doi.org/10.1074/jbc.C000447200

Imura, T., Nakano, I., Kornblum, H.I., Sofroniew, M. V., 2006. Phenotypic and functional heterogeneity of GFAP-expressing cells in vitro: Differential expression of LeX/CD15 by GFAP-expressing multipotent neural stem cells and non-neurogenic astrocytes. Glia 53, 277–293. https://doi.org/10.1002/glia.20281

Ingelsson, M., 2016. Alpha-synuclein oligomers-neurotoxic molecules in Parkinson's disease and other lewy body disorders. Front. Neurosci. https://doi.org/10.3389/fnins.2016.00408

Ischiropoulos, H., Beckman, J.S., 2003. Oxidative stress and nitration in neurodegeneration: Cause, effect, or association? J. Clin. Invest. 111, 163–169. https://doi.org/10.1172/JCI200317638

Ishihara, N., 2004. Mitofusin 1 and 2 play distinct roles in mitochondrial fusion reactions via GTPase activity. J. Cell Sci. 117, 6535–6546. https://doi.org/10.1242/jcs.01565

Islam, M.T., 2017. Oxidative stress and mitochondrial dysfunction-linked neurodegenerative disorders. Neurol. Res. 39, 73–82. https://doi.org/10.1080/01616412.2016.1251711

Itier, J.-M., 2003. Parkin gene inactivation alters behaviour and dopamine neurotransmission in the mouse. Hum. Mol. Genet. 12, 2277–2291. https://doi.org/10.1093/hmg/ddg239

Ito, H., Kamei, K., Iwamoto, I., Inaguma, Y., Garcia-Mata, R., Sztul, E., Kato, K., 2002. Inhibition of Proteasomes Induces Accumulation, Phosphorylation, and Recruitment of HSP27 and -Crystallin to Aggresomes. J. Biochem. 131, 593–603. https://doi.org/10.1093/oxfordjournals.jbchem.a003139

Itoh, K., Chiba, T., Takahashi, S., Ishii, T., Igarashi, K., Katoh, Y., Oyake, T., Hayashi, N., Satoh, K., Hatayama, I., Yamamoto, M., Nabeshima, Y., 1997. An Nrf2/Small Maf Heterodimer Mediates the Induction of Phase II Detoxifying Enzyme Genes through Antioxidant Response Elements. Biochem. Biophys. Res. Commun. 236, 313–322. https://doi.org/10.1006/bbrc.1997.6943

Itoh, K., Wakabayashi, N., Katoh, Y., Ishii, T., Igarashi, K., Engel, J.D., Yamamoto, M., 1999. Keap1 represses nuclear activation of antioxidant responsive elements by Nrf2 through binding to the amino-terminal Neh2 domain. Genes Dev. 13, 76–86. https://doi.org/10.1101/gad.13.1.76

Itoh, K., Wakabayashi, N., Katoh, Y., Ishii, T., O'Connor, T., Yamamoto, M., 2003. Keap1 regulates both cytoplasmic-nuclear shuttling and degradation of Nrf2 in response to electrophiles. Genes to Cells 8, 379–391. https://doi.org/10.1046/j.1365-2443.2003.00640.x

Ittner, L.M., Ke, Y.D., Delerue, F., Bi, M., Gladbach, A., van Eersel, J., Wölfing, H., Chieng, B.C., Christie, M.J., Napier, I.A., Eckert, A., Staufenbiel, M., Hardeman, E., Götz, J., 2010. Dendritic function of tau mediates amyloid-beta toxicity in Alzheimer's disease mouse models. Cell 142, 387–97. https://doi.org/10.1016/j.cell.2010.06.036

Ivankovic, D., Chau, K.-Y., Schapira, A.H. V., Gegg, M.E., 2016. Mitochondrial and lysosomal biogenesis are activated following PINK1/parkin-mediated mitophagy. J. Neurochem. 136, 388–402. https://doi.org/10.1111/jnc.13412

Iwata-Ichikawa, E., Kondo, Y., Miyazaki, I., Asanuma, M., Ogawa, N., 1999. Glial cells protect neurons against oxidative stress via transcriptional up-regulation of the glutathione synthesis. J. Neurochem. 72, 2334–2344. https://doi.org/10.1046/j.1471-4159.1999.0722334.x

Jacob, P., Hirt, H., Bendahmane, A., 2017. The heat-shock protein/chaperone network and multiple stress resistance. Plant Biotechnol. J. 15, 405–414. https://doi.org/10.1111/pbi.12659

Jády, A.G., Nagy, Á.M., Kőhidi, T., Ferenczi, S., Tretter, L., Madarász, E., 2016. Differentiation-Dependent Energy Production and Metabolite Utilization: A Comparative Study on Neural Stem Cells, Neurons, and

Astrocytes. Stem Cells Dev. 25, 995–1005. https://doi.org/10.1089/scd.2015.0388

Jaffrey, S.R., Erdjument-Bromage, H., Ferris, C.D., Tempst, P., Snyder, S.H., 2001. Protein S-nitrosylation: a physiological signal for neuronal nitric oxide. Nat. Cell Biol. 3, 193–197. https://doi.org/10.1038/35055104

Jain, A.K., Jaiswal, A.K., 2007. GSK-3β Acts Upstream of Fyn Kinase in Regulation of Nuclear Export and Degradation of NF-E2 Related Factor 2. J. Biol. Chem. 282, 16502–16510. https://doi.org/10.1074/jbc.M611336200

Jain, A.K., Jaiswal, A.K., 2006. Phosphorylation of Tyrosine 568 Controls Nuclear Export of Nrf2. J. Biol. Chem. 281, 12132–12142. https://doi.org/10.1074/jbc.M511198200

Jakaria, M., Park, S.-Y., Haque, M.E., Karthivashan, G., Kim, I.-S., Ganesan, P., Choi, D.-K., 2018. Neurotoxic Agent-Induced Injury in Neurodegenerative Disease Model: Focus on Involvement of Glutamate Receptors. Front. Mol. Neurosci. 11, 307. https://doi.org/10.3389/fnmol.2018.00307

Jang, J., Wang, Y., Kim, H.-S., Lalli, M.A., Kosik, K.S., 2014. Nrf2, a Regulator of the Proteasome, Controls Self-Renewal and Pluripotency in Human Embryonic Stem Cells. Stem Cells 32, 2616–2625. https://doi.org/10.1002/stem.1764

Jansen, A.H.P., Reits, E.A.J., Hol, E.M., 2014. The ubiquitin proteasome system in glia and its role in neurodegenerative diseases. Front. Mol. Neurosci. 7, 73. https://doi.org/10.3389/fnmol.2014.00073

Jelluma, N., 2006. Glucose Withdrawal Induces Oxidative Stress followed by Apoptosis in Glioblastoma Cells but not in Normal Human Astrocytes. Mol. Cancer Res. 4, 319–330. https://doi.org/10.1158/1541-7786.MCR-05-0061

Jenner, P., Olanow, C.W., 1996. Oxidative stress and the pathogenesis of Parkinson's disease. Neurology 47, S161-70. https://doi.org/10.1212/wnl.47.6_suppl_3.161s

Jha, M.K., Kim, J.-H., Song, G.J., Lee, W.-H., Lee, I.-K., Lee, H.-W., An, S.S.A., Kim, S., Suk, K., 2018. Functional dissection of astrocyte-secreted proteins: Implications in brain health and diseases. Prog. Neurobiol. 162, 37–69. https://doi.org/10.1016/j.pneurobio.2017.12.003

Jha, M.K., Seo, M., Kim, J.-H., Kim, B.-G., Cho, J.-Y., Suk, K., 2013. The secretome signature of reactive glial cells and its pathological implications. Biochim. Biophys. Acta - Proteins Proteomics 1834, 2418–2428. https://doi.org/10.1016/j.bbapap.2012.12.006

Jha, S.K., Jha, N.K., Kumar, D., Ambasta, R.K., Kumar, P., 2017. Linking mitochondrial dysfunction, metabolic syndrome and stress signaling in Neurodegeneration. Biochim. Biophys. Acta - Mol. Basis Dis. 1863, 1132–1146. https://doi.org/10.1016/j.bbadis.2016.06.015

Jhoo, J.H., Kim, H.-C., Nabeshima, T., Yamada, K., Shin, E.-J., Jhoo, W.-K., Kim, W., Kang, K.-S., Jo, S.A., Woo, J.I., 2004. β-Amyloid (1–42)-induced learning and memory deficits in mice: involvement of oxidative

burdens in the hippocampus and cerebral cortex. Behav. Brain Res. 155, 185–196. https://doi.org/10.1016/j.bbr.2004.04.012

Jiang, J., Nicoll, S.B., Lu, H.H., 2005. Co-culture of osteoblasts and chondrocytes modulates cellular differentiation in vitro. Biochem. Biophys. Res. Commun. 338, 762–770. https://doi.org/10.1016/j.bbrc.2005.10.025

Jiang, Q., Yan, Z., Feng, J., 2006. Neurotrophic Factors Stabilize Microtubules and Protect against Rotenone Toxicity on Dopaminergic Neurons. J. Biol. Chem. 281, 29391–29400. https://doi.org/10.1074/jbc.M602740200

Jimenez-Blasco, D., Santofimia-Castaño, P., Gonzalez, A., Almeida, A., Bolaños, J.P., 2015. Astrocyte NMDA receptors' activity sustains neuronal survival through a Cdk5–Nrf2 pathway. Cell Death Differ. 22, 1877–1889. https://doi.org/10.1038/cdd.2015.49

Jonckheere, A.I., Smeitink, J.A.M., Rodenburg, R.J.T., 2012. Mitochondrial ATP synthase: architecture, function and pathology. J. Inherit. Metab. Dis. 35, 211–225. https://doi.org/10.1007/s10545-011-9382-9

Jönsson, T.J., Johnson, L.C., Lowther, W.T., 2008. Structure of the sulphiredoxin–peroxiredoxin complex reveals an essential repair embrace. Nature 451, 98–101. https://doi.org/10.1038/nature06415

Joshi, G., A. Johnson, J., 2012. The Nrf2-ARE Pathway: A Valuable Therapeutic Target for the Treatment of Neurodegenerative Diseases. Recent Pat. CNS Drug Discov. 7, 218–229. https://doi.org/10.2174/157488912803252023

Joshi, G., Perluigi, M., Sultana, R., Agrippino, R., Calabrese, V., Butterfield, D.A., 2006. In vivo protection of synaptosomes by ferulic acid ethyl ester (FAEE) from oxidative stress mediated by 2,2-azobis(2-amidino-propane)dihydrochloride (AAPH) or Fe2+/H2O2: Insight into mechanisms of neuroprotection and relevance to oxidative stress-related . Neurochem. Int. 48, 318–327. https://doi.org/10.1016/j.neuint.2005.11.006

Ju, C., Gao, J., Hou, L., Wang, L., Zhang, F., Sun, F., Zhang, T., Xu, P., Shi, Z., Hu, F., Zhang, C., 2017. Neuroprotective effect of chondroitin sulfate on SH-SY5Y cells overexpressing wild-type or A53T mutant α-synuclein. Mol. Med. Rep. 16, 8721–8728. https://doi.org/10.3892/mmr.2017.7725

Juaristi, I., Llorente-Folch, I., Satrústegui, J., del Arco, A., 2019. Extracellular ATP and glutamate drive pyruvate production and energy demand to regulate mitochondrial respiration in astrocytes. Glia 67, 759–774. https://doi.org/10.1002/glia.23574

Jucker, M., Walker, L.C., 2013. Self-propagation of pathogenic protein aggregates in neurodegenerative diseases. Nature 501, 45–51. https://doi.org/10.1038/nature12481

Jung, C., Ichesco, E., Ratai, E.-M., Gonzalez, R.G., Burdo, T., Loggia, M.L., Harris, R.E., Napadow, V., 2020.

Magnetic resonance imaging of neuroinflammation in chronic pain. Pain 1. https://doi.org/10.1097/j.pain.0000000000001815

Junn, E., Jang, W.H., Zhao, X., Jeong, B.S., Mouradian, M.M., 2009. Mitochondrial localization of DJ-1 leads to enhanced neuroprotection. J. Neurosci. Res. 87, 123–129. https://doi.org/10.1002/jnr.21831

Kabiraj, P., Valenzuela, C.A., Marin, J.E., Ramirez, D.A., Mendez, L., Hwang, M.S., Varela-Ramirez, A., Fenelon, K., Narayan, M., Skouta, R., 2015. The Neuroprotective Role of Ferrostatin-1 Under Rotenone-Induced Oxidative Stress in Dopaminergic Neuroblastoma Cells. Protein J. 34, 349–358. https://doi.org/10.1007/s10930-015-9629-7

Kabuta, T., Setsuie, R., Mitsui, T., Kinugawa, A., Sakurai, M., Aoki, S., Uchida, K., Wada, K., 2008. Aberrant molecular properties shared by familial Parkinson's disease-associated mutant UCH-L1 and carbonyl-modified UCH-L1. Hum. Mol. Genet. https://doi.org/10.1093/hmg/ddn037

Kaczanowski, S., Klim, J., Zielenkiewicz, U., 2018. An Apoptotic and Endosymbiotic Explanation of the Warburg and the Inverse Warburg Hypotheses. Int. J. Mol. Sci. 19, 3100. https://doi.org/10.3390/ijms19103100

Kageyama, Y., Zhang, Z., Roda, R., Fukaya, M., Wakabayashi, J., Wakabayashi, N., Kensler, T.W., Reddy, P.H., Iijima, M., Sesaki, H., 2012. Mitochondrial division ensures the survival of postmitotic neurons by suppressing oxidative damage. J. Cell Biol. 197, 535–551. https://doi.org/10.1083/jcb.201110034

Kalyanaraman, B., Darley-Usmar, V., Davies, K.J.A., Dennery, P.A., Forman, H.J., Grisham, M.B., Mann, G.E., Moore, K., Roberts, L.J., Ischiropoulos, H., 2012. Measuring reactive oxygen and nitrogen species with fluorescent probes: challenges and limitations. Free Radic. Biol. Med. 52, 1–6. https://doi.org/10.1016/j.freeradbiomed.2011.09.030

Kane, L.A., Lazarou, M., Fogel, A.I., Li, Y., Yamano, K., Sarraf, S.A., Banerjee, S., Youle, R.J., 2014. PINK1 phosphorylates ubiquitin to activate Parkin E3 ubiquitin ligase activity. J. Cell Biol. 205, 143–153. https://doi.org/10.1083/jcb.201402104

Kang, S.-J., Kim, J.S., Park, S.M., 2018. Ubiquitin C-terminal Hydrolase L1 Regulates Lipid Raft-dependent Endocytosis. Exp. Neurobiol. 27, 377. https://doi.org/10.5607/en.2018.27.5.377

Kann, O., Kovács, R., 2007. Mitochondria and neuronal activity. Am. J. Physiol. Physiol. 292, C641–C657. https://doi.org/10.1152/ajpcell.00222.2006

Kanski, J., Aksenova, M., Stoyanova, A., Butterfield, D.A., 2002. Ferulic acid antioxidant protection against hydroxyl and peroxyl radical oxidation in synaptosomal and neuronal cell culture systems in vitro: structure-activity studies. J. Nutr. Biochem. 13, 273–281. https://doi.org/10.1016/S0955-2863(01)00215-7

Kao, Y.-C., Liao, Y.-C., Cheng, P.-L., Lee, C.-H., 2019. Neurite Retraction and Regrowth under Optical and

Chemical Stimulations, in: 2019 IEEE International Conference on BioPhotonics (BioPhotonics). IEEE, pp. 1–3. https://doi.org/10.1109/BioPhotonics.2019.8896752

Karbowski, M., 2010. Mitochondria on Guard: Role of Mitochondrial Fusion and Fission in the Regulation of Apoptosis, in: Advances in Experimental Medicine and Biology. pp. 131–142. https://doi.org/10.1007/978-1-4419-6706-0_8

Karmakar, S., Banik, N.L., Ray, S.K., 2008. Combination of all-trans retinoic acid and paclitaxel-induced differentiation and apoptosis in human glioblastoma U87MG xenografts in nude mice. Cancer 112, 596–607. https://doi.org/10.1002/cncr.23223

Kaspar, J.W., Jaiswal, A.K., 2011. Tyrosine phosphorylation controls nuclear export of Fyn, allowing Nrf2 activation of cytoprotective gene expression. FASEB J. 25, 1076–1087. https://doi.org/10.1096/fj.10-171553

Kaspar, J.W., Jaiswal, A.K., 2010a. Antioxidant-induced Phosphorylation of Tyrosine 486 Leads to Rapid Nuclear Export of Bach1 That Allows Nrf2 to Bind to the Antioxidant Response Element and Activate Defensive Gene Expression. J. Biol. Chem. 285, 153–162. https://doi.org/10.1074/jbc.M109.040022

Kaspar, J.W., Jaiswal, A.K., 2010b. An Autoregulatory Loop between Nrf2 and Cul3-Rbx1 Controls Their Cellular Abundance. J. Biol. Chem. 285, 21349–21358. https://doi.org/10.1074/jbc.M110.121863

Kaspar, J.W., Niture, S.K., Jaiswal, A.K., 2009. Nrf2:INrf2 (Keap1) signaling in oxidative stress. Free Radic. Biol. Med. 47, 1304–1309. https://doi.org/10.1016/j.freeradbiomed.2009.07.035

Katschinski, D.M., Boos, K., Schindler, S.G., Fandrey, J., 2000. Pivotal Role of Reactive Oxygen Species as Intracellular Mediators of Hyperthermia-induced Apoptosis. J. Biol. Chem. 275, 21094–21098. https://doi.org/10.1074/jbc.M001629200

Katsetos, C.D., Dráberová, E., Šmejkalová, B., Reddy, G., Bertrand, L., de Chadarévian, J.-P., Legido, A., Nissanov, J., Baas, P.W., Dráber, P., 2007. Class III β-Tubulin and γ-Tubulin are Co-expressed and Form Complexes in Human Glioblastoma Cells. Neurochem. Res. 32, 1387–1398. https://doi.org/10.1007/s11064-007-9321-1

Katsetos, C.D., Herman, M.M., Mörk, S.J., 2003. Class III β-tubulin in human development and cancer. Cell Motil. Cytoskeleton 55, 77–96. https://doi.org/10.1002/cm.10116

Kauppila, T.E.S., Kauppila, J.H.K., Larsson, N.-G., 2017. Mammalian Mitochondria and Aging: An Update. Cell Metab. 25, 57–71. https://doi.org/10.1016/j.cmet.2016.09.017

Kayser, J., Haslbeck, M., Dempfle, L., Krause, M., Grashoff, C., Buchner, J., Herrmann, H., Bausch, A.R., 2013. The Small Heat Shock Protein Hsp27 Affects Assembly Dynamics and Structure of Keratin Intermediate Filament Networks. Biophys. J. 105, 1778–1785. https://doi.org/10.1016/j.bpj.2013.09.007

Kazlauskaite, A., Kondapalli, C., Gourlay, R., Campbell, D.G., Ritorto, M.S., Hofmann, K., Alessi, D.R., Knebel,

A., Trost, M., Muqit, M.M.K., 2014. Parkin is activated by PINK1-dependent phosphorylation of ubiquitin at Ser 65. Biochem. J. 460, 127–141. https://doi.org/10.1042/BJ20140334

Keene, S.D., Greco, T.M., Parastatidis, I., Lee, S.-H., Hughes, E.G., Balice-Gordon, R.J., Speicher, D.W., Ischiropoulos, H., 2009. Mass spectrometric and computational analysis of cytokine-induced alterations in the astrocyte secretome. Proteomics 9, 768–782. https://doi.org/10.1002/pmic.200800385

Kempuraj, D., Thangavel, R., Natteru, P.A., Selvakumar, G.P., Saeed, D., Zahoor, H., Zaheer, S., Iyer, S.S., Zaheer, A., 2016. Neuroinflammation Induces Neurodegeneration. J. Neurol. Neurosurg. spine 1.

Kerschensteiner, M., Schwab, M.E., Lichtman, J.W., Misgeld, T., 2005. In vivo imaging of axonal degeneration and regeneration in the injured spinal cord. Nat. Med. 11, 572–577. https://doi.org/10.1038/nm1229

Khakh, B.S., Sofroniew, M. V, 2015. Diversity of astrocyte functions and phenotypes in neural circuits. Nat. Neurosci. 18, 942–952. https://doi.org/10.1038/nn.4043

Khalouei, S., Chow, A.M., Brown, I.R., 2014. Localization of heat shock protein HSPA6 (HSP70B') to sites of transcription in cultured differentiated human neuronal cells following thermal stress. J. Neurochem. 131, 743–754. https://doi.org/10.1111/jnc.12970

Khatib, T., Marini, P., Nunna, S., Chisholm, D.R., Whiting, A., Redfern, C., Greig, I.R., McCaffery, P., 2019. Genomic and non-genomic pathways are both crucial for peak induction of neurite outgrowth by retinoids. Cell Commun. Signal. 17, 40. https://doi.org/10.1186/s12964-019-0352-4

Kim, J.-H., Afridi, R., Lee, W.-H., Suk, K., 2020. Proteomic examination of the neuroglial secretome: lessons for the clinic. Expert Rev. Proteomics 14789450.2020.1745069. https://doi.org/10.1080/14789450.2020.1745069

Kim, J.-M., Cha, S.-H., Choi, Y.R., Jou, I., Joe, E.-H., Park, S.M., 2016. DJ-1 deficiency impairs glutamate uptake into astrocytes via the regulation of flotillin-1 and caveolin-1 expression. Sci. Rep. 6, 28823. https://doi.org/10.1038/srep28823

KIM, J., HAN, J., JANG, Y., KIM, S.J., LEE, M.J., RYU, M.J., KWEON, G.R., HEO, J.Y., 2015. High-capacity glycolytic and mitochondrial oxidative metabolisms mediate the growth ability of glioblastoma. Int. J. Oncol. 47, 1009–1016. https://doi.org/10.3892/ijo.2015.3101

Kim, R.H., Smith, P.D., Aleyasin, H., Hayley, S., Mount, M.P., Pownall, S., Wakeham, A., You-Ten, A.J., Kalia, S.K., Horne, P., Westaway, D., Lozano, A.M., Anisman, H., Park, D.S., Mak, T.W., 2005. Hypersensitivity of DJ-1-deficient mice to 1-methyl-4-phenyl-1,2,3,6-tetrahydropyrindine (MPTP) and oxidative stress. Proc. Natl. Acad. Sci. 102, 5215–5220. https://doi.org/10.1073/pnas.0501282102

Kim, S.-J., Park, Y.-J., Hwang, I.-Y., Youdim, M.B.H., Park, K.-S., Oh, Y.J., 2012. Nuclear translocation of DJ-1 during oxidative stress-induced neuronal cell death. Free Radic. Biol. Med. 53, 936–950. https://doi.org/10.1016/j.freeradbiomed.2012.05.035

Kim, S.R., Ha, Y.M., Kim, Y.M., Park, E.J., Kim, J.W., Park, S.W., Kim, H.J., Chung, H.T., Chang, K.C., 2015. Ascorbic acid reduces HMGB1 secretion in lipopolysaccharide-activated RAW 264.7 cells and improves survival rate in septic mice by activation of Nrf2/HO-1 signals. Biochem. Pharmacol. 95, 279–289. https://doi.org/10.1016/j.bcp.2015.04.007

Kiss, R., Zhu, M., Jójárt, B., Czajlik, A., Solti, K., Fórizs, B., Nagy, É., Zsila, F., Beke-Somfai, T., Tóth, G., 2017. Structural features of human DJ-1 in distinct Cys106 oxidative states and their relevance to its loss of function in disease. Biochim. Biophys. Acta - Gen. Subj. 1861, 2619–2629. https://doi.org/10.1016/j.bbagen.2017.08.017

Kitada, T., Asakawa, S., Hattori, N., Matsumine, H., Yamamura, Y., Minoshima, S., Yokochi, M., Mizuno, Y., Shimizu, N., 1998. Mutations in the parkin gene cause autosomal recessive juvenile parkinsonism. Nature 392, 605–608. https://doi.org/10.1038/33416

Kıray, H., Lindsay, S.L., Hosseinzadeh, S., Barnett, S.C., 2016. The multifaceted role of astrocytes in regulating myelination. Exp. Neurol. 283, 541–549. https://doi.org/10.1016/j.expneurol.2016.03.009

Klichko, V.I., Orr, W.C., Radyuk, S.N., 2016. The role of peroxiredoxin 4 in inflammatory response and aging. Biochim. Biophys. Acta - Mol. Basis Dis. 1862, 265–273. https://doi.org/10.1016/j.bbadis.2015.12.008

Kneynsberg, A., Collier, T.J., Manfredsson, F.P., Kanaan, N.M., 2016. Quantitative and semi-quantitative measurements of axonal degeneration in tissue and primary neuron cultures. J. Neurosci. Methods 266, 32–41. https://doi.org/10.1016/j.jneumeth.2016.03.004

Knott, A.B., Perkins, G., Schwarzenbacher, R., Bossy-Wetzel, E., 2008. Mitochondrial fragmentation in neurodegeneration. Nat. Rev. Neurosci. 9, 505–518. https://doi.org/10.1038/nrn2417

Kobayashi, M., Yamamoto, M., 2006. Nrf2-Keap1 regulation of cellular defense mechanisms against electrophiles and reactive oxygen species. Adv. Enzyme Regul. 46, 113–140. https://doi.org/10.1016/j.advenzreg.2006.01.007

Komander, D., Rape, M., 2012. The Ubiquitin Code. Annu. Rev. Biochem. 81, 203–229. https://doi.org/10.1146/annurev-biochem-060310-170328

Kondo, Y., Sasaki, T., Sato, Y., Amano, A., Aizawa, S., Iwama, M., Handa, S., Shimada, N., Fukuda, M., Akita, M., Lee, J., Jeong, K.-S., Maruyama, N., Ishigami, A., 2008. Vitamin C depletion increases superoxide generation in brains of SMP30/GNL knockout mice. Biochem. Biophys. Res. Commun. 377, 291–296. https://doi.org/10.1016/j.bbrc.2008.09.132

Kong, A.-N.T., Owuor, E., Yu, R., Hebbar, V., Chen, C., Hu, R., Mandlekar, S., 2001. Induction of xenobiotic enzymes by the map kinase pathway and the antioxidant or electrophile response element (ARE/EpRE) ,†, ‡. Drug Metab. Rev. 33, 255–271. https://doi.org/10.1081/DMR-120000652

Koprich, J.B., Reske-Nielsen, C., Mithal, P., Isacson, O., 2008. Neuroinflammation mediated by IL-1β increases

susceptibility of dopamine neurons to degeneration in an animal model of Parkinson's disease. J. Neuroinflammation 5, 8. https://doi.org/10.1186/1742-2094-5-8

Korovila, I., Hugo, M., Castro, J.P., Weber, D., Höhn, A., Grune, T., Jung, T., 2017. Proteostasis, oxidative stress and aging. Redox Biol. 13, 550–567. https://doi.org/10.1016/j.redox.2017.07.008

Koskenkorva-Frank, T.S., Weiss, G., Koppenol, W.H., Burckhardt, S., 2013. The complex interplay of iron metabolism, reactive oxygen species, and reactive nitrogen species: Insights into the potential of various iron therapies to induce oxidative and nitrosative stress. Free Radic. Biol. Med. 65, 1174–1194. https://doi.org/10.1016/j.freeradbiomed.2013.09.001

Koudriavtseva, T., Mainero, C., 2016. Neuroinflammation, neurodegeneration and regeneration in multiple sclerosis: intercorrelated manifestations of the immune response. Neural Regen. Res. 11, 1727. https://doi.org/10.4103/1673-5374.194804

Kovac, S., Angelova, P.R., Holmström, K.M., Zhang, Y., Dinkova-Kostova, A.T., Abramov, A.Y., 2015. Nrf2 regulates ROS production by mitochondria and NADPH oxidase. Biochim. Biophys. Acta - Gen. Subj. 1850, 794–801. https://doi.org/10.1016/j.bbagen.2014.11.021

Kovalevich, J., Langford, D., 2013. Considerations for the Use of SH-SY5Y Neuroblastoma Cells in Neurobiology, in: Methods in Molecular Biology. pp. 9–21. https://doi.org/10.1007/978-1-62703-640-5_2

Kowal, J., Arras, G., Colombo, M., Jouve, M., Morath, J.P., Primdal-Bengtson, B., Dingli, F., Loew, D., Tkach, M., Théry, C., 2016. Proteomic comparison defines novel markers to characterize heterogeneous populations of extracellular vesicle subtypes. Proc. Natl. Acad. Sci. 113, E968–E977. https://doi.org/10.1073/pnas.1521230113

Kowald, A., Kirkwood, T.B.L., 2011. Evolution of the mitochondrial fusion-fission cycle and its role in aging. Proc. Natl. Acad. Sci. 108, 10237–10242. https://doi.org/10.1073/pnas.1101604108

Kowald, A., Kirkwood, T.B.L., 2000. Accumulation of Defective Mitochondria through Delayed Degradation of Damaged Organelles and Its Possible Role in the Ageing of Post-mitotic and Dividing Cells. J. Theor. Biol. 202, 145–160. https://doi.org/10.1006/jtbi.1999.1046

Krance, S.M., Keng, P.C., Palis, J., Ballatori, N., 2010. Transient Glutathione Depletion Determines Terminal Differentiation in HL-60 Cells. Oxid. Med. Cell. Longev. 3, 53–60. https://doi.org/10.4161/oxim.3.1.10405

Kranich, O., Dringen, R., Sandberg, M., Hamprecht, B., 1998. Utilization of cysteine and cysteine precursors for the synthesis of glutathione in astroglial cultures: Preference for cystine. Glia 22, 11–18. https://doi.org/10.1002/(SICI)1098-1136(199801)22:1<11::AID-GLIA2>3.0.CO;2-B

Krishna, A., Biryukov, M., Trefois, C., Antony, P.M., Hussong, R., Lin, J., Heinäniemi, M., Glusman, G.,

Köglsberger, S., Boyd, O., van den Berg, B.H., Linke, D., Huang, D., Wang, K., Hood, L., Tholey, A., Schneider, R., Galas, D.J., Balling, R., May, P., 2014. Systems genomics evaluation of the SH-SY5Y neuroblastoma cell line as a model for Parkinson's disease. BMC Genomics 15, 1154. https://doi.org/10.1186/1471-2164-15-1154

Kritsiligkou, P., Chatzi, A., Charalampous, G., Mironov, A., Grant, C.M., Tokatlidis, K., 2017. Unconventional Targeting of a Thiol Peroxidase to the Mitochondrial Intermembrane Space Facilitates Oxidative Protein Folding. Cell Rep. 18, 2729–2741. https://doi.org/10.1016/j.celrep.2017.02.053

Kugler, W., Veenman, L., Shandalov, Y., Leschiner, S., Spanier, I., Lakomek, M., Gavish, M., 2008. Ligands of the mitochondrial 18 kDa translocator protein attenuate apoptosis of human glioblastoma cells exposed to erucylphosphohomocholine. Cell. Oncol. 30, 435–50. https://doi.org/10.3233/CLO-2008-0431

Kujoth, G.C., 2005. Mitochondrial DNA Mutations, Oxidative Stress, and Apoptosis in Mammalian Aging. Science (80-.). 309, 481–484. https://doi.org/10.1126/science.1112125

Kumar, D., Manek, R., Raghavan, V., Wang, K.K., 2018. Protein Characterization of Extracellular Microvesicles/Exosomes Released from Cytotoxin-Challenged Rat Cerebrocortical Mixed Culture and Mouse N2a Cells. Mol. Neurobiol. 55, 2112–2124. https://doi.org/10.1007/s12035-017-0474-x

Kumar, R., Jangir, D.K., Verma, G., Shekhar, S., Hanpude, P., Kumar, S., Kumari, R., Singh, N., Sarovar Bhavesh, N., Ranjan Jana, N., Kanti Maiti, T., 2017. S-nitrosylation of UCHL1 induces its structural instability and promotes α-synuclein aggregation. Sci. Rep. 7, 44558. https://doi.org/10.1038/srep44558

Kwak, M.-K., Wakabayashi, N., Greenlaw, J.L., Yamamoto, M., Kensler, T.W., 2003. Antioxidants Enhance Mammalian Proteasome Expression through the Keap1-Nrf2 Signaling Pathway. Mol. Cell. Biol. 23, 8786–8794. https://doi.org/10.1128/MCB.23.23.8786-8794.2003

Kwon, Y.T., Ciechanover, A., 2017. The Ubiquitin Code in the Ubiquitin-Proteasome System and Autophagy. Trends Biochem. Sci. 42, 873–886. https://doi.org/10.1016/j.tibs.2017.09.002

L'Episcopo, Francesca, Serapide, M.F., Tirolo, C., Testa, N., Caniglia, S., Morale, M.C., Pluchino, S., Marchetti, B., 2011. A Wnt1 regulated Frizzled-1/β-Catenin signaling pathway as a candidate regulatory circuit controlling mesencephalic dopaminergic neuron-astrocyte crosstalk: Therapeutical relevance for neuron survival and neuroprotection. Mol. Neurodegener. 6, 49. https://doi.org/10.1186/1750-1326-6-49

L'Episcopo, F., Tirolo, C., Testa, N., Caniglia, S., Morale, M.C., Cossetti, C., D'Adamo, P., Zardini, E., Andreoni, L., Ihekwaba, A.E.C., Serra, P.A., Franciotta, D., Martino, G., Pluchino, S., Marchetti, B., 2011. Reactive astrocytes and Wnt/β-catenin signaling link nigrostriatal injury to repair in 1-methyl-4-phenyl-1,2,3,6-tetrahydropyridine model of Parkinson's disease. Neurobiol. Dis. 41, 508–527. https://doi.org/10.1016/j.nbd.2010.10.023

Lackie, R.E., Maciejewski, A., Ostapchenko, V.G., Marques-Lopes, J., Choy, W.-Y., Duennwald, M.L., Prado, V.F., Prado, M.A.M., 2017. The Hsp70/Hsp90 Chaperone Machinery in Neurodegenerative Diseases. Front. Neurosci. 11, 254. https://doi.org/10.3389/fnins.2017.00254

Lafon-Cazal, M., Adjali, O., Galéotti, N., Poncet, J., Jouin, P., Homburger, V., Bockaert, J., Marin, P., 2003. Proteomic Analysis of Astrocytic Secretion in the Mouse. J. Biol. Chem. 278, 24438–24448. https://doi.org/10.1074/jbc.M211980200

Laganiere, J., Kells, A.P., Lai, J.T., Guschin, D., Paschon, D.E., Meng, X., Fong, L.K., Yu, Q., Rebar, E.J., Gregory, P.D., Bankiewicz, K.S., Forsayeth, J., Zhang, H.S., 2010. An engineered zinc finger protein activator of the endogenous glial cell line-derived neurotrophic factor gene provides functional neuroprotection in a rat model of Parkinson's disease. J. Neurosci. 30, 16469–74. https://doi.org/10.1523/JNEUROSCI.2440-10.2010

Lamarche, F., Signorini-Allibe, N., Gonthier, B., Barret, L., 2004. Influence of vitamin E, sodium selenite, and astrocyte-conditioned medium on neuronal survival after chronic exposure to ethanol. Alcohol 33, 127–38. https://doi.org/10.1016/j.alcohol.2004.09.001

Lambert, J.-P., Ivosev, G., Couzens, A.L., Larsen, B., Taipale, M., Lin, Z.-Y., Zhong, Q., Lindquist, S., Vidal, M., Aebersold, R., Pawson, T., Bonner, R., Tate, S., Gingras, A.-C., 2013. Mapping differential interactomes by affinity purification coupled with data-independent mass spectrometry acquisition. Nat. Methods 10, 1239–45. https://doi.org/10.1038/nmeth.2702

Lander, G.C., Estrin, E., Matyskiela, M.E., Bashore, C., Nogales, E., Martin, A., 2012. Complete subunit architecture of the proteasome regulatory particle. Nature 482, 186–191. https://doi.org/10.1038/nature10774

Langeveld, C.H., Schepens, E., Jongenelen, C.A.M., Stoof, J.C., Hjelle, O.P., Ottersen, O.P., Drukarch, B., 1996. Presence of glutathione immunoreactivity in cultured neurones and astrocytes. Neuroreport 7, 1833–1836. https://doi.org/10.1097/00001756-199607290-00029

Lantoine, J., Grevesse, T., Villers, A., Delhaye, G., Mestdagh, C., Versaevel, M., Mohammed, D., Bruyère, C., Alaimo, L., Lacour, S.P., Ris, L., Gabriele, S., 2016. Matrix stiffness modulates formation and activity of neuronal networks of controlled architectures. Biomaterials 89, 14–24. https://doi.org/10.1016/j.biomaterials.2016.02.041

Larsen, C.N., Krantz, B.A., Wilkinson, K.D., 1998. Substrate Specificity of Deubiquitinating Enzymes: Ubiquitin C-Terminal Hydrolases †. Biochemistry 37, 3358–3368. https://doi.org/10.1021/bi972274d

Larsen, N.J., Ambrosi, G., Mullett, S.J., Berman, S.B., Hinkle, D.A., 2011. DJ-1 knock-down impairs astrocyte mitochondrial function. Neuroscience 196, 251–264. https://doi.org/10.1016/j.neuroscience.2011.08.016

Lasker, K., Forster, F., Bohn, S., Walzthoeni, T., Villa, E., Unverdorben, P., Beck, F., Aebersold, R., Sali, A.,

Baumeister, W., 2012. Molecular architecture of the 26S proteasome holocomplex determined by an integrative approach. Proc. Natl. Acad. Sci. 109, 1380–1387. https://doi.org/10.1073/pnas.1120559109

Latronico, T., Pati, I., Ciavarella, R., Fasano, A., Mengoni, F., Lichtner, M., Vullo, V., Mastroianni, C.M., Liuzzi, G.M., 2018. In vitro effect of antiretroviral drugs on cultured primary astrocytes: analysis of neurotoxicity and matrix metalloproteinase inhibition. J. Neurochem. 144, 271–284. https://doi.org/10.1111/jnc.14269

Lau, L.W., Cua, R., Keough, M.B., Haylock-Jacobs, S., Yong, V.W., 2013. Pathophysiology of the brain extracellular matrix: a new target for remyelination. Nat. Rev. Neurosci. 14, 722–729. https://doi.org/10.1038/nrn3550

Lazarev, V.F., Nikotina, A.D., Mikhaylova, E.R., Nudler, E., Polonik, S.G., Guzhova, I. V., Margulis, B.A., 2016. Hsp70 chaperone rescues C6 rat glioblastoma cells from oxidative stress by sequestration of aggregating GAPDH. Biochem. Biophys. Res. Commun. 470, 766–771. https://doi.org/10.1016/j.bbrc.2015.12.076

Le Naour, F., Misek, D.E., Krause, M.C., Deneux, L., Giordano, T.J., Scholl, S., Hanash, S.M., 2001. Proteomics-based identification of RS/DJ-1 as a novel circulating tumor antigen in breast cancer. Clin. Cancer Res. 7, 3328–3335. https://doi.org/10.1002/prca.200600718

Leddy, H.A., Awad, H.A., Guilak, F., 2004. Molecular diffusion in tissue-engineered cartilage constructs: Effects of scaffold material, time, and culture conditions. J. Biomed. Mater. Res. 70B, 397–406. https://doi.org/10.1002/jbm.b.30053

Lee, C.S., Lee, C., Hu, T., Nguyen, J.M., Zhang, J., Martin, M. V., Vawter, M.P., Huang, E.J., Chan, J.Y., 2011. Loss of nuclear factor E2-related factor 1 in the brain leads to dysregulation of proteasome gene expression and neurodegeneration. Proc. Natl. Acad. Sci. 108, 8408–8413. https://doi.org/10.1073/pnas.1019209108

Lee, D., Ryu, K.-Y., 2017. Effect of cellular ubiquitin levels on the regulation of oxidative stress response and proteasome function via Nrf1. Biochem. Biophys. Res. Commun. 485, 234–240. https://doi.org/10.1016/j.bbrc.2017.02.105

Lee, J.-M., Calkins, M.J., Chan, K., Kan, Y.W., Johnson, J.A., 2003a. Identification of the NF-E2-related Factor-2-dependent Genes Conferring Protection against Oxidative Stress in Primary Cortical Astrocytes Using Oligonucleotide Microarray Analysis. J. Biol. Chem. 278, 12029–12038. https://doi.org/10.1074/jbc.M211558200

Lee, J.-M., Shih, A.Y., Murphy, T.H., Johnson, J.A., 2003b. NF-E2-related Factor-2 Mediates Neuroprotection against Mitochondrial Complex I Inhibitors and Increased Concentrations of Intracellular Calcium in Primary Cortical Neurons. J. Biol. Chem. 278, 37948–37956. https://doi.org/10.1074/jbc.M305204200

Lee, J.C., 1963. Electron microscopy of Wallerian degeneration. J. Comp. Neurol. 120, 65–79.

https://doi.org/10.1002/cne.901200107

Lee, P., Ulatowski, L.M., 2019. Vitamin E: Mechanism of transport and regulation in the CNS. IUBMB Life 71, 424–429. https://doi.org/10.1002/iub.1993

Lee, T.-C., Kashyap, R.L., 1994. Building Skeleton Models via 3-D Medial Surface/Axis Thinning Algorithms. Graph. Model. Image Process. 56, 462–78.

Lee, W.-C., Wong, H.-Y., Chai, Y.-Y., Shi, C.-W., Amino, N., Kikuchi, S., Huang, S.-H., 2012. Lipid peroxidation dysregulation in ischemic stroke: Plasma 4-HNE as a potential biomarker? Biochem. Biophys. Res. Commun. 425, 842–847. https://doi.org/10.1016/j.bbrc.2012.08.002

Lee, Y.-T.C., Hsu, S.-T.D., 2017. Familial Mutations and Post-translational Modifications of UCH-L1 in Parkinson's Disease and Neurodegenerative Disorders. Curr. Protein Pept. Sci. 18, 733–745. https://doi.org/10.2174/1389203717666160217143721

Lefaki, M., Papaevgeniou, N., Chondrogianni, N., 2017. Redox regulation of proteasome function. Redox Biol. 13, 452–458. https://doi.org/10.1016/j.redox.2017.07.005

Lemasters, J.J., 2014. Variants of mitochondrial autophagy: Types 1 and 2 mitophagy and micromitophagy (Type 3). Redox Biol. 2, 749–754. https://doi.org/10.1016/j.redox.2014.06.004

Lemire, J., Alhasawi, A., Appanna, V.P., Tharmalingam, S., Appanna, V.D., 2017. Metabolic defence against oxidative stress: the road less travelled so far. J. Appl. Microbiol. 123, 798–809. https://doi.org/10.1111/jam.13509

Leroy, E., Boyer, R., Auburger, G., Leube, B., Ulm, G., Mezey, E., Harta, G., Brownstein, M.J., Jonnalagada, S., Chernova, T., Dehejia, a, Lavedan, C., Gasser, T., Steinbach, P.J., Wilkinson, K.D., Polymeropoulos, M.H., 1998. The ubiquitin pathway in Parkinson's disease. Nature 395, 451–452. https://doi.org/10.1038/26652

Lev, N., Barhum, Y., Ben-Zur, T., Melamed, E., Steiner, I., Offen, D., 2013. Knocking Out DJ-1 Attenuates Astrocytes Neuroprotection Against 6-Hydroxydopamine Toxicity. J. Mol. Neurosci. 50, 542–550. https://doi.org/10.1007/s12031-013-9984-9

Levental, I., Georges, P.C., Janmey, P.A., 2007. Soft biological materials and their impact on cell function. Soft Matter 3, 299–306. https://doi.org/10.1039/B610522J

Levin, M., Udi, Y., Solomonov, I., Sagi, I., 2017. Next generation matrix metalloproteinase inhibitors — Novel strategies bring new prospects. Biochim. Biophys. Acta - Mol. Cell Res. 1864, 1927–1939. https://doi.org/10.1016/j.bbamcr.2017.06.009

Li, B., Harjani, J.R., Cormier, N.S., Madarati, H., Atkinson, J., Cosa, G., Pratt, D.A., 2013. Besting Vitamin E: Sidechain Substitution is Key to the Reactivity of Naphthyridinol Antioxidants in Lipid Bilayers. J. Am. Chem. Soc. 135, 1394–1405. https://doi.org/10.1021/ja309153x

Li, D., Han, B., Liu, Z., Zhao, D., 2001. Phase behavior of supercritical CO 2 /Styrene/Poly(ethylene terephthlate) (PET) system and preparation of polystyrene/PET composites. Polymer (Guildf). 42, 2331–2337. https://doi.org/10.1016/S0032-3861(00)00601-7

Li, H.M., Niki, T., Taira, T., Iguchi-Ariga, S.M.M., Ariga, H., 2005. Association of DJ-1 with chaperones and enhanced association and colocalization with mitochondrial Hsp70 by oxidative stress. Free Radic. Res. 39, 1091–1099. https://doi.org/10.1080/10715760500260348

Li, K., Li, J., Zheng, J., Qin, S., 2019. Reactive Astrocytes in Neurodegenerative Diseases. Aging Dis. 10, 664. https://doi.org/10.14336/AD.2018.0720

Li, M.-L., Defren, J., Brewer, G., 2013. Hsp27 and F-Box Protein -TrCP Promote Degradation of mRNA Decay Factor AUF1. Mol. Cell. Biol. 33, 2315–2326. https://doi.org/10.1128/MCB.00931-12

Li, W., James, M.O., McKenzie, S.C., Calcutt, N.A., Liu, C., Stacpoole, P.W., 2011. Mitochondrion as a Novel Site of Dichloroacetate Biotransformation by Glutathione Transferase ζ1. J. Pharmacol. Exp. Ther. 336, 87–94. https://doi.org/10.1124/jpet.110.173195

Li, Y., Xiao, Y., Liu, C., 2017. The Horizon of Materiobiology: A Perspective on Material-Guided Cell Behaviors and Tissue Engineering. Chem. Rev. 117, 4376–4421. https://doi.org/10.1021/acs.chemrev.6b00654

Liddell, J.R., Lehtonen, S., Duncan, C., Keksa-Goldsteine, V., Levonen, A.-L., Goldsteins, G., Malm, T., White, A.R., Koistinaho, J., Kanninen, K.M., 2016. Pyrrolidine dithiocarbamate activates the Nrf2 pathway in astrocytes. J. Neuroinflammation 13, 49. https://doi.org/10.1186/s12974-016-0515-9

Liddy, K.A., White, M.Y., Cordwell, S.J., 2013. Functional decorations: post-translational modifications and heart disease delineated by targeted proteomics. Genome Med. 5, 20. https://doi.org/10.1186/gm424

Lieberman, O.J., Frier, M.D., McGuirt, A.F., Griffey, C.J., Rafikian, E., Yang, M., Yamamoto, A., Borgkvist, A., Santini, E., Sulzer, D., 2020. Cell-type-specific regulation of neuronal intrinsic excitability by macroautophagy. Elife 9, e50843. https://doi.org/10.7554/eLife.50843

Lin, C.-Y., Lee, Y.-S., Lin, V.W., Silver, J., 2012. Fibronectin Inhibits Chronic Pain Development after Spinal Cord Injury. J. Neurotrauma 29, 589–599. https://doi.org/10.1089/neu.2011.2059

Lin, M.-Y., Sheng, Z.-H., 2015. Regulation of mitochondrial transport in neurons. Exp. Cell Res. 334, 35–44. https://doi.org/10.1016/j.yexcr.2015.01.004

Lin, M.T., Beal, M.F.F., 2006. Mitochondrial dysfunction and oxidative stress in neurodegenerative diseases. Nature 443, 787–795. https://doi.org/nature05292 [pii]\r10.1038/nature05292

Lin, Y., Zhang, J.-C., Yao, C.-Y., Wu, Y., Abdelgawad, A.F., Yao, S.-L., Yuan, S.-Y., 2016. Critical role of astrocytic interleukin-17 A in post-stroke survival and neuronal differentiation of neural precursor cells in adult mice. Cell Death Dis. 7, e2273–e2273. https://doi.org/10.1038/cddis.2015.284

Lindersson, E., Beedholm, R., Højrup, P., Moos, T., Gai, W., Hendil, K.B., Jensen, P.H., 2004. Proteasomal Inhibition by α-Synuclein Filaments and Oligomers. J. Biol. Chem. 279, 12924–12934. https://doi.org/10.1074/jbc.M306390200

Liu, K., Tedeschi, A., Park, K.K., He, Z., 2011. Neuronal Intrinsic Mechanisms of Axon Regeneration. Annu. Rev. Neurosci. 34, 131–152. https://doi.org/10.1146/annurev-neuro-061010-113723

Liu, Y., Wang, L., Long, Z., Zeng, L., Wu, Y., 2012. Protoplasmic Astrocytes Enhance the Ability of Neural Stem Cells to Differentiate into Neurons In Vitro. PLoS One 7, e38243. https://doi.org/10.1371/journal.pone.0038243

Liu, Z., Zhou, T., Ziegler, A.C., Dimitrion, P., Zuo, L., 2017. Oxidative Stress in Neurodegenerative Diseases: From Molecular Mechanisms to Clinical Applications. Oxid. Med. Cell. Longev. 2017, 1–11. https://doi.org/10.1155/2017/2525967

Livak, K.J., Schmittgen, T.D., 2001. Analysis of Relative Gene Expression Data Using Real-Time Quantitative PCR and the 2−ΔΔCT Method. Methods 25, 402–408. https://doi.org/10.1006/meth.2001.1262

Livnat-Levanon, N., Kevei, É., Kleifeld, O., Krutauz, D., Segref, A., Rinaldi, T., Erpapazoglou, Z., Cohen, M., Reis, N., Hoppe, T., Glickman, M.H., 2014. Reversible 26S Proteasome Disassembly upon Mitochondrial Stress. Cell Rep. 7, 1371–1380. https://doi.org/10.1016/j.celrep.2014.04.030

Livneh, I., Cohen-Kaplan, V., Cohen-Rosenzweig, C., Avni, N., Ciechanover, A., 2016. The life cycle of the 26S proteasome: from birth, through regulation and function, and onto its death. Cell Res. 26, 869–885. https://doi.org/10.1038/cr.2016.86

Ljubuncic, P., Gochman, E., Reznick, A.Z., 2010. Nitrosative Stress in Aging – Its Importance and Biological Implications in NF-κB Signaling, in: Aging and Age-Related Disorders. Humana Press, Totowa, NJ, pp. 27–54. https://doi.org/10.1007/978-1-60761-602-3_2

Lo Furno, D., Mannino, G., Giuffrida, R., Gili, E., Vancheri, C., Tarico, M.S., Perrotta, R.E., Pellitteri, R., 2018. Neural differentiation of human adipose-derived mesenchymal stem cells induced by glial cell conditioned media. J. Cell. Physiol. 233, 7091–7100. https://doi.org/10.1002/jcp.26632

Loeb, V., Yakunin, E., Saada, A., Sharon, R., 2010. The Transgenic Overexpression of α-Synuclein and Not Its Related Pathology Associates with Complex I Inhibition. J. Biol. Chem. 285, 7334–7343. https://doi.org/10.1074/jbc.M109.061051

Loos, B., Klionsky, D.J., Wong, E., 2017. Augmenting brain metabolism to increase macro- and chaperone-mediated autophagy for decreasing neuronal proteotoxicity and aging. Prog. Neurobiol. 156, 90–106. https://doi.org/10.1016/j.pneurobio.2017.05.001

Lopes, F.M., da Motta, L.L., De Bastiani, M.A., Pfaffenseller, B., Aguiar, B.W., de Souza, L.F., Zanatta, G., Vargas, D.M., Schönhofen, P., Londero, G.F., de Medeiros, L.M., Freire, V.N., Dafre, A.L., Castro, M.A.A.,

Parsons, R.B., Klamt, F., 2017. RA Differentiation Enhances Dopaminergic Features, Changes Redox Parameters, and Increases Dopamine Transporter Dependency in 6-Hydroxydopamine-Induced Neurotoxicity in SH-SY5Y Cells. Neurotox. Res. 31, 545–559. https://doi.org/10.1007/s12640-016-9699-0

Lopes, F.M., Schröder, R., Júnior, M.L.C. da F., Zanotto-Filho, A., Müller, C.B., Pires, A.S., Meurer, R.T., Colpo, G.D., Gelain, D.P., Kapczinski, F., Moreira, J.C.F., Fernandes, M. da C., Klamt, F., 2010. Comparison between proliferative and neuron-like SH-SY5Y cells as an in vitro model for Parkinson disease studies. Brain Res. 1337, 85–94. https://doi.org/10.1016/j.brainres.2010.03.102

Lopiano, L., Fasano, M., Giraudo, S., Digilio, G., Koenig, S.H., Torre, E., Bergamasco, B., Aime, S., 2000. Nuclear magnetic relaxation dispersion profiles of substantia nigra pars compacta in Parkinson's disease patients are consistent with protein aggregation. Neurochem.Int. 37, 331–336.

Lores-Arnaiz, S., Lombardi, P., Karadayian, A.G., Orgambide, F., Cicerchia, D., Bustamante, J., 2016. Brain cortex mitochondrial bioenergetics in synaptosomes and non-synaptic mitochondria during aging. Neurochem. Res. 41, 353–363. https://doi.org/10.1007/s11064-015-1817-5

Lou, G., Palikaras, K., Lautrup, S., Scheibye-Knudsen, M., Tavernarakis, N., Fang, E.F., 2020. Mitophagy and Neuroprotection. Trends Mol. Med. 26, 8–20. https://doi.org/10.1016/j.molmed.2019.07.002

Lovatt, D., Sonnewald, U., Waagepetersen, H.S., Schousboe, A., He, W., Lin, J.H.-C., Han, X., Takano, T., Wang, S., Sim, F.J., Goldman, S.A., Nedergaard, M., 2007. The Transcriptome and Metabolic Gene Signature of Protoplasmic Astrocytes in the Adult Murine Cortex. J. Neurosci. 27, 12255–12266. https://doi.org/10.1523/JNEUROSCI.3404-07.2007

Lu, S.C., 2013. Glutathione synthesis. Biochim. Biophys. Acta 1830, 3143–53. https://doi.org/10.1016/j.bbagen.2012.09.008

Lubbe, S., Morris, H.R., 2014. Recent advances in Parkinson's disease genetics. J. Neurol. 261, 259–266. https://doi.org/10.1007/s00415-013-7003-2

Lubińska, L., 1982. Patterns of Wallerian degeneration of myelinated fibres in short and long peripheral stumps and in isolated segments of rat phrenic nerve. Interpretation of the role of axoplasmic flow of the trophic factor. Brain Res. 233, 227–240. https://doi.org/10.1016/0006-8993(82)91199-4

Lubińska, L., 1977. Early course of wallerian degeneration in myelinated fibres of the rat phrenic nerve. Brain Res. 130, 47–63. https://doi.org/10.1016/0006-8993(77)90841-1

Lucius, R., Sievers, J., 1996. Postnatal retinal ganglion cells in vitro: protection against reactive oxygen species (ROS)-induced axonal degeneration by cocultured astrocytes. Brain Res. 743, 56–62. https://doi.org/10.1016/S0006-8993(96)01029-3

Ludtmann, M.H.R., Abramov, A.Y., 2016. Protein Misfolding and Aggregation: Implications for Mitochondrial

Dysfunction and Neurodegeneration, in: Mitochondrial Dysfunction in Neurodegenerative Disorders. Springer International Publishing, Cham, pp. 241–253. https://doi.org/10.1007/978-3-319-28637-2_10

Ludtmann, M.H.R., Angelova, P.R., Horrocks, M.H., Choi, M.L., Rodrigues, M., Baev, A.Y., Berezhnov, A. V., Yao, Z., Little, D., Banushi, B., Al-Menhali, A.S., Ranasinghe, R.T., Whiten, D.R., Yapom, R., Dolt, K.S., Devine, M.J., Gissen, P., Kunath, T., Jaganjac, M., Pavlov, E. V., Klenerman, D., Abramov, A.Y., Gandhi, S., 2018. α-synuclein oligomers interact with ATP synthase and open the permeability transition pore in Parkinson's disease. Nat. Commun. 9, 2293. https://doi.org/10.1038/s41467-018-04422-2

Luk, K.C., 2019. Oxidative stress and α-synuclein conspire in vulnerable neurons to promote Parkinson's disease progression. J. Clin. Invest. https://doi.org/10.1172/JCI130351

Luo, L., Guo, K., Fan, W., Lu, Y., Chen, L., Wang, Y., Shao, Y., Wu, G., Xu, J., Lü, L., 2017. Niche astrocytes promote the survival, proliferation and neuronal differentiation of co-transplanted neural stem cells following ischemic stroke in rats. Exp. Ther. Med. 13, 645–650. https://doi.org/10.3892/etm.2016.4016

Luth, E.S., Stavrovskaya, I.G., Bartels, T., Kristal, B.S., Selkoe, D.J., 2014. Soluble, Prefibrillar α-Synuclein Oligomers Promote Complex I-dependent, Ca 2+ -induced Mitochondrial Dysfunction. J. Biol. Chem. 289, 21490–21507. https://doi.org/10.1074/jbc.M113.545749

Macedo, M.G., Anar, B., Bronner, I.F., Cannella, M., Squitieri, F., Bonifati, V., Hoogeveen, A., Heutink, P., Rizzu, P., 2003. The DJ-1L166P mutant protein associated with early onset Parkinson's disease is unstable and forms higher-order protein complexes. Hum. Mol. Genet. 12, 2807–2816. https://doi.org/10.1093/hmg/ddg304

Maher, P., 2018. Potentiation of glutathione loss and nerve cell death by the transition metals iron and copper: Implications for age-related neurodegenerative diseases. Free Radic. Biol. Med. 115, 92–104. https://doi.org/10.1016/j.freeradbiomed.2017.11.015

Maiese, K., Li, F., Chong, Z.Z., Shang, Y.C., 2008. The Wnt signaling pathway: Aging gracefully as a protectionist? Pharmacol. Ther. 118, 58–81. https://doi.org/10.1016/j.pharmthera.2008.01.004

Maisonpierre, P., Belluscio, L., Squinto, S., Ip, N., Furth, M., Lindsay, R., Yancopoulos, G., 1990. Neurotrophin-3: a neurotrophic factor related to NGF and BDNF. Science (80-.). 247, 1446–1451. https://doi.org/10.1126/science.2321006

Makar, T.K., Nedergaard, M., Preuss, A., Gelbard, A.S., Perumal, A.S., Cooper, A.J.L., 2008. Vitamin E, Ascorbate, Glutathione, Glutathicne Disulfide, and Enzymes of Glutathione Metabolism in Cultures of Chick Astrocytes and Neurons: Evidence that Astrocytes Play an Important Role in Antioxidative Processes in the Brain. J. Neurochem. 62, 45–53. https://doi.org/10.1046/j.1471-4159.1994.62010045.x

Malone, P.E., Hernandez, M.R., 2007. 4-Hydroxynonenal, a product of oxidative stress, leads to an antioxidant response in optic nerve head astrocytes. Exp. Eye Res. 84, 444–454.

https://doi.org/10.1016/j.exer.2006.10.020

Manevich, Y., Shuvaeva, T., Dodia, C., Kazi, A., Feinstein, S.I., Fisher, A.B., 2009. Binding of peroxiredoxin 6 to substrate determines differential phospholipid hydroperoxide peroxidase and phospholipase A2 activities. Arch. Biochem. Biophys. 485, 139–149. https://doi.org/10.1016/j.abb.2009.02.008

Maniati, M.S., Maniati, M., Yousefi, T., Ahmadi-Ahangar, A., Tehrani, S.S., 2019. New insights into the role of microRNAs and long noncoding RNAs in most common neurodegenerative diseases. J. Cell. Biochem. 120, 8908–8918. https://doi.org/10.1002/jcb.28361

Manning-Bog, A.B., McCormack, A.L., Li, J., Uversky, V.N., Fink, A.L., Di Monte, D.A., 2002. The herbicide paraquat causes up-regulation and aggregation of α-synuclein in mice: Paraquat and α-synuclein. J. Biol. Chem. 277, 1641–1644. https://doi.org/10.1074/jbc.C100560200

Manocha, G.D., Floden, A.M., Puig, K.L., Nagamoto-Combs, K., Scherzer, C.R., Combs, C.K., 2017. Defining the contribution of neuroinflammation to Parkinson's disease in humanized immune system mice. Mol. Neurodegener. 12, 17. https://doi.org/10.1186/s13024-017-0158-z

Manzerra, P., Rush, S.J., Brown, I.R., 1997. Tissue-specific differences in heat shock protein hsc70 and hsp70 in the control and hyperthermic rabbit. J. Cell. Physiol. 170, 130–137. https://doi.org/10.1002/(SICI)1097-4652(199702)170:2<130::AID-JCP4>3.0.CO;2-P

Manzoni, C., 2017. The LRRK2–macroautophagy axis and its relevance to Parkinson's disease. Biochem. Soc. Trans. 45, 155–162. https://doi.org/10.1042/BST20160265

Maragakis, N.J., Rothstein, J.D., 2006. Mechanisms of Disease: astrocytes in neurodegenerative disease. Nat. Clin. Pract. Neurol. 2, 679–689. https://doi.org/10.1038/ncpneuro0355

Marchetti, B., L'Episcopo, F., Morale, M.C., Tirolo, C., Testa, N., Caniglia, S., Serapide, M.F., Pluchino, S., 2013. Uncovering novel actors in astrocyte-neuron crosstalk in Parkinson's disease: The Wnt/β-catenin signaling cascade as the common final pathway for neuroprotection and self-repair. Eur. J. Neurosci. 37, 1550–1563. https://doi.org/10.1111/ejn.12166

Marchetti, B., L'Episcopo, F., Tirolo, C., Testa, N., Caniglia, S., Morale, M.C., 2011. Vulnerability to Parkinson's Disease: Towards an Unifying Theory of Disease Etiology, in: Encyclopedia of Environmental Health. pp. 690–704. https://doi.org/http://dx.doi.org/10.1016/B978-0-444-52272-6.00079-9

Marí, M., Morales, A., Colell, A., García-Ruiz, C., Kaplowitz, N., Fernández-Checa, J.C., 2013. Mitochondrial glutathione: Features, regulation and role in disease. Biochim. Biophys. Acta - Gen. Subj. 1830, 3317–3328. https://doi.org/10.1016/j.bbagen.2012.10.018

Martinez-Ruiz, A., Villanueva, L., de Orduna, C.G., Lopez-Ferrer, D., Higueras, M.A., Tarin, C., Rodriguez-Crespo, I., Vazquez, J., Lamas, S., 2005. S-nitrosylation of Hsp90 promotes the inhibition of its ATPase and endothelial nitric oxide synthase regulatory activities. Proc. Natl. Acad. Sci. 102, 8525–8530.

https://doi.org/10.1073/pnas.0407294102

Martinez-Vicente, M., Cuervo, A.M., 2007. Autophagy and neurodegeneration: when the cleaning crew goes on strike. Lancet Neurol. 6, 352–361. https://doi.org/10.1016/S1474-4422(07)70076-5

Mayer, A.N., Wilkinson, K.D., 1989. Detection, resolution, and nomenclature of multiple ubiquitin carboxyl-terminal esterases from bovine calf thymus. Biochemistry 28, 166–172. https://doi.org/10.1021/bi00427a024

McBean, G., 2017. Cysteine, Glutathione, and Thiol Redox Balance in Astrocytes. Antioxidants 6, 62. https://doi.org/10.3390/antiox6030062

McGann, J.C., Mandel, G., 2018. Neuronal activity induces glutathione metabolism gene expression in astrocytes. Glia 66, 2024–2039. https://doi.org/10.1002/glia.23455

McLennan, H.R., Degli Esposti, M., 2000. The contribution of mitochondrial respiratory complexes to the production of reactive oxygen species. J. Bioenerg. Biomembr. 32, 153–62. https://doi.org/10.1023/A:1005507913372

McNaught, K.S.., Jenner, P., 2001. Proteasomal function is impaired in substantia nigra in Parkinson's disease. Neurosci. Lett. 297, 191–194. https://doi.org/10.1016/S0304-3940(00)01701-8

McNaught, K.S.P., Belizaire, R., Isacson, O., Jenner, P., Olanow, C.W., 2003. Altered proteasomal function in sporadic Parkinson's disease. Exp. Neurol. 179, 38–46. https://doi.org/10.1006/exnr.2002.8050

Mcnaught, K.S.P., Olanow, C.W., Halliwell, B., Isacson, O., Jenner, P., 2001. Failure of the ubiquitin–proteasome system in Parkinson's disease. Nat. Rev. Neurosci. 2, 589– 594.

Mehlen, P., Kretz-Remy, C., Préville, X., Arrigo, A.P., 1996. Human hsp27, Drosophila hsp27 and human alphaB-crystallin expression-mediated increase in glutathione is essential for the protective activity of these proteins against TNFalpha-induced cell death. EMBO J. 15, 2695–706.

Mele, L., Paino, F., Papaccio, F., Regad, T., Boocock, D., Stiuso, P., Lombardi, A., Liccardo, D., Aquino, G., Barbieri, A., Arra, C., Coveney, C., La Noce, M., Papaccio, G., Caraglia, M., Tirino, V., Desiderio, V., 2018. A new inhibitor of glucose-6-phosphate dehydrogenase blocks pentose phosphate pathway and suppresses malignant proliferation and metastasis in vivo. Cell Death Dis. 9, 572. https://doi.org/10.1038/s41419-018-0635-5

Mena, M. a, García de Yébenes, J., 2008. Glial cells as players in parkinsonism: the "good," the "bad," and the "mysterious" glia. Neuroscientist 14, 544–560. https://doi.org/10.1177/1073858408322839

Meredith, G.E., Totterdell, S., Potashkin, J.A., Surmeier, D.J., 2008. Modeling PD pathogenesis in mice: Advantages of a chronic MPTP protocol. Parkinsonism Relat. Disord. 14, S112–S115. https://doi.org/10.1016/j.parkreldis.2008.04.012

Merlini, G., Bellotti, V., 2003. Molecular Mechanisms of Amyloidosis. N. Engl. J. Med. 349, 583–596. https://doi.org/10.1056/NEJMra023144

Mey, J., Mccaffery, P., 2004. Retinoic Acid Signaling in the Nervous System of Adult Vertebrates. Neurosci. 10, 409–421. https://doi.org/10.1177/1073858404263520

Miki, Y., Shimoyama, S., Kon, T., Ueno, T., Hayakari, R., Tanji, K., Matsumiya, T., Tsushima, E., Mori, F., Wakabayashi, K., Tomiyama, M., 2018. Alteration of autophagy-related proteins in peripheral blood mononuclear cells of patients with Parkinson's disease. Neurobiol. Aging 63, 33–43. https://doi.org/10.1016/j.neurobiolaging.2017.11.006

Miklossy, J., Doudet, D.D., Schwab, C., Yu, S., McGeer, E.G., McGeer, P.L., 2006. Role of ICAM-1 in persisting inflammation in Parkinson disease and MPTP monkeys. Exp. Neurol. 197, 275–283. https://doi.org/10.1016/j.expneurol.2005.10.034

Miller, C.G., Holmgren, A., Arnér, E.S.J., Schmidt, E.E., 2018. NADPH-dependent and -independent disulfide reductase systems. Free Radic. Biol. Med. 127, 248–261. https://doi.org/10.1016/j.freeradbiomed.2018.03.051

Miller, D.W., Ahmad, R., Hague, S., Baptista, M.J., Canet-Aviles, R., McLendon, C., Carter, D.M., Zhu, P.P., Stadler, J., Chandran, J., Klinefelter, G.R., Blackstone, C., Cookson, M.R., 2003. L166P mutant DJ-1, causative for recessive Parkinson's disease, is degraded through the ubiquitin-proteasome system. J. Biol. Chem. 278, 36588–36595. https://doi.org/10.1074/jbc.M304272200

Mitsumoto, A., Nakagawa, Y., 2001. DJ-1 is an indicator for endogenous reactive oxygen species elicited by endotoxin. Free Radic. Res. 35, 885–93. https://doi.org/10.1080/10715760100301381

Mitsumoto, A., Nakagawa, Y., Takeuchi, A., Okawa, K., Iwamatsu, A., Takanezawa, Y., 2001. Oxidized forms of peroxiredoxins and DJ-1 on two-dimensional gels increased in response to sublethal levels of paraquat. Free Radic. Res. 35, 301–10. https://doi.org/10.1080/10715760100300831

Miyake, Y., Fukushima, W., Tanaka, K., Sasaki, S., Kiyohara, C., Tsuboi, Y., Yamada, T., Oeda, T., Miki, T., Kawamura, N., Sakae, N., Fukuyama, H., Hirota, Y., Nagai, M., 2011. Dietary intake of antioxidant vitamins and risk of Parkinson's disease: a case-control study in Japan. Eur. J. Neurol. 18, 106–113. https://doi.org/10.1111/j.1468-1331.2010.03088.x

Mizushima, N., Levine, B., Cuervo, A.M., Klionsky, D.J., 2008. Autophagy fights disease through cellular self-digestion. Nature 451, 1069–1075. https://doi.org/10.1038/nature06639

Mocchegiani, E., Costarelli, L., Giacconi, R., Malavolta, M., Basso, A., Piacenza, F., Ostan, R., Cevenini, E., Gonos, E.S., Franceschi, C., Monti, D., 2014. Vitamin E–gene interactions in aging and inflammatory age-related diseases: Implications for treatment. A systematic review. Ageing Res. Rev. 14, 81–101. https://doi.org/10.1016/j.arr.2014.01.001

Moeton, M., Stassen, O.M.J.A., Sluijs, J.A., van der Meer, V.W.N., Kluivers, L.J., van Hoorn, H., Schmidt, T., Reits, E.A.J., van Strien, M.E., Hol, E.M., 2016. GFAP isoforms control intermediate filament network dynamics, cell morphology, and focal adhesions. Cell. Mol. Life Sci. 73, 4101–4120. https://doi.org/10.1007/s00018-016-2239-5

Møller, I.M., Rogowska-Wrzesinska, A., Rao, R.S.P., 2011. Protein carbonylation and metal-catalyzed protein oxidation in a cellular perspective. J. Proteomics 74, 2228–2242. https://doi.org/10.1016/j.jprot.2011.05.004

Moncada, S., Bolanos, J.P., 2006. Nitric oxide, cell bioenergetics and neurodegeneration. J. Neurochem. 97, 1676–1689. https://doi.org/10.1111/j.1471-4159.2006.03988.x

Montagna, C., Cirotti, C., Rizza, S., Filomeni, G., 2020. When S -Nitrosylation Gets to Mitochondria: From Signaling to Age-Related Diseases. Antioxid. Redox Signal. ars.2019.7872. https://doi.org/10.1089/ars.2019.7872

Moore, N.H., Costa, L.G., Shaffer, S.A., Goodlett, D.R., Guizzetti, M., 2009. Shotgun proteomics implicates extracellular matrix proteins and protease systems in neuronal development induced by astrocyte cholinergic stimulation. J. Neurochem. 108, 891–908. https://doi.org/10.1111/j.1471-4159.2008.05836.x

Morçimen, Z.G., Taşdemir, Ş., Erdem, Ç., Güneş, F., Şendemir, A., 2019. Investıgatıon of the Adherence and Prolıferatıon Characterıstıcs of SH-SY5Y Neuron Model Cells on Graphene Foam Surfaces. Mater. Today Proc. 19, 40–46. https://doi.org/10.1016/j.matpr.2019.07.654

Moretti, M., Fraga, D.B., Rodrigues, A.L.S., 2017. Preventive and therapeutic potential of ascorbic acid in neurodegenerative diseases. CNS Neurosci. Ther. 23, 921–929. https://doi.org/10.1111/cns.12767

Morimoto, R.I., 2002. Dynamic remodeling of transcription complexes by molecular chaperones. Cell 110, 281–4. https://doi.org/10.1016/s0092-8674(02)00860-7

Moriyama, M., Kurebayashi, R., Kawabe, K., Takano, K., Nakamura, Y., 2016. Acetate Attenuates Lipopolysaccharide-Induced Nitric Oxide Production Through an Anti-Oxidative Mechanism in Cultured Primary Rat Astrocytes. Neurochem. Res. 41, 3138–3146. https://doi.org/10.1007/s11064-016-2038-2

Mostafavi-Pour, Z., Ramezani, F., Keshavarzi, F., Samadi, N., 2017. The role of quercetin and vitamin C in Nrf2-dependent oxidative stress production in breast cancer cells. Oncol. Lett. 13, 1965–1973. https://doi.org/10.3892/ol.2017.5619

Mothersill, C., Seymour, C.B., O'Brien, A., 2007. Induction of c-myc oncoprotein and of cellular proliferation by radiation in normal human urothelial cultures. Anticancer Res. 11, 1609–12. https://doi.org/10.1002/jor.20475

Motohashi, H., Yamamoto, M., 2004. Nrf2–Keap1 defines a physiologically important stress response

mechanism. Trends Mol. Med. 10, 549–557. https://doi.org/10.1016/j.molmed.2004.09.003

Müftüoglu, M., Elibol, B., Dalmizrak, Ö., Ercan, A., Kulaksiz, G., Ögüs, H., Dalkara, T., Özer, N., 2004. Mitochondrial complex I and IV activities in leukocytes from patients with parkin mutations. Mov. Disord. 19, 544–548. https://doi.org/10.1002/mds.10695

Murphy-Royal, C., Dupuis, J., Groc, L., Oliet, S.H.R., 2017. Astroglial glutamate transporters in the brain: Regulating neurotransmitter homeostasis and synaptic transmission. J. Neurosci. Res. 95, 2140–2151. https://doi.org/10.1002/jnr.24029

Murray, J., Taylor, S.W., Zhang, B., Ghosh, S.S., Capaldi, R.A., 2003. Oxidative Damage to Mitochondrial Complex I Due to Peroxynitrite. J. Biol. Chem. 278, 37223–37230. https://doi.org/10.1074/jbc.M305694200

Nagakubo, D., Taira, T., Kitaura, H., Ikeda, M., Tamai, K., Iguchi-Ariga, S.M., Ariga, H., 1997. DJ-1, a novel oncogene which transforms mouse NIH3T3 cells in cooperation with ras. Biochem. Biophys. Res. Commun. 231, 509–513. https://doi.org/10.1006/bbrc.1997.6132

Nakamura, H., Nakamura, K., Yodoi, J., 1997. REDOX REGULATION OF CELLULAR ACTIVATION. Annu. Rev. Immunol. 15, 351–369. https://doi.org/10.1146/annurev.immunol.15.1.351

Nakamura, T., Lipton, S.A., 2017. Aberrant Nitric Oxide Signaling Contributes to Protein Misfolding in Neurodegenerative Diseases via S-Nitrosylation and Tyrosine Nitration, in: Nitric Oxide. Elsevier, pp. 373–384. https://doi.org/10.1016/B978-0-12-804273-1.00027-2

Nakamura, T., Lipton, S.A., 2016. Protein S -Nitrosylation as a Therapeutic Target for Neurodegenerative Diseases. Trends Pharmacol. Sci. 37, 73–84. https://doi.org/10.1016/j.tips.2015.10.002

Nakamura, T., Tu, S., Akhtar, M.W., Sunico, C.R., Okamoto, S., Lipton, S.A., 2013. Aberrant Protein S-Nitrosylation in Neurodegenerative Diseases. Neuron 78, 596–614. https://doi.org/10.1016/j.neuron.2013.05.005

Nakata, T., Terada, S., Hirokawa, N., 1998. Visualization of the Dynamics of Synaptic Vesicle and Plasma Membrane Proteins in Living Axons. J. Cell Biol. 140, 659–674. https://doi.org/10.1083/jcb.140.3.659

Naoi, M., Maruyama, W., Yi, H., Inaba, K., Akao, Y., Shamoto-Nagai, M., 2009. Mitochondria in neurodegenerative disorders: Regulation of the redox state and death signaling leading to neuronal death and survival. J. Neural Transm. 116, 1371–1381. https://doi.org/10.1007/s00702-009-0309-7

Narendra, D., Tanaka, A., Suen, D.F., Youle, R.J., 2008. Parkin is recruited selectively to impaired mitochondria and promotes their autophagy. J. Cell Biol. 183, 795–803. https://doi.org/10.1083/jcb.200809125

Näsström, T., Fagerqvist, T., Barbu, M., Karlsson, M., Nikolajeff, F., Kasrayan, A., Ekberg, M., Lannfelt, L., Ingelsson, M., Bergström, J., 2011. The lipid peroxidation products 4-oxo-2-nonenal and 4-hydroxy-2-nonenal promote the formation of α-synuclein oligomers with distinct biochemical, morphological, and

functional properties. Free Radic. Biol. Med. 50, 428–437. https://doi.org/10.1016/j.freeradbiomed.2010.11.027

Navarro, A., Boveris, A., 2004. Rat brain and liver mitochondria develop oxidative stress and lose enzymatic activities on aging. Am. J. Physiol. Integr. Comp. Physiol. 287, R1244–R1249. https://doi.org/10.1152/ajpregu.00226.2004

Nedić, O., Rattan, S.I.S., Grune, T., Trougakos, I.P., 2013. Molecular effects of advanced glycation end products on cell signalling pathways, ageing and pathophysiology. Free Radic. Res. 47, 28–38. https://doi.org/10.3109/10715762.2013.806798

Neely, M.D., Sidell, K.R., Graham, D.G., Montine, T.J., 2002. The Lipid Peroxidation Product 4-Hydroxynonenal Inhibits Neurite Outgrowth, Disrupts Neuronal Microtubules, and Modifies Cellular Tubulin. J. Neurochem. 72, 2323–2333. https://doi.org/10.1046/j.1471-4159.1999.0722323.x

Nesti, C., Pardini, C., Barachini, S., D'Alessandro, D., Siciliano, G., Murri, L., Petrini, M., Vaglini, F., 2011. Human dental pulp stem cells protect mouse dopaminergic neurons against MPP+ or rotenone. Brain Res. 1367, 94–102. https://doi.org/10.1016/j.brainres.2010.09.042

Neukomm, L.J., Freeman, M.R., 2014. Diverse cellular and molecular modes of axon degeneration. Trends Cell Biol. 24, 515–523. https://doi.org/10.1016/j.tcb.2014.04.003

Neumann, M., Müller, V., Görner, K., Kretzschmar, H.A., Haass, C., Kahle, P.J., 2004. Pathological properties of the Parkinson's disease-associated protein DJ-1 in alpha-synucleinopathies and tauopathies: relevance for multiple system atrophy and Pick's disease. Acta Neuropathol. 107, 489–96. https://doi.org/10.1007/s00401-004-0834-2

Neviackas, J.A., Kerstein, M.D., 1976. Pancreatic enzyme response with an elemental diet. Surg. Gynecol. Obstet. 142, 71–4.

Newhouse, K., Hsuan, S.L., Chang, S.H., Cai, B., Wang, Y., Xia, Z., 2004. Rotenone-induced apoptosis is mediated by p38 and JNK MAP kinases in human dopaminergic SH-SY5Y cells. Toxicol. Sci. 79, 137–146. https://doi.org/10.1093/toxsci/kfh089

Nguyen, T., Nioi, P., Pickett, C.B., 2009. The Nrf2-Antioxidant Response Element Signaling Pathway and Its Activation by Oxidative Stress. J. Biol. Chem. 284, 13291–13295. https://doi.org/10.1074/jbc.R900010200

Nguyen, T., Sherratt, P.J., Nioi, P., Yang, C.S., Pickett, C.B., 2005. Nrf2 Controls Constitutive and Inducible Expression of ARE-driven Genes through a Dynamic Pathway Involving Nucleocytoplasmic Shuttling by Keap1. J. Biol. Chem. 280, 32485–32492. https://doi.org/10.1074/jbc.M503074200

Ni, H.-M., Williams, J.A., Ding, W.-X., 2015. Mitochondrial dynamics and mitochondrial quality control. Redox Biol. 4, 6–13. https://doi.org/10.1016/j.redox.2014.11.006

Nieoullon, A., 2011. Neurodegenerative diseases and neuroprotection: current views and prospects. J. Appl. Biomed. 9, 173–183. https://doi.org/10.2478/v10136-011-0013-4

Niki, E., 2014. Role of vitamin E as a lipid-soluble peroxyl radical scavenger: in vitro and in vivo evidence. Free Radic. Biol. Med. 66, 3–12. https://doi.org/10.1016/j.freeradbiomed.2013.03.022

Niki, E., 1990. Free radical initiators as source of water- or lipid-soluble peroxyl radicals. Methods Enzymol. 186, 100–108. https://doi.org/10.1016/0076-6879(90)86095-D

Nishiguchi, M., Tokugawa, K., Yamamoto, K., Akama, T., Nozawa, Y., Chaki, S., Ueki, T., Kameo, K., Okuyama, S., 2003. Increase in secretion of glial cell line-derived neurotrophic factor from glial cell lines by inhibitors of vacuolar ATPase. Neurochem. Int. 42, 493–498. https://doi.org/10.1016/S0197-0186(02)00139-0

Nishikawa, K., Li, H., Kawamura, R., Osaka, H., Wang, Y.L., Hara, Y., Hirokawa, T., Manago, Y., Amano, T., Noda, M., Aoki, S., Wada, K., 2003. Alterations of structure and hydrolase activity of parkinsonism-associated human ubiquitin carboxyl-terminal hydrolase L1 variants. Biochem. Biophys. Res. Commun. 304, 176–183. https://doi.org/10.1016/S0006-291X(03)00555-2

Nishikimi, M., 1975. Oxidation of ascorbic acid with superoxide anion generated by the xanthine-xanthine oxidase system. Biochem. Biophys. Res. Commun. 63, 463–468. https://doi.org/10.1016/0006-291X(75)90710-X

Nita, M., Grzybowski, A., 2016. The Role of the Reactive Oxygen Species and Oxidative Stress in the Pathomechanism of the Age-Related Ocular Diseases and Other Pathologies of the Anterior and Posterior Eye Segments in Adults. Oxid. Med. Cell. Longev. 2016, 1–23. https://doi.org/10.1155/2016/3164734

Nithianantharajah, J., 2004. Environmental enrichment results in cortical and subcortical changes in levels of synaptophysin and PSD-95 proteins. Neurobiol. Learn. Mem. 81, 200–210. https://doi.org/10.1016/j.nlm.2004.02.002

Niture, S.K., Jain, A.K., Shelton, P.M., Jaiswal, A.K., 2011. Src Subfamily Kinases Regulate Nuclear Export and Degradation of Transcription Factor Nrf2 to Switch Off Nrf2-mediated Antioxidant Activation of Cytoprotective Gene Expression. J. Biol. Chem. 286, 28821–28832. https://doi.org/10.1074/jbc.M111.255042

Niture, S.K., Khatri, R., Jaiswal, A.K., 2014. Regulation of Nrf2—an update. Free Radic. Biol. Med. 66, 36–44. https://doi.org/10.1016/j.freeradbiomed.2013.02.008

Nollen, E.A.A., Brunsting, J.F., Roelofsen, H., Weber, L.A., Kampinga, H.H., 1999. In Vivo Chaperone Activity of Heat Shock Protein 70 and Thermotolerance. Mol. Cell. Biol. 19, 2069–2079. https://doi.org/10.1128/MCB.19.3.2069

Nowak, P., Szczerbak, G., Dabrowska, J., Bortel, A., Biedka, I., Kostrzewa, R.M., 2006. Molecular mechanisms of levodopa action in animal models of Parkinson's disease. Neurol. Neurochir. Pol. 40, 517–25.

Nuytemans, K., Theuns, J., Cruts, M., Van Broeckhoven, C., 2010. Genetic etiology of Parkinson disease associated with mutations in the SNCA, PARK2, PINK1, PARK7, and LRRK2 genes: a mutation update. Hum. Mutat. 31, 763–780. https://doi.org/10.1002/humu.21277

O'Malley, E.K., Sieber, B.-A., Black, I.B., Dreyfus, C.F., 1992. Mesencephalic type I astrocytes mediate the survival of substantia nigra dopaminergic neurons in culture. Brain Res. 582, 65–70. https://doi.org/10.1016/0006-8993(92)90317-3

Obashi, K., Okabe, S., 2013. Regulation of mitochondrial dynamics and distribution by synapse position and neuronal activity in the axon. Eur. J. Neurosci. 38, 2350–2363. https://doi.org/10.1111/ejn.12263

Oberley, T.D., Verwiebe, E., Zhong, W., Kang, S.W., Rhee, S.G., 2001. Localization of the thioredoxin system in normal rat kidney. Free Radic. Biol. Med. 30, 412–424. https://doi.org/10.1016/S0891-5849(00)00486-X

Obeso, J.A., Stamelou, M., Goetz, C.G., Poewe, W., Lang, A.E., Weintraub, D., Burn, D., Halliday, G.M., Bezard, E., Przedborski, S., Lehericy, S., Brooks, D.J., Rothwell, J.C., Hallett, M., DeLong, M.R., Marras, C., Tanner, C.M., Ross, G.W., Langston, J.W., Klein, C., Bonifati, V., Jankovic, J., Lozano, A.M., Deuschl, G., Bergman, H., Tolosa, E., Rodriguez-Violante, M., Fahn, S., Postuma, R.B., Berg, D., Marek, K., Standaert, D.G., Surmeier, D.J., Olanow, C.W., Kordower, J.H., Calabresi, P., Schapira, A.H.V., Stoessl, A.J., 2017. Past, present, and future of Parkinson's disease: A special essay on the 200th Anniversary of the Shaking Palsy. Mov. Disord. 32, 1264–1310. https://doi.org/10.1002/mds.27115

Oettinghaus, B., Schulz, J.M., Restelli, L.M., Licci, M., Savoia, C., Schmidt, A., Schmitt, K., Grimm, A., Morè, L., Hench, J., Tolnay, M., Eckert, A., D'Adamo, P., Franken, P., Ishihara, N., Mihara, K., Bischofberger, J., Scorrano, L., Frank, S., 2016. Synaptic dysfunction, memory deficits and hippocampal atrophy due to ablation of mitochondrial fission in adult forebrain neurons. Cell Death Differ. 23, 18–28. https://doi.org/10.1038/cdd.2015.39

Ohashi, M., Hirano, T., Watanabe, K., Shoji, H., Ohashi, N., Baba, H., Endo, N., Kohno, T., 2016. Hydrogen peroxide modulates neuronal excitability and membrane properties in ventral horn neurons of the rat spinal cord. Neuroscience 331, 206–220. https://doi.org/10.1016/j.neuroscience.2016.06.033

Ohgaki, H., Kleihues, P., 2005. Population-Based Studies on Incidence, Survival Rates, and Genetic Alterations in Astrocytic and Oligodendroglial Gliomas. J. Neuropathol. Exp. Neurol. 64, 479–489. https://doi.org/10.1093/jnen/64.6.479

Ohtsuji, M., Katsuoka, F., Kobayashi, A., Aburatani, H., Hayes, J.D., Yamamoto, M., 2008. Nrf1 and Nrf2 Play Distinct Roles in Activation of Antioxidant Response Element-dependent Genes. J. Biol. Chem. 283, 33554–33562. https://doi.org/10.1074/jbc.M804597200

Oláh, S., Füle, M., Komlósi, G., Varga, C., Báldi, R., Barzó, P., Tamás, G., 2009. Regulation of cortical microcircuits by unitary GABA-mediated volume transmission. Nature 461, 1278–1281. https://doi.org/10.1038/nature08503

Oliveros, J.C., 2007. Venny. An interactive tool for comparing lists with Venn Diagrams [WWW Document]. BioinfoGP of CNB-CSIC.

Olshina, M.A., Ben-Nissan, G., Sharon, M., 2018. Functional regulation of proteins by 20S proteasome proteolytic processing. Cell Cycle 17, 393–394. https://doi.org/10.1080/15384101.2017.1414682

Olson, S.D., Kambal, A., Pollock, K., Mitchell, G.-M., Stewart, H., Kalomoiris, S., Cary, W., Nacey, C., Pepper, K., Nolta, J.A., 2012. Examination of mesenchymal stem cell-mediated RNAi transfer to Huntington's disease affected neuronal cells for reduction of huntingtin. Mol. Cell. Neurosci. 49, 271–281. https://doi.org/10.1016/j.mcn.2011.12.001

Onyango, I.G., Lu, J., Rodova, M., Lezi, E., Crafter, A.B., Swerdlow, R.H., 2010. Regulation of neuron mitochondrial biogenesis and relevance to brain health. Biochim. Biophys. Acta - Mol. Basis Dis. 1802, 228–234. https://doi.org/10.1016/j.bbadis.2009.07.014

Oshima, M., Seki, T., Kurauchi, Y., Hisatsune, A., Katsuki, H., 2019. Reciprocal Regulation of Chaperone-Mediated Autophagy/Microautophagy and Exosome Release. Biol. Pharm. Bull. 42, 1394–1401. https://doi.org/10.1248/bpb.b19-00316

Oswald, M.C.W., Garnham, N., Sweeney, S.T., Landgraf, M., 2018. Regulation of neuronal development and function by ROS. FEBS Lett. 592, 679–691. https://doi.org/10.1002/1873-3468.12972

Oudard, S., Arvelo, F., Miccoli, L., Apiou, F., Dutrillaux, A., Poisson, M., Dutrillaux, B., Poupon, M., 1996. High glycolysis in gliomas despite low hexokinase transcription and activity correlated to chromosome 10 loss. Br. J. Cancer 74, 839–845. https://doi.org/10.1038/bjc.1996.446

Outeiro, T.F., Klucken, J., Strathearn, K.E., Liu, F., Nguyen, P., Rochet, J.-C., Hyman, B.T., McLean, P.J., 2006. Small heat shock proteins protect against α-synuclein-induced toxicity and aggregation. Biochem. Biophys. Res. Commun. 351, 631–638. https://doi.org/10.1016/j.bbrc.2006.10.085

Öztürk, G., Cengiz, N., Erdoğan, E., Him, A., Oğuz, E.K., Yenidünya, E., Ayşit, N., 2013. Two distinct types of dying back axonal degeneration in vitro. Neuropathol. Appl. Neurobiol. 39, 362–376. https://doi.org/10.1111/j.1365-2990.2012.01295.x

Pacelli, C., De Rasmo, D., Signorile, A., Grattagliano, I., di Tullio, G., D'Orazio, A., Nico, B., Comi, G. Pietro, Ronchi, D., Ferranini, E., Pirolo, D., Seibel, P., Schubert, S., Gaballo, A., Villani, G., Cocco, T., 2011. Mitochondrial defect and PGC-1α dysfunction in parkin-associated familial Parkinson's disease. Biochim. Biophys. Acta - Mol. Basis Dis. 1812, 1041–1053. https://doi.org/10.1016/j.bbadis.2010.12.022

Padgett, C.M., Whorton, A.R., 1998. Cellular Responses to Nitric Oxide: Role of Protein S-Thiolation/Dethiolation. Arch. Biochem. Biophys. 358, 232–242. https://doi.org/10.1006/abbi.1998.0859

Påhlman, S., Hoehner, J.C., Nånberg, E., Hedborg, F., Fagerström, S., Gestblom, C., Johansson, I., Larsson, U., Lavenius, E., Örtoft, E., Söderholm, H., 1995. Differentiation and survival influences of growth factors in human neuroblastoma. Eur. J. Cancer 31, 453–458. https://doi.org/10.1016/0959-8049(95)00033-F

Påhlman, S., Ruusala, A.-I., Abrahamsson, L., Mattsson, M.E.K., Esscher, T., 1984. Retinoic acid-induced differentiation of cultured human neuroblastoma cells: a comparison with phorbolester-induced differentiation. Cell Differ. 14, 135–144. https://doi.org/10.1016/0045-6039(84)90038-1

Palacino, J.J., Sagi, D., Goldberg, M.S., Krauss, S., Motz, C., Wacker, M., Klose, J., Shen, J., 2004. Mitochondrial dysfunction and oxidative damage in parkin-deficient mice. J. Biol. Chem. 279, 18614–22. https://doi.org/10.1074/jbc.M401135200

Palozza, P., Krinsky, N.I., 1992. β-Carotene and α-tocopherol are synergistic antioxidants. Arch. Biochem. Biophys. 297, 184–187. https://doi.org/10.1016/0003-9861(92)90658-J

Pan, J., Kao, Y.-L., Joshi, S., Jeetendran, S., DiPette, D., Singh, U.S., 2005. Activation of Rac1 by phosphatidylinositol 3-kinase in vivo: role in activation of mitogen-activated protein kinase (MAPK) pathways and retinoic acid-induced neuronal differentiation of SH-SY5Y cells. J. Neurochem. 93, 571–583. https://doi.org/10.1111/j.1471-4159.2005.03106.x

Papadia, S., Soriano, F.X., Léveillé, F., Martel, M.-A., Dakin, K.A., Hansen, H.H., Kaindl, A., Sifringer, M., Fowler, J., Stefovska, V., Mckenzie, G., Craigon, M., Corriveau, R., Ghazal, P., Horsburgh, K., Yankner, B.A., Wyllie, D.J.A., Ikonomidou, C., Hardingham, G.E., 2008. Synaptic NMDA receptor activity boosts intrinsic antioxidant defenses. Nat. Neurosci. 11, 476–487. https://doi.org/10.1038/nn2071

Papi, A., Bartolini, G., Ammar, K., Guerra, F., Ferreri, A.M., Rocchi, P., Orlandi, M., 2007. Inhibitory effects of retinoic acid and IIF on growth, migration and invasiveness in the U87MG human glioblastoma cell line. Oncol. Rep. 18, 1015–21.

Pappert, E.J., Tangney, C.C., Goetz, C.G., Ling, Z.D., Lipton, J.W., Stebbins, G.T., Carvey, P.M., 1996. Alpha-tocopherol in the ventricular cerebrospinal fluid of Parkinson's disease patients: Dose-response study and correlations with plasma levels. Neurology 47, 1037–1042. https://doi.org/10.1212/WNL.47.4.1037

Paradies, G., Petrosillo, G., Paradies, V., Ruggiero, F.M., 2010. Oxidative stress, mitochondrial bioenergetics, and cardiolipin in aging. Free Radic. Biol. Med. 48, 1286–1295. https://doi.org/10.1016/j.freeradbiomed.2010.02.020

Park, J., Kerner, A., Burns, M.A., Lin, X.N., 2011. Microdroplet-Enabled Highly Parallel Co-Cultivation of Microbial Communities. PLoS One 6, e17019. https://doi.org/10.1371/journal.pone.0017019

Park, J., Lee, S.B., Lee, S.B., Kim, Y., Song, S., Kim, S., Bae, E., Kim, J.M., Shong, M.H., Kim, J.M., Chung, J.K., 2006. Mitochondrial dysfunction in Drosophila PINK1 mutants is complemented by parkin. Nature 441, 1157–1161. https://doi.org/10.1038/nature04788

Park, J., Seo, J., Won, J., Yeo, H.-G., Ahn, Y.-J., Kim, K., Jin, Y.B., Koo, B.-S., Lim, K.S., Jeong, K.-J., Kang, P., Lee, H.-Y., Baek, S.H., Jeon, C.-Y., Hong, J.-J., Huh, J.-W., Kim, Y.-H., Park, S.-J., Kim, S.-U., Lee, D.-S., Lee, S.-R., Lee, Y., 2019. Abnormal Mitochondria in a Non-human Primate Model of MPTP-induced Parkinson's Disease: Drp1 and CDK5/p25 Signaling. Exp. Neurobiol. 28, 414. https://doi.org/10.5607/en.2019.28.3.414

Park, M.H., Jo, M., Kim, Y.R., Lee, C.-K., Hong, J.T., 2016. Roles of peroxiredoxins in cancer, neurodegenerative diseases and inflammatory diseases. Pharmacol. Ther. 163, 1–23. https://doi.org/10.1016/j.pharmthera.2016.03.018

Park, S., Geddes, T.J., Javitch, J.A., Kuhn, D.M., 2003. Dopamine prevents nitration of tyrosine hydroxylase by peroxynitrite and nitrogen dioxide. Is nitrotyrosine formation an early step in dopamine neuronal damage? J. Biol. Chem. 278, 28736–28742. https://doi.org/10.1074/jbc.M304362200

Park, S.J., Lee, J.H., Kim, H.Y., Choi, Y.H., Park, J.S., Suh, Y.H., Park, S.M., Joe, E., Jou, I., 2012. Astrocytes, but not microglia, rapidly sense H_2O_2via STAT6 phosphorylation, resulting in cyclooxygenase-2 expression and prostaglandin release. J. Immunol. 188, 5132–41. https://doi.org/10.4049/jimmunol.1101600

Parkinson, J., 2002. An essay on the shaking palsy. 1817. J. Neuropsychiatry Clin. Neurosci. 14, 223–236; discussion 222. https://doi.org/10.1176/appi.neuropsych.14.2.223

Passmore, J.B., Pinho, S., Gomez-Lazaro, M., Schrader, M., 2017. The respiratory chain inhibitor rotenone affects peroxisomal dynamics via its microtubule-destabilising activity. Histochem. Cell Biol. 148, 331–341. https://doi.org/10.1007/s00418-017-1577-1

Patapoutian, A., Reichardt, L.F., 2000. Roles of Wnt proteins in neural development and maintenance. Curr. Opin. Neurobiol. 10, 392–399. https://doi.org/10.1016/S0959-4388(00)00100-8

Pathare, G.R., Nagy, I., Sledz, P., Anderson, D.J., Zhou, H.-J., Pardon, E., Steyaert, J., Forster, F., Bracher, A., Baumeister, W., 2014. Crystal structure of the proteasomal deubiquitylation module Rpn8-Rpn11. Proc. Natl. Acad. Sci. 111, 2984–2989. https://doi.org/10.1073/pnas.1400546111

Patra, R.., Swarup, D., Dwivedi, S.., 2001. Antioxidant effects of α tocopherol, ascorbic acid and l-methionine on lead induced oxidative stress to the liver, kidney and brain in rats. Toxicology 162, 81–88. https://doi.org/10.1016/S0300-483X(01)00345-6

Pavlovic, D., Markisic, M., Pavlovic, A., Lackovic, M., Bozic, M., 2014. Vitamin A and the nervous system. Arch. Biol. Sci. 66, 1585–1590. https://doi.org/10.2298/ABS1404585P

Pellerin, L., Magistretti, P.J., 1996. Excitatory Amino Acids Stimulate Aerobic Glycolysis in Astrocytes via an

Activation of the Na^+/K^+ ATPase. Dev. Neurosci. 18, 336–342. https://doi.org/10.1159/000111426

Peltzer, R.M., Kolli, H.B., Stocker, A., Cascella, M., 2018. Self-Assembly of α-Tocopherol Transfer Protein Nanoparticles: A Patchy Protein Model. J. Phys. Chem. B 122, 7066–7072. https://doi.org/10.1021/acs.jpcb.8b05936

Pendino, F., Flexor, M., Delhommeau, F., Buet, D., Lanotte, M., Segal-Bendirdjian, E., 2001. Retinoids down-regulate telomerase and telomere length in a pathway distinct from leukemia cell differentiation. Proc. Natl. Acad. Sci. 98, 6662–6667. https://doi.org/10.1073/pnas.111464998

Peng, K., Yang, L., Wang, J., Ye, F., Dan, G., Zhao, Y., Cai, Y., Cui, Z., Ao, L., Liu, J., Zou, Z., Sai, Y., Cao, J., 2017. The Interaction of Mitochondrial Biogenesis and Fission/Fusion Mediated by PGC-1α Regulates Rotenone-Induced Dopaminergic Neurotoxicity. Mol. Neurobiol. 54, 3783–3797. https://doi.org/10.1007/s12035-016-9944-9

Perea, G., Sur, M., Araque, A., 2014. Neuron-glia networks: integral gear of brain function. Front. Cell. Neurosci. 8, 378. https://doi.org/10.3389/fncel.2014.00378

Perez, V.I., Buffenstein, R., Masamsetti, V., Leonard, S., Salmon, A.B., Mele, J., Andziak, B., Yang, T., Edrey, Y., Friguet, B., Ward, W., Richardson, A., Chaudhuri, A., 2009. Protein stability and resistance to oxidative stress are determinants of longevity in the longest-living rodent, the naked mole-rat. Proc. Natl. Acad. Sci. 106, 3059–3064. https://doi.org/10.1073/pnas.0809620106

Perfeito, R., Ribeiro, M., Rego, A.C., 2017. Alpha-synuclein-induced oxidative stress correlates with altered superoxide dismutase and glutathione synthesis in human neuroblastoma SH-SY5Y cells. Arch. Toxicol. 91, 1245–1259. https://doi.org/10.1007/s00204-016-1788-6

Pernas, L., Scorrano, L., 2016. Mito-Morphosis: Mitochondrial Fusion, Fission, and Cristae Remodeling as Key Mediators of Cellular Function. Annu. Rev. Physiol. 78, 505–531. https://doi.org/10.1146/annurev-physiol-021115-105011

Perry, V.H., 2012. Innate Inflammation in Parkinson's Disease. Cold Spring Harb. Perspect. Med. 2, a009373–a009373. https://doi.org/10.1101/cshperspect.a009373

Persson, A.-K., Kim, I., Zhao, P., Estacion, M., Black, J.A., Waxman, S.G., 2013. Sodium Channels Contribute to Degeneration of Dorsal Root Ganglion Neurites Induced by Mitochondrial Dysfunction in an In Vitro Model of Axonal Injury. J. Neurosci. 33, 19250–19261. https://doi.org/10.1523/JNEUROSCI.2148-13.2013

Peth, A., Nathan, J.A., Goldberg, A.L., 2013. The ATP Costs and Time Required to Degrade Ubiquitinated Proteins by the 26 S Proteasome. J. Biol. Chem. 288, 29215–29222. https://doi.org/10.1074/jbc.M113.482570

Petit-Paitel, A., Brau, F., Cazareth, J., Chabry, J., 2009. Involvment of Cytosolic and Mitochondrial GSK-3β in

Mitochondrial Dysfunction and Neuronal Cell Death of MPTP/MPP+-Treated Neurons. PLoS One 4, e5491. https://doi.org/10.1371/journal.pone.0005491

Philips, T., Rothstein, J.D., 2017. Oligodendroglia: metabolic supporters of neurons. J. Clin. Invest. 127, 3271–3280. https://doi.org/10.1172/JCI90610

Pickart, C.M., Rose, I.A., 1985. Ubiquitin carboxyl-terminal hydrolase acts on ubiquitin carboxyl-terminal amides. J. Biol. Chem. 260, 7903–7910.

Pickrell, A.M., Pinto, M., Hida, A., Moraes, C.T., 2011. Striatal Dysfunctions Associated with Mitochondrial DNA Damage in Dopaminergic Neurons in a Mouse Model of Parkinson's Disease. J. Neurosci. 31, 17649–17658. https://doi.org/10.1523/JNEUROSCI.4871-11.2011

Pierozan, P., Biasibetti, H., Schmitz, F., Ávila, H., Fernandes, C.G., Pessoa-Pureur, R., Wyse, A.T.S., 2017. Neurotoxicity of Methylmercury in Isolated Astrocytes and Neurons: the Cytoskeleton as a Main Target. Mol. Neurobiol. 54, 5752–5767. https://doi.org/10.1007/s12035-016-0101-2

Piga, R., Saito, Y., Yoshida, Y., Niki, E., 2007. Cytotoxic effects of various stressors on PC12 cells: Involvement of oxidative stress and effect of antioxidants. Neurotoxicology 28, 67–75. https://doi.org/10.1016/j.neuro.2006.07.006

Piirainen, S., Youssef, A., Song, C., Kalueff, A. V., Landreth, G.E., Malm, T., Tian, L., 2017. Psychosocial stress on neuroinflammation and cognitive dysfunctions in Alzheimer's disease: the emerging role for microglia? Neurosci. Biobehav. Rev. 77, 148–164. https://doi.org/10.1016/j.neubiorev.2017.01.046

Pirkkala, L., Nykanen, P., Sistonen, L., 2001. Roles of the heat shock transcription factors in regulation of the heat shock response and beyond. FASEB J. 15, 1118–1131. https://doi.org/10.1096/fj00-0294rev

Pisanu, A., Lecca, D., Mulas, G., Wardas, J., Simbula, G., Spiga, S., Carta, A.R., 2014. Dynamic changes in pro- and anti-inflammatory cytokines in microglia after PPAR-γ agonist neuroprotective treatment in the MPTPp mouse model of progressive Parkinson's disease. Neurobiol. Dis. 71, 280–291. https://doi.org/10.1016/j.nbd.2014.08.011

Piston, D., Alvarez-Erviti, L., Bansal, V., Gargano, D., Yao, Z., Szabadkai, G., Odell, M., Puno, M.R., Björkblom, B., Maple-Grødem, J., Breuer, P., Kaut, O., Larsen, J.P., Bonn, S., Møller, S.G., Wüllner, U., Schapira, A.H. V, Gegg, M.E., 2017. DJ-1 is a redox sensitive adapter protein for high molecular weight complexes involved in regulation of catecholamine homeostasis. Hum. Mol. Genet. 26, 4028–4041. https://doi.org/10.1093/hmg/ddx294

Polymeropoulos, M.H., Lavedan, C., Leroy, E., Ide, S.E., Dehejia, A., Dutra, A., Pike, B., Root, H., Rubenstein, J., Boyer, R., Stenroos, E.S., Chandrasekharappa, S., Athanassiadou, A., Papapetropoulos, T., Johnson, W.G., Lazzarini, A.M., Duvoisin, R.C., Iorio, G. Di, Golbe, L.I., Nussbaum, R.L., 1997. Mutation in the α-Synuclein Gene Identified in Families with Parkinson's Disease. Science (80-.). 276, 2045–2047. https://doi.org/10.1126/science.276.5321.2045

Pontén, J., 1975. Neoplastic Human Glia Cells in Culture, in: Human Tumor Cells in Vitro. Springer US, Boston, MA, pp. 175–206. https://doi.org/10.1007/978-1-4757-1647-4_7

Poole, L.B., Hall, A., Nelson, K.J., 2011a. Overview of peroxiredoxins in oxidant defense and redox regulation. Curr. Protoc. Toxicol. Chapter 7, Unit7.9. https://doi.org/10.1002/0471140856.tx0709s49

Poole, L.B., Hall, A., Nelson, K.J., 2011b. Overview of peroxiredoxins in oxidant defense and redox regulation. Curr. Protoc. Toxicol. Chapter 7, Unit7.9. https://doi.org/10.1002/0471140856.tx0709s49

Popova, N.K., Ilchibaeva, T. V., Naumenko, V.S., 2017. Neurotrophic factors (BDNF and GDNF) and the serotonergic system of the brain. Biochem. 82, 308–317. https://doi.org/10.1134/S0006297917030099

Poprac, P., Jomova, K., Simunkova, M., Kollar, V., Rhodes, C.J., Valko, M., 2017. Targeting Free Radicals in Oxidative Stress-Related Human Diseases. Trends Pharmacol. Sci. 38, 592–607. https://doi.org/10.1016/j.tips.2017.04.005

Portera-Cailliau, C., Weimer, R.M., De Paola, V., Caroni, P., Svoboda, K., 2005. Diverse Modes of Axon Elaboration in the Developing Neocortex. PLoS Biol. 3, e272. https://doi.org/10.1371/journal.pbio.0030272

Posimo, J.M., Weilnau, J.N., Gleixner, A.M., Broeren, M.T., Weiland, N.L., Brodsky, J.L., Wipf, P., Leak, R.K., 2015. Heat shock protein defenses in the neocortex and allocortex of the telencephalon. Neurobiol. Aging 36, 1924–1937. https://doi.org/10.1016/j.neurobiolaging.2015.02.011

Pöyhönen, S., Er, S., Domanskyi, A., Airavaara, M., 2019. Effects of Neurotrophic Factors in Glial Cells in the Central Nervous System: Expression and Properties in Neurodegeneration and Injury. Front. Physiol. 10, 486. https://doi.org/10.3389/fphys.2019.00486

Presgraves, S.P., Ahmed, T., Borwege, S., Joyce, J.N., 2003. Terminally differentiated SH-SY5Y cells provide a model system for studying neuroprotective effects of dopamine agonists. Neurotox. Res. 5, 579–598. https://doi.org/10.1007/BF03033178

Press, C., Milbrandt, J., 2008. Nmnat Delays Axonal Degeneration Caused by Mitochondrial and Oxidative Stress. J. Neurosci. 28, 4861–4871. https://doi.org/10.1523/JNEUROSCI.0525-08.2008

Proffen, B.L., Haslauer, C.M., Harris, C.E., Murray, M.M., 2013. Mesenchymal Stem Cells from the Retropatellar Fat Pad and Peripheral Blood Stimulate ACL Fibroblast Migration, Proliferation, and Collagen Gene Expression. Connect. Tissue Res. 54, 14–21. https://doi.org/10.3109/03008207.2012.715701

Puspita, L., Chung, S.Y., Shim, J., 2017. Oxidative stress and cellular pathologies in Parkinson's disease. Mol. Brain 10, 53. https://doi.org/10.1186/s13041-017-0340-9

Pyka, M., Busse, C., Seidenbecher, C., Gundelfinger, E.D., Faissner, A., 2011. Astrocytes are crucial for survival and maturation of embryonic hippocampal neurons in a neuron-glia cell-insert coculture assay.

Synapse 65, 41–53. https://doi.org/10.1002/syn.20816

Quesada, A., Ogi, J., Schultz, J., Handforth, A., 2011. C-terminal mechano-growth factor induces heme oxygenase-1-mediated neuroprotection of SH-SY5Y cells via the protein kinase Cε/Nrf2 pathway. J. Neurosci. Res. 89, 394–405. https://doi.org/10.1002/jnr.22543

Quigney, D.J., Gorman, A.M., Samali, A., 2003. Heat shock protects PC12 cells against MPP+ toxicity. Brain Res. 993, 133–139. https://doi.org/10.1016/j.brainres.2003.09.004

Rabindran, S., Haroun, R., Clos, J., Wisniewski, J., Wu, C., 1993. Regulation of heat shock factor trimer formation: role of a conserved leucine zipper. Science (80-.). 259, 230–234. https://doi.org/10.1126/science.8421783

Radhakrishnan, S.K., den Besten, W., Deshaies, R.J., 2014. p97-dependent retrotranslocation and proteolytic processing govern formation of active Nrf1 upon proteasome inhibition. Elife 3, e01856. https://doi.org/10.7554/eLife.01856

Radi, R., 2013. Protein tyrosine nitration: Biochemical mechanisms and structural basis of functional effects. Acc. Chem. Res. 46, 550–559. https://doi.org/10.1021/ar300234c

Raff, M.C., 2002. Axonal Self-Destruction and Neurodegeneration. Science (80-.). 296, 868–871. https://doi.org/10.1126/science.1068613

Rahim, R.S., Chen, M., Nourse, C.C., Meedeniya, A.C.B., Crane, D.I., 2016. Mitochondrial changes and oxidative stress in a mouse model of Zellweger syndrome neuropathogenesis. Neuroscience 334, 201–213. https://doi.org/10.1016/j.neuroscience.2016.08.001

Rapin, J.R., Zaibi, M., Drieu, K., 1998. In vitro and in vivo effects of an extract of Ginkgo biloba (EGb 761), ginkgolide B, and bilobalide on apoptosis in primary cultures of rat hippocampal neurons. Drug Dev Res 45, 23–29.

Raps, S.P., Lai, J.C.K., Hertz, L., Cooper, A.J.L., 1989. Glutathione is present in high concentrations in cultured astrocytes but not in cultured neurons. Brain Res. 493, 398–401. https://doi.org/10.1016/0006-8993(89)91178-5

Rasband, M.N., 2016. Glial Contributions to Neural Function and Disease. Mol. Cell. Proteomics 15, 355–361. https://doi.org/10.1074/mcp.R115.053744

Ray, Paul D., Huang, B.-W., Tsuji, Y., 2012. Reactive oxygen species (ROS) homeostasis and redox regulation in cellular signaling. Cell. Signal. 24, 981–990. https://doi.org/10.1016/j.cellsig.2012.01.008

Ray, Paul D, Huang, B.-W., Tsuji, Y., 2012. Reactive oxygen species (ROS) homeostasis and redox regulation in cellular signaling. Cell. Signal. 24, 981–990. https://doi.org/10.1016/j.cellsig.2012.01.008

Raychaudhuri, S., Loew, C., Körner, R., Pinkert, S., Theis, M., Hayer-Hartl, M., Buchholz, F., Hartl, F.U., 2014.

Interplay of Acetyltransferase EP300 and the Proteasome System in Regulating Heat Shock Transcription Factor 1. Cell 156, 975–985. https://doi.org/10.1016/j.cell.2014.01.055

Raynes, R., Pomatto, L.C.D., Davies, K.J.A., 2016. Degradation of oxidized proteins by the proteasome: Distinguishing between the 20S, 26S, and immunoproteasome proteolytic pathways. Mol. Aspects Med. 50, 41–55. https://doi.org/10.1016/j.mam.2016.05.001

Razack, S., Kumar, K., Nallamuthu, I., Naika, M., Khanum, F., 2015. Antioxidant, Biomolecule Oxidation Protective Activities of Nardostachys jatamansi DC and Its Phytochemical Analysis by RP-HPLC and GC-MS. Antioxidants 4, 185–203. https://doi.org/10.3390/antiox4010185

Reczek, C.R., Chandel, N.S., 2015. ROS-dependent signal transduction. Curr. Opin. Cell Biol. https://doi.org/10.1016/j.ceb.2014.09.010

Redmann, M., Darley-Usmar, V., Zhang, J., 2016. The Role of Autophagy, Mitophagy and Lysosomal Functions in Modulating Bioenergetics and Survival in the Context of Redox and Proteotoxic Damage: Implications for Neurodegenerative Diseases. Aging Dis. 7, 150. https://doi.org/10.14336/AD.2015.0820

Redmann, M., Dodson, M., Boyer-Guittaut, M., Darley-Usmar, V., Zhang, J., 2014. Mitophagy mechanisms and role in human diseases. Int. J. Biochem. Cell Biol. 53, 127–133. https://doi.org/10.1016/j.biocel.2014.05.010

Reed, T., Perluigi, M., Sultana, R., Pierce, W.M., Klein, J.B., Turner, D.M., Coccia, R., Markesbery, W.R., Butterfield, D.A., 2008. Redox proteomic identification of 4-Hydroxy-2-nonenal-modified brain proteins in amnestic mild cognitive impairment: Insight into the role of lipid peroxidation in the progression and pathogenesis of Alzheimer's disease. Neurobiol. Dis. 30, 107–120. https://doi.org/10.1016/j.nbd.2007.12.007

Reed, T.T., 2011. Lipid peroxidation and neurodegenerative disease. Free Radic. Biol. Med. 51, 1302–1319. https://doi.org/10.1016/j.freeradbiomed.2011.06.027

Reed, T.T., Butterfield, D.A., 2017. Protein Carbonylation in Brains of Subjects with Selected Neurodegenerative Disorders, in: Protein Carbonylation. John Wiley & Sons, Inc., Hoboken, NJ, USA, pp. 167–205. https://doi.org/10.1002/9781119374947.ch8

Reeve, A., Meagher, M., Lax, N., Simcox, E., Hepplewhite, P., Jaros, E., Turnbull, D., 2013. The Impact of Pathogenic Mitochondrial DNA Mutations on Substantia Nigra Neurons. J. Neurosci. 33, 10790–10801. https://doi.org/10.1523/JNEUROSCI.3525-12.2013

Rego, A.C., Oliveira, C.R., 2003. Mitochondrial dysfunction and reactive oxygen species in excitotoxicity and apoptosis: implications for the pathogenesis of neurodegenerative diseases. Neurochem. Res. 28, 1563–74. https://doi.org/10.1023/a:1025682611389

Rehncrona, S., Smith, D.S., Åkesson, B., Westerberg, E., Siesjö, B.K., 1980. Peroxidative Changes in Brain

Cortical Fatty Acids and Phospholipids, as Characterized During Fe2+- and Ascorbic Acid-Stimulated Lipid Peroxidation In Vitro. J. Neurochem. 34, 1630–1638. https://doi.org/10.1111/j.1471-4159.1980.tb11254.x

Reinheckel, T., Ullrich, O., Sitte, N., Grune, T., 2000. Differential Impairment of 20S and 26S Proteasome Activities in Human Hematopoietic K562 Cells during Oxidative Stress. Arch. Biochem. Biophys. 377, 65–68. https://doi.org/10.1006/abbi.2000.1717

Ren, Y., Feng, J., 2007. Rotenone selectively kills serotonergic neurons through a microtubule-dependent mechanism. J. Neurochem. 103, 303–11. https://doi.org/10.1111/j.1471-4159.2007.04741.x

Renaud, J., Martinoli, M.-G., 2016. Development of an Insert Co-culture System of Two Cellular Types in the Absence of Cell-Cell Contact. J. Vis. Exp. https://doi.org/10.3791/54356

Rhee, S.G., 2016. Overview on Peroxiredoxin. Mol. Cells 39, 1–5. https://doi.org/10.14348/molcells.2016.2368

Rhee, S.G., Chae, H.Z., Kim, K., 2005. Peroxiredoxins: A historical overview and speculative preview of novel mechanisms and emerging concepts in cell signaling. Free Radic. Biol. Med. 38, 1543–1552. https://doi.org/10.1016/j.freeradbiomed.2005.02.026

Rhee, S.G., Jeong, W., Chang, T.-S., Woo, H.A., 2007. Sulfiredoxin, the cysteine sulfinic acid reductase specific to 2-Cys peroxiredoxin: its discovery, mechanism of action, and biological significance. Kidney Int. 72, S3–S8. https://doi.org/10.1038/sj.ki.5002380

Rice, M.E., 2000. Ascorbate regulation and its neuroprotective role in the brain. Trends Neurosci. 23, 209–216. https://doi.org/10.1016/S0166-2236(99)01543-X

Rice, M.E., Patel, J.C., Cragg, S.J., 2011. Dopamine release in the basal ganglia. Neuroscience 198, 112–137. https://doi.org/10.1016/j.neuroscience.2011.08.066

Rideout, H., Stefanis, L., 2002. Proteasomal Inhibition-Induced Inclusion Formation and Death in Cortical Neurons Require Transcription and Ubiquitination. Mol. Cell. Neurosci. 21, 223–238. https://doi.org/10.1006/mcne.2002.1173

Rideout, H.J., Larsen, K.E., Sulzer, D., Stefanis, L., 2001. Proteasomal inhibition leads to formation of ubiquitin/α-synuclein-immunoreactive inclusions in PC12 cells. J. Neurochem. 78, 899–908. https://doi.org/10.1046/j.1471-4159.2001.00474.x

Riemann, D., Petkova, A., Dresbach, T., Wallrafen, R., 2018. An Optical Assay for Synaptic Vesicle Recycling in Cultured Neurons Overexpressing Presynaptic Proteins. J. Vis. Exp. https://doi.org/10.3791/58043

Rieske, P., Augelli, B.J., Stawski, R., Gaughan, J., Azizi, S.A., Krynska, B., 2009. A population of human brain cells expressing phenotypic markers of more than one lineage can be induced in vitro to differentiate into mesenchymal cells. Exp. Cell Res. 315, 462–473. https://doi.org/10.1016/j.yexcr.2008.11.004

Riley, D.A., 1981. Ultrastructural evidence for axon retraction during the spontaneous elimination of polyneuronal innervation of the rat soleus muscle. J. Neurocytol. 10, 425–440. https://doi.org/10.1007/BF01262414

Rinaldi, T., Ricordy, R., Bolotin-Fukuhara, M., Frontali, L., 2002. Mitochondrial effects of the pleiotropic proteasomal mutation mpr1/rpn11 : uncoupling from cell cycle defects in extragenic revertants. Gene 286, 43–51. https://doi.org/10.1016/S0378-1119(01)00799-5

Rivera, I., Capone, R., Cauvi, D.M., Arispe, N., De Maio, A., 2018. Modulation of Alzheimer's amyloid β peptide oligomerization and toxicity by extracellular Hsp70. Cell Stress Chaperones 23, 269–279. https://doi.org/10.1007/s12192-017-0839-0

Rizzi, N., Brunialti, E., Cerri, S., Cermisoni, G., Levandis, G., Cesari, N., Maggi, A., Blandini, F., Ciana, P., 2018. In vivo imaging of early signs of dopaminergic neuronal death in an animal model of Parkinson's disease. Neurobiol. Dis. 114, 74–84. https://doi.org/10.1016/j.nbd.2018.02.005

Rogalla, T., Ehrnsperger, M., Preville, X., Kotlyarov, A., Lutsch, G., Ducasse, C., Paul, C., Wieske, M., Arrigo, A.-P., Buchner, J., Gaestel, M., 1999. Regulation of Hsp27 Oligomerization, Chaperone Function, and Protective Activity against Oxidative Stress/Tumor Necrosis Factor α by Phosphorylation. J. Biol. Chem. 274, 18947–18956. https://doi.org/10.1074/jbc.274.27.18947

Roqué, P.J., Dao, K., Costa, L.G., 2016. Microglia mediate diesel exhaust particle-induced cerebellar neuronal toxicity through neuroinflammatory mechanisms. Neurotoxicology 56, 204–214. https://doi.org/10.1016/j.neuro.2016.08.006

Rosenberg, G.A., 2002. Matrix metalloproteinases in neuroinflammation. Glia 39, 279–291. https://doi.org/10.1002/glia.10108

Rosewater, K., Sontheimer, H., 1994. Fibrous and protoplasmic astrocytes express GABAA receptors that differ in benzodiazepine pharmacology. Brain Res. 636, 73–80. https://doi.org/10.1016/0006-8993(94)90177-5

Ross, R.A., Spengler, B.A., Biedler, J.L., 1983. Coordinate morphological and biochemical interconversion of human neuroblastoma cells. J. Natl. Cancer Inst. 71, 741–7. https://doi.org/10.1093/jnci/71.4.741

Ruan, L., Zhou, C., Jin, E., Kucharavy, A., Zhang, Y., Wen, Z., Florens, L., Li, R., 2017. Cytosolic proteostasis through importing of misfolded proteins into mitochondria. Nature 543, 443–446. https://doi.org/10.1038/nature21695

Rubin, D.M., 1998. Active site mutants in the six regulatory particle ATPases reveal multiple roles for ATP in the proteasome. EMBO J. 17, 4909–4919. https://doi.org/10.1093/emboj/17.17.4909

Rudiger, S., 1997. Substrate specificity of the DnaK chaperone determined by screening cellulose-bound peptide libraries. EMBO J. 16, 1501–1507. https://doi.org/10.1093/emboj/16.7.1501

Rüdiger, S., Buchberger, A., Bukau, B., 1997. Interaction of Hsp70 chaperones with substrates. Nat. Struct. Mol. Biol. 4, 342–349. https://doi.org/10.1038/nsb0597-342

Ruszkiewicz, J., Albrecht, J., 2015. Changes in the mitochondrial antioxidant systems in neurodegenerative diseases and acute brain disorders. Neurochem. Int. 88, 66–72. https://doi.org/10.1016/j.neuint.2014.12.012

Ryan, B.J., Hoek, S., Fon, E.A., Wade-Martins, R., 2015. Mitochondrial dysfunction and mitophagy in Parkinson's: from familial to sporadic disease. Trends Biochem. Sci. 40, 200–210. https://doi.org/10.1016/j.tibs.2015.02.003

Ryter, S.W., Kim, H.P., Hoetzel, A., Park, J.W., Nakahira, K., Wang, X., Choi, A.M.K., 2007. Mechanisms of Cell Death in Oxidative Stress. Antioxid. Redox Signal. 9, 49–89. https://doi.org/10.1089/ars.2007.9.49

Sadeghian, M., Marinova-Mutafchieva, L., Broom, L., Davis, J.B., Virley, D., Medhurst, A.D., Dexter, D.T., 2012. Full and partial peroxisome proliferation-activated receptor-gamma agonists, but not delta agonist, rescue of dopaminergic neurons in the 6-OHDA Parkinsonian model is associated with inhibition of microglial activation and MMP expression. J. Neuroimmunol. 246, 69–77. https://doi.org/10.1016/j.jneuroim.2012.03.010

Sadowska-Bartosz, I., Ott, C., Grune, T., Bartosz, G., 2014. Posttranslational protein modifications by reactive nitrogen and chlorine species and strategies for their prevention and elimination. Free Radic. Res. 48, 1267–1284. https://doi.org/10.3109/10715762.2014.953494

Saeed, Y., Xie, B., Xu, J., Rehman, A., Hong, M., Hong, Q., Deng, Y., 2015. Glial U87 cells protect neuronal SH-SY5Y cells from indirect effect of radiation by reducing oxidative stress and apoptosis. Acta Biochim. Biophys. Sin. (Shanghai). 47, 250–257. https://doi.org/10.1093/abbs/gmv004

Saigoh, K., Wang, Y.L., Suh, J.G., Yamanishi, T., Sakai, Y., Kiyosawa, H., Harada, T., Ichihara, N., Wakana, S., Kikuchi, T., Wada, K., 1999. Intragenic deletion in the gene encoding ubiquitin carboxy-terminal hydrolase in gad mice. Nat. Genet. 23, 47–51. https://doi.org/10.1038/12647

Saito, Y., Miyasaka, T., Hatsuta, H., Takahashi-Niki, K., Hayashi, K., Mita, Y., Kusano-Arai, O., Iwanari, H., Ariga, H., Hamakubo, T., Yoshida, Y., Niki, E., Murayama, S., Ihara, Y., Noguchi, N., 2014. Immunostaining of Oxidized DJ-1 in Human and Mouse Brains. J. Neuropathol. Exp. Neurol. 73, 714–728. https://doi.org/10.1097/NEN.0000000000000087

Sakai, R., Suzuki, M., Ueyama, M., Takeuchi, T., Minakawa, E.N., Hayakawa, H., Baba, K., Mochizuki, H., Nagai, Y., 2019. E46K mutant α-synuclein is more degradation resistant and exhibits greater toxic effects than wild-type α-synuclein in Drosophila models of Parkinson's disease. PLoS One 14, e0218261. https://doi.org/10.1371/journal.pone.0218261

Saleh, Z., Menassa, J., Abbas, O., Atweh, S., Arayssi, T., 2010. Cranial nerve VI palsy as a rare initial presentation of systemic lupus erythematosus: case report and review of the literature. Lupus 19, 201–

5. https://doi.org/10.1177/0961203309345722

Salvadores, N., Sanhueza, M., Manque, P., Court, F.A., 2017. Axonal Degeneration during Aging and Its Functional Role in Neurodegenerative Disorders. Front. Neurosci. 11, 451. https://doi.org/10.3389/fnins.2017.00451

Samy, Z.A., Al-Abdullah, L., Turcani, M., Craik, J., Redzic, Z., 2018. Rat astrocytes during anoxia: Secretome profile of cytokines and chemokines. Brain Behav. 8, e01013. https://doi.org/10.1002/brb3.1013

Sanders, L.H., Timothy Greenamyre, J., 2013. Oxidative damage to macromolecules in human Parkinson disease and the rotenone model. Free Radic. Biol. Med. 62, 111–120. https://doi.org/10.1016/j.freeradbiomed.2013.01.003

Sandhu, J.K., Gardaneh, M., Iwasiow, R., Lanthier, P., Gangaraju, S., Ribecco-Lutkiewicz, M., Tremblay, R., Kiuchi, K., Sikorska, M., 2009. Astrocyte-secreted GDNF and glutathione antioxidant system protect neurons against 6OHDA cytotoxicity. Neurobiol. Dis. 33, 405–414. https://doi.org/10.1016/j.nbd.2008.11.016

Santambrogio, L., Cuervo, A.M., 2011. Chasing the elusive mammalian microautophagy. Autophagy 7, 652–654. https://doi.org/10.4161/auto.7.6.15287

Santos, A.L., Lindner, A.B., 2017. Protein Posttranslational Modifications: Roles in Aging and Age-Related Disease. Oxid. Med. Cell. Longev. 2017, 1–19. https://doi.org/10.1155/2017/5716409

Santos, D., Esteves, A.R., Silva, D.F., Januário, C., Cardoso, S.M., 2015. The Impact of Mitochondrial Fusion and Fission Modulation in Sporadic Parkinson's Disease. Mol. Neurobiol. 52, 573–586. https://doi.org/10.1007/s12035-014-8893-4

Sanz, A., 2016. Mitochondrial reactive oxygen species: Do they extend or shorten animal lifespan? Biochim. Biophys. Acta - Bioenerg. 1857, 1116–1126. https://doi.org/10.1016/j.bbabio.2016.03.018

Sarafian, T.A., Montes, C., Imura, T., Qi, J., Coppola, G., Geschwind, D.H., Sofroniew, M. V., 2010. Disruption of Astrocyte STAT3 Signaling Decreases Mitochondrial Function and Increases Oxidative Stress In Vitro. PLoS One 5, e9532. https://doi.org/10.1371/journal.pone.0009532

Sarkisian, M.R., Bartley, C.M., Chi, H., Nakamura, F., Hashimoto-Torii, K., Torii, M., Flavell, R.A., Rakic, P., 2006. MEKK4 Signaling Regulates Filamin Expression and Neuronal Migration. Neuron 52, 789–801. https://doi.org/10.1016/j.neuron.2006.10.024

Sarraf, S.A., Raman, M., Guarani-Pereira, V., Sowa, M.E., Huttlin, E.L., Gygi, S.P., Harper, J.W., 2013. Landscape of the PARKIN-dependent ubiquitylome in response to mitochondrial depolarization. Nature 496, 372–376. https://doi.org/10.1038/nature12043

Sauvageot, C., 2002. Molecular mechanisms controlling cortical gliogenesis. Curr. Opin. Neurobiol. 12, 244–249. https://doi.org/10.1016/S0959-4388(02)00322-7

Saxena, S., Caroni, P., 2007. Mechanisms of axon degeneration: From development to disease. Prog. Neurobiol. 83, 174–191. https://doi.org/10.1016/j.pneurobio.2007.07.007

Schafer, F.Q., Buettner, G.R., 2001. Redox environment of the cell as viewed through the redox state of the glutathione disulfide/glutathione couple. Free Radic. Biol. Med. 30, 1191–1212. https://doi.org/10.1016/S0891-5849(01)00480-4

Schapira, A.H., 2008. Mitochondria in the aetiology and pathogenesis of Parkinson's disease. Lancet Neurol. 7, 97–109. https://doi.org/10.1016/S1474-4422(07)70327-7

Schapira, A.H.V., Chaudhuri, K.R., Jenner, P., 2017. Non-motor features of Parkinson disease. Nat. Rev. Neurosci. 18, 435–450. https://doi.org/10.1038/nrn.2017.62

Schapira, A.H. V, Gegg, M., 2011. Mitochondrial Contribution to Parkinson's Disease Pathogenesis. Parkinsons. Dis. 2011, 1–7. https://doi.org/10.4061/2011/159160

Schmidlin, C.J., Dodson, M.B., Madhavan, L., Zhang, D.D., 2019. Redox regulation by NRF2 in aging and disease. Free Radic. Biol. Med. 134, 702–707. https://doi.org/10.1016/j.freeradbiomed.2019.01.016

Schneider, J.S., Denaro, F.J., 1988. Astrocytic Responses to the Dopaminergic Neurotoxin 1-Methyl-4-phenyl-1,2,3,6-tetrahydropyridine (MPTP) in Cat and Mouse Brain. J. Neuropathol. Exp. Neurol. 47, 452–458. https://doi.org/10.1097/00005072-198807000-00006

Schneider, L., Giordano, S., Zelickson, B.R., S. Johnson, M., A. Benavides, G., Ouyang, X., Fineberg, N., Darley-Usmar, V.M., Zhang, J., 2011. Differentiation of SH-SY5Y cells to a neuronal phenotype changes cellular bioenergetics and the response to oxidative stress. Free Radic. Biol. Med. 51, 2007–2017. https://doi.org/10.1016/j.freeradbiomed.2011.08.030

Schönfeld, P., Reiser, G., 2013. Why does Brain Metabolism not Favor Burning of Fatty Acids to Provide Energy? - Reflections on Disadvantages of the Use of Free Fatty Acids as Fuel for Brain. J. Cereb. Blood Flow Metab. 33, 1493–1499. https://doi.org/10.1038/jcbfm.2013.128

Schulz-Schaeffer, W.J., 2010. The synaptic pathology of α-synuclein aggregation in dementia with Lewy bodies, Parkinson's disease and Parkinson's disease dementia. Acta Neuropathol. 120, 131–143. https://doi.org/10.1007/s00401-010-0711-0

Schumacker, P.T., 2006. Reactive oxygen species in cancer cells: Live by the sword, die by the sword. Cancer Cell. https://doi.org/10.1016/j.ccr.2006.08.015

Sciarretta, F., Fulci, C., Palumbo, C., Aquilano, K., Pastore, A., Iorio, E., Lettieri-Barbato, D., Cicconi, R., Minutolo, A., Parravano, M., Gilardi, M., Varano, M., Caccuri, A.M., 2019. Glutathione transferase P silencing promotes neuronal differentiation of retinal R28 cells. J. Cell. Physiol. 234, 15885–15897. https://doi.org/10.1002/jcp.28246

Scrivo, A., Bourdenx, M., Pampliega, O., Cuervo, A.M., 2018. Selective autophagy as a potential therapeutic

target for neurodegenerative disorders. Lancet Neurol. 17, 802–815. https://doi.org/10.1016/S1474-4422(18)30238-2

Sedlak, T.W., Paul, B.D., Parker, G.M., Hester, L.D., Snowman, A.M., Taniguchi, Y., Kamiya, A., Snyder, S.H., Sawa, A., 2019. The glutathione cycle shapes synaptic glutamate activity. Proc. Natl. Acad. Sci. 116, 2701–2706. https://doi.org/10.1073/pnas.1817885116

Segura-Aguilar, J., Paris, I., Muñoz, P., Ferrari, E., Zecca, L., Zucca, F.A., 2014. Protective and toxic roles of dopamine in Parkinson's disease. J. Neurochem. 129, 898–915. https://doi.org/10.1111/jnc.12686

Seifert, G., Schilling, K., Steinhäuser, C., 2006. Astrocyte dysfunction in neurological disorders: a molecular perspective. Nat. Rev. Neurosci. 7, 194–206. https://doi.org/10.1038/nrn1870

Seniuk, N.A., Tatton, W.G., Greenwood, C.E., 1990. Dose-dependent destruction of the coeruleus-cortical and nigral-striatal projections by MPTP. Brain Res. 527, 7–20. https://doi.org/10.1016/0006-8993(90)91055-L

Shahmoradian, S.H., Lewis, A.J., Genoud, C., Hench, J., Moors, T.E., Navarro, P.P., Castaño-Díez, D., Schweighauser, G., Graff-Meyer, A., Goldie, K.N., Sütterlin, R., Huisman, E., Ingrassia, A., Gier, Y. de, Rozemuller, A.J.M., Wang, J., Paepe, A. De, Erny, J., Staempfli, A., Hoernschemeyer, J., Großerüschkamp, F., Niedieker, D., El-Mashtoly, S.F., Quadri, M., Van IJcken, W.F.J., Bonifati, V., Gerwert, K., Bohrmann, B., Frank, S., Britschgi, M., Stahlberg, H., Van de Berg, W.D.J., Lauer, M.E., 2019. Lewy pathology in Parkinson's disease consists of crowded organelles and lipid membranes. Nat. Neurosci. https://doi.org/10.1038/s41593-019-0423-2

Shamoto-Nagai, M., Hisaka, S., Naoi, M., Maruyama, W., 2018. Modification of α-synuclein by lipid peroxidation products derived from polyunsaturated fatty acids promotes toxic oligomerization: its relevance to Parkinson disease. J. Clin. Biochem. Nutr. 62, 207–212. https://doi.org/10.3164/jcbn.18-25

Shamoto-Nagai, M., Maruyama, W., Kato, Y., Isobe, K., Tanaka, M., Naoi, M., Osawa, T., 2003. An inhibitor of mitochondrial complex I, rotenone, inactivates proteasome by oxidative modification and induces aggregation of oxidized proteins in SH-SY5Y cells. J. Neurosci. Res. 74, 589–597. https://doi.org/10.1002/jnr.10777

Sharma, J., Johnston, M. V, Hossain, M., 2014. Sex differences in mitochondrial biogenesis determine neuronal death and survival in response to oxygen glucose deprivation and reoxygenation. BMC Neurosci. 15, 9. https://doi.org/10.1186/1471-2202-15-9

Sharma, N., Nehru, B., 2015. Characterization of the lipopolysaccharide induced model of Parkinson's disease: Role of oxidative stress and neuroinflammation. Neurochem. Int. 87, 92–105. https://doi.org/10.1016/j.neuint.2015.06.004

Shelton, P., Jaiswal, A.K., 2013. The transcription factor NF-E2-related Factor 2 (Nrf2): a protooncogene? FASEB J. 27, 414–423. https://doi.org/10.1096/fj.12-217257

Sherer, T.B., Betarbet, R., Testa, C.M., Seo, B.B., Richardson, J.R., Kim, J.H., Miller, G.W., Yagi, T., Matsuno-Yagi, A., Greenamyre, J.T., 2003. Mechanism of toxicity in rotenone models of Parkinson's disease. J. Neurosci. 23, 10756–10764. https://doi.org/23/34/10756 [pii]

Shi, S., Guo, Y., Lou, Y., Li, Q., Cai, X., Zhong, X., Li, H., 2017. Sulfiredoxin involved in the protection of peroxiredoxins against hyperoxidation in the early hyperglycaemia. Exp. Cell Res. 352, 273–280. https://doi.org/10.1016/j.yexcr.2017.02.015

Shiba-Fukushima, K., Imai, Y., Yoshida, S., Ishihama, Y., Kanao, T., Sato, S., Hattori, N., 2012. PINK1-mediated phosphorylation of the Parkin ubiquitin-like domain primes mitochondrial translocation of Parkin and regulates mitophagy. Sci. Rep. 2, 1002. https://doi.org/10.1038/srep01002

Shih, A.Y., Imbeault, S., Barakauskas, V., Erb, H., Jiang, L., Li, P., Murphy, T.H., 2005. Induction of the Nrf2-driven Antioxidant Response Confers Neuroprotection during Mitochondrial Stress in Vivo. J. Biol. Chem. 280, 22925–22936. https://doi.org/10.1074/jbc.M414635200

Shih, A.Y., Johnson, D.A., Wong, G., Kraft, A.D., Jiang, L., Erb, H., Johnson, J.A., Murphy, T.H., 2003. Coordinate regulation of glutathione biosynthesis and release by Nrf2-expressing glia potently protects neurons from oxidative stress. J. Neurosci. 23, 3394–406.

Shimura, H., Schlossmacher, M.G., Hattori, N., Frosch, M.P., Trockenbacher, a, Schneider, R., Mizuno, Y., Kosik, K.S., Selkoe, D.J., 2001. Ubiquitination of a new form of alpha-synuclein by parkin from human brain: implications for Parkinson's disease. Science 293, 263–269. https://doi.org/10.1126/science.1060627

Shimura, H., Tanaka, R., Urabe, T., Hattori, N., 2017. Heat Shock Protein 27 (HSP27) As a Therapeutic Target in Ischemic Stroke and Neurodegenerative Disorders. Juntendo Med. J. 63, 17–21. https://doi.org/10.14789/jmj.63.17

Shinohara, A., Ogawa, H., Matsuda, Y., Ushio, N., Ikeo, K., Ogawa, T., 1993. Cloning of human, mouse and fission yeast recombination genes homologous to RAD51 and recA. Nat. Genet. 4, 239–43. https://doi.org/10.1038/ng0793-239

Shipley, M.M., Mangold, C.A., Szpara, M.L., 2016. Differentiation of the SH-SY5Y Human Neuroblastoma Cell Line. J. Vis. Exp. https://doi.org/10.3791/53193

Shokolenko, I., Venediktova, N., Bochkareva, A., Wilson, G.L., Alexeyev, M.F., 2009. Oxidative stress induces degradation of mitochondrial DNA. Nucleic Acids Res. 37, 2539–2548. https://doi.org/10.1093/nar/gkp100

Shringarpure, R., Grune, T., Mehlhase, J., Davies, K.J.A., 2003. Ubiquitin Conjugation Is Not Required for the Degradation of Oxidized Proteins by Proteasome. J. Biol. Chem. 278, 311–318. https://doi.org/10.1074/jbc.M206279200

Shukla, R., 2007. Nitric Oxide in Neurodegeneration. Ann. Neurosci. 14, 13–20. https://doi.org/10.5214/ans.0972.7531.2007.140104

Silva-Islas, C.A., Maldonado, P.D., 2018. Canonical and non-canonical mechanisms of Nrf2 activation. Pharmacol. Res. 134, 92–99. https://doi.org/10.1016/j.phrs.2018.06.013

Silva Ramos, E., Motori, E., Brüser, C., Kühl, I., Yeroslaviz, A., Ruzzenente, B., Kauppila, J.H.K., Busch, J.D., Hultenby, K., Habermann, B.H., Jakobs, S., Larsson, N.-G., Mourier, A., 2019. Mitochondrial fusion is required for regulation of mitochondrial DNA replication. PLOS Genet. 15, e1008085. https://doi.org/10.1371/journal.pgen.1008085

Simpson, E.P., Henry, Y.K., Henkel, J.S., Smith, R.G., Appel, S.H., 2004. Increased lipid peroxidation in sera of ALS patients: A potential biomarker of disease burden. Neurology 62, 1758–1765. https://doi.org/10.1212/WNL.62.10.1758

Singleton, a B., Farrer, M., Johnson, J., Singleton, a, Hague, S., Kachergus, J., Hulihan, M., Peuralinna, T., Dutra, a, Nussbaum, R., Lincoln, S., Crawley, a, Hanson, M., Maraganore, D., Adler, C., Cookson, M.R., Muenter, M., Baptista, M., Miller, D., Blancato, J., Hardy, J., Gwinn-Hardy, K., 2003. alpha-Synuclein locus triplication causes Parkinson's disease. Science 302, 841. https://doi.org/10.1126/science.1090278

Skaper, S.D., Facci, L., 2018. Culture of Neonatal Rodent Microglia, Astrocytes, and Oligodendrocytes from the Cortex, Spinal Cord, and Cerebellum, in: Methods in Molecular Biology. pp. 49–61. https://doi.org/10.1007/978-1-4939-7571-6_4

Smirnoff, N., 2018. Ascorbic acid metabolism and functions: A comparison of plants and mammals. Free Radic. Biol. Med. 122, 116–129. https://doi.org/10.1016/j.freeradbiomed.2018.03.033

Smith, B.C., Marletta, M.A., 2012. Mechanisms of S-nitrosothiol formation and selectivity in nitric oxide signaling. Curr. Opin. Chem. Biol. 16, 498–506. https://doi.org/10.1016/j.cbpa.2012.10.016

Smith, K.J., Lassmann, H., 2002. The role of nitric oxide in multiple sclerosis. Lancet Nuerology 1, 232–41. https://doi.org/10.1016/S1474-4422(02)00102-3

Somara, S., Bitar, K.N., 2006. Phosphorylated HSP27 modulates the association of phosphorylated caldesmon with tropomyosin in colonic smooth muscle. Am. J. Physiol. Liver Physiol. 291, G630–G639. https://doi.org/10.1152/ajpgi.00350.2005

Song, D.D., Shults, C.W., Sisk, A., Rockenstein, E., Masliah, E., 2004. Enhanced substantia nigra mitochondrial pathology in human α-synuclein transgenic mice after treatment with MPTP. Exp. Neurol. 186, 158–172. https://doi.org/10.1016/S0014-4886(03)00342-X

Song, I.S., Kang, S.-S., Kim, E.-S., Park, H.-M., Choi, C.Y., Tchah, H., Kim, J.Y., 2014. Heat shock protein 27 phosphorylation is involved in epithelial cell apoptosis as well as epithelial migration during corneal

epithelial wound healing. Exp. Eye Res. 118, 36–41. https://doi.org/10.1016/j.exer.2013.11.002

Song, S., Miranda, C.J., Braun, L., Meyer, K., Frakes, A.E., Ferraiuolo, L., Likhite, S., Bevan, A.K., Foust, K.D., McConnell, M.J., Walker, C.M., Kaspar, B.K., 2016. Major histocompatibility complex class I molecules protect motor neurons from astrocyte-induced toxicity in amyotrophic lateral sclerosis. Nat. Med. 22, 397–403. https://doi.org/10.1038/nm.4052

Sorrentino, Z.A., Giasson, B.I., Chakrabarty, P., 2019. α-Synuclein and astrocytes: tracing the pathways from homeostasis to neurodegeneration in Lewy body disease. Acta Neuropathol. 138, 1–21. https://doi.org/10.1007/s00401-019-01977-2

Sotiriou, S., Gispert, S., Cheng, J., Wang, Y., Chen, A., Hoogstraten-Miller, S., Miller, G.F., Kwon, O., Levine, M., Guttentag, S.H., Nussbaum, R.L., 2002. Ascorbic-acid transporter Slc23a1 is essential for vitamin C transport into the brain and for perinatal survival. Nat. Med. 8, 514–517. https://doi.org/10.1038/0502-514

Spencer, K.C., Sy, J.C., Ramadi, K.B., Graybiel, A.M., Langer, R., Cima, M.J., 2017. Characterization of Mechanically Matched Hydrogel Coatings to Improve the Biocompatibility of Neural Implants. Sci. Rep. 7, 1952. https://doi.org/10.1038/s41598-017-02107-2

Spillantini, M.G., Schmidt, M.L., Lee, V.M., Trojanowski, J.Q., Jakes, R., Goedert, M., 1997. Alpha-synuclein in Lewy bodies. Nature 388, 839–40. https://doi.org/10.1038/42166

Stamler, J.S., Toone, E.J., Lipton, S.A., Sucher, N.J., 1997. (S)NO Signals: Translocation, Regulation, and a Consensus Motif. Neuron 18, 691–696. https://doi.org/10.1016/S0896-6273(00)80310-4

Stauch, K.L., Purnell, P.R., Fox, H.S., 2014. Aging synaptic mitochondria exhibit dynamic proteomic changes while maintaining bioenergetic function. Aging (Albany. NY). 6, 320–334. https://doi.org/10.18632/aging.100657

Steinert, J.R., Chernova, T., Forsythe, I.D., 2010. Nitric Oxide Signaling in Brain Function, Dysfunction, and Dementia. Neurosci. 16, 435–452. https://doi.org/10.1177/1073858410366481

Stevens, B., Allen, N.J., Vazquez, L.E., Howell, G.R., Christopherson, K.S., Nouri, N., Micheva, K.D., Mehalow, A.K., Huberman, A.D., Stafford, B., Sher, A., Litke, A.M., Lambris, J.D., Smith, S.J., John, S.W.M., Barres, B.A., 2007. The Classical Complement Cascade Mediates CNS Synapse Elimination. Cell 131, 1164–1178. https://doi.org/10.1016/j.cell.2007.10.036

Stöcker, S., Van Laer, K., Mijuskovic, A., Dick, T.P., 2018. The Conundrum of Hydrogen Peroxide Signaling and the Emerging Role of Peroxiredoxins as Redox Relay Hubs. Antioxid. Redox Signal. 28, 558–573. https://doi.org/10.1089/ars.2017.7162

Storch, a, Kaftan, A., Burkhardt, K., Schwarz, J., 2000. 6-Hydroxydopamine toxicity towards human SH-SY5Y dopaminergic neuroblastoma cells: independent of mitochondrial energy metabolism. J. Neural

Transm. 107, 0281–0293. https://doi.org/10.1007/s007020050023

Stott, S.R.W., Barker, R.A., 2014. Time course of dopamine neuron loss and glial response in the 6-OHDA striatal mouse model of Parkinson's disease. Eur. J. Neurosci. 39, 1042–1056. https://doi.org/10.1111/ejn.12459

Strobbe, D., Robinson, A.A., Harvey, K., Rossi, L., Ferraina, C., de Biase, V., Rodolfo, C., Harvey, R.J., Campanella, M., 2018. Distinct Mechanisms of Pathogenic DJ-1 Mutations in Mitochondrial Quality Control. Front. Mol. Neurosci. 11, 68. https://doi.org/10.3389/fnmol.2018.00068

Stroissnigg, H., Trančíková, A., Descovich, L., Fuhrmann, J., Kutschera, W., Kostan, J., Meixner, A., Nothias, F., Propst, F., 2007. S-nitrosylation of microtubule-associated protein 1B mediates nitric-oxide-induced axon retraction. Nat. Cell Biol. 9, 1035–1045. https://doi.org/10.1038/ncb1625

Su, B., Wang, X., Zheng, L., Perry, G., Smith, M.A., Zhu, X., 2010. Abnormal mitochondrial dynamics and neurodegenerative diseases. Biochim. Biophys. Acta - Mol. Basis Dis. 1802, 135–142. https://doi.org/10.1016/j.bbadis.2009.09.013

Sultana, R., Perluigi, M., Butterfield, D.A., 2013a. Lipid peroxidation triggers neurodegeneration: A redox proteomics view into the Alzheimer disease brain. Free Radic. Biol. Med. 62, 157–169. https://doi.org/10.1016/j.freeradbiomed.2012.09.027

Sultana, R., Perluigi, M., Butterfield, D.A., 2013b. Lipid peroxidation triggers neurodegeneration: A redox proteomics view into the Alzheimer disease brain. Free Radic. Biol. Med. 62, 157–169. https://doi.org/10.1016/j.freeradbiomed.2012.09.027

Sultanova, N., Kasarova, S., Nikolov, I., 2009. Dispersion Properties of Optical Polymers. Acta Phys. Pol. A 116, 585–587. https://doi.org/10.12693/APhysPolA.116.585

Sun, Y., Gu, Q.-P., Whanger, P.D., 2001. Selenoprotein W in overexpressed and underexpressed rat glial cells in culture. J. Inorg. Biochem. 84, 151–156. https://doi.org/10.1016/S0162-0134(00)00219-1

Sun, Y.E., Martinowich, K., Ge, W., 2003. Making and repairing the mammalian brain—signaling toward neurogenesis and gliogenesis. Semin. Cell Dev. Biol. 14, 161–168. https://doi.org/10.1016/S1084-9521(03)00007-7

Sung, K., Jimenez-Sanchez, M., 2020. Autophagy in Astrocytes and its Implications in Neurodegeneration. J. Mol. Biol. https://doi.org/10.1016/j.jmb.2019.12.041

Suzuki, T., Yamamoto, M., 2015. Molecular basis of the Keap1–Nrf2 system. Free Radic. Biol. Med. 88, 93–100. https://doi.org/10.1016/j.freeradbiomed.2015.06.006

Swarnkar, S., Goswami, P., Kamat, P.K., Gupta, S., Patro, I.K., Singh, S., Nath, C., 2012. Rotenone-induced apoptosis and role of calcium: a study on Neuro-2a cells. Arch. Toxicol. 86, 1387–1397. https://doi.org/10.1007/s00204-012-0853-z

Swerdlow, R.H., 2009. The Neurogenerative Mitochondriopathies. J. Alzheimers Dis. 17, 737–751. https://doi.org/10.3233/JAD-2009-1095.The

Syková, E., 2001. Glial diffusion barriers during aging and pathological states, in: Progress in Brain Research. pp. 339–363. https://doi.org/10.1016/S0079-6123(01)32087-3

Taghizadeh, M., Tamtaji, O.R., Dadgostar, E., Daneshvar Kakhaki, R., Bahmani, F., Abolhassani, J., Aarabi, M.H., Kouchaki, E., Memarzadeh, M.R., Asemi, Z., 2017. The effects of omega-3 fatty acids and vitamin E co-supplementation on clinical and metabolic status in patients with Parkinson's disease: A randomized, double-blind, placebo-controlled trial. Neurochem. Int. 108, 183–189. https://doi.org/10.1016/j.neuint.2017.03.014

Tagliaferro, P., Burke, R.E., 2016. Retrograde Axonal Degeneration in Parkinson Disease. J. Parkinsons. Dis. 6, 1–15. https://doi.org/10.3233/JPD-150769

Taira, T., Saito, Y., Niki, T., Iguchi-Ariga, S.M.M., Takahashi, K., Ariga, H., 2004. DJ-1 has a role in antioxidative stress to prevent cell death. EMBO Rep. 5, 213–218. https://doi.org/10.1038/sj.embor.7400074

Takahashi, K., Takisawa, S., Shimokado, K., Kono, N., Arai, H., Ishigami, A., 2017. Age-related changes of vitamin E: α-tocopherol levels in plasma and various tissues of mice and hepatic α-tocopherol transfer protein. Eur. J. Nutr. 56, 1317–1327. https://doi.org/10.1007/s00394-016-1182-4

Tambuyzer, B.R., Ponsaerts, P., Nouwen, E.J., 2009. Microglia: gatekeepers of central nervous system immunology. J. Leukoc. Biol. 85, 352–370. https://doi.org/10.1189/jlb.0608385

Tanaka, A., Cleland, M.M., Xu, S., Narendra, D.P., Suen, D.-F., Karbowski, M., Youle, R.J., 2010. Proteasome and p97 mediate mitophagy and degradation of mitofusins induced by Parkin. J. Cell Biol. 191, 1367–1380. https://doi.org/10.1083/jcb.201007013

Tappel, A.L., 1972. VITAMIN E AND FREE RADICAL PEROXIDATION OF LIPIDS. Ann. N. Y. Acad. Sci. 203, 12–28. https://doi.org/10.1111/j.1749-6632.1972.tb27851.x

Taso, O. V., Philippou, A., Moustogiannis, A., Zevolis, E., Koutsilieris, M., 2019. Lipid peroxidation products and their role in neurodegenerative diseases. Ann. Res. Hosp. 3, 2–2. https://doi.org/10.21037/arh.2018.12.02

Tatsuta, T., Langer, T., 2008. Quality control of mitochondria: protection against neurodegeneration and ageing. EMBO J. 27, 306–314. https://doi.org/10.1038/sj.emboj.7601972

Taylor, A.M., Wu, J., Tai, H.-C., Schuman, E.M., 2013. Axonal Translation of β-Catenin Regulates Synaptic Vesicle Dynamics. J. Neurosci. 33, 5584–5589. https://doi.org/10.1523/JNEUROSCI.2944-12.2013

Teismann, P., Schulz, J.B., 2004. Cellular pathology of Parkinson?s disease: astrocytes, microglia and inflammation. Cell Tissue Res. 318, 149–161. https://doi.org/10.1007/s00441-004-0944-0

Teppola, H., Sarkanen, J.-R., Jalonen, T.O., Linne, M.-L., 2016. Morphological Differentiation Towards Neuronal Phenotype of SH-SY5Y Neuroblastoma Cells by Estradiol, Retinoic Acid and Cholesterol. Neurochem. Res. 41, 731–747. https://doi.org/10.1007/s11064-015-1743-6

Terao, K., Niki, E., 1986. Damage to biological tissues induced by radical initiator 2,2′-azobis(2-amidinopropane) dihydrochloride and its inhibition by chain-breaking antioxidants. J. Free Radic. Biol. Med. 2, 193–201. https://doi.org/10.1016/S0748-5514(86)80070-8

Terman, A., Kurz, T., Navratil, M., Arriaga, E.A., Brunk, U.T., 2010. Mitochondrial Turnover and Aging of Long-Lived Postmitotic Cells: The Mitochondrial–Lysosomal Axis Theory of Aging. Antioxid. Redox Signal. 12, 503–535. https://doi.org/10.1089/ars.2009.2598

Testa, C.M., Sherer, T.B., Greenamyre, J.T., 2005. Rotenone induces oxidative stress and dopaminergic neuron damage in organotypic substantia nigra cultures. Mol. Brain Res. 134, 109–118. https://doi.org/10.1016/j.molbrainres.2004.11.007

Then, S.M., Wan Ngah, W.Z., Top, G.M., Mazlan, M., 2010. Comparison of the effects of α-tocopherol and γ-tocotrienol against oxidative stress in two different neuronal cultures. Sains Malaysiana 39, 145–156.

Thibaudeau, T.A., Anderson, R.T., Smith, D.M., 2018. A common mechanism of proteasome impairment by neurodegenerative disease-associated oligomers. Nat. Commun. 9, 1097. https://doi.org/10.1038/s41467-018-03509-0

Thomas, P.K., 1964. CHANGES IN THE ENDONEURIAL SHEATHS OF PERIPHERAL MYELINATED NERVE FIBRES DURING WALLERIAN DEGENERATION. J. Anat. 98, 175–82.

Thorne, N., Malik, N., Shah, S., Zhao, J., Class, B., Aguisanda, F., Southall, N., Xia, M., McKew, J.C., Rao, M., Zheng, W., 2016. High-Throughput Phenotypic Screening of Human Astrocytes to Identify Compounds That Protect Against Oxidative Stress. Stem Cells Transl. Med. 5, 613–627. https://doi.org/10.5966/sctm.2015-0170

Tofaris, G.K., Layfield, R., Spillantini, M.G., 2001. α-Synuclein metabolism and aggregation is linked to ubiquitin-independent degradation by the proteasome. FEBS Lett. 509, 22–26. https://doi.org/10.1016/S0014-5793(01)03115-5

Toledo, E.M., Colombres, M., Inestrosa, N.C., 2008. Wnt signaling in neuroprotection and stem cell differentiation. Prog. Neurobiol. 86, 281–296. https://doi.org/10.1016/j.pneurobio.2008.08.001

Tomozawa, Y., Appel, S.H., 1986. Soluble striatal extracts enhance development of mesencephalic dopaminergic neurons in vitro. Brain Res. 399, 111–124. https://doi.org/10.1016/0006-8993(86)90605-0

Tonelli, C., Chio, I.I.C., Tuveson, D.A., 2018. Transcriptional Regulation by Nrf2. Antioxid. Redox Signal. 29, 1727–1745. https://doi.org/10.1089/ars.2017.7342

Traber, M.G., Atkinson, J., 2007. Vitamin E, antioxidant and nothing more. Free Radic. Biol. Med. 43, 4–15. https://doi.org/10.1016/j.freeradbiomed.2007.03.024

Traber, M.G., Burton, G.W., Ingold, K.U., Kayden, H.J., 1990. RRR- and SRR-alpha-tocopherols are secreted without discrimination in human chylomicrons, but RRR-alpha-tocopherol is preferentially secreted in very low density lipoproteins. J. Lipid Res. 31, 675–85.

Trachootham, D., Lu, W., Ogasawara, M.A., Valle, N.R.-D., Huang, P., 2008. Redox Regulation of Cell Survival. Antioxid. Redox Signal. 10, 1343–1374. https://doi.org/10.1089/ars.2007.1957

Trachootham, D., Zhou, Y., Zhang, H., Demizu, Y., Chen, Z., Pelicano, H., Chiao, P.J., Achanta, G., Arlinghaus, R.B., Liu, J., Huang, P., 2006. Selective killing of oncogenically transformed cells through a ROS-mediated mechanism by β-phenylethyl isothiocyanate. Cancer Cell 10, 241–252. https://doi.org/10.1016/j.ccr.2006.08.009

Trougakos, I.P., Sesti, F., Tsakiri, E., Gorgoulis, V.G., 2013. Non-enzymatic post-translational protein modifications and proteostasis network deregulation in carcinogenesis. J. Proteomics 92, 274–298. https://doi.org/10.1016/j.jprot.2013.02.024

Tsao, J.W., Brown, M.C., Carden, M.J., McLean, W.G., Perry, V.H., 1994. Loss of the Compound Action Potential: an Electrophysiological, Biochemical and Morphological Study of Early Events in Axonal Degeneration in the C57BL/Ola Mouse. Eur. J. Neurosci. 6, 516–524. https://doi.org/10.1111/j.1460-9568.1994.tb00295.x

Tsuda, M., Toyomitsu, E., Komatsu, T., Masuda, T., Kunifusa, E., Nasu-Tada, K., Koizumi, S., Yamamoto, K., Ando, J., Inoue, K., 2008. Fibronectin/integrin system is involved in P2X4 receptor upregulation in the spinal cord and neuropathic pain after nerve injury. Glia 56, 579–585. https://doi.org/10.1002/glia.20641

Tu, Y.-J., Njus, D., Schlegel, H.B., 2017. A theoretical study of ascorbic acid oxidation and HOO˙/ O 2 ˙ − radical scavenging. Org. Biomol. Chem. 15, 4417–4431. https://doi.org/10.1039/C7OB00791D

Tufekci, K.U., Civi Bayin, E., Genc, S., Genc, K., 2011. The Nrf2/ARE Pathway: A Promising Target to Counteract Mitochondrial Dysfunction in Parkinson's Disease. Parkinsons. Dis. 2011, 1–14. https://doi.org/10.4061/2011/314082

Turner-Ivey, B., Manevich, Y., Schulte, J., Kistner-Griffin, E., Jezierska-Drutel, A., Liu, Y., Neumann, C.A., 2013. Role for Prdx1 as a specific sensor in redox-regulated senescence in breast cancer. Oncogene 32, 5302–5314. https://doi.org/10.1038/onc.2012.624

Turturici, G., Sconzo, G., Geraci, F., 2011. Hsp70 and Its Molecular Role in Nervous System Diseases. Biochem. Res. Int. 2011, 1–18. https://doi.org/10.1155/2011/618127

Twelves, D., Perkins, K.S.M., Counsell, C., 2003. Systematic review of incidence studies of Parkinson's disease.

Mov. Disord. 18, 19–31. https://doi.org/10.1002/mds.10305

Ulatowski, L., Dreussi, C., Noy, N., Barnholtz-Sloan, J., Klein, E., Manor, D., 2012. Expression of the α-tocopherol transfer protein gene is regulated by oxidative stress and common single-nucleotide polymorphisms. Free Radic. Biol. Med. 53, 2318–2326. https://doi.org/10.1016/j.freeradbiomed.2012.10.528

Unno, M., Mizushima, T., Morimoto, Y., Tomisugi, Y., Tanaka, K., Yasuoka, N., Tsukihara, T., 2002. The Structure of the Mammalian 20S Proteasome at 2.75 Å Resolution. Structure 10, 609–618. https://doi.org/10.1016/S0969-2126(02)00748-7

Uo, T., Dworzak, J., Kinoshita, C., Inman, D.M., Kinoshita, Y., Horner, P.J., Morrison, R.S., 2009. Drp1 levels constitutively regulate mitochondrial dynamics and cell survival in cortical neurons. Exp. Neurol. 218, 274–285. https://doi.org/10.1016/j.expneurol.2009.05.010

Utani, A., 2010. [Laminin alpha3 chain-derived peptide promotes keratinocyte migration and wound closure: clustering of syndecan-4 and integrin beta1]. Seikagaku. 82, 327–31. https://doi.org/10.1091/mbc.E08

Vaishnavi, S.N., Vlassenko, A.G., Rundle, M.M., Snyder, A.Z., Mintun, M.A., Raichle, M.E., 2010. Regional aerobic glycolysis in the human brain. Proc. Natl. Acad. Sci. 107, 17757–17762. https://doi.org/10.1073/pnas.1010459107

Valenta, T., Hausmann, G., Basler, K., 2012. The many faces and functions of β-catenin. EMBO J. 31, 2714–2736. https://doi.org/10.1038/emboj.2012.150

Valente, E.M., Abou-Sleiman, P.M., Caputo, V., Muqit, M.M.K., Harvey, K., Gispert, S., Ali, Z., Del Turco, D., Bentivoglio, A.R., Healy, D.G., Albanese, A., Nussbaum, R., Gonzalez-Maldonado, R., Deller, T., Salvi, S., Cortelli, P., Gilks, W.P., Latchman, D.S., Harvey, R.J., Dallapiccola, B., Auburger, G., Wood, N.W., 2004. Hereditary early-onset Parkinson's disease caused by mutations in PINK1. Science 304, 1158–60. https://doi.org/10.1126/science.1096284

van der Bliek, A.M., Shen, Q., Kawajiri, S., 2013. Mechanisms of Mitochondrial Fission and Fusion. Cold Spring Harb. Perspect. Biol. 5, a011072–a011072. https://doi.org/10.1101/cshperspect.a011072

van der Merwe, C., van Dyk, H.C., Engelbrecht, L., van der Westhuizen, F.H., Kinnear, C., Loos, B., Bardien, S., 2017. Curcumin Rescues a PINK1 Knock Down SH-SY5Y Cellular Model of Parkinson's Disease from Mitochondrial Dysfunction and Cell Death. Mol. Neurobiol. 54, 2752–2762. https://doi.org/10.1007/s12035-016-9843-0

van Horssen, J., Drexhage, J.A.R., Flor, T., Gerritsen, W., van der Valk, P., de Vries, H.E., 2010. Nrf2 and DJ1 are consistently upregulated in inflammatory multiple sclerosis lesions. Free Radic. Biol. Med. 49, 1283–1289. https://doi.org/10.1016/j.freeradbiomed.2010.07.013

van Horssen, J., van Schaik, P., Witte, M., 2019. Inflammation and mitochondrial dysfunction: A vicious circle

in neurodegenerative disorders? Neurosci. Lett. 710, 132931. https://doi.org/10.1016/j.neulet.2017.06.050

Van Laar, V.S., Berman, S.B., 2013. The interplay of neuronal mitochondrial dynamics and bioenergetics: Implications for Parkinson's disease. Neurobiol. Dis. 51, 43–55. https://doi.org/10.1016/j.nbd.2012.05.015

Vangala, J.R., Sotzny, F., Krüger, E., Deshaies, R.J., Radhakrishnan, S.K., 2016. Nrf1 can be processed and activated in a proteasome-independent manner. Curr. Biol. 26, R834–R835. https://doi.org/10.1016/j.cub.2016.08.008

Vargas, M.R., Johnson, J.A., 2009. The Nrf2–ARE cytoprotective pathway in astrocytes. Expert Rev. Mol. Med. 11, e17. https://doi.org/10.1017/S1462399409001094

Vargas, M.R., Pehar, M., Cassina, P., Beckman, J.S., Barbeito, L., 2006. Increased glutathione biosynthesis by Nrf2 activation in astrocytes prevents p75NTR-dependent motor neuron apoptosis. J. Neurochem. 97, 687–696. https://doi.org/10.1111/j.1471-4159.2006.03742.x

Ved, R., Saha, S., Westlund, B., Perier, C., Burnam, L., Sluder, A., Hoener, M., Rodrigues, C.M.P., Alfonso, A., Steer, C., Liu, L., Przedborski, S., Wolozin, B., 2005. Similar Patterns of Mitochondrial Vulnerability and Rescue Induced by Genetic Modification of α-Synuclein, Parkin, and DJ-1 in Caenorhabditis elegans. J. Biol. Chem. 280, 42655–42668. https://doi.org/10.1074/jbc.M505910200

Veenman, L., Alten, J., Linnemannstöns, K., Shandalov, Y., Zeno, S., Lakomek, M., Gavish, M., Kugler, W., 2010. Potential involvement of F0F1-ATP(synth)ase and reactive oxygen species in apoptosis induction by the antineoplastic agent erucylphosphohomocholine in glioblastoma cell lines. Apoptosis 15, 753–768. https://doi.org/10.1007/s10495-010-0460-5

Veenman, L., Shandalov, Y., Gavish, M., 2008. VDAC activation by the 18 kDa translocator protein (TSPO), implications for apoptosis. J. Bioenerg. Biomembr. 40, 199–205. https://doi.org/10.1007/s10863-008-9142-1

Ventre, M., Netti, P.A., 2016. Engineering Cell Instructive Materials To Control Cell Fate and Functions through Material Cues and Surface Patterning. ACS Appl. Mater. Interfaces 8, 14896–14908. https://doi.org/10.1021/acsami.5b08658

Venugopal, R., Jaiswal, a K., 1996. Nrf1 and Nrf2 positively and c-Fos and Fra1 negatively regulate the human antioxidant response element-mediated expression of NAD(P)H:quinone oxidoreductase1 gene. Proc. Natl. Acad. Sci. U. S. A. 93, 14960–14965. https://doi.org/10.1073/pnas.93.25.14960

Verkhratsky, A., Matteoli, M., Parpura, V., Mothet, J., Zorec, R., 2016. Astrocytes as secretory cells of the central nervous system: idiosyncrasies of vesicular secretion. EMBO J. 35, 239–257. https://doi.org/10.15252/embj.201592705

Verkhratsky, A., Sofroniew, M. V., Messing, A., DeLanerolle, N.C., Rempe, D., Rodríguez, J.J., Nedergaard, M., 2012. Neurological Diseases as Primary Gliopathies: A Reassessment of Neurocentrism. ASN Neuro 4, AN20120010. https://doi.org/10.1042/AN20120010

Verma, R., 2002. Role of Rpn11 Metalloprotease in Deubiquitination and Degradation by the 26S Proteasome. Science (80-.). 298, 611–615. https://doi.org/10.1126/science.1075898

Vilchez, D., Ros, S., Cifuentes, D., Pujadas, L., Vallès, J., García-Fojeda, B., Criado-García, O., Fernández-Sánchez, E., Medraño-Fernández, I., Domínguez, J., García-Rocha, M., Soriano, E., Rodríguez de Córdoba, S., Guinovart, J.J., 2007. Mechanism suppressing glycogen synthesis in neurons and its demise in progressive myoclonus epilepsy. Nat. Neurosci. 10, 1407–1413. https://doi.org/10.1038/nn1998

Vineetha, R.C., Archana, V., Binu, P., Arathi, P., Nair, R.H., 2018. L-Ascorbic Acid and α-Tocopherol Reduces Hepatotoxicity Associated with Arsenic Trioxide Chemotherapy by Modulating Nrf2 and Bcl2 Transcription Factors in Chang liver Cells. Nutr. Cancer 70, 684–696. https://doi.org/10.1080/01635581.2018.1460676

Virga, D.M., Capps, J., Vohra, B.P.S., 2018. Enteric Neurodegeneration is Mediated Through Independent Neuritic and Somal Mechanisms in Rotenone and MPP+ Toxicity. Neurochem. Res. 43, 2288–2303. https://doi.org/10.1007/s11064-018-2649-x

Visanji, N.P., Brotchie, J.M., Kalia, L. V., Koprich, J.B., Tandon, A., Watts, J.C., Lang, A.E., 2016. α-Synuclein-Based Animal Models of Parkinson's Disease: Challenges and Opportunities in a New Era. Trends Neurosci. 39, 750–762. https://doi.org/10.1016/j.tins.2016.09.003

Volterra, A., Meldolesi, J., 2005. Astrocytes, from brain glue to communication elements: the revolution continues. Nat. Rev. Neurosci. 6, 626–640. https://doi.org/10.1038/nrn1722

von Bartheld, C.S., Bahney, J., Herculano-Houzel, S., 2016. The search for true numbers of neurons and glial cells in the human brain: A review of 150 years of cell counting. J. Comp. Neurol. 524, 3865–3895. https://doi.org/10.1002/cne.24040

Voronkov, D.N., Khudoerkov, R.M., Dikalova, Y. V., Sheloukhova, L.I., 2016. Quantitative Evaluation of Changes in the Striatal Astrocyte Axons in Simulated Parkinsonism. Bull. Exp. Biol. Med. 160, 505–509. https://doi.org/10.1007/s10517-016-3208-6

Voronkov, D.N., Salkov, V.N., Anufriev, P.L., Khudoerkov, R.M., 2018. Lewy bodies in Parkinson's disease: histological, immunohistochemical, and interferometric examinations. Arkh. Patol. 80, 9. https://doi.org/10.17116/patol20188049

Vos, M., Verstreken, P., Klein, C., 2015. Stimulation of electron transport as potential novel therapy in Parkinson's disease with mitochondrial dysfunction: Figure 1. Biochem. Soc. Trans. 43, 275–279. https://doi.org/10.1042/BST20140325

Voth, W., Jakob, U., 2017. Stress-Activated Chaperones: A First Line of Defense. Trends Biochem. Sci. 42, 899–913. https://doi.org/10.1016/j.tibs.2017.08.006

Wai, T., Langer, T., 2016. Mitochondrial Dynamics and Metabolic Regulation. Trends Endocrinol. Metab. 27, 105–117. https://doi.org/10.1016/j.tem.2015.12.001

Walden, H., Muqit, M.M.K., 2017. Ubiquitin and Parkinson's disease through the looking glass of genetics. Biochem. J. 474, 1439–1451. https://doi.org/10.1042/BCJ20160498

Walker, L., Stefanis, L., Attems, J., 2019. Clinical and neuropathological differences between Parkinson's disease, Parkinson's disease dementia and dementia with Lewy bodies – current issues and future directions. J. Neurochem. 150, 467–474. https://doi.org/10.1111/jnc.14698

Walsh, C.T., Garneau-Tsodikova, S., Gatto, G.J., 2005. Protein Posttranslational Modifications: The Chemistry of Proteome Diversifications. Angew. Chemie Int. Ed. 44, 7342–7372. https://doi.org/10.1002/anie.200501023

Wang, B., Abraham, N., Gao, G., Yang, Q., 2016. Dysregulation of autophagy and mitochondrial function in Parkinson's disease. Transl. Neurodegener. 5, 19. https://doi.org/10.1186/s40035-016-0065-1

Wang, C., Telpoukhovskaia, M.A., Bahr, B.A., Chen, X., Gan, L., 2018. Endo-lysosomal dysfunction: a converging mechanism in neurodegenerative diseases. Curr. Opin. Neurobiol. 48, 52–58. https://doi.org/10.1016/j.conb.2017.09.005

Wang, D., Qian, L., Xiong, H., Liu, J., Neckameyer, W.S., Oldham, S., Xia, K., Wang, J., Bodmer, R., Zhang, Z., 2006. Antioxidants protect PINK1-dependent dopaminergic neurons in Drosophila. Proc. Natl. Acad. Sci. U. S. A. 103, 13520–5. https://doi.org/10.1073/pnas.0604661103

Wang, F., Awan, U., Wang, Y., Wang, L., Qing, H., Ma, H., Deng, Y., 2014. Damage of Neuroblastoma Cell SH-SY5Y Mediated by MPP+ Inhibits Proliferation of T-Cell Leukemia Jurkat by Co-Culture System. Int. J. Mol. Sci. 15, 10738–10750. https://doi.org/10.3390/ijms150610738

Wang, F., Ni, J., Wang, X., Xie, B., Feng, C., Zhao, S., Saeed, Y., Qing, H., Deng, Y., 2015. Salsolinol Damaged Neuroblastoma SH-SY5Y Cells Induce Proliferation of Human Monocyte THP-1 Cells Through the mTOR Pathway in a Co-culture System. Neurochem. Res. 40, 932–941. https://doi.org/10.1007/s11064-015-1547-8

Wang, H.L., Chou, A.H., Yeh, T.H., Li, A.H., Chen, Y.L., Kuo, Y.L., Tsai, S.R., Yu, S.T., 2007. PINK1 mutants associated with recessive Parkinson's disease are defective in inhibiting mitochondrial release of cytochrome c. Neurobiol. Dis. 28, 216–226. https://doi.org/10.1016/j.nbd.2007.07.010

Wang, J.T., Medress, Z.A., Barres, B.A., 2012. Axon degeneration: Molecular mechanisms of a self-destruction pathway. J. Cell Biol. 196, 7–18. https://doi.org/10.1083/jcb.201108111

Wang, J.T., Yin, L., Chen, Z., 2013. Neuroprotective role of fibronectin in neuron-glial extrasynaptic

transmission. Neural Regen. Res. 8, 376–82. https://doi.org/10.3969/j.issn.1673-5374.2013.04.010

Wang, L., Duan, Q., Wang, T., Ahmed, M., Zhang, N., Li, Y., Li, L., Yao, X., 2015. Mitochondrial Respiratory Chain Inhibitors Involved in ROS Production Induced by Acute High Concentrations of Iodide and the Effects of SOD as a Protective Factor. Oxid. Med. Cell. Longev. 2015, 1–14. https://doi.org/10.1155/2015/217670

Wang, L., Kisaalita, W.S., 2011. Administration of BDNF/ginsenosides combination enhanced synaptic development in human neural stem cells. J. Neurosci. Methods 194, 274–282. https://doi.org/10.1016/j.jneumeth.2010.10.025

Wang, R., Liu, C., 2019. All-trans retinoic acid therapy induces asymmetric division of glioma stem cells from the U87MG cell line. Oncol. Lett. https://doi.org/10.3892/ol.2019.10691

Wang, W., Yang, Y., Ying, C., Li, W., Ruan, H., Zhu, X., You, Y., Han, Y., Chen, R., Wang, Y., Li, M., 2007. Inhibition of glycogen synthase kinase-3β protects dopaminergic neurons from MPTP toxicity. Neuropharmacology 52, 1678–1684. https://doi.org/10.1016/j.neuropharm.2007.03.017

Wang, X.-F., Li, S., Chou, A.P., Bronstein, J.M., 2006. Inhibitory effects of pesticides on proteasome activity: Implication in Parkinson's disease. Neurobiol. Dis. 23, 198–205. https://doi.org/10.1016/j.nbd.2006.02.012

Wang, X., Qin, Z.-H., Leng, Y., Wang, Y., Jin, X., Chase, T.N., Bennett, M.C., 2002. Prostaglandin A1 inhibits rotenone-induced apoptosis in SH-SY5Y cells. J. Neurochem. 83, 1094–1102. https://doi.org/10.1046/j.1471-4159.2002.01224.x

Wang, Y., Branicky, R., Noë, A., Hekimi, S., 2018. Superoxide dismutases: Dual roles in controlling ROS damage and regulating ROS signaling. J. Cell Biol. 217, 1915–1928. https://doi.org/10.1083/jcb.201708007

Waragai, M., Wei, J., Fujita, M., Nakai, M., Ho, G.J., Masliah, E., Akatsu, H., Yamada, T., Hashimoto, M., 2006. Increased level of DJ-1 in the cerebrospinal fluids of sporadic Parkinson's disease. Biochem. Biophys. Res. Commun. 345, 967–972. https://doi.org/10.1016/j.bbrc.2006.05.011

Warburg, O., 1956. On the Origin of Cancer Cells. Science (80-.). 123, 309–314. https://doi.org/10.1126/science.123.3191.309

Warburg, O.H., 2010. The Classic: The Chemical Constitution of Respiration Ferment. Clin. Orthop. Relat. Res. 468, 2833–2839. https://doi.org/10.1007/s11999-010-1534-y

Waris, G., Ahsan, H., 2006. Reactive oxygen species: role in the development of cancer and various chronic conditions. J. Carcinog. 5, 14. https://doi.org/10.1186/1477-3163-5-14

Wei, H., Du, M., Bai, H., 2019. Correlations of Melatonin and Glutathione Levels with Oxidative Stress Mechanism in Parkinson' s Disease. Acta Acad. Med. Sin. 41, 183–187.

https://doi.org/10.3881/j.issn.1000-503X.10775

Wei, P.-C., Lee-Chen, G.-J., Chen, C.-M., Wu, Y.-R., Chen, Y.-J., Lin, J.-L., Lo, Y.-S., Yao, C.-F., Chang, K.-H., 2019. Neuroprotection of Indole-Derivative Compound NC001-8 by the Regulation of the NRF2 Pathway in Parkinson's Disease Cell Models. Oxid. Med. Cell. Longev. 2019, 1–15. https://doi.org/10.1155/2019/5074367

Weids, A.J., Ibstedt, S., Tamás, M.J., Grant, C.M., 2016. Distinct stress conditions result in aggregation of proteins with similar properties. Sci. Rep. 6, 24554. https://doi.org/10.1038/srep24554

Wellman, S.M., Eles, J.R., Ludwig, K.A., Seymour, J.P., Michelson, N.J., McFadden, W.E., Vazquez, A.L., Kozai, T.D.Y., 2018. A Materials Roadmap to Functional Neural Interface Design. Adv. Funct. Mater. 28, 1701269. https://doi.org/10.1002/adfm.201701269

Wells, R.G., 2008. The role of matrix stiffness in regulating cell behavior. Hepatology 47, 1394–1400. https://doi.org/10.1002/hep.22193

Wenzel, U., 2003. Ascorbic acid suppresses drug-induced apoptosis in human colon cancer cells by scavenging mitochondrial superoxide anions. Carcinogenesis 25, 703–712. https://doi.org/10.1093/carcin/bgh079

Werber, J., Wang, Y.J., Milligan, M., Li, X., Ji, J.A., 2011. Analysis of 2,2'-Azobis (2-amidinopropane) dihydrochloride degradation and hydrolysis in aqueous solutions. J. Pharm. Sci. 100, 3307–3315. https://doi.org/10.1002/jps.22578

Wilkinson, K.D., 1995. Roles of ubiquitinylation in proteolysis and cellular regulation. Annu. Rev. Nutr. 15, 161–89. https://doi.org/10.1146/annurev.nu.15.070195.001113

Wilkinson, K.D., Lee, K.M., Deshpande, S., Duerksen-Hughes, P., Boss, J.M., Pohl, J., 1989. The neuron-specific protein PGP 9.5 is a ubiquitin carboxyl-terminal hydrolase. Science 246, 670–673. https://doi.org/10.1126/science.2530630

Wilson, J., 1997. Antioxidant defense of the brain: a role for astrocytes. Can. J. Physiol. Pharmacol. 75, 1149–63.

Wilton, D.K., Dissing-Olesen, L., Stevens, B., 2019. Neuron-Glia Signaling in Synapse Elimination. Annu. Rev. Neurosci. 42, 107–127. https://doi.org/10.1146/annurev-neuro-070918-050306

Winklhofer, K.F., Henn, I.H., Kay-Jackson, P.C., Heller, U., Tatzelt, J., 2003. Inactivation of parkin by oxidative stress and C-terminal truncations: A protective role of molecular chaperones. J. Biol. Chem. 278, 47199–47208. https://doi.org/10.1074/jbc.M306769200

Winterbourn, C.C., 2015. Are free radicals involved in thiol-based redox signaling? Free Radic. Biol. Med. 80, 164–170. https://doi.org/10.1016/j.freeradbiomed.2014.08.017

Winterbourn, C.C., 2008. Reconciling the chemistry and biology of reactive oxygen species. Nat. Chem. Biol. 4, 278–286. https://doi.org/10.1038/nchembio.85

Winterbourn, C.C., Hampton, M.B., 2008. Thiol chemistry and specificity in redox signaling. Free Radic. Biol. Med. 45, 549–561. https://doi.org/10.1016/j.freeradbiomed.2008.05.004

Wood-Kaczmar, A., Gandhi, S., Yao, Z., Abramov, A.S.Y., Miljan, E.A., Keen, G., Stanyer, L., Hargreaves, I., Klupsch, K., Deas, E., Downward, J., Mansfield, L., Jat, P., Taylor, J., Heales, S., Duchen, M.R., Latchman, D., Tabrizi, S.J., Wood, N.W., 2008. PINK1 Is Necessary for Long Term Survival and Mitochondrial Function in Human Dopaminergic Neurons. PLoS One 3, e2455. https://doi.org/10.1371/journal.pone.0002455

Worden, E.J., Padovani, C., Martin, A., 2014. Structure of the Rpn11–Rpn8 dimer reveals mechanisms of substrate deubiquitination during proteasomal degradation. Nat. Struct. Mol. Biol. 21, 220–227. https://doi.org/10.1038/nsmb.2771

Wortmann, M., Schneider, M., Pircher, J., Hellfritsch, J., Aichler, M., Vegi, N., Kölle, P., Kuhlencordt, P., Walch, A., Pohl, U., Bornkamm, G.W., Conrad, M., Beck, H., 2013. Combined Deficiency in Glutathione Peroxidase 4 and Vitamin E Causes Multiorgan Thrombus Formation and Early Death in Mice. Circ. Res. 113, 408–417. https://doi.org/10.1161/CIRCRESAHA.113.279984

Wyss-Coray, T., Mucke, L., 2002. Inflammation in Neurodegenerative Disease—A Double-Edged Sword. Neuron 35, 419–432. https://doi.org/10.1016/S0896-6273(02)00794-8

Xia, C., Taylor, J.B., Spencer, S.R., Ketterer, B., 1993. The human glutathione S-transferase P1-1 gene: modulation of expression by retinoic acid and insulin. Biochem. J. 292 (Pt 3, 845–50. https://doi.org/10.1042/bj2920845

Xia, L., Wurmbach, E., Waxman, S., Jing, Y., 2006. Upregulation of Bfl-1/A1 in leukemia cells undergoing differentiation by all-trans retinoic acid treatment attenuates chemotherapeutic agent-induced apoptosis. Leukemia 20, 1009–1016. https://doi.org/10.1038/sj.leu.2404198

Xicoy, H., Wieringa, B., Martens, G.J.M., 2017. The SH-SY5Y cell line in Parkinson's disease research: a systematic review. Mol. Neurodegener. 12, 10. https://doi.org/10.1186/s13024-017-0149-0

Xu, C.-Y., Kang, W.-Y., Chen, Y.-M., Jiang, T.-F., Zhang, J., Zhang, L.-N., Ding, J.-Q., Liu, J., Chen, S.-D., 2017a. DJ-1 Inhibits α-Synuclein Aggregation by Regulating Chaperone-Mediated Autophagy. Front. Aging Neurosci. 9, 308. https://doi.org/10.3389/fnagi.2017.00308

Xu, C.-Y., Kang, W.-Y., Chen, Y.-M., Jiang, T.-F., Zhang, J., Zhang, L.-N., Ding, J.-Q., Liu, J., Chen, S.-D., 2017b. DJ-1 Inhibits α-Synuclein Aggregation by Regulating Chaperone-Mediated Autophagy. Front. Aging Neurosci. 9, 308. https://doi.org/10.3389/fnagi.2017.00308

Xu, S., Peng, G., Wang, Y., Fang, S., Karbowski, M., 2011. The AAA-ATPase p97 is essential for outer

mitochondrial membrane protein turnover. Mol. Biol. Cell 22, 291–300. https://doi.org/10.1091/mbc.e10-09-0748

Xu, Y.-M., Huang, D.-Y., Chiu, J.-F., Lau, A.T.Y., 2012. Post-Translational Modification of Human Heat Shock Factors and Their Functions: A Recent Update by Proteomic Approach. J. Proteome Res. 11, 2625–2634. https://doi.org/10.1021/pr201151a

Xun, Z., Lee, D.-Y., Lim, J., Canaria, C.A., Barnebey, A., Yanonne, S.M., McMurray, C.T., 2012. Retinoic acid-induced differentiation increases the rate of oxygen consumption and enhances the spare respiratory capacity of mitochondria in SH-SY5Y cells. Mech. Ageing Dev. 133, 176–185. https://doi.org/10.1016/j.mad.2012.01.008

Y., L., S., L., Y., Y., Z.J., B., 2016. Insufficient astrocyte-derived BDNF contributes to propofol-induced neuron death through AKT/GSK3beta/mitochondrial fission pathway in rats. Anesth. Analg.

Yakhine-Diop, S.M.S., Niso-Santano, M., Rodríguez-Arribas, M., Gómez-Sánchez, R., Martínez-Chacón, G., Uribe-Carretero, E., Navarro-García, J.A., Ruiz-Hurtado, G., Aiastui, A., Cooper, J.M., López de Munaín, A., Bravo-San Pedro, J.M., González-Polo, R.A., Fuentes, J.M., 2019. Impaired Mitophagy and Protein Acetylation Levels in Fibroblasts from Parkinson's Disease Patients. Mol. Neurobiol. 56, 2466–2481. https://doi.org/10.1007/s12035-018-1206-6

Yamamoto, T., Maruyama, W., Kato, Y., Yi, H., Shamoto-Nagai, M., Tanaka, M., Sato, Y., Naoi, M., 2002. Selective nitration of mitochondrial complex I by peroxynitrite: involvement in mitochondria dysfunction and cell death of dopaminergic SH-SY5Y cells. J. Neural Transm. 109, 1–13. https://doi.org/10.1007/s702-002-8232-1

Yang, J.-W., Rodrigo, R., Felipo, V., Lubec, G., 2005. Proteome Analysis of Primary Neurons and Astrocytes from Rat Cerebellum. J. Proteome Res. 4, 768–788. https://doi.org/10.1021/pr049774v

Yang, W., Li, S., Li, X.-J., 2019. A CRISPR monkey model unravels a unique function of PINK1 in primate brains. Mol. Neurodegener. 14, 17. https://doi.org/10.1186/s13024-019-0321-9

Yao, D., Gu, Z., Nakamura, T., Shi, Z.-Q., Ma, Y., Gaston, B., Palmer, L.A., Rockenstein, E.M., Zhang, Z., Masliah, E., Uehara, T., Lipton, S.A., 2004. Nitrosative stress linked to sporadic Parkinson's disease: S-nitrosylation of parkin regulates its E3 ubiquitin ligase activity. Proc. Natl. Acad. Sci. https://doi.org/10.1073/pnas.0404161101

Yeh, T.-H., Lee, D.Y., Gianino, S.M., Gutmann, D.H., 2009. Microarray analyses reveal regional astrocyte heterogeneity with implications for neurofibromatosis type 1 (NF1)-regulated glial proliferation. Glia 57, 1239–1249. https://doi.org/10.1002/glia.20845

Yeung, T., Georges, P.C., Flanagan, L.A., Marg, B., Ortiz, M., Funaki, M., Zahir, N., Ming, W., Weaver, V., Janmey, P.A., 2005. Effects of substrate stiffness on cell morphology, cytoskeletal structure, and adhesion. Cell Motil. Cytoskeleton 60, 24–34. https://doi.org/10.1002/cm.20041

Yin, P., Knolhoff, A.M., Rosenberg, H.J., Millet, L.J., Gillette, M.U., Sweedler, J. V., 2012. Peptidomic Analyses of Mouse Astrocytic Cell Lines and Rat Primary Cultured Astrocytes. J. Proteome Res. 11, 3965–3973. https://doi.org/10.1021/pr201066t

Yokota, T., Sugawara, K., Ito, K., Takahashi, R., Ariga, H., Mizusawa, H., 2003. Down regulation of DJ-1 enhances cell death by oxidative stress, ER stress, and proteasome inhibition. Biochem. Biophys. Res. Commun. 312, 1342–1348. https://doi.org/10.1016/j.bbrc.2003.11.056

Yokoyama, Y., Maruyama, K., Yamamoto, K., Omodaka, K., Yasuda, M., Himori, N., Ryu, M., Nishiguchi, K.M., Nakazawa, T., 2014. The role of calpain in an in vivo model of oxidative stress-induced retinal ganglion cell damage. Biochem. Biophys. Res. Commun. 451, 510–515. https://doi.org/10.1016/j.bbrc.2014.08.009

Yokozawa, T., Cho, E.J., Hara, Y., Kitani, K., 2000. Antioxidative activity of green tea treated with radical initiator 2, 2'-azobis(2-amidinopropane) dihydrochloride. J. Agric. Food Chem. 48, 5068–5073.

Yoon, I.S., Au, Q., Barber, J.R., Ng, S.C., Zhang, B., 2010. Development of a high-throughput screening assay for cytoprotective agents in rotenone-induced cell death. Anal. Biochem. 407, 205–210. https://doi.org/10.1016/j.ab.2010.08.011

Yoshida, H., Mimura, J., Imaizumi, T., Matsumiya, T., Ishikawa, A., Metoki, N., Tanji, K., Ota, K., Hayakari, R., Kosaka, K., Itoh, K., Satoh, K., 2011. Edaravone and carnosic acid synergistically enhance the expression of nerve growth factor in human astrocytes under hypoxia/reoxygenation. Neurosci. Res. 69, 291–298. https://doi.org/10.1016/j.neures.2010.12.016

Yoshii, S.R., Kishi, C., Ishihara, N., Mizushima, N., 2011. Parkin Mediates Proteasome-dependent Protein Degradation and Rupture of the Outer Mitochondrial Membrane. J. Biol. Chem. 286, 19630–19640. https://doi.org/10.1074/jbc.M110.209338

Youle, R.J., Narendra, D.P., 2011. Mechanisms of mitophagy. Nat. Rev. Mol. Cell Biol. 12, 9–14. https://doi.org/10.1038/nrm3028

Yu, B., Changsheng, Y., Wenjun, Z., Ben, L., Hai, Q., Jing, M., Guangwei, X., Shuhua, W., Fang, L., Aschner, M., Rongzhu, L., 2015. Differential protection of pre- versus post-treatment with curcumin, Trolox, and N -acetylcysteine against acrylonitrile-induced cytotoxicity in primary rat astrocytes. Neurotoxicology 51, 58–66. https://doi.org/10.1016/j.neuro.2015.09.011

Yu, H., Pan, W.-K., Zheng, B.-J., Wang, H.-J., Chen, X.-L., Liu, Y., Gao, Y., 2016. Decreased proliferative, migrative and neuro-differentiative potential of postnatal rat enteric neural crest-derived cells during culture in vitro. Exp. Cell Res. 343, 218–222. https://doi.org/10.1016/j.yexcr.2016.04.005

Yudkoff, M., Pleasure, D., Cregar, L., Lin, Z.-P., Nissim, Ilana, Stern, J., Nissim, Itzhak, 1990. Glutathione Turnover in Cultured Astrocytes: Studies with [15 N]Glutamate. J. Neurochem. 55, 137–145. https://doi.org/10.1111/j.1471-4159.1990.tb08831.x

Zabłocka, A., Mitkiewicz, M., Macała, J., Janusz, M., 2015. Neurotrophic Activity of Cultured Cell Line U87 is Up-Regulated by Proline-Rich Polypeptide Complex and Its Constituent Nonapeptide. Cell. Mol. Neurobiol. 35, 977–986. https://doi.org/10.1007/s10571-015-0192-8

Zagoura, D., Canovas-Jorda, D., Pistollato, F., Bremer-Hoffmann, S., Bal-Price, A., 2017. Evaluation of the rotenone-induced activation of the Nrf2 pathway in a neuronal model derived from human induced pluripotent stem cells. Neurochem. Int. 106, 62–73. https://doi.org/10.1016/j.neuint.2016.09.004

Zakharova, I., Sokolova, T., Vlasova, Y., Bayunova, L., Rychkova, M., Avrova, N., 2017. α-Tocopherol at Nanomolar Concentration Protects Cortical Neurons against Oxidative Stress. Int. J. Mol. Sci. 18, 216. https://doi.org/10.3390/ijms18010216

Zarkovic, K., 2003. 4-Hydroxynonenal and neurodegenerative diseases, in: Molecular Aspects of Medicine. pp. 293–303. https://doi.org/10.1016/S0098-2997(03)00024-4

Zelko, I.N., Mariani, T.J., Folz, R.J., 2002. Superoxide dismutase multigene family: a comparison of the CuZn-SOD (SOD1), Mn-SOD (SOD2), and EC-SOD (SOD3) gene structures, evolution, and expression. Free Radic. Biol. Med. 33, 337–349. https://doi.org/10.1016/S0891-5849(02)00905-X

Zeviani, M., 2004. Mitochondrial disorders. Brain 127, 2153–2172. https://doi.org/10.1093/brain/awh259

Zhang, C.-W., Adeline, H.B., Chai, B.-H., Hong, E.T.E., Ng, C.-H., Lim, K.-L., 2016. Pharmacological or Genetic Activation of Hsp70 Protects against Loss of Parkin Function. Neurodegener. Dis. 16, 304–316. https://doi.org/10.1159/000443668

Zhang, D.D., Hannink, M., 2003. Distinct Cysteine Residues in Keap1 Are Required for Keap1-Dependent Ubiquitination of Nrf2 and for Stabilization of Nrf2 by Chemopreventive Agents and Oxidative Stress. Mol. Cell. Biol. 23, 8137–8151. https://doi.org/10.1128/MCB.23.22.8137-8151.2003

Zhang, J., Ney, P.A., 2009. Role of BNIP3 and NIX in cell death, autophagy, and mitophagy. Cell Death Differ. 16, 939–946. https://doi.org/10.1038/cdd.2009.16

Zhang, L., Bartley, C.M., Gong, X., Hsieh, L.S., Lin, T. V., Feliciano, D.M., Bordey, A., 2014. MEK-ERK1/2-Dependent FLNA Overexpression Promotes Abnormal Dendritic Patterning in Tuberous Sclerosis Independent of mTOR. Neuron 84, 78–91. https://doi.org/10.1016/j.neuron.2014.09.009

Zhang, L., Shimoji, M., Thomas, B., Moore, D.J., Yu, S.-W., Marupudi, N.I., Torp, R., Torgner, I.A., Ottersen, O.P., Dawson, T.M., Dawson, V.L., 2005. Mitochondrial localization of the Parkinson's disease related protein DJ-1: implications for pathogenesis. Hum. Mol. Genet. 14, 2063–2073. https://doi.org/10.1093/hmg/ddi211

Zhang, R., Xu, M., Wang, Y., Xie, F., Zhang, G., Qin, X., 2017. Nrf2—a Promising Therapeutic Target for Defensing Against Oxidative Stress in Stroke. Mol. Neurobiol. 54, 6006–6017. https://doi.org/10.1007/s12035-016-0111-0

Zhang, S., Eitan, E., Mattson, M.P., 2017. Early involvement of lysosome dysfunction in the degeneration of cerebral cortical neurons caused by the lipid peroxidation product 4-hydroxynonenal. J. Neurochem. 140, 941–954. https://doi.org/10.1111/jnc.13957

Zhang, X.-L., Yuan, Y.-H., Shao, Q.-H., Wang, Z.-Z., Zhu, C.-G., Shi, J.-G., Ma, K.-L., Yan, X., Chen, N.-H., 2017. DJ-1 regulating PI3K-Nrf2 signaling plays a significant role in bibenzyl compound 20C-mediated neuroprotection against rotenone-induced oxidative insult. Toxicol. Lett. 271, 74–83. https://doi.org/10.1016/j.toxlet.2017.02.022

Zhang, Y., Sloan, S.A., Clarke, L.E., Caneda, C., Plaza, C.A., Blumenthal, P.D., Vogel, H., Steinberg, G.K., Edwards, M.S.B., Li, G., Duncan, J.A., Cheshier, S.H., Shuer, L.M., Chang, E.F., Grant, G.A., Gephart, M.G.H., Barres, B.A., 2016. Purification and Characterization of Progenitor and Mature Human Astrocytes Reveals Transcriptional and Functional Differences with Mouse. Neuron 89, 37–53. https://doi.org/10.1016/j.neuron.2015.11.013

Zhang, Z., Liu, L., Jiang, X., Zhai, S., Xing, D., 2016. The Essential Role of Drp1 and Its Regulation by S-Nitrosylation of Parkin in Dopaminergic Neurodegeneration: Implications for Parkinson's Disease. Antioxid. Redox Signal. 25, 609–622. https://doi.org/10.1089/ars.2016.6634

Zhao, J., Yu, S., Zheng, Y., Yang, H., Zhang, J., 2017. Oxidative Modification and Its Implications for the Neurodegeneration of Parkinson's Disease. Mol. Neurobiol. https://doi.org/10.1007/s12035-016-9743-3

Zheng, B., Liao, Z., Locascio, J.J., Lesniak, K.A., Roderick, S.S., Watt, M.L., Eklund, A.C., Zhang-James, Y., Kim, P.D., Hauser, M.A., Grünblatt, E., Moran, L.B., Mandel, S.A., Riederer, P., Miller, R.M., Federoff, H.J., Wüllner, U., Papapetropoulos, S., Youdim, M.B., Cantuti-Castelvetri, I., Young, A.B., Vance, J.M., Davis, R.L., Hedreen, J.C., Adler, C.H., Beach, T.G., Graeber, M.B., Middleton, F.A., Rochet, J.-C., Scherzer, C.R., Global PD Gene Expression (GPEX) Consortium, 2010. PGC-1α, a potential therapeutic target for early intervention in Parkinson's disease. Sci. Transl. Med. 2, 52–73. https://doi.org/10.1126/scitranslmed.3001059

Zheng, L., Michelson, Y., Freger, V., Avraham, Z., Venken, K.J.T., Bellen, H.J., Justice, M.J., Wides, R., 2011. Drosophila Ten-m and Filamin Affect Motor Neuron Growth Cone Guidance. PLoS One 6, e22956. https://doi.org/10.1371/journal.pone.0022956

ZHU, L., BI, W., LU, DAN, ZHANG, C., SHU, X., LU, DAXIANG, 2014. Luteolin inhibits SH-SY5Y cell apoptosis through suppression of the nuclear transcription factor-κB, mitogen-activated protein kinase and protein kinase B pathways in lipopolysaccharide-stimulated cocultured BV2 cells. Exp. Ther. Med. 7, 1065–1070. https://doi.org/10.3892/etm.2014.1564

Zimmermann, M., Gardoni, F., Marcello, E., Colciaghi, F., Borroni, B., Padovani, A., Cattabeni, F., Di Luca, M., 2004. Acetylcholinesterase inhibitors increase ADAM10 activity by promoting its trafficking in

neuroblastoma cell lines. J. Neurochem. 90, 1489–1499. https://doi.org/10.1111/j.1471-4159.2004.02680.x

Zuo, L., Koozechian, M.S., Chen, L.L., 2014. Characterization of reactive nitrogen species in allergic asthma. Ann. Allergy, Asthma Immunol. 112, 18–22. https://doi.org/10.1016/j.anai.2013.10.007

Zuo, L., Zhou, T., Pannell, B.K., Ziegler, A.C., Best, T.M., 2015. Biological and physiological role of reactive oxygen species - the good, the bad and the ugly. Acta Physiol. 214, 329–348. https://doi.org/10.1111/apha.12515

Aberle, H., Bauer, A., Stappert, J., Kispert, A., Kemler, R., 1997. β-catenin is a target for the ubiquitin-proteasome pathway. EMBO J. 16, 3797–804. https://doi.org/10.1093/emboj/16.13.3797

Abouelfetouh, A., Kondoh, T., Ehara, K., Kohmura, E., 2004. Morphological differentiation of bone marrow stromal cells into neuron-like cells after co-culture with hippocampal slice. Brain Res. 1029, 114–9. https://doi.org/10.1016/j.brainres.2004.07.092

Abramov, A.Y., 2004. β-Amyloid Peptides Induce Mitochondrial Dysfunction and Oxidative Stress in Astrocytes and Death of Neurons through Activation of NADPH Oxidase. J. Neurosci. 24, 565–75. https://doi.org/10.1523/jneurosci.4042-03.2004

Abramov, A.Y., Canevari, L., Duchen, M.R., 2003. Changes in intracellular calcium and glutathione in astrocytes as the primary mechanism of amyloid neurotoxicity. J. Neurosci. 23, 5088–95.

Adalbert, R., Coleman, M.P., 2013. Review: Axon pathology in age-related neurodegenerative disorders. Neuropathol. Appl. Neurobiol. 39, 90–108. https://doi.org/10.1111/j.1365-2990.2012.01308.x

Ahn, S.G., Thiele, D.J., 2003. Redox regulation of mammalian heat shock factor 1 is essential for Hsp gene activation and protection from stress. Genes Dev. 17, 516–28. https://doi.org/10.1101/gad.1044503

Åkerfelt, M., Trouillet, D., Mezger, V., Sistonen, L., 2007. Heat shock factors at a crossroad between stress and development, in: Annals of the New York Academy of Sciences. pp. 15–27. https://doi.org/10.1196/annals.1391.005

Åkerman, K.E.O., Scott, I.G., Andersson, L.C., 1984. Functional differentiation of a human ganglion cell derived neuroblastoma cell line SH-SY5Y induced by a phorbol ester (TPA). Neurochem. Int. 6, 77–80. https://doi.org/10.1016/0197-0186(84)90029-9

Alam, J., Stewart, D., Touchard, C., Boinapally, S., Choi, a M., Cook, J.L., 1999. Nrf2, a Cap'n'Collar transcription factor, regulates induction of the heme oxygenase-1 gene. J. Biol. Chem. 274, 26071–26078. https://doi.org/10.1074/jbc.274.37.26071

Alam, Z.I., Daniel, S.E., Lees, A.J., Marsden, D.C., Jenner, P., Halliwell, B., 1997. A generalised increase in protein carbonyls in the brain in Parkinson's but not incidental Lewy body disease. J. Neurochem. 69, 1326–1329. https://doi.org/10.1046/j.1471-4159.1997.69031326.x

Allaman, I., Bélanger, M., Magistretti, P.J., 2011. Astrocyte-neuron metabolic relationships: For better and for worse. Trends Neurosci. https://doi.org/10.1016/j.tins.2010.12.001

Allani, P.K., Sum, T., Bhansali, S.G., Mukherjee, S.K., Sonee, M., 2004. A comparative study of the effect of oxidative stress on the cytoskeleton in human cortical neurons. Toxicol. Appl. Pharmacol. 196, 29–36. https://doi.org/10.1016/j.taap.2003.12.010

Allen, M., Bjerke, M., Edlund, H., Nelander, S., Westermark, B., 2016. Origin of the U87MG glioma cell line: Good news and bad news. Sci. Transl. Med. 8, 354–7. https://doi.org/10.1126/scitranslmed.aaf6853

Allen, N.J., Barres, B.A., 2005. Signaling between glia and neurons: Focus on synaptic plasticity. Curr. Opin. Neurobiol. https://doi.org/10.1016/j.conb.2005.08.006

Amin, J., Ananthan, J., Voellmy, R., 1988. Key features of heat shock regulatory elements. Mol. Cell. Biol. 8, 3761–9. https://doi.org/10.1128/MCB.8.9.3761

Amor, S., Peferoen, L.A.N., Vogel, D.Y.S., Breur, M., van der Valk, P., Baker, D., van Noort, J.M., 2014. Inflammation in neurodegenerative diseases - an update. Immunology 142, 151–166. https://doi.org/10.1111/imm.12233

Anckar, J., Sistonen, L., 2011. Regulation of HSF 1 Function in the Heat Stress Response: Implications in Aging and Disease. Annu. Rev. Biochem. 80, 1089–115. https://doi.org/10.1146/annurev-biochem-060809-095203

Anckar, J., Sistonen, L., 2007. Heat shock factor 1 as a coordinator of stress and developmental pathways. Adv. Exp. Med. Biol. https://doi.org/10.1007/978-0-387-39975-1_8

Andreazza, A.C., Shao, L., Wang, J.-F., Young, L.T., 2010. Mitochondrial Complex I Activity and Oxidative Damage to Mitochondrial Proteins in the Prefrontal Cortex of Patients With Bipolar Disorder. Arch. Gen. Psychiatry 67, 360–8. https://doi.org/10.1001/archgenpsychiatry.2010.22

Angeli, J.P.F., Shah, R., Pratt, D.A., Conrad, M., 2017. Ferroptosis Inhibition: Mechanisms and Opportunities. Trends Pharmacol. Sci. https://doi.org/10.1016/j.tips.2017.02.005

Angelova, P.R., Horrocks, M.H., Klenerman, D., Gandhi, S., Abramov, A.Y., Shchepinov, M.S., 2015. Lipid peroxidation is essential for α-synuclein-induced cell death. J. Neurochem. 133, 582–9. https://doi.org/10.1111/jnc.13024

Anglade, P., 1997. Apoptosis and autophagy in nigral neurons of patients with Parkinson's disease. Histol. Histopathol. 12, 25–31.

Aon, M.A., Cortassa, S., Juhaszova, M., Sollott, S.J., 2016. Mitochondrial health, the epigenome and healthspan. Clin. Sci. 130, 1285–305. https://doi.org/10.1042/CS20160002

Ara, J., Przedborski, S., Naini, a B., Jackson-Lewis, V., Trifiletti, R.R., Horwitz, J., Ischiropoulos, H., 1998. Inactivation of tyrosine hydroxylase by nitration following exposure to peroxynitrite and 1-methyl-4-phenyl-1,2,3,6-tetrahydropyridine (MPTP). Proc. Natl. Acad. Sci. U. S. A. 95, 7659–7663. https://doi.org/10.1073/pnas.95.13.7659

Araki, T., Sasaki, Y., Milbrandt, J., 2004. Increased nuclear NAD biosynthesis and SIRT1 activation prevent axonal degeneration. Science (80-.). 205, 1010–3. https://doi.org/10.1126/science.1098014

Araque, A., 2008. Astrocytes process synaptic information. Neuron Glia Biol. 4, 3–10. https://doi.org/10.1017/s1740925x09000064

Araque, A., Carmignoto, G., Haydon, P.G., Oliet, S.H.R., Robitaille, R., Volterra, A., 2014. Gliotransmitters travel in time and space. Neuron. https://doi.org/10.1016/j.neuron.2014.02.007

Arbore, G., Kemper, C., Kolev, M., 2017. Intracellular complement – the complosome – in immune cell regulation. Mol. Immunol. https://doi.org/10.1016/j.molimm.2017.05.012

Arcangeli, A., Rosati, B., Crociani, O., Cherubini, A., Fontana, L., Passani, B., Wanke, E., Olivotto, M., 1999. Modulation of HERG current and herg gene expression during retinoic acid treatment of human neuroblastoma cells: Potentiating effects of BDNF. J. Neurobiol. 40, 214–25. https://doi.org/10.1002/(SICI)1097-4695(199908)40:2<214::AID-NEU7>3.0.CO;2-0

Armstrong, D., Browne, R., 1994. The Analysis of Free Radicals, Lipid Peroxides, Antioxidant Enzymes and Compounds Related to Oxidative Stress as Applied to the Clinical Chemistry Laboratory, in: 366. pp. 43–58. https://doi.org/10.1007/978-1-4615-1833-4_4

Au, Q., Kanchanastit, P., Barber, J.R., Ng, S.C., Zhang, B., 2008. High-content image-based screening for small-molecule chaperone amplifiers in heat shock. J. Biomol. Screen. 13, 953–9. https://doi.org/10.1177/1087057108326538

Auluck, P.K., Chan, H.Y.E., Trojanowski, J.Q., Lee, V.M.Y., Bonini, N.M., 2002. Chaperone suppression of alpha-synuclein toxicity in a Drosophila model for Parkinson's disease. Science 295, 865–8. https://doi.org/10.1126/science.1067389

Awasthi, Y.C., Sharma, R., Cheng, J.Z., Yang, Y., Sharma, A., Singhal, S.S., Awasthi, S., 2003. Role of 4-hydroxynonenal in stress-mediated apoptosis signaling, in: Molecular Aspects of Medicine. pp. 219–230. https://doi.org/10.1016/S0098-2997(03)00017-7

Bach, A.W., Lan, N.C., Johnson, D.L., Abell, C.W., Bembenek, M.E., Kwan, S.W., Seeburg, P.H., Shih, J.C., 1988. cDNA cloning of human liver monoamine oxidase A and B: molecular basis of differences in enzymatic properties. Proc Natl Acad Sci U S A 85, 4934–4938.

Bagri, A., Cheng, H.J., Yaron, A., Pleasure, S.J., Tessier-Lavigne, M., 2003. Stereotyped pruning of long hippocampal axon branches triggered by retraction inducers of the semaphorin family. Cell 113, 285–99. https://doi.org/10.1016/S0092-8674(03)00267-8

Balchin, D., Hayer-Hartl, M., Hartl, F.U., 2016. In vivo aspects of protein folding and quality control. Science (80-.). https://doi.org/10.1126/science.aac4354

Balgude, A.P., Yu, X., Szymanski, A., Bellamkonda, R. V, 2001. Agarose gel stiffness determines rate of DRG neurite extension in 3D cultures. Biomaterials 22, 1077–84.

Ballard, P.A., Tetrud, J.W., Langston, J.W., 1985. Permanent human parkinsonism due to 1-methyl-4-phenyl-1,2,3,6-tetrahydropyridine (MPTP): seven cases. Neurology 35, 949–56. https://doi.org/10.1212/WNL.35.7.949

Bandopadhyay, R., Kingsbury, A.E., Cookson, M.R., Reid, A.R., Evans, I.M., Hope, A.D., Pittman, A.M., Lashley, T., Canet-Aviles, R., Miller, D.W., McLendon, C., Strand, C., Leonard, A.J., Abou-Sleiman, P.M., Healy, D.G., Ariga, H., Wood, N.W., De Silva, R., Revesz, T., Hardy, J.A., Lees, A.J., 2004. The expression of DJ-1 (PARK7) in normal human CNS and idiopathic Parkinson's disease. Brain 127, 420–30. https://doi.org/10.1093/brain/awh054

Banker, G.A., 1980. Trophic interactions between astroglial cells and hippocampal neurons in culture. Science (80-.). 209, 809–10. https://doi.org/10.1126/science.7403847

Barcia, C., Sánchez Bahillo, A., Fernández-Villalba, E., Bautista, V., Poza Y Poza, M., Fernández-Barreiro, A., Hirsch, E.C., Herrero, M.T., 2004. Evidence of active microglia in substantia nigra pars compacta of parkinsonian monkeys 1 year after MPTP exposure. Glia 46, 402–409. https://doi.org/10.1002/glia.20015

Barja, G., López-Torres, M., Pérez-Campo, R., Rojas, C., Cadenas, S., Prat, J., Pamplona, R., 1994. Dietary vitamin C decreases endogenous protein oxidative damage, malondialdehyde, and lipid peroxidation and maintains fatty acid unsaturation in the guinea pig liver. Free Radic. Biol. Med. 17, 105–15. https://doi.org/10.1016/0891-5849(94)90108-2

Barkho, B.Z., Song, H., Aimone, J.B., Smrt, R.D., Kuwabara, T., Nakashima, K., Gage, F.H., Zhao, X., 2006. Identification of Astrocyte-expressed Factors That Modulate Neural Stem/Progenitor Cell Differentiation. Stem Cells Dev. 15, 407–21. https://doi.org/10.1089/scd.2006.15.407

Barrera, G., Pizzimenti, S., Ciamporcero, E.S., Daga, M., Ullio, C., Arcaro, A., Cetrangolo, G.P., Ferretti, C., Dianzani, C., Lepore, A., Gentile, F., 2015. Role of 4-Hydroxynonenal-Protein Adducts in Human Diseases. Antioxid. Redox Signal. 22, 1681–702. https://doi.org/10.1089/ars.2014.6166

Bassett, C.N., Neely, M.D., Sidell, K.R., Markesbery, W.R., Swift, L.L., Montine, T.J., 1999. Cerebrospinal fluid lipoproteins are more vulnerable to oxidation in Alzheimer's disease and are neurotoxic when oxidized ex vivo. Lipids 34, 1273–80. https://doi.org/10.1007/s11745-999-0478-1

Baxter, P.S., Hardingham, G.E., 2016. Adaptive regulation of the brain's antioxidant defences by neurons and astrocytes. Free Radic. Biol. Med. 100, 147–52. https://doi.org/10.1016/j.freeradbiomed.2016.06.027

Beach, T.G., Sue, L.I., Walker, D.G., Lue, L.F., Connor, D.J., Caviness, J.N., Sabbagh, M.N., Adler, C.H., 2007. Marked microglial reaction in normal aging human substantia nigra: Correlation with extraneuronal neuromelanin pigment deposits. Acta Neuropathol. 114, 419–424. https://doi.org/10.1007/s00401-007-0250-5

Beal, M.F., 2003. Mitochondria, oxidative damage, and inflammation in Parkinson's disease. Ann. N. Y. Acad. Sci. 991, 120–31. https://doi.org/10.1111/j.1749-6632.2003.tb07470.x

Beck, K.E., De Girolamo, L.A., Griffin, M., Billett, E.E., 2006. The role of tissue transglutaminase in 1-methyl-4-phenylpyridinium (MPP+)-induced toxicity in differentiated human SH-SY5Y neuroblastoma cells. Neurosci. Lett. 405, 46–51. https://doi.org/10.1016/j.neulet.2006.06.061

Beckwith, R., Estrin, E., Worden, E.J., Martin, A., 2013. Reconstitution of the 26S proteasome reveals functional asymmetries in its AAA+ unfoldase. Nat. Struct. Mol. Biol. 20, 1164–72. https://doi.org/10.1038/nsmb.2659

Bedford, L., Paine, S., Sheppard, P.W., Mayer, R.J., Roelofs, J., 2010. Assembly, structure, and function of the 26S proteasome. Trends Cell Biol. 20, 391–401. https://doi.org/10.1016/j.tcb.2010.03.007

Beere, H.M., Wolf, B.B., Cain, K., Mosser, D.D., Mahboubi, A., Kuwana, T., Tailor, P., Morimoto, R.I., Cohen, G.M., Green, D.R., 2000. Heat-shock protein 70 inhibits apoptosis by preventing recruitment of procaspase-9 to the Apaf-1 apoptosome. Nat. Cell Biol. 2, 469–75. https://doi.org/10.1038/35019501

Beilina, A., Van Der Brug, M., Ahmad, R., Kesavapany, S., Miller, D.W., Petsko, G. a, Cookson, M.R., 2005. Mutations in PTEN-induced putative kinase 1 associated with recessive parkinsonism have differential effects on protein stability. Proc. Natl. Acad. Sci. U. S. A. 102, 5703–5708. https://doi.org/10.1073/pnas.0500617102

Bellomo, G., Mirabelli, F., 1992. Oxidative Stress and Cytoskeletal Alterations. Ann. N. Y. Acad. Sci. 663, 97–109. https://doi.org/10.1111/j.1749-6632.1992.tb38653.x

Bellot, G., Garcia-Medina, R., Gounon, P., Chiche, J., Roux, D., Pouyssegur, J., Mazure, N.M., 2009. Hypoxia-Induced Autophagy Is Mediated through Hypoxia-Inducible Factor Induction of BNIP3 and BNIP3L via Their BH3 Domains. Mol. Cell. Biol. 29, 2570–81. https://doi.org/10.1128/MCB.00166-09

Belluzzi, E., Bisaglia, M., Lazzarini, E., Tabares, L.C., Beltramini, M., Bubacco, L., 2012. Human SOD2 modification by dopamine quinones affects enzymatic activity by promoting its aggregation: Possible implications for Parkinson's disease. PLoS One 7, 1–9. https://doi.org/10.1371/journal.pone.0038026

Ben-Yoseph, O., Boxer, P. a, Ross, B.D., 1996. Assessment of the role of the glutathione and pentose phosphate pathways in the protection of primary cerebrocortical cultures from oxidative stress. J. Neurochem. 66, 2329–37. https://doi.org/10.1046/j.1471-4159.1996.66062329.x

Ben-Yoseph, O., Boxer, P.A., Ross, B.D., 1994. Oxidative stress in the central nervous system: monitoring the metabolic response using the pentose phosphate pathway. Dev. Neurosci. 16, 328–336.

Ben Othman, S., Katsuno, N., Kitayama, A., Fujimura, M., Kitaguchi, K., Yabe, T., 2016. Water-soluble fractions from defatted sesame seeds protect human neuroblast cells against peroxyl radicals and hydrogen peroxide-induced oxidative stress. Free Radic. Res. 50, 949–958. https://doi.org/10.1080/10715762.2016.1207248

Benard, G., Karbowski, M., 2009. Mitochondrial fusion and division: Regulation and role in cell viability. Semin. Cell Dev. Biol. https://doi.org/10.1016/j.semcdb.2008.12.012

Bence, N.F., Sampat, R.M., Kopito, R.R., 2001. Impairment of the ubiquitin-proteasome system by protein aggregation. Science 292, 1552–5. https://doi.org/10.1126/science.292.5521.1552

Bendor, J.T., Logan, T.P., Edwards, R.H., 2013. The Function of α-Synuclein. Neuron 79, 1044–1066. https://doi.org/10.1016/j.neuron.2013.09.004

Benit, P., 2004. Mutant NDUFS3 subunit of mitochondrial complex I causes Leigh syndrome. J. Med. Genet. 41, 14–7. https://doi.org/10.1136/jmg.2003.014316

Bennett, M C, Bishop, J.F., Leng, Y., Chock, P.B., Chase, T.N., Mouradian, M.M., 1999. Degradation of alpha-synuclein by proteasome. J. Biol. Chem. 274, 33855–33858. https://doi.org/10.1074/jbc.274.48.33855

Bennett, M. Catherine, Bishop, J.F., Leng, Y., Chock, P.B., Chase, T.N., Mouradian, M.M., 1999. Degradation of a-synuclein by proteasome. J. Biol. Chem. 274, 33855–33858. https://doi.org/10.1074/jbc.274.48.33855

Benov, L., 2001. How superoxide radical damages the cell, in: Protoplasma. pp. 33–6. https://doi.org/10.1007/BF01289410

Berbusse, G.W., Woods, L.C., Vohra, B.P.S., Naylor, K., 2016. Mitochondrial Dynamics Decrease Prior to Axon Degeneration Induced by Vincristine and are Partially Rescued by Overexpressed cytNmnat1. Front. Cell. Neurosci. 10, 179. https://doi.org/10.3389/fncel.2016.00179

Berwick, D.C., Harvey, K., 2012. The importance of Wnt signalling for neurodegeneration in Parkinson's disease. Biochem. Soc. Trans. 40, 1123–8. https://doi.org/10.1042/bst20120122

Betarbet, R., Canet-Aviles, R.M., Sherer, T.B., Mastroberardino, P.G., McLendon, C., Kim, J.H., Lund, S., Na, H.M., Taylor, G., Bence, N.F., Kopito, R., Seo, B.B., Yagi, T., Yagi, A., Klinefelter, G., Cookson, M.R.,

Greenamyre, J.T., 2006. Intersecting pathways to neurodegeneration in Parkinson's disease: Effects of the pesticide rotenone on DJ-1, α-synuclein, and the ubiquitin-proteasome system. Neurobiol. Dis. 22, 404–20. https://doi.org/10.1016/j.nbd.2005.12.003

Betarbet, R., Sherer, T.B., Greenamyre, J.T., 2005. Ubiquitin–proteasome system and Parkinson's diseases. Exp. Neurol. 191, S17–S27. https://doi.org/10.1016/j.expneurol.2004.08.021

Betarbet, R., Sherer, T.B., Mackenzie, G., Garcia-osuna, M., Panov, A. V, Greenamyre, J.T., 2000. Chronic systemic pesticide exposure reproduces features of Parkinson's disease. Nat. Neurosci. 3, 1301–1306. https://doi.org/10.1038/81834

Biedler, J.L., Helson, L., Spengler, B.A., 1973. Morphology and Growth, Tumorigenicity, and Cytogenetics of Human Neuroblastoma Cells in Continuous Culture. Cancer Res. 33, 2643–52. https://doi.org/10.1007/PL00000826

Biedler, J.L., Roffler-Tarlov, S., Schachner, M., Freedman, L.S., 1978. Multiple neurotransmitter synthesis by human neuroblastoma cell lines and clones. Cancer Res. 38, 3751–7.

BIGNAMI, A., DAHL, D., 1976. THE ASTROGLIAL RESPONSE TO STABBING. IMMUNOFLUORESCENCE STUDIES WITH ANTIBODIES TO ASTROCYTE-SPECIFIC PROTEIN (GFA) IN MAMMALIAN AND SUBMAMMALIAN VERTEBRATES. Neuropathol. Appl. Neurobiol. 2, 99–110. https://doi.org/10.1111/j.1365-2990.1976.tb00488.x

Birben, E., Sahiner, U.M., Sackesen, C., Erzurum, S., Kalayci, O., 2012. Oxidative stress and antioxidant defense. World Allergy Organ. J. 5, 9–19. https://doi.org/10.1097/WOX.0b013e3182439613

Bisaglia, M., Mammi, S., Bubacco, L., 2007. Kinetic and structural analysis of the early oxidation products of dopamine: analysis of the interactions with alpha-synuclein. J Biol Chem 282, 15597–15605. https://doi.org/10.1074/jbc.M610893200

Biteau, B., Labarre, J., Toledano, M.B., 2003. ATP-dependent reduction of cysteine–sulphinic acid by S. cerevisiae sulphiredoxin. Nature 425, 980–984. https://doi.org/10.1038/nature02075

Bizzozero, O.A., 2009. Protein Carbonylation in Neurodegenerative and Demyelinating CNS Diseases, in: Handbook of Neurochemistry and Molecular Neurobiology. Springer US, Boston, MA, pp. 543–562. https://doi.org/10.1007/978-0-387-30375-8_23

Bjarkam, C.R., Nielsen, M.S., Glud, A.N., Rosendal, F., Mogensen, P., Bender, D., Doudet, D., Møller, A., Sørensen, J.C., 2008. Neuromodulation in a minipig MPTP model of Parkinson disease. Br. J. Neurosurg. 22, S9–S12. https://doi.org/10.1080/02688690802448285

Blank, C.L., McCreery, R., Wightman, M., Chey, W., Adams, R N, Reid, J., Smissman, E.E., Med Chem, J., S Tse, D.C., McCreery, R.L., Adams, Ralph N, 1975. Potential Oxidative Pathways of Brain Catecholaminest. Brain Catech. Biochem. Biophys. Res. Commun. J . Med. Chem. Biochem. J. Med. Chem. J . Med. Chem. J. Med. Chem 63152, 694543–37. https://doi.org/10.1021/jm00223a008

Blesa, J., Trigo-Damas, I., Quiroga-Varela, A., Jackson-Lewis, V.R., 2015. Oxidative stress and Parkinson's disease. Front. Neuroanat. 9, 91. https://doi.org/10.3389/fnana.2015.00091

Bogdanowicz, D.R., Lu, H.H., 2013. Studying cell-cell communication in co-culture. Biotechnol. J. 8, 395–396. https://doi.org/10.1002/biot.201300054

Boillée, S., Vande Velde, C., Cleveland, D.W., 2006. ALS: A Disease of Motor Neurons and Their Nonneuronal Neighbors. Neuron 52, 39–59. https://doi.org/10.1016/j.neuron.2006.09.018

Bolaños, J.P., Heales, S.J.R., Land, J.M., Clark, J.B., 1995. Effect of Peroxynitrite on the Mitochondrial Respiratory Chain: Differential Susceptibility of Neurones and Astrocytes in Primary Culture. J. Neurochem. 64, 1965–1972. https://doi.org/10.1046/j.1471-4159.1995.64051965.x

Bonifati, V, Rizzu, P., Van Baren, M.J., Schaap, O., Breedveld, G.J., Krieger, E., Dekker, M.C., Squitieri, F., Ibanez, P., Joosse, M., Van Dongen, J.W., Vanacore, N., Van Swieten, J.C., Brice, A., Meco, G., Van Duijn, C.M., Oostra, B.A., Heutink, P., 2003. Mutations in the DJ-1 Gene Associated with Autosomal Recessive

Early- Onset Parkinsonism. Science (80-.). 299, 256–259. https://doi.org/10.1126/science.1077209

Bonifati, Vincenzo, Rizzu, P., van Baren, M.J., Schaap, O., Breedveld, G.J., Krieger, E., Dekker, M.C.J., Squitieri, F., Ibanez, P., Joosse, M., van Dongen, J.W., Vanacore, N., van Swieten, J.C., Brice, A., Meco, G., van Duijn, C.M., Oostra, B. a, Heutink, P., 2003. Mutations in the DJ-1 gene associated with autosomal recessive early-onset parkinsonism. Science 299, 256–259. https://doi.org/10.1126/science.1077209

Borisov, V.B., 2002. Defects in mitochondrial respiratory complexes III and IV, and human pathologies. Mol. Aspects Med. 23, 385–412. https://doi.org/10.1016/S0098-2997(02)00013-4

Borrás, C., Gambini, J., López-Grueso, R., Pallardó, F. V., Viña, J., 2010. Direct antioxidant and protective effect of estradiol on isolated mitochondria. Biochim. Biophys. Acta - Mol. Basis Dis. 1802, 205–211. https://doi.org/10.1016/j.bbadis.2009.09.007

Borrás, C., Sastre, J., García-Sala, D., Lloret, A., Pallardó, F. V., Viña, J., 2003. Mitochondria from females exhibit higher antioxidant gene expression and lower oxidative damage than males. Free Radic. Biol. Med. 34, 546–552. https://doi.org/10.1016/S0891-5849(02)01356-4

Borst, J.W., Visser, N. V., Kouptsova, O., Visser, A.J.W.G., 2000a. Oxidation of unsaturated phospholipids in membrane bilayer mixtures is accompanied by membrane fluidity changes. Biochim. Biophys. Acta - Mol. Cell Biol. Lipids. https://doi.org/10.1016/S1388-1981(00)00084-6

Borst, J.W., Visser, N. V, Kouptsova, O., Visser, A.J.W.G., 2000b. Oxidation of unsaturated phospholipids in membrane bilayer mixtures is accompanied by membrane fluidity changes. Biochim. Biophys. Acta - Mol. Cell Biol. Lipids 1487, 61–73. https://doi.org/10.1016/S1388-1981(00)00084-6

Bournival, J., Plouffe, M., Renaud, J., Provencher, C., Martinoli, M.-G., 2012. Quercetin and Sesamin Protect Dopaminergic Cells from MPP + -Induced Neuroinflammation in a Microglial (N9)-Neuronal (PC12) Coculture System. Oxid. Med. Cell. Longev. 2012, 1–11. https://doi.org/10.1155/2012/921941

Braak, H., Braak, E., Yilmazer, D., Schultz, C., de Vos, R.A., Jansen, E.N., 1995. Nigral and extranigral pathology in Parkinson's disease. J. Neural Transm. Suppl. 46, 15–31.

Braak, H., Del Tredici, K., Rüb, U., De Vos, R.A.I., Jansen Steur, E.N.H., Braak, E., 2003. Staging of brain pathology related to sporadic Parkinson's disease. Neurobiol. Aging 24, 197–211. https://doi.org/10.1016/S0197-4580(02)00065-9

Bradshaw, T.Y., Romano, L.E.L., Duncan, E.J., Nethisinghe, S., Abeti, R., Michael, G.J., Giunti, P., Vermeer, S., Chapple, J.P., 2016. A reduction in Drp1-mediated fission compromises mitochondrial health in autosomal recessive spastic ataxia of Charlevoix Saguenay. Hum. Mol. Genet. 25, 3232–3244. https://doi.org/10.1093/hmg/ddw173

Breitzig, M., Bhimineni, C., Lockey, R., Kolliputi, N., 2016. 4-Hydroxy-2-nonenal: a critical target in oxidative stress? Am. J. Physiol. Physiol. 311, C537–C543. https://doi.org/10.1152/ajpcell.00101.2016

Brkic, M., Balusu, S., Libert, C., Vandenbroucke, R.E., 2015. Friends or Foes: Matrix Metalloproteinases and Their Multifaceted Roles in Neurodegenerative Diseases. Mediators Inflamm. 2015, 1–27. https://doi.org/10.1155/2015/620581

Bruck, N., Vitoux, D., Ferry, C., Duong, V., Bauer, A., de Thé, H., Rochette-Egly, C., 2009. A coordinated phosphorylation cascade initiated by p38MAPK/MSK1 directs RARα to target promoters. EMBO J. 28, 34–47. https://doi.org/10.1038/emboj.2008.256

Bruey, J.-M., Ducasse, C., Bonniaud, P., Ravagnan, L., Susin, S.A., Diaz-Latoud, C., Gurbuxani, S., Arrigo, A.-P., Kroemer, G., Solary, E., Garrido, C., 2000. Hsp27 negatively regulates cell death by interacting with cytochrome c. Nat. Cell Biol. 2, 645–652. https://doi.org/10.1038/35023595

Bryan, H.K., Olayanju, A., Goldring, C.E., Park, B.K., 2013. The Nrf2 cell defence pathway: Keap1-dependent and -independent mechanisms of regulation. Biochem. Pharmacol. 85, 705–717. https://doi.org/10.1016/j.bcp.2012.11.016

Buettner, G.R., 1993. The Pecking Order of Free Radicals and Antioxidants: Lipid Peroxidation, α-Tocopherol,

and Ascorbate. Arch. Biochem. Biophys. 300, 535–543. https://doi.org/10.1006/abbi.1993.1074

Bukau, B., Weissman, J., Horwich, A., 2006. Molecular Chaperones and Protein Quality Control. Cell 125, 443–451. https://doi.org/10.1016/j.cell.2006.04.014

Burbulla, L.F., Song, P., Mazzulli, J.R., Zampese, E., Wong, Y.C., Jeon, S., Santos, D.P., Blanz, J., Obermaier, C.D., Strojny, C., Savas, J.N., Kiskinis, E., Zhuang, X., Krüger, R., Surmeier, D.J., Krainc, D., 2017. Dopamine oxidation mediates mitochondrial and lysosomal dysfunction in Parkinson's disease. Science (80-.). 357, 1255–1261. https://doi.org/10.1126/science.aam9080

Burton, E., Prados, M., 1999. New chemotherapy options for the treatment of malignant gliomas. Curr. Opin. Oncol. 11, 157–61.

Burton, G.W., Ingold, K.U., 1986. Vitamin E: application of the principles of physical organic chemistry to the exploration of its structure and function. Acc. Chem. Res. 19, 194–201. https://doi.org/10.1021/ar00127a001

Bushong, E.A., Martone, M.E., Jones, Y.Z., Ellisman, M.H., 2002. Protoplasmic astrocytes in CA1 stratum radiatum occupy separate anatomical domains. J. Neurosci. 22, 183–92. https://doi.org/10.1023/A:1011172915691

Buzzard, K.A., Giaccia, A.J., Killender, M., Anderson, R.L., 1998. Heat Shock Protein 72 Modulates Pathways of Stress-induced Apoptosis. J. Biol. Chem. 273, 17147–17153. https://doi.org/10.1074/jbc.273.27.17147

Cabelli, D.E., Bielski, B.H.J., 1983. Kinetics and mechanism for the oxidation of ascorbic acid/ascorbate by HO2/O2- (hydroperoxyl/superoxide) radicals. A pulse radiolysis and stopped-flow photolysis study. J. Phys. Chem. 87, 1809–1812. https://doi.org/10.1021/j100233a031

Calabrese, V., Boyd-Kimball, D., Scapagnini, G., Butterfield, D.A., 2004. Nitric oxide and cellular stress response in brain aging and neurodegenerative disorders: The role of vitagenes. In Vivo (Brooklyn).

Calkins, M.J., Reddy, P.H., 2011. Assessment of newly synthesized mitochondrial DNA using BrdU labeling in primary neurons from Alzheimer's disease mice: Implications for impaired mitochondrial biogenesis and synaptic damage. Biochim. Biophys. Acta - Mol. Basis Dis. 1812, 1182–1189. https://doi.org/10.1016/j.bbadis.2011.04.006

Campello, S., Scorrano, L., 2010. Mitochondrial shape changes: orchestrating cell pathophysiology. EMBO Rep. 11, 678–684. https://doi.org/10.1038/embor.2010.115

Caneda-Ferrón, B., De Girolamo, L.A., Costa, T., Beck, K.E., Layfield, R., Billett, E.E., 2008. Assessment of the direct and indirect effects of MPP+ and dopamine on the human proteasome: implications for Parkinson's disease aetiology. J. Neurochem. 105, 225–38. https://doi.org/10.1111/j.1471-4159.2007.05130.x

Cannon, J.R., Greenamyre, J.T., 2013. Gene-environment interactions in Parkinson's disease: specific evidence in humans and mammalian models. Neurobiol. Dis. 57, 38–46. https://doi.org/10.1016/j.nbd.2012.06.025

Cañón, E., Cosgaya, J.M., Scsucova, S., Aranda, A., 2004. Rapid Effects of Retinoic Acid on CREB and ERK Phosphorylation in Neuronal Cells. Mol. Biol. Cell 15, 5583–5592. https://doi.org/10.1091/mbc.e04-05-0439

Carelli, V., Maresca, A., Caporali, L., Trifunov, S., Zanna, C., Rugolo, M., 2015. Mitochondria: Biogenesis and mitophagy balance in segregation and clonal expansion of mitochondrial DNA mutations. Int. J. Biochem. Cell Biol. 63, 21–24. https://doi.org/10.1016/j.biocel.2015.01.023

Carolindah, M.N., Rosli, R., Adam, A., Nordin, N., 2013. An Overview of in Vitro Research Models for Alzheimer'S Disease. Regen. Res. 2, 8–13.

Cartier, E. a, Parra, L. a, Baust, T.B., Quiroz, M., Salazar, G., Faundez, V., Egaña, L., Torres, G.E., 2010. A biochemical and functional protein complex involving dopamine synthesis and transport into synaptic vesicles. J. Biol. Chem. 285, 1957–66. https://doi.org/10.1074/jbc.M109.054510

Cásedas, G., Bennett, A.C., González-Burgos, E., Gómez-Serranillos, M.P., López, V., Smith, C., 2019. Polyphenol-associated oxidative stress and inflammation in a model of LPS-induced inflammation in glial cells: do we know enough for responsible compounding? Inflammopharmacology 27, 189–197. https://doi.org/10.1007/s10787-018-0549-y

Cassina, P., Cassina, A., Pehar, M., Castellanos, R., Gandelman, M., de Leon, A., Robinson, K.M., Mason, R.P., Beckman, J.S., Barbeito, L., Radi, R., 2008. Mitochondrial Dysfunction in SOD1G93A-Bearing Astrocytes Promotes Motor Neuron Degeneration: Prevention by Mitochondrial-Targeted Antioxidants. J. Neurosci. 28, 4115–4122. https://doi.org/10.1523/JNEUROSCI.5308-07.2008

Caudle, W.M., Colebrooke, R.E., Emson, P.C., Miller, G.W., 2008. Altered vesicular dopamine storage in Parkinson's disease: a premature demise. Trends Neurosci. 31, 303–308. https://doi.org/10.1016/j.tins.2008.02.010

Cebrián, C., Zucca, F.A., Mauri, P., Steinbeck, J.A., Studer, L., Scherzer, C.R., Kanter, E., Budhu, S., Mandelbaum, J., Vonsattel, J.P., Zecca, L., Loike, J.D., Sulzer, D., 2014. MHC-I expression renders catecholaminergic neurons susceptible to T-cell-mediated degeneration. Nat. Commun. 5, 3633. https://doi.org/10.1038/ncomms4633

Chacón, M.A., Varela-Nallar, L., Inestrosa, N.C., 2008. Frizzled-1 is involved in the neuroprotective effect of Wnt3a against Aβ oligomers. J. Cell. Physiol. 217, 215–227. https://doi.org/10.1002/jcp.21497

Chambon, P., 1996. A decade of molecular biology of retinoic acid receptors. FASEB J. 10, 940–54.

Chan, D.C., 2012. Fusion and Fission: Interlinked Processes Critical for Mitochondrial Health. Annu. Rev. Genet. 46, 265–287. https://doi.org/10.1146/annurev-genet-110410-132529

Chan, D.C., 2006. Mitochondria: Dynamic Organelles in Disease, Aging, and Development. Cell 125, 1241–1252. https://doi.org/10.1016/j.cell.2006.06.010

Chan, N.C., Salazar, A.M., Pham, A.H., Sweredoski, M.J., Kolawa, N.J., Graham, R.L.J., Hess, S., Chan, D.C., 2011. Broad activation of the ubiquitin–proteasome system by Parkin is critical for mitophagy. Hum. Mol. Genet. 20, 1726–1737. https://doi.org/10.1093/hmg/ddr048

Chang, K.-H., Cheng, M.-L., Chiang, M.-C., Chen, C.-M., 2018. Lipophilic antioxidants in neurodegenerative diseases. Clin. Chim. Acta 485, 79–87. https://doi.org/10.1016/j.cca.2018.06.031

Chaturvedi, M., Kaczmarek, L., 2014. MMP-9 Inhibition: a Therapeutic Strategy in Ischemic Stroke. Mol. Neurobiol. 49, 563–573. https://doi.org/10.1007/s12035-013-8538-z

Chaturvedi, R.K., Flint Beal, M., 2013. Mitochondrial Diseases of the Brain. Free Radic. Biol. Med. 63, 1–29. https://doi.org/10.1016/j.freeradbiomed.2013.03.018

Chen, C., Kong, A.-N.T., 2004. Dietary chemopreventive compounds and ARE/EpRE signaling. Free Radic. Biol. Med. 36, 1505–1516. https://doi.org/10.1016/j.freeradbiomed.2004.03.015

CHEN, G., BOWER, K.A., MA, C., FANG, S., THIELE, C.J., LUO, J., 2004. Glycogen synthase kinase 3β (GSK3β) mediates 6-hydroxydopamine-induced neuronal death. FASEB J. 18, 1162–1164. https://doi.org/10.1096/fj.04-1551fje

Chen, H., Chan, D.C., 2009. Mitochondrial dynamics-fusion, fission, movement, and mitophagy-in neurodegenerative diseases. Hum. Mol. Genet. 18, R169–R176. https://doi.org/10.1093/hmg/ddp326

Chen, H., Detmer, S.A., Ewald, A.J., Griffin, E.E., Fraser, S.E., Chan, D.C., 2003. Mitofusins Mfn1 and Mfn2 coordinately regulate mitochondrial fusion and are essential for embryonic development. J. Cell Biol. 160, 189–200. https://doi.org/10.1083/jcb.200211046

Chen, J., Zhang, Z., Cai, L., 2014. Diabetic Cardiomyopathy and Its Prevention by Nrf2: Current Status. Diabetes Metab. J. 38, 337. https://doi.org/10.4093/dmj.2014.38.5.337

Chen, T., Tan, J., Wan, Z., Zou, Y., Kessete Afewerky, H., Zhang, Z., Zhang, T., 2017. Effects of Commonly Used Pesticides in China on the Mitochondria and Ubiquitin-Proteasome System in Parkinson's Disease. Int. J. Mol. Sci. 18, 2507. https://doi.org/10.3390/ijms18122507

Chen, Y., Vartiainen, N.E., Ying, W., Chan, P.H., Koistinaho, J., Swanson, R.A., 2001. Astrocytes protect neurons from nitric oxide toxicity by a glutathione-dependent mechanism. J. Neurochem. 77, 1601–1610. https://doi.org/10.1046/j.1471-4159.2001.00374.x

Chen, Z.J., Sun, L.J., 2009. Nonproteolytic Functions of Ubiquitin in Cell Signaling. Mol. Cell 33, 275–286. https://doi.org/10.1016/j.molcel.2009.01.014

Cheng, J.T., Yang, C.F., Jou, T.C., 1988. Inhibitory effect of l-ascorbic acid on the growth of astrocytes in cell culture. Neuropharmacology 27, 1179–82. https://doi.org/10.1016/0028-3908(88)90014-7

Cheung, Y.-T., Lau, W.K.-W., Yu, M.-S., Lai, C.S.-W., Yeung, S.-C., So, K.-F., Chang, R.C.-C., 2009. Effects of all-trans-retinoic acid on human SH-SY5Y neuroblastoma as in vitro model in neurotoxicity research. Neurotoxicology 30, 127–135. https://doi.org/10.1016/j.neuro.2008.11.001

Cho, D.-H., Nakamura, T., Fang, J., Cieplak, P., Godzik, A., Gu, Z., Lipton, S.A., 2009. S-Nitrosylation of Drp1 Mediates β-Amyloid-Related Mitochondrial Fission and Neuronal Injury. Science (80-.). 324, 102–105. https://doi.org/10.1126/science.1171091

Cho, H.-Y., Reddy, S.P., Kleeberger, S.R., 2006. Nrf2 Defends the Lung from Oxidative Stress. Antioxid. Redox Signal. 8, 76–87. https://doi.org/10.1089/ars.2006.8.76

Choi, J., Conrad, C.C., Dai, R., Malakowsky, C.A., Talent, J.M., Carroll, C.A., Weintraub, S.T., Gracy, R.W., 2003. Vitamin E prevents oxidation of antiapoptotic proteins in neuronal cells. Proteomics 3, 73–77. https://doi.org/10.1002/pmic.200390011

Choi, J., Sullards, M.C., Olzmann, J.A., Rees, H.D., Weintraub, S.T., Bostwick, D.E., Gearing, M., Levey, A.I., Chin, L.-S., Li, L., 2006. Oxidative Damage of DJ-1 Is Linked to Sporadic Parkinson and Alzheimer Diseases. J. Biol. Chem. 281, 10816–10824. https://doi.org/10.1074/jbc.M509079200

Choi, S.W., Gerencser, A.A., Nicholls, D.G., 2009. Bioenergetic analysis of isolated cerebrocortical nerve terminals on a microgram scale: spare respiratory capacity and stochastic mitochondrial failure. J. Neurochem. 109, 1179–1191. https://doi.org/10.1111/j.1471-4159.2009.06055.x

Chou, A.P., Li, S., Fitzmaurice, A.G., Bronstein, J.M., 2010. Mechanisms of rotenone-induced proteasome inhibition. Neurotoxicology 31, 367–372. https://doi.org/10.1016/j.neuro.2010.04.006

Chouchani, E.T., Methner, C., Nadtochiy, S.M., Logan, A., Pell, V.R., Ding, S., James, A.M., Cochemé, H.M., Reinhold, J., Lilley, K.S., Partridge, L., Fearnley, I.M., Robinson, A.J., Hartley, R.C., Smith, R.A.J., Krieg, T., Brookes, P.S., Murphy, M.P., 2013. Cardioprotection by S-nitrosation of a cysteine switch on mitochondrial complex I. Nat. Med. 19, 753–759. https://doi.org/10.1038/nm.3212

Chu, C.T., 2010. A pivotal role for PINK1 and autophagy in mitochondrial quality control: implications for Parkinson disease. Hum. Mol. Genet. 19, R28–R37. https://doi.org/10.1093/hmg/ddq143

Ciani, L., Salinas, P.C., 2005. WNTS in the vertebrate nervous system: from patterning to neuronal connectivity. Nat. Rev. Neurosci. 6, 351–362. https://doi.org/10.1038/nrn1665

Ciechanover, A., Brundin, P., 2003. The ubiquitin proteasome system in neurodegenerative diseases: Sometimes the chicken, sometimes the egg. Neuron 40, 427–446. https://doi.org/10.1016/S0896-6273(03)00606-8

Clancy, R.M., Levartovsky, D., Leszczynska-Piziak, J., Yegudin, J., Abramson, S.B., 1994. Nitric oxide reacts with intracellular glutathione and activates the hexose monophosphate shunt in human neutrophils: evidence for S-nitrosoglutathione as a bioactive intermediary. Proc. Natl. Acad. Sci. 91, 3680–3684. https://doi.org/10.1073/pnas.91.9.3680

Clark, I.E., Dodson, M.W., Jiang, C., Cao, J.H., Huh, J.R., Seol, J.H., Yoo, S.J., Hay, B. a, Guo, M., 2006. Drosophila pink1 is required for mitochondrial function and interacts genetically with parkin. Nature 441, 1162–1166. https://doi.org/10.1038/nature04779

Clements, C.M., McNally, R.S., Conti, B.J., Mak, T.W., Ting, J.P., 2006. DJ-1, a cancer- and Parkinson's disease-associated protein, stabilizes the antioxidant transcriptional master regulator Nrf2. Proc Natl Acad Sci U

S A 103, 15091–15096. https://doi.org/10.1073/pnas.0607260103

Clements, R.T., Sodha, N.R., Feng, J., Mieno, S., Boodhwani, M., Ramlawi, B., Bianchi, C., Sellke, F.W., 2007. Phosphorylation and translocation of heat shock protein 27 and αB-crystallin in human myocardium after cardioplegia and cardiopulmonary bypass. J. Thorac. Cardiovasc. Surg. 134, 1461-1470.e3. https://doi.org/10.1016/j.jtcvs.2007.06.026

Cloos, P.A.C., Christgau, S., 2004. Post-translational modifications of proteins: Implications for aging, antigen recognition, and autoimmunity. Biogerontology. https://doi.org/10.1023/B:BGEN.0000031152.31352.8b

Cobb, C.A., Cole, M.P., 2015. Oxidative and nitrative stress in neurodegeneration. Neurobiol. Dis. 84, 4–21. https://doi.org/10.1016/j.nbd.2015.04.020

Cohen, G., Farooqui, R., Kesler, N., 1997. Parkinson disease: a new link between monoamine oxidase and mitochondrial electron flow. Proc. Natl. Acad. Sci. U. S. A. 94, 4890–4894.

Coleman, M.P., 2013. The challenges of axon survival: Introduction to the special issue on axonal degeneration. Exp. Neurol. 246, 1–5. https://doi.org/10.1016/j.expneurol.2013.06.007

Concannon, C.G., Orrenius, S., Samali, A., 2001. Hsp27 Inhibits Cytochrome c -Mediated Caspase Activation by Sequestering Both Pro-caspase-3 and Cytochrome c. Gene Expr. 9, 195–201. https://doi.org/10.3727/000000001783992605

Conrad, M., Friedmann Angeli, J.P., 2018. Glutathione Peroxidases, in: Comprehensive Toxicology. Elsevier, pp. 260–276. https://doi.org/10.1016/B978-0-12-801238-3.95621-6

Constantinescu, R., Constantinescu, A.T., Reichmann, H., Janetzky, B., 2007. Neuronal differentiation and long-term culture of the human neuroblastoma line SH-SY5Y. J. Neural Transm. Suppl. 72, 17–28. https://doi.org/10.1007/978-3-211-73574-9-3

Conway, K. a, Harper, J.D., Lansbury, P.T., 1998. Accelerated in vitro fibril formation by a mutant alpha-synuclein linked to early-onset Parkinson disease. Nat. Med. 4, 1318–1320. https://doi.org/10.1038/3311

Cox, A.G., Winterbourn, C.C., Hampton, M.B., 2010. Mitochondrial peroxiredoxin involvement in antioxidant defence and redox signalling. Biochem. J. 425, 313–325. https://doi.org/10.1042/BJ20091541

Coyle, J., Puttfarcken, P., 1993. Oxidative stress, glutamate, and neurodegenerative disorders. Science (80-.). 262, 689–695. https://doi.org/10.1126/science.7901908

Croisier, E., Moran, L.B., Dexter, D.T., Pearce, R.K.B., Graeber, M.B., 2005. Microglial inflammation in the parkinsonian substantia nigra: relationship to alpha-synuclein deposition. J. Neuroinflammation 2, 14. https://doi.org/10.1186/1742-2094-2-14

Cronin-Furman, E.N., Borland, M.K., Bergquist, K.E., Bennett, J.P., Trimmer, P.A., 2013. Mitochondrial quality, dynamics and functional capacity in Parkinson's disease cybrid cell lines selected for Lewy body expression. Mol. Neurodegener. 8, 6. https://doi.org/10.1186/1750-1326-8-6

Cruz-Garcia, D., Brouwers, N., Malhotra, V., Curwin, A.J., 2019. Reactive oxygen species (ROS) production triggers unconventional secretion of antioxidant enzymes. bioRxiv 628321. https://doi.org/10.1101/628321

Cuervo, A.M., Wong, E., 2014. Chaperone-mediated autophagy: roles in disease and aging. Cell Res. 24, 92–104. https://doi.org/10.1038/cr.2013.153

Cunningham, L.A., Wetzel, M., Rosenberg, G.A., 2005. Multiple roles for MMPs and TIMPs in cerebral ischemia. Glia 50, 329–339. https://doi.org/10.1002/glia.20169

D'Autréaux, B., Toledano, M.B., 2007. ROS as signalling molecules: mechanisms that generate specificity in ROS homeostasis. Nat. Rev. Mol. Cell Biol. 8, 813–824. https://doi.org/10.1038/nrm2256

Da Silva, F.L., Coelho Cerqueira, E., De Freitas, M.S., Gonçalves, D.L., Costa, L.T., Follmer, C., 2013. Vitamins K

interact with N-terminus α-synuclein and modulate the protein fibrillization in vitro. Exploring the interaction between quinones and α-synuclein. Neurochem. Int. 62, 103–112. https://doi.org/10.1016/j.neuint.2012.10.001

Dadakhujaev, S., Noh, H.S., Jung, E.J., Cha, J.Y., Baek, S.M., Ha, J.H., Kim, D.R., 2010. Autophagy protects the rotenone-induced cell death in α-synuclein overexpressing SH-SY5Y cells. Neurosci. Lett. 472, 47–52. https://doi.org/10.1016/j.neulet.2010.01.053

Daly, C., Sugimori, M., Moreira, J.E., Ziff, E.B., Llinas, R., 2000. Synaptophysin regulates clathrin-independent endocytosis of synaptic vesicles. Proc. Natl. Acad. Sci. 97, 6120–6125. https://doi.org/10.1073/pnas.97.11.6120

Damier, P., Hirsch, E.C., Zhang, P., Agid, Y., Javoy-Agid, F., 1993. Glutathione peroxidase, glial cells and Parkinson's disease. Neuroscience 52, 1–6. https://doi.org/10.1016/0306-4522(93)90175-F

Danbolt, N.C., 2001. Glutamate uptake. Prog. Neurobiol. https://doi.org/10.1016/S0301-0082(00)00067-8

Danial, N.N., Korsmeyer, S.J., 2004. Cell Death. Cell 116, 205–219. https://doi.org/10.1016/S0092-8674(04)00046-7

Darios, F., Corti, O., Lücking, C.B., Hampe, C., Muriel, M.P., Abbas, N., Gu, W.J., Hirsch, E.C., Rooney, T., Ruberg, M., Brice, A., 2003. Parkin prevents mitochondrial swelling and cytochrome c release in mitochondria-dependent cell death. Hum. Mol. Genet. 12, 517–526. https://doi.org/10.1093/hmg/ddg044

Darley-usmar, V.M., Hogg, N., O'leary, V.J., Wilson, M.T., Moncada, S., 1992. The Simultaneous Generation of Superoxide and Nitric Oxide Can Initiate Lipid Peroxidation in Human Low Density Lipoprotein. Free Radic. Res. Commun. 17, 9–20. https://doi.org/10.3109/10715769209061085

Das, A., Banik, N.L., Ray, S.K., 2009. Molecular Mechanisms of the Combination of Retinoid and Interferon-gamma for Inducing Differentiation and Increasing Apoptosis in Human Glioblastoma T98G and U87MG Cells. Neurochem. Res. 34, 87–101. https://doi.org/10.1007/s11064-008-9669-x

Das, A., Banik, N.L., Ray, S.K., 2008. Retinoids induced astrocytic differentiation with down regulation of telomerase activity and enhanced sensitivity to taxol for apoptosis in human glioblastoma T98G and U87MG cells. J. Neurooncol. 87, 9–22. https://doi.org/10.1007/s11060-007-9485-1

Dasuri, K., Zhang, L., Keller, J.N., 2013. Oxidative stress, neurodegeneration, and the balance of protein degradation and protein synthesis. Free Radic. Biol. Med. 62, 170–185. https://doi.org/10.1016/j.freeradbiomed.2012.09.016

Daubner, S.C., Le, T., Wang, S., 2011. Tyrosine hydroxylase and regulation of dopamine synthesis. Arch. Biochem. Biophys. 508, 1–12. https://doi.org/10.1016/j.abb.2010.12.017

Davis, C.W., Hawkins, B.J., Ramasamy, S., Irrinki, K.M., Cameron, B.A., Islam, K., Daswani, V.P., Doonan, P.J., Manevich, Y., Madesh, M., 2010. Nitration of the mitochondrial complex I subunit NDUFB8 elicits RIP1- and RIP3-mediated necrosis. Free Radic. Biol. Med. 48, 306–317. https://doi.org/10.1016/j.freeradbiomed.2009.11.001

de Farias, C.C., Maes, M., Bonifácio, K.L., Bortolasci, C.C., de Souza Nogueira, A., Brinholi, F.F., Matsumoto, A.K., do Nascimento, M.A., de Melo, L.B., Nixdorf, S.L., Lavado, E.L., Moreira, E.G., Barbosa, D.S., 2016. Highly specific changes in antioxidant levels and lipid peroxidation in Parkinson's disease and its progression: Disease and staging biomarkers and new drug targets. Neurosci. Lett. 617, 66–71. https://doi.org/10.1016/j.neulet.2016.02.011

De Grey, A.D.N.J., 2002. HO2•: The Forgotten Radical. DNA Cell Biol. 21, 251–257. https://doi.org/10.1089/104454902753759672

de Medeiros, L.M., De Bastiani, M.A., Rico, E.P., Schonhofen, P., Pfaffenseller, B., Wollenhaupt-Aguiar, B., Grun, L., Barbé-Tuana, F., Zimmer, E.R., Castro, M.A.A., Parsons, R.B., Klamt, F., 2019. Cholinergic Differentiation of Human Neuroblastoma SH-SY5Y Cell Line and Its Potential Use as an In vitro Model for Alzheimer's Disease Studies. Mol. Neurobiol. 1605–19. https://doi.org/10.1007/s12035-019-1605-3

de Oliveira, M.R., Brasil, F.B., Andrade, C.M.B., 2017. Naringenin Attenuates H2O2-Induced Mitochondrial Dysfunction by an Nrf2-Dependent Mechanism in SH-SY5Y Cells. Neurochem. Res. 42, 3341–3350. https://doi.org/10.1007/s11064-017-2376-8

de Pedro, N., Cantizani, J., Ortiz-López, F.J., González-Menéndez, V., Cautain, B., Rodríguez, L., Bills, G.F., Reyes, F., Genilloud, O., Vicente, F., 2016. Protective effects of isolecanoric acid on neurodegenerative in vitro models. Neuropharmacology 101, 538–548. https://doi.org/10.1016/j.neuropharm.2015.09.029

De Vos, K.J., Grierson, A.J., Ackerley, S., Miller, C.C.J., 2008. Role of Axonal Transport in Neurodegenerative Diseases. Annu. Rev. Neurosci. 31, 151–173. https://doi.org/10.1146/annurev.neuro.31.061307.090711

De Zutter, G.S., Davis, R.J., 2001. Pro-apoptotic gene expression mediated by the p38 mitogen-activated protein kinase signal transduction pathway. Proc. Natl. Acad. Sci. U. S. A. 98, 6168–6173. https://doi.org/10.1073/pnas.111027698

Deakin, M.R., Kovach, P.M., Stutts, K.J., Wightman, R.M., 1986. Heterogeneous mechanisms of the oxidation of catechols and ascorbic acid at carbon electrodes. Anal. Chem. 58, 1474–1480. https://doi.org/10.1021/ac00298a046

DeBalsi, K.L., Hoff, K.E., Copeland, W.C., 2017. Role of the mitochondrial DNA replication machinery in mitochondrial DNA mutagenesis, aging and age-related diseases. Ageing Res. Rev. 33, 89–104. https://doi.org/10.1016/j.arr.2016.04.006

Deeb, R.S., Nuriel, T., Cheung, C., Summers, B., Lamon, B.D., Gross, S.S., Hajjar, D.P., 2013. Characterization of a cellular denitrase activity that reverses nitration of cyclooxygenase. Am. J. Physiol. Circ. Physiol. 305, H687–H698. https://doi.org/10.1152/ajpheart.00876.2012

Delcourt, N., Jouin, P., Poncet, J., Demey, E., Mauger, E., Bockaert, J., Marin, P., Galéotti, N., 2005. Difference in Mass Analysis Using Labeled Lysines (DIMAL-K). Mol. Cell. Proteomics 4, 1085–1094. https://doi.org/10.1074/mcp.M500040-MCP200

Demasi, M., Davies, K.J.A., 2003. Proteasome inhibitors induce intracellular protein aggregation and cell death by an oxygen-dependent mechanism. FEBS Lett. 542, 89–94. https://doi.org/10.1016/S0014-5793(03)00353-3

Deng, Y.-N., Shi, J., Liu, J., Qu, Q.-M., 2013. Celastrol protects human neuroblastoma SH-SY5Y cells from rotenone-induced injury through induction of autophagy. Neurochem. Int. 63, 1–9. https://doi.org/10.1016/j.neuint.2013.04.005

Denton, K., Mou, Y., Xu, C.-C., Shah, D., Chang, J., Blackstone, C., Li, X.-J., 2018. Impaired mitochondrial dynamics underlie axonal defects in hereditary spastic paraplegias. Hum. Mol. Genet. 27, 2517–2530. https://doi.org/10.1093/hmg/ddy156

Desagher, S., Glowinski, J., Premont, J., 1996. Astrocytes protect neurons from hydrogen peroxide toxicity. J. Neurosci. 16, 2553–62.

Dexter, D.T., Carter, C.J., Wells, F.R., Javoy-Agid, F., Agid, Y., Lees, A., Jenner, P., Marsden, C.D., 1989. Basal Lipid Peroxidation in Substantia Nigra Is Increased in Parkinson's Disease. J. Neurochem. 52, 381–389. https://doi.org/10.1111/j.1471-4159.1989.tb09133.x

Dexter, D.T., Sian, J., Rose, S., Hindmarsh, J.G., Mann, V.M., Cooper, J.M., Wells, F.R., Daniel, S.E., Lees, a J., Schapira, a H., 1994. Indices of oxidative stress and mitochondrial function in individuals with incidental Lewy body disease. Ann. Neurol. 35, 38–44. https://doi.org/10.1002/ana.410350107

Dhakshinamoorthy, S., Jain, A.K., Bloom, D.A., Jaiswal, A.K., 2005. Bach1 Competes with Nrf2 Leading to Negative Regulation of the Antioxidant Response Element (ARE)-mediated NAD(P)H:Quinone Oxidoreductase 1 Gene Expression and Induction in Response to Antioxidants. J. Biol. Chem. 280, 16891–16900. https://doi.org/10.1074/jbc.M500166200

Dhakshinamoorthy, S., Jaiswal, a K., 2001. Functional characterization and role of INrf2 in antioxidant

response element-mediated expression and antioxidant induction of NAD(P)H:quinone oxidoreductase1 gene. Oncogene 20, 3906–3917. https://doi.org/10.1038/sj.onc.1204506

Di Cesare Mannelli, L., Zanardelli, M., Failli, P., Ghelardini, C., 2013. Oxaliplatin-induced oxidative stress in nervous system-derived cellular models: Could it correlate with in vivo neuropathy? Free Radic. Biol. Med. 61, 143–150. https://doi.org/10.1016/j.freeradbiomed.2013.03.019

Di Giacomo, G., Rizza, S., Montagna, C., Filomeni, G., 2012. Established Principles and Emerging Concepts on the Interplay between Mitochondrial Physiology and S -(De)nitrosylation: Implications in Cancer and Neurodegeneration. Int. J. Cell Biol. 2012, 1–20. https://doi.org/10.1155/2012/361872

Diaz, F., Fukui, H., Garcia, S., Moraes, C.T., 2006. Cytochrome c Oxidase Is Required for the Assembly/Stability of Respiratory Complex I in Mouse Fibroblasts. Mol. Cell. Biol. 26, 4872–4881. https://doi.org/10.1128/MCB.01767-05

Didonna, A., Benetti, F., 2015. Post-translational modifications in neurodegeneration. AIMS Biophys. 3, 27–49. https://doi.org/10.3934/biophy.2016.1.27

Ding, Q., Dimayuga, E., Martin, S., Bruce-Keller, A.J., Nukala, V., Cuervo, A.M., Keller, J.N., 2004. Characterization of chronic low-level proteasome inhibition on neural homeostasis. J. Neurochem. 86, 489–497. https://doi.org/10.1046/j.1471-4159.2003.01885.x

Dinkova-Kostova, A.T., Abramov, A.Y., 2015. The emerging role of Nrf2 in mitochondrial function. Free Radic. Biol. Med. 88, 179–188. https://doi.org/10.1016/j.freeradbiomed.2015.04.036

Dinkova-Kostova, A.T., Baird, L., Holmström, K.M., Meyer, C.J., Abramov, A.Y., 2015. The spatiotemporal regulation of the Keap1–Nrf2 pathway and its importance in cellular bioenergetics. Biochem. Soc. Trans. 43, 602–610. https://doi.org/10.1042/BST20150003

Dinkova-Kostova, A.T., Kostov, R. V., Kazantsev, A.G., 2018. The role of Nrf2 signaling in counteracting neurodegenerative diseases. FEBS J. 285, 3576–3590. https://doi.org/10.1111/febs.14379

Diot, A., Morten, K., Poulton, J., 2016. Mitophagy plays a central role in mitochondrial ageing. Mamm. Genome 27, 381–395. https://doi.org/10.1007/s00335-016-9651-x

Discher, D.E., 2005. Tissue Cells Feel and Respond to the Stiffness of Their Substrate. Science (80-.). 310, 1139–1143. https://doi.org/10.1126/science.1116995

Dodson, M., Liang, Q., Johnson, M.S., Redmann, M., Fineberg, N., Darley-Usmar, V.M., Zhang, J., 2013. Inhibition of glycolysis attenuates 4-hydroxynonenal-dependent autophagy and exacerbates apoptosis in differentiated SH-SY5Y neuroblastoma cells. Autophagy 9, 1996–2008. https://doi.org/10.4161/auto.26094

Dodson, M., Wani, W.Y., Redmann, M., Benavides, G.A., Johnson, M.S., Ouyang, X., Cofield, S.S., Mitra, K., Darley-Usmar, V., Zhang, J., 2017. Regulation of autophagy, mitochondrial dynamics, and cellular bioenergetics by 4-hydroxynonenal in primary neurons. Autophagy 13, 1828–1840. https://doi.org/10.1080/15548627.2017.1356948

Doetsch, F., 2003. The glial identity of neural stem cells. Nat. Neurosci. 6, 1127–1134. https://doi.org/10.1038/nn1144

Donaire, V., Niso, M., Morán, J.M., García, L., González-Polo, R.A., Soler, G., Fuentes, J.M., 2005. Heat shock proteins protect both MPP+ and paraquat neurotoxicity. Brain Res. Bull. 67, 509–514. https://doi.org/10.1016/j.brainresbull.2005.08.002

Donnelly, J.K., McLellan, K.M., Walker, J.L., Robinson, D.S., 1989. Superoxide dismutases in foods. A review. Food Chem. 33, 243–270. https://doi.org/10.1016/0308-8146(89)90036-8

Dooley, M.M., Sano, N., Kawashima, H., Nakamura, T., 1990. Effects of 2,2′-azobis (2-amidinopropane) hydrochloride in vivo and protection by vitamin E. Free Radic. Biol. Med. 9, 199–204. https://doi.org/10.1016/0891-5849(90)90028-H

Dorsey, E.R., Constantinescu, R., Thompson, J.P., Biglan, K.M., Holloway, R.G., Kieburtz, K., Marshall, F.J.,

Ravina, B.M., Schifitto, G., Siderowf, A., Tanner, C.M., 2007. Projected number of people with Parkinson disease in the most populous nations, 2005 through 2030. Neurology 68, 384–386. https://doi.org/10.1212/01.wnl.0000247740.47667.03

Dorsey, E.R., George, B.P., Leff, B., Willis, A.W., 2013. The coming crisis: Obtaining care for the growing burden of neurodegenerative conditions. Neurology 80, 1989–1996. https://doi.org/10.1212/WNL.0b013e318293e2ce

Dou, F., Netzer, W.J., Tanemura, K., Li, F., Hartl, F.U., Takashima, A., Gouras, G.K., Greengard, P., Xu, H., 2003. Chaperones increase association of tau protein with microtubules. Proc. Natl. Acad. Sci. 100, 721–726. https://doi.org/10.1073/pnas.242720499

Douglas, P.M., Dillin, A., 2010. Protein homeostasis and aging in neurodegeneration. J. Cell Biol. 190, 719–729. https://doi.org/10.1083/jcb.201005144

Dowell, J.A., Johnson, J.A., 2013. Mechanisms of Nrf2 Protection in Astrocytes as Identified by Quantitative Proteomics and siRNA Screening. PLoS One 8, e70163. https://doi.org/10.1371/journal.pone.0070163

Drechsel, D.A., Patel, M., 2010. Respiration-dependent H 2 O 2 Removal in Brain Mitochondria via the Thioredoxin/Peroxiredoxin System. J. Biol. Chem. 285, 27850–27858. https://doi.org/10.1074/jbc.M110.101196

Dringen, R., Gutterer, J.M., Hirrlinger, J., 2000. Glutathione metabolism in brain. Eur. J. Biochem. 267, 4912–4916. https://doi.org/10.1046/j.1432-1327.2000.01597.x

Dringen, R., Hamprecht, B., 1997. Involvement of glutathione peroxidase and catalase in the disposal of exogenous hydrogen peroxide by cultured astroglial cells. Brain Res. 759, 67–75. https://doi.org/10.1016/S0006-8993(97)00233-3

Dringen, R., Hirrlinger, J., 2003. Glutathione pathways in the brain. Biol. Chem. 384, 505–16. https://doi.org/10.1515/BC.2003.059

Dringen, R., Kranich, O., Hamprecht, B., 1997. The gamma-glutamyl transpeptidase inhibitor acivicin preserves glutathione released by astroglial cells in culture. Neurochem. Res. 22, 727–33. https://doi.org/10.1023/a:1027310328310

Dringen, R., Pawlowski, P.G., Hirrlinger, J., 2005. Peroxide detoxification by brain cells. J. Neurosci. Res. 79, 157–65. https://doi.org/10.1002/jnr.20280

Dringen, R., Pfeiffer, B., Hamprecht, B., 1999. Synthesis of the antioxidant glutathione in neurons: supply by astrocytes of CysGly as precursor for neuronal glutathione. J. Neurosci. 19, 562–9. https://doi.org/10.1523/JNEUROSCI.19-02-00562.1999

Dröge, W., 2002. Free radicals in the physiological control of cell function. Physiol. Rev. 82, 47–95. https://doi.org/10.1152/physrev.00018.2001

Drukarch, B., Schepens, E., Jongenelen, C.A.., Stoof, J.., Langeveld, C.., 1997. Astrocyte-mediated enhancement of neuronal survival is abolished by glutathione deficiency. Brain Res. 770, 123–130. https://doi.org/10.1016/S0006-8993(97)00790-7

Drukarch, B., Schepens, E., Stoof, J.C., Langeveld, C.H., Van Muiswinkel, F.L., 1998. Astrocyte-enhanced neuronal survival is mediated by scavenging of extracellular reactive oxygen species. Free Radic. Biol. Med. 25, 217–220. https://doi.org/10.1016/S0891-5849(98)00050-1

Du, F., Yu, Q., Chen, A., Chen, D., Yan, S.S., 2018. Astrocytes Attenuate Mitochondrial Dysfunctions in Human Dopaminergic Neurons Derived from iPSC. Stem Cell Reports 10, 366–374. https://doi.org/10.1016/j.stemcr.2017.12.021

Du, J., Cullen, J.J., Buettner, G.R., 2012. Ascorbic acid: Chemistry, biology and the treatment of cancer. Biochim. Biophys. Acta - Rev. Cancer 1826, 443–457. https://doi.org/10.1016/j.bbcan.2012.06.003

Echtay, K.S., Murphy, M.P., Smith, R.A.J., Talbot, D.A., Brand, M.D., 2002. Superoxide Activates Mitochondrial Uncoupling Protein 2 from the Matrix Side. J. Biol. Chem. 277, 47129–47135.

https://doi.org/10.1074/jbc.M208262200

Edmondson, D.E., 2014. Hydrogen peroxide produced by mitochondrial monoamine oxidase catalysis: biological implications. Curr. Pharm. Des. 20, 155–160. https://doi.org/10.2174/13816128113190990406

Edsjö, A., Lavenius, E., Nilsson, H., Hoehner, J.C., Simonsson, P., Culp, L.A., Martinsson, T., Larsson, C., Påhlman, S., 2003. Expression of trkB in Human Neuroblastoma in Relation to MYCN Expression and Retinoic Acid Treatment. Lab. Investig. 83, 813–823. https://doi.org/10.1097/01.LAB.0000074895.48776.D8

Ehrnhoefer, D.E., Wong, B.K.Y., Hayden, M.R., 2011. Convergent pathogenic pathways in Alzheimer's and Huntington's diseases: shared targets for drug development. Nat. Rev. Drug Discov. 10, 853–867. https://doi.org/10.1038/nrd3556

Ehrnsperger, M., 1997. Binding of non-native protein to Hsp25 during heat shock creates a reservoir of folding intermediates for reactivation. EMBO J. 16, 221–229. https://doi.org/10.1093/emboj/16.2.221

Encinas, Mario, Iglesias, M., Liu, Y., Wang, H., Muhaisen, A., Ceña, V., Gallego, C., Comella, J.X., 2002. Sequential Treatment of SH-SY5Y Cells with Retinoic Acid and Brain-Derived Neurotrophic Factor Gives Rise to Fully Differentiated, Neurotrophic Factor-Dependent, Human Neuron-Like Cells. J. Neurochem. 75, 991–1003. https://doi.org/10.1046/j.1471-4159.2000.0750991.x

Encinas, M., Iglesias, M., Llecha, N., Comella, J.X., 2002. Extracellular-Regulated Kinases and Phosphatidylinositol 3-Kinase Are Involved in Brain-Derived Neurotrophic Factor-Mediated Survival and neuritogenesis of the Neuroblastoma Cell Line SH-SY5Y. J. Neurochem. 73, 1409–1421. https://doi.org/10.1046/j.1471-4159.1999.0731409.x

Engele, J., Schubert, D., Bohn, M.C., 1991. Conditioned media derived from glial cell lines promote survival and differentiation of dopaminergic neurons in vitro: Role of mesencephalic glia. J. Neurosci. Res. 30, 359–371. https://doi.org/10.1002/jnr.490300212

Engler, A.J., Griffin, M.A., Sen, S., Bönnemann, C.G., Sweeney, H.L., Discher, D.E., 2004. Myotubes differentiate optimally on substrates with tissue-like stiffness. J. Cell Biol. 166, 877–887. https://doi.org/10.1083/jcb.200405004

Eroglu, C., Barres, B.A., 2010. Regulation of synaptic connectivity by glia. Nature 468, 223–231. https://doi.org/10.1038/nature09612

Espinosa-Diez, C., Miguel, V., Mennerich, D., Kietzmann, T., Sánchez-Pérez, P., Cadenas, S., Lamas, S., 2015. Antioxidant responses and cellular adjustments to oxidative stress. Redox Biol. 6, 183–197. https://doi.org/10.1016/j.redox.2015.07.008

Esposito, F., Ammendola, R., Faraonio, R., Russo, T., Cimino, F., 2004. Redox Control of Signal Transduction, Gene Expression and Cellular Senescence. Neurochem. Res. 29, 617–628. https://doi.org/10.1023/B:NERE.0000014832.78725.1a

Esser, C., Alberti, S., Höhfeld, J., 2004. Cooperation of molecular chaperones with the ubiquitin/proteasome system. Biochim. Biophys. Acta - Mol. Cell Res. 1695, 171–188. https://doi.org/10.1016/j.bbamcr.2004.09.020

Esterbauer, H., Schaur, R.J., Zollner, H., 1991. Chemistry and biochemistry of 4-hydroxynonenal, malonaldehyde and related aldehydes. Free Radic. Biol. Med. 11, 81–128. https://doi.org/10.1016/0891-5849(91)90192-6

Esterbauer, H., Zollern, H., 1989. Methods for determination of aldehydic lipid peroxidation products. Free Radic. Biol. Med. 7, 197–203. https://doi.org/10.1016/0891-5849(89)90015-4

Fan, G.-H., Qi, C., Chen, S.-D., 2005. Heat shock proteins reduce toxicity of 1-methyl-4-phenylpyridinium ion in SK-N-SH cells. J. Neurosci. Res. 82, 551–562. https://doi.org/10.1002/jnr.20656

Fariss, M.W., Chan, C.B., Patel, M., Van Houten, B., Orrenius, S., 2005. Role of mitochondria in toxic oxidative

stress. Mol. Interv. 5, 94–111. https://doi.org/10.1124/mi.5.2.7

Feany, M.B., Bender, W.W., 2000. A Drosophila model of Parkinson's disease. Nature 404, 394–398. https://doi.org/10.1038/35006074

Feitosa, C.M., da Silva Oliveira, G.L., do Nascimento Cavalcante, A., Morais Chaves, S.K., Rai, M., 2018. Determination of Parameters of Oxidative Stress in vitro Models of Neurodegenerative Diseases-A Review. Curr. Clin. Pharmacol. 13, 100–109. https://doi.org/10.2174/1574884713666180301091612

Feng, J., 2006. Microtubule: A Common Target for Parkin and Parkinson's Disease Toxins. Neurosci. 12, 469–476. https://doi.org/10.1177/1073858406293853

Ferreira, M., Massano, J., 2017. An updated review of Parkinson's disease genetics and clinicopathological correlations. Acta Neurol. Scand. 135, 273–284. https://doi.org/10.1111/ane.12616

Ferreira, P.S., Nogueira, T.B., Costa, V.M., Branco, P.S., Ferreira, L.M., Fernandes, E., Bastos, M.L., Meisel, A., Carvalho, F., Capela, J.P., 2013. Neurotoxicity of "ecstasy" and its metabolites in human dopaminergic differentiated SH-SY5Y cells. Toxicol. Lett. 216, 159–170. https://doi.org/10.1016/j.toxlet.2012.11.015

Ferreira, T.A., Blackman, A. V, Oyrer, J., Jayabal, S., Chung, A.J., Watt, A.J., Sjöström, P.J., van Meyel, D.J., 2014. Neuronal morphometry directly from bitmap images. Nat. Methods 11, 982–984. https://doi.org/10.1038/nmeth.3125

Filomeni, G., Graziani, I., De Zio, D., Dini, L., Centonze, D., Rotilio, G., Ciriolo, M.R., 2012. Neuroprotection of kaempferol by autophagy in models of rotenone-mediated acute toxicity: possible implications for Parkinson's disease. Neurobiol. Aging 33, 767–785. https://doi.org/10.1016/j.neurobiolaging.2010.05.021

Filosto, M., Scarpelli, M., Cotelli, M.S., Vielmi, V., Todeschini, A., Gregorelli, V., Tonin, P., Tomelleri, G., Padovani, A., 2011. The role of mitochondria in neurodegenerative diseases. J. Neurol. 258, 1763–1774. https://doi.org/10.1007/s00415-011-6104-z

Finley, D., 2009. Recognition and processing of ubiquitin-protein conjugates by the proteasome. Annu. Rev. Biochem. 78, 477–513. https://doi.org/10.1146/annurev.biochem.78.081507.101607

Fischer, F., Hamann, A., Osiewacz, H.D., 2012. Mitochondrial quality control: an integrated network of pathways. Trends Biochem. Sci. 37, 284–292. https://doi.org/10.1016/j.tibs.2012.02.004

Fisher, A.B., 2011. Peroxiredoxin 6: A Bifunctional Enzyme with Glutathione Peroxidase and Phospholipase A 2 Activities. Antioxid. Redox Signal. 15, 831–844. https://doi.org/10.1089/ars.2010.3412

Fitzgerald, J.C., Ufer, C., De Girolamo, L.A., Kuhn, H., Billett, E.E., 2007. Monoamine oxidase-A modulates apoptotic cell death induced by staurosporine in human neuroblastoma cells. J. Neurochem. 103, 2189–2199. https://doi.org/10.1111/j.1471-4159.2007.04921.x

Fitzgerald, J.C., Ugun-Klusek, A., Allen, G., De Girolamo, L.A., Hargreaves, I., Ufer, C., Abramov, A.Y., Billett, E.E., 2014. Monoamine oxidase-A knockdown in human neuroblastoma cells reveals protection against mitochondrial toxins. FASEB J. 28, 218–229. https://doi.org/10.1096/fj.13-235481

Flanagan, L.A., Ju, Y.-E., Marg, B., Osterfield, M., Janmey, P.A., 2002. Neurite branching on deformable substrates. Neuroreport 13, 2411–2415. https://doi.org/10.1097/00001756-200212200-00007

Foppoli, C., Coccia, R., Cini, C., Rosei, M.A., 1997. Catecholamines oxidation by xanthine oxidase. Biochim. Biophys. Acta - Gen. Subj. 1334, 200–206. https://doi.org/10.1016/S0304-4165(96)00093-1

Fornai, F., Schlüter, O.M., Lenzi, P., Gesi, M., Ruffoli, R., Ferrucci, M., Lazzeri, G., Busceti, C.L., Pontarelli, F., Battaglia, G., Pellegrini, A., Nicoletti, F., Ruggieri, S., Paparelli, A., Südhof, T.C., 2005. Parkinson-like syndrome induced by continuous MPTP infusion: convergent roles of the ubiquitin-proteasome system and alpha-synuclein. Proc. Natl. Acad. Sci. U. S. A. 102, 3413–3418. https://doi.org/10.1073/pnas.0409713102

Forno, L.S., DeLanney, L.E., Irwin, I., Monte, D. Di, Langston, J.W., 1992. Chapter 36: Astrocytes and Parkinson's disease, in: Progress in Brain Research. pp. 429–436. https://doi.org/10.1016/S0079-

6123(08)61770-7

Forno, L.S., Langston, J.W., DeLanney, L.E., Irwin, I., Ricaurte, G. a, 1986. Locus ceruleus lesions and eosinophilic inclusions in MPTP-treated monkeys. Ann. Neurol. 20, 449–455. https://doi.org/10.1002/ana.410200403

Forster, J.I., Köglsberger, S., Trefois, C., Boyd, O., Baumuratov, A.S., Buck, L., Balling, R., Antony, P.M.A., 2016. Characterization of Differentiated SH-SY5Y as Neuronal Screening Model Reveals Increased Oxidative Vulnerability. J. Biomol. Screen. 21, 496–509. https://doi.org/10.1177/1087057115625190

Franco-Iborra, S., Vila, M., Perier, C., 2018. Mitochondrial Quality Control in Neurodegenerative Diseases: Focus on Parkinson's Disease and Huntington's Disease. Front. Neurosci. 12, 342. https://doi.org/10.3389/fnins.2018.00342

Franco-Iborra, S., Vila, M., Perier, C., 2016. The Parkinson Disease Mitochondrial Hypothesis. Neurosci. 22, 266–277. https://doi.org/10.1177/1073858415574600

Franklin, T.B., Krueger-Naug, A.M., Clarke, D.B., Arrigo, A.-P., Currie, R.W., 2005. The role of heat shock proteins Hsp70 and Hsp27 in cellular protection of the central nervous system. Int. J. Hyperth. 21, 379–392. https://doi.org/10.1080/02656730500069955

Fratelli, M., Demol, H., Puype, M., Casagrande, S., Eberini, I., Salmona, M., Bonetto, V., Mengozzi, M., Duffieux, F., Miclet, E., Bachi, A., Vandekerckhove, J., Gianazza, E., Ghezzi, P., 2002. Identification by redox proteomics of glutathionylated proteins in oxidatively stressed human T lymphocytes. Proc. Natl. Acad. Sci. 99, 3505–3510. https://doi.org/10.1073/pnas.052592699

Fridovich, I., 1995. Superoxide Radical and Superoxide Dismutases. Annu. Rev. Biochem. 64, 97–112. https://doi.org/10.1146/annurev.bi.64.070195.000525

Friedman, J.R., Nunnari, J., 2014. Mitochondrial form and function. Nature 505, 335–343. https://doi.org/10.1038/nature12985

Frucht, S., Greene, P.E., Weiner, W.J., Olanow, C.W., Watts, R.L., Koller, W.C., Kieburtz, K., Griggs, R.C., 2002. An algorithm (decision tree) for the management of Parkinson's disease (2001): Treatment guidelines. Neurology 58, 156–157. https://doi.org/10.1212/WNL.58.1.156

Fukui, H., Moraes, C.T., 2007. Extended polyglutamine repeats trigger a feedback loop involving the mitochondrial complex III, the proteasome and huntingtin aggregates. Hum. Mol. Genet. 16, 783–797. https://doi.org/10.1093/hmg/ddm023

Fukuzawa, K., Matsuura, K., Tokumura, A., Suzuki, A., Terao, J., 1997. Kinetics and Dynamics of Singlet Oxygen Scavenging by α-Tocopherol in Phospholipid Model Membranes. Free Radic. Biol. Med. 22, 923–930. https://doi.org/10.1016/S0891-5849(96)00485-6

Fuxe, K., Manger, P., Genedani, S., Agnati, L., 2006. The nigrostriatal DA pathway and Parkinson's disease, in: Parkinson's Disease and Related Disorders. Springer Vienna, Vienna, pp. 71–83. https://doi.org/10.1007/978-3-211-45295-0_13

Gai, W.P., Yuan, H.X., Li, X.Q., Power, J.T., Blumbergs, P.C., Jensen, P.H., 2000. In situ and in vitro study of colocalization and segregation of alpha-synuclein, ubiquitin, and lipids in Lewy bodies. Exp. Neurol. 166, 324–333. https://doi.org/10.1006/exnr.2000.7527

Gallo, E.F., Iadecola, C., 2011. Neuronal Nitric Oxide Contributes to Neuroplasticity-Associated Protein Expression through cGMP, Protein Kinase G, and Extracellular Signal-Regulated Kinase. J. Neurosci. 31, 6947–6955. https://doi.org/10.1523/JNEUROSCI.0374-11.2011

Galzigna, L., De Iuliis, A., Zanatta, L., 2000. Enzymatic dopamine peroxidation in substantia nigra of human brain. Clin. Chim. Acta 300, 131–138. https://doi.org/10.1016/S0009-8981(00)00313-2

Gan, L., Vargas, M.R., Johnson, D.A., Johnson, J.A., 2012. Astrocyte-Specific Overexpression of Nrf2 Delays Motor Pathology and Synuclein Aggregation throughout the CNS in the Alpha-Synuclein Mutant (A53T) Mouse Model. J. Neurosci. 32, 17775–17787. https://doi.org/10.1523/JNEUROSCI.3049-12.2012

Gandhi, S., Abramov, A.Y., 2012. Mechanism of Oxidative Stress in Neurodegeneration. Oxid. Med. Cell. Longev. 2012, 1–11. https://doi.org/10.1155/2012/428010

Gandhi, S., Wood, N.W., 2005. Molecular pathogenesis of Parkinson's disease. Hum. Mol. Genet. 14, 2749–2755. https://doi.org/10.1093/hmg/ddi308

García-García, F., Ponce, S., Brown, R., Cussen, V., Krueger, J.M., 2005. Sleep disturbances in the rotenone animal model of Parkinson disease. Brain Res. 1042, 160–168. https://doi.org/10.1016/j.brainres.2005.02.036

Garrido, C., Paul, C., Seigneuric, R., Kampinga, H.H., 2012. The small heat shock proteins family: The long forgotten chaperones. Int. J. Biochem. Cell Biol. 44, 1588–1592. https://doi.org/10.1016/j.biocel.2012.02.022

Gaschler, M.M., Stockwell, B.R., 2017. Lipid peroxidation in cell death. Biochem. Biophys. Res. Commun. 482, 419–425. https://doi.org/10.1016/j.bbrc.2016.10.086

George, R., Griffin, J.W., 1994. Delayed Macrophage Responses and Myelin Clearance during Wallerian Degeneration in the Central Nervous System: The Dorsal Radiculotomy Model. Exp. Neurol. 129, 225–236. https://doi.org/10.1006/exnr.1994.1164

Georges, P.C., Miller, W.J., Meaney, D.F., Sawyer, E.S., Janmey, P.A., 2006. Matrices with Compliance Comparable to that of Brain Tissue Select Neuronal over Glial Growth in Mixed Cortical Cultures. Biophys. J. 90, 3012–3018. https://doi.org/10.1529/biophysj.105.073114

Georgiou, G., 2003. BIOCHEMISTRY: An Overoxidation Journey with a Return Ticket. Science (80-.). 300, 592–594. https://doi.org/10.1126/science.1084976

Gerencser, A.A., Neilson, A., Choi, S.W., Edman, U., Yadava, N., Oh, R.J., Ferrick, D.A., Nicholls, D.G., Brand, M.D., 2009. Quantitative Microplate-Based Respirometry with Correction for Oxygen Diffusion. Anal. Chem. 81, 6868–6878. https://doi.org/10.1021/ac900881z

Ghasemi, M., Fatemi, A., 2014. Pathologic role of glial nitric oxide in adult and pediatric neuroinflammatory diseases. Neurosci. Biobehav. Rev. 45, 168–182. https://doi.org/10.1016/j.neubiorev.2014.06.002

Giasson, B.I., 2000. Oxidative Damage Linked to Neurodegeneration by Selective alpha -Synuclein Nitration in Synucleinopathy Lesions. Science (80-.). 290, 985–989. https://doi.org/10.1126/science.290.5493.985

Gidalevitz, T., 2006. Progressive Disruption of Cellular Protein Folding in Models of Polyglutamine Diseases. Science (80-.). 311, 1471–1474. https://doi.org/10.1126/science.1124514

Giordano, S., Dodson, M., Ravi, S., Redmann, M., Ouyang, X., Darley Usmar, V.M., Zhang, J., 2014. Bioenergetic adaptation in response to autophagy regulators during rotenone exposure. J. Neurochem. 131, 625–633. https://doi.org/10.1111/jnc.12844

Girotto, S., Sturlese, M., Bellanda, M., Tessari, I., Cappellini, R., Bisaglia, M., Bubacco, L., Mammi, S., 2012. Dopamine-derived quinones affect the structure of the redox sensor DJ-1 through modifications at Cys-106 and Cys-53. J. Biol. Chem. 287, 18738–18749. https://doi.org/10.1074/jbc.M111.311589

Glass, J.D., Brushart, T.M., George, E.B., Griffin, J.W., 1993. Prolonged survival of transected nerve fibres in C57BL/Ola mice is an intrinsic characteristic of the axon. J. Neurocytol. 22, 311–321. https://doi.org/10.1007/BF01195555

Glick, D., Zhang, W., Beaton, M., Marsboom, G., Gruber, M., Simon, M.C., Hart, J., Dorn, G.W., Brady, M.J., Macleod, K.F., 2012. BNip3 Regulates Mitochondrial Function and Lipid Metabolism in the Liver. Mol. Cell. Biol. 32, 2570–2584. https://doi.org/10.1128/MCB.00167-12

Glickman, M.H., Ciechanover, A., 2002. The Ubiquitin-Proteasome Proteolytic Pathway: Destruction for the Sake of Construction. Physiol. Rev. 82, 373–428. https://doi.org/10.1152/physrev.00027.2001

Glickman, M.H., Rubin, D.M., Coux, O., Wefes, I., Pfeifer, G., Cjeka, Z., Baumeister, W., Fried, V.A., Finley, D., 1998. A Subcomplex of the Proteasome Regulatory Particle Required for Ubiquitin-Conjugate Degradation and Related to the COP9-Signalosome and eIF3. Cell 94, 615–623.

https://doi.org/10.1016/S0092-8674(00)81603-7

Glinka, Y.Y., Youdim, M.B.H., 1995. Inhibition of mitochondrial complexes I and IV by 6-hydroxydopamine. Eur. J. Pharmacol. Environ. Toxicol. Pharmacol. 292, 329–332. https://doi.org/10.1016/0926-6917(95)90040-3

Goedert, M., 2001. Alpha-synuclein and neurodegenerative diseases. Nat. Rev. Neurosci. 2, 492–501. https://doi.org/10.1038/35081564

Goedert, M., Jakes, R., Spillantini, M.G., 2017. The Synucleinopathies: Twenty Years On. J. Parkinsons. Dis. 7, S51–S69. https://doi.org/10.3233/JPD-179005

Goldbaum, O., Riedel, M., Stahnke, T., Richter-Landsberg, C., 2009. The small heat shock protein HSP25 protects astrocytes against stress induced by proteasomal inhibition. Glia 57, 1566–1577. https://doi.org/10.1002/glia.20870

Goldberg, M.S., Pisani, A., Haburcak, M., Vortherms, T.A., Kitada, T., Costa, C., Tong, Y., Martella, G., Tscherter, A., Martins, A., Bernardi, G., Roth, B.L., Pothos, E.N., Calabresi, P., Shen, J., 2005. Nigrostriatal dopaminergic deficits and hypokinesia caused by inactivation of the familial parkinsonism-linked gene DJ-1. Neuron 45, 489–496. https://doi.org/10.1016/j.neuron.2005.01.041

Goldring, C., Casini, A.F., Maellaro, E., Del Bello, B., Comporti, M., 1993. Determination of 4-hydroxynonenal by high-performance liquid chromatography with electrochemical detection. Lipids 28, 141–145. https://doi.org/10.1007/BF02535778

Gomez-Lazaro, M., Bonekamp, N.A., Galindo, M.F., Jordán, J., Schrader, M., 2008. 6-Hydroxydopamine (6-OHDA) induces Drp1-dependent mitochondrial fragmentation in SH-SY5Y cells. Free Radic. Biol. Med. 44, 1960–1969. https://doi.org/10.1016/j.freeradbiomed.2008.03.009

Gómez-Piña, V., Martínez, E., Fernández-Ruíz, I., del Fresno, C., Soares-Schanoski, A., Jurado, T., Siliceo, M., Toledano, V., Fernández-Palomares, R., García-Rio, F., Arnalich, F., Biswas, S.K., López-Collazo, E., 2012. Role of MMPs in orchestrating inflammatory response in human monocytes via a TREM-1-PI3K-NF-κB pathway. J. Leukoc. Biol. 91, 933–945. https://doi.org/10.1189/jlb.0711340

Gómez-Tortosa, E., Newell, K., Irizarry, M.C., Sanders, J.L., Hyman, B.T., 2000. Alpha-Synuclein immunoreactivity in dementia with Lewy bodies: morphological staging and comparison with ubiquitin immunostaining. Acta Neuropathol. 99, 352–7. https://doi.org/10.1007/s004010051135

Gordon, M.D., Nusse, R., 2006. Wnt Signaling: Multiple Pathways, Multiple Receptors, and Multiple Transcription Factors. J. Biol. Chem. 281, 22429–22433. https://doi.org/10.1074/jbc.R600015200

Gorell, J.M., Johnson, C.C., Rybicki, B.A., Peterson, E.L., Richardson, R.J., 1998. The risk of Parkinson's disease with exposure to pesticides, farming, well water, and rural living. Neurology 50, 1346–1350. https://doi.org/10.1212/WNL.50.5.1346

Gorisse, L., Pietrement, C., Vuiblet, V., Schmelzer, C.E.H., Köhler, M., Duca, L., Debelle, L., Fornès, P., Jaisson, S., Gillery, P., 2016. Protein carbamylation is a hallmark of aging. Proc. Natl. Acad. Sci. 113, 1191–1196. https://doi.org/10.1073/pnas.1517096113

Gorman, A.M., Heavey, B., Creagh, E., Cotter, T.G., Samali, A., 1999. Antioxidant-mediated inhibition of the heat shock response leads to apoptosis. FEBS Lett. 445, 98–102. https://doi.org/10.1016/S0014-5793(99)00094-0

Goswami, P., Gupta, S., Joshi, N., Sharma, S., Singh, S., 2015. Astrocyte activation and neurotoxicity: A study in different rat brain regions and in rat C6 astroglial cells. Environ. Toxicol. Pharmacol. 40, 122–139. https://doi.org/10.1016/j.etap.2015.06.001

Goto, S., Kawakatsu, M., Izumi, S., Urata, Y., Kageyama, K., Ihara, Y., Koji, T., Kondo, T., 2009. Glutathione S-transferase π localizes in mitochondria and protects against oxidative stress. Free Radic. Biol. Med. 46, 1392–1403. https://doi.org/10.1016/j.freeradbiomed.2009.02.025

Gotoh, N., Niki, E., 1992. Rates of interactions of superoxide with vitamin E, vitamin C and related

compounds as measured by chemiluminescence. Biochim. Biophys. Acta - Gen. Subj. 1115, 201–207. https://doi.org/10.1016/0304-4165(92)90054-X

Gottschall, P.E., Deb, S., 1996. Regulation of Matrix Metalloproteinase Expression in Astrocytes, Microglia and Neurons. Neuroimmunomodulation 3, 69–75. https://doi.org/10.1159/000097229

Gottschall, P.E., Yu, X., 2002. Cytokines Regulate Gelatinase A and B (Matrix Metalloproteinase 2 and 9) Activity in Cultured Rat Astrocytes. J. Neurochem. 64, 1513–1520. https://doi.org/10.1046/j.1471-4159.1995.64041513.x

Graham, D.G., 1978. Oxidative pathways for catecholamines in the genesis of neuromelanin and cytotoxic quinones. Mol. Pharmacol. 14, 633–643. https://doi.org/10.1097/00005072-197809000-00155

Graham, D.G., Tiffany, S.M., Bell Jr., W.R., Gutknecht, W.F., 1978. Autoxidation versus covalent binding of quinones as the mechanism of toxicity of dopamine, 6-hydroxydopamine, and related compounds toward C1300 neuroblastoma cells in vitro. Mol. Pharmacol. 14, 644–653. https://doi.org/10.1111/j.1365-2842.1978.tb00386.x

Greco, T.M., Seeholzer, S.H., Mak, A., Spruce, L., Ischiropoulos, H., 2010. Quantitative Mass Spectrometry-based Proteomics Reveals the Dynamic Range of Primary Mouse Astrocyte Protein Secretion. J. Proteome Res. 9, 2764–2774. https://doi.org/10.1021/pr100134n

Green, D.R., Van Houten, B., 2011. SnapShot: Mitochondrial Quality Control. Cell 147, 950-950.e1. https://doi.org/10.1016/j.cell.2011.10.036

Greene, J.C., Whitworth, A.J., Kuo, I., Andrews, L.A., Feany, M.B., Pallanck, L.J., 2003. Mitochondrial pathology and apoptotic muscle degeneration in Drosophila parkin mutants. Proc. Natl. Acad. Sci. U. S. A. 100, 4078–83. https://doi.org/10.1073/pnas.0737556100

GRIFFIN, J.W., GEORGE, E.B., HSIEH, S.-T., GLASS, J.D., 1995. Axonal degeneration and disorders of the axonal cytoskeleton, in: The Axon. Oxford University Press, pp. 375–390. https://doi.org/10.1093/acprof:oso/9780195082937.003.0020

Griffith, O.W., Meister, A., 1979. Potent and specific inhibition of glutathione synthesis by buthionine sulfoximine (S-n-butyl homocysteine sulfoximine). J. Biol. Chem. 254, 7558–60.

Grimm, A., Eckert, A., 2017. Brain aging and neurodegeneration: from a mitochondrial point of view. J. Neurochem. 143, 418–431. https://doi.org/10.1111/jnc.14037

Grimm, A., Friedland, K., Eckert, A., 2016. Mitochondrial dysfunction: the missing link between aging and sporadic Alzheimer's disease. Biogerontology 17, 281–296. https://doi.org/10.1007/s10522-015-9618-4

GROBSTEIN, C., 1953. Morphogenetic Interaction between Embryonic Mouse Tissues separated by a Membrane Filter. Nature 172, 869–871. https://doi.org/10.1038/172869a0

Groll, M., Bajorek, M., Köhler, A., Moroder, L., Rubin, D.M., Huber, R., Glickman, M.H., Finley, D., 2000. A gated channel into the proteasome core particle. Nat. Struct. Biol. 7, 1062–1067. https://doi.org/10.1038/80992

Groll, M., Ditzel, L., Löwe, J., Stock, D., Bochtler, M., Bartunik, H.D., Huber, R., 1997. Structure of 20S proteasome from yeast at 2.4Å resolution. Nature 386, 463–471. https://doi.org/10.1038/386463a0

Grünblatt, E., Mandel, S., Youdim, M.B., 2000. MPTP and 6-hydroxydopamine-induced neurodegeneration as models for Parkinson's disease: neuroprotective strategies. J. Neurol. 247 Suppl, II95-102. https://doi.org/10.1007/pl00022909

Grune, T., Catalgol, B., Licht, A., Ermak, G., Pickering, A.M., Ngo, J.K., Davies, K.J.A., 2011. HSP70 mediates dissociation and reassociation of the 26S proteasome during adaptation to oxidative stress. Free Radic. Biol. Med. 51, 1355–1364. https://doi.org/10.1016/j.freeradbiomed.2011.06.015

Guerra, F., Girolimetti, G., Beli, R., Mitruccio, M., Pacelli, C., Ferretta, A., Gasparre, G., Cocco, T., Bucci, C., 2019. Synergistic Effect of Mitochondrial and Lysosomal Dysfunction in Parkinson's Disease. Cells 8,

452. https://doi.org/10.3390/cells8050452

Gunawardena, S., Goldstein, L.S.B., 2005. Polyglutamine Diseases and Transport Problems. Arch. Neurol. 62, 46. https://doi.org/10.1001/archneur.62.1.46

Guo, A., Zhao, Y., Wang, Y., Wang, Q., 2016. Cattle encephalon glycoside and ignotin injection promoted synthesis of glial cell line-derived neurotrophic factor by astrocytes that protected against neuronal damage induced by AAPH 9, 1794–1800.

Guo, K., Lu, J., Huang, Y., Wu, M., Zhang, L., Yu, H., Zhang, M., Bao, Y., He, J.C., Chen, H., Jia, W., 2015. Protective Role of PGC-1α in Diabetic Nephropathy Is Associated with the Inhibition of ROS through Mitochondrial Dynamic Remodeling. PLoS One 10, e0125176. https://doi.org/10.1371/journal.pone.0125176

Gutbier, S., Spreng, A.-S., Delp, J., Schildknecht, S., Karreman, C., Suciu, I., Brunner, T., Groettrup, M., Leist, M., 2018. Prevention of neuronal apoptosis by astrocytes through thiol-mediated stress response modulation and accelerated recovery from proteotoxic stress. Cell Death Differ. 25, 2101–2117. https://doi.org/10.1038/s41418-018-0229-x

Hajieva, P., Mocko, J.B., Moosmann, B., Behl, C., 2009. Novel imine antioxidants at low nanomolar concentrations protect dopaminergic cells from oxidative neurotoxicity. J. Neurochem. 110, 118–132. https://doi.org/10.1111/j.1471-4159.2009.06114.x

Hall, A., Nelson, K., Poole, L.B., Karplus, P.A., 2011. Structure-based Insights into the Catalytic Power and Conformational Dexterity of Peroxiredoxins. Antioxid. Redox Signal. 15, 795–815. https://doi.org/10.1089/ars.2010.3624

Hall, E.D., 1987. Intensive anti-oxidant pretreatment retards motor nerve degeneration. Brain Res. 413, 175–178. https://doi.org/10.1016/0006-8993(87)90166-1

Halliwell, B., 2003. Oxidative stress in cell culture: an under-appreciated problem? FEBS Lett. 540, 3–6. https://doi.org/10.1016/S0014-5793(03)00235-7

Halliwell, B., Foyer, C.H., 1976. Ascorbic acid, metal ions and the superoxide radical. Biochem. J. 155, 697–700. https://doi.org/10.1042/bj1550697

Halliwell, B., Gutteridge, J.M.C., 1991. Free radicals in biology and medicine, second edition. Free Radic. Biol. Med. 10, 449–450. https://doi.org/10.1016/0891-5849(91)90055-8

Hamazaki, J., Hirayama, S., Murata, S., 2015. Redundant Roles of Rpn10 and Rpn13 in Recognition of Ubiquitinated Proteins and Cellular Homeostasis. PLOS Genet. 11, e1005401. https://doi.org/10.1371/journal.pgen.1005401

Hamberger, A., 1970. COMPARATIVE STUDIES ON MITOCHONDRIA ISOLATED FROM NEURON-ENRICHED AND GLIA-ENRICHED FRACTIONS OF RABBIT AND BEEF BRAIN. J. Cell Biol. 45, 221–234. https://doi.org/10.1083/jcb.45.2.221

Han, D., Jin, J., Woo, J., Min, H., Kim, Y., 2014. Proteomic analysis of mouse astrocytes and their secretome by a combination of FASP and StageTip-based, high pH, reversed-phase fractionation. Proteomics 14, 1604–1609. https://doi.org/10.1002/pmic.201300495

Han, X.-J., Lu, Y.-F., Li, S.-A., Kaitsuka, T., Sato, Y., Tomizawa, K., Nairn, A.C., Takei, K., Matsui, H., Matsushita, M., 2008. CaM kinase Iα–induced phosphorylation of Drp1 regulates mitochondrial morphology. J. Cell Biol. 182, 573–585. https://doi.org/10.1083/jcb.200802164

HANSSON, E., RÖNNBÄCK, L., 2003. Glial neuronal signaling in the central nervous system. FASEB J. 17, 341–348. https://doi.org/10.1096/fj.02-0429rev

Haque, A., Das, A., Hajiaghamohseni, L.M., Younger, A., Banik, N.L., Ray, S.K., 2007. Induction of apoptosis and immune response by all-trans retinoic acid plus interferon-gamma in human malignant glioblastoma T98G and U87MG cells. Cancer Immunol. Immunother. 56, 615–625. https://doi.org/10.1007/s00262-006-0219-6

Haroon, S., Vermulst, M., 2016. Linking mitochondrial dynamics to mitochondrial protein quality control. Curr. Opin. Genet. Dev. 38, 68–74. https://doi.org/10.1016/j.gde.2016.04.004

Harris, J., Deen, N., Zamani, S., Hasnat, M.A., 2018. Mitophagy and the release of inflammatory cytokines. Mitochondrion 41, 2–8. https://doi.org/10.1016/j.mito.2017.10.009

Harris, P.S., Roy, S.R., Coughlan, C., Orlicky, D.J., Liang, Y., Shearn, C.T., Roede, J.R., Fritz, K.S., 2015. Chronic ethanol consumption induces mitochondrial protein acetylation and oxidative stress in the kidney. Redox Biol. 6, 33–40. https://doi.org/10.1016/j.redox.2015.06.021

Harrison, F.E., May, J.M., 2009. Vitamin C function in the brain: vital role of the ascorbate transporter SVCT2. Free Radic. Biol. Med. 46, 719–730. https://doi.org/10.1016/j.freeradbiomed.2008.12.018

Hartl, F.U., Bracher, A., Hayer-Hartl, M., 2011. Molecular chaperones in protein folding and proteostasis. Nature 475, 324–332. https://doi.org/10.1038/nature10317

Hastings, T.G., 2002. Enzymatic Oxidation of Dopamine: The Role of Prostaglandin H Synthase. J. Neurochem. 64, 919–924. https://doi.org/10.1046/j.1471-4159.1995.64020919.x

Hattingen, E., Magerkurth, J., Pilatus, U., Mozer, A., Seifried, C., Steinmetz, H., Zanella, F., Hilker, R., 2009. Phosphorus and proton magnetic resonance spectroscopy demonstrates mitochondrial dysfunction in early and advanced Parkinson's disease. Brain 132, 3285–97. https://doi.org/10.1093/brain/awp293

Hauser, D.N., Dukes, A.A., Mortimer, A.D., Hastings, T.G., 2013. Dopamine quinone modifies and decreases the abundance of the mitochondrial selenoprotein glutathione peroxidase 4. Free Radic. Biol. Med. 65, 419–427. https://doi.org/10.1016/j.freeradbiomed.2013.06.030

Hauser, D.N., Hastings, T.G., 2013. Mitochondrial dysfunction and oxidative stress in Parkinson's disease and monogenic parkinsonism. Neurobiol. Dis. https://doi.org/10.1016/j.nbd.2012.10.011

Haut, S., Brivet, M., Touati, G., Rustin, P., Lebon, S., Garcia-Cazorla, A., Saudubray, J.M., Boutron, A., Legrand, A., Slama, A., 2003. A deletion in the human QP-C gene causes a complex III deficiency resulting in hypoglycaemia and lactic acidosis. Hum. Genet. 113, 118–22. https://doi.org/10.1007/s00439-003-0946-0

Haydon, P.G., 2001. Glia: listening and talking to the synapse. Nat. Rev. Neurosci. 2, 185–193. https://doi.org/10.1038/35058528

He, F., Zuo, L., 2015. Redox Roles of Reactive Oxygen Species in Cardiovascular Diseases. Int. J. Mol. Sci. 16, 27770–27780. https://doi.org/10.3390/ijms161126059

He, Y., Yu, W., Baas, P.W., 2002. Microtubule reconfiguration during axonal retraction induced by nitric oxide. J. Neurosci. 22, 5982–91. https://doi.org/20026604

Hegazy, A.M., El-Sayed, E.M., Ibrahim, K.S., Abdel-Azeem, A.S., 2019. Dietary antioxidant for disease prevention corroborated by the Nrf2 pathway. J. Complement. Integr. Med. https://doi.org/10.1515/jcim-2018-0161

Heikkila, R.E., Cohen, G., 1973. 6-Hydroxydopamine: Evidence for Superoxide Radical as an Oxidative Intermediate. Science (80-.). 181, 456–457. https://doi.org/10.1126/science.181.4098.456

Heikkila, R.E., Nicklas, W.J., Vyas, I., Duvoisin, R.C., 1985. Dopaminergic toxicity of rotenone and the 1-methyl-4-phenylpyridinium ion after their stereotaxic administration to rats: Implication for the mechanism of 1-methyl-4-phenyl-1,2,3,6-tetrahydropyridine toxicity. Neurosci. Lett. 62, 389–394. https://doi.org/10.1016/0304-3940(85)90580-4

Heneka, M.T., Kummer, M.P., Latz, E., 2014. Innate immune activation in neurodegenerative disease. Nat. Rev. Immunol. 14, 463–477. https://doi.org/10.1038/nri3705

Herculano-Houzel, S., 2009. The human brain in numbers: a linearly scaled-up primate brain. Front. Hum. Neurosci. 3, 31. https://doi.org/10.3389/neuro.09.031.2009

Herrero-Mendez, A., Almeida, A., Fernández, E., Maestre, C., Moncada, S., Bolaños, J.P., 2009. The

bioenergetic and antioxidant status of neurons is controlled by continuous degradation of a key glycolytic enzyme by APC/C–Cdh1. Nat. Cell Biol. 11, 747–752. https://doi.org/10.1038/ncb1881

Hertz, L., Peng, L., Dienel, G.A., 2007. Energy Metabolism in Astrocytes: High Rate of Oxidative Metabolism and Spatiotemporal Dependence on Glycolysis/Glycogenolysis. J. Cereb. Blood Flow Metab. 27, 219–249. https://doi.org/10.1038/sj.jcbfm.9600343

Higdon, A., Diers, A.R., Oh, J.Y., Landar, A., Darley-Usmar, V.M., 2012. Cell signalling by reactive lipid species: new concepts and molecular mechanisms. Biochem. J. 442, 453–64. https://doi.org/10.1042/BJ20111752

Higgins, D.S., Greenamyre, J.T., 1996. [3H]dihydrorotenone binding to NADH: ubiquinone reductase (complex I) of the electron transport chain: an autoradiographic study. J. Neurosci. 16, 3807–16.

Hinkle, J.T., Dawson, V.L., Dawson, T.M., 2019. The A1 astrocyte paradigm: New avenues for pharmacological intervention in neurodegeneration. Mov. Disord. 34, 959–969. https://doi.org/10.1002/mds.27718

Hinshaw, D.B., Miller, M.T., Omann, G.M., Beals, T.F., Hyslop, P.A., 1993. A cellular model of oxidant-mediated neuronal injury. Brain Res. 615, 13–26. https://doi.org/10.1016/0006-8993(93)91110-E

Hirsch, E.C., Hunot, S., 2009. Neuroinflammation in Parkinson's disease: a target for neuroprotection? Lancet Neurol. 8, 382–397. https://doi.org/10.1016/S1474-4422(09)70062-6

Hod, Y., Pentyala, S.N., Whyard, T.C., El-Maghrabi, M.R., 1999. Identification and characterization of a novel protein that regulates RNA-protein interaction. J. Cell. Biochem. 72, 435–444. https://doi.org/10.1002/(SICI)1097-4644(19990301)72:3<435::AID-JCB12>3.0.CO;2-H [pii]

Höftberger, R., Aboul-Enein, F., Brueck, W., Lucchinetti, C., Rodriguez, M., Schmidbauer, M., Jellinger, K., Lassmann, H., 2004. Expression of Major Histocompatibility Complex class I Molecules on the Different Cell Types in Multiple Sclerosis Lesions. Brain Pathol. 14, 43–50. https://doi.org/10.1111/j.1750-3639.2004.tb00496.x

Hogg, N., Kalyanaraman, B., 1999. Nitric Oxide and Lipid Peroxidation. Biochim. Biophys. Acta - Bioenerg. 1411, 378–384. https://doi.org/10.1016/S0005-2728(99)00027-4

Hogg, N., Singh, R.J., Kalyanaraman, B., 1996. The role of glutathione in the transport and catabolism of nitric oxide. FEBS Lett. 382, 223–228. https://doi.org/10.1016/0014-5793(96)00086-5

Hohn, A., Leibrock, J., Bailey, K., Barde, Y.-A., 1990. Identification and characterization of a novel member of the nerve growth factor/brain-derived neurotrophic factor family. Nature 344, 339–341. https://doi.org/10.1038/344339a0

Holley, A.K., Dhar, S.K., St. Clair, D.K., 2010. Manganese superoxide dismutase vs. p53: Regulation of mitochondrial ROS. Mitochondrion 10, 649–661. https://doi.org/10.1016/j.mito.2010.06.003

Hong, Z., Shi, M., Chung, K.A., Quinn, J.F., Peskind, E.R., Galasko, D., Jankovic, J., Zabetian, C.P., Leverenz, J.B., Baird, G., Montine, T.J., Hancock, A.M., Hwang, H., Pan, C., Bradner, J., Kang, U.J., Jensen, P.H., Zhang, J., 2010. DJ-1 and α-synuclein in human cerebrospinal fluid as biomarkers of Parkinson's disease. Brain 133, 713–726. https://doi.org/10.1093/brain/awq008

Hongo, H., Kihara, T., Kume, T., Izumi, Y., Niidome, T., Sugimoto, H., Akaike, A., 2012. Glycogen synthase kinase-3β activation mediates rotenone-induced cytotoxicity with the involvement of microtubule destabilization. Biochem. Biophys. Res. Commun. 426, 94–99. https://doi.org/10.1016/j.bbrc.2012.08.042

Hosomi, A., Goto, K., Kondo, H., Iwatsubo, T., Yokota, T., Ogawa, M., Arita, M., Aoki, J., Arai, H., Inoue, K., 1998. Localization of α-tocopherol transfer protein in rat brain. Neurosci. Lett. 256, 159–162. https://doi.org/10.1016/S0304-3940(98)00785-X

Houenou, L.J., Li, L., Lei, M., Kent, C.R., Tytell, M., 1996. Exogenous heat shock cognate protein Hsc 70 prevents axotomy-induced death of spinal sensory neurons. Cell Stress Chaperones 1, 161–6. https://doi.org/10.1379/1466-1268(1996)001<0161:ehscph>2.3.co;2

Hough, R., Pratt, G., Rechsteiner, M., 1986. Ubiquitin-lysozyme conjugates. Identification and characterization of an ATP-dependent protease from rabbit reticulocyte lysates. J. Biol. Chem. 261, 2400–2408.

Hu, X., Zhang, D., Pang, H., Caudle, W.M., Li, Y., Gao, H., Liu, Y., Qian, L., Wilson, B., Di Monte, D.A., Ali, S.F., Zhang, J., Block, M.L., Hong, J.-S., 2008. Macrophage antigen complex-1 mediates reactive microgliosis and progressive dopaminergic neurodegeneration in the MPTP model of Parkinson's disease. J. Immunol. 181, 7194–204. https://doi.org/10.4049/jimmunol.181.10.7194

Huang, E.J., Reichardt, L.F., 2003. Trk Receptors: Roles in Neuronal Signal Transduction. Annu. Rev. Biochem. 72, 609–642. https://doi.org/10.1146/annurev.biochem.72.121801.161629

Huang, H.-C., Nguyen, T., Pickett, C.B., 2000. Regulation of the antioxidant response element by protein kinase C-mediated phosphorylation of NF-E2-related factor 2. Proc. Natl. Acad. Sci. 97, 12475–12480. https://doi.org/10.1073/pnas.220418997

Huang, Y., Li, W., Su, Z., Kong, A.-N.T., 2015. The complexity of the Nrf2 pathway: beyond the antioxidant response. J. Nutr. Biochem. 26, 1401–1413. https://doi.org/10.1016/j.jnutbio.2015.08.001

Huang, Z., Huang, P., Panahian, N., Dalkara, T., Fishman, M., Moskowitz, M., 1994. Effects of cerebral ischemia in mice deficient in neuronal nitric oxide synthase. Science (80-.). 265, 1883–1885. https://doi.org/10.1126/science.7522345

Hudson, G., Amati-Bonneau, P., Blakely, E.L., Stewart, J.D., He, L., Schaefer, A.M., Griffiths, P.G., Ahlqvist, K., Suomalainen, A., Reynier, P., McFarland, R., Turnbull, D.M., Chinnery, P.F., Taylor, R.W., 2008. Mutation of OPA1 causes dominant optic atrophy with external ophthalmoplegia, ataxia, deafness and multiple mitochondrial DNA deletions: a novel disorder of mtDNA maintenance. Brain 131, 329–337. https://doi.org/10.1093/brain/awm272

Husnjak, K., Elsasser, S., Zhang, N., Chen, X., Randles, L., Shi, Y., Hofmann, K., Walters, K.J., Finley, D., Dikic, I., 2008. Proteasome subunit Rpn13 is a novel ubiquitin receptor. Nature 453, 481–488. https://doi.org/10.1038/nature06926

Hynes, R.O., 2009. The Extracellular Matrix: Not Just Pretty Fibrils. Science (80-.). 326, 1216–1219. https://doi.org/10.1126/science.1176009

Hyun, D.H., Lee, M.H., Hattori, N., Kubo, S.I., Mizuno, Y., Halliwell, B., Jenner, P., 2002. Effect of wild-type or mutant parkin on oxidative damage, nitric oxide, antioxidant defenses, and the proteasome. J. Biol. Chem. 277, 28572–28577. https://doi.org/10.1074/jbc.M200666200

Ichimura, Y., Kominami, E., Tanaka, K., Komatsu, M., 2008. Selective turnover of p62/A170/SQSTM1 by autophagy. Autophagy 4, 1063–1066. https://doi.org/10.4161/auto.6826

Ikeda, Y., Tsuji, S., Satoh, A., Ishikura, M., Shirasawa, T., Shimizu, T., 2008. Protective effects of astaxanthin on 6-hydroxydopamine-induced apoptosis in human neuroblastoma SH-SY5Y cells. J. Neurochem. 107, 1730–1740. https://doi.org/10.1111/j.1471-4159.2008.05743.x

Imai, Y., Soda, M., Takahashi, R., 2000. Parkin suppresses unfolded protein stress-induced cell death through its E3 ubiquitin-protein ligase activity. J. Biol. Chem. 275, 35661–35664. https://doi.org/10.1074/jbc.C000447200

Imura, T., Nakano, I., Kornblum, H.I., Sofroniew, M. V., 2006. Phenotypic and functional heterogeneity of GFAP-expressing cells in vitro: Differential expression of LeX/CD15 by GFAP-expressing multipotent neural stem cells and non-neurogenic astrocytes. Glia 53, 277–293. https://doi.org/10.1002/glia.20281

Irizarry, M.C., 2015. Nigral and Cortical Lewy Bodies and Dystrophic Nigral Neurites in Parkinson's Disease and Cortical Lewy Body Disease Contain alpha-synuclein Immunoreactivity. J. Neurophathology Exp. Neurol. 1, 1689–1699. https://doi.org/10.1017/CBO9781107415324.004

Ischiropoulos, H., Beckman, J.S., 2003. Oxidative stress and nitration in neurodegeneration: Cause, effect, or association? J. Clin. Invest. 111, 163–169. https://doi.org/10.1172/JCI200317638

Ishihara, N., 2004. Mitofusin 1 and 2 play distinct roles in mitochondrial fusion reactions via GTPase activity. J. Cell Sci. 117, 6535–6546. https://doi.org/10.1242/jcs.01565

Islam, M.T., 2017. Oxidative stress and mitochondrial dysfunction-linked neurodegenerative disorders. Neurol. Res. 39, 73–82. https://doi.org/10.1080/01616412.2016.1251711

Itier, J.-M., 2003. Parkin gene inactivation alters behaviour and dopamine neurotransmission in the mouse. Hum. Mol. Genet. 12, 2277–2291. https://doi.org/10.1093/hmg/ddg239

Ito, H., Kamei, K., Iwamoto, I., Inaguma, Y., Garcia-Mata, R., Sztul, E., Kato, K., 2002. Inhibition of Proteasomes Induces Accumulation, Phosphorylation, and Recruitment of HSP27 and -Crystallin to Aggresomes. J. Biochem. 131, 593–603. https://doi.org/10.1093/oxfordjournals.jbchem.a003139

Itoh, K., Chiba, T., Takahashi, S., Ishii, T., Igarashi, K., Katoh, Y., Oyake, T., Hayashi, N., Satoh, K., Hatayama, I., Yamamoto, M., Nabeshima, Y., 1997. An Nrf2/Small Maf Heterodimer Mediates the Induction of Phase II Detoxifying Enzyme Genes through Antioxidant Response Elements. Biochem. Biophys. Res. Commun. 236, 313–322. https://doi.org/10.1006/bbrc.1997.6943

Itoh, K., Wakabayashi, N., Katoh, Y., Ishii, T., Igarashi, K., Engel, J.D., Yamamoto, M., 1999. Keap1 represses nuclear activation of antioxidant responsive elements by Nrf2 through binding to the amino-terminal Neh2 domain. Genes Dev. 13, 76–86. https://doi.org/10.1101/gad.13.1.76

Itoh, K., Wakabayashi, N., Katoh, Y., Ishii, T., O'Connor, T., Yamamoto, M., 2003. Keap1 regulates both cytoplasmic-nuclear shuttling and degradation of Nrf2 in response to electrophiles. Genes to Cells 8, 379–391. https://doi.org/10.1046/j.1365-2443.2003.00640.x

Ittner, L.M., Ke, Y.D., Delerue, F., Bi, M., Gladbach, A., van Eersel, J., Wölfing, H., Chieng, B.C., Christie, M.J., Napier, I.A., Eckert, A., Staufenbiel, M., Hardeman, E., Götz, J., 2010. Dendritic function of tau mediates amyloid-beta toxicity in Alzheimer's disease mouse models. Cell 142, 387–97. https://doi.org/10.1016/j.cell.2010.06.036

Iwata-Ichikawa, E., Kondo, Y., Miyazaki, I., Asanuma, M., Ogawa, N., 1999. Glial cells protect neurons against oxidative stress via transcriptional up-regulation of the glutathione synthesis. J. Neurochem. 72, 2334–2344. https://doi.org/10.1046/j.1471-4159.1999.0722334.x

Jády, A.G., Nagy, Á.M., Kőhidi, T., Ferenczi, S., Tretter, L., Madarász, E., 2016. Differentiation-Dependent Energy Production and Metabolite Utilization: A Comparative Study on Neural Stem Cells, Neurons, and Astrocytes. Stem Cells Dev. 25, 995–1005. https://doi.org/10.1089/scd.2015.0388

Jaffrey, S.R., Erdjument-Bromage, H., Ferris, C.D., Tempst, P., Snyder, S.H., 2001. Protein S-nitrosylation: a physiological signal for neuronal nitric oxide. Nat. Cell Biol. 3, 193–197. https://doi.org/10.1038/35055104

Jain, A.K., Jaiswal, A.K., 2007. GSK-3β Acts Upstream of Fyn Kinase in Regulation of Nuclear Export and Degradation of NF-E2 Related Factor 2. J. Biol. Chem. 282, 16502–16510. https://doi.org/10.1074/jbc.M611336200

Jain, A.K., Jaiswal, A.K., 2006. Phosphorylation of Tyrosine 568 Controls Nuclear Export of Nrf2. J. Biol. Chem. 281, 12132–12142. https://doi.org/10.1074/jbc.M511198200

Jang, J., Wang, Y., Kim, H.-S., Lalli, M.A., Kosik, K.S., 2014. Nrf2, a Regulator of the Proteasome, Controls Self-Renewal and Pluripotency in Human Embryonic Stem Cells. Stem Cells 32, 2616–2625. https://doi.org/10.1002/stem.1764

Jankovic, J., 2008. Parkinson's disease: clinical features and diagnosis. J. Neurol. Neurosurg. & Psychiatry 79, 368–76.

Jansen, A.H.P., Reits, E.A.J., Hol, E.M., 2014. The ubiquitin proteasome system in glia and its role in neurodegenerative diseases. Front. Mol. Neurosci. 7, 73. https://doi.org/10.3389/fnmol.2014.00073

Jelluma, N., 2006. Glucose Withdrawal Induces Oxidative Stress followed by Apoptosis in Glioblastoma Cells but not in Normal Human Astrocytes. Mol. Cancer Res. 4, 319–330. https://doi.org/10.1158/1541-

7786.MCR-05-0061

Jenner, P., Olanow, C.W., 1996. Oxidative stress and the pathogenesis of Parkinson's disease. Neurology 47, S161-70. https://doi.org/10.1212/wnl.47.6_suppl_3.161s

Jha, M.K., Kim, J.-H., Song, G.J., Lee, W.-H., Lee, I.-K., Lee, H.-W., An, S.S.A., Kim, S., Suk, K., 2018. Functional dissection of astrocyte-secreted proteins: Implications in brain health and diseases. Prog. Neurobiol. 162, 37–69. https://doi.org/10.1016/j.pneurobio.2017.12.003

Jha, M.K., Seo, M., Kim, J.-H., Kim, B.-G., Cho, J.-Y., Suk, K., 2013. The secretome signature of reactive glial cells and its pathological implications. Biochim. Biophys. Acta - Proteins Proteomics 1834, 2418–2428. https://doi.org/10.1016/j.bbapap.2012.12.006

Jha, S.K., Jha, N.K., Kumar, D., Ambasta, R.K., Kumar, P., 2017. Linking mitochondrial dysfunction, metabolic syndrome and stress signaling in Neurodegeneration. Biochim. Biophys. Acta - Mol. Basis Dis. 1863, 1132–1146. https://doi.org/10.1016/j.bbadis.2016.06.015

Jhoo, J.H., Kim, H.-C., Nabeshima, T., Yamada, K., Shin, E.-J., Jhoo, W.-K., Kim, W., Kang, K.-S., Jo, S.A., Woo, J.I., 2004. β-Amyloid (1–42)-induced learning and memory deficits in mice: involvement of oxidative burdens in the hippocampus and cerebral cortex. Behav. Brain Res. 155, 185–196. https://doi.org/10.1016/j.bbr.2004.04.012

Jiang, J., Nicoll, S.B., Lu, H.H., 2005. Co-culture of osteoblasts and chondrocytes modulates cellular differentiation in vitro. Biochem. Biophys. Res. Commun. 338, 762–770. https://doi.org/10.1016/j.bbrc.2005.10.025

Jiang, Q., Yan, Z., Feng, J., 2006. Neurotrophic Factors Stabilize Microtubules and Protect against Rotenone Toxicity on Dopaminergic Neurons. J. Biol. Chem. 281, 29391–29400. https://doi.org/10.1074/jbc.M602740200

Jimenez-Blasco, D., Santofimia-Castaño, P., Gonzalez, A., Almeida, A., Bolaños, J.P., 2015. Astrocyte NMDA receptors' activity sustains neuronal survival through a Cdk5–Nrf2 pathway. Cell Death Differ. 22, 1877–1889. https://doi.org/10.1038/cdd.2015.49

Johnston, J.P., 1968. Some observations upon a new inhibitor of monoamine oxidase in brain tissue. Biochem Pharmacol 17, 1285–1297. https://doi.org/10.1016/0006-2952(68)90066-X

Jonckheere, A.I., Smeitink, J.A.M., Rodenburg, R.J.T., 2012. Mitochondrial ATP synthase: architecture, function and pathology. J. Inherit. Metab. Dis. 35, 211–225. https://doi.org/10.1007/s10545-011-9382-9

Jönsson, T.J., Johnson, L.C., Lowther, W.T., 2008. Structure of the sulphiredoxin–peroxiredoxin complex reveals an essential repair embrace. Nature 451, 98–101. https://doi.org/10.1038/nature06415

Joshi, G., A. Johnson, J., 2012. The Nrf2-ARE Pathway: A Valuable Therapeutic Target for the Treatment of Neurodegenerative Diseases. Recent Pat. CNS Drug Discov. 7, 218–229. https://doi.org/10.2174/157488912803252023

Joshi, G., Perluigi, M., Sultana, R., Agrippino, R., Calabrese, V., Butterfield, D.A., 2006. In vivo protection of synaptosomes by ferulic acid ethyl ester (FAEE) from oxidative stress mediated by 2,2-azobis(2-amidino-propane)dihydrochloride (AAPH) or Fe2+/H2O2: Insight into mechanisms of neuroprotection and relevance to oxidative stress-related . Neurochem. Int. 48, 318–327. https://doi.org/10.1016/j.neuint.2005.11.006

Ju, C., Gao, J., Hou, L., Wang, L., Zhang, F., Sun, F., Zhang, T., Xu, P., Shi, Z., Hu, F., Zhang, C., 2017. Neuroprotective effect of chondroitin sulfate on SH-SY5Y cells overexpressing wild-type or A53T mutant α-synuclein. Mol. Med. Rep. 16, 8721–8728. https://doi.org/10.3892/mmr.2017.7725

Juaristi, I., Llorente-Folch, I., Satrústegui, J., del Arco, A., 2019. Extracellular ATP and glutamate drive pyruvate production and energy demand to regulate mitochondrial respiration in astrocytes. Glia 67, 759–774. https://doi.org/10.1002/glia.23574

Jucker, M., Walker, L.C., 2013. Self-propagation of pathogenic protein aggregates in neurodegenerative diseases. Nature 501, 45–51. https://doi.org/10.1038/nature12481

Junn, E., Jang, W.H., Zhao, X., Jeong, B.S., Mouradian, M.M., 2009. Mitochondrial localization of DJ-1 leads to enhanced neuroprotection. J. Neurosci. Res. 87, 123–129. https://doi.org/10.1002/jnr.21831

Junn, E., Mouradian, M.M., 2001. Apoptotic signaling in dopamine-induced cell death: the role of oxidative stress, p38 mitogen-activated protein kinase, cytochrome c and caspases. J. Neurochem. 78, 374–383. https://doi.org/10.1046/j.1471-4159.2001.00425.x

Kabiraj, P., Valenzuela, C.A., Marin, J.E., Ramirez, D.A., Mendez, L., Hwang, M.S., Varela-Ramirez, A., Fenelon, K., Narayan, M., Skouta, R., 2015. The Neuroprotective Role of Ferrostatin-1 Under Rotenone-Induced Oxidative Stress in Dopaminergic Neuroblastoma Cells. Protein J. 34, 349–358. https://doi.org/10.1007/s10930-015-9629-7

Kabuta, T., Setsuie, R., Mitsui, T., Kinugawa, A., Sakurai, M., Aoki, S., Uchida, K., Wada, K., 2008. Aberrant molecular properties shared by familial Parkinson's disease-associated mutant UCH-L1 and carbonyl-modified UCH-L1. Hum. Mol. Genet. https://doi.org/10.1093/hmg/ddn037

Kageyama, Y., Zhang, Z., Roda, R., Fukaya, M., Wakabayashi, J., Wakabayashi, N., Kensler, T.W., Reddy, P.H., Iijima, M., Sesaki, H., 2012. Mitochondrial division ensures the survival of postmitotic neurons by suppressing oxidative damage. J. Cell Biol. 197, 535–551. https://doi.org/10.1083/jcb.201110034

Kakimura, J.-I., Kitamura, Y., Takata, K., Umeki, M., Suzuki, S., Shibagaki, K., Taniguchi, T., Nomura, Y., Gebicke-Haerter, P.J., Smith, M.A., Perry, G., Shimohama, S., 2002. Microglial activation and amyloid-beta clearance induced by exogenous heat-shock proteins. FASEB J. 16, 601–3. https://doi.org/10.1096/fj.01-0530fje

Kalyanaraman, B., Darley-Usmar, V., Davies, K.J.A., Dennery, P.A., Forman, H.J., Grisham, M.B., Mann, G.E., Moore, K., Roberts, L.J., Ischiropoulos, H., 2012. Measuring reactive oxygen and nitrogen species with fluorescent probes: challenges and limitations. Free Radic. Biol. Med. 52, 1–6. https://doi.org/10.1016/j.freeradbiomed.2011.09.030

Kane, L.A., Lazarou, M., Fogel, A.I., Li, Y., Yamano, K., Sarraf, S.A., Banerjee, S., Youle, R.J., 2014. PINK1 phosphorylates ubiquitin to activate Parkin E3 ubiquitin ligase activity. J. Cell Biol. 205, 143–153. https://doi.org/10.1083/jcb.201402104

Kann, O., Kovács, R., 2007. Mitochondria and neuronal activity. Am. J. Physiol. Physiol. 292, C641–C657. https://doi.org/10.1152/ajpcell.00222.2006

Kanski, J., Aksenova, M., Stoyanova, A., Butterfield, D.A., 2002. Ferulic acid antioxidant protection against hydroxyl and peroxyl radical oxidation in synaptosomal and neuronal cell culture systems in vitro: structure-activity studies. J. Nutr. Biochem. 13, 273–281. https://doi.org/10.1016/S0955-2863(01)00215-7

Kaplan, D.R., Matsumoto, K., Lucarelli, E., Thielet, C.J., 1993. Induction of TrkB by retinoic acid mediates biologic responsiveness to BDNF and differentiation of human neuroblastoma cells. Neuron 11, 321–331. https://doi.org/10.1016/0896-6273(93)90187-V

Karbowski, M., 2010. Mitochondria on Guard: Role of Mitochondrial Fusion and Fission in the Regulation of Apoptosis, in: Advances in Experimental Medicine and Biology. pp. 131–142. https://doi.org/10.1007/978-1-4419-6706-0_8

Karmakar, S., Banik, N.L., Ray, S.K., 2008. Combination of all-trans retinoic acid and paclitaxel-induced differentiation and apoptosis in human glioblastoma U87MG xenografts in nude mice. Cancer 112, 596–607. https://doi.org/10.1002/cncr.23223

Kaspar, J.W., Jaiswal, A.K., 2011. Tyrosine phosphorylation controls nuclear export of Fyn, allowing Nrf2 activation of cytoprotective gene expression. FASEB J. 25, 1076–1087. https://doi.org/10.1096/fj.10-171553

Kaspar, J.W., Jaiswal, A.K., 2010a. Antioxidant-induced Phosphorylation of Tyrosine 486 Leads to Rapid

Nuclear Export of Bach1 That Allows Nrf2 to Bind to the Antioxidant Response Element and Activate Defensive Gene Expression. J. Biol. Chem. 285, 153–162. https://doi.org/10.1074/jbc.M109.040022

Kaspar, J.W., Jaiswal, A.K., 2010b. An Autoregulatory Loop between Nrf2 and Cul3-Rbx1 Controls Their Cellular Abundance. J. Biol. Chem. 285, 21349–21358. https://doi.org/10.1074/jbc.M110.121863

Kaspar, J.W., Niture, S.K., Jaiswal, A.K., 2009. Nrf2:INrf2 (Keap1) signaling in oxidative stress. Free Radic. Biol. Med. 47, 1304–1309. https://doi.org/10.1016/j.freeradbiomed.2009.07.035

Katschinski, D.M., Boos, K., Schindler, S.G., Fandrey, J., 2000. Pivotal Role of Reactive Oxygen Species as Intracellular Mediators of Hyperthermia-induced Apoptosis. J. Biol. Chem. 275, 21094–21098. https://doi.org/10.1074/jbc.M001629200

Katsetos, C.D., Dráberová, E., Šmejkalová, B., Reddy, G., Bertrand, L., de Chadarévian, J.-P., Legido, A., Nissanov, J., Baas, P.W., Dráber, P., 2007. Class III β-Tubulin and γ-Tubulin are Co-expressed and Form Complexes in Human Glioblastoma Cells. Neurochem. Res. 32, 1387–1398. https://doi.org/10.1007/s11064-007-9321-1

Katsetos, C.D., Herman, M.M., Mörk, S.J., 2003. Class III β-tubulin in human development and cancer. Cell Motil. Cytoskeleton 55, 77–96. https://doi.org/10.1002/cm.10116

Kauppila, T.E.S., Kauppila, J.H.K., Larsson, N.-G., 2017. Mammalian Mitochondria and Aging: An Update. Cell Metab. 25, 57–71. https://doi.org/10.1016/j.cmet.2016.09.017

Kayser, J., Haslbeck, M., Dempfle, L., Krause, M., Grashoff, C., Buchner, J., Herrmann, H., Bausch, A.R., 2013. The Small Heat Shock Protein Hsp27 Affects Assembly Dynamics and Structure of Keratin Intermediate Filament Networks. Biophys. J. 105, 1778–1785. https://doi.org/10.1016/j.bpj.2013.09.007

Kazlauskaite, A., Kondapalli, C., Gourlay, R., Campbell, D.G., Ritorto, M.S., Hofmann, K., Alessi, D.R., Knebel, A., Trost, M., Muqit, M.M.K., 2014. Parkin is activated by PINK1-dependent phosphorylation of ubiquitin at Ser 65. Biochem. J. 460, 127–141. https://doi.org/10.1042/BJ20140334

Keene, S.D., Greco, T.M., Parastatidis, I., Lee, S.-H., Hughes, E.G., Balice-Gordon, R.J., Speicher, D.W., Ischiropoulos, H., 2009. Mass spectrometric and computational analysis of cytokine-induced alterations in the astrocyte secretome. Proteomics 9, 768–782. https://doi.org/10.1002/pmic.200800385

Keller, J.., Huang, F.., Markesbery, W.., 2000. Decreased levels of proteasome activity and proteasome expression in aging spinal cord. Neuroscience 98, 149–156. https://doi.org/10.1016/S0306-4522(00)00067-1

Kensler, T.W., Wakabayashi, N., Biswal, S., 2007. Cell Survival Responses to Environmental Stresses Via the Keap1-Nrf2-ARE Pathway. Annu. Rev. Pharmacol. Toxicol. 47, 89–116. https://doi.org/10.1146/annurev.pharmtox.46.120604.141046

Kerschensteiner, M., Schwab, M.E., Lichtman, J.W., Misgeld, T., 2005. In vivo imaging of axonal degeneration and regeneration in the injured spinal cord. Nat. Med. 11, 572–577. https://doi.org/10.1038/nm1229

Khakh, B.S., Sofroniew, M. V, 2015. Diversity of astrocyte functions and phenotypes in neural circuits. Nat. Neurosci. 18, 942–952. https://doi.org/10.1038/nn.4043

Khatib, T., Marini, P., Nunna, S., Chisholm, D.R., Whiting, A., Redfern, C., Greig, I.R., McCaffery, P., 2019. Genomic and non-genomic pathways are both crucial for peak induction of neurite outgrowth by retinoids. Cell Commun. Signal. 17, 40. https://doi.org/10.1186/s12964-019-0352-4

Kim, J.-M., Cha, S.-H., Choi, Y.R., Jou, I., Joe, E.-H., Park, S.M., 2016. DJ-1 deficiency impairs glutamate uptake into astrocytes via the regulation of flotillin-1 and caveolin-1 expression. Sci. Rep. 6, 28823. https://doi.org/10.1038/srep28823

KIM, J., HAN, J., JANG, Y., KIM, S.J., LEE, M.J., RYU, M.J., KWEON, G.R., HEO, J.Y., 2015. High-capacity glycolytic and mitochondrial oxidative metabolisms mediate the growth ability of glioblastoma. Int. J. Oncol. 47, 1009–1016. https://doi.org/10.3892/ijo.2015.3101

Kim, R.H., Smith, P.D., Aleyasin, H., Hayley, S., Mount, M.P., Pownall, S., Wakeham, A., You-Ten, A.J., Kalia,

S.K., Horne, P., Westaway, D., Lozano, A.M., Anisman, H., Park, D.S., Mak, T.W., 2005. Hypersensitivity of DJ-1-deficient mice to 1-methyl-4-phenyl-1,2,3,6-tetrahydropyrindine (MPTP) and oxidative stress. Proc. Natl. Acad. Sci. 102, 5215–5220. https://doi.org/10.1073/pnas.0501282102

Kim, S.-J., Park, Y.-J., Hwang, I.-Y., Youdim, M.B.H., Park, K.-S., Oh, Y.J., 2012. Nuclear translocation of DJ-1 during oxidative stress-induced neuronal cell death. Free Radic. Biol. Med. 53, 936–950. https://doi.org/10.1016/j.freeradbiomed.2012.05.035

Kim, S.R., Ha, Y.M., Kim, Y.M., Park, E.J., Kim, J.W., Park, S.W., Kim, H.J., Chung, H.T., Chang, K.C., 2015. Ascorbic acid reduces HMGB1 secretion in lipopolysaccharide-activated RAW 264.7 cells and improves survival rate in septic mice by activation of Nrf2/HO-1 signals. Biochem. Pharmacol. 95, 279–289. https://doi.org/10.1016/j.bcp.2015.04.007

Kiss, R., Zhu, M., Jójárt, B., Czajlik, A., Solti, K., Fórizs, B., Nagy, É., Zsila, F., Beke-Somfai, T., Tóth, G., 2017. Structural features of human DJ-1 in distinct Cys106 oxidative states and their relevance to its loss of function in disease. Biochim. Biophys. Acta - Gen. Subj. 1861, 2619–2629. https://doi.org/10.1016/j.bbagen.2017.08.017

Kitada, T., Asakawa, S., Hattori, N., Matsumine, H., Yamamura, Y., Minoshima, S., Yokochi, M., Mizuno, Y., Shimizu, N., 1998. Mutations in the parkin gene cause autosomal recessive juvenile parkinsonism. Nature 392, 605–608. https://doi.org/10.1038/33416

Knott, A.B., Perkins, G., Schwarzenbacher, R., Bossy-Wetzel, E., 2008. Mitochondrial fragmentation in neurodegeneration. Nat. Rev. Neurosci. 9, 505–518. https://doi.org/10.1038/nrn2417

Kobayashi, M., Yamamoto, M., 2006. Nrf2-Keap1 regulation of cellular defense mechanisms against electrophiles and reactive oxygen species. Adv. Enzyme Regul. 46, 113–140. https://doi.org/10.1016/j.advenzreg.2006.01.007

Komander, D., Rape, M., 2012. The Ubiquitin Code. Annu. Rev. Biochem. 81, 203–229. https://doi.org/10.1146/annurev-biochem-060310-170328

Kondo, Y., Sasaki, T., Sato, Y., Amano, A., Aizawa, S., Iwama, M., Handa, S., Shimada, N., Fukuda, M., Akita, M., Lee, J., Jeong, K.-S., Maruyama, N., Ishigami, A., 2008. Vitamin C depletion increases superoxide generation in brains of SMP30/GNL knockout mice. Biochem. Biophys. Res. Commun. 377, 291–296. https://doi.org/10.1016/j.bbrc.2008.09.132

Kong, A.-N.T., Owuor, E., Yu, R., Hebbar, V., Chen, C., Hu, R., Mandlekar, S., 2001. Induction of xenobiotic enzymes by the map kinase pathway and the antioxidant or electrophile response element (ARE/EpRE) ,†, ‡. Drug Metab. Rev. 33, 255–271. https://doi.org/10.1081/DMR-120000652

Koopman, W.J.H., Verkaart, S., Visch, H.-J., van der Westhuizen, F.H., Murphy, M.P., van den Heuvel, L.W.P.J., Smeitink, J. a M., Willems, P.H.G.M., 2005. Inhibition of complex I of the electron transport chain causes O 2 − ·-mediated mitochondrial outgrowth. Am. J. Physiol. Physiol. 288, C1440–C1450. https://doi.org/10.1152/ajpcell.00607.2004

Koprich, J.B., Reske-Nielsen, C., Mithal, P., Isacson, O., 2008. Neuroinflammation mediated by IL-1β increases susceptibility of dopamine neurons to degeneration in an animal model of Parkinson's disease. J. Neuroinflammation 5, 8. https://doi.org/10.1186/1742-2094-5-8

Korovila, I., Hugo, M., Castro, J.P., Weber, D., Höhn, A., Grune, T., Jung, T., 2017. Proteostasis, oxidative stress and aging. Redox Biol. 13, 550–567. https://doi.org/10.1016/j.redox.2017.07.008

Koskenkorva-Frank, T.S., Weiss, G., Koppenol, W.H., Burckhardt, S., 2013. The complex interplay of iron metabolism, reactive oxygen species, and reactive nitrogen species: Insights into the potential of various iron therapies to induce oxidative and nitrosative stress. Free Radic. Biol. Med. 65, 1174–1194. https://doi.org/10.1016/j.freeradbiomed.2013.09.001

Kovac, S., Angelova, P.R., Holmström, K.M., Zhang, Y., Dinkova-Kostova, A.T., Abramov, A.Y., 2015. Nrf2 regulates ROS production by mitochondria and NADPH oxidase. Biochim. Biophys. Acta - Gen. Subj. 1850, 794–801. https://doi.org/10.1016/j.bbagen.2014.11.021

Kovalevich, J., Langford, D., 2013. Considerations for the Use of SH-SY5Y Neuroblastoma Cells in Neurobiology, in: Methods in Molecular Biology. pp. 9–21. https://doi.org/10.1007/978-1-62703-640-5_2

Kowal, J., Arras, G., Colombo, M., Jouve, M., Morath, J.P., Primdal-Bengtson, B., Dingli, F., Loew, D., Tkach, M., Théry, C., 2016. Proteomic comparison defines novel markers to characterize heterogeneous populations of extracellular vesicle subtypes. Proc. Natl. Acad. Sci. 113, E968–E977. https://doi.org/10.1073/pnas.1521230113

Kowald, A., Kirkwood, T.B.L., 2011. Evolution of the mitochondrial fusion-fission cycle and its role in aging. Proc. Natl. Acad. Sci. 108, 10237–10242. https://doi.org/10.1073/pnas.1101604108

KOWALD, A., KIRKWOOD, T.B.L., 2000. Accumulation of Defective Mitochondria through Delayed Degradation of Damaged Organelles and Its Possible Role in the Ageing of Post-mitotic and Dividing Cells. J. Theor. Biol. 202, 145–160. https://doi.org/10.1006/jtbi.1999.1046

Krance, S.M., Keng, P.C., Palis, J., Ballatori, N., 2010. Transient Glutathione Depletion Determines Terminal Differentiation in HL-60 Cells. Oxid. Med. Cell. Longev. 3, 53–60. https://doi.org/10.4161/oxim.3.1.10405

Kranich, O., Dringen, R., Sandberg, M., Hamprecht, B., 1998. Utilization of cysteine and cysteine precursors for the synthesis of glutathione in astroglial cultures: Preference for cystine. Glia 22, 11–18. https://doi.org/10.1002/(SICI)1098-1136(199801)22:1<11::AID-GLIA2>3.0.CO;2-B

Krishna, A., Biryukov, M., Trefois, C., Antony, P.M., Hussong, R., Lin, J., Heinäniemi, M., Glusman, G., Köglsberger, S., Boyd, O., van den Berg, B.H., Linke, D., Huang, D., Wang, K., Hood, L., Tholey, A., Schneider, R., Galas, D.J., Balling, R., May, P., 2014. Systems genomics evaluation of the SH-SY5Y neuroblastoma cell line as a model for Parkinson's disease. BMC Genomics 15, 1154. https://doi.org/10.1186/1471-2164-15-1154

Kritsiligkou, P., Chatzi, A., Charalampous, G., Mironov, A., Grant, C.M., Tokatlidis, K., 2017. Unconventional Targeting of a Thiol Peroxidase to the Mitochondrial Intermembrane Space Facilitates Oxidative Protein Folding. Cell Rep. 18, 2729–2741. https://doi.org/10.1016/j.celrep.2017.02.053

Kugler, W., Veenman, L., Shandalov, Y., Leschiner, S., Spanier, I., Lakomek, M., Gavish, M., 2008. Ligands of the mitochondrial 18 kDa translocator protein attenuate apoptosis of human glioblastoma cells exposed to erucylphosphohomocholine. Cell. Oncol. 30, 435–50. https://doi.org/10.3233/CLO-2008-0431

Kuhn, D.M., Arthur, R., 1998. Dopamine inactivates tryptophan hydroxylase and forms a redox-cycling quinoprotein: possible endogenous toxin to serotonin neurons. J. Neurosci. 18, 7111–7117.

Kujoth, G.C., 2005. Mitochondrial DNA Mutations, Oxidative Stress, and Apoptosis in Mammalian Aging. Science (80-.). 309, 481–484. https://doi.org/10.1126/science.1112125

Kumar, R., Jangir, D.K., Verma, G., Shekhar, S., Hanpude, P., Kumar, S., Kumari, R., Singh, N., Sarovar Bhavesh, N., Ranjan Jana, N., Kanti Maiti, T., 2017. S-nitrosylation of UCHL1 induces its structural instability and promotes α-synuclein aggregation. Sci. Rep. 7, 44558. https://doi.org/10.1038/srep44558

Kwak, M.-K., Wakabayashi, N., Greenlaw, J.L., Yamamoto, M., Kensler, T.W., 2003. Antioxidants Enhance Mammalian Proteasome Expression through the Keap1-Nrf2 Signaling Pathway. Mol. Cell. Biol. 23, 8786–8794. https://doi.org/10.1128/MCB.23.23.8786-8794.2003

L'Episcopo, Francesca, Serapide, M.F., Tirolo, C., Testa, N., Caniglia, S., Morale, M.C., Pluchino, S., Marchetti, B., 2011. A Wnt1 regulated Frizzled-1/β-Catenin signaling pathway as a candidate regulatory circuit controlling mesencephalic dopaminergic neuron-astrocyte crosstalk: Therapeutical relevance for neuron survival and neuroprotection. Mol. Neurodegener. 6, 49. https://doi.org/10.1186/1750-1326-6-49

L'Episcopo, F., Tirolo, C., Testa, N., Caniglia, S., Morale, M.C., Cossetti, C., D'Adamo, P., Zardini, E., Andreoni, L., Ihekwaba, A.E.C., Serra, P.A., Franciotta, D., Martino, G., Pluchino, S., Marchetti, B., 2011. Reactive

astrocytes and Wnt/β-catenin signaling link nigrostriatal injury to repair in 1-methyl-4-phenyl-1,2,3,6-tetrahydropyridine model of Parkinson's disease. Neurobiol. Dis. 41, 508–527. https://doi.org/10.1016/j.nbd.2010.10.023

Lackie, R.E., Maciejewski, A., Ostapchenko, V.G., Marques-Lopes, J., Choy, W.-Y., Duennwald, M.L., Prado, V.F., Prado, M.A.M., 2017. The Hsp70/Hsp90 Chaperone Machinery in Neurodegenerative Diseases. Front. Neurosci. 11, 254. https://doi.org/10.3389/fnins.2017.00254

Lafon-Cazal, M., Adjali, O., Galéotti, N., Poncet, J., Jouin, P., Homburger, V., Bockaert, J., Marin, P., 2003. Proteomic Analysis of Astrocytic Secretion in the Mouse. J. Biol. Chem. 278, 24438–24448. https://doi.org/10.1074/jbc.M211980200

Laganiere, J., Kells, A.P., Lai, J.T., Guschin, D., Paschon, D.E., Meng, X., Fong, L.K., Yu, Q., Rebar, E.J., Gregory, P.D., Bankiewicz, K.S., Forsayeth, J., Zhang, H.S., 2010. An engineered zinc finger protein activator of the endogenous glial cell line-derived neurotrophic factor gene provides functional neuroprotection in a rat model of Parkinson's disease. J. Neurosci. 30, 16469–74. https://doi.org/10.1523/JNEUROSCI.2440-10.2010

Lamarche, F., Signorini-Allibe, N., Gonthier, B., Barret, L., 2004. Influence of vitamin E, sodium selenite, and astrocyte-conditioned medium on neuronal survival after chronic exposure to ethanol. Alcohol 33, 127–38. https://doi.org/10.1016/j.alcohol.2004.09.001

Lambert, J.-P., Ivosev, G., Couzens, A.L., Larsen, B., Taipale, M., Lin, Z.-Y., Zhong, Q., Lindquist, S., Vidal, M., Aebersold, R., Pawson, T., Bonner, R., Tate, S., Gingras, A.-C., 2013. Mapping differential interactomes by affinity purification coupled with data-independent mass spectrometry acquisition. Nat. Methods 10, 1239–45. https://doi.org/10.1038/nmeth.2702

Lander, G.C., Estrin, E., Matyskiela, M.E., Bashore, C., Nogales, E., Martin, A., 2012. Complete subunit architecture of the proteasome regulatory particle. Nature 482, 186–191. https://doi.org/10.1038/nature10774

Langeveld, C.H., Schepens, E., Jongenelen, C.A.M., Stoof, J.C., Hjelle, O.P., Ottersen, O.P., Drukarch, B., 1996. Presence of glutathione immunoreactivity in cultured neurones and astrocytes. Neuroreport 7, 1833–1836. https://doi.org/10.1097/00001756-199607290-00029

Larsen, C.N., Krantz, B.A., Wilkinson, K.D., 1998. Substrate Specificity of Deubiquitinating Enzymes: Ubiquitin C-Terminal Hydrolases †. Biochemistry 37, 3358–3368. https://doi.org/10.1021/bi972274d

Larsen, C.N., Price, J.S., Wilkinson, K.D., 1996. Substrate binding and catalysis by ubiquitin C-terminal hydrolases: Identification of two active site residues. Biochemistry 35, 6735–6744. https://doi.org/10.1021/bi960099f

Larsen, N.J., Ambrosi, G., Mullett, S.J., Berman, S.B., Hinkle, D.A., 2011. DJ-1 knock-down impairs astrocyte mitochondrial function. Neuroscience 196, 251–264. https://doi.org/10.1016/j.neuroscience.2011.08.016

Lasker, K., Forster, F., Bohn, S., Walzthoeni, T., Villa, E., Unverdorben, P., Beck, F., Aebersold, R., Sali, A., Baumeister, W., 2012. Molecular architecture of the 26S proteasome holocomplex determined by an integrative approach. Proc. Natl. Acad. Sci. 109, 1380–1387. https://doi.org/10.1073/pnas.1120559109

Lau, L.W., Cua, R., Keough, M.B., Haylock-Jacobs, S., Yong, V.W., 2013. Pathophysiology of the brain extracellular matrix: a new target for remyelination. Nat. Rev. Neurosci. 14, 722–729. https://doi.org/10.1038/nrn3550

Le Naour, F., Misek, D.E., Krause, M.C., Deneux, L., Giordano, T.J., Scholl, S., Hanash, S.M., 2001. Proteomics-based identification of RS/DJ-1 as a novel circulating tumor antigen in breast cancer. Clin. Cancer Res. 7, 3328–3335. https://doi.org/10.1002/prca.200600718

Leddy, H.A., Awad, H.A., Guilak, F., 2004. Molecular diffusion in tissue-engineered cartilage constructs: Effects of scaffold material, time, and culture conditions. J. Biomed. Mater. Res. 70B, 397–406. https://doi.org/10.1002/jbm.b.30053

Lee, C.S., Lee, C., Hu, T., Nguyen, J.M., Zhang, J., Martin, M. V., Vawter, M.P., Huang, E.J., Chan, J.Y., 2011. Loss of nuclear factor E2-related factor 1 in the brain leads to dysregulation of proteasome gene expression and neurodegeneration. Proc. Natl. Acad. Sci. 108, 8408–8413. https://doi.org/10.1073/pnas.1019209108

Lee, C.S., Song, E.H., Park, S.Y., Han, E.S., 2003. Combined effect of dopamine and MPP+ on membrane permeability in mitochondria and cell viability in PC12 cells. Neurochem. Int. 43, 147–154. https://doi.org/10.1016/S0197-0186(02)00214-0

Lee, D., Ryu, K.-Y., 2017. Effect of cellular ubiquitin levels on the regulation of oxidative stress response and proteasome function via Nrf1. Biochem. Biophys. Res. Commun. 485, 234–240. https://doi.org/10.1016/j.bbrc.2017.02.105

Lee, J.-M., Calkins, M.J., Chan, K., Kan, Y.W., Johnson, J.A., 2003a. Identification of the NF-E2-related Factor-2-dependent Genes Conferring Protection against Oxidative Stress in Primary Cortical Astrocytes Using Oligonucleotide Microarray Analysis. J. Biol. Chem. 278, 12029–12038. https://doi.org/10.1074/jbc.M211558200

Lee, J.-M., Shih, A.Y., Murphy, T.H., Johnson, J.A., 2003b. NF-E2-related Factor-2 Mediates Neuroprotection against Mitochondrial Complex I Inhibitors and Increased Concentrations of Intracellular Calcium in Primary Cortical Neurons. J. Biol. Chem. 278, 37948–37956. https://doi.org/10.1074/jbc.M305204200

Lee, J.C., 1963. Electron microscopy of Wallerian degeneration. J. Comp. Neurol. 120, 65–79. https://doi.org/10.1002/cne.901200107

Lee, J.R., Kim, J.K., Lee, S.J., Kim, K.P., 2009. Role of protein tyrosine nitration in neurodegenerative diseases and atherosclerosis. Arch. Pharm. Res. 32, 1109–1118. https://doi.org/10.1007/s12272-009-1802-0

Lee, T.-C., Kashyap, R.L., 1994. Building Skeleton Models via 3-D Medial Surface/Axis Thinning Algorithms. Graph. Model. Image Process. 56, 462–78.

Lee, W.-C., Wong, H.-Y., Chai, Y.-Y., Shi, C.-W., Amino, N., Kikuchi, S., Huang, S.-H., 2012. Lipid peroxidation dysregulation in ischemic stroke: Plasma 4-HNE as a potential biomarker? Biochem. Biophys. Res. Commun. 425, 842–847. https://doi.org/10.1016/j.bbrc.2012.08.002

Lemasters, J.J., 2014. Variants of mitochondrial autophagy: Types 1 and 2 mitophagy and micromitophagy (Type 3). Redox Biol. 2, 749–754. https://doi.org/10.1016/j.redox.2014.06.004

Leroy, E., Boyer, R., Auburger, G., Leube, B., Ulm, G., Mezey, E., Harta, G., Brownstein, M.J., Jonnalagada, S., Chernova, T., Dehejia, a, Lavedan, C., Gasser, T., Steinbach, P.J., Wilkinson, K.D., Polymeropoulos, M.H., 1998. The ubiquitin pathway in Parkinson's disease. Nature 395, 451–452. https://doi.org/10.1038/26652

Lev, N., Barhum, Y., Ben-Zur, T., Melamed, E., Steiner, I., Offen, D., 2013. Knocking Out DJ-1 Attenuates Astrocytes Neuroprotection Against 6-Hydroxydopamine Toxicity. J. Mol. Neurosci. 50, 542–550. https://doi.org/10.1007/s12031-013-9984-9

Levental, I., Georges, P.C., Janmey, P.A., 2007. Soft biological materials and their impact on cell function. Soft Matter 3, 299–306. https://doi.org/10.1039/B610522J

Levin, M., Udi, Y., Solomonov, I., Sagi, I., 2017. Next generation matrix metalloproteinase inhibitors — Novel strategies bring new prospects. Biochim. Biophys. Acta - Mol. Cell Res. 1864, 1927–1939. https://doi.org/10.1016/j.bbamcr.2017.06.009

Li, B., Harjani, J.R., Cormier, N.S., Madarati, H., Atkinson, J., Cosa, G., Pratt, D.A., 2013. Besting Vitamin E: Sidechain Substitution is Key to the Reactivity of Naphthyridinol Antioxidants in Lipid Bilayers. J. Am. Chem. Soc. 135, 1394–1405. https://doi.org/10.1021/ja309153x

Li, D., Han, B., Liu, Z., Zhao, D., 2001. Phase behavior of supercritical CO 2 /Styrene/Poly(ethylene terephthlate) (PET) system and preparation of polystyrene/PET composites. Polymer (Guildf). 42, 2331–2337. https://doi.org/10.1016/S0032-3861(00)00601-7

Li, H.M., Niki, T., Taira, T., Iguchi-Ariga, S.M.M., Ariga, H., 2005. Association of DJ-1 with chaperones and enhanced association and colocalization with mitochondrial Hsp70 by oxidative stress. Free Radic. Res. 39, 1091–1099. https://doi.org/10.1080/10715760500260348

Li, M.-L., Defren, J., Brewer, G., 2013. Hsp27 and F-Box Protein -TrCP Promote Degradation of mRNA Decay Factor AUF1. Mol. Cell. Biol. 33, 2315–2326. https://doi.org/10.1128/MCB.00931-12

Li, W., James, M.O., McKenzie, S.C., Calcutt, N.A., Liu, C., Stacpoole, P.W., 2011. Mitochondrion as a Novel Site of Dichloroacetate Biotransformation by Glutathione Transferase ζ1. J. Pharmacol. Exp. Ther. 336, 87–94. https://doi.org/10.1124/jpet.110.173195

Li, Y., Xiao, Y., Liu, C., 2017. The Horizon of Materiobiology: A Perspective on Material-Guided Cell Behaviors and Tissue Engineering. Chem. Rev. 117, 4376–4421. https://doi.org/10.1021/acs.chemrev.6b00654

Liddell, J.R., Lehtonen, S., Duncan, C., Keksa-Goldsteine, V., Levonen, A.-L., Goldsteins, G., Malm, T., White, A.R., Koistinaho, J., Kanninen, K.M., 2016. Pyrrolidine dithiocarbamate activates the Nrf2 pathway in astrocytes. J. Neuroinflammation 13, 49. https://doi.org/10.1186/s12974-016-0515-9

Liddy, K.A., White, M.Y., Cordwell, S.J., 2013. Functional decorations: post-translational modifications and heart disease delineated by targeted proteomics. Genome Med. 5, 20. https://doi.org/10.1186/gm424

Lin, C.-Y., Lee, Y.-S., Lin, V.W., Silver, J., 2012. Fibronectin Inhibits Chronic Pain Development after Spinal Cord Injury. J. Neurotrauma 29, 589–599. https://doi.org/10.1089/neu.2011.2059

Lin, L., Doherty, D., Lile, J., Bektesh, S., Collins, F., 1993. GDNF: a glial cell line-derived neurotrophic factor for midbrain dopaminergic neurons. Science (80-.). 260, 1130–1132. https://doi.org/10.1126/science.8493557

Lin, M.-Y., Sheng, Z.-H., 2015. Regulation of mitochondrial transport in neurons. Exp. Cell Res. 334, 35–44. https://doi.org/10.1016/j.yexcr.2015.01.004

Lin, M.T., Beal, M.F.F., 2006. Mitochondrial dysfunction and oxidative stress in neurodegenerative diseases. Nature 443, 787–795. https://doi.org/nature05292 [pii]\r10.1038/nature05292

Lindersson, E., Beedholm, R., Højrup, P., Moos, T., Gai, W., Hendil, K.B., Jensen, P.H., 2004. Proteasomal Inhibition by α-Synuclein Filaments and Oligomers. J. Biol. Chem. 279, 12924–12934. https://doi.org/10.1074/jbc.M306390200

Linert, W., Herlinger, E., Jameson, R.F., Kienzl, E., Jellinger, K., Youdim, M.B.H., 1996. Dopamine, 6-hydroxydopamine, iron, and dioxygen - Their mutual interactions and possible implication in the development of Parkinson's disease. Biochim. Biophys. Acta - Mol. Basis Dis. 1316, 160–168. https://doi.org/10.1016/0925-4439(96)00020-8

Liu, K., Tedeschi, A., Park, K.K., He, Z., 2011. Neuronal Intrinsic Mechanisms of Axon Regeneration. Annu. Rev. Neurosci. 34, 131–152. https://doi.org/10.1146/annurev-neuro-061010-113723

Liu, Y., Wang, L., Long, Z., Zeng, L., Wu, Y., 2012. Protoplasmic Astrocytes Enhance the Ability of Neural Stem Cells to Differentiate into Neurons In Vitro. PLoS One 7, e38243. https://doi.org/10.1371/journal.pone.0038243

Liu, Z., Zhou, T., Ziegler, A.C., Dimitrion, P., Zuo, L., 2017. Oxidative Stress in Neurodegenerative Diseases: From Molecular Mechanisms to Clinical Applications. Oxid. Med. Cell. Longev. 2017, 1–11. https://doi.org/10.1155/2017/2525967

Livak, K.J., Schmittgen, T.D., 2001. Analysis of Relative Gene Expression Data Using Real-Time Quantitative PCR and the 2−ΔΔCT Method. Methods 25, 402–408. https://doi.org/10.1006/meth.2001.1262

Livnat-Levanon, N., Kevei, É., Kleifeld, O., Krutauz, D., Segref, A., Rinaldi, T., Erpapazoglou, Z., Cohen, M., Reis, N., Hoppe, T., Glickman, M.H., 2014. Reversible 26S Proteasome Disassembly upon Mitochondrial Stress. Cell Rep. 7, 1371–1380. https://doi.org/10.1016/j.celrep.2014.04.030

Ljubuncic, P., Gochman, E., Reznick, A.Z., 2010. Nitrosative Stress in Aging – Its Importance and Biological Implications in NF-κB Signaling, in: Aging and Age-Related Disorders. Humana Press, Totowa, NJ, pp.

27–54. https://doi.org/10.1007/978-1-60761-602-3_2

Loeb, V., Yakunin, E., Saada, A., Sharon, R., 2010. The Transgenic Overexpression of α-Synuclein and Not Its Related Pathology Associates with Complex I Inhibition. J. Biol. Chem. 285, 7334–7343. https://doi.org/10.1074/jbc.M109.061051

Lopes, F.M., Schröder, R., Júnior, M.L.C. da F., Zanotto-Filho, A., Müller, C.B., Pires, A.S., Meurer, R.T., Colpo, G.D., Gelain, D.P., Kapczinski, F., Moreira, J.C.F., Fernandes, M. da C., Klamt, F., 2010. Comparison between proliferative and neuron-like SH-SY5Y cells as an in vitro model for Parkinson disease studies. Brain Res. 1337, 85–94. https://doi.org/10.1016/j.brainres.2010.03.102

Lopiano, L., Fasano, M., Giraudo, S., Digilio, G., Koenig, S.H., Torre, E., Bergamasco, B., Aime, S., 2000. Nuclear magnetic relaxation dispersion profiles of substantia nigra pars compacta in Parkinson's disease patients are consistent with protein aggregation. Neurochem.Int. 37, 331–336.

Lores-Arnaiz, S., Lombardi, P., Karadayian, A.G., Orgambide, F., Cicerchia, D., Bustamante, J., 2016. Brain cortex mitochondrial bioenergetics in synaptosomes and non-synaptic mitochondria during aging. Neurochem. Res. 41, 353–363. https://doi.org/10.1007/s11064-015-1817-5

Lovatt, D., Sonnewald, U., Waagepetersen, H.S., Schousboe, A., He, W., Lin, J.H.-C., Han, X., Takano, T., Wang, S., Sim, F.J., Goldman, S.A., Nedergaard, M., 2007. The Transcriptome and Metabolic Gene Signature of Protoplasmic Astrocytes in the Adult Murine Cortex. J. Neurosci. 27, 12255–12266. https://doi.org/10.1523/JNEUROSCI.3404-07.2007

Lu, S.C., 2013. Glutathione synthesis. Biochim. Biophys. Acta 1830, 3143–53. https://doi.org/10.1016/j.bbagen.2012.09.008

Lubbe, S., Morris, H.R., 2014. Recent advances in Parkinson's disease genetics. J. Neurol. 261, 259–266. https://doi.org/10.1007/s00415-013-7003-2

Lubińska, L., 1982. Patterns of Wallerian degeneration of myelinated fibres in short and long peripheral stumps and in isolated segments of rat phrenic nerve. Interpretation of the role of axoplasmic flow of the trophic factor. Brain Res. 233, 227–240. https://doi.org/10.1016/0006-8993(82)91199-4

Lubińska, L., 1977. Early course of wallerian degeneration in myelinated fibres of the rat phrenic nerve. Brain Res. 130, 47–63. https://doi.org/10.1016/0006-8993(77)90841-1

Lucas, J.H., 1987. Proximal segment retraction increases the probability of nerve cell survival after dendrite transection. Brain Res. 425, 384–387. https://doi.org/10.1016/0006-8993(87)90526-9

Lucius, R., Sievers, J., 1996. Postnatal retinal ganglion cells in vitro: protection against reactive oxygen species (ROS)-induced axonal degeneration by cocultured astrocytes. Brain Res. 743, 56–62. https://doi.org/10.1016/S0006-8993(96)01029-3

Ludtmann, M.H.R., Angelova, P.R., Horrocks, M.H., Choi, M.L., Rodrigues, M., Baev, A.Y., Berezhnov, A. V., Yao, Z., Little, D., Banushi, B., Al-Menhali, A.S., Ranasinghe, R.T., Whiten, D.R., Yapom, R., Dolt, K.S., Devine, M.J., Gissen, P., Kunath, T., Jaganjac, M., Pavlov, E. V., Klenerman, D., Abramov, A.Y., Gandhi, S., 2018. α-synuclein oligomers interact with ATP synthase and open the permeability transition pore in Parkinson's disease. Nat. Commun. 9, 2293. https://doi.org/10.1038/s41467-018-04422-2

Luth, E.S., Stavrovskaya, I.G., Bartels, T., Kristal, B.S., Selkoe, D.J., 2014. Soluble, Prefibrillar α-Synuclein Oligomers Promote Complex I-dependent, Ca 2+ -induced Mitochondrial Dysfunction. J. Biol. Chem. 289, 21490–21507. https://doi.org/10.1074/jbc.M113.545749

Luzio, J.P., Pryor, P.R., Bright, N.A., 2007. Lysosomes: fusion and function. Nat. Rev. Mol. Cell Biol. 8, 622–632. https://doi.org/10.1038/nrm2217

Macedo, M.G., Anar, B., Bronner, I.F., Cannella, M., Squitieri, F., Bonifati, V., Hoogeveen, A., Heutink, P., Rizzu, P., 2003. The DJ-1L166P mutant protein associated with early onset Parkinson's disease is unstable and forms higher-order protein complexes. Hum. Mol. Genet. 12, 2807–2816. https://doi.org/10.1093/hmg/ddg304

Maiese, K., Li, F., Chong, Z.Z., Shang, Y.C., 2008. The Wnt signaling pathway: Aging gracefully as a protectionist? Pharmacol. Ther. 118, 58–81. https://doi.org/10.1016/j.pharmthera.2008.01.004

Maisonpierre, P., Belluscio, L., Squinto, S., Ip, N., Furth, M., Lindsay, R., Yancopoulos, G., 1990. Neurotrophin-3: a neurotrophic factor related to NGF and BDNF. Science (80-.). 247, 1446–1451. https://doi.org/10.1126/science.2321006

Makar, T.K., Nedergaard, M., Preuss, A., Gelbard, A.S., Perumal, A.S., Cooper, A.J.L., 2008. Vitamin E, Ascorbate, Glutathione, Glutathicne Disulfide, and Enzymes of Glutathione Metabolism in Cultures of Chick Astrocytes and Neurons: Evidence that Astrocytes Play an Important Role in Antioxidative Processes in the Brain. J. Neurochem. 62, 45–53. https://doi.org/10.1046/j.1471-4159.1994.62010045.x

Malone, P.E., Hernandez, M.R., 2007. 4-Hydroxynonenal, a product of oxidative stress, leads to an antioxidant response in optic nerve head astrocytes. Exp. Eye Res. 84, 444–454. https://doi.org/10.1016/j.exer.2006.10.020

Malyshev, I.Y., Malugin, A. V., Golubeva, L.Y., Zenina, T.A., Manukhina, E.B., Mikoyan, V.D., Vanin, A.F., 1996. Nitric oxide donor induces HSP70 accumulation in the heart and in cultured cells. FEBS Lett. 391, 21–23. https://doi.org/10.1016/0014-5793(96)00691-6

Manevich, Y., Shuvaeva, T., Dodia, C., Kazi, A., Feinstein, S.I., Fisher, A.B., 2009. Binding of peroxiredoxin 6 to substrate determines differential phospholipid hydroperoxide peroxidase and phospholipase A2 activities. Arch. Biochem. Biophys. 485, 139–149. https://doi.org/10.1016/j.abb.2009.02.008

Manning-Bog, A.B., McCormack, A.L., Li, J., Uversky, V.N., Fink, A.L., Di Monte, D.A., 2002. The herbicide paraquat causes up-regulation and aggregation of α-synuclein in mice: Paraquat and α-synuclein. J. Biol. Chem. 277, 1641–1644. https://doi.org/10.1074/jbc.C100560200

Manzerra, P., Rush, S.J., Brown, I.R., 1997. Tissue-specific differences in heat shock protein hsc70 and hsp70 in the control and hyperthermic rabbit. J. Cell. Physiol. 170, 130–137. https://doi.org/10.1002/(SICI)1097-4652(199702)170:2<130::AID-JCP4>3.0.CO;2-P

Maragakis, N.J., Rothstein, J.D., 2006. Mechanisms of Disease: astrocytes in neurodegenerative disease. Nat. Clin. Pract. Neurol. 2, 679–689. https://doi.org/10.1038/ncpneuro0355

Marchetti, B., L'Episcopo, F., Morale, M.C., Tirolo, C., Testa, N., Caniglia, S., Serapide, M.F., Pluchino, S., 2013. Uncovering novel actors in astrocyte-neuron crosstalk in Parkinson's disease: The Wnt/β-catenin signaling cascade as the common final pathway for neuroprotection and self-repair. Eur. J. Neurosci. 37, 1550–1563. https://doi.org/10.1111/ejn.12166

Marchetti, B., L'Episcopo, F., Tirolo, C., Testa, N., Caniglia, S., Morale, M.C., 2011. Vulnerability to Parkinson's Disease: Towards an Unifying Theory of Disease Etiology, in: Encyclopedia of Environmental Health. pp. 690–704. https://doi.org/http://dx.doi.org/10.1016/B978-0-444-52272-6.00079-9

Marcuccilli, C.J., Mathur, S.K., Morimoto, R.I., Miller, R.J., 1996. Regulatory differences in the stress response of hippocampal neurons and glial cells after heat shock. J. Neurosci. 16, 478–85.

Marí, M., Morales, A., Colell, A., García-Ruiz, C., Kaplowitz, N., Fernández-Checa, J.C., 2013. Mitochondrial glutathione: Features, regulation and role in disease. Biochim. Biophys. Acta - Gen. Subj. 1830, 3317–3328. https://doi.org/10.1016/j.bbagen.2012.10.018

Markesbery, W.R., Lovell, M.A., 1998. Four-hydroxynonenal, a product of lipid peroxidation, is increased in the brain in Alzheimer's disease. Neurobiol. Aging 19, 33–36. https://doi.org/10.1016/S0197-4580(98)00009-8

Martinez-Ruiz, A., Villanueva, L., de Orduna, C.G., Lopez-Ferrer, D., Higueras, M.A., Tarin, C., Rodriguez-Crespo, I., Vazquez, J., Lamas, S., 2005. S-nitrosylation of Hsp90 promotes the inhibition of its ATPase and endothelial nitric oxide synthase regulatory activities. Proc. Natl. Acad. Sci. 102, 8525–8530. https://doi.org/10.1073/pnas.0407294102

Martinez-Vicente, M., Cuervo, A.M., 2007. Autophagy and neurodegeneration: when the cleaning crew goes

on strike. Lancet Neurol. 6, 352–361. https://doi.org/10.1016/S1474-4422(07)70076-5

Masoud, S.T., Vecchio, L.M., Bergeron, Y., Hossain, M.M., Nguyen, L.T., Bermejo, M.K., Kile, B., Sotnikova, T.D., Siesser, W.B., Gainetdinov, R.R., Wightman, R.M., Caron, M.G., Richardson, J.R., Miller, G.W., Ramsey, A.J., Cyr, M., Salahpour, A., 2015. Increased expression of the dopamine transporter leads to loss of dopamine neurons, oxidative stress and l-DOPA reversible motor deficits. Neurobiol. Dis. 74, 66–75. https://doi.org/10.1016/j.nbd.2014.10.016

Matsumoto, K., Wada, R.K., Yamashiro, J.M., Kaplan, D.R., Thiele, C.J., 1995. Expression of Brain-derived Neurotrophic Factor and p145TrkBAffects Survival, Differentiation, and Invasiveness of Human Neuroblastoma Cells. Cancer Res. 55, 1798–1806.

Mayer, A.N., Wilkinson, K.D., 1989. Detection, resolution, and nomenclature of multiple ubiquitin carboxyl-terminal esterases from bovine calf thymus. Biochemistry 28, 166–172. https://doi.org/10.1021/bi00427a024

McGeer, P.L., Itagaki, S., Boyes, B.E., McGeer, E.G., 1988. Reactive microglia are positive for HLA-DR in the substantia nigra of Parkinson's and Alzheimer's disease brains. Neurology 38, 1285–1291. https://doi.org/10.1212/WNL.38.8.1285

McLennan, H.R., Degli Esposti, M., 2000. The contribution of mitochondrial respiratory complexes to the production of reactive oxygen species. J. Bioenerg. Biomembr. 32, 153–62. https://doi.org/10.1023/A:1005507913372

McNaught, K.S.., Jenner, P., 2001a. Proteasomal function is impaired in substantia nigra in Parkinson's disease. Neurosci. Lett. 297, 191–194. https://doi.org/10.1016/S0304-3940(00)01701-8

McNaught, K.S.., Jenner, P., 2001b. Proteasomal function is impaired in substantia nigra in Parkinson's disease. Neurosci. Lett. 297, 191–194. https://doi.org/10.1016/S0304-3940(00)01701-8

McNaught, K.S.P., Belizaire, R., Isacson, O., Jenner, P., Olanow, C.W., 2003. Altered proteasomal function in sporadic Parkinson's disease. Exp. Neurol. 179, 38–46. https://doi.org/10.1006/exnr.2002.8050

Mcnaught, K.S.P., Olanow, C.W., Halliwell, B., Isacson, O., Jenner, P., 2001. Failure of the ubiquitin–proteasome system in Parkinson's disease. Nat. Rev. Neurosci. 2, 589– 594.

Meacham, G.C., Patterson, C., Zhang, W., Younger, J.M., Cyr, D.M., 2001. The Hsc70 co-chaperone CHIP targets immature CFTR for proteasomal degradation. Nat. Cell Biol. 3, 100–105. https://doi.org/10.1038/35050509

Mehlen, P., Kretz-Remy, C., Préville, X., Arrigo, A.P., 1996. Human hsp27, Drosophila hsp27 and human alphaB-crystallin expression-mediated increase in glutathione is essential for the protective activity of these proteins against TNFalpha-induced cell death. EMBO J. 15, 2695–706.

Mele, L., Paino, F., Papaccio, F., Regad, T., Boocock, D., Stiuso, P., Lombardi, A., Liccardo, D., Aquino, G., Barbieri, A., Arra, C., Coveney, C., La Noce, M., Papaccio, G., Caraglia, M., Tirino, V., Desiderio, V., 2018. A new inhibitor of glucose-6-phosphate dehydrogenase blocks pentose phosphate pathway and suppresses malignant proliferation and metastasis in vivo. Cell Death Dis. 9, 572. https://doi.org/10.1038/s41419-018-0635-5

Mena, M. a, García de Yébenes, J., 2008. Glial cells as players in parkinsonism: the "good," the "bad," and the "mysterious" glia. Neuroscientist 14, 544–560. https://doi.org/10.1177/1073858408322839

Menegon, A., Board, P.G., Blackburn, A.C., Mellick, G.D., Couteur, D.G. Le, 1998. Parkinson's disease, pesticides, and glutathione transferase polymorphisms. Lancet 352, 1344–1346. https://doi.org/10.1016/S0140-6736(98)03453-9

Meredith, G.E., Totterdell, S., Potashkin, J.A., Surmeier, D.J., 2008. Modeling PD pathogenesis in mice: Advantages of a chronic MPTP protocol. Parkinsonism Relat. Disord. 14, S112–S115. https://doi.org/10.1016/j.parkreldis.2008.04.012

Merlini, G., Bellotti, V., 2003. Molecular Mechanisms of Amyloidosis. N. Engl. J. Med. 349, 583–596.

https://doi.org/10.1056/NEJMra023144

Mey, J., Mccaffery, P., 2004. Retinoic Acid Signaling in the Nervous System of Adult Vertebrates. Neurosci. 10, 409–421. https://doi.org/10.1177/1073858404263520

Miki, M., Tamai, H., Mino, M., Yamamoto, Y., Niki, E., 1987. Free-radical chain oxidation of rat red blood cells by molecular oxygen and its inhibition by α-tocopherol. Arch. Biochem. Biophys. 258, 373–380. https://doi.org/10.1016/0003-9861(87)90358-4

Miki, Y., Shimoyama, S., Kon, T., Ueno, T., Hayakari, R., Tanji, K., Matsumiya, T., Tsushima, E., Mori, F., Wakabayashi, K., Tomiyama, M., 2018. Alteration of autophagy-related proteins in peripheral blood mononuclear cells of patients with Parkinson's disease. Neurobiol. Aging 63, 33–43. https://doi.org/10.1016/j.neurobiolaging.2017.11.006

Miklossy, J., Doudet, D.D., Schwab, C., Yu, S., McGeer, E.G., McGeer, P.L., 2006. Role of ICAM-1 in persisting inflammation in Parkinson disease and MPTP monkeys. Exp. Neurol. 197, 275–283. https://doi.org/10.1016/j.expneurol.2005.10.034

Miller, D.W., Ahmad, R., Hague, S., Baptista, M.J., Canet-Aviles, R., McLendon, C., Carter, D.M., Zhu, P.P., Stadler, J., Chandran, J., Klinefelter, G.R., Blackstone, C., Cookson, M.R., 2003. L166P mutant DJ-1, causative for recessive Parkinson's disease, is degraded through the ubiquitin-proteasome system. J. Biol. Chem. 278, 36588–36595. https://doi.org/10.1074/jbc.M304272200

Mitsumoto, A., Nakagawa, Y., 2001. DJ-1 is an indicator for endogenous reactive oxygen species elicited by endotoxin. Free Radic. Res. 35, 885–93. https://doi.org/10.1080/10715760100301381

Mitsumoto, A., Nakagawa, Y., Takeuchi, A., Okawa, K., Iwamatsu, A., Takanezawa, Y., 2001. Oxidized forms of peroxiredoxins and DJ-1 on two-dimensional gels increased in response to sublethal levels of paraquat. Free Radic. Res. 35, 301–10. https://doi.org/10.1080/10715760100300831

Miyake, Y., Fukushima, W., Tanaka, K., Sasaki, S., Kiyohara, C., Tsuboi, Y., Yamada, T., Oeda, T., Miki, T., Kawamura, N., Sakae, N., Fukuyama, H., Hirota, Y., Nagai, M., 2011. Dietary intake of antioxidant vitamins and risk of Parkinson's disease: a case-control study in Japan. Eur. J. Neurol. 18, 106–113. https://doi.org/10.1111/j.1468-1331.2010.03088.x

Mizuno, Y., Ohta, S., Tanaka, M., Takamiya, S., Suzuki, K., Sato, T., Oya, H., Ozawa, T., Kagawa, Y., 1989. Deficiencies in Complex I subunits of the respiratory chain in Parkinson's disease. Biochem. Biophys. Res. Commun. 163, 1450–1455. https://doi.org/10.1016/0006-291X(89)91141-8

Mizushima, N., Levine, B., Cuervo, A.M., Klionsky, D.J., 2008. Autophagy fights disease through cellular self-digestion. Nature 451, 1069–1075. https://doi.org/10.1038/nature06639

Mocchegiani, E., Costarelli, L., Giacconi, R., Malavolta, M., Basso, A., Piacenza, F., Ostan, R., Cevenini, E., Gonos, E.S., Franceschi, C., Monti, D., 2014. Vitamin E–gene interactions in aging and inflammatory age-related diseases: Implications for treatment. A systematic review. Ageing Res. Rev. 14, 81–101. https://doi.org/10.1016/j.arr.2014.01.001

Molina-Jiménez, M.F., Sánchez-Reus, M.I., Andres, D., Cascales, M., Benedi, J., 2004. Neuroprotective effect of fraxetin and myricetin against rotenone-induced apoptosis in neuroblastoma cells. Brain Res. 1009, 9–16. https://doi.org/10.1016/j.brainres.2004.02.065

Møller, I.M., Rogowska-Wrzesinska, A., Rao, R.S.P., 2011. Protein carbonylation and metal-catalyzed protein oxidation in a cellular perspective. J. Proteomics 74, 2228–2242. https://doi.org/10.1016/j.jprot.2011.05.004

Moncada, S., Bolanos, J.P., 2006. Nitric oxide, cell bioenergetics and neurodegeneration. J. Neurochem. 97, 1676–1689. https://doi.org/10.1111/j.1471-4159.2006.03988.x

Moore, N.H., Costa, L.G., Shaffer, S.A., Goodlett, D.R., Guizzetti, M., 2009. Shotgun proteomics implicates extracellular matrix proteins and protease systems in neuronal development induced by astrocyte cholinergic stimulation. J. Neurochem. 108, 891–908. https://doi.org/10.1111/j.1471-4159.2008.05836.x

Morimoto, R.I., 2002. Dynamic remodeling of transcription complexes by molecular chaperones. Cell 110, 281–4. https://doi.org/10.1016/s0092-8674(02)00860-7

Morimoto, R.I., 1998. Regulation of the heat shock transcriptional response: cross talk between a family of heat shock factors, molecular chaperones, and negative regulators. Genes Dev. 12, 3788–3796. https://doi.org/10.1101/gad.12.24.3788

Mostafavi-Pour, Z., Ramezani, F., Keshavarzi, F., Samadi, N., 2017. The role of quercetin and vitamin C in Nrf2-dependent oxidative stress production in breast cancer cells. Oncol. Lett. 13, 1965–1973. https://doi.org/10.3892/ol.2017.5619

Mothersill, C., Seymour, C.B., O'Brien, A., 2007. Induction of c-myc oncoprotein and of cellular proliferation by radiation in normal human urothelial cultures. Anticancer Res. 11, 1609–12. https://doi.org/10.1002/jor.20475

Motohashi, H., Yamamoto, M., 2004. Nrf2–Keap1 defines a physiologically important stress response mechanism. Trends Mol. Med. 10, 549–557. https://doi.org/10.1016/j.molmed.2004.09.003

Muchowski, P.J., Wacker, J.L., 2005. Modulation of neurodegeneration by molecular chaperones. Nat. Rev. Neurosci. 6, 11–22. https://doi.org/10.1038/nrn1587

Müftüoglu, M., Elibol, B., Dalmizrak, Ö., Ercan, A., Kulaksiz, G., Ögüs, H., Dalkara, T., Özer, N., 2004. Mitochondrial complex I and IV activities in leukocytes from patients with parkin mutations. Mov. Disord. 19, 544–548. https://doi.org/10.1002/mds.10695

Muller, D.P., Goss-Sampson, M.A., 1990. Neurochemical, neurophysiological, and neuropathological studies in vitamin E deficiency. Crit. Rev. Neurobiol. 5, 239–63.

Muñoz, P., Huenchuguala, S., Paris, I., Segura-Aguilar, J., 2012. Dopamine Oxidation and Autophagy. Parkinsons. Dis. 2012, 1–13. https://doi.org/10.1155/2012/920953

Murray, J., Taylor, S.W., Zhang, B., Ghosh, S.S., Capaldi, R.A., 2003. Oxidative Damage to Mitochondrial Complex I Due to Peroxynitrite. J. Biol. Chem. 278, 37223–37230. https://doi.org/10.1074/jbc.M305694200

Nagakubo, D., Taira, T., Kitaura, H., Ikeda, M., Tamai, K., Iguchi-Ariga, S.M., Ariga, H., 1997. DJ-1, a novel oncogene which transforms mouse NIH3T3 cells in cooperation with ras. Biochem. Biophys. Res. Commun. 231, 509–513. https://doi.org/10.1006/bbrc.1997.6132

Nakamura, H., Nakamura, K., Yodoi, J., 1997. REDOX REGULATION OF CELLULAR ACTIVATION. Annu. Rev. Immunol. 15, 351–369. https://doi.org/10.1146/annurev.immunol.15.1.351

Nakamura, T., Tu, S., Akhtar, M.W., Sunico, C.R., Okamoto, S., Lipton, S.A., 2013. Aberrant Protein S-Nitrosylation in Neurodegenerative Diseases. Neuron 78, 596–614. https://doi.org/10.1016/j.neuron.2013.05.005

Nakata, T., Terada, S., Hirokawa, N., 1998. Visualization of the Dynamics of Synaptic Vesicle and Plasma Membrane Proteins in Living Axons. J. Cell Biol. 140, 659–674. https://doi.org/10.1083/jcb.140.3.659

Naoi, M., Maruyama, W., Yi, H., Inaba, K., Akao, Y., Shamoto-Nagai, M., 2009. Mitochondria in neurodegenerative disorders: Regulation of the redox state and death signaling leading to neuronal death and survival. J. Neural Transm. 116, 1371–1381. https://doi.org/10.1007/s00702-009-0309-7

Narendra, D., Tanaka, A., Suen, D.F., Youle, R.J., 2008. Parkin is recruited selectively to impaired mitochondria and promotes their autophagy. J. Cell Biol. 183, 795–803. https://doi.org/10.1083/jcb.200809125

Näsström, T., Fagerqvist, T., Barbu, M., Karlsson, M., Nikolajeff, F., Kasrayan, A., Ekberg, M., Lannfelt, L., Ingelsson, M., Bergström, J., 2011. The lipid peroxidation products 4-oxo-2-nonenal and 4-hydroxy-2-nonenal promote the formation of α-synuclein oligomers with distinct biochemical, morphological, and functional properties. Free Radic. Biol. Med. 50, 428–437. https://doi.org/10.1016/j.freeradbiomed.2010.11.027

Navarro, A., Boveris, A., 2004. Rat brain and liver mitochondria develop oxidative stress and lose enzymatic

activities on aging. Am. J. Physiol. Integr. Comp. Physiol. 287, R1244–R1249. https://doi.org/10.1152/ajpregu.00226.2004

Nedić, O., Rattan, S.I.S., Grune, T., Trougakos, I.P., 2013. Molecular effects of advanced glycation end products on cell signalling pathways, ageing and pathophysiology. Free Radic. Res. 47, 28–38. https://doi.org/10.3109/10715762.2013.806798

Neely, M.D., Sidell, K.R., Graham, D.G., Montine, T.J., 2002. The Lipid Peroxidation Product 4-Hydroxynonenal Inhibits Neurite Outgrowth, Disrupts Neuronal Microtubules, and Modifies Cellular Tubulin. J. Neurochem. 72, 2323–2333. https://doi.org/10.1046/j.1471-4159.1999.0722323.x

Nesti, C., Pardini, C., Barachini, S., D'Alessandro, D., Siciliano, G., Murri, L., Petrini, M., Vaglini, F., 2011. Human dental pulp stem cells protect mouse dopaminergic neurons against MPP+ or rotenone. Brain Res. 1367, 94–102. https://doi.org/10.1016/j.brainres.2010.09.042

Neukomm, L.J., Freeman, M.R., 2014. Diverse cellular and molecular modes of axon degeneration. Trends Cell Biol. 24, 515–523. https://doi.org/10.1016/j.tcb.2014.04.003

Neumann, M., Müller, V., Görner, K., Kretzschmar, H.A., Haass, C., Kahle, P.J., 2004. Pathological properties of the Parkinson's disease-associated protein DJ-1 in alpha-synucleinopathies and tauopathies: relevance for multiple system atrophy and Pick's disease. Acta Neuropathol. 107, 489–96. https://doi.org/10.1007/s00401-004-0834-2

Neviackas, J.A., Kerstein, M.D., 1976. Pancreatic enzyme response with an elemental diet. Surg. Gynecol. Obstet. 142, 71–4.

Newhouse, K., Hsuan, S.L., Chang, S.H., Cai, B., Wang, Y., Xia, Z., 2004. Rotenone-induced apoptosis is mediated by p38 and JNK MAP kinases in human dopaminergic SH-SY5Y cells. Toxicol. Sci. 79, 137–146. https://doi.org/10.1093/toxsci/kfh089

Nguyen, T., Nioi, P., Pickett, C.B., 2009. The Nrf2-Antioxidant Response Element Signaling Pathway and Its Activation by Oxidative Stress. J. Biol. Chem. 284, 13291–13295. https://doi.org/10.1074/jbc.R900010200

Nguyen, T., Sherratt, P.J., Nioi, P., Yang, C.S., Pickett, C.B., 2005. Nrf2 Controls Constitutive and Inducible Expression of ARE-driven Genes through a Dynamic Pathway Involving Nucleocytoplasmic Shuttling by Keap1. J. Biol. Chem. 280, 32485–32492. https://doi.org/10.1074/jbc.M503074200

Ni, H.-M., Williams, J.A., Ding, W.-X., 2015. Mitochondrial dynamics and mitochondrial quality control. Redox Biol. 4, 6–13. https://doi.org/10.1016/j.redox.2014.11.006

Nieoullon, A., 2011. Neurodegenerative diseases and neuroprotection: current views and prospects. J. Appl. Biomed. 9, 173–183. https://doi.org/10.2478/v10136-011-0013-4

Niki, E., 2014. Role of vitamin E as a lipid-soluble peroxyl radical scavenger: in vitro and in vivo evidence. Free Radic. Biol. Med. 66, 3–12. https://doi.org/10.1016/j.freeradbiomed.2013.03.022

Niki, E., 1990. Free radical initiators as source of water- or lipid-soluble peroxyl radicals. Methods Enzymol. 186, 100–108. https://doi.org/10.1016/0076-6879(90)86095-D

Niki, E., Noguchi, N., Tsuchihashi, H., Gotoh, N., 1995. Interaction among vitamin C, vitamin E, and β-carotene, in: American Journal of Clinical Nutrition. pp. 1322–1326.

Nishiguchi, M., Tokugawa, K., Yamamoto, K., Akama, T., Nozawa, Y., Chaki, S., Ueki, T., Kameo, K., Okuyama, S., 2003. Increase in secretion of glial cell line-derived neurotrophic factor from glial cell lines by inhibitors of vacuolar ATPase. Neurochem. Int. 42, 493–498. https://doi.org/10.1016/S0197-0186(02)00139-0

Nishikawa, K., Li, H., Kawamura, R., Osaka, H., Wang, Y.L., Hara, Y., Hirokawa, T., Manago, Y., Amano, T., Noda, M., Aoki, S., Wada, K., 2003. Alterations of structure and hydrolase activity of parkinsonism-associated human ubiquitin carboxyl-terminal hydrolase L1 variants. Biochem. Biophys. Res. Commun. 304, 176–183. https://doi.org/10.1016/S0006-291X(03)00555-2

Nishikimi, M., 1975. Oxidation of ascorbic acid with superoxide anion generated by the xanthine-xanthine oxidase system. Biochem. Biophys. Res. Commun. 63, 463–468. https://doi.org/10.1016/0006-291X(75)90710-X

Nita, M., Grzybowski, A., 2016. The Role of the Reactive Oxygen Species and Oxidative Stress in the Pathomechanism of the Age-Related Ocular Diseases and Other Pathologies of the Anterior and Posterior Eye Segments in Adults. Oxid. Med. Cell. Longev. 2016, 1–23. https://doi.org/10.1155/2016/3164734

Nithianantharajah, J., 2004. Environmental enrichment results in cortical and subcortical changes in levels of synaptophysin and PSD-95 proteins. Neurobiol. Learn. Mem. 81, 200–210. https://doi.org/10.1016/j.nlm.2004.02.002

Niture, S.K., Jain, A.K., Shelton, P.M., Jaiswal, A.K., 2011. Src Subfamily Kinases Regulate Nuclear Export and Degradation of Transcription Factor Nrf2 to Switch Off Nrf2-mediated Antioxidant Activation of Cytoprotective Gene Expression. J. Biol. Chem. 286, 28821–28832. https://doi.org/10.1074/jbc.M111.255042

Niture, S.K., Jaiswal, A.K., 2009. Prothymosin-α Mediates Nuclear Import of the INrf2/Cul3·Rbx1 Complex to Degrade Nuclear Nrf2. J. Biol. Chem. 284, 13856–13868. https://doi.org/10.1074/jbc.M808084200

Niture, S.K., Khatri, R., Jaiswal, A.K., 2014. Regulation of Nrf2—an update. Free Radic. Biol. Med. 66, 36–44. https://doi.org/10.1016/j.freeradbiomed.2013.02.008

Nixon, R.A., 2006. Autophagy in neurodegenerative disease: friend, foe or turncoat? Trends Neurosci. 29, 528–535. https://doi.org/10.1016/j.tins.2006.07.003

Nollen, E.A.A., Brunsting, J.F., Roelofsen, H., Weber, L.A., Kampinga, H.H., 1999. In Vivo Chaperone Activity of Heat Shock Protein 70 and Thermotolerance. Mol. Cell. Biol. 19, 2069–2079. https://doi.org/10.1128/MCB.19.3.2069

Nowak, P., Szczerbak, G., Dabrowska, J., Bortel, A., Biedka, I., Kostrzewa, R.M., 2006. Molecular mechanisms of levodopa action in animal models of Parkinson's disease. Neurol. Neurochir. Pol. 40, 517–25.

Nuytemans, K., Theuns, J., Cruts, M., Van Broeckhoven, C., 2010. Genetic etiology of Parkinson disease associated with mutations in the SNCA, PARK2, PINK1, PARK7, and LRRK2 genes: a mutation update. Hum. Mutat. 31, 763–780. https://doi.org/10.1002/humu.21277

O'Malley, E.K., Sieber, B.-A., Black, I.B., Dreyfus, C.F., 1992. Mesencephalic type I astrocytes mediate the survival of substantia nigra dopaminergic neurons in culture. Brain Res. 582, 65–70. https://doi.org/10.1016/0006-8993(92)90317-3

Obashi, K., Okabe, S., 2013. Regulation of mitochondrial dynamics and distribution by synapse position and neuronal activity in the axon. Eur. J. Neurosci. 38, 2350–2363. https://doi.org/10.1111/ejn.12263

Oberley, T.D., Verwiebe, E., Zhong, W., Kang, S.W., Rhee, S.G., 2001. Localization of the thioredoxin system in normal rat kidney. Free Radic. Biol. Med. 30, 412–424. https://doi.org/10.1016/S0891-5849(00)00486-X

Obeso, J.A., Stamelou, M., Goetz, C.G., Poewe, W., Lang, A.E., Weintraub, D., Burn, D., Halliday, G.M., Bezard, E., Przedborski, S., Lehericy, S., Brooks, D.J., Rothwell, J.C., Hallett, M., DeLong, M.R., Marras, C., Tanner, C.M., Ross, G.W., Langston, J.W., Klein, C., Bonifati, V., Jankovic, J., Lozano, A.M., Deuschl, G., Bergman, H., Tolosa, E., Rodriguez-Violante, M., Fahn, S., Postuma, R.B., Berg, D., Marek, K., Standaert, D.G., Surmeier, D.J., Olanow, C.W., Kordower, J.H., Calabresi, P., Schapira, A.H.V., Stoessl, A.J., 2017. Past, present, and future of Parkinson's disease: A special essay on the 200th Anniversary of the Shaking Palsy. Mov. Disord. 32, 1264–1310. https://doi.org/10.1002/mds.27115

Oettinghaus, B., Schulz, J.M., Restelli, L.M., Licci, M., Savoia, C., Schmidt, A., Schmitt, K., Grimm, A., Morè, L., Hench, J., Tolnay, M., Eckert, A., D'Adamo, P., Franken, P., Ishihara, N., Mihara, K., Bischofberger, J., Scorrano, L., Frank, S., 2016. Synaptic dysfunction, memory deficits and hippocampal atrophy due to ablation of mitochondrial fission in adult forebrain neurons. Cell Death Differ. 23, 18–28.

https://doi.org/10.1038/cdd.2015.39

Ohgaki, H., Kleihues, P., 2005. Population-Based Studies on Incidence, Survival Rates, and Genetic Alterations in Astrocytic and Oligodendroglial Gliomas. J. Neuropathol. Exp. Neurol. 64, 479–489. https://doi.org/10.1093/jnen/64.6.479

Ohtsuji, M., Katsuoka, F., Kobayashi, A., Aburatani, H., Hayes, J.D., Yamamoto, M., 2008. Nrf1 and Nrf2 Play Distinct Roles in Activation of Antioxidant Response Element-dependent Genes. J. Biol. Chem. 283, 33554–33562. https://doi.org/10.1074/jbc.M804597200

Oláh, S., Füle, M., Komlósi, G., Varga, C., Báldi, R., Barzó, P., Tamás, G., 2009. Regulation of cortical microcircuits by unitary GABA-mediated volume transmission. Nature 461, 1278–1281. https://doi.org/10.1038/nature08503

Oliveros, J.C., 2007. Venny. An interactive tool for comparing lists with Venn Diagrams [WWW Document]. BioinfoGP of CNB-CSIC.

Olshina, M.A., Ben-Nissan, G., Sharon, M., 2018. Functional regulation of proteins by 20S proteasome proteolytic processing. Cell Cycle 17, 393–394. https://doi.org/10.1080/15384101.2017.1414682

Olson, S.D., Kambal, A., Pollock, K., Mitchell, G.-M., Stewart, H., Kalomoiris, S., Cary, W., Nacey, C., Pepper, K., Nolta, J.A., 2012. Examination of mesenchymal stem cell-mediated RNAi transfer to Huntington's disease affected neuronal cells for reduction of huntingtin. Mol. Cell. Neurosci. 49, 271–281. https://doi.org/10.1016/j.mcn.2011.12.001

Onyango, I.G., Lu, J., Rodova, M., Lezi, E., Crafter, A.B., Swerdlow, R.H., 2010. Regulation of neuron mitochondrial biogenesis and relevance to brain health. Biochim. Biophys. Acta - Mol. Basis Dis. 1802, 228–234. https://doi.org/10.1016/j.bbadis.2009.07.014

Orlowski, M., Meister, A., 1970. The γ-Glutamyl Cycle: A Possible Transport System for Amino Acids. Proc. Natl. Acad. Sci. 67, 1248–1255. https://doi.org/10.1073/pnas.67.3.1248

Ou, X.-M., Chen, K., Shih, J.C., 2006. Monoamine oxidase A and repressor R1 are involved in apoptotic signaling pathway. Proc. Natl. Acad. Sci. U. S. A. 103, 10923–8. https://doi.org/10.1073/pnas.0601515103

Oudard, S., Arvelo, F., Miccoli, L., Apiou, F., Dutrillaux, A., Poisson, M., Dutrillaux, B., Poupon, M., 1996. High glycolysis in gliomas despite low hexokinase transcription and activity correlated to chromosome 10 loss. Br. J. Cancer 74, 839–845. https://doi.org/10.1038/bjc.1996.446

Outeiro, T.F., Klucken, J., Strathearn, K.E., Liu, F., Nguyen, P., Rochet, J.-C., Hyman, B.T., McLean, P.J., 2006. Small heat shock proteins protect against α-synuclein-induced toxicity and aggregation. Biochem. Biophys. Res. Commun. 351, 631–638. https://doi.org/10.1016/j.bbrc.2006.10.085

Öztürk, G., Cengiz, N., Erdoğan, E., Him, A., Oğuz, E.K., Yenidünya, E., Ayşit, N., 2013. Two distinct types of dying back axonal degeneration in vitro. Neuropathol. Appl. Neurobiol. 39, 362–376. https://doi.org/10.1111/j.1365-2990.2012.01295.x

Pacelli, C., De Rasmo, D., Signorile, A., Grattagliano, I., di Tullio, G., D'Orazio, A., Nico, B., Comi, G. Pietro, Ronchi, D., Ferranini, E., Pirolo, D., Seibel, P., Schubert, S., Gaballo, A., Villani, G., Cocco, T., 2011. Mitochondrial defect and PGC-1α dysfunction in parkin-associated familial Parkinson's disease. Biochim. Biophys. Acta - Mol. Basis Dis. 1812, 1041–1053. https://doi.org/10.1016/j.bbadis.2010.12.022

Padgett, C.M., Whorton, A.R., 1998. Cellular Responses to Nitric Oxide: Role of Protein S-Thiolation/Dethiolation. Arch. Biochem. Biophys. 358, 232–242. https://doi.org/10.1006/abbi.1998.0859

Påhlman, S., Hoehner, J.C., Nånberg, E., Hedborg, F., Fagerström, S., Gestblom, C., Johansson, I., Larsson, U., Lavenius, E., Örtoft, E., Söderholm, H., 1995. Differentiation and survival influences of growth factors in human neuroblastoma. Eur. J. Cancer 31, 453–458. https://doi.org/10.1016/0959-8049(95)00033-F

Påhlman, S., Ruusala, A.-I., Abrahamsson, L., Mattsson, M.E.K., Esscher, T., 1984. Retinoic acid-induced differentiation of cultured human neuroblastoma cells: a comparison with phorbolester-induced differentiation. Cell Differ. 14, 135–144. https://doi.org/10.1016/0045-6039(84)90038-1

Palacino, J.J., Sagi, D., Goldberg, M.S., Krauss, S., Motz, C., Wacker, M., Klose, J., Shen, J., 2004. Mitochondrial dysfunction and oxidative damage in parkin-deficient mice. J. Biol. Chem. 279, 18614–22. https://doi.org/10.1074/jbc.M401135200

Palozza, P., Krinsky, N.I., 1992. β-Carotene and α-tocopherol are synergistic antioxidants. Arch. Biochem. Biophys. 297, 184–187. https://doi.org/10.1016/0003-9861(92)90658-J

Pampaloni, F., Reynaud, E.G., Stelzer, E.H.K., 2007. The third dimension bridges the gap between cell culture and live tissue. Nat. Rev. Mol. Cell Biol. 8, 839–845. https://doi.org/10.1038/nrm2236

Pan, J., Kao, Y.-L., Joshi, S., Jeetendran, S., DiPette, D., Singh, U.S., 2005. Activation of Rac1 by phosphatidylinositol 3-kinase in vivo: role in activation of mitogen-activated protein kinase (MAPK) pathways and retinoic acid-induced neuronal differentiation of SH-SY5Y cells. J. Neurochem. 93, 571–583. https://doi.org/10.1111/j.1471-4159.2005.03106.x

Papadia, S., Soriano, F.X., Léveillé, F., Martel, M.-A., Dakin, K.A., Hansen, H.H., Kaindl, A., Sifringer, M., Fowler, J., Stefovska, V., Mckenzie, G., Craigon, M., Corriveau, R., Ghazal, P., Horsburgh, K., Yankner, B.A., Wyllie, D.J.A., Ikonomidou, C., Hardingham, G.E., 2008. Synaptic NMDA receptor activity boosts intrinsic antioxidant defenses. Nat. Neurosci. 11, 476–487. https://doi.org/10.1038/nn2071

Papi, A., Bartolini, G., Ammar, K., Guerra, F., Ferreri, A.M., Rocchi, P., Orlandi, M., 2007. Inhibitory effects of retinoic acid and IIF on growth, migration and invasiveness in the U87MG human glioblastoma cell line. Oncol. Rep. 18, 1015–21.

Pappert, E.J., Tangney, C.C., Goetz, C.G., Ling, Z.D., Lipton, J.W., Stebbins, G.T., Carvey, P.M., 1996. Alpha-tocopherol in the ventricular cerebrospinal fluid of Parkinson's disease patients: Dose-response study and correlations with plasma levels. Neurology 47, 1037–1042. https://doi.org/10.1212/WNL.47.4.1037

Paradies, G., Petrosillo, G., Paradies, V., Ruggiero, F.M., 2010. Oxidative stress, mitochondrial bioenergetics, and cardiolipin in aging. Free Radic. Biol. Med. 48, 1286–1295. https://doi.org/10.1016/j.freeradbiomed.2010.02.020

Park, J., Kerner, A., Burns, M.A., Lin, X.N., 2011. Microdroplet-Enabled Highly Parallel Co-Cultivation of Microbial Communities. PLoS One 6, e17019. https://doi.org/10.1371/journal.pone.0017019

Park, J., Lee, S.B., Lee, S.B., Kim, Y., Song, S., Kim, S., Bae, E., Kim, J.M., Shong, M.H., Kim, J.M., Chung, J.K., 2006. Mitochondrial dysfunction in Drosophila PINK1 mutants is complemented by parkin. Nature 441, 1157–1161. https://doi.org/10.1038/nature04788

Park, M.H., Jo, M., Kim, Y.R., Lee, C.-K., Hong, J.T., 2016. Roles of peroxiredoxins in cancer, neurodegenerative diseases and inflammatory diseases. Pharmacol. Ther. 163, 1–23. https://doi.org/10.1016/j.pharmthera.2016.03.018

Park, S., Geddes, T.J., Javitch, J.A., Kuhn, D.M., 2003. Dopamine prevents nitration of tyrosine hydroxylase by peroxynitrite and nitrogen dioxide. Is nitrotyrosine formation an early step in dopamine neuronal damage? J. Biol. Chem. 278, 28736–28742. https://doi.org/10.1074/jbc.M304362200

Park, S.J., Lee, J.H., Kim, H.Y., Choi, Y.H., Park, J.S., Suh, Y.H., Park, S.M., Joe, E., Jou, I., 2012. Astrocytes, but not microglia, rapidly sense H_2O_2via STAT6 phosphorylation, resulting in cyclooxygenase-2 expression and prostaglandin release. J. Immunol. 188, 5132–41. https://doi.org/10.4049/jimmunol.1101600

Parker, W.D., Swerdlow, R.H., 1998. Mitochondrial Dysfunction in Idiopathic Parkinson Disease. Am. J. Hum. Genet. 62, 758–762. https://doi.org/10.1086/301812

Parkinson, J., 2002. An essay on the shaking palsy. 1817. J. Neuropsychiatry Clin. Neurosci. 14, 223–236; discussion 222. https://doi.org/10.1176/appi.neuropsych.14.2.223

Patapoutian, A., Reichardt, L.F., 2000. Roles of Wnt proteins in neural development and maintenance. Curr. Opin. Neurobiol. 10, 392–399. https://doi.org/10.1016/S0959-4388(00)00100-8

Pathare, G.R., Nagy, I., Sledz, P., Anderson, D.J., Zhou, H.-J., Pardon, E., Steyaert, J., Forster, F., Bracher, A., Baumeister, W., 2014. Crystal structure of the proteasomal deubiquitylation module Rpn8-Rpn11. Proc. Natl. Acad. Sci. 111, 2984–2989. https://doi.org/10.1073/pnas.1400546111

Patra, R.., Swarup, D., Dwivedi, S.., 2001. Antioxidant effects of α tocopherol, ascorbic acid and l-methionine on lead induced oxidative stress to the liver, kidney and brain in rats. Toxicology 162, 81–88. https://doi.org/10.1016/S0300-483X(01)00345-6

Pavlovic, D., Markisic, M., Pavlovic, A., Lackovic, M., Bozic, M., 2014. Vitamin A and the nervous system. Arch. Biol. Sci. 66, 1585–1590. https://doi.org/10.2298/ABS1404585P

Pelham, H.R.B., 1982. A regulatory upstream promoter element in the Drosophila Hsp 70 heat-shock gene. Cell 30, 517–528. https://doi.org/10.1016/0092-8674(82)90249-5

Pellerin, L., Magistretti, P.J., 1996. Excitatory Amino Acids Stimulate Aerobic Glycolysis in Astrocytes via an Activation of the Na^+/K^+ ATPase. Dev. Neurosci. 18, 336–342. https://doi.org/10.1159/000111426

Pendino, F., Flexor, M., Delhommeau, F., Buet, D., Lanotte, M., Segal-Bendirdjian, E., 2001. Retinoids down-regulate telomerase and telomere length in a pathway distinct from leukemia cell differentiation. Proc. Natl. Acad. Sci. 98, 6662–6667. https://doi.org/10.1073/pnas.111464998

Peng, K., Yang, L., Wang, J., Ye, F., Dan, G., Zhao, Y., Cai, Y., Cui, Z., Ao, L., Liu, J., Zou, Z., Sai, Y., Cao, J., 2017. The Interaction of Mitochondrial Biogenesis and Fission/Fusion Mediated by PGC-1α Regulates Rotenone-Induced Dopaminergic Neurotoxicity. Mol. Neurobiol. 54, 3783–3797. https://doi.org/10.1007/s12035-016-9944-9

Perea, G., Sur, M., Araque, A., 2014. Neuron-glia networks: integral gear of brain function. Front. Cell. Neurosci. 8, 378. https://doi.org/10.3389/fncel.2014.00378

Perez, V.I., Buffenstein, R., Masamsetti, V., Leonard, S., Salmon, A.B., Mele, J., Andziak, B., Yang, T., Edrey, Y., Friguet, B., Ward, W., Richardson, A., Chaudhuri, A., 2009. Protein stability and resistance to oxidative stress are determinants of longevity in the longest-living rodent, the naked mole-rat. Proc. Natl. Acad. Sci. 106, 3059–3064. https://doi.org/10.1073/pnas.0809620106

Perfeito, R., Ribeiro, M., Rego, A.C., 2017. Alpha-synuclein-induced oxidative stress correlates with altered superoxide dismutase and glutathione synthesis in human neuroblastoma SH-SY5Y cells. Arch. Toxicol. 91, 1245–1259. https://doi.org/10.1007/s00204-016-1788-6

Pernas, L., Scorrano, L., 2016. Mito-Morphosis: Mitochondrial Fusion, Fission, and Cristae Remodeling as Key Mediators of Cellular Function. Annu. Rev. Physiol. 78, 505–531. https://doi.org/10.1146/annurev-physiol-021115-105011

Perng, M.D., Cairns, L., van den IJssel, P., Prescott, A., Hutcheson, A.M., Quinlan, R.A., 1999. Intermediate filament interactions can be altered by HSP27 and alphaB-crystallin. J. Cell Sci. 112 (Pt 1, 2099–112.

Perry, V.H., 2012. Innate Inflammation in Parkinson's Disease. Cold Spring Harb. Perspect. Med. 2, a009373–a009373. https://doi.org/10.1101/cshperspect.a009373

Persson, A.-K., Kim, I., Zhao, P., Estacion, M., Black, J.A., Waxman, S.G., 2013. Sodium Channels Contribute to Degeneration of Dorsal Root Ganglion Neurites Induced by Mitochondrial Dysfunction in an In Vitro Model of Axonal Injury. J. Neurosci. 33, 19250–19261. https://doi.org/10.1523/JNEUROSCI.2148-13.2013

Peth, A., Nathan, J.A., Goldberg, A.L., 2013. The ATP Costs and Time Required to Degrade Ubiquitinated Proteins by the 26 S Proteasome. J. Biol. Chem. 288, 29215–29222. https://doi.org/10.1074/jbc.M113.482570

Petit-Paitel, A., Brau, F., Cazareth, J., Chabry, J., 2009. Involvment of Cytosolic and Mitochondrial GSK-3β in Mitochondrial Dysfunction and Neuronal Cell Death of MPTP/MPP+-Treated Neurons. PLoS One 4,

e5491. https://doi.org/10.1371/journal.pone.0005491

Petit, A., Kawarai, T., Paitel, E., Sanjo, N., Maj, M., Scheid, M., Chen, F., Gu, Y., Hasegawa, H., Salehi-Rad, S., Wang, L., Rogaeva, E., Fraser, P., Robinson, B., St. George-Hyslop, P., Tandon, A., 2005. Wild-type PINK1 prevents basal and induced neuronal apoptosis, a protective effect abrogated by Parkinson disease-related mutations. J. Biol. Chem. 280, 34025–34032. https://doi.org/10.1074/jbc.M505143200

Petrosillo, G., Ruggiero, F.M., Di Venosa, N., Paradies, G., 2003. Decreased complex III activity in mitochondria isolated from rat heart subjected to ischemia and reperfusion: role of reactive oxygen species and cardiolipin. FASEB J. 17, 714–6.

Petrucelli, L., 2004. CHIP and Hsp70 regulate tau ubiquitination, degradation and aggregation. Hum. Mol. Genet. 13, 703–714. https://doi.org/10.1093/hmg/ddh083

Pickart, C.M., Rose, I.A., 1985. Ubiquitin carboxyl-terminal hydrolase acts on ubiquitin carboxyl-terminal amides. J. Biol. Chem. 260, 7903–7910.

Pickrell, A.M., Pinto, M., Hida, A., Moraes, C.T., 2011. Striatal Dysfunctions Associated with Mitochondrial DNA Damage in Dopaminergic Neurons in a Mouse Model of Parkinson's Disease. J. Neurosci. 31, 17649–17658. https://doi.org/10.1523/JNEUROSCI.4871-11.2011

Pieczenik, S.R., Neustadt, J., 2007. Mitochondrial dysfunction and molecular pathways of disease. Exp. Mol. Pathol. 83, 84–92. https://doi.org/10.1016/j.yexmp.2006.09.008

Piga, R., Saito, Y., Yoshida, Y., Niki, E., 2007. Cytotoxic effects of various stressors on PC12 cells: Involvement of oxidative stress and effect of antioxidants. Neurotoxicology 28, 67–75. https://doi.org/10.1016/j.neuro.2006.07.006

PIRKKALA, L., NYKÄNEN, P., SISTONEN, L., 2001. Roles of the heat shock transcription factors in regulation of the heat shock response and beyond. FASEB J. 15, 1118–1131. https://doi.org/10.1096/fj00-0294rev

Pisanu, A., Lecca, D., Mulas, G., Wardas, J., Simbula, G., Spiga, S., Carta, A.R., 2014. Dynamic changes in pro- and anti-inflammatory cytokines in microglia after PPAR-γ agonist neuroprotective treatment in the MPTPp mouse model of progressive Parkinson's disease. Neurobiol. Dis. 71, 280–291. https://doi.org/10.1016/j.nbd.2014.08.011

Piston, D., Alvarez-Erviti, L., Bansal, V., Gargano, D., Yao, Z., Szabadkai, G., Odell, M., Puno, M.R., Björkblom, B., Maple-Grødem, J., Breuer, P., Kaut, O., Larsen, J.P., Bonn, S., Møller, S.G., Wüllner, U., Schapira, A.H. V, Gegg, M.E., 2017. DJ-1 is a redox sensitive adapter protein for high molecular weight complexes involved in regulation of catecholamine homeostasis. Hum. Mol. Genet. 26, 4028–4041. https://doi.org/10.1093/hmg/ddx294

Polymeropoulos, M.H., Lavedan, C., Leroy, E., Ide, S.E., Dehejia, A., Dutra, A., Pike, B., Root, H., Rubenstein, J., Boyer, R., Stenroos, E.S., Chandrasekharappa, S., Athanassiadou, A., Papapetropoulos, T., Johnson, W.G., Lazzarini, A.M., Duvoisin, R.C., Iorio, G. Di, Golbe, L.I., Nussbaum, R.L., 1997. Mutation in the α-Synuclein Gene Identified in Families with Parkinson's Disease. Science (80-.). 276, 2045–2047. https://doi.org/10.1126/science.276.5321.2045

Pontén, J., 1975. Neoplastic Human Glia Cells in Culture, in: Human Tumor Cells in Vitro. Springer US, Boston, MA, pp. 175–206. https://doi.org/10.1007/978-1-4757-1647-4_7

Poole, L.B., Hall, A., Nelson, K.J., 2011a. Overview of peroxiredoxins in oxidant defense and redox regulation. Curr. Protoc. Toxicol. Chapter 7, Unit7.9. https://doi.org/10.1002/0471140856.tx0709s49

Poole, L.B., Hall, A., Nelson, K.J., 2011b. Overview of peroxiredoxins in oxidant defense and redox regulation. Curr. Protoc. Toxicol. Chapter 7, Unit7.9. https://doi.org/10.1002/0471140856.tx0709s49

Portera-Cailliau, C., Weimer, R.M., De Paola, V., Caroni, P., Svoboda, K., 2005. Diverse Modes of Axon Elaboration in the Developing Neocortex. PLoS Biol. 3, e272. https://doi.org/10.1371/journal.pbio.0030272

Posimo, J.M., Weilnau, J.N., Gleixner, A.M., Broeren, M.T., Weiland, N.L., Brodsky, J.L., Wipf, P., Leak, R.K.,

2015. Heat shock protein defenses in the neocortex and allocortex of the telencephalon. Neurobiol. Aging 36, 1924–1937. https://doi.org/10.1016/j.neurobiolaging.2015.02.011

Povlishock, J.T., 1993. Pathobiology of traumatically induced axonal injury in animals and man. Ann. Emerg. Med. 22, 980–986. https://doi.org/10.1016/S0196-0644(05)82738-6

Presgraves, S.P., Ahmed, T., Borwege, S., Joyce, J.N., 2003. Terminally differentiated SH-SY5Y cells provide a model system for studying neuroprotective effects of dopamine agonists. Neurotox. Res. 5, 579–598. https://doi.org/10.1007/BF03033178

Press, C., Milbrandt, J., 2008. Nmnat Delays Axonal Degeneration Caused by Mitochondrial and Oxidative Stress. J. Neurosci. 28, 4861–4871. https://doi.org/10.1523/JNEUROSCI.0525-08.2008

Proffen, B.L., Haslauer, C.M., Harris, C.E., Murray, M.M., 2013. Mesenchymal Stem Cells from the Retropatellar Fat Pad and Peripheral Blood Stimulate ACL Fibroblast Migration, Proliferation, and Collagen Gene Expression. Connect. Tissue Res. 54, 14–21. https://doi.org/10.3109/03008207.2012.715701

Puspita, L., Chung, S.Y., Shim, J., 2017. Oxidative stress and cellular pathologies in Parkinson's disease. Mol. Brain 10, 53. https://doi.org/10.1186/s13041-017-0340-9

Pyka, M., Busse, C., Seidenbecher, C., Gundelfinger, E.D., Faissner, A., 2011. Astrocytes are crucial for survival and maturation of embryonic hippocampal neurons in a neuron-glia cell-insert coculture assay. Synapse 65, 41–53. https://doi.org/10.1002/syn.20816

Qiu, J.H., Asai, a, Chi, S., Saito, N., Hamada, H., Kirino, T., 2000. Proteasome inhibitors induce cytochrome c-caspase-3-like protease-mediated apoptosis in cultured cortical neurons. J. Neurosci. 20, 259–265.

Quesada, A., Ogi, J., Schultz, J., Handforth, A., 2011. C-terminal mechano-growth factor induces heme oxygenase-1-mediated neuroprotection of SH-SY5Y cells via the protein kinase Cε/Nrf2 pathway. J. Neurosci. Res. 89, 394–405. https://doi.org/10.1002/jnr.22543

Quigney, D.J., Gorman, A.M., Samali, A., 2003. Heat shock protects PC12 cells against MPP+ toxicity. Brain Res. 993, 133–139. https://doi.org/10.1016/j.brainres.2003.09.004

Rabindran, S., Haroun, R., Clos, J., Wisniewski, J., Wu, C., 1993. Regulation of heat shock factor trimer formation: role of a conserved leucine zipper. Science (80-.). 259, 230–234. https://doi.org/10.1126/science.8421783

Radhakrishnan, S.K., den Besten, W., Deshaies, R.J., 2014. p97-dependent retrotranslocation and proteolytic processing govern formation of active Nrf1 upon proteasome inhibition. Elife 3, e01856. https://doi.org/10.7554/eLife.01856

Radi, R., 2013. Protein tyrosine nitration: Biochemical mechanisms and structural basis of functional effects. Acc. Chem. Res. 46, 550–559. https://doi.org/10.1021/ar300234c

Radi, R., Beckman, J.S., Bush, K.M., Freeman, B.A., 1991. Peroxynitrite-induced membrane lipid peroxidation: The cytotoxic potential of superoxide and nitric oxide. Arch. Biochem. Biophys. 288, 481–487. https://doi.org/10.1016/0003-9861(91)90224-7

Raff, M.C., 2002. Axonal Self-Destruction and Neurodegeneration. Science (80-.). 296, 868–871. https://doi.org/10.1126/science.1068613

Rapin, J.R., Zaibi, M., Drieu, K., 1998. In vitro and in vivo effects of an extract of Ginkgo biloba (EGb 761), ginkgolide B, and bilobalide on apoptosis in primary cultures of rat hippocampal neurons. Drug Dev Res 45, 23–29.

Raps, S.P., Lai, J.C.K., Hertz, L., Cooper, A.J.L., 1989. Glutathione is present in high concentrations in cultured astrocytes but not in cultured neurons. Brain Res. 493, 398–401. https://doi.org/10.1016/0006-8993(89)91178-5

Ray, Paul D., Huang, B.-W., Tsuji, Y., 2012. Reactive oxygen species (ROS) homeostasis and redox regulation in cellular signaling. Cell. Signal. 24, 981–990. https://doi.org/10.1016/j.cellsig.2012.01.008

Ray, Paul D, Huang, B.-W., Tsuji, Y., 2012. Reactive oxygen species (ROS) homeostasis and redox regulation in cellular signaling. Cell. Signal. 24, 981–990. https://doi.org/10.1016/j.cellsig.2012.01.008

Raychaudhuri, S., Loew, C., Körner, R., Pinkert, S., Theis, M., Hayer-Hartl, M., Buchholz, F., Hartl, F.U., 2014. Interplay of Acetyltransferase EP300 and the Proteasome System in Regulating Heat Shock Transcription Factor 1. Cell 156, 975–985. https://doi.org/10.1016/j.cell.2014.01.055

Razack, S., Kumar, K., Nallamuthu, I., Naika, M., Khanum, F., 2015. Antioxidant, Biomolecule Oxidation Protective Activities of Nardostachys jatamansi DC and Its Phytochemical Analysis by RP-HPLC and GC-MS. Antioxidants 4, 185–203. https://doi.org/10.3390/antiox4010185

Reczek, C.R., Chandel, N.S., 2015. ROS-dependent signal transduction. Curr. Opin. Cell Biol. https://doi.org/10.1016/j.ceb.2014.09.010

Redmann, M., Darley-Usmar, V., Zhang, J., 2016. The Role of Autophagy, Mitophagy and Lysosomal Functions in Modulating Bioenergetics and Survival in the Context of Redox and Proteotoxic Damage: Implications for Neurodegenerative Diseases. Aging Dis. 7, 150. https://doi.org/10.14336/AD.2015.0820

Redmann, M., Dodson, M., Boyer-Guittaut, M., Darley-Usmar, V., Zhang, J., 2014. Mitophagy mechanisms and role in human diseases. Int. J. Biochem. Cell Biol. 53, 127–133. https://doi.org/10.1016/j.biocel.2014.05.010

Reed, T., Perluigi, M., Sultana, R., Pierce, W.M., Klein, J.B., Turner, D.M., Coccia, R., Markesbery, W.R., Butterfield, D.A., 2008. Redox proteomic identification of 4-Hydroxy-2-nonenal-modified brain proteins in amnestic mild cognitive impairment: Insight into the role of lipid peroxidation in the progression and pathogenesis of Alzheimer's disease. Neurobiol. Dis. 30, 107–120. https://doi.org/10.1016/j.nbd.2007.12.007

Reed, T.T., 2011. Lipid peroxidation and neurodegenerative disease. Free Radic. Biol. Med. 51, 1302–1319. https://doi.org/10.1016/j.freeradbiomed.2011.06.027

Reeve, A., Meagher, M., Lax, N., Simcox, E., Hepplewhite, P., Jaros, E., Turnbull, D., 2013. The Impact of Pathogenic Mitochondrial DNA Mutations on Substantia Nigra Neurons. J. Neurosci. 33, 10790–10801. https://doi.org/10.1523/JNEUROSCI.3525-12.2013

Rego, A.C., Oliveira, C.R., 2003. Mitochondrial dysfunction and reactive oxygen species in excitotoxicity and apoptosis: implications for the pathogenesis of neurodegenerative diseases. Neurochem. Res. 28, 1563–74. https://doi.org/10.1023/a:1025682611389

Rehncrona, S., Smith, D.S., Åkesson, B., Westerberg, E., Siesjö, B.K., 1980. Peroxidative Changes in Brain Cortical Fatty Acids and Phospholipids, as Characterized During Fe2+- and Ascorbic Acid-Stimulated Lipid Peroxidation In Vitro. J. Neurochem. 34, 1630–1638. https://doi.org/10.1111/j.1471-4159.1980.tb11254.x

Reinheckel, T., Ullrich, O., Sitte, N., Grune, T., 2000. Differential Impairment of 20S and 26S Proteasome Activities in Human Hematopoietic K562 Cells during Oxidative Stress. Arch. Biochem. Biophys. 377, 65–68. https://doi.org/10.1006/abbi.2000.1717

Ren, Y., Feng, J., 2007. Rotenone selectively kills serotonergic neurons through a microtubule-dependent mechanism. J. Neurochem. 103, 303–11. https://doi.org/10.1111/j.1471-4159.2007.04741.x

Renaud, J., Martinoli, M.-G., 2016. Development of an Insert Co-culture System of Two Cellular Types in the Absence of Cell-Cell Contact. J. Vis. Exp. https://doi.org/10.3791/54356

Renkawek, K., Bosman, G.I.C.G.M., de Jong, W.W., 1994. Expression of small heat-shock protein hsp 27 in reactive gliosis in Alzheimer disease and other types of dementia. Acta Neuropathol. 87, 511–519. https://doi.org/10.1007/BF00294178

Renkawek, K., Stege, G.J.J., Bosman, G.J.C.G.M., 1999. Dementia, gliosis and expression of the small heat shock proteins hsp27 and αB-crystallin in Parkinson's disease. Neuroreport 10, 2273–2276. https://doi.org/10.1097/00001756-199908020-00009

Rhee, S.G., Chae, H.Z., Kim, K., 2005. Peroxiredoxins: A historical overview and speculative preview of novel mechanisms and emerging concepts in cell signaling. Free Radic. Biol. Med. 38, 1543–1552. https://doi.org/10.1016/j.freeradbiomed.2005.02.026

Rhee, S.G., Jeong, W., Chang, T.-S., Woo, H.A., 2007. Sulfiredoxin, the cysteine sulfinic acid reductase specific to 2-Cys peroxiredoxin: its discovery, mechanism of action, and biological significance. Kidney Int. 72, S3–S8. https://doi.org/10.1038/sj.ki.5002380

Rice, M.E., 2000. Ascorbate regulation and its neuroprotective role in the brain. Trends Neurosci. 23, 209–216. https://doi.org/10.1016/S0166-2236(99)01543-X

Rice, M.E., Patel, J.C., Cragg, S.J., 2011. Dopamine release in the basal ganglia. Neuroscience 198, 112–137. https://doi.org/10.1016/j.neuroscience.2011.08.066

RIDEOUT, H., STEFANIS, L., 2002. Proteasomal Inhibition-Induced Inclusion Formation and Death in Cortical Neurons Require Transcription and Ubiquitination. Mol. Cell. Neurosci. 21, 223–238. https://doi.org/10.1006/mcne.2002.1173

Rideout, H.J., Larsen, K.E., Sulzer, D., Stefanis, L., 2001. Proteasomal inhibition leads to formation of ubiquitin/α-synuclein-immunoreactive inclusions in PC12 cells. J. Neurochem. 78, 899–908. https://doi.org/10.1046/j.1471-4159.2001.00474.x

Riederer, P., Konradi, C., Schay, V., Kienzl, E., Birkmayer, G., Danielczyk, W., Sofic, E., Youdim, M.B., 1987. Localization of MAO-A and MAO-B in human brain: a step in understanding the therapeutic action of L-deprenyl. Adv. Neurol. 45, 111–8.

Rieske, P., Augelli, B.J., Stawski, R., Gaughan, J., Azizi, S.A., Krynska, B., 2009. A population of human brain cells expressing phenotypic markers of more than one lineage can be induced in vitro to differentiate into mesenchymal cells. Exp. Cell Res. 315, 462–473. https://doi.org/10.1016/j.yexcr.2008.11.004

Riley, D.A., 1981. Ultrastructural evidence for axon retraction during the spontaneous elimination of polyneuronal innervation of the rat soleus muscle. J. Neurocytol. 10, 425–440. https://doi.org/10.1007/BF01262414

Rinaldi, T., Ricordy, R., Bolotin-Fukuhara, M., Frontali, L., 2002. Mitochondrial effects of the pleiotropic proteasomal mutation mpr1/rpn11 : uncoupling from cell cycle defects in extragenic revertants. Gene 286, 43–51. https://doi.org/10.1016/S0378-1119(01)00799-5

Rivera, I., Capone, R., Cauvi, D.M., Arispe, N., De Maio, A., 2018. Modulation of Alzheimer's amyloid β peptide oligomerization and toxicity by extracellular Hsp70. Cell Stress Chaperones 23, 269–279. https://doi.org/10.1007/s12192-017-0839-0

Rizzi, N., Brunialti, E., Cerri, S., Cermisoni, G., Levandis, G., Cesari, N., Maggi, A., Blandini, F., Ciana, P., 2018. In vivo imaging of early signs of dopaminergic neuronal death in an animal model of Parkinson's disease. Neurobiol. Dis. 114, 74–84. https://doi.org/10.1016/j.nbd.2018.02.005

Rogalla, T., Ehrnsperger, M., Preville, X., Kotlyarov, A., Lutsch, G., Ducasse, C., Paul, C., Wieske, M., Arrigo, A.-P., Buchner, J., Gaestel, M., 1999. Regulation of Hsp27 Oligomerization, Chaperone Function, and Protective Activity against Oxidative Stress/Tumor Necrosis Factor α by Phosphorylation. J. Biol. Chem. 274, 18947–18956. https://doi.org/10.1074/jbc.274.27.18947

Rogers, J., Mastroeni, D., Leonard, B., Joyce, J., Grover, A., 2007. Neuroinflammation in Alzheimer's Disease and Parkinson's Disease: Are Microglia Pathogenic in Either Disorder?, in: International Review of Neurobiology. pp. 235–246. https://doi.org/10.1016/S0074-7742(07)82012-5

Rosenberg, G.A., 2002. Matrix metalloproteinases in neuroinflammation. Glia 39, 279–291. https://doi.org/10.1002/glia.10108

Rosenberg, P.A., Aizenman, E., 1989. Hundred-fold increase in neuronal vulnerability to glutamate toxicity in astrocyte-poor cultures of rat cerebral cortex. Neurosci. Lett. 103, 162–168. https://doi.org/10.1016/0304-3940(89)90569-7

Rosewater, K., Sontheimer, H., 1994. Fibrous and protoplasmic astrocytes express GABAA receptors that differ in benzodiazepine pharmacology. Brain Res. 636, 73–80. https://doi.org/10.1016/0006-8993(94)90177-5

Ross, R.A., Biedler, J.L., 1985. Presence and regulation of tyrosinase activity in human neuroblastoma cell variants in vitro. Cancer Res. 45, 1628–32.

Ross, R.A., Spengler, B.A., Biedler, J.L., 1983. Coordinate morphological and biochemical interconversion of human neuroblastoma cells. J. Natl. Cancer Inst. 71, 741–7. https://doi.org/10.1093/jnci/71.4.741

Rousseau, F., Serrano, L., Schymkowitz, J.W.H., 2006. How Evolutionary Pressure Against Protein Aggregation Shaped Chaperone Specificity. J. Mol. Biol. 355, 1037–1047. https://doi.org/10.1016/j.jmb.2005.11.035

Ruan, L., Zhou, C., Jin, E., Kucharavy, A., Zhang, Y., Wen, Z., Florens, L., Li, R., 2017. Cytosolic proteostasis through importing of misfolded proteins into mitochondria. Nature 543, 443–446. https://doi.org/10.1038/nature21695

Rubin, D.M., 1998. Active site mutants in the six regulatory particle ATPases reveal multiple roles for ATP in the proteasome. EMBO J. 17, 4909–4919. https://doi.org/10.1093/emboj/17.17.4909

Rudiger, S., 1997. Substrate specificity of the DnaK chaperone determined by screening cellulose-bound peptide libraries. EMBO J. 16, 1501–1507. https://doi.org/10.1093/emboj/16.7.1501

Rüdiger, S., Buchberger, A., Bukau, B., 1997. Interaction of Hsp70 chaperones with substrates. Nat. Struct. Mol. Biol. 4, 342–349. https://doi.org/10.1038/nsb0597-342

Ruszkiewicz, J., Albrecht, J., 2015. Changes in the mitochondrial antioxidant systems in neurodegenerative diseases and acute brain disorders. Neurochem. Int. 88, 66–72. https://doi.org/10.1016/j.neuint.2014.12.012

Ryan, B.J., Hoek, S., Fon, E.A., Wade-Martins, R., 2015. Mitochondrial dysfunction and mitophagy in Parkinson's: from familial to sporadic disease. Trends Biochem. Sci. 40, 200–210. https://doi.org/10.1016/j.tibs.2015.02.003

Ryter, S.W., Kim, H.P., Hoetzel, A., Park, J.W., Nakahira, K., Wang, X., Choi, A.M.K., 2007. Mechanisms of Cell Death in Oxidative Stress. Antioxid. Redox Signal. 9, 49–89. https://doi.org/10.1089/ars.2007.9.49

Sadeghian, M., Marinova-Mutafchieva, L., Broom, L., Davis, J.B., Virley, D., Medhurst, A.D., Dexter, D.T., 2012. Full and partial peroxisome proliferation-activated receptor-gamma agonists, but not delta agonist, rescue of dopaminergic neurons in the 6-OHDA Parkinsonian model is associated with inhibition of microglial activation and MMP expression. J. Neuroimmunol. 246, 69–77. https://doi.org/10.1016/j.jneuroim.2012.03.010

Sadowska-Bartosz, I., Ott, C., Grune, T., Bartosz, G., 2014. Posttranslational protein modifications by reactive nitrogen and chlorine species and strategies for their prevention and elimination. Free Radic. Res. 48, 1267–1284. https://doi.org/10.3109/10715762.2014.953494

Saeed, Y., Xie, B., Xu, J., Rehman, A., Hong, M., Hong, Q., Deng, Y., 2015. Glial U87 cells protect neuronal SH-SY5Y cells from indirect effect of radiation by reducing oxidative stress and apoptosis. Acta Biochim. Biophys. Sin. (Shanghai). 47, 250–257. https://doi.org/10.1093/abbs/gmv004

Saigoh, K., Wang, Y.L., Suh, J.G., Yamanishi, T., Sakai, Y., Kiyosawa, H., Harada, T., Ichihara, N., Wakana, S., Kikuchi, T., Wada, K., 1999. Intragenic deletion in the gene encoding ubiquitin carboxy-terminal hydrolase in gad mice. Nat. Genet. 23, 47–51. https://doi.org/10.1038/12647

Saito, Y., Miyasaka, T., Hatsuta, H., Takahashi-Niki, K., Hayashi, K., Mita, Y., Kusano-Arai, O., Iwanari, H., Ariga, H., Hamakubo, T., Yoshida, Y., Niki, E., Murayama, S., Ihara, Y., Noguchi, N., 2014. Immunostaining of Oxidized DJ-1 in Human and Mouse Brains. J. Neuropathol. Exp. Neurol. 73, 714–728. https://doi.org/10.1097/NEN.0000000000000087

Saleh, Z., Menassa, J., Abbas, O., Atweh, S., Arayssi, T., 2010. Cranial nerve VI palsy as a rare initial presentation of systemic lupus erythematosus: case report and review of the literature. Lupus 19, 201–

5. https://doi.org/10.1177/0961203309345722

Salińska, E., Danysz, W., Łazarewicz, J.W., 2005. The role of excitotoxicity in neurodegeneration. Folia Neuropathol. 43, 322–39. https://doi.org/5375 [pii]

Salvadores, N., Sanhueza, M., Manque, P., Court, F.A., 2017. Axonal Degeneration during Aging and Its Functional Role in Neurodegenerative Disorders. Front. Neurosci. 11, 451. https://doi.org/10.3389/fnins.2017.00451

Sanders, L.H., Timothy Greenamyre, J., 2013. Oxidative damage to macromolecules in human Parkinson disease and the rotenone model. Free Radic. Biol. Med. 62, 111–120. https://doi.org/10.1016/j.freeradbiomed.2013.01.003

Sandhu, J.K., Gardaneh, M., Iwasiow, R., Lanthier, P., Gangaraju, S., Ribecco-Lutkiewicz, M., Tremblay, R., Kiuchi, K., Sikorska, M., 2009. Astrocyte-secreted GDNF and glutathione antioxidant system protect neurons against 6OHDA cytotoxicity. Neurobiol. Dis. 33, 405–414. https://doi.org/10.1016/j.nbd.2008.11.016

Santambrogio, L., Cuervo, A.M., 2011. Chasing the elusive mammalian microautophagy. Autophagy 7, 652–654. https://doi.org/10.4161/auto.7.6.15287

Santos, A.L., Lindner, A.B., 2017. Protein Posttranslational Modifications: Roles in Aging and Age-Related Disease. Oxid. Med. Cell. Longev. 2017, 1–19. https://doi.org/10.1155/2017/5716409

Santos, D., Esteves, A.R., Silva, D.F., Januário, C., Cardoso, S.M., 2015. The Impact of Mitochondrial Fusion and Fission Modulation in Sporadic Parkinson's Disease. Mol. Neurobiol. 52, 573–586. https://doi.org/10.1007/s12035-014-8893-4

Sarafian, T.A., Montes, C., Imura, T., Qi, J., Coppola, G., Geschwind, D.H., Sofroniew, M. V., 2010. Disruption of Astrocyte STAT3 Signaling Decreases Mitochondrial Function and Increases Oxidative Stress In Vitro. PLoS One 5, e9532. https://doi.org/10.1371/journal.pone.0009532

Sarkisian, M.R., Bartley, C.M., Chi, H., Nakamura, F., Hashimoto-Torii, K., Torii, M., Flavell, R.A., Rakic, P., 2006. MEKK4 Signaling Regulates Filamin Expression and Neuronal Migration. Neuron 52, 789–801. https://doi.org/10.1016/j.neuron.2006.10.024

Sarraf, S.A., Raman, M., Guarani-Pereira, V., Sowa, M.E., Huttlin, E.L., Gygi, S.P., Harper, J.W., 2013. Landscape of the PARKIN-dependent ubiquitylome in response to mitochondrial depolarization. Nature 496, 372–376. https://doi.org/10.1038/nature12043

Sastre, J., Millan, A., de la Asuncion, J.G., Pla, R., Juan, G., Pallardo, F. V., O'Connor, E., Martin, J.A., Droy-Lefaix, M.-T., Viña, J., 1998. A Ginkgo Biloba Extract (EGb 761) Prevents Mitochondrial Aging by Protecting Against Oxidative Stress. Free Radic. Biol. Med. 24, 298–304. https://doi.org/10.1016/S0891-5849(97)00228-1

Sauer, H., Wartenberg, M., Hescheler, J., 2001. Reactive Oxygen Species as Intracellular Messengers During Cell Growth and Differentiation. Cell. Physiol. Biochem. 11, 173–186. https://doi.org/10.1159/000047804

Saura, J., Parés, M., Bové, J., Pezzi, S., Alberch, J., Marin, C., Tolosa, E., Martí, M.J., 2003. Intranigral infusion of interleukin-1β activates astrocytes and protects from subsequent 6-hydroxydopamine neurotoxicity. J. Neurochem. 85, 651–661. https://doi.org/10.1046/j.1471-4159.2003.01676.x

Sauvageot, C., 2002. Molecular mechanisms controlling cortical gliogenesis. Curr. Opin. Neurobiol. 12, 244–249. https://doi.org/10.1016/S0959-4388(02)00322-7

Saxena, S., Caroni, P., 2007. Mechanisms of axon degeneration: From development to disease. Prog. Neurobiol. 83, 174–191. https://doi.org/10.1016/j.pneurobio.2007.07.007

Sayre, L.M., Zelasko, D.A., Harris, P.L., Perry, G., Salomon, R.G., Smith, M.A., 1997. 4-Hydroxynonenal-derived advanced lipid peroxidation end products are increased in Alzheimer's disease. J. Neurochem. 68, 2092–2097. https://doi.org/10.1046/j.1471-4159.1997.68052092.x

Schafer, F.Q., Buettner, G.R., 2001. Redox environment of the cell as viewed through the redox state of the glutathione disulfide/glutathione couple. Free Radic. Biol. Med. 30, 1191–1212. https://doi.org/10.1016/S0891-5849(01)00480-4

Schapira, A.H., 2008. Mitochondria in the aetiology and pathogenesis of Parkinson's disease. Lancet Neurol. 7, 97–109. https://doi.org/10.1016/S1474-4422(07)70327-7

Schapira, A.H.V., Chaudhuri, K.R., Jenner, P., 2017. Non-motor features of Parkinson disease. Nat. Rev. Neurosci. 18, 435–450. https://doi.org/10.1038/nrn.2017.62

Schapira, A.H. V, Gegg, M., 2011. Mitochondrial Contribution to Parkinson's Disease Pathogenesis. Parkinsons. Dis. 2011, 1–7. https://doi.org/10.4061/2011/159160

Scharr, D.G., Sieber, B.-A., Dreyfus, C.F., Black, I.B., 1993. Regional and Cell-Specific Expression of GDNF in Rat Brain. Exp. Neurol. 124, 368–371. https://doi.org/10.1006/exnr.1993.1207

Schneider, J.S., Denaro, F.J., 1988. Astrocytic Responses to the Dopaminergic Neurotoxin 1-Methyl-4-phenyl-1,2,3,6-tetrahydropyridine (MPTP) in Cat and Mouse Brain. J. Neuropathol. Exp. Neurol. 47, 452–458. https://doi.org/10.1097/00005072-198807000-00006

Schneider, J.S., Rothblat, D.S., DiStefano, L., 1994. Volume transmission of dopamine over large distances may contribute to recovery from experimental parkinsonism. Brain Res. 643, 86–91. https://doi.org/10.1016/0006-8993(94)90012-4

Schneider, L., Giordano, S., Zelickson, B.R., S. Johnson, M., A. Benavides, G., Ouyang, X., Fineberg, N., Darley-Usmar, V.M., Zhang, J., 2011. Differentiation of SH-SY5Y cells to a neuronal phenotype changes cellular bioenergetics and the response to oxidative stress. Free Radic. Biol. Med. 51, 2007–2017. https://doi.org/10.1016/j.freeradbiomed.2011.08.030

Schoeniger, L.O., Andreoni, K.A., Ott, G.R., Risby, T.H., Bulkley, G.B., Udelsman, R., Burdick, J.F., Buchman, T.G., 1994. Induction of heat-shock gene expression in postischemic pig liver depends on superoxide generation. Gastroenterology 106, 177–184. https://doi.org/10.1016/S0016-5085(94)95209-4

Schönfeld, P., Reiser, G., 2013. Why does Brain Metabolism not Favor Burning of Fatty Acids to Provide Energy? - Reflections on Disadvantages of the Use of Free Fatty Acids as Fuel for Brain. J. Cereb. Blood Flow Metab. 33, 1493–1499. https://doi.org/10.1038/jcbfm.2013.128

Schulz-Schaeffer, W.J., 2010. The synaptic pathology of α-synuclein aggregation in dementia with Lewy bodies, Parkinson's disease and Parkinson's disease dementia. Acta Neuropathol. 120, 131–143. https://doi.org/10.1007/s00401-010-0711-0

Schumacker, P.T., 2006. Reactive oxygen species in cancer cells: Live by the sword, die by the sword. Cancer Cell. https://doi.org/10.1016/j.ccr.2006.08.015

Seemüller, E., Lupas, a, Stock, D., Löwe, J., Huber, R., Baumeister, W., 1995. Proteasome from Thermoplasma acidophilum: a threonine protease. Science 268, 579–582. https://doi.org/10.1126/science.7725107

Segura-Aguilar, J., 1996. Peroxidase activity of liver microsomal vitamin D 25-hydroxylase and cytochrome P450 1A2 catalyzes 25-hydroxylation of vitamin D3 and oxidation of dopamine to aminochrome. Biochem. Mol. Med. 58, 122–9. https://doi.org/10.1006/bmme.1996.0039

Segura-Aguilar, J., Paris, I., Muñoz, P., Ferrari, E., Zecca, L., Zucca, F.A., 2014. Protective and toxic roles of dopamine in Parkinson's disease. J. Neurochem. 129, 898–915. https://doi.org/10.1111/jnc.12686

Seifert, G., Schilling, K., Steinhäuser, C., 2006. Astrocyte dysfunction in neurological disorders: a molecular perspective. Nat. Rev. Neurosci. 7, 194–206. https://doi.org/10.1038/nrn1870

Selkoe, D.J., 2002. Alzheimer's Disease Is a Synaptic Failure. Science (80-.). 298, 789–791. https://doi.org/10.1126/science.1074069

Seniuk, N.A., Tatton, W.G., Greenwood, C.E., 1990. Dose-dependent destruction of the coeruleus-cortical and nigral-striatal projections by MPTP. Brain Res. 527, 7–20. https://doi.org/10.1016/0006-8993(90)91055-L

Shamoto-Nagai, M., Hisaka, S., Naoi, M., Maruyama, W., 2018. Modification of α-synuclein by lipid peroxidation products derived from polyunsaturated fatty acids promotes toxic oligomerization: its relevance to Parkinson disease. J. Clin. Biochem. Nutr. 62, 207–212. https://doi.org/10.3164/jcbn.18-25

Shamoto-Nagai, M., Maruyama, W., Kato, Y., Isobe, K., Tanaka, M., Naoi, M., Osawa, T., 2003. An inhibitor of mitochondrial complex I, rotenone, inactivates proteasome by oxidative modification and induces aggregation of oxidized proteins in SH-SY5Y cells. J. Neurosci. Res. 74, 589–597. https://doi.org/10.1002/jnr.10777

Sharma, J., Johnston, M. V, Hossain, M., 2014. Sex differences in mitochondrial biogenesis determine neuronal death and survival in response to oxygen glucose deprivation and reoxygenation. BMC Neurosci. 15, 9. https://doi.org/10.1186/1471-2202-15-9

Sharma, N., Nehru, B., 2015. Characterization of the lipopolysaccharide induced model of Parkinson's disease: Role of oxidative stress and neuroinflammation. Neurochem. Int. 87, 92–105. https://doi.org/10.1016/j.neuint.2015.06.004

Shelton, P., Jaiswal, A.K., 2013. The transcription factor NF-E2-related Factor 2 (Nrf2): a protooncogene? FASEB J. 27, 414–423. https://doi.org/10.1096/fj.12-217257

Sherer, T.B., Betarbet, R., Stout, A.K., Lund, S., Baptista, M., Panov, A. V, Cookson, M.R., Greenamyre, J.T., 2002. An in vitro model of Parkinson's disease: linking mitochondrial impairment to altered alpha-synuclein metabolism and oxidative damage. J. Neurosci. 22, 7006–7015. https://doi.org/20026721\r22/16/7006 [pii]

Sherer, T.B., Betarbet, R., Testa, C.M., Seo, B.B., Richardson, J.R., Kim, J.H., Miller, G.W., Yagi, T., Matsuno-Yagi, A., Greenamyre, J.T., 2003. Mechanism of toxicity in rotenone models of Parkinson's disease. J. Neurosci. 23, 10756–10764. https://doi.org/23/34/10756 [pii]

Sherman, M.Y., Goldberg, A.L., 2001. Cellular Defenses against Unfolded Proteins. Neuron 29, 15–32. https://doi.org/10.1016/S0896-6273(01)00177-5

Shiba-Fukushima, K., Imai, Y., Yoshida, S., Ishihama, Y., Kanao, T., Sato, S., Hattori, N., 2012. PINK1-mediated phosphorylation of the Parkin ubiquitin-like domain primes mitochondrial translocation of Parkin and regulates mitophagy. Sci. Rep. 2, 1002. https://doi.org/10.1038/srep01002

Shih, A.Y., Imbeault, S., Barakauskas, V., Erb, H., Jiang, L., Li, P., Murphy, T.H., 2005. Induction of the Nrf2-driven Antioxidant Response Confers Neuroprotection during Mitochondrial Stress in Vivo. J. Biol. Chem. 280, 22925–22936. https://doi.org/10.1074/jbc.M414635200

Shih, A.Y., Johnson, D.A., Wong, G., Kraft, A.D., Jiang, L., Erb, H., Johnson, J.A., Murphy, T.H., 2003. Coordinate regulation of glutathione biosynthesis and release by Nrf2-expressing glia potently protects neurons from oxidative stress. J. Neurosci. 23, 3394–406.

Shimura, H., Schlossmacher, M.G., Hattori, N., Frosch, M.P., Trockenbacher, a, Schneider, R., Mizuno, Y., Kosik, K.S., Selkoe, D.J., 2001. Ubiquitination of a new form of alpha-synuclein by parkin from human brain: implications for Parkinson's disease. Science 293, 263–269. https://doi.org/10.1126/science.1060627

Shinohara, A., Ogawa, H., Matsuda, Y., Ushio, N., Ikeo, K., Ogawa, T., 1993. Cloning of human, mouse and fission yeast recombination genes homologous to RAD51 and recA. Nat. Genet. 4, 239–43. https://doi.org/10.1038/ng0793-239

Shokolenko, I., Venediktova, N., Bochkareva, A., Wilson, G.L., Alexeyev, M.F., 2009. Oxidative stress induces degradation of mitochondrial DNA. Nucleic Acids Res. 37, 2539–2548. https://doi.org/10.1093/nar/gkp100

Shringarpure, R., Grune, T., Mehlhase, J., Davies, K.J.A., 2003. Ubiquitin Conjugation Is Not Required for the Degradation of Oxidized Proteins by Proteasome. J. Biol. Chem. 278, 311–318. https://doi.org/10.1074/jbc.M206279200

Shukla, R., 2007. Nitric Oxide in Neurodegeneration. Ann. Neurosci. 14, 13–20.

https://doi.org/10.5214/ans.0972.7531.2007.140104

Simpson, E.P., Henry, Y.K., Henkel, J.S., Smith, R.G., Appel, S.H., 2004. Increased lipid peroxidation in sera of ALS patients: A potential biomarker of disease burden. Neurology 62, 1758–1765. https://doi.org/10.1212/WNL.62.10.1758

Singleton, a B., Farrer, M., Johnson, J., Singleton, a, Hague, S., Kachergus, J., Hulihan, M., Peuralinna, T., Dutra, a, Nussbaum, R., Lincoln, S., Crawley, a, Hanson, M., Maraganore, D., Adler, C., Cookson, M.R., Muenter, M., Baptista, M., Miller, D., Blancato, J., Hardy, J., Gwinn-Hardy, K., 2003. alpha-Synuclein locus triplication causes Parkinson's disease. Science 302, 841. https://doi.org/10.1126/science.1090278

Slezak, M., Pfrieger, F.W., 2003. New roles for astrocytes: Regulation of CNS synaptogenesis. Trends Neurosci. 26, 531–535. https://doi.org/10.1016/j.tins.2003.08.005

Smirnoff, N., 2018. Ascorbic acid metabolism and functions: A comparison of plants and mammals. Free Radic. Biol. Med. 122, 116–129. https://doi.org/10.1016/j.freeradbiomed.2018.03.033

Smith, B.C., Marletta, M.A., 2012. Mechanisms of S-nitrosothiol formation and selectivity in nitric oxide signaling. Curr. Opin. Chem. Biol. 16, 498–506. https://doi.org/10.1016/j.cbpa.2012.10.016

Smith, K.J., Lassmann, H., 2002. The role of nitric oxide in multiple sclerosis. Lancet Nuerology 1, 232–41. https://doi.org/10.1016/S1474-4422(02)00102-3

Snyder, H., Mensah, K., Theisler, C., Lee, J., Matouschek, A., Wolozin, B., 2003. Aggregated and Monomeric α-Synuclein Bind to the S6′ Proteasomal Protein and Inhibit Proteasomal Function. J. Biol. Chem. 278, 11753–11759. https://doi.org/10.1074/jbc.M208641200

Somara, S., Bitar, K.N., 2006. Phosphorylated HSP27 modulates the association of phosphorylated caldesmon with tropomyosin in colonic smooth muscle. Am. J. Physiol. Liver Physiol. 291, G630–G639. https://doi.org/10.1152/ajpgi.00350.2005

Song, D.D., Shults, C.W., Sisk, A., Rockenstein, E., Masliah, E., 2004. Enhanced substantia nigra mitochondrial pathology in human α-synuclein transgenic mice after treatment with MPTP. Exp. Neurol. 186, 158–172. https://doi.org/10.1016/S0014-4886(03)00342-X

Song, I.S., Kang, S.-S., Kim, E.-S., Park, H.-M., Choi, C.Y., Tchah, H., Kim, J.Y., 2014. Heat shock protein 27 phosphorylation is involved in epithelial cell apoptosis as well as epithelial migration during corneal epithelial wound healing. Exp. Eye Res. 118, 36–41. https://doi.org/10.1016/j.exer.2013.11.002

Song, S., Miranda, C.J., Braun, L., Meyer, K., Frakes, A.E., Ferraiuolo, L., Likhite, S., Bevan, A.K., Foust, K.D., McConnell, M.J., Walker, C.M., Kaspar, B.K., 2016. Major histocompatibility complex class I molecules protect motor neurons from astrocyte-induced toxicity in amyotrophic lateral sclerosis. Nat. Med. 22, 397–403. https://doi.org/10.1038/nm.4052

Sorrentino, Z.A., Giasson, B.I., Chakrabarty, P., 2019. α-Synuclein and astrocytes: tracing the pathways from homeostasis to neurodegeneration in Lewy body disease. Acta Neuropathol. 138, 1–21. https://doi.org/10.1007/s00401-019-01977-2

Sotiriou, S., Gispert, S., Cheng, J., Wang, Y., Chen, A., Hoogstraten-Miller, S., Miller, G.F., Kwon, O., Levine, M., Guttentag, S.H., Nussbaum, R.L., 2002. Ascorbic-acid transporter Slc23a1 is essential for vitamin C transport into the brain and for perinatal survival. Nat. Med. 8, 514–517. https://doi.org/10.1038/0502-514

Spencer, J.P., Jenner, P., Daniel, S.E., Lees, a J., Marsden, D.C., Halliwell, B., 1998. Conjugates of catecholamines with cysteine and GSH in Parkinson's disease: possible mechanisms of formation involving reactive oxygen species. J. Neurochem. 71, 2112–2122. https://doi.org/10.1046/j.1471-4159.1998.71052112.x

Spillantini, M.G., Crowther, R.A., Jakes, R., Hasegawa, M., Goedert, M., 1998. α -Synuclein in filamentous inclusions of Lewy bodies from Parkinson's disease and dementia with Lewy bodies. Proc. Natl. Acad. Sci. 95, 6469–6473. https://doi.org/10.1073/pnas.95.11.6469

Spillantini, M.G., Schmidt, M.L., Lee, V.M., Trojanowski, J.Q., Jakes, R., Goedert, M., 1997. Alpha-synuclein in Lewy bodies. Nature 388, 839–40. https://doi.org/10.1038/42166

Squier, T.C., 2001. Oxidative stress and protein aggregation during biological aging. Exp. Gerontol. 36, 1539–1550. https://doi.org/10.1016/S0531-5565(01)00139-5

Stamler, J.S., Toone, E.J., Lipton, S.A., Sucher, N.J., 1997. (S)NO Signals: Translocation, Regulation, and a Consensus Motif. Neuron 18, 691–696. https://doi.org/10.1016/S0896-6273(00)80310-4

Stauch, K.L., Purnell, P.R., Fox, H.S., 2014. Aging synaptic mitochondria exhibit dynamic proteomic changes while maintaining bioenergetic function. Aging (Albany. NY). 6, 320–334. https://doi.org/10.18632/aging.100657

Steinert, J.R., Chernova, T., Forsythe, I.D., 2010. Nitric Oxide Signaling in Brain Function, Dysfunction, and Dementia. Neurosci. 16, 435–452. https://doi.org/10.1177/1073858410366481

Stevens, B., Allen, N.J., Vazquez, L.E., Howell, G.R., Christopherson, K.S., Nouri, N., Micheva, K.D., Mehalow, A.K., Huberman, A.D., Stafford, B., Sher, A., Litke, A.M., Lambris, J.D., Smith, S.J., John, S.W.M., Barres, B.A., 2007. The Classical Complement Cascade Mediates CNS Synapse Elimination. Cell 131, 1164–1178. https://doi.org/10.1016/j.cell.2007.10.036

Storch, a, Kaftan, A., Burkhardt, K., Schwarz, J., 2000. 6-Hydroxydopamine toxicity towards human SH-SY5Y dopaminergic neuroblastoma cells: independent of mitochondrial energy metabolism. J. Neural Transm. 107, 0281–0293. https://doi.org/10.1007/s007020050023

Stott, S.R.W., Barker, R.A., 2014. Time course of dopamine neuron loss and glial response in the 6-OHDA striatal mouse model of Parkinson's disease. Eur. J. Neurosci. 39, 1042–1056. https://doi.org/10.1111/ejn.12459

Strobbe, D., Robinson, A.A., Harvey, K., Rossi, L., Ferraina, C., de Biase, V., Rodolfo, C., Harvey, R.J., Campanella, M., 2018. Distinct Mechanisms of Pathogenic DJ-1 Mutations in Mitochondrial Quality Control. Front. Mol. Neurosci. 11, 68. https://doi.org/10.3389/fnmol.2018.00068

Stroissnigg, H., Trančíková, A., Descovich, L., Fuhrmann, J., Kutschera, W., Kostan, J., Meixner, A., Nothias, F., Propst, F., 2007. S-nitrosylation of microtubule-associated protein 1B mediates nitric-oxide-induced axon retraction. Nat. Cell Biol. 9, 1035–1045. https://doi.org/10.1038/ncb1625

Su, B., Wang, X., Zheng, L., Perry, G., Smith, M.A., Zhu, X., 2010. Abnormal mitochondrial dynamics and neurodegenerative diseases. Biochim. Biophys. Acta - Mol. Basis Dis. 1802, 135–142. https://doi.org/10.1016/j.bbadis.2009.09.013

Sultana, R., Perluigi, M., Butterfield, D.A., 2013a. Lipid peroxidation triggers neurodegeneration: A redox proteomics view into the Alzheimer disease brain. Free Radic. Biol. Med. 62, 157–169. https://doi.org/10.1016/j.freeradbiomed.2012.09.027

Sultana, R., Perluigi, M., Butterfield, D.A., 2013b. Lipid peroxidation triggers neurodegeneration: A redox proteomics view into the Alzheimer disease brain. Free Radic. Biol. Med. 62, 157–169. https://doi.org/10.1016/j.freeradbiomed.2012.09.027

Sultanova, N., Kasarova, S., Nikolov, I., 2009. Dispersion Properties of Optical Polymers. Acta Phys. Pol. A 116, 585–587. https://doi.org/10.12693/APhysPolA.116.585

Sun, J., Morgan, M., Shen, R.-F., Steenbergen, C., Murphy, E., 2007. Preconditioning Results in S -Nitrosylation of Proteins Involved in Regulation of Mitochondrial Energetics and Calcium Transport. Circ. Res. 101, 1155–1163. https://doi.org/10.1161/CIRCRESAHA.107.155879

Sun, Y., Gu, Q.-P., Whanger, P.D., 2001. Selenoprotein W in overexpressed and underexpressed rat glial cells in culture. J. Inorg. Biochem. 84, 151–156. https://doi.org/10.1016/S0162-0134(00)00219-1

Sun, Y.E., Martinowich, K., Ge, W., 2003. Making and repairing the mammalian brain—signaling toward neurogenesis and gliogenesis. Semin. Cell Dev. Biol. 14, 161–168. https://doi.org/10.1016/S1084-9521(03)00007-7

Suzuki, T., Yamamoto, M., 2015. Molecular basis of the Keap1–Nrf2 system. Free Radic. Biol. Med. 88, 93–100. https://doi.org/10.1016/j.freeradbiomed.2015.06.006

Swarnkar, S., Goswami, P., Kamat, P.K., Gupta, S., Patro, I.K., Singh, S., Nath, C., 2012. Rotenone-induced apoptosis and role of calcium: a study on Neuro-2a cells. Arch. Toxicol. 86, 1387–1397. https://doi.org/10.1007/s00204-012-0853-z

Swerdlow, R.H., 2009. The Neurogenerative Mitochondriopathies. J. Alzheimers Dis. 17, 737–751. https://doi.org/10.3233/JAD-2009-1095.The

Syková, E., 2001. Glial diffusion barriers during aging and pathological states, in: Progress in Brain Research. pp. 339–363. https://doi.org/10.1016/S0079-6123(01)32087-3

Tagliaferro, P., Burke, R.E., 2016. Retrograde Axonal Degeneration in Parkinson Disease. J. Parkinsons. Dis. 6, 1–15. https://doi.org/10.3233/JPD-150769

Taira, T., Saito, Y., Niki, T., Iguchi-Ariga, S.M.M., Takahashi, K., Ariga, H., 2004. DJ-1 has a role in antioxidative stress to prevent cell death. EMBO Rep. 5, 213–218. https://doi.org/10.1038/sj.embor.7400074

Takahashi, T., Yamashita, H., Nakamura, T., Nagano, Y., Nakamura, S., 2002. Tyrosine 125 of α-synuclein plays a critical role for dimerization following nitrative stress. Brain Res. 938, 73–80. https://doi.org/10.1016/S0006-8993(02)02498-8

Tambuyzer, B.R., Ponsaerts, P., Nouwen, E.J., 2009. Microglia: gatekeepers of central nervous system immunology. J. Leukoc. Biol. 85, 352–370. https://doi.org/10.1189/jlb.0608385

Tanaka, A., Cleland, M.M., Xu, S., Narendra, D.P., Suen, D.-F., Karbowski, M., Youle, R.J., 2010. Proteasome and p97 mediate mitophagy and degradation of mitofusins induced by Parkin. J. Cell Biol. 191, 1367–1380. https://doi.org/10.1083/jcb.201007013

Tanaka, K., Hashimoto, T., Tokumaru, S., Iguchi, H., Kojo, and S., 1997. Interactions between Vitamin C and Vitamin E Are Observed in Tissues of Inherently Scorbutic Rats. J. Nutr. 127, 2060–2064. https://doi.org/10.1093/jn/127.10.2060

Tanner, C.M., 1999. Parkinson Disease in Twins<SUBTITLE>An Etiologic Study</SUBTITLE>. JAMA 281, 341. https://doi.org/10.1001/jama.281.4.341

Tappel, A.L., 1972. VITAMIN E AND FREE RADICAL PEROXIDATION OF LIPIDS. Ann. N. Y. Acad. Sci. 203, 12–28. https://doi.org/10.1111/j.1749-6632.1972.tb27851.x

Tatsuta, T., Langer, T., 2008. Quality control of mitochondria: protection against neurodegeneration and ageing. EMBO J. 27, 306–314. https://doi.org/10.1038/sj.emboj.7601972

Taylor, A.M., Wu, J., Tai, H.-C., Schuman, E.M., 2013. Axonal Translation of β-Catenin Regulates Synaptic Vesicle Dynamics. J. Neurosci. 33, 5584–5589. https://doi.org/10.1523/JNEUROSCI.2944-12.2013

Teismann, P., Schulz, J.B., 2004. Cellular pathology of Parkinson?s disease: astrocytes, microglia and inflammation. Cell Tissue Res. 318, 149–161. https://doi.org/10.1007/s00441-004-0944-0

Teppola, H., Sarkanen, J.-R., Jalonen, T.O., Linne, M.-L., 2016. Morphological Differentiation Towards Neuronal Phenotype of SH-SY5Y Neuroblastoma Cells by Estradiol, Retinoic Acid and Cholesterol. Neurochem. Res. 41, 731–747. https://doi.org/10.1007/s11064-015-1743-6

Terao, K., Niki, E., 1986. Damage to biological tissues induced by radical initiator 2,2′-azobis(2-amidinopropane) dihydrochloride and its inhibition by chain-breaking antioxidants. J. Free Radic. Biol. Med. 2, 193–201. https://doi.org/10.1016/S0748-5514(86)80070-8

Terman, A., Kurz, T., Navratil, M., Arriaga, E.A., Brunk, U.T., 2010. Mitochondrial Turnover and Aging of Long-Lived Postmitotic Cells: The Mitochondrial–Lysosomal Axis Theory of Aging. Antioxid. Redox Signal. 12, 503–535. https://doi.org/10.1089/ars.2009.2598

Testa, C.M., Sherer, T.B., Greenamyre, J.T., 2005. Rotenone induces oxidative stress and dopaminergic neuron damage in organotypic substantia nigra cultures. Mol. Brain Res. 134, 109–118.

https://doi.org/10.1016/j.molbrainres.2004.11.007

Then, S.M., Wan Ngah, W.Z., Top, G.M., Mazlan, M., 2010. Comparison of the effects of α-tocopherol and γ-tocotrienol against oxidative stress in two different neuronal cultures. Sains Malaysiana 39, 145–156.

Theodore, M., Kawai, Y., Yang, J., Kleshchenko, Y., Reddy, S.P., Villalta, F., Arinze, I.J., 2008. Multiple Nuclear Localization Signals Function in the Nuclear Import of the Transcription Factor Nrf2. J. Biol. Chem. 283, 8984–8994. https://doi.org/10.1074/jbc.M709040200

THOMAS, P.K., 1964. CHANGES IN THE ENDONEURIAL SHEATHS OF PERIPHERAL MYELINATED NERVE FIBRES DURING WALLERIAN DEGENERATION. J. Anat. 98, 175–82.

Thompson, C.M., Capdevila, J.H., Strobel, H.W., 2000. Recombinant cytochrome P450 2D18 metabolism of dopamine and arachidonic acid. J. Pharmacol. Exp. Ther. 294, 1120–1130.

Tofaris, G.K., Layfield, R., Spillantini, M.G., 2001. α-Synuclein metabolism and aggregation is linked to ubiquitin-independent degradation by the proteasome. FEBS Lett. 509, 22–26. https://doi.org/10.1016/S0014-5793(01)03115-5

Toledo, E.M., Colombres, M., Inestrosa, N.C., 2008. Wnt signaling in neuroprotection and stem cell differentiation. Prog. Neurobiol. 86, 281–296. https://doi.org/10.1016/j.pneurobio.2008.08.001

Tomozawa, Y., Appel, S.H., 1986. Soluble striatal extracts enhance development of mesencephalic dopaminergic neurons in vitro. Brain Res. 399, 111–124. https://doi.org/10.1016/0006-8993(86)90605-0

Toyama, T., Shinkai, Y., Yazawa, A., Kakehashi, H., Kaji, T., Kumagai, Y., 2014. Glutathione-mediated reversibility of covalent modification of ubiquitin carboxyl-terminal hydrolase L1 by 1,2-naphthoquinone through Cys152, but not Lys4. Chem. Biol. Interact. 214, 41–48. https://doi.org/10.1016/j.cbi.2014.02.008

Traber, M.G., Atkinson, J., 2007. Vitamin E, antioxidant and nothing more. Free Radic. Biol. Med. 43, 4–15. https://doi.org/10.1016/j.freeradbiomed.2007.03.024

Traber, M.G., Burton, G.W., Ingold, K.U., Kayden, H.J., 1990. RRR- and SRR-alpha-tocopherols are secreted without discrimination in human chylomicrons, but RRR-alpha-tocopherol is preferentially secreted in very low density lipoproteins. J. Lipid Res. 31, 675–85.

Trachootham, D., Lu, W., Ogasawara, M.A., Valle, N.R.-D., Huang, P., 2008. Redox Regulation of Cell Survival. Antioxid. Redox Signal. 10, 1343–1374. https://doi.org/10.1089/ars.2007.1957

Trachootham, D., Zhou, Y., Zhang, H., Demizu, Y., Chen, Z., Pelicano, H., Chiao, P.J., Achanta, G., Arlinghaus, R.B., Liu, J., Huang, P., 2006. Selective killing of oncogenically transformed cells through a ROS-mediated mechanism by β-phenylethyl isothiocyanate. Cancer Cell 10, 241–252. https://doi.org/10.1016/j.ccr.2006.08.009

Trougakos, I.P., Sesti, F., Tsakiri, E., Gorgoulis, V.G., 2013. Non-enzymatic post-translational protein modifications and proteostasis network deregulation in carcinogenesis. J. Proteomics 92, 274–298. https://doi.org/10.1016/j.jprot.2013.02.024

Tsang, A.H.K., Chung, K.K.K., 2009. Oxidative and nitrosative stress in Parkinson's disease. Biochim. Biophys. Acta - Mol. Basis Dis. 1792, 643–650. https://doi.org/10.1016/j.bbadis.2008.12.006

Tsao, J.W., Brown, M.C., Carden, M.J., McLean, W.G., Perry, V.H., 1994. Loss of the Compound Action Potential: an Electrophysiological, Biochemical and Morphological Study of Early Events in Axonal Degeneration in the C57BL/Ola Mouse. Eur. J. Neurosci. 6, 516–524. https://doi.org/10.1111/j.1460-9568.1994.tb00295.x

Tsuda, M., Toyomitsu, E., Komatsu, T., Masuda, T., Kunifusa, E., Nasu-Tada, K., Koizumi, S., Yamamoto, K., Ando, J., Inoue, K., 2008. Fibronectin/integrin system is involved in P2X4 receptor upregulation in the spinal cord and neuropathic pain after nerve injury. Glia 56, 579–585. https://doi.org/10.1002/glia.20641

Tu, Y.-J., Njus, D., Schlegel, H.B., 2017. A theoretical study of ascorbic acid oxidation and HOO˙/ O 2 ˙ − radical scavenging. Org. Biomol. Chem. 15, 4417–4431. https://doi.org/10.1039/C7OB00791D

Tufekci, K.U., Civi Bayin, E., Genc, S., Genc, K., 2011. The Nrf2/ARE Pathway: A Promising Target to Counteract Mitochondrial Dysfunction in Parkinson's Disease. Parkinsons. Dis. 2011, 1–14. https://doi.org/10.4061/2011/314082

Turner-Ivey, B., Manevich, Y., Schulte, J., Kistner-Griffin, E., Jezierska-Drutel, A., Liu, Y., Neumann, C.A., 2013. Role for Prdx1 as a specific sensor in redox-regulated senescence in breast cancer. Oncogene 32, 5302–5314. https://doi.org/10.1038/onc.2012.624

Turturici, G., Sconzo, G., Geraci, F., 2011. Hsp70 and Its Molecular Role in Nervous System Diseases. Biochem. Res. Int. 2011, 1–18. https://doi.org/10.1155/2011/618127

Twelves, D., Perkins, K.S.M., Counsell, C., 2003. Systematic review of incidence studies of Parkinson's disease. Mov. Disord. 18, 19–31. https://doi.org/10.1002/mds.10305

Twig, G., Shirihai, O.S., 2011. The Interplay Between Mitochondrial Dynamics and Mitophagy. Antioxid. Redox Signal. 14, 1939–1951. https://doi.org/10.1089/ars.2010.3779

Tydlacka, S., Wang, C.-E., Wang, X., Li, S., Li, X.-J., 2008. Differential Activities of the Ubiquitin-Proteasome System in Neurons versus Glia May Account for the Preferential Accumulation of Misfolded Proteins in Neurons. J. Neurosci. 28, 13285–13295. https://doi.org/10.1523/JNEUROSCI.4393-08.2008

Ulatowski, L., Dreussi, C., Noy, N., Barnholtz-Sloan, J., Klein, E., Manor, D., 2012. Expression of the α-tocopherol transfer protein gene is regulated by oxidative stress and common single-nucleotide polymorphisms. Free Radic. Biol. Med. 53, 2318–2326. https://doi.org/10.1016/j.freeradbiomed.2012.10.528

Unno, M., Mizushima, T., Morimoto, Y., Tomisugi, Y., Tanaka, K., Yasuoka, N., Tsukihara, T., 2002. The Structure of the Mammalian 20S Proteasome at 2.75 Å Resolution. Structure 10, 609–618. https://doi.org/10.1016/S0969-2126(02)00748-7

Uo, T., Dworzak, J., Kinoshita, C., Inman, D.M., Kinoshita, Y., Horner, P.J., Morrison, R.S., 2009. Drp1 levels constitutively regulate mitochondrial dynamics and cell survival in cortical neurons. Exp. Neurol. 218, 274–285. https://doi.org/10.1016/j.expneurol.2009.05.010

Utani, A., 2010. [Laminin alpha3 chain-derived peptide promotes keratinocyte migration and wound closure: clustering of syndecan-4 and integrin beta1]. Seikagaku. 82, 327–31. https://doi.org/10.1091/mbc.E08

Vaishnavi, S.N., Vlassenko, A.G., Rundle, M.M., Snyder, A.Z., Mintun, M.A., Raichle, M.E., 2010. Regional aerobic glycolysis in the human brain. Proc. Natl. Acad. Sci. 107, 17757–17762. https://doi.org/10.1073/pnas.1010459107

Valenta, T., Hausmann, G., Basler, K., 2012. The many faces and functions of β-catenin. EMBO J. 31, 2714–2736. https://doi.org/10.1038/emboj.2012.150

Valente, E.M., Abou-Sleiman, P.M., Caputo, V., Muqit, M.M.K., Harvey, K., Gispert, S., Ali, Z., Del Turco, D., Bentivoglio, A.R., Healy, D.G., Albanese, A., Nussbaum, R., Gonzalez-Maldonado, R., Deller, T., Salvi, S., Cortelli, P., Gilks, W.P., Latchman, D.S., Harvey, R.J., Dallapiccola, B., Auburger, G., Wood, N.W., 2004. Hereditary early-onset Parkinson's disease caused by mutations in PINK1. Science 304, 1158–60. https://doi.org/10.1126/science.1096284

van der Bliek, A.M., Shen, Q., Kawajiri, S., 2013. Mechanisms of Mitochondrial Fission and Fusion. Cold Spring Harb. Perspect. Biol. 5, a011072–a011072. https://doi.org/10.1101/cshperspect.a011072

van der Merwe, C., van Dyk, H.C., Engelbrecht, L., van der Westhuizen, F.H., Kinnear, C., Loos, B., Bardien, S., 2017. Curcumin Rescues a PINK1 Knock Down SH-SY5Y Cellular Model of Parkinson's Disease from Mitochondrial Dysfunction and Cell Death. Mol. Neurobiol. 54, 2752–2762. https://doi.org/10.1007/s12035-016-9843-0

van Horssen, J., Drexhage, J.A.R., Flor, T., Gerritsen, W., van der Valk, P., de Vries, H.E., 2010. Nrf2 and DJ1

are consistently upregulated in inflammatory multiple sclerosis lesions. Free Radic. Biol. Med. 49, 1283–1289. https://doi.org/10.1016/j.freeradbiomed.2010.07.013

Van Laar, V.S., Berman, S.B., 2013. The interplay of neuronal mitochondrial dynamics and bioenergetics: Implications for Parkinson's disease. Neurobiol. Dis. 51, 43–55. https://doi.org/10.1016/j.nbd.2012.05.015

Van Wagoner, N.J., Oh, J.W., Repovic, P., Benveniste, E.N., 1999. Interleukin-6 (IL-6) production by astrocytes: autocrine regulation by IL-6 and the soluble IL-6 receptor. J. Neurosci. 19, 5236–44.

Vangala, J.R., Sotzny, F., Krüger, E., Deshaies, R.J., Radhakrishnan, S.K., 2016. Nrf1 can be processed and activated in a proteasome-independent manner. Curr. Biol. 26, R834–R835. https://doi.org/10.1016/j.cub.2016.08.008

Vargas, M.R., Johnson, D.A., Sirkis, D.W., Messing, A., Johnson, J.A., 2008. Nrf2 Activation in Astrocytes Protects against Neurodegeneration in Mouse Models of Familial Amyotrophic Lateral Sclerosis. J. Neurosci. 28, 13574–13581. https://doi.org/10.1523/JNEUROSCI.4099-08.2008

Vargas, M.R., Johnson, J.A., 2009. The Nrf2–ARE cytoprotective pathway in astrocytes. Expert Rev. Mol. Med. 11, e17. https://doi.org/10.1017/S1462399409001094

Vargas, M.R., Pehar, M., Cassina, P., Beckman, J.S., Barbeito, L., 2006. Increased glutathione biosynthesis by Nrf2 activation in astrocytes prevents p75NTR-dependent motor neuron apoptosis. J. Neurochem. 97, 687–696. https://doi.org/10.1111/j.1471-4159.2006.03742.x

Vargas, M.R., Pehar, M., Cassina, P., Martínez-Palma, L., Thompson, J.A., Beckman, J.S., Barbeito, L., 2005. Fibroblast Growth Factor-1 Induces Heme Oxygenase-1 via Nuclear Factor Erythroid 2-related Factor 2 (Nrf2) in Spinal Cord Astrocytes. J. Biol. Chem. 280, 25571–25579. https://doi.org/10.1074/jbc.M501920200

Ved, R., Saha, S., Westlund, B., Perier, C., Burnam, L., Sluder, A., Hoener, M., Rodrigues, C.M.P., Alfonso, A., Steer, C., Liu, L., Przedborski, S., Wolozin, B., 2005. Similar Patterns of Mitochondrial Vulnerability and Rescue Induced by Genetic Modification of α-Synuclein, Parkin, and DJ-1 in Caenorhabditis elegans. J. Biol. Chem. 280, 42655–42668. https://doi.org/10.1074/jbc.M505910200

Veenman, L., Alten, J., Linnemannstöns, K., Shandalov, Y., Zeno, S., Lakomek, M., Gavish, M., Kugler, W., 2010. Potential involvement of F0F1-ATP(synth)ase and reactive oxygen species in apoptosis induction by the antineoplastic agent erucylphosphohomocholine in glioblastoma cell lines. Apoptosis 15, 753–768. https://doi.org/10.1007/s10495-010-0460-5

Veenman, L., Shandalov, Y., Gavish, M., 2008. VDAC activation by the 18 kDa translocator protein (TSPO), implications for apoptosis. J. Bioenerg. Biomembr. 40, 199–205. https://doi.org/10.1007/s10863-008-9142-1

Venugopal, R., Jaiswal, a K., 1996. Nrf1 and Nrf2 positively and c-Fos and Fra1 negatively regulate the human antioxidant response element-mediated expression of NAD(P)H:quinone oxidoreductase1 gene. Proc. Natl. Acad. Sci. U. S. A. 93, 14960–14965. https://doi.org/10.1073/pnas.93.25.14960

Verkhratsky, A., Matteoli, M., Parpura, V., Mothet, J., Zorec, R., 2016. Astrocytes as secretory cells of the central nervous system: idiosyncrasies of vesicular secretion. EMBO J. 35, 239–257. https://doi.org/10.15252/embj.201592705

Verkhratsky, A., Sofroniew, M. V., Messing, A., DeLanerolle, N.C., Rempe, D., Rodríguez, J.J., Nedergaard, M., 2012. Neurological Diseases as Primary Gliopathies: A Reassessment of Neurocentrism. ASN Neuro 4, AN20120010. https://doi.org/10.1042/AN20120010

Verma, R., 2002. Role of Rpn11 Metalloprotease in Deubiquitination and Degradation by the 26S Proteasome. Science (80-.). 298, 611–615. https://doi.org/10.1126/science.1075898

Vilchez, D., Ros, S., Cifuentes, D., Pujadas, L., Vallès, J., García-Fojeda, B., Criado-García, O., Fernández-Sánchez, E., Medraño-Fernández, I., Domínguez, J., García-Rocha, M., Soriano, E., Rodríguez de Córdoba, S., Guinovart, J.J., 2007. Mechanism suppressing glycogen synthesis in neurons and its demise

in progressive myoclonus epilepsy. Nat. Neurosci. 10, 1407–1413. https://doi.org/10.1038/nn1998

Vineetha, R.C., Archana, V., Binu, P., Arathi, P., Nair, R.H., 2018. L-Ascorbic Acid and α-Tocopherol Reduces Hepatotoxicity Associated with Arsenic Trioxide Chemotherapy by Modulating Nrf2 and Bcl2 Transcription Factors in Chang liver Cells. Nutr. Cancer 70, 684–696. https://doi.org/10.1080/01635581.2018.1460676

Virga, D.M., Capps, J., Vohra, B.P.S., 2018. Enteric Neurodegeneration is Mediated Through Independent Neuritic and Somal Mechanisms in Rotenone and MPP+ Toxicity. Neurochem. Res. 43, 2288–2303. https://doi.org/10.1007/s11064-018-2649-x

Voges, D., Zwickl, P., Baumeister, W., 1999. The 26S proteasome: a molecular machine designed for controlled proteolysis. Annu. Rev. Biochem. 68, 1015–68. https://doi.org/10.1146/annurev.biochem.68.1.1015

Volterra, A., Meldolesi, J., 2005. Astrocytes, from brain glue to communication elements: the revolution continues. Nat. Rev. Neurosci. 6, 626–640. https://doi.org/10.1038/nrn1722

Voronkov, D.N., Khudoerkov, R.M., Dikalova, Y. V., Sheloukhova, L.I., 2016. Quantitative Evaluation of Changes in the Striatal Astrocyte Axons in Simulated Parkinsonism. Bull. Exp. Biol. Med. 160, 505–509. https://doi.org/10.1007/s10517-016-3208-6

Vos, M., Verstreken, P., Klein, C., 2015. Stimulation of electron transport as potential novel therapy in Parkinson's disease with mitochondrial dysfunction: Figure 1. Biochem. Soc. Trans. 43, 275–279. https://doi.org/10.1042/BST20140325

Wai, T., Langer, T., 2016. Mitochondrial Dynamics and Metabolic Regulation. Trends Endocrinol. Metab. 27, 105–117. https://doi.org/10.1016/j.tem.2015.12.001

Wakabayashi, K., Engelender, S., Yoshimoto, M., Tsuji, S., Ross, C.A., Takahashi, H., 2000a. Synphilin-1 is present in lewy bodies in Parkinson's disease. Ann. Neurol. 47, 521–523. https://doi.org/10.1002/1531-8249(200004)47:4<521::AID-ANA18>3.0.CO;2-B

Wakabayashi, K., Hayashi, S., Yoshimoto, M., Kudo, H., Takahashi, H., 2000b. NACP/α-synuclein-positive filamentous inclusions in astrocytes and oligodendrocytes of Parkinson's disease brains. Acta Neuropathol. 99, 14–20. https://doi.org/10.1007/PL00007400

Walsh, C.T., Garneau-Tsodikova, S., Gatto, G.J., 2005. Protein Posttranslational Modifications: The Chemistry of Proteome Diversifications. Angew. Chemie Int. Ed. 44, 7342–7372. https://doi.org/10.1002/anie.200501023

Wang, C., Telpoukhovskaia, M.A., Bahr, B.A., Chen, X., Gan, L., 2018. Endo-lysosomal dysfunction: a converging mechanism in neurodegenerative diseases. Curr. Opin. Neurobiol. 48, 52–58. https://doi.org/10.1016/j.conb.2017.09.005

Wang, D., Qian, L., Xiong, H., Liu, J., Neckameyer, W.S., Oldham, S., Xia, K., Wang, J., Bodmer, R., Zhang, Z., 2006. Antioxidants protect PINK1-dependent dopaminergic neurons in Drosophila. Proc. Natl. Acad. Sci. U. S. A. 103, 13520–5. https://doi.org/10.1073/pnas.0604661103

Wang, F., Awan, U., Wang, Y., Wang, L., Qing, H., Ma, H., Deng, Y., 2014. Damage of Neuroblastoma Cell SH-SY5Y Mediated by MPP+ Inhibits Proliferation of T-Cell Leukemia Jurkat by Co-Culture System. Int. J. Mol. Sci. 15, 10738–10750. https://doi.org/10.3390/ijms150610738

Wang, F., Hao, H., Zhao, S., Zhang, Y., Liu, Q., Liu, H., Liu, S., Yuan, Q., Bing, L., Ling, E.-A., Hao, A., 2011. Roles of activated astrocyte in neural stem cell proliferation and differentiation. Stem Cell Res. 7, 41–53. https://doi.org/10.1016/j.scr.2011.03.004

Wang, F., Ni, J., Wang, X., Xie, B., Feng, C., Zhao, S., Saeed, Y., Qing, H., Deng, Y., 2015. Salsolinol Damaged Neuroblastoma SH-SY5Y Cells Induce Proliferation of Human Monocyte THP-1 Cells Through the mTOR Pathway in a Co-culture System. Neurochem. Res. 40, 932–941. https://doi.org/10.1007/s11064-015-1547-8

Wang, H.L., Chou, A.H., Yeh, T.H., Li, A.H., Chen, Y.L., Kuo, Y.L., Tsai, S.R., Yu, S.T., 2007. PINK1 mutants associated with recessive Parkinson's disease are defective in inhibiting mitochondrial release of cytochrome c. Neurobiol. Dis. 28, 216–226. https://doi.org/10.1016/j.nbd.2007.07.010

Wang, J., Edmondson, D.E., 2011. Topological probes of monoamine oxidases A and B in rat liver mitochondria: Inhibition by TEMPO-substituted pargyline analogues and inactivation by proteolysis. Biochemistry 50, 2499–2505. https://doi.org/10.1021/bi101722b

Wang, J.T., Medress, Z.A., Barres, B.A., 2012. Axon degeneration: Molecular mechanisms of a self-destruction pathway. J. Cell Biol. 196, 7–18. https://doi.org/10.1083/jcb.201108111

Wang, J.T., Yin, L., Chen, Z., 2013. Neuroprotective role of fibronectin in neuron-glial extrasynaptic transmission. Neural Regen. Res. 8, 376–82. https://doi.org/10.3969/j.issn.1673-5374.2013.04.010

Wang, L., Duan, Q., Wang, T., Ahmed, M., Zhang, N., Li, Y., Li, L., Yao, X., 2015. Mitochondrial Respiratory Chain Inhibitors Involved in ROS Production Induced by Acute High Concentrations of Iodide and the Effects of SOD as a Protective Factor. Oxid. Med. Cell. Longev. 2015, 1–14. https://doi.org/10.1155/2015/217670

Wang, L., Kisaalita, W.S., 2011. Administration of BDNF/ginsenosides combination enhanced synaptic development in human neural stem cells. J. Neurosci. Methods 194, 274–282. https://doi.org/10.1016/j.jneumeth.2010.10.025

Wang, W., Yang, Y., Ying, C., Li, W., Ruan, H., Zhu, X., You, Y., Han, Y., Chen, R., Wang, Y., Li, M., 2007. Inhibition of glycogen synthase kinase-3β protects dopaminergic neurons from MPTP toxicity. Neuropharmacology 52, 1678–1684. https://doi.org/10.1016/j.neuropharm.2007.03.017

Wang, X.-F., Li, S., Chou, A.P., Bronstein, J.M., 2006. Inhibitory effects of pesticides on proteasome activity: Implication in Parkinson's disease. Neurobiol. Dis. 23, 198–205. https://doi.org/10.1016/j.nbd.2006.02.012

Wang, X., Qin, Z.-H., Leng, Y., Wang, Y., Jin, X., Chase, T.N., Bennett, M.C., 2002. Prostaglandin A1 inhibits rotenone-induced apoptosis in SH-SY5Y cells. J. Neurochem. 83, 1094–1102. https://doi.org/10.1046/j.1471-4159.2002.01224.x

Waragai, M., Wei, J., Fujita, M., Nakai, M., Ho, G.J., Masliah, E., Akatsu, H., Yamada, T., Hashimoto, M., 2006. Increased level of DJ-1 in the cerebrospinal fluids of sporadic Parkinson's disease. Biochem. Biophys. Res. Commun. 345, 967–972. https://doi.org/10.1016/j.bbrc.2006.05.011

Warburg, O., 1956. On the Origin of Cancer Cells. Science (80-.). 123, 309–314. https://doi.org/10.1126/science.123.3191.309

Warburg, O.H., 2010. The Classic: The Chemical Constitution of Respiration Ferment. Clin. Orthop. Relat. Res. 468, 2833–2839. https://doi.org/10.1007/s11999-010-1534-y

Waris, G., Ahsan, H., 2006. Reactive oxygen species: role in the development of cancer and various chronic conditions. J. Carcinog. 5, 14. https://doi.org/10.1186/1477-3163-5-14

WEINHOUSE, S., WARBURG, O., BURK, D., SCHADE, A.L., 1956. On Respiratory Impairment in Cancer Cells. Science (80-.). 124, 267–272. https://doi.org/10.1126/science.124.3215.267

Weissman, a M., 2001. Themes and variations on ubiquitylation. Nat. Rev. Mol. Cell Biol. 2, 169–178. https://doi.org/10.1038/35056563

Wells, R.G., 2008. The role of matrix stiffness in regulating cell behavior. Hepatology 47, 1394–1400. https://doi.org/10.1002/hep.22193

Wenzel, U., 2003. Ascorbic acid suppresses drug-induced apoptosis in human colon cancer cells by scavenging mitochondrial superoxide anions. Carcinogenesis 25, 703–712. https://doi.org/10.1093/carcin/bgh079

Werber, J., Wang, Y.J., Milligan, M., Li, X., Ji, J.A., 2011. Analysis of 2,2'-Azobis (2-amidinopropane) dihydrochloride degradation and hydrolysis in aqueous solutions. J. Pharm. Sci. 100, 3307–3315.

https://doi.org/10.1002/jps.22578

Wild, A.C., Moinova, H.R., Mulcahy, R.T., 1999. Regulation of gamma-glutamylcysteine synthetase subunit gene expression by the transcription factor Nrf2. J. Biol. Chem. 274, 33627–36. https://doi.org/10.1074/jbc.274.47.33627

Wilkinson, K.D., 1995. Roles of ubiquitinylation in proteolysis and cellular regulation. Annu. Rev. Nutr. 15, 161–89. https://doi.org/10.1146/annurev.nu.15.070195.001113

Wilkinson, K.D., Lee, K.M., Deshpande, S., Duerksen-Hughes, P., Boss, J.M., Pohl, J., 1989. The neuron-specific protein PGP 9.5 is a ubiquitin carboxyl-terminal hydrolase. Science 246, 670–673. https://doi.org/10.1126/science.2530630

Wilson, J., 1997. Antioxidant defense of the brain: a role for astrocytes. Can. J. Physiol. Pharmacol. 75, 1149–63.

Winklhofer, K.F., Henn, I.H., Kay-Jackson, P.C., Heller, U., Tatzelt, J., 2003. Inactivation of parkin by oxidative stress and C-terminal truncations: A protective role of molecular chaperones. J. Biol. Chem. 278, 47199–47208. https://doi.org/10.1074/jbc.M306769200

Winterbourn, C.C., 2015. Are free radicals involved in thiol-based redox signaling? Free Radic. Biol. Med. 80, 164–170. https://doi.org/10.1016/j.freeradbiomed.2014.08.017

Winterbourn, C.C., 2008. Reconciling the chemistry and biology of reactive oxygen species. Nat. Chem. Biol. 4, 278–286. https://doi.org/10.1038/nchembio.85

Winterbourn, C.C., Hampton, M.B., 2008. Thiol chemistry and specificity in redox signaling. Free Radic. Biol. Med. 45, 549–561. https://doi.org/10.1016/j.freeradbiomed.2008.05.004

Wood-Kaczmar, A., Gandhi, S., Yao, Z., Abramov, A.S.Y., Miljan, E.A., Keen, G., Stanyer, L., Hargreaves, I., Klupsch, K., Deas, E., Downward, J., Mansfield, L., Jat, P., Taylor, J., Heales, S., Duchen, M.R., Latchman, D., Tabrizi, S.J., Wood, N.W., 2008. PINK1 Is Necessary for Long Term Survival and Mitochondrial Function in Human Dopaminergic Neurons. PLoS One 3, e2455. https://doi.org/10.1371/journal.pone.0002455

Worden, E.J., Padovani, C., Martin, A., 2014. Structure of the Rpn11–Rpn8 dimer reveals mechanisms of substrate deubiquitination during proteasomal degradation. Nat. Struct. Mol. Biol. 21, 220–227. https://doi.org/10.1038/nsmb.2771

Wortmann, M., Schneider, M., Pircher, J., Hellfritsch, J., Aichler, M., Vegi, N., Kölle, P., Kuhlencordt, P., Walch, A., Pohl, U., Bornkamm, G.W., Conrad, M., Beck, H., 2013. Combined Deficiency in Glutathione Peroxidase 4 and Vitamin E Causes Multiorgan Thrombus Formation and Early Death in Mice. Circ. Res. 113, 408–417. https://doi.org/10.1161/CIRCRESAHA.113.279984

Wyss-Coray, T., Mucke, L., 2002. Inflammation in Neurodegenerative Disease—A Double-Edged Sword. Neuron 35, 419–432. https://doi.org/10.1016/S0896-6273(02)00794-8

Xia, C., Taylor, J.B., Spencer, S.R., Ketterer, B., 1993. The human glutathione S-transferase P1-1 gene: modulation of expression by retinoic acid and insulin. Biochem. J. 292 (Pt 3, 845–50. https://doi.org/10.1042/bj2920845

Xia, L., Wurmbach, E., Waxman, S., Jing, Y., 2006. Upregulation of Bfl-1/A1 in leukemia cells undergoing differentiation by all-trans retinoic acid treatment attenuates chemotherapeutic agent-induced apoptosis. Leukemia 20, 1009–1016. https://doi.org/10.1038/sj.leu.2404198

Xu, C.-Y., Kang, W.-Y., Chen, Y.-M., Jiang, T.-F., Zhang, J., Zhang, L.-N., Ding, J.-Q., Liu, J., Chen, S.-D., 2017a. DJ-1 Inhibits α-Synuclein Aggregation by Regulating Chaperone-Mediated Autophagy. Front. Aging Neurosci. 9, 308. https://doi.org/10.3389/fnagi.2017.00308

Xu, C.-Y., Kang, W.-Y., Chen, Y.-M., Jiang, T.-F., Zhang, J., Zhang, L.-N., Ding, J.-Q., Liu, J., Chen, S.-D., 2017b. DJ-1 Inhibits α-Synuclein Aggregation by Regulating Chaperone-Mediated Autophagy. Front. Aging Neurosci. 9, 308. https://doi.org/10.3389/fnagi.2017.00308

Xu, S., Peng, G., Wang, Y., Fang, S., Karbowski, M., 2011. The AAA-ATPase p97 is essential for outer mitochondrial membrane protein turnover. Mol. Biol. Cell 22, 291–300. https://doi.org/10.1091/mbc.e10-09-0748

Xu, Y.-M., Huang, D.-Y., Chiu, J.-F., Lau, A.T.Y., 2012. Post-Translational Modification of Human Heat Shock Factors and Their Functions: A Recent Update by Proteomic Approach. J. Proteome Res. 11, 2625–2634. https://doi.org/10.1021/pr201151a

Xu, Y., Stokes, A.H., Roskoski, R., Vrana, K.E., 1998. Dopamine, in the presence of tyrosinase, covalently modifies and inactivates tyrosine hydroxylase. J. Neurosci. Res. 54, 691–697. https://doi.org/10.1002/(SICI)1097-4547(19981201)54:5<691::AID-JNR14>3.0.CO;2-F

Xun, Z., Lee, D.-Y., Lim, J., Canaria, C.A., Barnebey, A., Yanonne, S.M., McMurray, C.T., 2012. Retinoic acid-induced differentiation increases the rate of oxygen consumption and enhances the spare respiratory capacity of mitochondria in SH-SY5Y cells. Mech. Ageing Dev. 133, 176–185. https://doi.org/10.1016/j.mad.2012.01.008

Yamamoto, T., Maruyama, W., Kato, Y., Yi, H., Shamoto-Nagai, M., Tanaka, M., Sato, Y., Naoi, M., 2002. Selective nitration of mitochondrial complex I by peroxynitrite: involvement in mitochondria dysfunction and cell death of dopaminergic SH-SY5Y cells. J. Neural Transm. 109, 1–13. https://doi.org/10.1007/s702-002-8232-1

Yang, J.-W., Rodrigo, R., Felipo, V., Lubec, G., 2005. Proteome Analysis of Primary Neurons and Astrocytes from Rat Cerebellum. J. Proteome Res. 4, 768–788. https://doi.org/10.1021/pr049774v

Yao, D., Gu, Z., Nakamura, T., Shi, Z.-Q., Ma, Y., Gaston, B., Palmer, L.A., Rockenstein, E.M., Zhang, Z., Masliah, E., Uehara, T., Lipton, S.A., 2004. Nitrosative stress linked to sporadic Parkinson's disease: S-nitrosylation of parkin regulates its E3 ubiquitin ligase activity. Proc. Natl. Acad. Sci. https://doi.org/10.1073/pnas.0404161101

Yeh, T.-H., Lee, D.Y., Gianino, S.M., Gutmann, D.H., 2009. Microarray analyses reveal regional astrocyte heterogeneity with implications for neurofibromatosis type 1 (NF1)-regulated glial proliferation. Glia 57, 1239–1249. https://doi.org/10.1002/glia.20845

Yeung, T., Georges, P.C., Flanagan, L.A., Marg, B., Ortiz, M., Funaki, M., Zahir, N., Ming, W., Weaver, V., Janmey, P.A., 2005. Effects of substrate stiffness on cell morphology, cytoskeletal structure, and adhesion. Cell Motil. Cytoskeleton 60, 24–34. https://doi.org/10.1002/cm.20041

Yin, P., Knolhoff, A.M., Rosenberg, H.J., Millet, L.J., Gillette, M.U., Sweedler, J. V., 2012. Peptidomic Analyses of Mouse Astrocytic Cell Lines and Rat Primary Cultured Astrocytes. J. Proteome Res. 11, 3965–3973. https://doi.org/10.1021/pr201066t

Yokota, T., Sugawara, K., Ito, K., Takahashi, R., Ariga, H., Mizusawa, H., 2003. Down regulation of DJ-1 enhances cell death by oxidative stress, ER stress, and proteasome inhibition. Biochem. Biophys. Res. Commun. 312, 1342–1348. https://doi.org/10.1016/j.bbrc.2003.11.056

Yokoyama, Y., Maruyama, K., Yamamoto, K., Omodaka, K., Yasuda, M., Himori, N., Ryu, M., Nishiguchi, K.M., Nakazawa, T., 2014. The role of calpain in an in vivo model of oxidative stress-induced retinal ganglion cell damage. Biochem. Biophys. Res. Commun. 451, 510–515. https://doi.org/10.1016/j.bbrc.2014.08.009

Yokozawa, T., Cho, E.J., Hara, Y., Kitani, K., 2000. Antioxidative activity of green tea treated with radical initiator 2, 2'-azobis(2-amidinopropane) dihydrochloride. J. Agric. Food Chem. 48, 5068–5073.

Yoon, I.S., Au, Q., Barber, J.R., Ng, S.C., Zhang, B., 2010. Development of a high-throughput screening assay for cytoprotective agents in rotenone-induced cell death. Anal. Biochem. 407, 205–210. https://doi.org/10.1016/j.ab.2010.08.011

Yoritaka, a, Hattori, N., Uchida, K., Tanaka, M., Stadtman, E.R., Mizuno, Y., 1996. Immunohistochemical detection of 4-hydroxynonenal protein adducts in Parkinson disease. Proc. Natl. Acad. Sci. 93, 2696–2701. https://doi.org/10.1073/pnas.93.7.2696

Yoshida, H., Mimura, J., Imaizumi, T., Matsumiya, T., Ishikawa, A., Metoki, N., Tanji, K., Ota, K., Hayakari, R., Kosaka, K., Itoh, K., Satoh, K., 2011. Edaravone and carnosic acid synergistically enhance the expression of nerve growth factor in human astrocytes under hypoxia/reoxygenation. Neurosci. Res. 69, 291–298. https://doi.org/10.1016/j.neures.2010.12.016

Yoshii, S.R., Kishi, C., Ishihara, N., Mizushima, N., 2011. Parkin Mediates Proteasome-dependent Protein Degradation and Rupture of the Outer Mitochondrial Membrane. J. Biol. Chem. 286, 19630–19640. https://doi.org/10.1074/jbc.M110.209338

Youle, R.J., Narendra, D.P., 2011. Mechanisms of mitophagy. Nat. Rev. Mol. Cell Biol. 12, 9–14. https://doi.org/10.1038/nrm3028

Yu, B., Changsheng, Y., Wenjun, Z., Ben, L., Hai, Q., Jing, M., Guangwei, X., Shuhua, W., Fang, L., Aschner, M., Rongzhu, L., 2015. Differential protection of pre- versus post-treatment with curcumin, Trolox, and N -acetylcysteine against acrylonitrile-induced cytotoxicity in primary rat astrocytes. Neurotoxicology 51, 58–66. https://doi.org/10.1016/j.neuro.2015.09.011

Yudkoff, M., Pleasure, D., Cregar, L., Lin, Z.-P., Nissim, Ilana, Stern, J., Nissim, Itzhak, 1990. Glutathione Turnover in Cultured Astrocytes: Studies with [15 N]Glutamate. J. Neurochem. 55, 137–145. https://doi.org/10.1111/j.1471-4159.1990.tb08831.x

Zabłocka, A., Mitkiewicz, M., Macała, J., Janusz, M., 2015. Neurotrophic Activity of Cultured Cell Line U87 is Up-Regulated by Proline-Rich Polypeptide Complex and Its Constituent Nonapeptide. Cell. Mol. Neurobiol. 35, 977–986. https://doi.org/10.1007/s10571-015-0192-8

Zagoura, D., Canovas-Jorda, D., Pistollato, F., Bremer-Hoffmann, S., Bal-Price, A., 2017. Evaluation of the rotenone-induced activation of the Nrf2 pathway in a neuronal model derived from human induced pluripotent stem cells. Neurochem. Int. 106, 62–73. https://doi.org/10.1016/j.neuint.2016.09.004

Zakharova, I., Sokolova, T., Vlasova, Y., Bayunova, L., Rychkova, M., Avrova, N., 2017. α-Tocopherol at Nanomolar Concentration Protects Cortical Neurons against Oxidative Stress. Int. J. Mol. Sci. 18, 216. https://doi.org/10.3390/ijms18010216

Zarkovic, K., 2003. 4-Hydroxynonenal and neurodegenerative diseases, in: Molecular Aspects of Medicine. pp. 293–303. https://doi.org/10.1016/S0098-2997(03)00024-4

Zeevalk, G.D., Razmpour, R., Bernard, L.P., 2008. Glutathione and Parkinson's disease: Is this the elephant in the room? Biomed. Pharmacother. 62, 236–249. https://doi.org/10.1016/j.biopha.2008.01.017

Zelko, I.N., Mariani, T.J., Folz, R.J., 2002. Superoxide dismutase multigene family: a comparison of the CuZn-SOD (SOD1), Mn-SOD (SOD2), and EC-SOD (SOD3) gene structures, evolution, and expression. Free Radic. Biol. Med. 33, 337–349. https://doi.org/10.1016/S0891-5849(02)00905-X

Zeviani, M., 2004. Mitochondrial disorders. Brain 127, 2153–2172. https://doi.org/10.1093/brain/awh259

Zhang, D.D., Hannink, M., 2003. Distinct Cysteine Residues in Keap1 Are Required for Keap1-Dependent Ubiquitination of Nrf2 and for Stabilization of Nrf2 by Chemopreventive Agents and Oxidative Stress. Mol. Cell. Biol. 23, 8137–8151. https://doi.org/10.1128/MCB.23.22.8137-8151.2003

Zhang, J., Ney, P.A., 2009. Role of BNIP3 and NIX in cell death, autophagy, and mitophagy. Cell Death Differ. 16, 939–946. https://doi.org/10.1038/cdd.2009.16

Zhang, L., Bartley, C.M., Gong, X., Hsieh, L.S., Lin, T. V., Feliciano, D.M., Bordey, A., 2014. MEK-ERK1/2-Dependent FLNA Overexpression Promotes Abnormal Dendritic Patterning in Tuberous Sclerosis Independent of mTOR. Neuron 84, 78–91. https://doi.org/10.1016/j.neuron.2014.09.009

Zhang, L., Shimoji, M., Thomas, B., Moore, D.J., Yu, S.-W., Marupudi, N.I., Torp, R., Torgner, I.A., Ottersen, O.P., Dawson, T.M., Dawson, V.L., 2005. Mitochondrial localization of the Parkinson's disease related protein DJ-1: implications for pathogenesis. Hum. Mol. Genet. 14, 2063–2073. https://doi.org/10.1093/hmg/ddi211

Zhang, R., Xu, M., Wang, Y., Xie, F., Zhang, G., Qin, X., 2017. Nrf2—a Promising Therapeutic Target for

Defensing Against Oxidative Stress in Stroke. Mol. Neurobiol. 54, 6006–6017. https://doi.org/10.1007/s12035-016-0111-0

Zhang, S., Eitan, E., Mattson, M.P., 2017. Early involvement of lysosome dysfunction in the degeneration of cerebral cortical neurons caused by the lipid peroxidation product 4-hydroxynonenal. J. Neurochem. 140, 941–954. https://doi.org/10.1111/jnc.13957

Zhang, X.-L., Yuan, Y.-H., Shao, Q.-H., Wang, Z.-Z., Zhu, C.-G., Shi, J.-G., Ma, K.-L., Yan, X., Chen, N.-H., 2017. DJ-1 regulating PI3K-Nrf2 signaling plays a significant role in bibenzyl compound 20C-mediated neuroprotection against rotenone-induced oxidative insult. Toxicol. Lett. 271, 74–83. https://doi.org/10.1016/j.toxlet.2017.02.022

Zhang, Y., Sloan, S.A., Clarke, L.E., Caneda, C., Plaza, C.A., Blumenthal, P.D., Vogel, H., Steinberg, G.K., Edwards, M.S.B., Li, G., Duncan, J.A., Cheshier, S.H., Shuer, L.M., Chang, E.F., Grant, G.A., Gephart, M.G.H., Barres, B.A., 2016. Purification and Characterization of Progenitor and Mature Human Astrocytes Reveals Transcriptional and Functional Differences with Mouse. Neuron 89, 37–53. https://doi.org/10.1016/j.neuron.2015.11.013

Zhang, Z.-X., Román, G.C., 1993. Worldwide Occurrence of Parkinson's Disease: An Updated Review. Neuroepidemiology 12, 195–208. https://doi.org/10.1159/000110318

Zhang, Z., Liu, L., Jiang, X., Zhai, S., Xing, D., 2016. The Essential Role of Drp1 and Its Regulation by S-Nitrosylation of Parkin in Dopaminergic Neurodegeneration: Implications for Parkinson's Disease. Antioxid. Redox Signal. 25, 609–622. https://doi.org/10.1089/ars.2016.6634

Zhao, L., Longo-Guess, C., Harris, B.S., Lee, J.-W., Ackerman, S.L., 2005. Protein accumulation and neurodegeneration in the woozy mutant mouse is caused by disruption of SIL1, a cochaperone of BiP. Nat. Genet. 37, 974–979. https://doi.org/10.1038/ng1620

Zheng, B., Liao, Z., Locascio, J.J., Lesniak, K.A., Roderick, S.S., Watt, M.L., Eklund, A.C., Zhang-James, Y., Kim, P.D., Hauser, M.A., Grünblatt, E., Moran, L.B., Mandel, S.A., Riederer, P., Miller, R.M., Federoff, H.J., Wüllner, U., Papapetropoulos, S., Youdim, M.B., Cantuti-Castelvetri, I., Young, A.B., Vance, J.M., Davis, R.L., Hedreen, J.C., Adler, C.H., Beach, T.G., Graeber, M.B., Middleton, F.A., Rochet, J.-C., Scherzer, C.R., Global PD Gene Expression (GPEX) Consortium, 2010. PGC-1α, a potential therapeutic target for early intervention in Parkinson's disease. Sci. Transl. Med. 2, 52–73. https://doi.org/10.1126/scitranslmed.3001059

Zheng, L., Michelson, Y., Freger, V., Avraham, Z., Venken, K.J.T., Bellen, H.J., Justice, M.J., Wides, R., 2011. Drosophila Ten-m and Filamin Affect Motor Neuron Growth Cone Guidance. PLoS One 6, e22956. https://doi.org/10.1371/journal.pone.0022956

Zhou, Z.D., Refai, F.S., Xie, S.P., Ng, S.H., Chan, C.H.S., Ho, P.G.H., Zhang, X.D., Lim, T.M., Tan, E.K., 2014. Mutant PINK1 upregulates tyrosine hydroxylase and dopamine levels, leading to vulnerability of dopaminergic neurons. Free Radic. Biol. Med. 68, 220–233. https://doi.org/10.1016/j.freeradbiomed.2013.12.015

ZHU, L., BI, W., LU, DAN, ZHANG, C., SHU, X., LU, DAXIANG, 2014. Luteolin inhibits SH-SY5Y cell apoptosis through suppression of the nuclear transcription factor-κB, mitogen-activated protein kinase and protein kinase B pathways in lipopolysaccharide-stimulated cocultured BV2 cells. Exp. Ther. Med. 7, 1065–1070. https://doi.org/10.3892/etm.2014.1564

Zhu, Z.-H., Yang, R., Fu, X., Wang, Y.-Q., Wu, G.-C., 2006. Astrocyte-conditioned medium protecting hippocampal neurons in primary cultures against corticosterone-induced damages via PI3-K/Akt signal pathway. Brain Res. 1114, 1–10. https://doi.org/10.1016/j.brainres.2006.07.070

Zhuang, Z.P., Marks, B., McCauley, R.B., 1992. The insertion of monoamine oxidase A into the outer membrane of rat liver mitochondria. J. Biol. Chem. 267, 591–596.

Zimmermann, M., Gardoni, F., Marcello, E., Colciaghi, F., Borroni, B., Padovani, A., Cattabeni, F., Di Luca, M., 2004. Acetylcholinesterase inhibitors increase ADAM10 activity by promoting its trafficking in neuroblastoma cell lines. J. Neurochem. 90, 1489–1499. https://doi.org/10.1111/j.1471-

4159.2004.02680.x

Zuo, L., Koozechian, M.S., Chen, L.L., 2014. Characterization of reactive nitrogen species in allergic asthma. Ann. Allergy, Asthma Immunol. 112, 18–22. https://doi.org/10.1016/j.anai.2013.10.007

Zuo, L., Zhou, T., Pannell, B.K., Ziegler, A.C., Best, T.M., 2015. Biological and physiological role of reactive oxygen species - the good, the bad and the ugly. Acta Physiol. 214, 329–348. https://doi.org/10.1111/apha.12515

CHAPTER 8

SUPPLEMENTARY DATA

Table 8.2 Differentially identified proteins in AAPH or rotenone treated U-87MG lysates using mass spectrometry. *U-87MG cells were differentiated over 5 days and then treated with 1 mM AAPH or 0.5 µM rotenone for 48 hours and lysate was subjected to mass spectrometry.*

Secondary Name	Accession Number	AAPH fold change	Secondary Name	Accession Number	Rotenone fold change
Adipocyte plasma membrane-associated protein	Q9HDC9	7.8	**Deoxyribonuclease-2-alpha**	O00115	17.9
Ras-related protein Rab-43	Q86YS6	6.2	**Peroxisomal carnitine O-octanoyltransferase**	Q9UKG9	5.0
Interleukin-1 beta	P01584	3.4	**Prostaglandin G/H synthase 2**	P35354	4.1
Cytochrome P450 1B1	Q16678	3.1	**Interleukin-8**	P10145	3.9
E3 ubiquitin-protein ligase Itchy homolog	Q96J02	2.5	**Hemoglobin subunit alpha**	P69905	3.1
Heme oxygenase 1	P09601	2.2	**ADP-ribosylation factor-like protein 6-interacting protein 1**	Q15041	3.0
Sphingomyelin phosphodiesterase	P17405	2.1	**Growth/differentiation factor 15**	Q99988	2.9
45 kDa calcium-binding protein	Q9BRK5	2.0	**Pentraxin-related protein PTX3**	P26022	2.8
Proline synthase co-transcribed bacterial homolog protein	O94903	2.0	**Annexin A7**	P20073	2.6
T-cell differentiation antigen CD6	P30203	2.0	**Proepiregulin**	O14944	2.5
Multiple inositol polyphosphate phosphatase 1	Q9UNW1	2.0	**Histone H2A.Z**	P0C0S5	2.4
Cathepsin D	P07339	1.9	**Podocalyxin**	O00592	2.3
Insulin-like growth factor-binding protein 7	Q16270	1.9	**General transcription factor IIF subunit 1**	P35269	2.1
Palmitoyl-protein thioesterase 1	P50897	1.8	**Annexin A6**	P08133	2.1
Integral membrane protein 2C	Q9NQX7	1.7	**Thrombomodulin**	P07204	2.1
Anthrax toxin receptor 2	P58335	1.7	**Uncharacterized protein C11orf98**	E9PRG8	2.0
Cytochrome c oxidase subunit 5A, mitochondrial	P20674	1.7	**Large neutral amino acids transporter small subunit 1**	Q01650	2.0
Raftlin	Q14699	1.7	**D-tyrosyl-tRNA(Tyr) deacylase 1**	Q8TEA8	2.0
fMet-Leu-Phe receptor	P21462	1.6	**Zinc transporter SLC39A7**	Q92504	1.9
Golgi apparatus protein 1	Q92896	1.6	**WD repeat-containing protein 43**	Q15061	1.9
Aldehyde dehydrogenase family 3 member B1	P43353	1.6	**Tissue factor pathway inhibitor 2**	P48307	1.9
Tissue alpha-L-fucosidase	P04066	1.6	**Solute carrier family 43 member 3**	Q8NBI5	1.8
Acid ceramidase	Q13510	1.5	**Fibroblast growth factor 2**	P09038	1.7
Reticulon-3	O95197	1.5	**DNA-(apurinic or apyrimidinic site) lyase**	P27695	1.7
ORM1-like protein 2	Q53FV1	1.5	**Transmembrane protein 41B**	Q5BJD5	1.7
Keratin, type I cuticular Ha1	Q15323	1.5	**ADP/ATP translocase 3**	P12236	1.7

Acyl-CoA desaturase	O00767	1.5	**CD44 antigen**	P16070	1.7
Keratin, type I cytoskeletal 14	P02533	1.5	**MICOS complex subunit MIC10**	Q5TGZ0	1.7
HLA class II histocompatibility antigen, DP alpha 1 chain	P20036	1.4	**40S ribosomal protein S25**	P62851	1.6
Guanine nucleotide-binding protein G(i) subunit alpha-1	P63096	1.4	**26S proteasome non-ATPase regulatory subunit 8**	P48556	1.6
5'-nucleotidase domain-containing protein 2	Q9H857	1.4	**Alpha-2-HS-glycoprotein**	P02765	1.6
Osteoclast-stimulating factor 1	Q92882	1.4	**Secretory carrier-associated membrane protein 3**	O14828	1.6
KDEL motif-containing protein 2	Q7Z4H8	1.4	**Secretory carrier-associated membrane protein 2**	O15127	1.6
Glycogenin-1	P46976	1.4	**Phospholipid phosphatase 3**	O14495	1.6
Neuropilin-2	O60462	1.4	**4F2 cell-surface antigen heavy chain**	P08195	1.6
Sulfatase-modifying factor 2	Q8NBJ7	1.4	**Glucose-6-phosphate exchanger SLC37A4**	O43826	1.6
GDP-fucose protein O-fucosyltransferase 2	Q9Y2G5	1.4	**ADP/ATP translocase 2**	P05141	1.6
Transmembrane 9 superfamily member 2	Q99805	1.4	**40S ribosomal protein S17**	P08708	1.6
Protein-glutamine gamma-glutamyltransferase 2	P21980	1.4	**Translocon-associated protein subunit alpha**	P43307	1.6
Ras-related protein Rap-2a	P10114	1.4	**Transmembrane emp24 domain-containing protein 10**	P49755	1.6
Glucosamine-6-phosphate isomerase 1	P46926	1.4	**Histone H2B type 1-L**	Q99880	1.5
Protein FAM210B	Q96KR6	1.3	**Transmembrane emp24 domain-containing protein 7**	Q9Y3B3	1.5
Sorting nexin-2	O60749	1.3	**78 kDa glucose-regulated protein**	P11021	1.5
N-acetylglucosamine-6-sulfatase	P15586	1.3	**Calcium-binding mitochondrial carrier protein SCaMC-1**	Q6NUK1	1.5
Ras-related protein Rap-1A	P62834	1.3	**Prohibitin-2**	Q99623	1.5
Long-chain-fatty-acid--CoA ligase 4	O60488	1.3	**Acid ceramidase**	Q13510	1.5
Myeloid-derived growth factor	Q969H8	1.3	**Phosphate carrier protein, mitochondrial**	Q00325	1.5
Gamma-secretase subunit APH-1B	Q8WW43	1.3	**ADP/ATP translocase 1**	P12235	1.5
Scavenger receptor class B member 1	Q8WTV0	1.3	**Prohibitin**	P35232	1.5
Epididymal secretory protein E1	P61916	1.3	**Transmembrane emp24 domain-containing protein 2**	Q15363	1.5
Protein FAM3C	Q92520	1.3	**60S ribosomal protein L9**	P32969	1.5
Lysosome membrane protein 2	Q14108	1.3	**Cathepsin L1**	P07711	1.5
MLN64 N-terminal domain homolog	O95772	1.3	**Translocating chain-associated membrane protein 1**	Q15629	1.5

NADH dehydrogenase [ubiquinone] 1 alpha subcomplex subunit 6	P56556	1.3	**Very-long-chain (3R)-3-hydroxyacyl-CoA dehydratase 3**	Q9P035	1.5
Lysosomal acid phosphatase	P11117	1.2	**Prenylated Rab acceptor protein 1**	Q9UI14	1.5
Ras-related protein Rab-7a	P51149	1.2	**Transmembrane emp24 domain-containing protein 5**	Q9Y3A6	1.5
Ras-related protein Rab-27B	O00194	1.2	**Transmembrane emp24 domain-containing protein 4**	Q7Z7H5	1.5
FAD synthase	Q8NFF5	1.2	**CAAX prenyl protease 1 homolog**	O75844	1.5
Serine/threonine-protein phosphatase PP1-beta catalytic subunit	P62140	-1.2	**Protein NDRG1**	Q92597	1.5
40S ribosomal protein S9	P46781	-1.3	**40S ribosomal protein S15**	P62841	1.5
40S ribosomal protein S24	P62847	-1.3	**Transmembrane emp24 domain-containing protein 9**	Q9BVK6	1.5
BET1 homolog	O15155	-1.3	**Ethanolaminephosphotransferase 1**	Q9C0D9	1.5
60S ribosomal protein L4	P36578	-1.3	**Ribosomal L1 domain-containing protein 1**	O76021	1.5
Transcription factor BTF3 homolog 4	Q96K17	-1.3	**40S ribosomal protein S10**	P46783	1.5
CD44 antigen	P16070	-1.3	**Mitochondrial 2-oxoglutarate/malate carrier protein**	Q02978	1.5
60S ribosomal protein L23	P62829	-1.3	**Stromal interaction molecule 2**	Q9P246	1.5
60S ribosomal protein L18	Q07020	-1.3	**Transmembrane protein 41A**	Q96HV5	1.5
Endothelial differentiation-related factor 1	O60869	-1.3	**Transmembrane 9 superfamily member 3**	Q9HD45	1.5
Perilipin-3	O60664	-1.3	**Sideroflexin-1**	Q9H9B4	1.5
Cytoplasmic dynein 1 heavy chain 1	Q14204	-1.3	**Reticulon-4**	Q9NQC3	1.5
60S ribosomal protein L28	P46779	-1.3	**Thioredoxin-dependent peroxide reductase, mitochondrial**	P30048	1.5
Calfacilitin	Q96CP7	-1.3	**Translocation protein SEC62**	Q99442	1.5
Poly(rC)-binding protein 1	Q15365	-1.3	**3-ketodihydrosphingosine reductase**	Q06136	1.5
Signal recognition particle 9 kDa protein	P49458	-1.3	**Protein jagunal homolog 1**	Q8N5M9	1.4
Spectrin beta chain, non-erythrocytic 1	Q01082	-1.3	**Minor histocompatibility antigen H13**	Q8TCT9	1.4
WASH complex subunit 5	Q12768	-1.3	**Transmembrane protein 70, mitochondrial**	Q9BUB7	1.4
Caveolin-1	Q03135	-1.3	**Calcium-binding mitochondrial carrier protein Aralar1**	O75746	1.4
ATP synthase subunit O, mitochondrial	P48047	-1.3	**Cytochrome b**	P00156	1.4
Eukaryotic translation initiation factor 4E type 2	O60573	-1.3	**LETM1 and EF-hand domain-containing protein 1, mitochondrial**	O95202	1.4
Spectrin alpha chain, non-erythrocytic 1	Q13813	-1.3	**Gamma-glutamyl hydrolase**	Q92820	1.4

LIM and SH3 domain protein 1	Q14847	-1.3	**Transmembrane emp24 domain-containing protein 1**	Q13445	1.4
Basigin	P35613	-1.3	**Translocon-associated protein subunit gamma**	Q9UNL2	1.4
60S ribosomal protein L34	P49207	-1.3	**Zinc transporter 7**	Q8NEW0	1.4
Eukaryotic translation initiation factor 3 subunit E	P60228	-1.3	**Epoxide hydrolase 1**	P07099	1.4
40S ribosomal protein S8	P62241	-1.3	**Type-1 angiotensin II receptor-associated protein**	Q6RW13	1.4
Transmembrane protein 109	Q9BVC6	-1.3	**Endoplasmic reticulum resident protein 29**	P30040	1.4
Migration and invasion enhancer 1	Q9BRT3	-1.4	**Sideroflexin-3**	Q9BWM7	1.4
40S ribosomal protein S6	P62753	-1.4	**Sigma non-opioid intracellular receptor 1**	Q99720	1.4
39S ribosomal protein L41, mitochondrial	Q8IXM3	-1.4	**Caveolin-1**	Q03135	1.4
RNA-binding protein PNO1	Q9NRX1	-1.4	**CMP-N-acetylneuraminate-beta-galactosamide-alpha-2,3-sialyltransferase 1**	Q11201	1.4
60S ribosomal protein L23a	P62750	-1.4	**Nicotinamide phosphoribosyltransferase**	P43490	1.4
Caprin-1	Q14444	-1.4	**Transmembrane protein 65**	Q6PI78	1.4
Serine/arginine-rich splicing factor 3	P84103	-1.4	**Dolichol kinase**	Q9UPQ8	1.4
Heat shock protein beta-1	P04792	-1.4	**ER membrane protein complex subunit 4**	Q5J8M3	1.4
Sorcin	P30626	-1.4	**High affinity cationic amino acid transporter 1**	P30825	1.4
Protein kish-A	Q8TBQ9	-1.4	**2,4-dienoyl-CoA reductase, mitochondrial**	Q16698	1.4
Serine/arginine-rich splicing factor 2	Q01130	-1.4	**Transmembrane 9 superfamily member 4**	Q92544	1.4
Keratin, type I cytoskeletal 9	P35527	-1.4	**Perilipin-3**	O60664	1.4
Nuclear pore complex protein Nup205	Q92621	-1.4	**Alpha-mannosidase 2**	Q16706	1.4
Ephrin-B2	P52799	-1.4	**B-cell receptor-associated protein 31**	P51572	1.4
Insulin-like growth factor 2 mRNA-binding protein 2	Q9Y6M1	-1.4	**ER membrane protein complex subunit 2**	Q15006	1.4
Eukaryotic translation initiation factor 3 subunit A	Q14152	-1.4	**Acetyl-coenzyme A transporter 1**	O00400	1.4
Eukaryotic translation initiation factor 3 subunit C	Q99613	-1.4	**Neutral cholesterol ester hydrolase 1**	Q6PIU2	1.4
Soluble calcium-activated nucleotidase 1	Q8WVQ1	-1.4	**Translocator protein**	P30536	1.4
Cytoplasmic FMR1-interacting protein 1	Q7L576	-1.4	**ATP synthase subunit gamma, mitochondrial**	P36542	1.4
60S ribosomal protein L6	Q02878	-1.4	**Cytochrome P450 20A1**	Q6UW02	1.4
40S ribosomal protein S30	P62861	-1.4	**Tissue alpha-L-fucosidase**	P04066	1.4
Interleukin enhancer-binding factor 2	Q12905	-1.4	**Mitochondrial fission process protein 1**	Q9UDX5	1.4
40S ribosomal protein S19	P39019	-1.4	**Thioredoxin-related transmembrane protein 2**	Q9Y320	1.4

Myosin-9	P35579	-1.4	**Ras-related protein Rab-4B**	P61018	1.4
Interleukin enhancer-binding factor 3	Q12906	-1.4	**Neutral amino acid transporter B(0)**	Q15758	1.4
Heterogeneous nuclear ribonucleoprotein L	P14866	-1.4	**Major prion protein**	P04156	1.4
Eukaryotic translation initiation factor 4 gamma 2	P78344	-1.4	**39S ribosomal protein L48, mitochondrial**	Q96GC5	1.4
Probable global transcription activator SNF2L1	P28370	-1.5	**Glutamate dehydrogenase 1, mitochondrial**	P00367	1.4
Filamin-A	P21333	-1.5	**Secretory carrier-associated membrane protein 4**	Q969E2	1.4
Neuroblast differentiation-associated protein AHNAK	Q09666	-1.5	**Calcium-binding mitochondrial carrier protein SCaMC-2**	Q6KCM7	1.4
Eukaryotic translation initiation factor 4 gamma 1	Q04637	-1.5	**UDP-glucuronic acid decarboxylase 1**	Q8NBZ7	1.4
Charged multivesicular body protein 4b	Q9H444	-1.5	**Calcium-binding mitochondrial carrier protein Aralar2**	Q9UJS0	1.4
Actin-related protein 2/3 complex subunit 5	O15511	-1.5	**Fumarate hydratase, mitochondrial**	P07954	1.4
ATP-dependent RNA helicase DDX3X	O00571	-1.5	**Transmembrane protein 33**	P57088	1.4
Abl interactor 1	Q8IZP0	-1.5	**ATP-dependent Clp protease proteolytic subunit, mitochondrial**	Q16740	1.4
Splicing factor 3B subunit 6	Q9Y3B4	-1.5	**Protein SET**	Q01105	1.4
Serine/threonine-protein phosphatase PGAM5, mitochondrial	Q96HS1	-1.5	**Heat shock 70 kDa protein 1-like**	P34931	1.4
Heterogeneous nuclear ribonucleoprotein K	P61978	-1.5	**Sodium/myo-inositol cotransporter**	P53794	1.4
rRNA 2'-O-methyltransferase fibrillarin	P22087	-1.5	**Annexin A1**	P04083	1.4
Dihydropyrimidinase-related protein 2	Q16555	-1.5	**ATP synthase F(0) complex subunit B1, mitochondrial**	P24539	1.4
ATP-dependent RNA helicase DDX18	Q9NVP1	-1.5	**Peroxisomal membrane protein PEX16**	Q9Y5Y5	1.4
Small nuclear ribonucleoprotein F	P62306	-1.5	**Translocon-associated protein subunit delta**	P51571	1.4
Ribosomal L1 domain-containing protein 1	O76021	-1.5	**Protein RFT1 homolog**	Q96AA3	1.4
Protein quaking	Q96PU8	-1.5	**UPF0160 protein MYG1, mitochondrial**	Q9HB07	1.4
Macrophage migration inhibitory factor	P14174	-1.5	**Glycerol-3-phosphate dehydrogenase, mitochondrial**	P43304	1.4
Microtubule-associated protein 1B	P46821	-1.5	**Adipocyte plasma membrane-associated protein**	Q9HDC9	1.4
Activated RNA polymerase II transcriptional coactivator p15	P53999	-1.5	**Dehydrogenase/reductase SDR family member 7**	Q9Y394	1.4
Microtubule-associated protein 4	P27816	-1.5	**Lysosomal acid phosphatase**	P11117	1.4

Mitochondrial fission factor	Q9GZY8	-1.5	**Peroxisomal membrane protein PMP34**	O43808	1.4
Selenoprotein S	Q9BQE4	-1.5	**Lanosterol synthase**	P48449	1.4
Nucleoporin SEH1	Q96EE3	-1.5	**Superoxide dismutase [Mn], mitochondrial**	P04179	1.4
Tumor susceptibility gene 101 protein	Q99816	-1.5	**ATP synthase subunit beta, mitochondrial**	P06576	1.4
Microtubule-associated proteins 1A/1B light chain 3B	Q9GZQ8	-1.6	**Mitochondrial dicarboxylate carrier**	Q9UBX3	1.4
Inositol 1,4,5-trisphosphate receptor type 1	Q14643	-1.6	**60 kDa heat shock protein, mitochondrial**	P10809	1.4
Symplekin	Q92797	-1.6	**Leucine-rich repeat-containing protein 59**	Q96AG4	1.4
Mitochondrial import receptor subunit TOM22 homolog	Q9NS69	-1.6	**Succinate dehydrogenase [ubiquinone] flavoprotein subunit, mitochondrial**	P31040	1.4
Probable ATP-dependent RNA helicase DDX6	P26196	-1.6	**Signal peptidase complex catalytic subunit SEC11A**	P67812	1.4
Protein transport protein Sec31A	O94979	-1.6	**Dol-P-Man:Man(5)GlcNAc(2)-PP-Dol alpha-1,3-mannosyltransferase**	Q92685	1.3
TBC1 domain family member 20	Q96BZ9	-1.6	**Ras-related protein Rab-14**	P61106	1.3
Heterogeneous nuclear ribonucleoproteins A2/B1	P22626	-1.6	**ATP synthase subunit alpha, mitochondrial**	P25705	1.3
Major vault protein	Q14764	-1.6	**Aspartate aminotransferase, mitochondrial**	P00505	1.3
Vimentin	P08670	-1.6	**ER membrane protein complex subunit 3**	Q9P0I2	1.3
U2 small nuclear ribonucleoprotein A'	P09661	-1.6	**Vesicle transport protein GOT1B**	Q9Y3E0	1.3
Dihydropyrimidinase-related protein 3	Q14195	-1.6	**Lysosome membrane protein 2**	Q14108	1.3
Dolichyl-diphosphooligosaccharide--protein glycosyltransferase subunit DAD1	P61803	-1.7	**Carnitine O-palmitoyltransferase 1, liver isoform**	P50416	1.3
Annexin A4	P09525	-1.7	**Mannose-P-dolichol utilization defect 1 protein**	O75352	1.3
Probable rRNA-processing protein EBP2	Q99848	-1.7	**Activated RNA polymerase II transcriptional coactivator p15**	P53999	1.3
40S ribosomal protein S26	P62854	-1.7	**Surfeit locus protein 4**	O15260	1.3
Heterogeneous nuclear ribonucleoprotein H3	P31942	-1.7	**Growth hormone-inducible transmembrane protein**	Q9H3K2	1.3
Probable ATP-dependent RNA helicase DDX17	Q92841	-1.7	**Vacuole membrane protein 1**	Q96GC9	1.3
Cell cycle and apoptosis regulator protein 2	Q8N163	-1.7	**Protein transport protein Sec61 subunit alpha isoform 1**	P61619	1.3
Protein LSM12 homolog	Q3MHD2	-1.7	**Thioredoxin-related transmembrane protein 1**	Q9H3N1	1.3
Protein TFG	Q92734	-1.7	**NIF3-like protein 1**	Q9GZT8	1.3
40S ribosomal protein S21	P63220	-1.7	**Reticulon-1**	Q16799	1.3

Heterogeneous nuclear ribonucleoprotein R	O43390	-1.7	**ER membrane protein complex subunit 6**	Q9BV81	1.3
Far upstream element-binding protein 2	Q92945	-1.7	**Stomatin-like protein 2, mitochondrial**	Q9UJZ1	1.3
Septin-7	Q16181	-1.7	**Sphingosine-1-phosphate phosphatase 1**	Q9BX95	1.3
Zyxin	Q15942	-1.7	**Quinone oxidoreductase**	Q08257	1.3
Serine/arginine-rich splicing factor 1	Q07955	-1.7	**Prenylcysteine oxidase 1**	Q9UHG3	1.3
Immunoglobulin superfamily member 8	Q969P0	-1.7	**Signal peptidase complex subunit 3**	P61009	1.3
CAD protein	P27708	-1.7	**Protein disulfide-isomerase A6**	Q15084	1.3
Septin-2	Q15019	-1.7	**Microsomal glutathione S-transferase 1**	P10620	1.3
Annexin A2	P07355	-1.7	**Ubiquinol-cytochrome-c reductase complex assembly factor 1**	Q9NVA1	1.3
Src substrate cortactin	Q14247	-1.7	**Hydroxyacyl-coenzyme A dehydrogenase, mitochondrial**	Q16836	1.3
Clathrin light chain A	P09496	-1.7	**Ras-related protein Ral-A**	P11233	1.3
Polyadenylate-binding protein 1	P11940	-1.8	**60S ribosomal protein L22**	P35268	1.3
Septin-9	Q9UHD8	-1.8	**CDGSH iron-sulfur domain-containing protein 2**	Q8N5K1	1.3
Far upstream element-binding protein 3	Q96I24	-1.8	**Eukaryotic translation initiation factor 2 subunit 3**	P41091	1.3
Golgin subfamily A member 2	Q08379	-1.8	**Sodium/potassium-transporting ATPase subunit alpha-1**	P05023	1.3
Serine/arginine-rich splicing factor 7	Q16629	-1.8	**Malate dehydrogenase, mitochondrial**	P40926	1.3
Large proline-rich protein BAG6	P46379	-1.8	**Ras-related protein Rab-2A**	P61019	1.3
Heterogeneous nuclear ribonucleoprotein A3	P51991	-1.8	**Putative 60S ribosomal protein L39-like 5**	Q59GN2	1.2
Nuclear pore complex protein Nup160	Q12769	-1.9	**PRA1 family protein 3**	O75915	1.2
Polymerase I and transcript release factor	Q6NZI2	-1.9	**40S ribosomal protein S3a**	P61247	1.2
Polyadenylate-binding protein 4	Q13310	-1.9	**40S ribosomal protein S3**	P23396	1.2
Clathrin heavy chain 1	Q00610	-1.9	**GH3 domain-containing protein**	Q8N2G8	1.2
ATP-dependent RNA helicase DDX24	Q9GZR7	-1.9	**Endoplasmin**	P14625	1.2
Histone H1x	Q92522	-1.9	**NADH-cytochrome b5 reductase 3**	P00387	1.2
Serine/arginine-rich splicing factor 10	O75494	-1.9	**40S ribosomal protein S19**	P39019	1.2
Plectin	Q15149	-1.9	**V-type proton ATPase subunit d 1**	P61421	1.2
Nuclear pore complex protein Nup88	Q99567	-1.9	**Transferrin receptor protein 1**	P02786	-1.2
40S ribosomal protein S28	P62857	-1.9	**Protein Mpv17**	P39210	-1.2
BAG family molecular chaperone regulator 2	O95816	-1.9	**Cytoskeleton-associated protein 4**	Q07065	-1.2

Exosome complex component RRP43	Q96B26	-1.9	**Peptidyl-prolyl cis-trans isomerase FKBP9**	O95302	-1.2
AMP deaminase 2	Q01433	-2.0	**Zinc finger RNA-binding protein**	Q96KR1	-1.3
Tubulin beta-3 chain	Q13509	-2.0	**Delta-1-pyrroline-5-carboxylate synthase**	P54886	-1.3
CCR4-NOT transcription complex subunit 7	Q9UIV1	-2.0	**60S acidic ribosomal protein P0**	P05388	-1.3
Tubulin alpha-1C chain	Q9BQE3	-2.0	**Ras-related protein Rap-1A**	P62834	-1.3
Transformer-2 protein homolog beta	P62995	-2.0	**Ragulator complex protein LAMTOR3**	Q9UHA4	-1.3
Protein S100-A10	P60903	-2.0	**SUMO-conjugating enzyme UBC9**	P63279	-1.3
Scaffold attachment factor B1	Q15424	-2.0	**40S ribosomal protein S8**	P62241	-1.3
Tubulin beta-2A chain	Q13885	-2.0	**Long-chain-fatty-acid--CoA ligase 3**	O95573	-1.3
Tubulin alpha-1A chain	Q71U36	-2.1	**E3 ubiquitin-protein ligase NEDD4**	P46934	-1.3
Tubulin beta chain	P07437	-2.1	**60S ribosomal protein L3**	P39023	-1.3
Zinc finger protein 285	Q96NJ3	-2.1	**GTP-binding protein SAR1a**	Q9NR31	-1.3
Protein S100-A6	P06703	-2.1	**Dolichyl-diphosphooligosaccharide--protein glycosyltransferase subunit DAD1**	P61803	-1.3
Tubulin beta-6 chain	Q9BUF5	-2.3	**60S ribosomal protein L18a**	Q02543	-1.3
Four and a half LIM domains protein 2	Q14192	-2.3	**ADP-ribosylation factor 5**	P84085	-1.3
Small nuclear ribonucleoprotein Sm D3	P62318	-2.3	**Endothelial differentiation-related factor 1**	O60869	-1.3
Prelamin-A/C	P02545	-2.4	**Rho-related GTP-binding protein RhoC**	P08134	-1.3
Serine/arginine-rich splicing factor 9	Q13242	-2.4	**Peptidyl-prolyl cis-trans isomerase A**	P62937	-1.3
Small nuclear ribonucleoprotein-associated proteins B and B'	P14678	-2.4	**Protein SGT1 homolog**	Q9Y2Z0	-1.3
Tubulin beta-4B chain	P68371	-2.5	**Dihydropyrimidinase-related protein 2**	Q16555	-1.3
MICAL-like protein 1	Q8N3F8	-2.9	**Signal recognition particle 9 kDa protein**	P49458	-1.3
Transcription factor p65	Q04206	-3.6	**Stromal interaction molecule 1**	Q13586	-1.3
FK506-binding protein 15	Q5T1M5	-4.0	**39S ribosomal protein L38, mitochondrial**	Q96DV4	-1.3
Suppressor of SWI4 1 homolog	Q9NQ55	-4.2	**Peptidyl-prolyl cis-trans isomerase FKBP10**	Q96AY3	-1.4
Protein S100-A13	Q99584	-4.8	**Mitofusin-1**	Q8IWA4	-1.4
Pleckstrin homology-like domain family A member 3	Q9Y5J5	-5.1	**Spectrin alpha chain, non-erythrocytic 1**	Q13813	-1.4
Protein 4.1	P11171	-5.9	**Bifunctional glutamate/proline--tRNA ligase**	P07814	-1.4

Zinc finger RNA-binding protein	Q96KR1	-6.5	**Serine/threonine-protein phosphatase PP1-alpha catalytic subunit**	P62136	-1.4
Phosphatidate cytidylyltransferase, mitochondrial	Q96BW9	-7.5	**Heterogeneous nuclear ribonucleoprotein K**	P61978	-1.4
			Eukaryotic translation initiation factor 4E	P06730	-1.4
			Osteoclast-stimulating factor 1	Q92882	-1.4
			Filamin-B	O75369	-1.4
			39S ribosomal protein S18a, mitochondrial	Q9NVS2	-1.4
			40S ribosomal protein S24	P62847	-1.4
			Aspartate--tRNA ligase, cytoplasmic	P14868	-1.4
			Ubiquitin-conjugating enzyme E2 variant 2	Q15819	-1.4
			Alpha-2-macroglobulin receptor-associated protein	P30533	-1.4
			Beta-galactosidase	P16278	-1.4
			Dihydrolipoyl dehydrogenase, mitochondrial	P09622	-1.4
			Low-density lipoprotein receptor	P01130	-1.4
			Regulation of nuclear pre-mRNA domain-containing protein 1B	Q9NQG5	-1.4
			NADH dehydrogenase [ubiquinone] iron-sulfur protein 3, mitochondrial	O75489	-1.4
			RNA-binding protein PNO1	Q9NRX1	-1.4
			Alpha-actinin-1	P12814	-1.4
			Isoleucine--tRNA ligase, cytoplasmic	P41252	-1.4
			Serine palmitoyltransferase 1	O15269	-1.4
			Peripheral plasma membrane protein CASK	O14936	-1.4
			Unconventional myosin-Ic	O00159	-1.4
			Poly(rC)-binding protein 1	Q15365	-1.4
			Dihydropyrimidinase-related protein 3	Q14195	-1.4
			28S ribosomal protein S29, mitochondrial	P51398	-1.4
			WD repeat and FYVE domain-containing protein 1	Q8IWB7	-1.4
			Protein-glutamine gamma-glutamyltransferase 2	P21980	-1.4
			Leucine--tRNA ligase, cytoplasmic	Q9P2J5	-1.4
			28S ribosomal protein S23, mitochondrial	Q9Y3D9	-1.4

	HLA class II histocompatibility antigen gamma chain	P04233	-1.4
	Procollagen-lysine,2-oxoglutarate 5-dioxygenase 2	O00469	-1.5
	Methylcrotonoyl-CoA carboxylase subunit alpha, mitochondrial	Q96RQ3	-1.5
	Double-stranded RNA-binding protein Staufen homolog 1	O95793	-1.5
	39S ribosomal protein L23, mitochondrial	Q16540	-1.5
	Epsin-1	Q9Y6I3	-1.5
	40S ribosomal protein S26	P62854	-1.5
	ADP-ribosylation factor 6	P62330	-1.5
	Filamin-A	P21333	-1.5
	Ras-related protein Rab-32	Q13637	-1.5
	Ras-related protein Rab-13	P51153	-1.5
	60S ribosomal protein L23	P62829	-1.5
	ATP-dependent 6-phosphofructokinase, platelet type	Q01813	-1.5
	Mannosyl-oligosaccharide glucosidase	Q13724	-1.5
	Serine/threonine-protein phosphatase PP1-beta catalytic subunit	P62140	-1.5
	Leucine-rich PPR motif-containing protein, mitochondrial	P42704	-1.5
	Protein mago nashi homolog 2	Q96A72	-1.5
	Procollagen-lysine,2-oxoglutarate 5-dioxygenase 1	Q02809	-1.5
	Filamin-C	Q14315	-1.5
	14-3-3 protein zeta/delta	P63104	-1.5
	Lipase maturation factor 2	Q9BU23	-1.5
	Interferon-induced, double-stranded RNA-activated protein kinase	P19525	-1.5
	Staphylococcal nuclease domain-containing protein 1	Q7KZF4	-1.5
	14-3-3 protein theta	P27348	-1.5
	Poly(rC)-binding protein 2	Q15366	-1.5
	Poliovirus receptor	P15151	-1.5
	Talin-1	Q9Y490	-1.5
	Plectin	Q15149	-1.5
	[3-methyl-2-oxobutanoate dehydrogenase [lipoamide]] kinase, mitochondrial	O14874	-1.5

	Interferon-inducible double-stranded RNA-dependent protein kinase activator A	O75569	-1.5
	Adenosylhomocysteinase 2	O43865	-1.5
	Alpha-actinin-4	O43707	-1.5
	ADP-ribosylation factor 4	P18085	-1.5
	60S ribosomal protein L34	P49207	-1.5
	NADH dehydrogenase [ubiquinone] 1 alpha subcomplex subunit 13	Q9P0J0	-1.5
	Nucleolin	P19338	-1.5
	Actin-related protein 2/3 complex subunit 3	O15145	-1.5
	Gamma-adducin	Q9UEY8	-1.5
	Spliceosome RNA helicase DDX39B	Q13838	-1.5
	Protein transport protein Sec31A	O94979	-1.5
	Microtubule-associated proteins 1A/1B light chain 3B	Q9GZQ8	-1.5
	Adenylate kinase 2, mitochondrial	P54819	-1.6
	CCR4-NOT transcription complex subunit 1	A5YKK6	-1.6
	Metalloreductase STEAP3	Q658P3	-1.6
	Tubulin beta chain	P07437	-1.6
	ATP-dependent 6-phosphofructokinase, muscle type	P08237	-1.6
	Protein S100-A10	P60903	-1.6
	Fatty acid synthase	P49327	-1.6
	Mitochondrial fission factor	Q9GZY8	-1.6
	Hexokinase-1	P19367	-1.6
	Procollagen galactosyltransferase 1	Q8NBJ5	-1.6
	Prolyl 3-hydroxylase 3	Q8IVL6	-1.6
	Protein S100-A11	P31949	-1.6
	39S ribosomal protein L49, mitochondrial	Q13405	-1.6
	Coronin-1B	Q9BR76	-1.6
	Armadillo repeat-containing X-linked protein 3	Q9UH62	-1.6
	EH domain-containing protein 2	Q9NZN4	-1.6
	C-1-tetrahydrofolate synthase, cytoplasmic	P11586	-1.6
	Lysyl oxidase homolog 1	Q08397	-1.6
	Thioredoxin-related transmembrane protein 4	Q9H1E5	-1.6
	Glutathione S-transferase kappa 1	Q9Y2Q3	-1.6

	Voltage-dependent anion-selective channel protein 1	P21796	-1.6
	40S ribosomal protein S21	P63220	-1.6
	Cellular nucleic acid-binding protein	P62633	-1.6
	Eukaryotic translation initiation factor 4 gamma 1	Q04637	-1.6
	Protein quaking	Q96PU8	-1.6
	Clathrin heavy chain 1	Q00610	-1.6
	Tubulin beta-3 chain	Q13509	-1.6
	General vesicular transport factor p115	O60763	-1.7
	Isocitrate dehydrogenase [NADP], mitochondrial	P48735	-1.7
	ATP-dependent RNA helicase DDX3X	O00571	-1.7
	Tubulin alpha-1C chain	Q9BQE3	-1.7
	Beta-2-microglobulin	P61769	-1.7
	Ubiquitin carboxyl-terminal hydrolase 10	Q14694	-1.7
	SRA stem-loop-interacting RNA-binding protein, mitochondrial	Q9GZT3	-1.7
	ORM1-like protein 2	Q53FV1	-1.7
	Polyadenylate-binding protein 1	P11940	-1.7
	Fragile X mental retardation syndrome-related protein 1	P51114	-1.7
	39S ribosomal protein L3, mitochondrial	P09001	-1.7
	NADH dehydrogenase [ubiquinone] iron-sulfur protein 7, mitochondrial	O75251	-1.7
	Dimethyladenosine transferase 2, mitochondrial	Q9H5Q4	-1.7
	Protein SEC13 homolog	P55735	-1.7
	Cytochrome c oxidase assembly protein COX11, mitochondrial	Q9Y6N1	-1.7
	Prostaglandin E synthase 3	Q15185	-1.7
	Nucleophosmin	P06748	-1.7
	Coronin-1C	Q9ULV4	-1.7
	Eukaryotic initiation factor 4A-III	P38919	-1.7
	Scaffold attachment factor B1	Q15424	-1.7
	Elongin-B	Q15370	-1.7
	Prolow-density lipoprotein receptor-related protein 1	Q07954	-1.7
	Ras-related protein R-Ras2	P62070	-1.7
	Protein S100-A6	P06703	-1.7

	tRNA pseudouridine synthase A, mitochondrial	Q9Y606	-1.8
	40S ribosomal protein S28	P62857	-1.8
	ER membrane protein complex subunit 7	Q9NPA0	-1.8
	Bax inhibitor 1	P55061	-1.8
	DnaJ homolog subfamily C member 13	O75165	-1.8
	Myosin regulatory light chain 12A	P19105	-1.8
	Actin-related protein 2/3 complex subunit 5	O15511	-1.8
	E3 ubiquitin-protein ligase TRIP12	Q14669	-1.8
	Glycosyltransferase 8 domain-containing protein 1	Q68CQ7	-1.8
	X-ray repair cross-complementing protein 5	P13010	-1.8
	Kinesin-like protein KIF3B	O15066	-1.8
	Coiled-coil domain-containing protein 58	Q4VC31	-1.8
	X-ray repair cross-complementing protein 6	P12956	-1.8
	Ribosomal protein S6 kinase alpha-3	P51812	-1.8
	Polymerase delta-interacting protein 2	Q9Y2S7	-1.8
	Carboxypeptidase D	O75976	-1.8
	Cytochrome b5	P00167	-1.8
	Ubiquitin-associated protein 2-like	Q14157	-1.8
	Dynein light chain 1, cytoplasmic	P63167	-1.8
	Polyadenylate-binding protein 4	Q13310	-1.8
	Tyrosine-protein kinase Yes	P07947	-1.8
	Lysyl oxidase homolog 2	Q9Y4K0	-1.8
	Myosin-9	P35579	-1.8
	Elongation factor Tu, mitochondrial	P49411	-1.8
	60S ribosomal protein L38	P63173	-1.8
	Macrophage migration inhibitory factor	P14174	-1.8
	Adenylate kinase 4, mitochondrial	P27144	-1.9
	OCIA domain-containing protein 2	Q56VL3	-1.9
	Chitobiosyldiphosphodolichol beta-mannosyltransferase	Q9BT22	-1.9
	Nuclear pore complex protein Nup88	Q99567	-1.9
	Sorcin	P30626	-1.9
	Short-chain dehydrogenase/reductase 3	O75911	-1.9

	Very long-chain specific acyl-CoA dehydrogenase, mitochondrial	P49748	-1.9
	PDZ and LIM domain protein 5	Q96HC4	-1.9
	Insulin-like growth factor 2 mRNA-binding protein 2	Q9Y6M1	-1.9
	Solute carrier family 35 member E1	Q96K37	-1.9
	HLA class I histocompatibility antigen, B-44 alpha chain	P30481	-1.9
	Probable ATP-dependent RNA helicase DDX47	Q9H0S4	-1.9
	Tumor susceptibility gene 101 protein	Q99816	-1.9
	Catenin delta-1	O60716	-1.9
	General transcription factor IIE subunit 1	P29083	-1.9
	Symplekin	Q92797	-1.9
	Retinol dehydrogenase 11	Q8TC12	-2.0
	ADP-ribosylation factor-like protein 1	P40616	-2.0
	GTP-binding protein RAD	P55042	-2.0
	Acyl-CoA synthetase family member 2, mitochondrial	Q96CM8	-2.0
	Ubiquitin carboxyl-terminal hydrolase 5	P45974	-2.0
	Exocyst complex component 5	O00471	-2.0
	Cytochrome P450 1B1	Q16678	-2.0
	Serpin H1	P50454	-2.0
	Synaptonemal complex protein SC65	Q92791	-2.0
	Heterogeneous nuclear ribonucleoprotein H2	P55795	-2.0
	Rho GTPase-activating protein 1	Q07960	-2.0
	Eukaryotic initiation factor 4A-I	P60842	-2.0
	GTP-binding protein Rheb	Q15382	-2.0
	Tubulin beta-4B chain	P68371	-2.1
	Heterogeneous nuclear ribonucleoprotein H3	P31942	-2.1
	eIF-2-alpha kinase activator GCN1	Q92616	-2.1
	Golgi resident protein GCP60	Q9H3P7	-2.1
	Acyl-CoA dehydrogenase family member 9, mitochondrial	Q9H845	-2.1
	Vigilin	Q00341	-2.1
	HLA class I histocompatibility antigen, A-2 alpha chain	P01892	-2.1
	ATP-dependent Clp protease ATP-binding	O76031	-2.2

	subunit clpX-like, mitochondrial		
	Protein ABHD11	Q8NFV4	-2.2
	Peptidyl-prolyl cis-trans isomerase FKBP8	Q14318	-2.2
	Eukaryotic translation initiation factor 4 gamma 2	P78344	-2.2
	Transcription intermediary factor 1-beta	Q13263	-2.2
	ATP-dependent RNA helicase DDX39A	O00148	-2.2
	Mothers against decapentaplegic homolog 3	P84022	-2.2
	Clusterin	P10909	-2.2
	RNA-binding protein 3	P98179	-2.2
	SPARC	P09486	-2.3
	Serine/arginine-rich splicing factor 9	Q13242	-2.3
	Tubulin beta-2A chain	Q13885	-2.4
	Pyruvate carboxylase, mitochondrial	P11498	-2.4
	Heterogeneous nuclear ribonucleoproteins C1/C2	P07910	-2.4
	Phospholipase D3	Q8IV08	-2.5
	Heat shock protein beta-1	P04792	-2.6
	Transducin beta-like protein 2	Q9Y4P3	-2.6
	Cytochrome c	P99999	-2.6
	Tubulin alpha-1A chain	Q71U36	-2.6
	Tubulin beta-6 chain	Q9BUF5	-2.7
	E3 ubiquitin/ISG15 ligase TRIM25	Q14258	-2.7
	Follistatin-related protein 1	Q12841	-2.8
	NADH dehydrogenase [ubiquinone] 1 alpha subcomplex subunit 9, mitochondrial	Q16795	-2.9
	NADH-ubiquinone oxidoreductase 75 kDa subunit, mitochondrial	P28331	-2.9
	Fibronectin type III domain-containing protein 3B	Q53EP0	-3.0
	DNA topoisomerase 2-alpha	P11388	-3.2
	28S ribosomal protein S18b, mitochondrial	Q9Y676	-3.2
	Large proline-rich protein BAG6	P46379	-3.2
	Protein TBRG4	Q969Z0	-3.3
	Copine-1	Q99829	-3.4
	5'-nucleotidase domain-containing protein 2	Q9H857	-3.4

	Corticosteroid 11-beta-dehydrogenase isozyme 1	P28845	-3.5
	Growth arrest and DNA damage-inducible proteins-interacting protein 1	Q8TAE8	-3.6
	NADH dehydrogenase [ubiquinone] flavoprotein 2, mitochondrial	P19404	-3.6
	Glutaminase kidney isoform, mitochondrial	O94925	-3.7
	Conserved oligomeric Golgi complex subunit 7	P83436	-3.8
	Pleckstrin homology-like domain family A member 3	Q9Y5J5	-4.1
	Thymidine kinase, cytosolic	P04183	-4.1
	Cell differentiation protein RCD1 homolog	Q92600	-4.3
	Phosphatidate cytidylyltransferase, mitochondrial	Q96BW9	-4.5
	Vesicle transport protein SEC20	Q12981	-4.7
	Grancalcin	P28676	-4.8
	Translation factor GUF1, mitochondrial	Q8N442	-4.9
	Integral membrane protein 2C	Q9NQX7	-5.2
	Cytochrome P450 26B1	Q9NR63	-5.4
	NADH dehydrogenase [ubiquinone] 1 alpha subcomplex subunit 6	P56556	-5.5
	NADH dehydrogenase [ubiquinone] flavoprotein 1, mitochondrial	P49821	-5.5
	E3 ubiquitin-protein ligase ZFP91	Q96JP5	-5.7
	Ubiquitin-associated domain-containing protein 2	Q8NBM4	-6.0
	Chondroitin sulfate synthase 1	Q86X52	-6.8
	Ankyrin repeat and LEM domain-containing protein 2	Q86XL3	-8.1
	Acyl-CoA desaturase	O00767	-9.5
	Protein-lysine 6-oxidase	P28300	-12.1
	Selenoprotein N	Q9NZV5	-12.2
	28S ribosomal protein S24, mitochondrial	Q96EL2	-17.7
	Cat eye syndrome critical region protein 5	Q9BXW7	-23.2
	PDZ domain-containing protein GIPC1	O14908	-46.8

Table 8.2 Differentially identified proteins in AAPH or rotenone treated U-87MG secretomes using mass spectrometry. *U-87MG cells were differentiated over 5 days and then treated with 1 mM AAPH or 0.5 µM rotenone for 48 hours and secretome was collected and subjected to mass spectrometry.*

Secondary Name	Accession Number	AAPH fold change	Secondary name	Accession Number	Rotenone fold change
Protein S100-A11	P31949	77.7	**Actin-related protein 2**	P61160	27.5
Histone H2A type 1-J	Q99878	33.3	**BolA-like protein 2**	Q9H3K6	20.2
Eukaryotic translation initiation factor 2 subunit 1	P05198	28.3	**COP9 signalosome complex subunit 4**	Q9BT78	12.3
Histone H2A type 2-A	Q6FI13	18.0	**Glucose-6-phosphate 1-dehydrogenase**	P11413	11.1
F-actin-capping protein subunit beta	P47756	16.7	**Alanine--tRNA ligase, cytoplasmic**	P49588	10.5
Neuroblast differentiation-associated protein AHNAK	Q09666	16.6	**Nucleoside diphosphate kinase A**	P15531	9.9
Syndecan-4	P31431	15.0	**Elongation factor 1-beta**	P24534	8.9
Heat shock protein 105 kDa	Q92598	14.4	**Serotransferrin**	P02787	8.4
Guanine nucleotide-binding protein G(s) subunit alpha isoforms XLas	Q5JWF2	12.4	**Lysine--tRNA ligase**	Q15046	8.4
Elongation factor 1-beta	P24534	12.1	**SKI family transcriptional corepressor 2**	Q2VWA4	7.6
Protein DJ-1	Q99497	12.0	**40S ribosomal protein S16**	P62249	7.4
Activated RNA polymerase II transcriptional coactivator p15	P53999	11.6	**Stanniocalcin-2**	O76061	7.0
6-phosphogluconate dehydrogenase, decarboxylating	P52209	10.9	**40S ribosomal protein S20**	P60866	6.9
Ras-related protein Rab-2A	P61019	10.7	**Nucleophosmin**	P06748	6.3
Gamma-enolase	P09104	10.7	**Peptidyl-prolyl cis-trans isomerase FKBP1A**	P62942	6.2
Reticulocalbin-1	Q15293	10.2	**Histone H2A type 1-C**	Q93077	6.1
Alpha-2-antiplasmin	P08697	10.2	**Eukaryotic translation initiation factor 3 subunit B**	P55884	5.9
Calpain small subunit 1	P04632	9.8	**Superoxide dismutase [Cu-Zn]**	P00441	5.8
Barrier-to-autointegration factor	O75531	9.6	**Kynureninase**	Q16719	5.5
Ras-related protein Rab-1B	Q9H0U4	8.9	**Heterogeneous nuclear ribonucleoprotein Q**	O60506	5.5
Histidine--tRNA ligase, cytoplasmic	P12081	8.4	**Major vault protein**	Q14764	5.4
Superoxide dismutase [Cu-Zn]	P00441	8.0	**Galectin-3**	P17931	5.4
Integrator complex subunit 4	Q96HW7	8.0	**Proliferation-associated protein 2G4**	Q9UQ80	5.2
40S ribosomal protein S14	P62263	7.8	**40S ribosomal protein S14**	P62263	5.2
Keratin, type I cytoskeletal 9	P35527	7.5	**Malate dehydrogenase, mitochondrial**	P40926	5.0
Cysteine--tRNA ligase, cytoplasmic	P49589	7.5	**Caldesmon**	Q05682	5.0
D-3-phosphoglycerate dehydrogenase	O43175	7.3	**Heat shock protein 105 kDa**	Q92598	4.9
Fatty acid synthase	P49327	6.8	**Apolipoprotein B-100**	P04114	4.7

Filamin-B	O75369	6.7	**28 kDa heat- and acid-stable phosphoprotein**	Q13442	4.5
ADP/ATP translocase 2	P05141	6.7	**Nucleosome assembly protein 1-like 1**	P55209	4.4
Transaldolase	P37837	6.5	**Tryptophan--tRNA ligase, cytoplasmic**	P23381	4.4
Reticulocalbin-3	Q96D15	6.2	**Desmoplakin**	P15924	4.4
Collagen alpha-1(II) chain	P02458	6.1	**40S ribosomal protein S25**	P62851	4.3
Purine nucleoside phosphorylase	P00491	5.9	**Activated RNA polymerase II transcriptional coactivator p15**	P53999	4.2
Lactoylglutathione lyase	Q04760	5.6	**Guanine nucleotide-binding protein G(s) subunit alpha isoforms XLas**	Q5JWF2	4.2
Ezrin	P15311	5.4	**Glycine--tRNA ligase**	P41250	4.1
Clathrin heavy chain 1	Q00610	5.3	**Eukaryotic translation initiation factor 4H**	Q15056	4.0
Serine/arginine-rich splicing factor 1	Q07955	5.0	**Glucose-6-phosphate isomerase**	P06744	4.0
Biliverdin reductase A	P53004	5.0	**Fatty acid synthase**	P49327	4.0
Desmoplakin	P15924	4.7	**Uroporphyrinogen decarboxylase**	P06132	3.9
60S ribosomal protein L19	P84098	4.6	**Adenylyl cyclase-associated protein 1**	Q01518	3.9
Nucleophosmin	P06748	4.5	**Ubiquitin-conjugating enzyme E2 variant 2**	Q15819	3.8
Aldehyde dehydrogenase family 1 member A3	P47895	4.5	**Tenascin**	P24821	3.8
C-type lectin domain family 11 member A	Q9Y240	4.3	**Filamin-B**	O75369	3.8
40S ribosomal protein S21	P63220	4.3	**60S ribosomal protein L4**	P36578	3.8
Tropomyosin alpha-1 chain	P09493	4.3	**60S ribosomal protein L5**	P46777	3.7
Eukaryotic translation initiation factor 3 subunit B	P55884	4.2	**Ezrin**	P15311	3.7
Actin-related protein 2	P61160	4.2	**Rab GDP dissociation inhibitor beta**	P50395	3.7
Osteopontin	P10451	4.2	**Glucosidase 2 subunit beta**	P14314	3.7
Importin subunit beta-1	Q14974	4.2	**Tubulin alpha-1C chain**	Q9BQE3	3.6
Hexokinase-1	P19367	4.1	**Cysteine--tRNA ligase, cytoplasmic**	P49589	3.6
40S ribosomal protein S28	P62857	4.0	**LIM and SH3 domain protein 1**	Q14847	3.6
Stanniocalcin-2	O76061	3.9	**Barrier-to-autointegration factor**	O75531	3.6
Eukaryotic translation initiation factor 3 subunit A	Q14152	3.9	**60S ribosomal protein L19**	P84098	3.5
Basigin	P35613	3.9	**Calpain-2 catalytic subunit**	P17655	3.4
Protein SET	Q01105	3.9	**Eukaryotic translation initiation factor 3 subunit A**	Q14152	3.3
LIM and SH3 domain protein 1	Q14847	3.8	**Ras-related protein Rab-10**	P61026	3.3
SKI family transcriptional corepressor 2	Q2VWA4	3.8	**Hexokinase-1**	P19367	3.3
Eukaryotic translation initiation factor 4 gamma 1	Q04637	3.7	**Acidic leucine-rich nuclear phosphoprotein 32 family member B**	Q92688	3.3

Ectonucleotide pyrophosphatase/phospho diesterase family member 2	Q13822	3.6	**ATP-dependent 6-phosphofructokinase, platelet type**	Q01813	3.3
40S ribosomal protein S5	P46782	3.6	**Heterogeneous nuclear ribonucleoprotein D0**	Q14103	3.3
Lysine--tRNA ligase	Q15046	3.6	**40S ribosomal protein S3**	P23396	3.3
40S ribosomal protein S18	P62269	3.6	**Rab GDP dissociation inhibitor alpha**	P31150	3.2
Neutral alpha-glucosidase AB	Q14697	3.5	**Lactoylglutathione lyase**	Q04760	3.2
ADP-ribosylation factor 4	P18085	3.5	**60S ribosomal protein L18**	Q07020	3.1
Ubiquitin thioesterase OTUB1	Q96FW1	3.5	**Spermine synthase**	P52788	3.1
Histone H2A type 1-C	Q93077	3.4	**Aldose reductase**	P15121	3.1
Ras-related protein Rab-7a	P51149	3.3	**Stress-induced-phosphoprotein 1**	P31948	3.0
60S ribosomal protein L12	P30050	3.3	**Ubiquitin-conjugating enzyme E2 L3**	P68036	3.0
Metalloproteinase inhibitor 1	P01033	3.2	**C-type lectin domain family 11 member A**	Q9Y240	3.0
Tryptophan--tRNA ligase, cytoplasmic	P23381	3.1	**Phosphoserine aminotransferase**	Q9Y617	3.0
Caldesmon	Q05682	3.1	**Alpha-enolase**	P06733	3.0
Alanine--tRNA ligase, cytoplasmic	P49588	3.1	**Protein S100-A6**	P06703	2.9
Calpain-2 catalytic subunit	P17655	3.1	**40S ribosomal protein S18**	P62269	2.9
Uroporphyrinogen decarboxylase	P06132	3.0	**Reticulocalbin-1**	Q15293	2.9
Coactosin-like protein	Q14019	3.0	**Thymosin beta-10**	P63313	2.9
CD82 antigen	P27701	2.9	**Gamma-enolase**	P09104	2.9
Ras-related protein Rab-10	P61026	2.9	**Filamin-C**	Q14315	2.8
60S acidic ribosomal protein P2	P05387	2.8	**40S ribosomal protein S2**	P15880	2.8
Hippocalcin-like protein 1	P37235	2.6	**Protein S100-A11**	P31949	2.8
Complement C1s subcomponent	P09871	2.6	**Thioredoxin**	P10599	2.7
Plasminogen activator inhibitor 1 RNA-binding protein	Q8NC51	2.6	**Tubulin-specific chaperone A**	O75347	2.7
Heterogeneous nuclear ribonucleoprotein Q	O60506	2.5	**14-3-3 protein beta/alpha**	P31946	2.6
Heterogeneous nuclear ribonucleoprotein K	P61978	2.5	**Elongation factor 1-delta**	P29692	2.6
Coatomer subunit delta	P48444	2.4	**Vimentin**	P08670	2.6
Guanine nucleotide-binding protein G(I)/G(S)/G(O) subunit gamma-12	Q9UBI6	2.4	**Myosin-9**	P35579	2.6
Procollagen C-endopeptidase enhancer 2	Q9UKZ9	2.4	**Myosin regulatory light chain 12A**	P19105	2.6
GPALPP motifs-containing protein 1	Q8IXQ4	2.3	**Stathmin**	P16949	2.5
Rho GDP-dissociation inhibitor 1	P52565	2.3	**Tropomyosin alpha-1 chain**	P09493	2.5
L-lactate dehydrogenase B chain	P07195	2.3	**78 kDa glucose-regulated protein**	P11021	2.5
Tenascin	P24821	2.3	**Actin-related protein 2/3 complex subunit 1B**	O15143	2.5
Tumor protein D54	O43399	2.2	**Galectin-1**	P09382	2.5

Stress-70 protein, mitochondrial	P38646	2.2	**Neuroblast differentiation-associated protein AHNAK**	Q09666	2.4
Heterogeneous nuclear ribonucleoprotein R	O43390	2.2	**Proteasome activator complex subunit 1**	Q06323	2.4
Laminin subunit gamma-1	P11047	2.2	**Fructose-bisphosphate aldolase A**	P04075	2.4
Coronin-1C	Q9ULV4	2.2	**ADP-ribosylation factor 1**	P84077	2.4
Collagen alpha-2(VI) chain	P12110	2.1	**F-actin-capping protein subunit beta**	P47756	2.4
Adenylate kinase 2, mitochondrial	P54819	2.1	**Stress-70 protein, mitochondrial**	P38646	2.4
Apolipoprotein B-100	P04114	2.1	**Elongation factor 1-gamma**	P26641	2.4
Hemoglobin subunit alpha	P69905	2.1	**Guanine nucleotide-binding protein G(I)/G(S)/G(O) subunit gamma-12**	Q9UBI6	2.4
Flavin reductase (NADPH)	P30043	2.0	**Actin, alpha skeletal muscle**	P68133	2.3
Phosphoserine aminotransferase	Q9Y617	2.0	**Glyceraldehyde-3-phosphate dehydrogenase**	P04406	2.3
Reticulon-4	Q9NQC3	2.0	**Acylamino-acid-releasing enzyme**	P13798	2.3
Complement C1r subcomponent	P00736	1.9	**Synaptic vesicle membrane protein VAT-1 homolog**	Q99536	2.3
Peroxiredoxin-1	Q06830	1.9	**Glutathione S-transferase omega-1**	P78417	2.3
Retinoic acid receptor responder protein 1	P49788	1.9	**Coactosin-like protein**	Q14019	2.3
Tubulin alpha-4A chain	P68366	1.9	**Actin, cytoplasmic 2**	P63261	2.3
Translationally-controlled tumor protein	P13693	1.9	**ADP/ATP translocase 2**	P05141	2.3
Extracellular matrix protein 1	Q16610	1.9	**Eukaryotic translation initiation factor 3 subunit E**	P60228	2.2
Versican core protein	P13611	1.8	**Protein DJ-1**	Q99497	2.2
Calsyntenin-1	O94985	1.8	**Basigin**	P35613	2.2
Filamin-A	P21333	1.8	**Adenylate kinase 2, mitochondrial**	P54819	2.2
Sulfhydryl oxidase 1	O00391	1.8	**14-3-3 protein theta**	P27348	2.2
Spermine synthase	P52788	1.8	**Calpain small subunit 1**	P04632	2.2
Actin-related protein 3B	Q9P1U1	1.7	**Serine/arginine-rich splicing factor 1**	Q07955	2.2
Histone H2B type 1-L	Q99880	1.7	**Prothymosin alpha**	P06454	2.1
ICOS ligand	O75144	1.7	**Putative trypsin-6**	Q8NHM4	2.1
Transitional endoplasmic reticulum ATPase	P55072	1.6	**Trypsin-2**	P07478	2.1
Heterogeneous nuclear ribonucleoprotein A3	P51991	1.6	**Aldehyde dehydrogenase family 1 member A3**	P47895	2.1
Nucleoside diphosphate kinase A	P15531	1.6	**StAR-related lipid transfer protein 9**	Q9P2P6	2.1
Multifunctional protein ADE2	P22234	1.6	**60 kDa heat shock protein, mitochondrial**	P10809	2.1
Transgelin-2	P37802	1.6	**6-phosphogluconate dehydrogenase, decarboxylating**	P52209	2.1

Peptidyl-prolyl cis-trans isomerase B	P23284	1.5	**Triosephosphate isomerase**	P60174	2.0
Latent-transforming growth factor beta-binding protein 1	Q14766	1.5	**Microtubule-associated protein 4**	P27816	2.0
Cation-independent mannose-6-phosphate receptor	P11717	1.5	**Transaldolase**	P37837	2.0
Periostin	Q15063	1.5	**NAD(P)H dehydrogenase [quinone] 1**	P15559	2.0
Apolipoprotein E	P02649	1.5	**Malate dehydrogenase, cytoplasmic**	P40925	2.0
Acylamino-acid-releasing enzyme	P13798	1.5	**Fructose-bisphosphate aldolase C**	P09972	2.0
Insulin-like growth factor-binding protein 2	P18065	1.5	**Multifunctional protein ADE2**	P22234	2.0
Myosin light polypeptide 6	P60660	1.5	**Clathrin heavy chain 1**	Q00610	2.0
Sushi repeat-containing protein SRPX	P78539	1.5	**Brain acid soluble protein 1**	P80723	2.0
Brain acid soluble protein 1	P80723	1.5	**Peptidyl-prolyl cis-trans isomerase A**	P62937	2.0
Collagen alpha-1(V) chain	P20908	1.5	**Eukaryotic translation initiation factor 4 gamma 1**	Q04637	2.0
Eukaryotic translation initiation factor 4H	Q15056	1.4	**Reticulon-4**	Q9NQC3	2.0
Galectin-3-binding protein	Q08380	1.4	**Profilin-1**	P07737	2.0
Eukaryotic translation initiation factor 3 subunit D	O15371	1.4	**Annexin A5**	P08758	2.0
40S ribosomal protein S16	P62249	1.4	**Heterogeneous nuclear ribonucleoprotein A1**	P09651	1.9
Small ubiquitin-related modifier 2	P61956	1.4	**Phosphoglycerate kinase 1**	P00558	1.9
Coagulation factor IX	P00740	1.4	**Transgelin-2**	P37802	1.9
72 kDa type IV collagenase	P08253	1.4	**Receptor of activated protein C kinase 1**	P63244	1.9
Leukemia inhibitory factor	P15018	1.4	**Tumor protein D54**	O43399	1.9
Collagen alpha-2(I) chain	P08123	1.4	**Ubiquitin-like modifier-activating enzyme 1**	P22314	1.9
Pregnancy zone protein	P20742	1.4	**14-3-3 protein epsilon**	P62258	1.9
Vinculin	P18206	1.4	**Pyruvate kinase PKM**	P14618	1.9
Prothymosin alpha	P06454	1.4	**Ras-related protein Rab-7a**	P51149	1.9
Serine protease HTRA1	Q92743	1.4	**Protein-glutamine gamma-glutamyltransferase 2**	P21980	1.9
Beta-2-microglobulin	P61769	1.4	**Tubulin beta-4B chain**	P68371	1.8
Phospholipid transfer protein	P55058	1.4	**Annexin A1**	P04083	1.8
Insulin-like growth factor II	P01344	1.4	**Plasminogen activator inhibitor 1 RNA-binding protein**	Q8NC51	1.8
Hepatocyte growth factor activator	Q04756	1.4	**Inter-alpha-trypsin inhibitor heavy chain H3**	Q06033	1.8
Amyloid beta A4 protein	P05067	1.4	**Peroxiredoxin-5, mitochondrial**	P30044	1.8
SPARC	P09486	1.4	**Tubulin beta-6 chain**	Q9BUF5	1.8

EGF-containing fibulin-like extracellular matrix protein 1	Q12805	1.3	**40S ribosomal protein S10**	P46783	1.8
Molybdopterin synthase catalytic subunit	O96007	1.3	**T-complex protein 1 subunit theta**	P50990	1.8
Cartilage oligomeric matrix protein	P49747	1.3	**Vinculin**	P18206	1.8
Thrombospondin-1	P07996	1.3	**Peroxiredoxin-1**	Q06830	1.8
Elongation factor 1-gamma	P26641	1.3	**Cystatin-B**	P04080	1.8
Afamin	P43652	1.3	**10 kDa heat shock protein, mitochondrial**	P61604	1.8
Protein FAM47E	Q6ZV65	1.3	**Moesin**	P26038	1.8
Tropomyosin alpha-3 chain	P06753	1.3	**Serine/threonine-protein phosphatase 5**	P53041	1.8
Coagulation factor V	P12259	1.3	**Heat shock protein HSP 90-alpha**	P07900	1.8
Cystatin-C	P01034	1.3	**Guanine nucleotide-binding protein G(I)/G(S)/G(T) subunit beta-1**	P62873	1.8
Transforming growth factor-beta-induced protein ig-h3	Q15582	1.3	**Cofilin-1**	P23528	1.8
WD repeat-containing protein 1	O75083	1.3	**Biliverdin reductase A**	P53004	1.8
Complement factor I	P05156	1.3	**GTP-binding nuclear protein Ran**	P62826	1.8
Collagen alpha-1(VI) chain	P12109	1.3	**Ubiquitin-60S ribosomal protein L40**	P62987	1.8
Lysyl oxidase homolog 2	Q9Y4K0	1.3	**Actin-related protein 3B**	Q9P1U1	1.7
Fibrinogen gamma chain	P02679	1.3	**Protein SET**	Q01105	1.7
Retinol-binding protein 4	P02753	1.3	**L-lactate dehydrogenase A chain**	P00338	1.7
Heparin cofactor 2	P05546	1.3	**Peroxiredoxin-6**	P30041	1.7
Lactotransferrin	P02788	1.3	**Myosin light polypeptide 6**	P60660	1.7
Lumican	P51884	1.3	**Transitional endoplasmic reticulum ATPase**	P55072	1.7
Clusterin	P10909	1.3	**Ras-related protein Rab-2A**	P61019	1.7
Collagen alpha-1(I) chain	P02452	1.3	**Transketolase**	P29401	1.7
Plasminogen activator inhibitor 1	P05121	1.3	**WD repeat-containing protein 1**	O75083	1.6
Collagen alpha-3(VI) chain	P12111	1.3	**Adenosylhomocysteinase**	P23526	1.6
Sacsin	Q9NZJ4	1.3	**Small ubiquitin-related modifier 2**	P61956	1.6
Tetranectin	P05452	1.3	**Alpha-actinin-4**	O43707	1.6
CD44 antigen	P16070	1.3	**D-3-phosphoglycerate dehydrogenase**	O43175	1.6
Prothrombin	P00734	1.3	**Importin subunit beta-1**	Q14974	1.6
Thrombospondin-2	P35442	1.3	**Tropomyosin alpha-4 chain**	P67936	1.6
Vitronectin	P04004	1.3	**Ubiquitin carboxyl-terminal hydrolase isozyme L1**	P09936	1.6
ATP-binding cassette sub-family A member 10	Q8WWZ4	1.3	**Putative elongation factor 1-alpha-like 3**	Q5VTE0	1.6
Sex hormone-binding globulin	P04278	1.2	**Ras-related protein Rab-1B**	Q9H0U4	1.6

Fibronectin	P02751	1.2	**Flavin reductase (NADPH)**	P30043	1.6
Apolipoprotein M	O95445	1.2	**Elongation factor 1-alpha 1**	P68104	1.6
Beta-2-syntrophin	Q13425	1.2	**Peroxiredoxin-2**	P32119	1.5
E3 ubiquitin-protein ligase MARCH4	Q9P2E8	1.2	**Filamin-A**	P21333	1.5
Plasminogen	P00747	1.2	**Nicotinamide phosphoribosyltransferase**	P43490	1.5
Collagen alpha-1(III) chain	P02461	1.2	**14-3-3 protein zeta/delta**	P63104	1.5
Insulin-like growth factor-binding protein 7	Q16270	1.2	**Rho GDP-dissociation inhibitor 1**	P52565	1.5
Alpha-1B-glycoprotein	P04217	1.2	**Phosphatidylethanolamine-binding protein 1**	P30086	1.5
Complement C3	P01024	1.2	**L-lactate dehydrogenase B chain**	P07195	1.5
Apolipoprotein C-III	P02656	1.2	**Talin-1**	Q9Y490	1.5
Fibulin-1	P23142	1.2	**Heat shock protein HSP 90-beta**	P08238	1.5
Complement C5	P01031	1.2	**Phosphoglycerate mutase 1**	P18669	1.5
Alpha-2-macroglobulin	P01023	1.2	**Puromycin-sensitive aminopeptidase**	P55786	1.5
ADP-ribosylation factor 1	P84077	1.2	**Tubulin alpha-1B chain**	P68363	1.5
Antithrombin-III	P01008	1.2	**Heat shock cognate 71 kDa protein**	P11142	1.5
Talin-1	Q9Y490	1.2	**14-3-3 protein gamma**	P61981	1.5
Serotransferrin	P02787	1.2	**Ribonuclease inhibitor**	P13489	1.5
Trafficking protein particle complex subunit 6A	O75865	1.2	**Eukaryotic translation initiation factor 2 subunit 1**	P05198	1.4
Inter-alpha-trypsin inhibitor heavy chain H3	Q06033	1.2	**Nucleoside diphosphate kinase B**	P22392	1.4
Single-pass membrane and coiled-coil domain-containing protein 2	A6NFE2	1.2	**Beta-2-syntrophin**	Q13425	1.4
Pigment epithelium-derived factor	P36955	1.2	**Sterol 26-hydroxylase, mitochondrial**	Q02318	1.4
Inter-alpha-trypsin inhibitor heavy chain H4	Q14624	1.2	**T-complex protein 1 subunit gamma**	P49368	1.4
Complement component C7	P10643	1.2	**Apolipoprotein A-I**	P02647	1.4
PiggyBac transposable element-derived protein 5	Q8N414	1.2	**Annexin A2**	P07355	1.4
Vimentin	P08670	1.1	**60S ribosomal protein L27a**	P46776	1.4
Vitamin D-binding protein	P02774	1.1	**HLA class I histocompatibility antigen, B-44 alpha chain**	P30481	1.4
Putative trypsin-6	Q8NHM4	1.1	**Collagen alpha-1(III) chain**	P02461	1.4
60 kDa heat shock protein, mitochondrial	P10809	1.1	**Endoplasmin**	P14625	1.4
Trypsin-2	P07478	1.1	**40S ribosomal protein S12**	P25398	1.4
Heat shock 70 kDa protein 1B	P0DMV9	-1.1	**CD82 antigen**	P27701	1.4
E3 ubiquitin-protein ligase BRE1B	O75150	-1.2	**E3 ubiquitin-protein ligase MARCH4**	Q9P2E8	1.4
Beta-2-glycoprotein 1	P02749	-1.2	**Elongation factor 2**	P13639	1.4
Tubulin-specific chaperone A	O75347	-1.2	**Calmodulin-3**	P0DP25	1.4

Gelsolin	P06396	-1.2	**Glutaredoxin-1**	P35754	1.4
Nicotinamide phosphoribosyltransferase	P43490	-1.2	**Fascin**	Q16658	1.3
Alpha-fetoprotein	P02771	-1.2	**40S ribosomal protein S28**	P62857	1.3
Complement component C9	P02748	-1.2	**Protein disulfide-isomerase**	P07237	1.3
45 kDa calcium-binding protein	Q9BRK5	-1.2	**Parathymosin**	P20962	1.3
Inorganic pyrophosphatase 2, mitochondrial	Q9H2U2	-1.2	**Tubulin alpha-4A chain**	P68366	1.3
Histone H4	P62805	-1.2	**14-3-3 protein eta**	Q04917	1.3
Hemopexin	P02790	-1.2	**Tropomyosin alpha-3 chain**	P06753	1.2
Apolipoprotein A-I	P02647	-1.2	**CD44 antigen**	P16070	1.2
Peroxiredoxin-2	P32119	-1.2	**Trafficking protein particle complex subunit 6A**	O75865	1.2
Myotrophin	P58546	-1.2	**Sacsin**	Q9NZJ4	1.2
Ubiquitin carboxyl-terminal hydrolase isozyme L1	P09936	-1.3	**Aldo-keto reductase family 1 member C1**	Q04828	1.2
Proteasome subunit alpha type-6	P60900	-1.3	**Eukaryotic initiation factor 4A-I**	P60842	1.2
Tropomyosin alpha-4 chain	P67936	-1.3	**Copper-transporting ATPase 2**	P35670	-1.1
Nucleosome assembly protein 1-like 1	P55209	-1.3	**Metallothionein-1E**	P04732	-1.2
Annexin A5	P08758	-1.3	**Tetranectin**	P05452	-1.2
Basement membrane-specific heparan sulfate proteoglycan core protein	P98160	-1.3	**SH3 domain-binding glutamic acid-rich-like protein 3**	Q9H299	-1.2
Heat shock cognate 71 kDa protein	P11142	-1.3	**Fibrinogen beta chain**	P02675	-1.2
Alpha-amylase 2B	P19961	-1.3	**PiggyBac transposable element-derived protein 5**	Q8N414	-1.2
Inter-alpha-trypsin inhibitor heavy chain H2	P19823	-1.3	**Molybdopterin synthase catalytic subunit**	O96007	-1.3
Hemoglobin subunit beta	P68871	-1.3	**Afamin**	P43652	-1.3
Endoplasmin	P14625	-1.3	**Calumenin**	O43852	-1.3
Chloride intracellular channel protein 1	O00299	-1.3	**E3 ubiquitin-protein ligase BRE1B**	O75150	-1.3
Alpha-2-HS-glycoprotein	P02765	-1.3	**Apolipoprotein C-III**	P02656	-1.3
Pantetheinase	O95497	-1.3	**Insulin-like growth factor-binding protein 3**	P17936	-1.3
Carboxypeptidase A4	Q9UI42	-1.3	**Inter-alpha-trypsin inhibitor heavy chain H4**	Q14624	-1.4
Protein S100-A6	P06703	-1.3	**Complement component C7**	P10643	-1.4
Phosphoglycerate kinase 1	P00558	-1.3	**Collagen alpha-1(I) chain**	P02452	-1.4
Nucleoside diphosphate kinase B	P22392	-1.3	**ICOS ligand**	O75144	-1.4
Cystatin-B	P04080	-1.3	**Procollagen C-endopeptidase enhancer 2**	Q9UKZ9	-1.4
Myosin regulatory light chain 12A	P19105	-1.3	**Leukemia inhibitory factor**	P15018	-1.4
Metallothionein-1E	P04732	-1.3	**Complement C5**	P01031	-1.4
Insulin-like growth factor-binding protein 3	P17936	-1.3	**Insulin-like growth factor II**	P01344	-1.4
14-3-3 protein zeta/delta	P63104	-1.4	**Fibulin-1**	P23142	-1.5

MOB kinase activator 1A	Q9H8S9	-1.4	**Alpha-2-antiplasmin**	P08697	-1.5
Moesin	P26038	-1.4	**Heat shock 70 kDa protein 1B**	P0DMV9	-1.5
Alpha-enolase	P06733	-1.4	**TLR4 interactor with leucine rich repeats**	Q7L0X0	-1.5
Cofilin-1	P23528	-1.4	**Lumican**	P51884	-1.5
Annexin A2	P07355	-1.4	**Alpha-2-macroglobulin**	P01023	-1.5
Parathymosin	P20962	-1.4	**Collagen alpha-1(XI) chain**	P12107	-1.5
14-3-3 protein theta	P27348	-1.4	**Protein Z-dependent protease inhibitor**	Q9UK55	-1.5
Eukaryotic initiation factor 4A-I	P60842	-1.4	**Serine/threonine-protein phosphatase 2A catalytic subunit alpha isoform**	P67775	-1.5
Glutaredoxin-1	P35754	-1.4	**60S acidic ribosomal protein P2**	P05387	-1.5
Fibrinogen beta chain	P02675	-1.4	**ATP-binding cassette sub-family A member 10**	Q8WWZ4	-1.5
Phosphatidylethanolamine-binding protein 1	P30086	-1.4	**Fibrinogen gamma chain**	P02679	-1.5
Elongation factor 1-alpha 1	P68104	-1.4	**Cathepsin B**	P07858	-1.5
Fructose-bisphosphate aldolase C	P09972	-1.4	**Coronin-1C**	Q9ULV4	-1.5
Glutathione S-transferase omega-1	P78417	-1.4	**Apolipoprotein E**	P02649	-1.6
Alpha-actinin-4	O43707	-1.4	**Inter-alpha-trypsin inhibitor heavy chain H1**	P19827	-1.6
Glutathione S-transferase P	P09211	-1.4	**Hemopexin**	P02790	-1.6
SH3 domain-binding glutamic acid-rich-like protein 3	Q9H299	-1.4	**Hemoglobin subunit alpha**	P69905	-1.6
Cathepsin B	P07858	-1.4	**Pigment epithelium-derived factor**	P36955	-1.6
Putative elongation factor 1-alpha-like 3	Q5VTE0	-1.4	**Complement component C9**	P02748	-1.6
Heat shock protein HSP 90-alpha	P07900	-1.4	**Hepatocyte growth factor activator**	Q04756	-1.6
Eukaryotic translation initiation factor 5A-1	P63241	-1.4	**Gelsolin**	P06396	-1.6
Transketolase	P29401	-1.4	**Pentraxin-related protein PTX3**	P26022	-1.6
Inter-alpha-trypsin inhibitor heavy chain H1	P19827	-1.4	**Vitamin K-dependent protein S**	P07225	-1.6
60S ribosomal protein L22	P35268	-1.4	**Protein disulfide-isomerase A3**	P30101	-1.6
Fructose-bisphosphate aldolase A	P04075	-1.4	**Coagulation factor V**	P12259	-1.6
Elongation factor 2	P13639	-1.4	**HLA class I histocompatibility antigen, B-59 alpha chain**	Q29940	-1.6
Histone H3.1	P68431	-1.4	**Vitamin D-binding protein**	P02774	-1.6
Glyceraldehyde-3-phosphate dehydrogenase	P04406	-1.5	**Nucleolin**	P19338	-1.6
Pyruvate kinase PKM	P14618	-1.5	**Prothrombin**	P00734	-1.6
GTP-binding nuclear protein Ran	P62826	-1.5	**Cartilage oligomeric matrix protein**	P49747	-1.6
Aldo-keto reductase family 1 member C1	Q04828	-1.5	**Hemoglobin subunit beta**	P68871	-1.7
Prosaposin	P07602	-1.5	**Complement factor I**	P05156	-1.7

14-3-3 protein eta	Q04917	-1.5	**Heat shock protein beta-1**	P04792	-1.7
L-lactate dehydrogenase A chain	P00338	-1.5	**Heparin cofactor 2**	P05546	-1.7
Complement factor B	P00751	-1.5	**Complement C4-A**	P0C0L4	-1.7
Profilin-1	P07737	-1.5	**Basement membrane-specific heparan sulfate proteoglycan core protein**	P98160	-1.7
Galectin-1	P09382	-1.5	**Apolipoprotein M**	O95445	-1.7
Calumenin	O43852	-1.5	**Alpha-fetoprotein**	P02771	-1.7
Heat shock protein beta-1	P04792	-1.5	**Thrombospondin-1**	P07996	-1.7
Aldose reductase	P15121	-1.5	**Reticulocalbin-3**	Q96D15	-1.7
Triosephosphate isomerase	P60174	-1.5	**Histone H2B type 1-L**	Q99880	-1.7
HLA class I histocompatibility antigen, B-59 alpha chain	Q29940	-1.5	**Complement factor B**	P00751	-1.7
Stanniocalcin-1	P52823	-1.5	**EGF-containing fibulin-like extracellular matrix protein 1**	Q12805	-1.7
Tubulin alpha-1B chain	P68363	-1.5	**Protein FAM47E**	Q6ZV65	-1.7
Peroxiredoxin-6	P30041	-1.5	**Periostin**	Q15063	-1.7
Peptidyl-prolyl cis-trans isomerase A	P62937	-1.5	**Aspartate aminotransferase, cytoplasmic**	P17174	-1.7
Myosin-9	P35579	-1.6	**Collagen alpha-1(II) chain**	P02458	-1.8
Pentraxin-related protein PTX3	P26022	-1.6	**Peptidyl-prolyl cis-trans isomerase FKBP4**	Q02790	-1.8
Annexin A1	P04083	-1.6	**Hemoglobin subunit gamma-2**	P69892	-1.8
Protein disulfide-isomerase	P07237	-1.6	**Hippocalcin-like protein 1**	P37235	-1.8
14-3-3 protein gamma	P61981	-1.6	**Syndecan-4**	P31431	-1.8
Interleukin-8	P10145	-1.6	**Vitronectin**	P04004	-1.8
Laminin subunit beta-1	P07942	-1.6	**Histone H4**	P62805	-1.8
Protein disulfide-isomerase A3	P30101	-1.6	**Antithrombin-III**	P01008	-1.8
40S ribosomal protein S12	P25398	-1.6	**Insulin-like growth factor-binding protein 2**	P18065	-1.8
Thioredoxin	P10599	-1.6	**Coagulation factor IX**	P00740	-1.8
Nuclear ubiquitous casein and cyclin-dependent kinase substrate 1	Q9H1E3	-1.6	**Complement C3**	P01024	-1.8
Actin, cytoplasmic 2	P63261	-1.7	**Cation-independent mannose-6-phosphate receptor**	P11717	-1.8
StAR-related lipid transfer protein 9	Q9P2P6	-1.7	**Inter-alpha-trypsin inhibitor heavy chain H2**	P19823	-1.9
78 kDa glucose-regulated protein	P11021	-1.7	**Plasminogen activator inhibitor 1**	P05121	-1.9
Insulin-like growth factor-binding protein 6	P24592	-1.8	**Proteasome subunit alpha type-6**	P60900	-1.9
Macrophage migration inhibitory factor	P14174	-1.8	**Pantetheinase**	O95497	-1.9
Cathepsin L1	P07711	-1.8	**Coagulation factor XIII A chain**	P00488	-1.9
10 kDa heat shock protein, mitochondrial	P61604	-1.8	**Plasminogen**	P00747	-1.9
Heat shock protein HSP 90-beta	P08238	-1.9	**Ubiquitin thioesterase OTUB1**	Q96FW1	-1.9

14-3-3 protein beta/alpha	P31946	-1.9	**Serine protease HTRA1**	Q92743	-2.0
Thymosin beta-10	P63313	-1.9	**Glia-derived nexin**	P07093	-2.0
Serine/threonine-protein phosphatase 2A catalytic subunit alpha isoform	P67775	-1.9	**Histone H1.5**	P16401	-2.0
Tubulin beta-4B chain	P68371	-2.0	**60S ribosomal protein L22**	P35268	-2.0
Nucleolin	P19338	-2.0	**Collagen alpha-2(VI) chain**	P12110	-2.0
28 kDa heat- and acid-stable phosphoprotein	Q13442	-2.0	**Beta-2-glycoprotein 1**	P02749	-2.0
Copper-transporting ATPase 2	P35670	-2.0	**Delta(3,5)-Delta(2,4)-dienoyl-CoA isomerase, mitochondrial**	Q13011	-2.1
Interleukin enhancer-binding factor 2	Q12905	-2.0	**Collagen alpha-3(VI) chain**	P12111	-2.1
14-3-3 protein epsilon	P62258	-2.0	**Collagen alpha-2(I) chain**	P08123	-2.1
Metallothionein-2	P02795	-2.0	**Protein DENND6A**	Q8IWF6	-2.1
60S ribosomal protein L27a	P46776	-2.1	**UPF0160 protein MYG1, mitochondrial**	Q9HB07	-2.1
Synaptic vesicle membrane protein VAT-1 homolog	Q99536	-2.1	**60S ribosomal protein L12**	P30050	-2.1
Actin, cytoplasmic 1	P60709	-2.1	**Peptidyl-prolyl cis-trans isomerase B**	P23284	-2.2
Histone H1.5	P16401	-2.1	**Amyloid beta A4 protein**	P05067	-2.2
Pachytene checkpoint protein 2 homolog	Q15645	-2.1	**Versican core protein**	P13611	-2.2
T-complex protein 1 subunit gamma	P49368	-2.2	**Retinol-binding protein 4**	P02753	-2.2
Protein DENND6A	Q8IWF6	-2.2	**Beta-2-microglobulin**	P61769	-2.2
Serum albumin	P02768	-2.2	**Heterogeneous nuclear ribonucleoprotein R**	O43390	-2.2
Integrin beta-1	P05556	-2.3	**Eukaryotic translation initiation factor 5A-1**	P63241	-2.2
Cathepsin D	P07339	-2.3	**Transforming growth factor-beta-induced protein ig-h3**	Q15582	-2.3
Stress-induced-phosphoprotein 1	P31948	-2.3	**Cathepsin L1**	P07711	-2.3
40S ribosomal protein S2	P15880	-2.4	**Thrombospondin-4**	P35443	-2.4
Hepatocyte growth factor-like protein	P26927	-2.4	**Collagen alpha-1(VI) chain**	P12109	-2.5
Actin-related protein 2/3 complex subunit 3	O15145	-2.4	**Single-pass membrane and coiled-coil domain-containing protein 2**	A6NFE2	-2.5
Stathmin	P16949	-2.5	**Collagen alpha-1(V) chain**	P20908	-2.5
Proteasome subunit alpha type-2	P25787	-2.5	**Lactotransferrin**	P02788	-2.5
Glucose-6-phosphate isomerase	P06744	-2.5	**Cathepsin D**	P07339	-2.5
Metalloproteinase inhibitor 2	P16035	-2.6	**Serine/threonine-protein phosphatase 2A 55 kDa regulatory subunit B alpha isoform**	P63151	-2.5
Malate dehydrogenase, mitochondrial	P40926	-2.6	**Alpha-2-HS-glycoprotein**	P02765	-2.5
Adenylyl cyclase-associated protein 1	Q01518	-2.6	**Clusterin**	P10909	-2.5
Elongation factor 1-delta	P29692	-2.7	**40S ribosomal protein S4, X isoform**	P62701	-2.5

Ubiquitin-conjugating enzyme E2 variant 2	Q15819	-2.7	**Nuclear ubiquitous casein and cyclin-dependent kinase substrate 1**	Q9H1E3	-2.6
Filamin-C	Q14315	-2.8	**Ras-related C3 botulinum toxin substrate 1**	P63000	-2.6
Adenosylhomocysteinase	P23526	-2.9	**Lysyl oxidase homolog 2**	Q9Y4K0	-2.6
Aspartate aminotransferase, cytoplasmic	P17174	-3.0	**GPALPP motifs-containing protein 1**	Q8IXQ4	-2.7
Prelamin-A/C	P02545	-3.0	**SPARC**	P09486	-2.7
Rab GDP dissociation inhibitor beta	P50395	-3.0	**Interleukin-8**	P10145	-2.8
Ubiquitin-60S ribosomal protein L40	P62987	-3.1	**Fibronectin**	P02751	-2.8
40S ribosomal protein S20	P60866	-3.1	**Sulfhydryl oxidase 1**	O00391	-2.8
Peptidyl-prolyl cis-trans isomerase FKBP4	Q02790	-3.1	**Prosaposin**	P07602	-2.9
Acidic leucine-rich nuclear phosphoprotein 32 family member B	Q92688	-3.2	**Histone H3.1**	P68431	-2.9
Actin-related protein 2/3 complex subunit 1B	O15143	-3.2	**Ectonucleotide pyrophosphatase/phosphodiesterase family member 2**	Q13822	-2.9
Proteasome subunit alpha type-3	P25788	-3.3	**Sex hormone-binding globulin**	P04278	-2.9
Heterogeneous nuclear ribonucleoprotein D0	Q14103	-3.4	**Phospholipid transfer protein**	P55058	-2.9
Proteasome activator complex subunit 1	Q06323	-3.4	**Calsyntenin-1**	O94985	-3.0
Protein-glutamine gamma-glutamyltransferase 2	P21980	-3.4	**Insulin-like growth factor-binding protein 7**	Q16270	-3.0
Mitochondrial import receptor subunit TOM70	O94826	-3.4	**Hepatocyte growth factor-like protein**	P26927	-3.0
Actin, alpha skeletal muscle	P68133	-3.4	**Cystatin-C**	P01034	-3.1
Galectin-3	P17931	-3.4	**Pregnancy zone protein**	P20742	-3.1
Latexin	Q9BS40	-3.5	**Procollagen-lysine,2-oxoglutarate 5-dioxygenase 2**	O00469	-3.1
Granulocyte colony-stimulating factor	P09919	-3.5	**Galectin-3-binding protein**	Q08380	-3.2
Protein Z-dependent protease inhibitor	Q9UK55	-3.5	**72 kDa type IV collagenase**	P08253	-3.2
Coagulation factor XIII A chain	P00488	-3.5	**60S ribosomal protein L7**	P18124	-3.2
Guanine nucleotide-binding protein G(I)/G(S)/G(T) subunit beta-1	P62873	-3.5	**Growth/differentiation factor 15**	Q99988	-3.3
Peptidyl-prolyl cis-trans isomerase FKBP1A	P62942	-3.5	**Latexin**	Q9BS40	-3.4
Glia-derived nexin	P07093	-3.5	**Insulin-like growth factor-binding protein 6**	P24592	-3.5
Ribonuclease inhibitor	P13489	-3.5	**Xaa-Pro aminopeptidase 1**	Q9NQW7	-3.5
UPF0160 protein MYG1, mitochondrial	Q9HB07	-3.6	**Metalloproteinase inhibitor 2**	P16035	-3.5
Procollagen-lysine,2-oxoglutarate 5-dioxygenase 1	Q02809	-3.6	**60S acidic ribosomal protein P1**	P05386	-3.5
Calmodulin-3	P0DP25	-3.9	**Complement C1s subcomponent**	P09871	-3.5

40S ribosomal protein S10	P46783	-3.9	**45 kDa calcium-binding protein**	Q9BRK5	-3.6
Sterol 26-hydroxylase, mitochondrial	Q02318	-3.9	**Actin-related protein 2/3 complex subunit 3**	O15145	-3.6
Serine/threonine-protein phosphatase 2A 55 kDa regulatory subunit B alpha isoform	P63151	-3.9	**Purine nucleoside phosphorylase**	P00491	-3.7
Xaa-Pro aminopeptidase 1	Q9NQW7	-4.0	**Complement C1r subcomponent**	P00736	-3.7
Puromycin-sensitive aminopeptidase	P55786	-4.0	**Macrophage migration inhibitory factor**	P14174	-3.8
Kynureninase	Q16719	-4.0	**Metalloproteinase inhibitor 1**	P01033	-3.9
Rab GDP dissociation inhibitor alpha	P31150	-4.1	**Heterogeneous nuclear ribonucleoprotein K**	P61978	-3.9
40S ribosomal protein S25	P62851	-4.1	**Alpha-1B-glycoprotein**	P04217	-4.0
60S ribosomal protein L4	P36578	-4.2	**Integrator complex subunit 4**	Q96HW7	-4.3
Eukaryotic translation initiation factor 3 subunit E	P60228	-4.2	**Retinoic acid receptor responder protein 1**	P49788	-4.5
Growth/differentiation factor 15	Q99988	-4.2	**Macrophage colony-stimulating factor 1**	P09603	-4.6
Microtubule-associated protein 4	P27816	-4.2	**Laminin subunit gamma-1**	P11047	-4.8
Peroxiredoxin-5, mitochondrial	P30044	-4.3	**Histidine--tRNA ligase, cytoplasmic**	P12081	-4.8
Thrombospondin-4	P35443	-4.3	**Inorganic pyrophosphatase**	Q15181	-5.1
40S ribosomal protein S3	P23396	-4.4	**Histone H2A type 2-A**	Q6FI13	-5.3
Malate dehydrogenase, cytoplasmic	P40925	-4.4	**Extracellular matrix protein 1**	Q16610	-5.5
Receptor of activated protein C kinase 1	P63244	-4.5	**Heterogeneous nuclear ribonucleoprotein A3**	P51991	-5.5
T-complex protein 1 subunit theta	P50990	-4.6	**Neutral alpha-glucosidase AB**	Q14697	-5.5
Ras-related C3 botulinum toxin substrate 1	P63000	-4.6	**Sushi repeat-containing protein SRPX**	P78539	-5.7
Ubiquitin-like modifier-activating enzyme 1	P22314	-4.8	**Serum albumin**	P02768	-5.7
Programmed cell death 6-interacting protein	Q8WUM4	-4.8	**Proteasome subunit alpha type-3**	P25788	-5.8
Glutathione synthetase	P48637	-4.8	**Serine/threonine-protein phosphatase 2A 65 kDa regulatory subunit A alpha isoform**	P30153	-5.9
60S acidic ribosomal protein P1	P05386	-4.9	**Myotrophin**	P58546	-5.9
Ras-related protein Rab-11B	Q15907	-5.0	**Mitochondrial import receptor subunit TOM70**	O94826	-6.0
TLR4 interactor with leucine rich repeats	Q7L0X0	-5.1	**Ras-related protein Rab-11B**	Q15907	-6.1
T-complex protein 1 subunit eta	Q99832	-5.3	**Procollagen-lysine,2-oxoglutarate 5-dioxygenase 1**	Q02809	-6.2
Glycine--tRNA ligase	P41250	-5.4	**40S ribosomal protein S5**	P46782	-6.2
Heterogeneous nuclear ribonucleoprotein A1	P09651	-5.4	**Interleukin enhancer-binding factor 2**	Q12905	-6.7
Phosphoglycerate mutase 1	P18669	-5.7	**Integrin beta-1**	P05556	-6.8
Collagen alpha-1(XI) chain	P12107	-5.8	**Prelamin-A/C**	P02545	-6.9

Macrophage colony-stimulating factor 1	P09603	-5.9	**Metallothionein-2**	P02795	-6.9
Serine/threonine-protein phosphatase 5	P53041	-5.9	**Alpha-amylase 2B**	P19961	-7.1
Major vault protein	Q14764	-6.0	**Coatomer subunit delta**	P48444	-7.4
ATP-dependent 6-phosphofructokinase, platelet type	Q01813	-6.1	**Laminin subunit beta-1**	P07942	-7.4
Ubiquitin-conjugating enzyme E2 L3	P68036	-6.4	**Stanniocalcin-1**	P52823	-7.5
COP9 signalosome complex subunit 4	Q9BT78	-6.5	**Thrombospondin-2**	P35442	-7.5
Thioredoxin reductase 1, cytoplasmic	Q16881	-6.5	**Serine/arginine-rich splicing factor 3**	P84103	-7.9
Hemoglobin subunit gamma-2	P69892	-6.6	**T-complex protein 1 subunit eta**	Q99832	-7.9
60S ribosomal protein L7	P18124	-6.6	**Thioredoxin reductase 1, cytoplasmic**	Q16881	-8.1
Glucose-6-phosphate 1-dehydrogenase	P11413	-6.8	**Actin, cytoplasmic 1**	P60709	-8.6
Serine/threonine-protein phosphatase 2A 65 kDa regulatory subunit A alpha isoform	P30153	-7.0	**Fibrillin-1**	P35555	-8.7
HLA class I histocompatibility antigen, B-44 alpha chain	P30481	-7.6	**Granulocyte colony-stimulating factor**	P09919	-8.7
60S ribosomal protein L5	P46777	-7.7	**Keratin, type I cytoskeletal 9**	P35527	-9.6
Fibrillin-1	P35555	-7.9	**Suprabasin**	Q6UWP8	-11.2
Vitamin K-dependent protein S	P07225	-8.0	**Inorganic pyrophosphatase 2, mitochondrial**	Q9H2U2	-11.4
Proliferation-associated protein 2G4	Q9UQ80	-8.1	**40S ribosomal protein S21**	P63220	-12.3
Tubulin beta-6 chain	Q9BUF5	-8.3	**Programmed cell death 6-interacting protein**	Q8WUM4	-12.5
40S ribosomal protein S4, X isoform	P62701	-8.5	**ADP-ribosylation factor 4**	P18085	-12.7
Delta(3,5)-Delta(2,4)-dienoyl-CoA isomerase, mitochondrial	Q13011	-9.5	**Translationally-controlled tumor protein**	P13693	-14.1
Procollagen-lysine,2-oxoglutarate 5-dioxygenase 2	O00469	-10.6	**Osteopontin**	P10451	-15.1
Suprabasin	Q6UWP8	-11.2	**MOB kinase activator 1A**	Q9H8S9	-16.3
Glucosidase 2 subunit beta	P14314	-11.8	**Glutathione synthetase**	P48637	-19.3
60S ribosomal protein L18	Q07020	-13.6	**Glutathione S-transferase P**	P09211	-19.6
Serine/arginine-rich splicing factor 3	P84103	-14.9	**Latent-transforming growth factor beta-binding protein 1**	Q14766	-20.2
BolA-like protein 2	Q9H3K6	-16.7	**Proteasome subunit alpha type-2**	P25787	-25.6
Fascin	Q16658	-17.2	**Eukaryotic translation initiation factor 3 subunit D**	O15371	-31.5
Tubulin alpha-1C chain	Q9BQE3	-17.4	**Chloride intracellular channel protein 1**	O00299	-37.4

NAD(P)H dehydrogenase [quinone] 1	P15559	-26.2	**Pachytene checkpoint protein 2 homolog**	Q15645	-44.6
Inorganic pyrophosphatase	Q15181	-26.9	**Carboxypeptidase A4**	Q9UI42	-78.5
Complement C4-A	P0C0L4	-36.4	**Histone H2A type 1-J**	Q99878	-87.8